

POSTERS GROUP 2

P13-2 - Tuesday, October 30, 2012, 16:00 - 16:30, Poster Exhibition Area

Physics & Instrumentation & Data Analysis: Instrumentation

P0670

Quantitative ^{124}I -PET: Evaluation of Prompt Gamma Coincidence Correction on a Clinical PET/CT system

P. Braad¹, S. B. Hansen², H. Thisgaard¹, P. Høiland-Carlson¹; ¹Odense University Hospital, Odense C, DENMARK, ²Århus University Hospital, Århus, DENMARK.

Objective: Quantitative Iodine-124-PET/CT is a highly promising tool for pre-therapeutic tumour dosimetry before Iodine-131 radionuclide therapy. However, imaging is complicated by prompt gamma coincidences (PGC) that add an undesired background activity to the images. An option for PGC-correction is available as part of the modelled scatter correction on the GE Discovery 690 PET/CT system. We evaluated the effect of this correction on image quality. **Materials and methods:** ^{124}I -spatial resolution was measured using the NEMA NU-2 standard. Six spherical inserts with volumes between 0.52 and 26.52ml were filled with a homogeneous aqueous solution of ^{124}I and placed inside the NEMA/IEC torso phantom. ^{124}I -activity was assessed in reconstructed PET/CT images of the phantom and the contrast recovery of each lesion was determined. The background of an 18cm high, 20cm diameter cylindrical phantom with three non-radioactive 5cm diameter cylindrical rods (teflon, air and water) was filled with a homogeneous aqueous ^{124}I -solution. Four 4cm cylindrical ROIs were placed in the background of the PET/CT images and noise and uniformity were assessed. Similar regions were placed over each 5cm diameter rod and spill-in of activity into the rods was determined. All reconstructions were done with and without PGC-correction, and all assessments of ^{124}I -activities were compared to gamma ray spectroscopy measurements. **Results:** The spatial resolution was measured to 5.5mm axially and 4.7mm transversally. Visual image quality was greatly improved by PGC correction. Contrast recovery was improved by 4% for the smallest lesion and 6% for the largest lesion. The total activity assessed from the reconstructed images with and without PGC-correction was 98% and 90%, respectively, of the expected value. Without PGC correction, the uniformity in the cylindrical phantom was clearly biased by an overcorrection of scatter in the central ROI and only 75% of the expected activity concentration was recovered. With PGC correction, uniformity and quantification was improved, though activity assessed in the central part of the phantom was 11% higher than expected. Excess activity was also measured in the "cold" cylindrical inserts, indicating that PGC and scatter was slightly under-corrected. **Conclusion:** PGC correction improves image quality and quantification accuracy. High quantitative accuracy can be expected when the activity is limited to a few isolated lesions. In imaging situations with a high ^{124}I -background, quantification is challenged. A better modelling of PGC in the scatter correction could improve the situation.

P0671

Digital signal processing unit for nuclear detection system

S. Sajedi¹, M. Farahani², N. Zeraatkar², H. Arabi³, N. Naderi¹, M. Ay⁴; ¹Pato Negar Persia Co., Tehran, IRAN, ISLAMIC REPUBLIC OF, ²Research Center for Science and Technology in Medicine, Tehran University of Medical Sciences and Pato Negar Persia Co., Tehran, IRAN, ISLAMIC REPUBLIC OF, ³Research Center for Science and Technology in Medicine, Tehran University of Medical Sciences and Pato Negar Persia Co., Tehran, IRAN, ISLAMIC REPUBLIC OF, ⁴Department of Medical Physics and Biomedical Engineering and Research Center for Science and Technology in Medicine and Research Institute for Nuclear Medicine, Tehran University of Medical Sciences, Tehran, IRAN, ISLAMIC REPUBLIC OF.

Aim: Development of digital processors widens the topic of pulse processing methods in nuclear detectors for appropriate data generation. In most applications, utilized particular method does not highly impact the data quality, whereas in some scenarios, such as in the presence of high count rates or high frequency pulses, this issue merits extra consideration. In this study, a new approach for pulse processing in spectroscopy has been implemented. **Materials and methods:** A new Non-Linear Recursive Filter (NLRF) was presented for spectroscopy applications. The filter exploits the constant shape of the output signal from PMT and, using non-linear equations, extracts the pulse's main characteristics. The obtained non-linear functions were not analytically feasible to resolve, so they were implemented by employing look-up tables. The filter has powerful pileup recovery ability instead of pileup rejection by predicting pulse tails and subtracting them from the following pulses. The algorithm was first simulated and then implemented in FPGA platform. Designated hardware was constructed by a low noise 12-bit ADC, a Spartan-3 FPGA

from Xilinx as processing unit, and a large-volume (512Mb) SDRAM for storing look-up tables. **Results:** The results based on spectroscopy application showed pileup recovery ability instead of traditional pileup rejection. The filter generated acceptable spectrum shape for count rates more than 1Mcps whereas the FWHM of photo peak was increased 60% from 200kcps to 1.2Mcps. The required frequency to run this filter was around the detector's time constant (e.g. 300ns for NaI(Tl) crystal). **Conclusion:** This filter in comparison to the other pileup rejection algorithms, shows competitive results considering very simple hardware required for implementation. Since, the sampling frequency utilized in this filter is about ten times smaller than the frequency required for processing NaI(Tl) detector (we used 3.3MHz which shall be minimally 30MHz according to the Nyquist frequency of the output pulse), it seems the roll of filter will be bold on fast detectors where sampling frequency may be critical for digital processing.

P0672

Use of a Printed Subresolution Sandwich Phantom for Simulation of FDG PET Images

B. Berthon¹, R. B. Holmes², C. Marshall¹, E. Spezi³; ¹Cardiff University - PETIC, Cardiff, UNITED KINGDOM, ²University Hospital Bristol NHS Foundation Trust, Cardiff, UNITED KINGDOM, ³Department of Medical Physics - Velindre Cancer Centre, Cardiff, UNITED KINGDOM.

Aims: Data simulation is an essential step in any PET study, especially in the validation of quantitative analysis techniques intended for clinical application. Software simulation allows the generation of known realistic ground truth but does not include the actual scanning process. Subresolution printed phantoms allow the simulation of realistic uptake patterns and provide a physical object to be scanned, thereby including the scanner in the simulation process. A small number of studies have demonstrated the usefulness of this approach in SPECT simulation, but the short half-life of ^{18}F , high-energy emission, lower availability and higher resolution makes PET simulation more challenging. This study aimed at investigating the feasibility of this type of phantoms applied to ^{18}F -FDG PET imaging. **Materials and methods:** Brain patterns with different ratios of printed intensity for grey and white matter segments have been derived from BrainWeb MRI segmentation maps and printed with a HP Deskjet 930 printer using black ink mixed with ^{18}F -FDG. The printed slices were assembled in a sub-resolution sandwich phantom consisting of elliptical 2mm Perspex sheets and imaged on a GE 690 Discovery PET-CT scanner. Reconstruction used time of flight information and CT-based attenuation correction. **Results:** After reconstruction using clinical settings phantom scans appear realistic on visual inspection. However, when voxel-based analysis is used to compare phantom data with 77 FDG PET scans of controls taken from the Alzheimer's Disease Neuroimaging Initiative (ADNI), the phantom data do not accurately match the control data. **Conclusions:** Further work is required to produce phantom scans that appear normal when compared to control scans. This will involve scanning of a wider range of simulated grey to white matter uptake ratios and to use the phantom - control data comparison to further refine the printout templates. However, this work has demonstrated the feasibility of simulating FDG PET brain scans using a printed subresolution sandwich phantom. The phantom has the potential to be successfully used for the simulation of normal and abnormal FDG uptake in the head and neck area. Furthermore, it could be used as a reference tool for (1) the evaluation of the performance of PET scanners, (2) the validation of segmentation algorithms, (3) the generation of realistic simulated dementia lesions.

P0673

Can Radiation Exposure Measurement by GM Counter be Used Interchangeably with Dose Calibrator to Assess the Completeness of Y90-microsphere Therapy?

M. F. Bozkurt, G. Demir, B. Volkan Salanci, O. Ugur; Hacettepe University Faculty of Medicine, Ankara, TURKEY.

Aim: Y90-microsphere therapy serves as an efficient treatment option for primary and metastatic liver tumors. There may be some obstacles regarding the intraarterial dose administration which limits the complete infusion of the calculated dose. Activity measurement from the dose vial by a dose calibrator which is set for Y90 energy extrapolatively, is the most used method to measure the administered dose to patient. However, it is not an ideal method with regard to Y90 being a pure beta emitter and needs liquid scintillator counters indeed. Also, dealing with the vial increases the personnel contamination risk. The aim of this study is to assess whether exposure rates read by Geiger-Müller (GM) detectors can be used to calculate the completeness of Y90 microsphere treatment as a more practical method. **Materials and Methods:** Between 2008-2012 a total of 97 patients (64m, mean age:56±10y) underwent Y90-resin microsphere treatment. Radiation exposure measurements by a GM counter were done at a certain distance from 4 sides of the transport set both before and after the treatment. In 12 out of 97 patients (12%) full therapy dose could not be administered mostly due to arterial spasm. In all these patients the residual activities in the vial were measured both by dose calibrator and also by GM counter by the same pretherapy

measurement technique. Pre and post-therapy counts from dose calibrator and GM counter were compared to each other to assess the use of interchangeable use. **Results:** The activity measurements from the full vial in all 97 patients at pre-therapy setting in mCi units by the dose calibrator correlated well with the exposure rate measurements of the same vial in mR/hr units by GM counter (Pearson, 0.96, $p=0.01$). In 12 patients to whom the full therapy dose could not be administered, the residual activity measurements by dose calibrator also correlated well with the exposure rate measurements by GM counter in the post-therapy setting (Spearman $\rho=0.95$, $p=0.02$). **Conclusion:** Our results may indicate that radiation exposure rate measurements by using a GM counter correlates very well with activity measurement directly by using a dose calibrator. The interchangeable use of GM counter may be more advantageous than dose calibrators as being a more practical and safer method with regard to avoiding direct hand contact which minimizes the risk of personnel contamination during Y90 microsphere treatment.

P0674

Striatal semi-quantification in ^{99m}Tc - ^{123}I dual-isotope SPECT acquired with a CZT-camera versus an Anger camera: a first brain-phantom study

D. Papathanassiou¹, D. Vilain², T. Blaire³, A. Bailliez²; ¹Institut Jean-Godinot, Reims, FRANCE, ²Hôpital Foch, Suresnes, FRANCE, ³Polyclinique du Bois, Lille, FRANCE.

Aim: Exploring if the energy resolution of a novel CZT-camera makes it possible to measure striatal radioactivity concentration ratios more accurately than with a conventional Anger gamma-camera, using dual-isotope acquisition. A brain phantom was used in order to simulate a striatal neurotransmission assessment combined with a perfusion SPECT. **Materials and methods:** Three cortical and three diencephalic compartments (0.8 to 11.6 ml) of a two dimensional Hoffman Multi-Compartment Brain Phantom (Data Spectrum) were filled with water containing different concentrations of ^{123}I (20 to 300 MBq/ml), and (except for one cortical compartment) 300 MBq/ml of ^{99m}Tc leading to $^{99m}\text{Tc}/^{123}\text{I}$ ratios varying from 1 to 12. Dual-isotope SPECT images were acquired with an ultrafast Alcyone (Discovery 530 NMC, GE Healthcare) CZT-camera and a Hawkeye HD SPECT/CT camera (GE Healthcare). Acquisition parameters were respectively 8 minutes duration and 120 (20 s) projections. Circular (0.652 cm²) regions of interest (ROI) were manually positioned on the CZT-camera SPECT image and copied on the Anger-camera SPECT image. They were used for measurements of both nuclides activity, corrected for radioactive decay. Diencephalic (caudate or putamen)/cortical (frontal, parietal, temporal, occipital) ROIs ratios and the caudate/putamen ratio were computed using ^{123}I and ^{99m}Tc values, obtained with both devices. The difference between the true ratio and the measured ratio, expressed as a percentage, was analysed for nine ratios. A non parametric test (permutation test for paired replicates) was used for evaluation of statistical significance. **Results:** The mean difference between the true and the calculated ratios for the CZT and Anger cameras was respectively -26.01 and -34.80 ($p=0.04$) with ^{99m}Tc , and was -19.69 and -51.10 ($p=0.02$) with ^{123}I . With both cameras and both nuclides, the percentage error was larger for the caudate than for the putamen (whose volumes are 0.8 and 3.2 ml respectively). **Conclusion:** The striatal semi-quantification with a CZT camera seems at least as acceptable as with an Anger camera in a ^{99m}Tc - ^{123}I dual-isotope acquisition. The error was even smaller in our study (especially for ^{123}I), probably due to spatial resolution (as far as the partial volume effect is involved) and the better energy resolution inherent to the new system.

P0675

What value should we use for the heart to mediastinum ratio?

F. Zanarini¹, P. Cella², J. O'Brien³, L. Clarke⁴; ¹Bristol Royal Infirmary, Bristol, UNITED KINGDOM, ²GE Healthcare, Milwaukee, WI, UNITED STATES, ³Birmingham City Hospital, Birmingham, UNITED KINGDOM, ⁴GE Healthcare, Amersham, UNITED KINGDOM.

Aim AdreView Myocardial Imaging for Risk Evaluation in Heart Failure (ADMIRE-HF) study (1) suggested that using ^{123}I MIBG (AdreView), patients with H/M ratio of less than 1.6 are at higher risk of major cardiac events. Another study (2) investigated H/M ratios using low energy high resolution (LEHR) collimators. The aim of this study is to investigate variation in heart/mediastinum (H/M) ratio across different camera systems and collimators. **Material and methods** A planar phantom was designed by GE Healthcare to depict the left ventricle, lungs and liver. A flood phantom was also constructed to be used as the scatter/attenuator. Both phantoms were filled with ^{123}I in a water solution. The flood phantom was filled with solution of lower concentration. Images of the phantom were acquired with and without the flood using LEHR and medium energy general purpose (MEGP) collimators on different camera systems. The acquisition parameters of 128x128, no zoom and 20% window were used. A background region of 7x7 pixels for mediastinum and a region around myocardium were drawn. The ratio of average counts per pixel in myocardium and mediastinum was calculated for each set of images. **Result** The preliminary results show that the calculated ratio using LEHR collimators was 2.07 ± 0.13 . However, the ratio using an SMV/GE camera was 2.34.

When the phantom was imaged in conjunction with the flood the calculated ratio was 1.88 ± 0.13 . The ratios using MEGP collimators were calculated to be 2.70 ± 0.15 and 2.39 ± 0.03 when imaging the phantom only and the phantom with the flood respectively. **Conclusion** The difference between the results with and without the flood and also the ratio for some camera systems highlights the need for a range of ratios to be considered in order to use the H/M ratio in clinical settings. However, the ratio between modern cameras was consistent. Care must be taken when older camera systems are used. The results for different cameras will need further investigation. 1) Journal of the American College of Cardiology 2010;55:2212-2221. 2) Journal of the American College of Cardiology 2010;55:2769-2777.

P0676

Precision of the measurements of distal fall-off of dose profiles in carbon ion therapy with a dedicated in-room PET system

N. Belcari^{1,2}, G. Sportelli², N. Camarlinghi², K. Straub², S. Ferretti¹, N. Marino¹, G. A. P. Cirrone³, G. Cuttone³, F. Romano³, V. Rosso^{1,2}, A. Del Guerra^{1,2}; ¹University of Pisa, Pisa, ITALY, ²INFN, Pisa, ITALY, ³INFN-LNS, Catania, ITALY.

Aim We have developed a dedicated PET system to monitor the dose delivered in hadrontherapy treatments by measuring the activity distribution of beta+ emitters produced in tissue during the particle irradiation. Our aim is to study the lower limit of the delivered dose for monitoring the distal fall-off of the dose profiles with a precision of better than 1 mm using 12C beams. **Materials and methods** The DoPET system consisted of two planar detector heads comprising up to four independent modules each, arranged in a 2x2 geometry. The modules are made up of 23x23 LYSO crystal matrix (2 mm pitch), with a total active area of 46 mm x 46 mm, coupled to multi-anode photomultiplier tubes (Hamamatsu H8500) and read out by a dedicated electronics. Data acquisition is performed by DAQ boards, one for each detector, hosted on a FPGA-based motherboard. Data are then streamed to a PC via USB connection. The total Field of View of the DoPET system is about 10 cm (high) x 10 cm (wide) x 10 cm (transaxial). The system was used to measure the activity distribution produced by proton and carbon ion beams at the INFN-LNS hadrontherapy facility CATANA (Catania, Italy). Particles were produced with a maximum energy of 62 MeV/A and their range was varied using range shifters. Irradiations of PMMA and tissue equivalent phantoms were performed delivering the typical dose as for clinical treatment (up to about 15 Gy, such as in ocular melanoma treatments). By exploiting the count rate performance offered by our system, we have also studied the feasibility of in-beam (i.e. data acquisition during hadronic beam irradiation) PET measurements and compared the results with a more conventional in-room (i.e. data acquisition started just after the end of the irradiation) measurement approach. **Results and Conclusions** The DoPET system has demonstrated to be able to reconstruct the position of the distal fall-off of the activity distribution with a precision of better than 1 mm with carbon ion beams. Thanks to the high modularity of the system it was also possible to use part of the information from annihilation photons during beam irradiation that is usually lost in in-room measurements.

P14-2 - Tuesday, October 30, 2012, 16:00 - 16:30, Poster Exhibition Area

Physics & Instrumentation & Data Analysis: Image Reconstruction

P0677

Application of A Intraoperative Dual-Gamma-Probe System in the Sentinel Lymph Node Detection: A Monte Carlo Simulation Study

C. H. Lin¹, K. Chuang¹, S. Lu¹, H. Lin¹, M. Jan²; ¹Biomedical Engineering and Environmental Sciences, National Tsing-Hua Uni., Hsinchu, TAIWAN, ²Institute of Nuclear Energy Research, Taoyuan, TAIWAN.

Aim: Gamma probe has been widely applied to assist in sentinel lymph node (SLN) tumor detection, resection, and radio-immunotherapy guide. However, it cannot provide 3-D information and it is highly sensitive to noise. These factors limit the employment of the device. In order to improve the diagnostic rate and success rate of operation, and to provide more precise spatial and quantitative information, a robust, convenient and real time 3-D imaging system is necessary, especially for intraoperative SLN tumor detection. **Materials and Methods:** A dual photon emission computed tomography (DuPECT) system was developed for multiple-emission-isotopes that were applied to detect the SLNs (tumor size ranged between 2mm to 50 mm) during operation. The DuPECT system composed of two detectors, one with a slat collimator, the other with a fan-beam collimator. Both collimators were made of tungsten with a hole diameter of 1.6 mm and length of 58 mm. Both collimators can be easily manipulated independently. The collimators define the direction of the incident photons. The source position can be located by

calculating the intersection of the line-plane pair, defined by slat- and fan-beam collimators, respectively. The effect of various focal lengths of the fan-beam collimator was investigated. Se-75, a multiple-emission-isotope, was placed at the focal point and different off-focal points within the FOV for assessing the system performance. The system was modeled with a SimSET/GATE software, a Monte Carlo code established by our laboratory. Results: The results indicate that the fan-beam collimator with a focal length of 150 mm provided the most acceptable detection efficiency and special resolution. A transaxial resolution of 3.2 mm can be achieved with detection efficiency of 2.2×10^{-5} for a source located at the focal point. Furthermore, the system has a high true event rate of 95.8%. The effective area of the FOV was 83 mm. Note that most of the SLN tumors sizes are usually in the range of 2 mm to 50 mm, that just fall within the FOV of the DuPECT system. Conclusions: The preliminary results indicate that images obtained with the DuPECT system provided 3-D information, higher signal-to-noise ratio, and better transaxial resolution. Despite the limitations of a loss of axial resolution and low detection efficiency, we conclude this system has a great potential to improve the diagnosis and the removal rate of SNL tumors in the operation room.

P0678

Comparison of two iterative reconstruction algorithms used in SPECT acquisition for somatostatin receptor' detectability

F. Voltini, F. Zito, G. Marotta, L. Florimonte, P. Gerundini; IRCCS Fondazione Cà Granda Ospedale Maggiore, Milan, ITALY.

Aim. The choice of algorithm used for SPECT images reconstruction may be crucial for lesion detectability. The aim of this work was to evaluate the performance in somatostatin receptors' lesions detectability of two iterative algorithms. **Material and Methods.** γ -camera SYMBIA-S (Siemens) was used for data acquisition. SPECT patient examination was simulated using an Alderson phantom containing lungs, heart, liver and 8 spherical inserts reproduced tumoral foci: 2 thorax, 4 external wall of liver, 2 abdomen. Mediastinum and abdomen were filled with ^{111}In water solution with 0.59 kBq/ml, and liver with 5.2 kBq/ml. Five lesions (volumes $1 \pm 2\text{ml}$) were filled with 74 kBq/ml and the smallest (0.5ml) with 444 kBq/ml. SPECT phantom acquisitions were performed by circular-orbits (CO) and body-contour (BC). The iterative algorithm implemented in SYMBIA are: Osem-2D and Flash-3DTM. The reconstruction parameters were 20 sub-sets combined respectively with 5, 10, 15, 20, 30 iterations (IT) and Gauss postfiltering. The images were evaluated by two observers which detected the lesions and assigned to each of them a score on 5 points scale, to grade the detectability from 1 (doubt) to 5 (very good). Fixed the orbit, to analyze differences between Osem-2D and Flash-3DTM with the same iterations, a paired t-test (PT1) was assessed between correspondent scores of each lesion. The differences between studies OC and BC were examined with paired t-test (PT2) between correspondent scores of each lesion for the sets of images reconstructed with the same algorithm and number IT. For each set of reconstructed images the mean of the scores values (MSC) was calculated as figure of merit, to summarize lesion detectability. **Results.** The observers detected 6 foci of 8 for all sets of images for both the algorithms and both orbits. Two of three lesions of 0.5ml, adherent to the liver, were not recognized, while one close to the liver but not adherent was identified. The test PT1 was significant ($P < 0.05$) for all the sets of images considered while PT2 was significant only for images reconstructed with 20 IT and 30 IT. The lesions with volumes between $1 \pm 2\text{ml}$ were always detected. The ranges of MSC values for images reconstructed with different number of iterations with Osem-2D were for OC: 4.4 ± 4.2 for BC: 3.7 ± 3.8 while for Flash-3DTM were for OC: 4.7 ± 4.8 and for BC: 4.0 ± 4.5 . Highest values of MSC for OC (4.2) were reached for Osem-2D with 20 IT while for Flash-3DTM with 10 IT OC (4.8). **Conclusion.** Flash-3D show better lesion detectability than OSEM-2D. SPECT examination with circular orbit and Flash-3D are preferable for somatostatin receptors' detectability. Optimization of iterations is mandatory to achieve the best image quality. Further increase of iterations for both algorithms and particularly for Flash-3DTM and BC creates important artefacts.

P0679

Performance evaluation of 3D dynamic RAMLA reconstruction for brain PET imaging

M. Ibaraki¹, K. Matsubara¹, T. Mizuta², T. Kinoshita¹; ¹Akita Research Institute of Brain and Blood Vessels, Akita, JAPAN, ²Shimadzu Corporation, Kyoto, JAPAN.

Aim: For brain PET imaging, improved characteristics of image contrast and noise while keeping the quantitative accuracy are required for a newly-developed image reconstruction algorithm. The aim of the study was to evaluate 3D-implemented dynamic row-action maximum likelihood algorithm (3D-DRAMA) [Tanaka, PMB 2003, 2010] in terms of the image contrast-noise characteristics and the quantitative accuracy for brain PET, by comparing the conventional 2D-DRAMA (FORE-DRAMA), which has been validated against 2D FBP reconstruction [Ibaraki, ANM 2009]. A bootstrap-based method was applied to estimate the pixel-level statistical noises of human brain PET images [Dahlbom, IEEE TNS 2002; Buvat, PMB 2002]. **Materials and Methods:** A GSO-based 3D PET scanner was used [Ibaraki,

JNM 2008]. DRAMA reconstruction is a modified version of RAMLA using a subset-dependent relaxation parameter for noise suppression. In the present study, 3D-DRAMA was compared to FORE-DRAMA. For the assessment of the image contrast-noise characteristics, ^{18}F -FDG PET data obtained from a healthy volunteer (60min-uptake, 5min scanning) were analyzed. In this analysis, the striatum-to-white matter count ratio and the bootstrap-derived pixel noises in the white matter region were used as indices of image contrast and image noises, respectively. ^{15}O -H₂O PET data set obtained from healthy volunteers ($n=17$) were used to show the applicability of 3D-DRAMA to the quantitative CBF measurement. **Results:** The image contrast-noise characteristic curves derived from the FDG PET data were calculated as a function of the number-of-iterations ($N_{it} = 1-10$), and were compared between 3D-DRAMA and FORE-DRAMA. Larger the number-of-iterations provided higher contrast and greater noise. 3D-DRAMA provided better characteristic curves with higher contrast and lower noise compared to FORE-DRAMA. On average, with no post-reconstruction filtering, image noises were approximately 25% smaller in 3D-DRAMA than FORE-DRAMA at the condition of same image contrast. When post-reconstruction filtering with 4-mm FWHM Gaussian kernel was applied, however, the advantages of 3D-DRAMA were reduced: approximately 10% smaller noises with 3D-DRAMA. Region of interests analysis of CBF maps derived from the ^{15}O -H₂O reconstruction images showed excellent agreement of CBF values between 3D-DRAMA and FORE-DRAMA. For 3D-DRAMA, average gray-matter and white-matter CBF values were 45.3 ± 4.4 and 20.6 ± 2.8 (mL/100 mL/min), respectively. These values were comparable to the CBF values by FORE-DRAMA: 46.1 ± 4.6 and 20.4 ± 2.9 (mL/100 mL/min). **Conclusion:** 3D-DRAMA is applicable to quantitative brain PET study, and is superior to conventional FORE-DRAMA in terms of the trade-off between image noise and contrast.

P0680

The Influence of resolution recovery during image reconstruction on quantitative brain SPECT imaging

A. Emami-Ardekani¹, F. Kalantari², H. Rajabi², M. Ay¹, A. Fard-Esfahani¹, M. Eftekhari¹, K. Razavi¹, D. Beiki¹, L. Sadeghian¹, B. Fallahi¹, M. Saghani¹, P. Geramifard¹; ¹Research Institute for Nuclear Medicine, Tehran, IRAN, ISLAMIC REPUBLIC OF, ²Department of Medical Physics, Tarbiat Modares University, Tehran, Iran, Tehran, IRAN, ISLAMIC REPUBLIC OF.

Partial volume effect due to the poor spatial resolution of single photon emission tomography (SPET), significantly restricts the absolute quantification of the regional brain uptake and limits the accuracy of the absolute measurement of the blood flow. In this study we assessed the importance of compensation for the collimator-detector response (CDR) in the 99mTc-ECD brain SPET by incorporating system response in the ordered-subsets expectation maximization (OSEM) reconstruction algorithm. By placing a point source of 99mTc in the different distances from the face of the collimator, CDRs were found and modelled using Gaussian functions. A fillable slice of the brain phantom was designed and filled by 99mTc. Projections acquired from the phantoms and also 4 patients who underwent the 99mTc-ECD brain SPET were used in this study. 3D OSEM algorithm was used to reconstruct the images. System blurring functions were modeled during the reconstruction in both projection and backprojection steps. Our results were compared with the conventional resolution recovery using Metz filter in the filtered backprojection (FBP). Visual inspection was done by the six nuclear medicine specialists. Quantitative analysis was also done by calculating the contrast and the count density in the reconstructed images. For the phantom images, background counts and noise were decreased by 3D OSEM compared to FBP-Metz method. Quantitatively, the ratio of the occupied hot region to the cold region of the reconstructed image by FBP-Metz was 1.14. This value was decreased from 1.12 to 0.86 for 3D OSEM of 2 and 30 iterations respectively. The reference value was 0.85 for the planar image. For clinical images, hot to cold (grey to white matter) the count ratio was increased from 1.44 in FBP-Metz to 3.2 and 4 in 3D OSEM with 10 and 20 iterations respectively. Based on the interpretability of images, the best scores (3.79 ± 0.51) by the physicians were given to the images reconstructed by 3D OSEM and 10 iterations. This value was 0.63 ± 0.77 for FBP-Metz images. By incorporating the distance dependent CDRs during 3D OSEM, it is possible to reconstruct the brain images with much higher resolution and quantitative accuracy compared to the conventional resolution recovery method (FBP-Metz). It is however important to make a trade-off between noise and resolution by determining an optimum iteration number.

P0681

Comparison of Myocardial Blood Flow quantification for 13NH3 and 3D-PET by using different image reconstruction algorithms (3D-Reprojection, 3D-OSEM, 3D-OSEM with Time-of-Flight and 3D-Point-Spread-Function) and De-Grado Model.

L. Presotto¹, E. Busnardo², V. Bettinardi³, C. Landoni⁴, P. Todeschini², O. Rimoldi⁵, M. C. Gilardi⁶, L. Gianolli⁷; ¹Scientific institute San Raffaele dpt. of Nuclear Medicine; Un. of Milano-Bicocca dpt. of Physics, Milano, ITALY, ²Scientific institute San Raffaele dpt. of Nuclear Medicine, Milano, ITALY,

³Scientific institute San Raffaele dpt. of Nuclear Medicine; IBFM-CNR Institute for Molecular Biomedicine and Physiology, Milano; Segrate, ITALY, ⁴Scientific institute San Raffaele dpt. of Nuclear Medicine; Un. of Milano-Bicocca dpt. of Surgical Science, Milano, ITALY, ⁵IBFM-CNR Institute for Molecular Biomedicine and Physiology, Segrate, ITALY, ⁶Scientific institute San Raffaele dpt. of Nuclear Medicine; IBFM-CNR Institute for Molecular Biomedicine and Physiology; Tecnomed Foundation, Milano; Segrate; Monza, ITALY.

Aim: To compare the absolute quantification of Myocardial Blood Flow (MBF) with 13NH₃ and 3D-PET by using different image reconstruction algorithms (3D-Reprojection, 3D-OSEM, 3D-OSEM with Time-of-Flight and 3D-PET Point-Spread-Function) and De-Grado Model. Materials and methods: 22 patients with different cardiomyopathies (hypertensive, ischemic, hypertrophic and dilatative) underwent a 3D-PET (Discovery-690; GEMS, Milwaukee, USA) at rest and during vasodilatory stress after dipyridamol infusion (0.56 mg/kg/4 min). After the injection of 370 MBq of 13NH₃, a 3D-PET dynamic scan was acquired with framing: 9x10s, 6x15s, 3x20s, 2x30s, and 1x900s. Off-line the 3D-PET data were reconstructed by using different reconstruction algorithms and parameter configurations as follow: a) 3D-Reprojection, with the smallest possible filter imposed by the Nyquist limit, 3D-OSEM with two different number of iterations: b) 3 iterations and c) 5 iterations, and d) 3D-OSEM accounting also for Time-Of-Flight and 3D-PET Point-Spread-Function. Quantification was performed with PMOD software (v3.1, PMOD Technologies, Zurich) using the De-Grado 1-compartment model. Two analysis were conducted. At first, VOIs of the blood pool and myocardial tissue were drawn on images a; subsequently they were applied onto reconstructions b, c, and d. In the second analysis, new VOIs were drawn on each differently reconstructed image set, in order to evaluate whether the reconstruction method could affect the delineation of the VOIs. Comparison were made by Bland Altman plots. Results: The analysis performed using the same VOIs showed no significant mean difference between method a (used as reference) b and c. With method d a mean difference of +5% was observed. Standard deviations between the chosen reconstruction and method a were [Rest,Stress]: b[4.5%,6.5%], c[4.2%,6.1%], d[5.5%,9.2%]. Using different VOIs the analysis of mean differences gave identical results. The standard deviations, indicating the inter-algorithm variability, increased to b[8.2%,6.3%], c[7.1%,7.7%], d[7%,9.1%]. The spill-over fraction was minimized by method d: -20% compared to a and -31% compared to b. Method c had the same values as a. Conclusion: Absolute quantification of MBF with 13NH₃, 3D-PET and De-Grado model is consistently stable across different image reconstruction methods. The most innovative reconstruction algorithm, including Time-Of-Flight information and 3D-PET Point-Spread-Function, is slightly biased compared with 3D-RP and needs less spillover correction. The between-algorithms variability remained limited to less than 9%. Thus, MBF quantification can be considered clinically robust to different image reconstruction techniques.

P0682

Reduction of CT Exposure for Low-Dose CT Imaging by Iterative CT Reconstruction

O. S. Grosser, D. Czuczvara, H. Wissel, K. Laatz, G. Ulrich, C. Furth, J. Ruf, H. Amthauer; University Hospital Magdeburg, Magdeburg, GERMANY.

Aim The low-dose CT scan of modern hybrid imaging systems (e.g., PET/CT, SPECT/CT) is the state-of-the-art for attenuation correction and morphological registration to diagnostic imaging. The reduction of the CT-related exposure to ionizing radiation for each patient is focus of a permanent optimization process. In this concerns, a feasible approach is the utilization of enhanced CT reconstruction algorithms in low-dose CT imaging formerly exclusively available for high-end CT devices. Therefore, aim of the study is the evaluation of an iterative CT reconstruction algorithm (ASIR[®], GE Healthcare, Haifa, Israel) regarding their usability for optimization of image quality and exposure for low dose CT imaging.

Material and Methods CT imaging was performed by a SPECT/CT (NM/CT 670, GE Medical, Haifa, Israel) with a full diagnostic multi-slice CT (16 slices) to be used for low dose CT imaging for attenuation correction. Phantom examinations were performed using a Catphan[®] 500 phantom (Phantom Lab, Salem, NY, USA) with different segments containing homogeneity as well as density (Acrylic, Teflon, Air, Polyethylene) inserts. CT imaging was performed with a tube voltage of 80, 100, 120 and 140 kV. Energy doses (CTDI_{vol}) ranged from 0.5 mGy up to 10.9 mGy ($t_{rot}=0.8$ s, pitch=1.375, slicing=3.75 mm). Images were reconstructed by standard Filtered Back Projection (FBP) and by the ASIR algorithm with different settings (40%, 50%, 60%). Noise and Contrast-to-Noise ratio (CNR) were estimated for both reconstruction algorithms. Noise was estimated inside the homogeneity insert and CNR was estimated for the different density inserts. Statistical analysis was performed by Wilcoxon-Rank-Test ($p \leq 0.05$). **Results** ASIR reconstructed images provide a significant decreased noise ($p = 0.008$) compared to FBP reconstruction (FBP/ASIR50%, CTDI_{vol}= 2.2 mGy, R= 13.6±1.2/9.4±0.8; CTDI_{vol}= 4.4 mGy, R= 9.8±0.6/6.8±0.4). Noise of ASIR reconstructed images scanned with CTDI_{vol}= 2.2 mGy was comparable to FBP reconstructed scans measured with CTDI_{vol}= 4.4 mGy ($p = 0.001$). CNR is improved significant by using ASIR (e.g., Acrylic, CTDI_{vol}= 2.2 mGy, FBP/ASIR, CNR= 9.0±0.9/12.7±1.1, $p = 0.03$; CTDI_{vol}= 4.4 mGy, FBP/ASIR, CNR=

14.4±1.1/20.8±1.8, $p = 0.01$). The CNR of the density inserts scanned with CTDI_{vol}= 2.2 mGy and ASIR (Level=50%) reconstructed is not significant ($p = 0.11$) decreased regarding FBP reconstructed images from scans with twice energy dose (CTDI_{vol}= 4.4 mGy). **Conclusion** In general, image quality of low-dose CT will be improved by iterative (ASIR) reconstruction. Particularly, ASIR reconstructed images provide a decreased noise level and an improved CNR when compared to the FBP reconstruction.

P0683

Influence of time of flight reconstruction algorithm on SUV measurements in PET/CT

J. Deportos¹, A. Fernandez¹, A. Ruiz², I. Gich³, M. Khodaverdi⁴, M. A. Gonzalez⁵, L. Geraldo¹, I. Carrio¹; ¹Hospital de la Santa Creu i Sant Pau. Servei de Medicina Nuclear., Barcelona, SPAIN, ²Hospital de la Santa Creu i Sant Pau. Servei de Radiofísica., Barcelona, SPAIN, ³Hospital de la Santa Creu i Sant Pau. Servei de Epidemiologia., Barcelona, SPAIN, ⁴GS&S-International, Philips Healthcare, Hamburg, GERMANY, ⁵Philips Healthcare, Madrid, SPAIN.

AIM: To evaluate if Time-of-Flight (ToF) reconstruction in ¹⁸F-FDG PET/CT scans has an impact in metabolic quantification using maximal Standardized Uptake Value (SUV_{max}) in comparison to nonToF reconstruction. **METHODS:** 100 consecutive patients (mean 59, range: 12-87 y; 45 men) with primary or recurrent malignancy were scheduled for ¹⁸F-FDG PET. Imaging was acquired with a Philips Gemini TF hybrid scanner with ToF technology. PET-CT was performed 67 min after iv injection of 249 MBq of ¹⁸F FDG. Body mass index (BMI) was calculated for each patient. PET raw data were reconstructed using ToF correction algorithms and also without ToF correction (nonToF). Metabolic activity in lung and liver (low activity background areas) and three hypermetabolic regions (pathological or physiological areas defined as SUV_{max} higher than 2,5) were subsequently evaluated. SUV_{max} was measured in a 30 mm volumetric region of interest drawn on a identical slice location of both ToF and nonToF sets of images. Intraclass Correlation Coefficient (ICC) was calculated in order to assess the conformity of both ToF and nonToF measurements of metabolic activity in the different localizations. Multiple Linear Regression (MLR) was also used to model the linear relationship between a dependent variable (SUV in ToF and nonToF) and other independent variables (BMI, dose and time acquisition). **RESULTS:** The mean of SUV_{max} measured in lung in ToF and nonToF studies was 1,16 and 1,15 respectively; in the liver, values were 3,24 and 3,08 and in hypermetabolic areas 5,56 and 5,34. Mean differences were 1%, 4,8% and 4% respectively. ICC values of ToF and nonToF estimation were 0,821 in lung SUV_{max}, 0,866 in liver SUV_{max} and 0,988 in whole hypermetabolic regions ($p < 0,001$ in all determinations). These results show a good correlation between SUV values obtained with or without ToF correction, and demonstrate no influence of reconstruction algorithm. In patients with BMI > 25, mean difference between TOF and nonTOF was higher in liver (8%) than in the rest of localizations (lower than 5%). MLR model shows a global influence of BMI depending on reconstruction algorithm in lung and liver ($R = 0,896$; $p < 0,001$) but not in the rest of localizations. No influence of dose or time acquisition was observed. **CONCLUSION:** Our results show a strong correlation in SUV_{max} values between ToF and nonToF corrected PET/CT, especially in high activity localizations. BMI has an influence in SUV_{max} determination depending on ToF correction in low activity areas with higher SUV_{max} in ToF reconstructions.

P0684

Half-time or half-dose gated SPECT: Impact of OSEM with resolution recovery on the assessment of myocardial perfusion and global left ventricular function

F. Mohammed, H. K. Mohan, D. Sharp, L. Livieratos; Guy's and St Thomas' Hospitals, London, UNITED KINGDOM.

Recent molybdenum shortages together with ongoing efforts for reducing radiation exposure to patients undergoing radionuclide imaging such as gated SPECT (GSPECT) have driven efforts for administering less activity while preserving diagnostic quality by state-of-the-art image reconstruction. This prospective study investigated a commercial 3D-OSEM algorithm with distance-dependent resolution recovery (RR) at half the usual acquisition times, equivalent to half the usual injected activity. Data from 24 patients (10 male, 59+/-11yr) with established (n= 5) or suspected ischemic heart disease undergoing a two-day adenosine/99mTc-sestamibi protocol were acquired on Phillips Precedence-16 camera concurrently at full and half duration, with low-dose CT attenuation correction (CTAC). Data were reconstructed with 3D-OSEM-RR (5 iterations x 8 subsets, CTAC/non-AC) and FBP (Butterworth, order=5/cut-off:0.5/non-AC). Parameters were established on phantom and preliminary patient data. Images were assessed by an experienced physician with summed stress/rest and difference scores (SSS, SRS, SDS), LV volumes and ejection fraction calculated by QGS. Reproducibility data were also available on a Philips FORTE camera for this cohort. There was statistically significant agreement between half-time and full-time scans for qualitative (final report 93.3% no-difference, 4.3% change) and quantitative results for rest/stress

LVEF ($p=0.26 / 0.63$) and perfusion scores: SSS ($p=0.70$), SRS ($p=0.87$) and SDS ($p=0.20$). Disagreements were noted in EDV at rest and stress, and ESV volumes at stress though similar to the reproducibility data. Half-time images with 3D-OSEM-RR produced clinically comparable results to full time scans. Further patients are being recruited for this study.

P15-2 - Tuesday, October 30, 2012, 16:00 - 16:30, Poster Exhibition Area

Physics & Instrumentation & Data Analysis: Data Analysis & Management

P0685

Evaluation of 3D Discrete Angles Rotation Degradations for Myocardial Perfusion Imaging

H. Der Sarkissian¹, J. Guédon¹, P. Tervé², N. Normand¹, I. Svalbe³,
¹LUNAM Université, Université de Nantes, IRCCyN UMR CNRS 6597, Nantes, FRANCE, ²Keosys, Nantes, FRANCE, ³Monash Univ., Melbourne, AUSTRALIA.

Introduction: Myocardial perfusion imaging (MPI) is a reference technique for coronary artery disease (CAD) diagnosis. This paper focuses onto 3D PET image processing prior to quantification. For visualization and quantitative image analysis, the transaxial reconstructed tomographic images have to be properly rotated to be presented in the standard horizontal-long axis, vertical-long axis and small-axis views. This specific 3D rotation step induces an interpolation and the resulting degradation must be carefully quantified so that it can be minimized. **Material and methods:** Continuous rotation on a discrete grid introduces bias in rotated data due to the lack of perfect match from the initial grid to the rotated one. It follows that a discrete 3D angle description (defined through integer displacements along the x, y and z axes) can always be sufficient to assess the rotation. A method for the error quantization of a rotation method is successive rotations followed by inverse rotation of the opposite angle. The resulting image is different from the original one and the distance between them is used as an indicator of the algorithm performance. We have investigated and compared two classes of rotation algorithms: (classical) continuous rotation with bilinear interpolation versus discrete rotation algorithm based on Finite Radon Transform (FRT). The FRT is a discrete and exact form of the Radon transform using discrete angles. The underlying idea is to rotate the data not in the image space, but in the discrete projection space which offers an intrinsic rotational structure. Since the FRT is exact, the inverse transform is also exact and no information is lost between the projection and the backprojection of rotated data. FRT based rotations allows for permuting 2D projection data to implement a 3D rotation, which requires significantly less computation. This provides us fast and accurate reorientation algorithm. **Results:** Tests were conducted both onto a 3D PET FDG cardiac volume and on synthetic data. The L2 distance between original and rotated data was computed inside a volume of interest. Any 3D continuous rotation can be decomposed into two discrete 2D angles, with arbitrarily close precision, through a ratio of integers chosen from the Farey-Harros series. This technique is compared to classical interpolation with or without data oversampling in the final paper. **Conclusions:** We propose a discrete, 2D projection-based operator to achieve precise, high quality rotation of 3D tomographic data. Our algorithm compares favorably to the continuous rotation using interpolation of adjacent voxels.

P0686

[¹⁸F]Fluciclatide (RGD Peptide) PET in Metastatic Breast Cancer: Impact of Labeled Metabolites on Patlak Analysis and Qualification of the Use of Image-Derived Blood Input

A. M. Ringheim¹, M. P. Miller², R. Owenius³, ¹Instituto do Cérebro, Hospital Israelita Albert Einstein, São Paulo, BRAZIL, ²GE Healthcare, Medical Diagnostics R&D, Amersham, UNITED KINGDOM, ³GE Healthcare, Medical Diagnostics R&D, Uppsala, SWEDEN.

Aim: The in vivo kinetics of the Arg-Gly-Asp (RGD) peptide ligand [¹⁸F]fluciclatide in metastatic breast cancer patients was investigated from positron emission tomography (PET) using Patlak graphical analysis, where different scenarios regarding the uptake and binding of labeled metabolites were tested. In addition, the validity of replacing arterial blood sampling with image-derived blood curves was explored. **Materials and Methods:** The net-irreversible retention rate constant K_i was calculated for metastatic tumors and healthy tissues using the Patlak model configured according to the following assumptions: labeled metabolites do not enter into tissue (model A); labeled metabolites enter into tissue and bind to target (model B); and labeled metabolites enter into tissue but do not bind to target (model C). Image-derived blood curves were also compared with the arterial blood sampling data as well as being applied in the Patlak analysis. **Results:** The uptake and binding of labeled metabolites differed between non-liver (i.e. lung and breast) lesions and liver lesions. For non-liver lesions, model C (which is correcting for metabolites) showed closest similarity with model A, whereas for liver lesions,

model C showed most similarity with model B. The same trends were observed for normal non-liver and liver tissues. Use of an image-derived blood input function resulted in an overestimation of Patlak K_i of 10-13%. **Conclusion:** Different uptake and binding patterns of labeled metabolites from [¹⁸F]fluciclatide are shown in liver and non-liver lesions and normal tissues, implying that labeled metabolites enter more easily into liver tissues than into non-liver tissues. Moreover, an image-derived blood input function can be used in Patlak graphical analysis of [¹⁸F]fluciclatide data when the heart is in the image field of view, removing the need for arterial blood sampling in future studies.

P0687

Influence of automatic tube current modulation on attenuation correction of PET images

D. D'Ambrosio, L. Depaoli, L. Moro, D. Panizza, I. Carne, C. Fuccio, G. Trifiro, D. Fantinato; Fondazione S. Maugeri, Pavia, ITALY.

Aim: Automatic tube current modulation (ATCM) technique is nowadays widely used in most of CT systems as providing constant image quality reducing patient radiation dose. This technique is also available in PET/CT scanners. The main goal of this work is to investigate the influence of ATCM on attenuation correction of PET images. **Materials and methods:** PET/CT images of an anthropomorphic phantom (RS-800, RSD) were acquired using Discovery690 VCT scanner (GE Healthcare). The phantom was filled with about 100MBq of ¹⁸F-FDG (background:myocardium:liver:hepatic lesion=1:15:3:18) and was acquired in a supine position in the center of field of view. Several reference images were acquired: AP, PA and LL scouts. Three CT acquisitions were performed using 80mA, 30-120mA and 30-180mA ATCM ranges, for each scout. Other acquisition parameters were 120kVp, slice thickness=3.75mm and noise index=25. Time-of-flight PET data were acquired and reconstructed by VuePointFX+SharpIR iterative algorithm. In order to know the ATCM for used CT protocols, tube current and exposure were plotted versus phantom longitudinal axis. Volume of interests (VOIs) were drawn over abdomen, lungs, ventricle, myocardium, liver and hepatic lesion of PET images. The effect of different attenuation map on corrected PET images was evaluated. The percentage difference ($D_{\%}$) of the VOIs mean value was calculated with respect to the same VOI drawn over no ATCM-CT based attenuation corrected PET. Liver and tumor VOI statistics were also used to evaluate maximum tumor/liver ratio (T/L). Coefficient of variation (CV) was also calculated to estimate noise in each VOI. **Results:** $D_{\%}$ measured in lung VOI was in a range of 0.6%-1.1%. More precisely, it was lower for AP scout and higher for PA and LL for both the ATCM CT protocols. Liver and tumor analysis showed $D_{\%}$ in the range of [-0.04, 0.21]% and [-0.12, 0.02]%, respectively. Maximum T/L was equal to 5.7 independently by CT protocol used. Myocardium and ventricle $D_{\%}$ were in the range of [-0.89, 0.01]% and [-0.05, 0.21]%, respectively. Abdomen VOI analysis showed an absolute $D_{\%}$ below 0.05%. CV values measured in each VOI over PET images were independent on the tube current and scout image used in CT acquisition. **Conclusion:** The absolute percentage difference measured on PET images for some ATCM-based CT clinical protocols was below 1.1%. Therefore, results of this preliminary study showed an almost negligible influence of ATCM-based CT images on attenuation correction of PET images.

P0688

Simulation of extra-cardiac uptake in myocardial perfusion imaging

D. Minarik, E. Trägårdh; Skåne University Hospital, Malmö, SWEDEN.

Background: Tc-labelled myocardial perfusion agents are cleared by the liver and excreted by the biliary system. Increased intestinal or gastric activity may create a problem in the visual and quantitative interpretation of the inferior wall. The objective was to determine when interpretation of the studies is affected by the extra-cardiac activity, and when re-examination is necessary. **Methods:** The SIMIND Monte Carlo code with the XCAT-phantom was used to simulate myocardial perfusion images. Inferior defects of 3, 4 and 6% of the left ventricle were simulated. Extra-cardiac uptake was simulated using a spherical 4cm hot spot with three different concentrations of Tc compared to the myocardium: 1) visually the same intensity, i.e. slightly less concentration in the hotspot 2) visually twice the intensity and 3) visually half the intensity in the hotspot. The hot spot was placed below the heart, and the position was changed from 10 mm to 0 mm from the inferior cardiac wall, with 2 mm intervals. Images without hot spot were used as reference. Images were created by simulating 32 angles in a 180 arc, starting from 45° right anterior oblique position and reconstructed using the OSEM algorithm (4 iterations, 8 subsets) and a gaussian post filter. The EXINI heart software was used to evaluate the extent and severity of the defects. **Results:** For the same intensity simulations, severity started to decrease when the hot spot was closer than 6 mm, i.e. the spillout from the hot spot to the heart started to affect the computerized interpretation. For small defect sizes (3%), the extent decreased when the hot spot was localized less than 6 mm from the heart. For the simulation with twice the intensity in the hot spot, severity started to decrease at 8 mm, and completely filled the smaller defects at 6 mm, i.e. no defect was detected by the computerized

interpretation. The same effect was found for larger defects, but instead at 4 mm, and 2 mm. For the simulation with half the hot spot intensity, a slight decrease in extent and severity for the smallest defect was found at 2 mm. No change in extent or severity was seen for the larger defects. Conclusions: Re-examination should be considered when the extra-cardiac intensity is equal to or twice the myocardium intensity, at a distance of 0.5 respectively 1 cardiac wall thicknesses. For extra-cardiac intensities half the myocardium, no re-examination is necessary.

P0689

Comparison of CBAC and CTAC in quantification of uptake with Florbetapir imaging

J. Peyrat¹, G. Platsch², C. Hayden³, A. Joshi⁴, M. Mintun⁵, M. E. Casey³, J. Declerck¹; ¹Siemens Molecular Imaging, Oxford, UNITED KINGDOM, ²Siemens AG, Erlangen, GERMANY, ³Siemens Molecular Imaging, Knoxville, TN, UNITED STATES, ⁴Avid Radiopharmaceuticals, Oxford, PA, UNITED STATES, ⁵Avid Radiopharmaceuticals, Philadelphia, PA, UNITED STATES.

Aim: Calculated brain attenuation correction (CBAC) is a method to reconstruct brain PET images without transmission scan such as CT. The aim is to evaluate the difference between calculated brain (CBAC) and CT-based (CTAC) attenuation correction on the quantitative analysis of Florbetapir imaging with the computation of cortex-to-cerebellum **standard uptake value ratio (SUVR)**. **Materials and methods:** Florbetapir PET scans were reconstructed with both CBAC and CTAC using OSEM method with 3 iterations, 21 subsets and 5mm FWHM. Cortex-to-cerebellum SUVR is computed with an automatic method, implemented in the syngo.PET Amyloid Plaque software (Siemens Healthcare), based on a reference semi-automatic method described in Fleisher et al. [Archives of Neurology 2011]. This automatic method has already been shown to provide SUVR results highly correlated to the one obtained with Fleisher's method by Peyrat et al. [SNM 2012]. The cortex-to-cerebellum SUVR computed from CTAC- and CBAC- based PET reconstructions are compared, as well as the regional SUVR within the six regions (anterior cingulate gyrus, frontal lobe, parietal lobe, posterior cingulate gyrus, precuneus, and temporal lobe) used to compute the cortex-to-cerebellum SUVR. The differences of regional SUVRs are analyzed among a population of 17 patients, 10 scanned with a Siemens Biograph TruePoint and 7 with a Biograph mCT. **Results:** The cortex-to-cerebellum SUVR quantification of Florbetapir images with syngo.PET Amyloid Plaque using CBAC is highly correlated to the SUVR quantification using CTAC ($y=1.0159x-0.0235$, $R^2 = 0.9793$). Nevertheless, a systematic overestimation of regional SUVR in the anterior brain regions (frontal lobe: +8.0%, anterior cingulate gyrus 4.7%) and underestimation of regional SUVR in the posterior brain regions (parietal lobe: -4.6%, posterior cingulate gyrus: -5.5%, precuneus: -5.2%) are observed and confirmed with a Wilcoxon paired samples test ($p<0.006$). The temporal lobe, a bigger and more central region, does not show such bias (-0.5%, $p=0.487$), so does the overall cortex-to-cerebellum SUVR (-0.5%, $p=0.632$). **Conclusion:** The cortex-to-cerebellum SUVR quantification of Florbetapir images with syngo.PET Amyloid Plaque using CTAC and CBAC reconstructions shows high correlation. However, there are local differences with an overestimation of regional SUVR in the anterior brain regions and an underestimation of regional SUVR in the posterior brain regions.

P0690

Tumour-Background Separation In Breast Molecular Imaging(BMI) using Bayesian Probability Based(BPB) Modelling

M. Carroll; Royal Liverpool University Hospital, Liverpool, UK

Objectives: The application of BMI using Tc99m labelled sestamibi(MIBI) for the routine screening of women with dense breasts is an important and growing area in nuclear medicine. BMI may demonstrate increased sensitivity in tumour detection compared to mammography in women with dense breasts but has the potential severe disadvantage of increased radiation dose, the average dose from mammography is 0.56mSv compared to 6.5mSv for a 20 mCi dose in BMI. Hence in order to achieve a comparable radiation dose to mammography of 0.65 mSv the injected activity in BMI needs to be of the order of 2mCi. To achieve sensitive detection at a dose of 2mCi we propose BPB as an adjunct to solid state gamma cameras as a means of achieving high sensitivity with low radiation dose. **Methods:** We model the spatially varying background within a MIBI image by a bivariate thin plate spline(TPS). A TPS is a weighted sum of translations of radially symmetric basis functions augmented by a linear term. $TPS(x) = E(x) + \sum_{i=1}^N \lambda_i f_i(x-x_i)$, where x are 2D pixel coordinates and $E(x) = c_0 + c_1x + c_2y$ is the planar term. The N supporting points, (x_i, y_i) are densely chosen along the breast image outline but sparsely for the image interior to minimize the potential impact of large tumour sites on the resulting background model. The background is estimated from the TPS over the whole breast image and potential tumour signals are modelled as statistical outliers in this background field. **Results:** A simulated field comprising 33 sources was generated where the shape of each source was described by a 2D Gaussian function whose variance determined the source size diameter. The

sources had counts ranging from 50 to 500. The sources were embedded within a relatively complex background signal derived from an example MIBI image set and modelled by its associated TPS field. True detection was 26 out of 33 with an associated 3 false positive signals. **Conclusion:** Bayesian based statistical detection in BMI may contribute to the overall objective of reducing radiation dose in BMI by enhancing the detection of tumour signals in low count images. TPS modeling with outlier detection presents an objective, operator independent approach to tumour detection in BMI where each potential source detection has an associated probabilistic measure.

P0691

Comparison of Different ROI Selections in 123I-β-CIT DAT Studies

S. Turunen¹, E. Hippeläinen¹, J. Eerola-Rautio², P. Nikkinen¹, A. Ahonen¹; ¹HUSLAB, Division of Clinical Physiology and Nuclear Medicine, Helsinki, FINLAND, ²Department of Medicine, Division of Neurology, Helsinki, FINLAND.

Aims: The common aim in the analysis of DAT SPECT studies is to determine the specific binding ratio of the striatum (caudate nuclei and putamina) vs. the brain background activity. The selection of ROI size, shape and location has a large impact on the results of these calculations. Manually drawn ROIs can easily adapt to patient-specific anatomy, but the inter-observer variability can be large. The opposite is true for pre-made anatomical ROI models. Large box ROIs containing the whole striatum provide robust information, but with the loss of separate caudatus and putamen ROIs that provide crucial information especially in the early stages of Parkinson's disease. This study aims to compare the analysis of clinical patients with manual ROIs, previously created ROI models, and box ROIs utilizing the "Southampton method", which has been proposed for the analysis of 123I-FP-CIT studies. **Methods:** 94 patients with suspected Parkinson's disease or tremor symptoms were retrospectively selected for the study. They had undergone a DAT SPECT study using 123I-β-CIT imaged 24 hours post injection. Good clinical practice was followed in all preparations. After a brief follow-up (2-8 months) two patient groups were formed using the clinical outcome of each patient: one group with near-certain DAT abnormalities (PD group, $n=13$) and another with near-certainly normal DAT physiology (normal group, $n=21$). Both groups were analyzed using manually drawn ROIs, previously made anatomical ROI models, and the Southampton method, i.e. large box ROIs that contain all striatum-related counts. The power of each analysis method to recognize the PD group patients was compared. **Results:** The manual ROIs agreed with the clinical outcome in 9 out of 13 PD group patients using the caudatus ROIs alone, and all 13 using the putamen ROIs. The anatomical ROI models achieved the same results, with minimal differences in the PD group, but larger in the normal group, when comparing with the manual ROI method. The Southampton method recognized 12 PD group patients. **Conclusions:** Manual ROIs and anatomical ROI models performed equally, and somewhat better than the Southampton method. The manual method performs better in the normal group as it can trace individual anatomy, but it apparently had no such advantage in the PD group. As the pre-made ROI models are easier to use and less prone to inter-observer differences, they are the method of choice. However, the Southampton method provides an easy way to increase the robustness of the analysis in 123I-β-CIT studies.

P0692

Mathematically Simulated Phantom for PET Kinetic Modelling

H. Merisaari, S. V. Nesterov, V. Oikonen, M. Teräs, C. Han; Turku PET Centre, Turku University Hospital, FINLAND.

Purpose: In order to better study the heart physiology and pathology, researchers need better analysis tools, among which are PET analysis software tools. To ensure that PET analysis software provides correct results digital phantoms can be successfully used. At the Turku PET Centre, we developed a mathematically simulated phantom and published it on our Centre's website; it is absolutely free, and it also includes several common-used cardiac tracer related kinetic models. **Methods:** The anatomic structures of left and right ventricular myocardium and cavities are generated based on typical human heart anatomy. Input function is taken based on tracer-specific study data. Kinetic model is simulated based on our in-house simulation programs. Output format is standard DICOM format image data, which can be used to evaluate SPECT or PET heart analysis software that supports rest-stress study analysis. **Results:** We analyzed phantom data using Carimas 2. Polarmap segmentation volumes are compared with phantom containing predefined values distributed in myocardium according to the 17-AHA standard: basal 35%, mid-cavity 35%, apical 30%. Modelling parameters of water, acetate and ammonia resemble the values placed in simulated digital phantom data. **Conclusions:** The results show that our developed mathematical simulated cardiac PET kinetic phantom is useful for evaluating the cardiac PET analysis tools for purpose of evaluating polarmap mapping convention, and modeling performance. It is free and can be found on Turku PET Centre web pages.

P0693

Evaluation of Inter- and Intra-Observer Variation when Processing Left Ventricular Ejection Fraction and Volumes on Two Different SPECT Gamma Camera Systems

B. Zerahn, C. Huang; Herlev University Hospital, Copenhagen County, Herlev, DENMARK.

Aim Determination of left ventricular ejection fraction (LVEF) by steady state ^{99m}Tc -HSA radionuclide ventriculography (MUGA) can among other purposes be used to monitor potentially cardiotoxic side effects of chemotherapy. In order to test whether the introduction of a new type of gamma camera system will improve the ability to detect changes in LVEF we assessed inter-observer and intra-observer variation when processing MUGA's acquired on two different types of gamma cameras. **Materials and methods** The study is intended to comprise 80 patients of which 50 patients (45 women) have been included so far with a mean age of 58.0 years ± 12.6 (1 SD). Forty-seven patients were monitored for potential cardiotoxicity of chemotherapy and three patients during treatment for cardiomyopathy. Patients had two sequential MUGAs on a dual head dedicated cardiac gamma camera with a sodium iodine crystal (CMD) (Cardio MD, Philips) and a CZT detector camera (Disc) (Discovery 530c, GE). Each acquisition was analysed twice by each of two experienced technologists (A and B). Inter- and intra-observer variation was calculated for each camera system. **Results** The mean intra-observer variation for observer A and B on the CMD was 1.74 ± 0.23 (SEM)% and $1.83 \pm 0.27\%$, respectively. For the Disc-system the corresponding intra-observer variations were $1.06 \pm 0.11\%$ and $0.80 \pm 0.09\%$, respectively. The mean absolute intra-observer differences for both observers were significantly lower for the Disc-system compared to the CMD ($p = 0.017$ and $p < 0.001$, respectively). The inter-observer variation for the first and the second series of observer A vs. B on the CMD were $3.22 \pm 0.46\%$ and $2.40 \pm 0.42\%$, respectively. For the Disc-system the corresponding inter-observer variations were $1.42 \pm 0.20\%$ and $1.44 \pm 0.21\%$, respectively. The mean absolute inter-observer differences for both observer series were significantly lower for the Disc-system compared to the CMD ($p = 0.047$ and $p < 0.017$, respectively). Furthermore, the mean LVEF assessed on the CMD was significantly higher compared to the Disc-system (65.6 ± 1.4 vs. 59.1 ± 1.4 , $p < 0.001$). This is due to the CMD-system overestimating the left ventricular end-diastolic-volume compared to the Disc-system with 15.9 ± 2.24 mL ($p < 0.001$), whereas there was no difference between the two systems with regard to the assessment of left ventricular end-systolic-volume. **Conclusion** The CZT detector camera system (Disc) has significantly better intra- and inter-observer variation characteristics compared to the sodium iodine crystal SPECT camera system (CMD). The latter estimates LVEF higher than the CZT detector camera system, due to an higher left ventricular end-diastolic-volume.

P0694

Using Curve Prediction to Improve Patient Throughput in Renography

J. B. Hermansen, B. Zerahn; Herlev University Hospital, Copenhagen County, Herlev, DENMARK.

Aim To develop an algorithm capable of accurately estimating the outcome of renographies on the fly, in order to shorten the acquisition time for normal patients. **Materials & Methods** A mathematical model was created using MatLab (v. R2011a, MathWorks, Sweden), based on literature on the pharmacokinetic behaviour of ^{99m}Tc -MAG3 in the kidneys. Based on this model an algorithm for predicting the descending tail of the renography curve was developed. A random subset of 29 normal renographies was selected from a large body of normal renographies, from which the raw acquisition data was analysed using the developed algorithm and model. At our institution the quantitative analysis of ^{99m}Tc -MAG3 renographies consists of three measurements: Time to maximum (TTM), function distribution (FD) and remaining activity after 20 minutes in percentage of the activity at TTM (RA_{20}). Given the normal limits at our institution, it is possible to determine whether both TTM and FD are normal after 270 seconds. Therefore only the RA_{20} needs to be modelled and predicted in order to terminate the acquisition before the scheduled 20 minute acquisition time. The algorithm reads the renography curve as it progresses, continually expanding the curve segment used for estimation. The RA_{20} estimation algorithm continuously updates the prediction, and displays the predicted renography curve along with the related confidence intervals (with user variable α -value). When the chosen confidence level is reached predicting that the RA_{20} will be within normal limits, the algorithm notifies the user and suggests that the acquisition be terminated. **Results** The developed algorithm was able to correctly estimate whether the RA_{20} is within normal limits in 28 cases (96.6%) with an α -value of 0.95 and in 26 cases (89.7%) with an α -value of 0.995. The estimation was based on the renography curve from TTM to 10 minutes after injection. **Conclusion** It has been shown that the predictive renography algorithm is robust and that it is possible to terminate the acquisition 10 minutes prior to scheduled for a normal renography in approximately 9 out of 10 cases, with a high level of confidence. As approximately 25% of all renographies at our institution are normal, this algorithm could potentially increase patient

throughput. The negative predictive value of this method is subsequently being tested.

P0695

Protocol Optimization to Further Reduce Intra- and Inter-animal Variability in microPET Rat Brain Image Quantification

S. Deleye¹, D. Smits¹, L. Wyffels¹, J. Verhaeghe¹, T. Wyckhuys¹, X. Langlois², M. Schmidt², S. Dedeurwaerdere¹, S. Stroobants¹, S. Staelens¹; ¹University of Antwerp, Antwerp, BELGIUM, ²Janssen Pharmaceutica, Beerse, BELGIUM.

INTRODUCTION In preclinical molecular imaging studies the variability within and between subjects has already been assessed in the organs of mice [Jan] and in mice tumors [Dandekar] while others have looked at impact of animal handling [Fueger] and optimizing experimental protocols [Schiffer] as well as investigating administration route, dietary condition and blood glucose level [Wong]. In this study we investigate the confounding factors of the rat brain 18F-FDG uptake. **METHODS** To assess the intra-variability we scanned tail-vein injected rats twice with at least 48 hours in between. We calculated the ratio of the whole brain uptake (Wb) versus the cerebellum (Cb) and the SUV of the Wb. To test the inter-variability we scanned 13 rats in a standardized protocol: i.v. injection under anesthesia, ≤ 12 h fasted, heated, a glucose measurement before (glu1) and after (glu2) the scan and a blood sample at 45 min p.i. (Cp). Again we calculated the SUV for Wb and the Wb/Cb ratio. Furthermore we now also normalized the results against injected dose (%ID/g) and the Cp in combination with glu1, glu2 and the mean glucose measurement (mglu). **RESULTS** The intra-subject COV was 2% and 7% respectively for the relative and the absolute quantification. The inter-variability COV for the Wb/Cb ratio, the SUV and %ID/g was respectively 2.6, 15.8 and 15.9%. Normalizing to the SUV and the glucose measurements were 20.6, 27.8 and 15.2% for mglu, glu1 and glu2 respectively. The glu2 measurements were significantly higher than glu1. Normalizing to the Cp increased the variability to 38.2, 43.9 and 33% for mglu, glu1 and glu2 respectively since a high variability in the gamma counting results (COV=45%). **CONCLUSION** When using a standardized protocol an intra-subject variation of 7% can be reached for SUV and 2% with a ratio. Also to reach a low inter-variability, using a ratio is recommendable. Normalizing to glucose before the scan and/or a single plasma sample gives rise to the highest variability. %ID/g, SUV and SUV-glu2 result in the lowest inter-subject variability. 1. Jan, 2004. Accuracy and variability of quantitative values obtained for mouse imaging using the microPET 2. Dandekar, 2006. Reproducibility of 18FDG microPET studies in mouse tumor xenografts 3. Fueger, 2006. Impact of animal handling on the results of the 18FDG PET studies in mice 4. Schiffer, 2007. Optimizing experimental protocols for quantitative imaging with 18FDG in rodents 5. Wong, 2011. Effects of administration route, dietary condition, and glucose level on uptake of 18F-FDG in mice

P16-2 - Tuesday, October 30, 2012, 16:00 - 16:30, Poster Exhibition Area

Physics & Instrumentation & Data Analysis: Radiation Exposure & Protection

P0696

Optimisation of Radiation Protection for Yttrium-90 and Lutetium-177 Peptide Therapy Administration: 3 Year Experience.

R. C. Fernandez¹, L. Price², C. Sibley-Allen¹, L. Livieratos¹, S. J. Allen¹; ¹Guy's & St Thomas' NHS Foundation Trust, London, UNITED KINGDOM, ²King's College London, London, UNITED KINGDOM.

Introduction The use of peptides labelled with beta particle emitting radionuclides, such as yttrium-90 (^{90}Y) and lutetium-177 (^{177}Lu), to treat neuroendocrine tumours has increased dramatically in recent years. There are inherent complications in using both ^{90}Y and ^{177}Lu due to the physical characteristics of the emitted radiation. This study shares our three year experience of performing both ^{90}Y and ^{177}Lu peptide therapies, with particular focus on techniques/equipment to minimise occupational exposure during therapeutic administration. This is particularly relevant given the pending ICRP recommendation for reduction of the eye lens equivalent dose limit. **Method** 52 ^{90}Y -dotatate (prescribed activity: 3.7GBq/m² body surface area) and 36 ^{177}Lu -dotatate (prescribed activity: 7.4GBq) therapies were administered over a three year period. Bespoke Perspex/lead shielding was developed in-house for the ^{90}Y / ^{177}Lu infusion system. All staff involved in the administration procedure wore ED2+ (Thermo Scientific) electronic personal dosimeters (EPDs) measuring whole-body depth/skin doses ($\text{H}_p[10]/\text{H}_s[0.07]$ respectively). Additionally, physicists wore ED2 (Aegis)/NED (Unfors) real-time, automatic EPDs at the fingertips during the therapeutic administration to isolate the specific tasks contributing to extremity exposure during the procedure. **Results** As anticipated, due to increased handling of radionuclides during assay and connection/dismantling of the infusion system, physicists received the highest

whole-body/extremity doses during the administration procedure. Mean[SD] whole-body $H_p[10]/H_p[10]$ per administration varied depending on staff group and radionuclide; physicists (2.7/35.9[3.8/74.9] μ Sv vs. 4.5/5.5[3.3/4.5] μ Sv), clinicians (2.2/14.9[6.2/23.2] μ Sv vs. 4.1/4.2[2.5/2.2] μ Sv) and nurses (0.5/1.4[0.9/1.6] μ Sv vs. 2.5/1.7[2.2/1.1] μ Sv) for ^{90}Y vs. ^{177}Lu respectively. X-ray aprons (0.2mm lead-equivalent thickness) worn during ^{90}Y administrations afforded mean whole-body $H_p[10]/H_p[0.07]$ dose reduction of 93.8%/99.4% respectively. Mean[SD] physicist extremity dose per administration was 64.6[6.4] μ Sv vs. 133.4[93.7] μ Sv for $^{90}\text{Y}/^{177}\text{Lu}$ respectively. Mean[SD] percentage contribution to extremity dose from connecting administration syringe to infusion tubing was 23.0[12.2]% vs. 41.5[16.5]% for $^{90}\text{Y}/^{177}\text{Lu}$ respectively, whilst assay of residual activity in tubing post-administration contributed 31.0[19.1]% vs. 17.1[25.3]% for $^{90}\text{Y}/^{177}\text{Lu}$ respectively. 10mm thick Perspex/lead half-cylinders placed over the administration syringe barrel during infusion reduced surface dose-rate, as measured by extremity EPD, by >99% for both ^{90}Y and ^{177}Lu . Mean[SD] residual activity in tubing post-administration could be reduced from 4.0[3.1]% of the patient administered activity to 2.9[0.8]% by using shorter tubing and optimised flushing of lines. **Conclusion** There are a number of important practical considerations prior to commencing ^{90}Y and ^{177}Lu peptide therapy. Appropriate shielding, both personal and surrounding infusion equipment, together with suitable monitoring devices and staff training can significantly reduce radiation exposure and ensure that effective/equivalent dose limits are not exceeded.

P0697

Security evaluation of an epilepsy monitoring unit in implantation technique of ictal SPECT

A. Mestre-Fusco¹, M. Lacruz², M. Suarez-Piñera¹, J. Ruiz³, M. Rubio⁴, J. Capellades⁵; ¹Nuclear Medicine CRC-Mar. Hospital del Mar. Parc de Salut Mar., Barcelona, SPAIN, ²Radiophysics-Radioprotection. Hospital del Mar. Parc de Salut Mar. Universitat Pompeu Fabra, Barcelona, SPAIN, ³Radiophysics-Radioprotection CRC-Mar., Barcelona, SPAIN, ⁴ACPRO, Barcelona, SPAIN, ⁵Radiology & Nuclear Medicine. Hospital del Mar. Parc de Salut Mar., Barcelona, SPAIN.

AIM: Ictal SPECT studies are performed in epilepsy monitoring units (EMU) that usually are located externally at nuclear medicine department. Security evaluation includes risks of exposition/contamination in monodose transport and risks of tracer injection in the EMU. **MATERIAL AND METHODS:** 1.- Thickness (Pb-shield) was estimated in radiotracer transport. 2.- Transport circuit was defined according to legislation. 3.- Integrated Dose of another patient in the same room was estimated and contamination risk was studied. Radiation exposure risks were calculated depending on: dose rate from injected patient in different distances (Radionuclide Protection Data Handbook 2002), location of another patient or medical staff, work charge (patients/week⁻¹) and radionuclide decay based on integrated equivalent dose (H_{int}). The possibility of located (surface $\phi=10$ cm) or extended ($\phi=100$ cm) contamination were considered. Mean value of resuspended factor ($1\cdot10^{-7}$) was used to calculate ambient radiation exposure and depending on committed dose equivalent (Real Decreto 783/2001). The obtained values were less than annual limits defined by national regulations. **Specifications:** Cover walls and floor with vinyl waterproof material, closed at the surface and easy decontamination. **RESULTS** A thickness of 6.2 mm of Pb-shield is estimated as an acceptable value in radiotracer transport. It is not necessary an additional shield implantation in the original concrete structure building because of the accumulated annual dose for all radiation workers is less than established limits. EMU is classified as Controlled Area with contamination risk and annex areas are classified as Non-designated Areas, free access. **CONCLUSION:** Implantation technique of ictal SPECT includes security evaluation in radiation exposition, contamination risk in radiotracer transport and safety administration dose in the EMU.

P0698

[F-18]FDG dose reduction paradigm at Yale New Haven Hospital

D. Ersahin¹, L. H. Staib¹, F. d'Errico¹, D. Menard², D. W. Cheng¹; ¹Yale University School of Medicine, New Haven, CT, UNITED STATES, ²Yale New Haven Hospital, New Haven, CT, UNITED STATES.

In an effort to minimize the [F-18]FDG patient dose burden while preserving quantitation, we reprocessed our clinical PET/CT scans and assessed the standard uptake values (SUV) as a function of imaging time. It was our hope that a practical protocol could be developed balancing imaging time and dose, so that each patient will benefit from a significant reduction in radiation burden from positron decay. Over 70 clinical PET/CT studies with different diagnoses performed using 555 MBq (15 mCi) [F-18]FDG were reprocessed. All acquisitions were made in list mode, and images were reconstructed at 0.5, 1, 1.5, 2, 2.5, and 3 minutes per bed position. Two board certified nuclear medicine physicians, with knowledge of the clinical diagnoses, evaluated each study for image quality and selected appropriate lesions to be evaluated for size, maximum SUV (SUVmax), and average SUV (SUVavg) at each time interval. A large region of interest was drawn in the normal liver and SUVavg as well as SUVmax were quantified to serve as a reference for

biodistribution. For comparisons with other lesions at the same time point, we have normalized our SUVmax and SUVavg of each lesion to the value obtained at the 3 minute acquisition. Our data demonstrated statistically significant differences in lesions with normalized SUVmax and SUVavg obtained at 0.5 minute reconstruction compared to our reference 3 minute reconstruction. In addition, a plot of normalized SUVs against acquisition time demonstrated that the standard deviation in composite as well as in subcategories of lesions decreased as the time of acquisition approached 3 minutes, with excellent agreement between 2, 2.5 and 3 minute acquisitions. In summary, our results assured valid comparisons of SUVmax and SUVavg in lesions from our old protocol using 555 MBq (15 mCi) [F-18]FDG to our new protocol using 370 MBq (10 mCi) [F-18]FDG and a 3 minute acquisition (equivalent to a 2 minute acquisition in the old protocol), important in longitudinal studies and even more so in evaluation of treatment response. Hence, our patients benefitted in terms of a radiation burden reduced by 33%. Our current efforts seek correlations between patient acquisitions and data from a parallel study using an ECT phantom.

P0699

Introduction of a monitoring system for radioactive waste: one year experience.

R. Stoico, P. Baruzzi, G. Gianduia, F. Leoni, K. Siczek, L. S. Maffioli; Ospedale Civile di Legnano, Legnano, ITALY.

AIM: This study describes one year experience at Legnano Hospital in radioactive waste management by the introduction of radioactivity monitoring portal system. **MATERIAL AND METHODS:** The Brumola portal system for the monitoring of radioactivity was installed in October 2010 closed to hospital temporary waste storage. A 6-mm-thick leaden wall was made in order to store radioactive waste exceeding alarm threshold. The alarm threshold was defined during installation by the use of radioactive sources ^{137}Cs and ^{99m}Tc . New alarm thresholds based on halipack geometry and possible activity values for low energies were defined in January 2011. In February 2011 started daily registration. An intra-hospital procedure was set to manage waste: temporary store in clinical departments for at least 3 days. An external team of workers is concerning with the collection and transport the containers (halipack) to the storage-room. An intra-training program was performed to them. One year experience in the use of radioactive waste monitoring portal system was collected from February 2011 until 2012. The halipack number exceeding threshold alarms was registered for each month. The medical departments involved in the production and detention of halipacks were identified. They were related to the number of patients undergone nuclear medicine examination. A cut-off was defined in order to identify the medical departments that better apply the radioactive waste management program. The program was about the detention of halipack in due time for ^{99m}Tc decay. **RESULTS:** Halipack/months collection showed a decrease of detention during the time. The clinical departments involved in detention of radioactive waste containers were Neurosurgery, General Surgery, Interventional Cardiology, Vascular Surgery, Day Surgery, Neurology, Orthopedics, Emergency Unit, Oncology, Urology and General Medicine departments. One halipack/5 patients ratio was calculated as a mean value of halipack/patients ratio of all clinical departments. New 1:20 ratio was defined as cut-off. Neurology, General Surgery and B General Medicine were to be strictly closed to new cut-off. No contaminated halipacks were registered from Nuclear Medicine Department. **CONCLUSIONS:** The systematic control of halipacks reduces the risk to discharge contaminated waste to the environment. A lower number of contaminated halipacks is registered during the last year: this demonstrates good application of the procedures. However, a periodic cleaning workers retraining is needed to improve the waste management. The introduction of radioactive waste monitoring portal system allowed to control the radioactive waste flux. It removed the risk of contaminated discharge waste stop and operating costs to the incinerator.

P0700

X-rays Dosimetry of Laboratory Animals using Organic Scintillators and Time-Correlated Single Photon Counting (TCSPC) Technique

T. Sohler¹, M. Munier¹, M. Torres¹, A. Sayeh², J. Jung¹, **P. Choquet**², R. Barillon¹; ¹Institut Pluridisciplinaire Hubert Curien, STRASBOURG, FRANCE, ²Hopitaux Universitaires de Strasbourg, STRASBOURG, FRANCE.

AIM: Availability of dedicated apparatus for small animal imaging has increased dramatically during the last ten years. The main advantage of imaging is based on the possibility of longitudinal follow-up, keeping the animal alive throughout experiments. Among all modalities, XRay microCT had gained a wide interest due to its high spatial resolution associated with a reasonable acquisition time. Merged with functional techniques, it also allows for anatomical coregistration and nowadays microPET (microSPECT) are systematically combined with a microCT. However, the question of dosimetry is of importance and necessitates a measurement or an evaluation as many biological processes could be altered by

ionizing radiations. We propose a new approach for measuring continuously during acquisitions the dose received by small animals. **METHODS:** Measurements were done using the Time-Correlated Single Photon Counting (TCSPC) technique. This allows taking into account not only the primary and secondary ionizations induced by radiation, responsible of charge pair creation, but also the molecular excitation phenomena. Organic scintillator was linked via an optical fiber (HCP1000), completed by a 50/50 light splitter, to two photomultiplier tubes R3235/01 (Hamamatsu Photonics, Hamamatsu, Japan), each followed by a discriminator (Ortec 584, Oak Ridge, USA). The output signals were guided to a time to amplitude converter (Ortec 566), associated to a counting unit, gathering coincidence events. Several measurements were achieved using X-ray source of a microCT (GE eXplore Vision CT120, Waukesha, USA) with different couples voltage/current and with different phantoms. Comparisons were done with an ionization chamber (DIADOS E, PTW, Freiburg, Germany). **RESULTS:** There is a very good correlation between measurements with organic scintillators and ionization chamber. A higher sensitivity to X-rays doses has also been observed. As a result, dose measurement is more accurate when compared to that acquired by an ionization chamber. No artefact was noticed when the scintillator is placed near the animal, allowing to make simultaneously acquisition and dose measurement. **CONCLUSION:** Our first results show that organic scintillators combined with TCSPC technique is a very promising method for preclinical dose and dose profile measurements. Moreover, the TCSPC technique, used here for the first time in dosimetry, is a very promising alternative choice to the ionization chamber.

P0701

Impact of Smart mA technique on patient's CT dose in PET/CT diagnostics

M. Bienkiewicz¹, K. Napierska, I. Raciborska, M. Gadzicki, M. Górską-Chrząstek; Voxel Medical Diagnostic Centre, PET Lab, Łódź, POLAND.

Aim A number of strategies are available to minimise the radiation burden for a patient undergoing a CT scan for PET attenuation correction and anatomic correspondence with PET findings. The aim was to assess the effectiveness of a Smart mA technique with Auto mA modulation in optimising CT radiation dose in PET/CT diagnostics, based on one year use of Discovery 600 PET/CT scanner in Voxel Medical Diagnostic Centre. Material and method Retrospective analysis of CT dose reports of 750 PET/CT examinations. Standardised measures of radiation in CT environment - CTDIvol values were analysed with respect to patients' characteristics: sex (329M; 421F), body weight (from 30 to 142kg), body height (from 141 to 194cm) and parameters of CT exposure (mA range limitation - 180mA, tube potential settings: 100kV(17 cases), 120kV (688 cases), 140kV (45 cases)), noise level-25%). Results Values of CTDIvol in the range 2.93 to 15.69 mGy (7.75±2.23) were significantly dependent on characteristics of patients body size and parameters of CT exposure. As expected, the cases of obese patients scanned with use of higher tube potential (140kV) reported significantly higher CTDIvol (14.09mGy ±1.02) than standard procedures with potential of 120kV (7.42mGy ±1.47) or slim patients scans with use of 100kV (3.59mGy ±0.28). In all subjects, CTDIvol values very highly correlated with characteristics of patients body size, among which patients' body mass index (BMI) was the most representative. Analysis of CTDIvol of 688 scans (295M; 393F) with the most often used settings of 120kV (180mA range limitation) showed high positive correlation with patients BMI ($r=0.85$). In addition, in male patients we found higher CTDIvol values in comparison to female cases holding the same BMI. Multiple analysis of regression showed significant impact of both BMI and gender explaining over 77% of variation of BMI:gender+0.31-CTDIvol values: CTDIvol=0.88+0.63 Analysis of selected cases suggested that highest values of CTDI were caused by inaccurate positioning of the patients' bed. This was especially the case for males with increased abdomen girth. Conclusions 1. Smart mA technique with Auto mA modulation that actively changes the CT parameters as the patient is imaged was found to be effective in adopting the current potential to patients' body size, therefore optimising radiation burden 2. Patient's positioning (the height of patient's bed) seems to be crucial in optimising patient's dose. Practical implications and possible theoretical interpretations of identified effects are further discussed.

P0702

Optimization of the radiation protection in a single nuclear medicine unit.

M. Tomaszuk¹, A. Kozyra², A. Sowa-Staszczak¹, W. Lenda-Tracz¹, B. Glowa¹, A. Hubalewska-Dydejczyk¹; ¹Jagiellonian University Collegium Medicum, Krakow, POLAND, ²AGH, University of Science and Technology, Faculty of Physics and Applied Computer Science, Krakow, POLAND.

Introduction: Because the number of performed clinical procedures in nuclear medicine is increasing, also the role of radiation protection is growing. Most often individual thermoluminescent detectors are used for the effective dose assessment in nuclear medicine units. However this measurement gives information after 3 months without the knowledge what happened in each day of work. The aim of this study was to investigate the radiation exposure and the quality of radiation

protection concerning each group of nuclear medicine staff at our department by electronic personal dosimeters and to optimize it. Material and method: The personal dose equivalent for whole body Hp(10) was evaluated in the period of nearly two months in terms of nuclear medicine physician (group A, n = 1), technical staff responsible for radiopharmaceuticals preparation (group B, n = 5), technical staff responsible for performing examinations (group C, n = 5) and nurse (group D, n = 1). 50 measurements by electronic personal dosimeter in time of consecutive 50 days were performed in each group. In time of this study standard activities of handling radiopharmaceuticals labeled with ^{99m}Tc or ¹³¹I for diagnostic purposes and Na¹³¹I for therapeutic and diagnostic purposes were used. Results: The mean radiation background in different rooms varied from 0.058μSv/h (physicians room) to 0.198μSv/h (hot lab). Mean (min - max) Hp(10) measured in each group was as follows: A - 1.2μSv (0 - 6), B - 6.1μSv (2 - 29), C - 5.8μSv (1 - 16) and D - 6.2μSv (2 - 17). The highest values of Hp(10) in A group were related to myocardial perfusion procedure, in group B - various part of the radioiodine treatment procedure, in groups C and D - bone scintigraphy procedure. Careful analyses of data with taking into consideration the type and the number of examinations each day will be presented at the conference. Conclusion: The exposure can differ significantly for different groups of workers. Also in each examined group different procedures caused higher exposure. Information about to whom, when and where the most significant exposure is observed is the first step for the radiation safety procedures optimization.

P0703

Doses for patient's family members undergoing PET-CT examination

A. Wyszomirska¹, L. Luniak², G. Kamieniarz², R. Kopeć³, M. Ruchała⁴, R. Czepczyński¹, J. Sowiński⁴, M. Budzanowski³; ¹Dept. of PET/CT, Euromedic, Poznań, POLAND, ²Department of Computer Physics, Physics Department, Adam Mickiewicz University, Poznań, POLAND, ³Laboratory of Individual and Environmental Dosimetry Institute of Nuclear Physics, Polish Academy of Sciences, Krakow, POLAND, ⁴Dept. of Endocrinology, Poznań University of Medical Sciences, Poznań, POLAND.

Introduction In radiation protection, dose may be either 'normative', characterizing the health risk (cannot be directly measured) or used for practical purposes (operational values that can be measured). Aim The aim of this study was to measure the radiation doses for family members of patients undergoing PET-CT examinations using 18F-FDG. Materials and methods Experimental measurements of deep personal dose equivalent Hp (10), which is a conservative approximation of the effective dose to the whole body, were taken by highly sensitive thermoluminescent detectors MCP-N (LiF: Mg, Cu, P) in a cassette-type dosimeter DI-02. The main measurement concerned the dose which receive persons in the patient's vicinity. The study group consisted of 30 individuals who were family members of the patients, i.e. patients' spouses and children arriving at our PET-CT Department were qualified. All the qualified persons declared staying with the patients in their homes for about 24 hours after the PET-CT examination. Measurement time was 24 hours. Measurements of dose equivalent Hp (10) at a distance of 1 meter from the patient, 90 minutes after administration of 18F-FDG were performed. Measurements of the dose received by the patient himself were performed also as control. Results The average value of measured individual dose equivalent for the family members of patients was 0.24 ± 0.04 mSv. Theoretical estimates of the value of whole-body dose to the patient's family members, at a fixed distance from the source of 1 m and 0.5 m are several times higher than the average values measured for the whole body. Mean values of these levels were 0.83 ± 0.15 mSv and 3.31 ± 0.59 mSv respectively. Results of the measurement of dose equivalent rate at distance of 1 meter from the patient 90 minutes after administration of 18F-FDG were on average 17.36 ± 3.55 μSv/h. Dose equivalent rate was correlated with the applied activity. The individual dose equivalents measured at the body surface of patients undergoing PET-CT were 1.09 ± 0.20 mSv. The doses measured by dosimeters at the patients' body surface were much lower than the theoretical dose for PET procedures using F-18 FDG, which amounted to 7.18 ± 1.21 mSv. Conclusions Family members of patients undergoing a PET-CT using 18F-FDG receive an average dose about of 0.24 mSv. The measurement results confirmed that a patient after PET-CT does not pose any severe risk to their vicinity in terms of radiation protection.

P0704

The use of detailed risk assessments with dose-rate surveys, dose modelling, risk reduction strategies and regulatory compliance checklists as tools for staff training, dose reduction and the minimisation of risk during the administration of 131I-mIBG and 177Lu-DOTATATE

T. A. Söderlund¹, M. D. Aldridge¹, S. Michopoulou¹, Z. Saad¹, R. Sajjan¹, A. Haroon¹, C. Walker², J. E. Gains², M. N. Gaze², J. B. Bomanji¹, W. A. Waddington¹; ¹Institute of Nuclear Medicine, UCL Hospitals, London, UNITED KINGDOM, ²Department of Oncology, UCL Hospitals, London, UNITED KINGDOM.

Purpose ^{131}I -mIBG and ^{177}Lu -DOTATATE are well-established adult and paediatric therapies at UCLH. A recent review of their radiation risk assessments led to development of a set of tools to permit more detailed assessment of the staff dose and risk for each step of the two procedures. With this knowledge, effort was directed towards effecting 1) dose reduction for key steps contributing the highest doses to the full procedure dose and 2) minimisation of the risk of incidents at each step. **Methods** Detailed review of risk assessments was performed by: i) Generating a spreadsheet for each procedure identifying the major stages and then individual steps. L/M/H risk rating was assigned and practical actions to further reduce dose and/or risk identified and evaluated. Critically, this was performed with a comprehensive instantaneous dose rate (IDR) survey for each procedure including measurement of time taken by staff at each step. This allowed modelling of individual contributions to total dose, which strongly directed the strategy for dose and risk reduction. Audit of staff dose records was also conducted, and used to highlight further changes. ii) Development of detailed checklists with multiple signoffs for use at each administration; ensuring that all major points of compliance with regulatory requirements and the clinical protocol are addressed and formally documented. Input was obtained from the multidisciplinary team. **Results** Implementation of the changes identified in procedures, techniques, shielding and equipment led to an overall reduction in the risk of incidents associated with both procedures. For ^{131}I -mIBG a reduction in total staff dose of 1 $\mu\text{Sv}/\text{GBq}$ was obtained - for the maximum administered activity of 26.4 GBq, total staff dose fell from 127 to 100 μSv per procedure. For ^{177}Lu -DOTATATE, an inherently low staff dose procedure, no difference was obtained (total dose <1 $\mu\text{Sv}/\text{GBq}$). Audit of staff doses highlighted the importance of contingency plans for reducing staff dose following an incident. The revised risk assessment and data from i) and ii) have also been used to extend the knowledge of current staff and are key tools for training new staff. **Conclusion** An overall reduction in staff dose and greater appreciation of the very wide range of radiation risks associated with these procedures, and the nature and origin of their causes (practical, clinical and regulatory) have been obtained. The results and outputs have been and will continue to be used as key tools for the training of staff.

P0705

Optimization in 4D CT/PET acquisitions

A. Mari, M. Valenti, S. Maggi, M. Cardinali, G. Ascoli; AOU Ospedali Riuniti Ancona, Ancona, ITALY.

The diffusion of PET imaging in radiotherapy and increase of IGRT treatments create even more a request for 4D imaging also for planning. Technology development now permit this kind of acquisition and image management. Our experience showed first a great dose exposure for patient. We tried to reduce patient dose optimizing image quality with parameter acquisition. We worked on GE Discovery 690 and RPM Respiratory gating system. First step was to not increase 18FDG activity for these exams and optimizing acquisition parameters (numbers of bed, acquisition time and number of phases), second step was to optimizing CT acquisition (cycle time, dose, image noise). A great constraints for our optimization was patient comfort in order to keep a good immobilization, that aspect had prior impact on time acquisition (for PET and also for CT). For PET we reached a good optimization with 4 phase acquisition with 2 minutes for bed, without activity administration increase (9 mCi/kg, acquisition after 45 min of administration). For CT, available only in retrospective mode (cine acquisition) we reduced mA as low as possible (usually under 100 mA, with SmartmA and AutoMA switched on and a noise index of 30), we applied iterative algorithms at medium level (Asir 30%) and a minimum increase of cycle time respect respiratory cycle (0.5-1.0 sec depending on regularity of cycle). At least we tried to acquire at maximum 2 bed, and to coaching patient breath in order to reduce and regularize respiratory cycle. We started with a CTDI/respiratory cycle of 13.4 mGy/s (DLP 1014 mGy) and we reached a mean value of 7.34 mGy/s (mean DLP 600mGy). Image noise at hepatic tissue increased from 25HU to 35 HU without information loss. We perceived that PET acquisition doesn't need great optimization but we would try to reduce furthermore time acquisition, and increase number of phases (in order to reduce movement artefact and improve length acquisition), CT need great care to be optimized because of retrospective acquisition and is strongly dependent of respiratory cycle length, but have more tools to reach a good optimization. That was a process really time consuming for acquisition set up and optimization but give a lot of important information to accurately localize lesions and to choice the better treatment.

P17-2 - Tuesday, October 30, 2012, 16:00 - 16:30, Poster Exhibition Area

Physics & Instrumentation & Data Analysis: Quality Control & NEMA

P0706

Validation of autoradiochromatography as safe alternative technique to beta counting for determination of radiochemical

purity of 90Y-ibritumomab tiuxetan

M. Di Franco¹, T. Scotognella¹, E. Martinengo², T. Angusti², C. Rabbia¹, V. Podio²; ¹Hospital Pharmacy, San Luigi Hospital, Turin, ITALY, ²Nuclear Medicine Unit, San Luigi Hospital, Turin, ITALY.

AIM 90Y-ibritumomab tiuxetan (Zevalin; Bayer, Germany) is a murine monoclonal antibody conjugated to pure beta minus emitter radionuclide yttrium-90; it is approved for radioimmunotherapy in patients with relapsed or refractory follicular non-Hodgkin's lymphoma. 90Y-ibritumomab tiuxetan labeling is a safe procedure, with complex activity determination (bremsstrahlung component and geometric corrections) and sequential addition of various reagents. Emathological toxicity due to beta minus radiation can occur after Zevalin administration if radiochemical purity (R.P.) is too low (95% as minimum acceptable). All these variables make mandatory R.P. control of Zevalin. Thin layer chromatography silica gel impregnated glass fibre (ITLC-SG) revealed by beta counter is the analytical method recommended by manufacturer. Scintillation liquid (a mixture of aromatic hydrocarbons) is added to samples before analysis, with dangerous exposure of operators to carcinogenic exhalations. This work aims to validate autoradiochromatography as alternative safe technique to determine R.P. of 90Y-ibritumomab tiuxetan. **MATERIALS AND METHODS** Eight preparations were checked for labeling yield by ITLC-SG (Varian; Agilent Technologies, USA) using saline solution as mobile phase. Detection by beta counter was compared to detection by a storage phosphor system (Cyclone Plus; PerkinElmer, USA) able to perform filmless autoradiography of ITLC samples. Three R.P. tests were performed for each preparation and arithmetic mean calculated for every set of measures from the same labeling and detection system. All R.P. tests were performed on samples obtained by a 1:100 dilution of the preparation in saline solution, to obviate to high sensibility of beta counter. In autoradiochromatographic analysis phosphor screen was impressed by TLC samples for one minute, scanned by laser system and finally a high resolution digitized image was created as an image file, quantitatively analyzed by OptiQuant™ software. **RESULTS:** Our results from storage phosphor system and beta counter produced 0.7% as maximum difference between arithmetic medias. In general, precision related to TLC analysis is of the order of 1.0%, limit to define equivalence between two TLC methods for R.P. determination. Consequently, the two methods of detection analyzed can be considered equivalent and interchangeable. **CONCLUSION** An alternative method of detection in R.P. analysis of 90Y-ibritumomab tiuxetan safer for operators was found. Direct detection of yttrium-90 beta minus radiation, employing very toxic liquid of scintillation, can be substituted by indirect autoradiochromatographic analysis, advantageous in terms of safety and accuracy in quantitative analysis and less time consuming.

P0707

Evaluation of different stationary phases as replacement for Instant Thin Layer Chromatography silica gel impregnated glass fibre (ITLC-SG) for radiochemical purity (R.P.) determination on radiopharmaceuticals from cold kits

M. Di Franco¹, T. Scotognella¹, E. Martinengo², T. Angusti², C. Rabbia¹, V. Podio²; ¹Hospital Pharmacy, San Luigi Hospital, Turin, ITALY, ²Nuclear Medicine Unit, San Luigi Hospital, Turin, ITALY.

Aim: European Pharmacopoeia and radiopharmaceutical manufacturers specify Instant Thin Layer Chromatography silica gel impregnated glass fibre (ITLC-SG) as stationary phase for measuring R.P. of most radiopharmaceuticals from kit. During 2008 Pall Corporation, at that time the only world producer of ITLC-SG, stopped manufacturing this product. Existing stocks could run out in a few months, even before a satisfactory replacement could be identified. The objective of this work was to find an alternative and suitable stationary phase, as replacement for Pall support. Materials and methods: We tested supports with chemical features theoretically able to generate chromatographic separations similar to Pall strips thanks to adsorbment and partition mechanisms. Analyzed radiopharmaceuticals from cold kits were labeled with technetium-99m (99mTc), indium-111 (111In) and yttrium-90 (90Y). 99mTc-HDP (hydroxymethylendiphosphonate) and 99mTc-MAG3 (mertiatide) were the first studied radiopharmaceuticals. We tested HPTLC (high performance thin layer chromatography) Lichrospher and HPTLC cellulose (Merck), traditional TLC and HPTLC (Merck), Wathman paper grade 1 Chr and Wathman paper grade 3MM Chr. Finally, we tested ITLC-SG manufactured by Varian (Agilent Technologies, USA), the new owners of Pall's patent. Results: 99mTc-HDP analysis showed consistent tales of elution, especially for reduced hydrolyzed technetium (99mTcO₂); big trouble was also the long time of elution (40-50 min). Only Varian ITLC-SG gave suitable separations for 99mTc-HDP in few minutes. Separations were adequate for 99mTc-MAG3 (only 99mTcO₂ could not be analyzed by Lichrospher because elution stopped at half run) but in all occurrences time of elution was too high. Wathman paper grade 1 Chr did not give clear results, while Wathman paper grade 3MM Chr could not separate neither pertechnetate nor 99mTcO₂. Varian ITLC-SG gave suitable and reproducible separations both for 99mTc-HDP and 99mTc-MAG3, with less than 1% difference in 99mTcO₂ determination and a maximum of +3% in pertechnetate determination by Varian supports compared to Pall results. Then we compared Varian to Pall ITLC-SG also on other

radiopharmaceuticals. ^{99m}Tc -ECD (ethylcysteinate dimer) and $^{90\text{Y}}$ -ibritumomab tiuxetan evidenced a separation respectively of pertechnetate and free yttrium-90 superior of maximum 1% by Pall strips. Results from ^{99m}Tc -albumin macroaggregates, ^{99m}Tc -albumin nanocolloids and ^{111}In -pentetate showed total agreement between the two supports. Conclusion: Even if results from Varian strips were not completely satisfactory for all radiopharmaceuticals, Varian supports were the most satisfying and their similar chemical characteristics to Pall strips, resulted in quite comparable quantitative separation of impurities and elution times. For this reason, in 2010 we chose Varian ITC-SG as replacement of Pall supports.

P0708

Contrast and background variability evaluations by varying target to background activity concentration ratio, for PET/CT acquisition with IEC NEMA Body PET Phantom.

L. Gallo¹, E. Bolla¹, S. Bissoli², F. Chierichetti²; ¹Medical Physics Department, General Hospital, Castelfranco Veneto, ITALY, ²Nuclear Medicine-PET Center, General Hospital, Castelfranco Veneto, ITALY.

Introduction Nema Body Phantom allows PET evaluation for variations of percent contrast to background (CNT%) using small spheric fillable inserts of different diameters, varying from 10 to 37 mm. The assessment of CNT% depending on Target to Background Ratio (T/B) is a very time consuming procedure and produces more uncertainties because any T/B value requires a complete emptying and a new refilling of phantom and inserts; every time new measurements of T & B activities are necessary and when statistical counting becomes poor there is an error propagation. **Aim of the study** To evaluate CNT% and background variability at various T/B ratios by a single phantom preparation, making a trick misleading PET acquisition based on the use of two radiotracers with different half-life (^{11}C and ^{18}F) while acquiring for ^{18}F protocol to obtain a range of T/B values from 21,5 to 1,0. **Material and Methods** We used ^{11}C (half-life 20,4 minutes) to fill hot spheres and ^{18}F (half-life 109,8 minutes) to fill background. Radioisotope activities were measured both on dose calibrator and on gammacounter. The initial activity concentrations were 37,5 kBq/ml and 1,75 kBq/ml for spheres and background, respectively (T/B = 21,5). Target activity decreases faster than background, so acquisitions were repeated until T/B ratio was less than 1,0. Acquisitions and reconstructions were performed by a PET/CT scanner (Siemens Biograph LSO, Sensation 16), according to clinical protocols and images were analyzed using an IDL software. Calculation algorithms are the same one required by NEMA NU2 2007 image quality test. Analysis was performed by drawing circular ROIs on the hot spheres and throughout the background. Corrections were applied for the different physical properties of the two radiotracers to obtain CNT% and background variability. In addition, a visual analysis was performed by two separate nuclear physicians with a score attribution to evaluate the contrast visibility threshold as function of T/B and sphere diameter. **Results** For background activity concentration greater than 1,0 kBq/ml and T/B greater than 2,0, data analysis showed that CNT% is quite independent on T/B values. For background concentrations below 1,0 kBq/ml, statistical fluctuations increased and images were too noisy. Insert visibility depended on sphere diameter and reduced progressively at T/B values of about 2,5. **Conclusions** This method allowed us to study some important imaging parameters with a small time consuming procedure and with less measurement uncertainties.

P0709

Gamma Camera QC Programs with ImageJ

G. D. James, A. Jennings, W. H. Thomson, J. O'Brien; City Hospital, Birmingham, UNITED KINGDOM.

Aim Gamma camera QC is often performed according to manufacturer's specifications and data analysed using manufacturer's software. This invalidates cross comparison between different gamma camera manufacturers. Also, some QC tests are difficult to analyse on the manufacturer's standard software platforms. **Method** We have developed in-house gamma camera QC analysis programs designed to run on an independent DICOM image analysis platform (ImageJ). The data is analysed according to standard literature including NEMA, IAEA and AAPM. The following tests are included: NEMA image uniformity, centre of rotation, line spread function and linearity, point spread function and head alignment, planar sensitivity, quantitative bar phantom analysis, pulse height analysis, multiple window spatial registration, and coefficient of variation flood analysis. The programs have automatic data archiving that allows trend analysis to be performed for every test. Equipment performance can therefore be monitored over time. **Results** All programs have been validated against commercially available software where possible. Some differences were found ($p < 0.05$). The programs have also been tested with artificial data. In recent use, head alignment on a newly installed gamma camera was shown to be unacceptable ($\Delta Y=8\text{mm}$) but passed manufacturer's tests. The programs also detected image uniformity problems that the manufacturer's software missed. **Conclusion** These analysis programs are a simple and convenient way to perform quality assurance tests on any gamma

camera system. They give independent analysis and a consistent approach between different manufacturers. The programs can be easily integrated into any nuclear medicine department's local QC protocol.

P18-2 - Tuesday, October 30, 2012, 16:00 - 16:30, Poster Exhibition Area

Physics & Instrumentation & Data Analysis: Standardisation

P0710

Interobserver variability of heart-to-mediastinum ratio in I-123 MIBG sympathetic imaging

B. F. Bulten, R. L. F. van der Palen, H. W. M. van Laarhoven, L. Kapusta, A. M. C. Mavinkurve-Groothuis, L. de Geus-Oei; Radboud University Nijmegen Medical Centre, Nijmegen, NETHERLANDS.

Objectives: Several factors contribute to the variation in heart/mediastinum (H/M) ratios reported by different institutions. One of these is the method of region of interest (ROI) placement that is used. The current study evaluates the interpatient variability of two ROI definition methods described in the literature to calculate H/M ratio in pediatric patients. In these patients a standardized approach could be valuable to predict cardiotoxicity due to chemotherapy. **Methods:** In 30 pediatric neuroblastoma patients who underwent I-123 MIBG scintigraphy, two methods of ROI placement were used: 'whole heart ROI', in which the whole heart is included in the ROI, and 'small anterior wall ROI', placing a 20 pixel ROI along the left ventricular anterior wall (LVAW). These two methods were performed by two independent observers on both 4 and 24 hours postinjection (p.i.) images of every patient. H/M ratios and corresponding intraclass correlation coefficients (ICC's) were calculated. **Results:** At 4 hours p.i. the interobserver ICC's were 0.88 (95% CI: 0.58-0.96) for small LVAW ROI H/M ratio measurements and 0.96 (95% CI: 0.90-0.98) for whole heart ROI H/M ratio. At 24 hours p.i. ICC's were 0.91 (95% CI: 0.72-0.97) for small LVAW ROI H/M ratio and 0.95 (95% CI: 0.90-0.98) for whole heart ROI H/M ratio. **Conclusions:** We recommend to use the 'whole heart ROI definition method' in pediatric patients, since this leads to the most optimal interobserver agreement in calculating H/M ratios.

P0711

Preliminary utilisation of RadLex terms onto nuclear medicine imaging reports

H. Lee, G. Koh, J. H. Kim, Y. Lee, K. H. Hwang, S. G. Kim; Gil Hospital, Gachon University, Incheon, KOREA, REPUBLIC OF.

BACKGROUND RSNA RadLex is a lexicon of the unified radiology terms for radiologists and it serves as a standard of terminology. In nuclear medicine there has not been one like it. Even in our institution each nuclear medicine physician has his/her own preferred terms when making imaging reports. However it is important to establish a standard terminology for a variety of reasons. The aim of this study was to evaluate whether nuclear medicine imaging reporting terms used in our institution can be mapped onto RadLex terms so as to stick to the standard. **METHOD** The everyday nuclear medicine imaging reports of 5-month duration were reviewed and each word or term was looked up at the RadLex Term Browser site (<http://www.radlex.org> ver 3.5). Imaging reports included both gamma camera images and PET/CT images and we evaluated all the words in each report. Every word was classified into one of the three groups, that is, lexical, semantic or no mapping and those in the first two groups were recorded with RID of RadLex. **DISCUSSION** Calculating the number of RadLex-mapped terms upon the total number of terms in each sentence, 25-75% were successfully mapped to RadLex, that is, classified into lexical or semantic group. However, more than 25% of the terms were not mapped and these included ones describing anatomy, shape, location, or size etc. and on the other hand with different usage or meaning from radiology making the translated sentence awkward. **CONCLUSION** In terms of imaging reports, it is important to use standard terms in order not to deliver ambiguous meaning. As RadLex is a standard for radiology therefore nuclear medicine specific terms essentially do not belong to it, however, could be represented by means of alternative RadLex terms, although not all.

P0712

Effect of acquisition time on the measurement of SUV parameter

A. Wyszomirska¹, R. Czepczyński¹, A. Salyga¹, J. Sowiński², K. Wypychowska¹, T. Sobota¹, I. Guzikowska-Ruszkowska³, K. Obuchowski¹, K. Ciborowski¹, P. Barć⁴, G. Kamieniarz², S. Cichocka⁴, M. Ruchala²; ¹Dept. of PET/CT, Euromedic, Poznań, POLAND, ²Dept. of Endocrinology, Poznań University of Medical Sciences, Poznań, POLAND, ³Dept. of Radiology, Poznań University of Medical Sciences, Poznań, POLAND, ⁴Department of

Computer Physics, Physics Department, Adam Mickiewicz University, Poznań, POLAND.

Introduction The value of the SUV parameter depends on the radiopharmaceutical uptake in the region of interest (ROI), as well as on the body weight or body surface area. Theoretically, acquisition time should affect the quality of the images. The impact of acquisition time was discussed in the literature, but the performed analyses were qualitative. **Aim** Investigation of the relation between the time of acquisition and the SUV parameter was the aim of this study. **Materials and methods** PET-CT images of different patients performed in our institution, and an image of the whole body NEMA phantom were used. During the analysis maximum SUV was evaluated, for images with different acquisition times per field of view (FOV). For each performed examination, eight images in the following times of the acquisition in FOV: 30, 60, 90, 120, 150, 180, 210, 240 s were evaluated. SUV parameters were measured for four regions of interest in the patients' bodies. In case of the phantom, measurements of cold and hot spheres as well as of the background were performed. The results of the measurements were analyzed statistically using Friedman and Dunn tests. Results Statistical analysis confirmed the impact of acquisition time on the value of SUV for all kinds of SUV (body weight, lean body mass, body surface area). A relation between the acquisition times of 30–120 s per FOV was documented. In the range of 150–240 s per 15 cm-FOV dependence has been demonstrated only in reference to shorter times. Decrease in maximum SUV values for the time interval 30–120 s was observed. With the increase of acquisition times above 120 s, the value of SUV parameter oscillated around the mean value. Conclusions Acquisition time in the range of 30–120 s per FOV significantly affects the value of SUV. Extension of acquisition time above 150 s does not affect this value. These results allow to conclude that the optimal time of acquisition is 150 s per FOV.

P0713

Reliability and stability of liver SUV values in the context of a retrospective multicentre study

S. Chauvie¹, L. Kostakoglu², A. Biggi¹, F. Bergesio¹, E. Lanzi¹, M. Gregianin³, M. Huthings⁴, M. Meignan⁵, A. Gallamini¹, S. Barrington⁶, ¹S. Croce e Carle Hospital, Cuneo, ITALY, ²Mount Sinai Medical Center, New York, NY, UNITED STATES, ³Oncology Institute of Veneto, Padova, ITALY, ⁴Rigshospitalet, Copenhagen, DENMARK, ⁵CHU H.Mondor, Paris, FRANCE, ⁶St. Thomas Hospital, London, UNITED KINGDOM.

Liver uptake is an important reference background in assessment of response for PERCIST and the Deauville criteria. The purpose of this study was to analyze the reliability of the liver as a reference organ. 430 PET scans, from 17 institutions worldwide included in the International Validation Study in lymphoma were assessed. SUV mean and SUV max were measured in a 3cm ROI in the liver. The coefficient of variation (CV) for 3 independent readers for SUV mean and max for 20 consecutive scans acquired on the same scanner was 0.03 and 0.06 respectively. Higher variation was observed when 7 readers reviewed the entire dataset of 430 PET scans acquired on multiple scanners with a CV of 0.06 and 0.08 for SUV mean and max. The intrinsic variability of the SUV, expressed as the standard deviation of the voxel SUV, in the 20 patients was 0.25 SUV units. The normalized variability of the SUV in the liver in all 430 patients was 0.38 and 0.58 for SUV mean and max respectively. The SUV mean and max for all patients was 1.86 ± 0.48 and 2.63 ± 0.69 respectively. No relationship was found between liver SUV and injected activity, patient weight or height. There was a significant difference in SUV mean and max for subjects with BMI >25 compared to <25 ($p < 0.05$). A strong correlation ($p < 0.01$) was found between mean and max SUV in the liver and uptake time. Scans had SUV mean and max with time <75 minutes of 2.01 ± 0.50 and 2.76 ± 0.66 respectively and with time >75 minutes of 1.77 ± 0.45 and 2.54 ± 0.70 respectively. There was a strong correlation ($R^2 = 0.66$) between SUV mean and max in liver and mediastinal blood pool. In conclusion, the liver is a reliable reference organ for response assessment and SUV mean is less variable than SUV max. SUV is significantly affected by uptake time and SUV in liver and MBPS are strongly correlated.

P19-2 - Tuesday, October 30, 2012, 16:00 - 16:30, Poster Exhibition Area

Physics & Instrumentation & Data Analysis: New & Innovative

P0714

Gated studies of patients with pacemakers using device OMH 002SYNC

H. Trojanova¹, O. Lang¹, J. Antos², M. Bilwachs³, ¹Charles Univ., 3rd School of Medicine, Prague, CZECH REPUBLIC, ²Orbit Merret, Prague, CZECH REPUBLIC, ³Charles Univ., 1st School of Medicine, Prague, CZECH REPUBLIC.

Aim: Cardiac evaluations by the imaging method are ECG-gated to be able to record and compare images in the same phases of the heart cycle. However, triggering mechanisms may be incapable properly identify the R wave in some patients (e.g. those with a pacemaker, mainly with dual-chamber stimulation). Device OMH 002SYNC generates triggering signal derived from pulse wave and can be used instead of ECG. **Material and methods:** We developed a new method for generation of the triggering signal for synchronized acquisition of heart images. The generation of triggering signal based on a recording of physiological signals from arteries (pulse wave) has the advantage against the ECG gated signals in that it is not negatively influenced by the pacemaker activity or other disturbing effects. Pulse wave is expressed by the saw tooth curve, which is an ideal controlling function enabling to exactly time a generation of triggering signal at the bottom turning point. The device OMH 002SYNC generate a triggering signal with amplitude 10V or 2.5V which is acceptable for most SPECT and PET cameras. We tested the function of this device by comparing it with the ECG trigger on patients without pacemakers. Data were processed by ECToolbox and BPGs on Xeleris computer and paired t-test and correlation were used for comparison. **Results:** Values of EF, EDV, ESV were compared in 30 myocardial perfusion SPECT and 2 planar and SPECT ventriculography examinations for both type of triggering. The LV curves from both gating types were practically identical when heart cycle was divided into 16 or more images. When only 8 images per heart cycle were used the time per one image is relatively long and therefore the images are acquired in slightly shifted time intervals. Regardless of that correlation for EF was 0.955, for EDV 0.987 and for ESV 0.991 ($p = 0.000$ for all correlations). Mean paired difference for EF was -0.034 ($t = -5.6$, $p = 0.000$), for EDV 5.9 ($t = 2.7$, $p = 0.012$) and for ESV 7.9 ($t = 4.0$, $p = 0.000$). **Conclusion:** Triggering of data acquisition by OMH 002SYNC is feasible. Quantitative data of heart function correlate highly with the data calculated with ECG trigger and the differences are not statistically significant in a wide range of values. This device could be very useful in patients with ECG abnormalities and especially those with a pacemaker.

P0715

A phantom study of gamma-probe-based freehand functional imaging for stereotactic navigated interventions

S. Kerschbaumer, C. Gstettner, R. Lipp, R. Aigner; Medical University of Graz, Division of Nuclear Medicine, Graz, AUSTRIA.

The aim of the study was to verify the precision of stereotactic navigation and visualization system declipseSPECT (SurgicEye GmbH, Munich, Germany) and furthermore to optimize and to implement the comprehensive workflow to improve surgical interventions. The declipseSPECT follows the idea to use SPECT/CT (LEHR collimator, 2x30 positions for 30 seconds, Symbia T16, Siemens Medical Solutions USA, Inc., Malvern, PA) data combined with a gamma probe (Type CXS-Sz40, Crystal Photonics GmbH, Berlin, Germany). This allows intra-operatively to project the 3D nuclear medical images in addition to a 3D visualization of the radioactive tracer uptake detected with the gamma probe (augmented reality). Three different types of phantoms were used filled with Tc99m (0.5 up to 400MBq) and with different shapes (line 0.3ml, spherical 0.6 - 30ml, flask 20ml), to correlate distance measurement using the gamma probe as a navigation device in comparison to measurement results from the camera workstation (Syngo Workstation, Siemens Medical Solutions USA, Inc., Malvern, PA). The navigation system and the gamma probe were calibrated using calibrators (3D chessboard and probe calibration target) and 10MBq of Tc99m (140keV, energy window $\pm 10\%$). The SPECT/CT-dataset from the camera was transferred to the declipseSPECT. The system registers the different modalities and the phantoms position (or patient position) using a reflecting target which has to be present in the SPECT/CT dataset. On the Syngo workstation the distance was taken between several markers on the phantom and in the center of the source. On the navigation system the gamma probe was positioned on the marker and the distance to the center of the source is displayed by the declipseSPECT. The mean deviation for the spheres in a depth between 7 and 21 cm was 1.6 ± 1.0 mm (maximum 2.0 ± 0.9 mm), for the line source in a depth between 4 and 18 cm 1.4 ± 0.8 mm (maximum 1.9 ± 0.3 mm) and for the flasks in a depth between 5 and 17 cm 0.7 ± 0.6 mm (maximum 1.0 ± 1.1 mm). Considering the additional uncertainty of the registration, the values shows outstanding precision compared to the specified values of the navigation system itself. The range of 1-2mm is state of the art and sufficient also in comparison to the spatial resolution of the SPECT. The use of the gamma probe combined with stereotactic navigation in addition to the diagnostic scintigraphy is an expedient methodical enhancement for the use of the nuclear medical 3D-data in surgical interventions.

P0716

Preciseness of the injection technique in ROLL (Radioguided Occult Lesion Localization): a multimodal imaging Quality Control (QC)

A. Ricci, A. Sglavo, A. Anitori, S. Chiusaroli, S. Maccafeo, F. Fiore Melacrinis, S. Trivisonne, P. Frittelli, L. Chiatti, R. Schiavo; Belcolle Hospital, Viterbo, ITALY.

Aim ROLL is a surgical technique, commonly used in breast care units to detect non-palpable lesion during breast cancer treatment. Efficacy of this procedure is usually verified by the pathologist by demonstration of a complete tumor excision with a sufficient margin of healthy tissue. X-ray of the specimen, only in the presence of clusters of centrally located microcalcifications, will help to evaluate the overall precision of the localization procedure, but will not test the precision of the injection technique (stereotactic or US guided) as the small amount of ^{99m}Tc -MAA may spread along the borders of the lesion or reflow after needle removal. Our purpose was to validate a QC method, based on multimodal imaging (X-ray, SPECT, MR, phosphor storage imaging), for “a posteriori” verification of the correct centering and intra or perilesion activity administration, with no significant margination. **Materials and methods** Surgical specimen from three patients undergoing breast tumor excision, according to ROLL technique (^{99m}Tc -MAA, 20 MBq in 0.2 mL), were examined by the pathologist to evaluate the accuracy of the excision and then studied with SPECT (128x128, 180°, 64 step, 20 sec/step) and MR (T1-weighted). Isocontour 10% threshold colour maps were applied on transaxial reconstructed SPECT images (FBP, Butterworth 0.45;8) to identify the margins of the excised specimen. SPECT/MR coregistration (Syngo, SIEMENS), based on a “home made” external localizing system, was then performed in order to obtain fusion imaging and allow the localization of both the maximum activity and the tumoral lesion. All the specimen were then studied with a Storage Phosphor Imaging System (Cyclone Plus - Perkin Elmer), commonly used for radiopharmaceutical purity control, and by X-ray (mammogram). Post-processing correlation of the “Cyclone” and mammograms images was then performed by an open-source software (ImageJ 1.44), allowing 2D anatomical correlation between lesion and maximum activity. Distances between maximum activity and the margins of the excised lesions were measured in all the specimen. **Results** Correct measurement of the distance between the injected maximum activity, the center of the lesion and the excision margins was successfully performed in all the specimen. Differences between “activity-centered” and histopathologic distance measurement were less than 5 mm; **Conclusion** A multimodal validation of the injection technique in ROLL procedure is feasible both using SPECT/MR fusion imaging or a 2D postprocessing of storage phosphor-obtained and mammogram images. These methods could be taken in account as a QC test in an radiosurgery physician quality assurance program.

P20-2 - Tuesday, October 30, 2012, 16:00 - 16:30, Poster Exhibition Area

Molecular & Multimodal Imaging: PET/CT

P0717

The Relationship Between Lymph Node Staging and Tumor SUVmax in NSCLC

T. A. Balci¹, H. Komek², M. Cengiz³, H. Kaya³; ¹Damla Hospital, Department of Nuclear Medicine, Elazig, TURKEY, ²Training Hospital, Department of Nuclear Medicine, Elazig, TURKEY, ³Dicle University Medical Faculty, Department of Nuclear Medicine, Elazig, TURKEY.

Introduction: F-18 fluoro-2-deoxy-D-glucose (FDG) uptake in the small sized or borderline lymph nodes will guide the clinician in decision making of the patient's medical and surgical treatment. For this purpose, we evaluated the relationship between the nodular stage and FDG uptake in non-small cell lung cancers (NSCLC).

Materials and Methods: Seventy three patients who were histopathologically diagnosed as NSCLC between July 2009-July 2011 and scanned with PET/CT were evaluated retrospectively. PET/CT imaging in patients with at least 4 hours of fasting and blood glucose levels under 150 mg/dL was performed from the part of the body between the vertex and 1/3 of the thigh at 45-60 minutes following the injection of 370-555 MBq (10-15 mCi) F-18 fluoro-2-deoxy-D-glucose (FDG). SUVmax was determined in tumor tissue and mediastinal lymph nodes in addition to visual evaluation of PET/CT slices. Staging with FDG PET/CT was done according to the Tumor-Node-Metastasis (TNM) (lymph node stage N0, N1, N2, N3). Cut-off value was accepted as 2.5 for the SUVmax. **Results:** Ten female (13.7%) and 63 male (86.3%) patients were included in this study. Mean age was 61.4±9.6 years (between 32 to 83 years). Distribution of patients according to lymph node staging were as follows: N0:11 patients (15.1%), N1:11 (15.1%), N2:20 (27.4%), N3:31 (42.5%). According to lymph node staging, SUVmax values on tumor tissue were as follows: N0:10.2±3.7, N1:11.5±3.9, N2:14.4±5.2, N3:16.8±8.5. A significant correlation between the lymph node stage and SUVmax of tumor tissue ($r=0.302$, $p=0.009$) was determined statistically. **Conclusion:** There is a significant correlation in positive manner between the lymph node staging and the amount of FDG uptake in the tumor, i.e. SUVmax of tumor tissue in NSCLC. Nodular stage increases as with increasing SUVmax in tumor tissue.

P0718

Changes of F-18 FDG uptake in the spinal cord on serial PET/CT of healthy population

H. Song¹, A. Chong¹, J. Oh¹, J. Kim¹, S. Kang¹, J. Ha², B. Byun³, S. Hong³, J. Min³, H. Bom¹; ¹Department of Nuclear Medicine, Chonnam National University Hospital, Hak-dong, Dong-gu, Gwangju, KOREA, REPUBLIC OF, ²Department of Nuclear Medicine, Chosun University Hospital, Seoseok-dong, Dong-gu, Gwangju, KOREA, REPUBLIC OF, ³Department of Nuclear Medicine, Chonnam National University Hwasun Hospital, IIsim-ri Hwasun-eup, Hwasun-gun, Jeollanam-Do, KOREA, REPUBLIC OF.

Purpose: There has not been sufficient information of FDG uptake in spinal cord in healthy population without cancer history. We tried to determine the pattern of FDG uptake in spinal nerve in them and we asked whether the FDG uptake in spinal cord changed significantly on follow-up PET/CT. **Materials and Methods:** We enrolled all healthy subjects who underwent PET/CT twice for cancer screening. We excluded who had vertebral or neurologic disease or motion artifact. SUVmax of spinal cord of each mid-vertebral body level was obtained by drawing ROI on axial image with assist of fusion image of PET/CT. For analysis, the cord-to-background ratio (CTB) was used ($\text{CTB} = \text{SUVmax of each level} / \text{SUVmax of L5 level}$). By using mean CTB, pattern of spinal uptake was determined. Wilcoxon signed rank test was done for comparison of two serial PET/CT. Difference of CTB in sex, age and intervals of two PET/CTs was analyzed. **Result:** Total 60 PET/CTs of 30 people were enrolled. The mean interval between two PET/CTs was 2.7 years (± 0.93). Mean CTB showed decreasing pattern from cervical to lumbar vertebrae. There were two peaks at lower cervical level (C4-6) and at lower thoracic level (T12). On follow-up PET/CT, significant change was shown at the level of C6 and T10 vertebra ($p<0.005$). Sex or age were not significantly correlated to CTB. **Conclusion:** FDG uptake along spinal cord decreases along cervical to lumbar vertebra with two peaks at lower cervical and lower thoracic areas. This is the first study which showed that FDG uptake of spinal cord changes significantly on follow-up PET/CT at the level of C6 and T11 vertebra ($p<0.005$). This finding is valuable as baseline reference in follow-up of metabolic change of spinal cord.

P0719

Introduction with newly available radiopharmaceutical F-18 NaF and Bone PET/CT: Initial private center experience.

O. Carikci, S. Yilmaz, S. Gokart; Lifemed Medical Center, Kadikoy/Istanbul, TURKEY.

Aim: F-18 NaF is recently available in Turkey for routine practice as a bone imaging radiopharmaceutical. The aim of this study is to reveal initial experience with a newly introduced era of bone imaging agent. **Materials&Methods:** Whole body F-18 NaF PET/CT studies of 57 patients; 13 male and 44 female, aged between 14 to 89, scanned and reported are enclosed in this study. Fifty five patients were diagnosed and treated for extraosseous malignant disorders; 40 patients with breast cancer, 8 with prostate cancer, 3 with lung cancer, 2 with colon cancer, 1 with gastric cancer, 1 with thyroid cancer, 1 with thymic carcinoma and 1 with bladder cancer; two patients were having two primary synchronous malignancy. Two patients referred as having primary bone tumors are also included in the study. Retrospective analysis of F-18 NaF PET/CT results of these patients are enclosed and evaluated. **Results:** Twenty six studies were reported as normal, being without any metastatic or malignant bone disease. Multiple metastases, which is accepted as more than 3 lesions, were detected in images of 14 patients. Ten patients were found to have solitary bone metastasis, as well as 2 patients had two metastases and 3 patients had three metastases. From two patients referred as having primary bone tumor one had normal scan and the other one had multiple bony mass lesions. A previously unknown pathological fracture in femoral neck is determined in one patient. Three unknown primary benign bone lesions were detected in scans of three separate patients, and also increased F-18 NaF accumulation were seen in sagittal sinus calcification, atherosclerosis in femoral arteries, and hydatid cyst in three other separate patients. Inflammatory/degenerative joint disease was noticed and reported in 49 patients. **Conclusion:** F-18 NaF is a newly available, highly sensitive and efficient radiopharmaceutical in Turkey; so the favorable imaging performance and the clinical utility of F-18 NaF PET/CT should support the reconsideration of F-18 NaF PET/CT as a routine bone-imaging agent in a wider range of patient population.

P0720

Multivariate analyses for prognostic evaluation with C-11 methionine PET/CT for primary non-small-cell lung carcinoma treated by carbon ion radiotherapy

S. Toubaru¹, K. Yoshikawa¹, S. Ohashi¹, M. Hasebe¹, H. Ishikawa¹, K. Tamura¹, K. Tanimoto¹, S. Kandatsu¹, N. Yamamoto¹, T. Fukumura¹, T. Saga¹, K. Kawaguchi², Y. Hamada², T. Kamada²; ¹National Institute of Radiological Sciences, Chiba, JAPAN, ²Tsurumi University, Yokohama, JAPAN.

Purpose: We evaluated whether or not early prediction of the occurrence of local recurrence and metastasis as well as prognosis (disease-specific survival) is possible regarding patients with primary non-small-cell lung cancer treated by carbon ion radiotherapy (CIRT) by PET/CT using L-methyl-[11C]-methionine (MET). **Methods:**

One hundred forty-six cases that underwent MET-PET/CT study prior to CIRT were prospectively investigated. One hundred thirty-one cases of them also underwent second MET-PET/CT study three months following the completion of CIRT. MET accumulation of the tumor was evaluated using the semiquantitative tumor to normal tissue ratio (TNR). A univariate and multivariate analysis were carried out regarding TNR of the tumor as well as several other clinical factors (age, gender, and tumor size). Results: The average TNR prior to treatment and TNR following treatment was 3.8 (± 2.0) and 2.6 (± 1.2), respectively, showing a significant decline in the TNR following treatment. Upon univariate analysis, a high TNR prior to treatment was a significant factor for occurrence of local recurrence, metastasis and disease-specific survival. Cut-off values were 4.85 ($p=0.006$), 2.70 ($p=0.02$) and 4.51 ($p=0.002$), respectively. A high TNR following treatment was a significant factor for occurrence of local recurrence (Cut-off value=3.10, $p=0.003$). In the outcome of multivariate analysis, TNR prior to treatment and age were significant factors influencing the occurrence of metastasis. Regarding disease-specific survival, TNR prior to treatment was the factor with significant influence. TNR following treatment was the factor significantly influencing local recurrence. That is to say, TNR prior to treatment was a significant factor for metastasis and disease-specific survival upon both univariate analysis and multivariate analysis. In the same manner, TNR following treatment was a significant factor regarding local recurrence in both analyses. Conclusion: MET accumulation measured by PET/CT was a factor significantly related to the occurrence of local recurrence and metastasis as well as early prognosis regarding CIRT for primary non-small-cell lung cancer, thus suggesting it is useful for determining therapeutic efficacy.

P0721

The Role of ^{68}Ga -DOTATOC Positron Emission Tomography/Computed Tomography in the Localization of Ectopic Adrenocorticotropin-secreting Tumors

L. Gilardi, M. Colandrea, D. Militano, G. Paganelli; European Institute of Oncology, Milano, ITALY.

Aim: To determine the role of ^{68}Ga -DOTATOC PET/CT in the localization of Ectopic ACTH-Secreting (EAS) tumors. **Materials and Method:** We retrospectively evaluated five patients who underwent ^{68}Ga -DOTATOC PET/CT for clinical and biochemical evidence of EAS tumors. PET/CT scans were visually assessed. Any ^{68}Ga -DOTATOC uptake higher than the surrounding normal tissues was considered as a positive result. PET/CT data were compared with histology, when available, and follow-up outcomes. **Results:** In four patients PET/CT identified a lesion in the lungs. Surgery was performed in three cases and a final diagnosis of typical carcinoid was histologically confirmed. In the fourth patient the clinical and instrumental follow-up indicated the diagnosis of lung ACTH secreting tumor. Remarkably, all these patients were previously submitted to a ^{111}In -pentetreotide scintigraphy that failed to localize the EAS tumors. The fifth patient showed focal accumulation in left adrenal gland that was considered suspect as for disease localization. After surgery, the diagnosis was adrenal hyperplasia. **Conclusions:** ^{68}Ga -DOTATOC PET/CT could be an useful tool in the localization of EAS tumors and can be used instead of somatostatin receptor scintigraphy in the initial evaluation of this disease due to its better diagnostic performance. Organs with physiological uptake of the radiotracer should be evaluated with caution to avoid false positive results.

P0722

Should we use metabolic information of FDG PET/CT to improve the choice of target lesions in malignant lymphoma?

F. Ricard, C. Tychy-Pinel, F. Giammarile, C. Houzard, F. Réty; Centre Hospitalier Lyon Sud, Pierre Bénite, FRANCE.

Introduction: Malignant lymphoma is a heterogeneous and widespread disease. The morphological follow-up is based on the choice of 6 target lesions at baseline on enhanced CT (eCT) that will be reassessed during follow-up. This means that a small amount of lesions has to be representative of the whole patient. Nowadays FDG PET/CT is commonly used for the initial staging in Hodgkin and diffuse large B cell lymphomas and we can wonder if metabolic information should be integrated in the choice of these target lesions. **Materials and Methods:** 59 patients with aggressive lymphoma were retrospectively included. Interpretation of enhanced CT alone was first carried out by radiologists, then a combined analysis of eCT and FDG PET/CT (eCT+PET) was done by imaging specialists in both FDG PET and CT interpretation. They chose nodal target lesions, with a maximum of 6 lesions per patient, based on morphological aspect for eCT readers and on metabolic aspect for eCT+PET readers. Each target lesion was measured at baseline and follow-up and corresponding results were compared to a clinical gold standard (GS). Interobserver agreement and comparison to the GS were assessed with kappa (K) and intraclass correlation (ICC) statistics and significant values were assessed with Student's test. **Results:** The distribution of target nodal areas was equivalent among eCT and eCT+PET readers (ICC = 0.97 and 0.99) with a maximum of target lesions chosen in cervical and mediastinal areas. However, choosing lesions with eCT+PET led to heterogeneity in the size of target lesions when compared with eCT

alone ($p=0.03$). Agreement for assessing the morphological decrease in size of target lesions at follow-up was equivalent between eCT and eCT+PET readers (K = 0.85 and 0.84), as well as the percentage of morphological variation between baseline and follow-up. When comparing the degree of morphological response, there was a better reproducibility of eCT (K = 0.70 vs 0.59) and a global equivalence of eCT and eCT+PET when comparing to the GS (K = 0.40 - 0.63 vs 0.50 - 0.56). **Conclusions:** The choice of target lesions in malignant lymphoma based on metabolic information is an alternative to the usual choice of target lesions with morphologic information. Even if choosing lesions with PET/CT leads to heterogeneity in the size of target lesions, the percentage of morphological response and the agreement with the clinical gold standard are equivalent when targeting with eCT or eCT+PET.

P0723

Role of ^{18}F -FDG PET/CT in the Evaluation of Axillary Lymph Nodes After Neoadjuvant Therapy in Patients with Breast Cancer

L. Gilardi, C. De Cicco, M. Colandrea, L. L. Travaini, S. Vassallo, D. Familiari, V. Bagnardi, D. Paolucci, G. Paganelli; European Institute of Oncology, Milano, ITALY.

Aim: The main objective of this study was to determine the role of ^{18}F -2-fluoro-2-deoxy-D-glucose positron emission tomography (FDG PET) in the evaluation of axillary lymph nodes after neoadjuvant therapy in patients with breast cancer.

Materials and methods: Sixty-five patients with primary breast cancer clinically classified as cT2, cT3 or cT4a-c cN0-N2 or cN3 M0 with a positive baseline FDG PET scan both in the site of primary tumour and axillary lymph nodes underwent neoadjuvant therapy. Afterwards a second FDG PET scan was performed. In case of persistent axillary FDG uptake, patients underwent directly an axillary lymph node dissection (ALND). When FDG PET scan was negative for axillary involvement, SNB was performed to evaluate axillary lymph node status and a total ALND followed only in case of SN positivity. **Results:** Specificity and positive predictive value of FDG PET for detection of axillary lymph node metastases after neoadjuvant therapy were 93% (95% confidence interval: 76-99%) and 86% (95% confidence interval: 57-98%) respectively. Whereas sensitivity, negative predictive value and diagnostic accuracy were NOT adequate for a correct staging (32, 49 and 57% respectively). **Conclusion:** The poor sensitivity of FDG PET in detecting axillary lymph node metastases makes SNB mandatory in case of a negative scan. Positive predictive value proved to be relatively high, suggesting a role of FDG PET in selecting patients candidate for ALND after neoadjuvant therapy, avoiding SNB.

P0724

Deep Inspiration Breath Hold ^{18}F -FDG PET-CT in evaluating lung lesions: preliminary results

E. Puta, V. Massetti, M. Andreoli, A. Mostarda, A. Soffientini, S. Ren Kaiser, C. Pizzocaro, U. Guerra; Fondazione Poliambulanza- Istituto Ospedaliero, Brescia, ITALY.

Aim: Deep Inspiration Breath Hold (DIBH) PET-CT technique is under investigation for its contribution to a more accurate detection and diagnosis of lung lesions. The aim of this study was to investigate the clinical feasibility of a single 20-s acquisition of DIBH ^{18}F -FDG PET-CT and the comparison between PET-CT in DIBH and free breathing (FB) in the detection of lung lesions. **Materials and methods:** The PET-CT study was performed using a LSO TOF PET-CT scanner, 4 rings (Siemens Medical Solution). From 10.05.2011 to 03.01.2012, twenty-five patients with pulmonary lesions underwent a standard whole body ^{18}F -FDG PET-CT scan followed by a single bed thorax acquisition PET-CT in DIBH. The patients were asked to hold their breath in DIBH, for 10s during the CT scan and 20s for the PET. The cut-off of 15-20s for the PET acquisition was determined by a phantom study prior to the clinical study. The displacement of lung lesions between PET and CT images, the maximum lesion standardized uptake value SUVmax in FB and DIBH PET-CT were recorded. The percent difference in SUVmax between the FB and DIBH scans was calculated and defined as %BH-index. **Results:** 23/25 patients were able to complete the PET-CT acquisition in DIBH and 27 lung lesions were studied. In 19/27 lesions there was misalignment between PET and CT images in FB. PET-CT in DIBH showed a significant increase of SUVmax compared to FB for these 19 lesions ($p=0.0002$). In the remaining 8/27 lesions there was matching between PET and CT images in FB and showed no significant statistical difference between DIBH and FB PET-CT in SUVmax ($p=0.83$). There was observed a correlation between the %BH-index and lesion displacement between PET and CT images ($R^2=0.324$, $p=0.01$) which was significantly higher for lesions having a displacement > 8mm ($p=0.002$). The comparison of lesion displacement, SUVmax in DIBH and the %BH-index showed a statistically significant increase for the lesions in the lower lung area than in the upper lung area respectively ($p=0.034$; $p=0.013$ and $p=0.013$). **Conclusion:** The single 20-s acquisition of DIBH PET CT is a feasible technique for lung lesion detection in the clinical setting (23/25 pts) and requires only a minor increase in examination time without particular patient training. 20s DIBH provided more

precise measurement of SUVmax, especially for lesions in the lower lung lobes which had a greater displacement between PET and CT images in FB.

P0725

F-18 FDG PET/CT Studies in Patients Receiving Treatment for Tuberculosis: A Six Month Follow-Up Study

A. Ellmann, A. Du Plessis, L. Nolan, D. Kriel, G. Walzl, J. Warwick; Stellenbosch University, Cape Town, SOUTH AFRICA.

FDG PET/CT studies cannot differentiate between tuberculosis and malignancy, as high FDG uptake is found in both conditions. The exact role of FDG PET/CT in the evaluation of tuberculosis patients is not clearly defined. Few papers in the literature report the value of FDG PET in monitoring treatment response in TB patients. We report on findings at baseline and up to 6 months follow-up after the initiation of TB treatment. Methods: HIV negative patients who presented clinically with active pulmonary tuberculosis were referred for serial FDG PET/CT studies, before therapy was started (baseline), after one month and after six months of anti-TB treatment. The three scans were compared. Results: On the baseline study (n=42 patients) 76% of patients had multiple sites of disease in both lungs, with chest lymph node (LN) uptake in 55%. Extrapulmonary activity was noted in 8 cases (19%), including one case of extrapulmonary TB, four with extrathoracic LN uptake, and one with a malignant rib lesion. At one month follow-up the majority of patients (48%) had a mixed pattern of FDG uptake, with some areas improving, and some areas demonstrating more intense uptake in the lungs. LN uptake was also variable. The majority of patients still demonstrated LN FDG uptake. At the time of preparing the abstract, six month follow-up was only done in 31 patients. The FDG uptake normalised in only 5 patients, while it improved in the majority of cases (65%) with 4 cases with a mixed pattern. Only 3 patients had residual LN uptake. Discussion: Although the exact role of FDG PET/CT studies is not clearly defined, our study is the first to document the response of pulmonary TB using PET/CT in a large group of patients. The study confirmed avid FDG uptake in TB lung lesions in all patients at baseline. PET/CT following 1 month of therapy does not show improvement from baseline. All patients demonstrated improvement in FDG uptake after 6 months of therapy, however the majority still showed residual activity at 6 months, the significance of which requires further study. PET/CT studies may have some value in the follow-up of specific groups of patients receiving treatment for active pulmonary TB. Extrapulmonary TB was an infrequent finding in this high risk patient group, suggesting that increased risk of false positive oncology studies due to extrapulmonary TB in HIV negative patients in South Africa may be overstated.

P0726

Unusual Findings in PET/CT and Cardiac MRI Lead to the Diagnosis in a Patient with Pyrexia of Unknown Origin.

K. Adlington, D. Pencharz, T. Wagner; Royal Free Hospital, London, UNITED KINGDOM.

Introduction: We report on a patient who presented with pyrexia of unknown origin (PUO) and complex imaging findings on CT chest/abdomen/pelvis (C/A/P), cardiac MRI (CMR) and whole body FDG PET/CT. The latter was key in helping to reach a diagnosis. Case report description: A 30 year old Ethiopian man presented on 1/11/11 with weight loss, intermittent fevers and chest pain. CT C/A/P on 3/11/11 showed mediastinal, hilar and axillary lymphadenopathy, splenomegaly (14.3cm) and a moderate pericardial effusion. Lymphoma was thought to be the most likely cause of the findings. He was diagnosed with HIV infection (viral load 93 000 copies/ml, CD4 count 148) and commenced on anti retrovirals. However he had ongoing fevers for which no cause was found. Infection screen, axillary lymph node biopsy on 7/11/11, pericardiocentesis on 11/11/11 and inguinal lymph node biopsy on 18/11/11 were all non-diagnostic. Due to his PUO he had a whole body FDGPET/CT scan on 16/11/11 which showed high-grade uptake in a mediastinal mass and diffuse pericardial involvement, as well as moderate uptake in axillary and inguinal lymph nodes. The unusual mediastinal and pericardial uptake on PET/CT led to CMR on 5/12/11. CMR demonstrated a large mediastinal mass extending from the aortic arch up to the atria, encasing the left atrium and extending into the pericardium. On 17/12/11 the patient had a Video Assisted Thoracic Surgical (VATS) biopsy of the mediastinal mass. It was found to contain pus and mycobacterium tuberculosis was identified in the samples obtained. The patient was started on antituberculous therapy with good response. Conclusion: Diffuse pericardial uptake on PET/CT is unusual and led to CMR and identification of a suitable biopsy site. PET/CT is a powerful tool in the management of patients with PUO.

P0727

Failure To Detect Endometriosis with FDG PET-CT

C. Aprile, B. Gardella, I. Calvino, G. Cavenaghi, G. Carletti; Fond. Policlinico S.Matteo, IRCCS, Pavia, ITALY.

Aim: There are several case report suggesting some utility of FDG-PET in the detection of endometriosis, while other authors on small pts series did not find a sufficient accuracy. Aim of this work was to evaluate the clinical impact of FDG PET-CT in the detection of deep endometriosis. Material and Method: Twelve consecutive patients (median age 38.5 yrs, range 27-50) with clinical suspicion of endometriosis underwent a diagnostic pre-operative work-up, including trans vaginal sonography (TVS) and/or MRI, CA125 serum assay and FDG PET-CT in the follicular phase. Nine patients underwent a laparoscopic surgery after a median delay of 9 (range 2-29) days from PET study. In one patient TVS/MRI did not confirm endometriosis at pre-operative visit, surgery was postponed in another premenopausal patient with severe comorbidity and one was lost to follow up. Results: Laparoscopic surgery revealed endometriosis localizations in all 9 patients and all the specimens were confirmed by pathology. Of the 9 patients, 5 had documented I stage, 2 II stage e 2 IV stage according to AFS classification. In the nine patients underwent surgery, CA125 serum levels were normal in 3, slightly elevated in 4 and increased in 3. FDG did not accumulate in any of these localizations, even in patients with elevated serum level of CA 125; while gave one false positive and one equivocal result in two patients, surgery and further follow-up did not reveal any abnormality in these patients, probably due to inflammatory changes or physiologic changes due to menstrual cycle. Another patient presented a moderate lung uptake, not confirmed by contrast enhanced CT and by follow-up. Conclusion: Our results further confirm the reports by Fastrez and Setubal, which showed a very poor accuracy of FDG PET-CT in the detection of pelvic endometriosis. Interestingly in patients with elevated CA125 serum levels FDG did not give true positive results mediated by inflammatory changes of the peritoneum. On the other hand the three false positive results were observed in patients with elevated CA125 levels, inflammatory changes and luteal hemorrhagic cyst in one pt..

P0728

Superiority of F-18 NaF PET/CT scan upon Tc-99m MDP bone scintigraphy in prostatic cancer patients with low PSA levels: a case report.

S. Yilmaz, O. Carikci, S. Gokart; Lifemed Medical Center, Kadikoy/Istanbul, TURKEY.

Aim: Samarium-153 lexidronam (Sm-153) is a highly efficient therapeutic radiopharmaceutical used in palliation of pain, caused by bone metastases. The aim of this abstract is to share our clinic's experience in one patient imaged by two different imaging modalities; both Tc-99m MDP bone scintigraphy and F-18 NaF PET/CT, and also images obtained after bone pain palliation treatment with Sm-153. Materials & Methods: Sixty two year old male patient with diagnosis of prostate cancer, determined at November 2010 and had been treated with bilateral orchiectomy and radiation therapy. He has been referred to our clinic for bone pain palliation, which was unresponsive to pain medication. Results: Bone scintigraphy of the patient performed in another center a few days ago before patient admission was reported as without any osteoblastic metastases. With the knowledge of normal findings, patient has been questioned again and he answered that he had severe pain, unresponsive to pain medication. As the bone scan of patient was reported as normal, hard copy images of that bone scan was revised by two nuclear medicine specialists and confirmed as without any osteoblastic metastases. The patient's PSA level was 5.2 ng/ml at the time of bone scan. To evaluate the existence of any metastasis, F-18 NaF PET/CT scan has been performed to patient in our clinic. F-18 NaF PET/CT study revealed widespread sclerotic metastases throughout the whole skeleton, most of them showing mildly increased NaF accumulation. The question bore in mind that the metastases may be under scintigraphic resolution limits, but the lesions bigger than 1 cm in widest diameter seen at CT slices can not be visualised in bone scan retrospectively. After PET/CT scan, metastatic disease had been stated and bone pain palliation treatment with 1 mCi/kg Sm-153 treatment has been given intravenously to patient. After Sm-153 treatment, whole body imaging also has been done, and lesions detected at F-18 NaF PET/CT displayed mildly increased Sm-153 accumulation. Conclusion: The sensitivity and specificity of Tc99m MDP bone scintigraphy known as low at PSA levels of <10 ng/ml. Our patient had a normal bone scintigraphy result while his PSA level was 5.2 ng/ml, but as an imaging modality of much higher sensitivity, F-18 NaF PET/CT study has revealed widespread sclerotic metastases throughout the skeleton. At this point, our findings suggest that F-18 NaF PET/CT should be the first screening choice for bone metastases, especially in patients with low PSA levels.

P0729

3D CT-Histogram analysis enables to distinguish affected and FDG-negative lymph nodes in patients with lung cancer

P. Flechsig¹, C. Kratochwil², J. Moltz³, C. Heussel⁴, H. Kauczor¹, U. Haberkorn², F. L. Giesel²; ¹University of Heidelberg, Diagnostic and Interventional Radiology, Heidelberg, GERMANY, ²University of Heidelberg, Heidelberg, GERMANY, ³Fraunhofer Institut, Bremen, GERMANY, ⁴Thoraxklinik Heidelberg, Heidelberg, GERMANY.

Purpose: Patients with lung cancer often describe chronic lung diseases (i.e. COPD), so that mediastinal lymph nodes present a positive FDG-uptake due to inflammatory pathogenesis. However, FDG-PET is the leading imaging modality for N-Staging in lung cancer patients and therefore in unclear FDG-PET status 3D CT histogram analysis might give an additional value to distinguish unclear PET findings. In this investigation 3D CT histogram analysis was used to identify metastatic lymphnode involvement in lung cancer patients in correlation to FDG-PET/CT. **Materials and Methods:** 38 lymph nodes of 32 patients aged 43–76 years (16 male, median age 58) diagnosed with lung cancer were investigated. FDG-PET/CT (Biograph 6 PET/CT) was performed prior to surgery/biopsy according to clinical schedule. Lymph node assessments were acquired using FDG-uptake (SUVmax) and 3D CT histogram analysis on the basis of non-enhanced CT scans. For computing the histograms, the lymph nodes were segmented by a semi-automatic method; if necessary, the segmentation result was corrected manually. Both imaging finding were correlated to the histological gold standard (histology: 24 times adenocarcinoma, 5 times squamous cell carcinoma, 3 times neuroendocrine carcinoma). **Results:** 21 positive and 17 negative histological proven lymph nodes were successfully analyzed by 3D CT histogram (Figure 1a). The histological positive lymph nodes presented a median CT HU value of 34.5 (min -29,8 / max 59,1) while histological negative lymph nodes presented a median CT HU value of 7.6 (min -21.0 / max 87.4; Figure 1b). Findings were independent of the FDG-uptake value. **Conclusion:** 3D Histogram analysis seems to be a very promising and valuable imaging surrogate for N-staging stratification in patients with lung cancer with unclear glucose utilisation in FDG-PET.

P0730

Impact of F18-FDG-PET/CT on treatment planning in non-surgical cancer patients before oncological microtherapy

J. M. Rogasch, C. Furth, G. Ulrich, K. Mohnike, I. G. Steffen, E. Kettner, J. Ruf, J. Rieke, H. Amthauer; Klinik für Radiologie und Nuklearmedizin, Universitätsklinik Magdeburg A.ö.R., Otto-von-Guericke Universität, Magdeburg, GERMANY.

PURPOSE: Before local microtherapy [e.g., radiofrequency ablation (RFA), brachytherapy or irreversible electroporation (IRE)] of primary tumors and metastases, patients have to be carefully evaluated to decide whether this is the adequate treatment and/or to optimize further treatment planning. In this study, we determined the value of whole-body FDG-PET/CT for planning of microtherapy and/or change of the therapeutic approach. **PATIENTS, METHODS:** In this study, 19 patients (f, 7; m, 12) referred for microtherapy [RFA, n=4; brachytherapy, n=11; IRE, n=3, and selective internal radiotherapy (SIRT), n=1] suffering from primary malignancies or metastases thereof [colorectal cancer (CRC), n=11; renal cell cancer (RCC), n=2; cholangiocellular carcinoma (CC), n=2; others, n=4] were included retrospectively. Staging was carried out by conventional imaging methods (CIM; thoracic and abdominal CT, liver MRI) and FDG-PET/CT. The examinations were analyzed in a consensus reading by two observers. Based on the staging information, therapeutic decisions were made by an interdisciplinary tumor board. The influence of the additional FDG-PET/CT on the therapy management was assessed and subsequently validated by imaging, clinical follow up and histopathology (if available). Standard statistical parameters were calculated. **RESULTS:** Compared to CIM, discrepant findings on FDG-PET/CT led to major changes in the therapeutic approach (e.g., local ablative vs. surgery vs. systemic therapy vs. best supportive care) in 8/19 patients (42.1%). In 5/19 patients (26.3%), the clinical target volume (CTV) was altered due to an improved delineation of viable lesions (n=3) or detection of additional lesions (n=2). In 6/19 patients (31.6%), no changes in the therapeutic approach were observed. **CONCLUSION:** In the evaluation of patients before highly innovative microtherapy procedures, FDG-PET/CT depicted relevant findings supplementary to CIM. Subsequently, FDG-PET/CT seems to be of high value for both planning of the microtherapeutic procedure and decision making in further clinical course.

P0731

A parathyroid Adenoma Presenting as a Hypermetabolic Mediastinal Mass on F-18 FDG PET-CT

N. P. Karahan, O. Ozdogan, G. Capa Kaya, H. Durak; Dokuzeylul University Faculty of Medicine Nuclear Medicine Department, IZMIR, TURKEY.

A 66 year-old male patient with a mass in the superior mediastinum on thorax CT was referred for F18-fluoro-2-deoxyglucose positron emission tomography (F-18 FDG PET) for metabolic characterization of the lesion. The mass which was located on right upper paratracheal region was hypermetabolic (SUVmax: 7.3). It was reported as a lymph node with a probable malignant potential. The patient underwent surgery. The lesion was resected and the final histopathologic diagnosis was a parathyroid adenoma. There was not any parathyroid hormone levels studied before surgery. The patient was hypercalcemic (Ca: 13.9 mg/dl) preoperatively. The patient's calcium levels decline postoperatively to normal levels (9.0 mg/dl). The PTH level was normal (63 pg/ml). The F-18 FDG PET study is useful for localization of primary and recurrent parathyroid carcinomas. Although rare, intrathyroidal parathyroid adenomas were also declared to demonstrate high

metabolic activity on F-18 FDG PET study. In our case we detected a high F-18 FDG uptake in an ectopic parathyroid adenoma. PET study using F-18 FDG may be beneficial to localize ectopic parathyroid glands in patients with hyperparathyroidism.

P0732

18F-FDG PET/CT Breath-Hold Acquisition in Metabolic Evaluation of Solitary Pulmonary Nodules: An Alternative Method to Respiratory Gating

M. Queneau¹, S. Petras², D. Lussato¹, M. Guernou¹, K. Farid³, B. Songy¹; ¹Centre Cardiologique du Nord, Paris, FRANCE, ²Institut Curie, Paris, FRANCE, ³Hôpital Hôtel-Dieu, Paris, FRANCE.

Objectives To evaluate the effect of the 18F-FDG PET/CT short deep-inspiration breath-hold acquisition in metabolic evaluation of solitary pulmonary nodules before treatment decision. **Methods** PET/CT scans were performed for metabolic evaluation of solitary pulmonary nodules (SPN) in 31 patients. We studied 22M/9F with mean age of 63 years (range: 40–80) having radiologically suspicious nodules ≤3 cm during their scheduled staging examinations. The scans were performed on Discovery PET/CT 690 (GE Healthcare) scanner 60 min after iv injection of 18F-FDG (4MBq/kg). The standard whole body (WB) acquisition was followed by a short 30 sec deep-inspiration breath-hold (BH) acquisition. The OSEM iterative reconstruction was used to generate images. The SUVmax values measured by standard VOI method were obtained for each lesion in WB and BH studies to calculate the SUVmax percentage difference (% Diff SUVmax = SUVmax BH-SUVmax WB/ SUVmax WB). **Results** Thirty-one morphologically suspected SPN were studied, mean nodule size was 13 mm (6–29). Seventeen SPN (55%) were diagnosed in the right and 14 (45%) in the left lungs. The SUVmax mean value was 2,4 (0,5–10,5) in WB and 3,3 (0,6 to 15,5) in BH studies (p=0,01). There was an increase of SUVmax values in BH scans in comparison to WB studies from 0,4–7,7 (mean 0,9). The mean % Diff SUVmax for all patients was 22% and their values increased more in subjects having SUVmax≥2,0 in WB scans (54%), than in those showing SUVmax<2 (4%). **Conclusions** The short 30 sec deep-inspiration breath-hold FDG acquisition is an alternative method to respiratory gating on new generation PET/CT scanners showing high counts rate with reduced injected doses. This technique improves metabolic evaluation of solitary pulmonary nodules before treatment decision.

P0733

Clinical value of 18F-FDG PET/CT in the management of suspected infection and fever of unknown origin: experience in 38 patients

E. Greco¹, C. Di Leo¹, L. Pagani¹, A. Cantù¹, M. Picchio², C. Messa³; ¹A. Manzoni Hospital, Lecco, ITALY, ²San Raffaele Scientific Institute, Milan, ITALY, ³San Gerardo Hospital, Monza, ITALY.

AIM: to evaluate the clinical impact of ¹⁸F-FDG PET/CT on the diagnosis and management of selected patients with suspected infection and fever of unknown origin (FUO). **MATERIALS AND METHODS:** Thirty-eight patients (22 men, 16 women; age range: 21–85 years) with clinical and diagnostic suspect of bone or vascular graft infection (n=27) and FUO (n=11) were studied by ¹⁸F-FDG PET/CT and retrospectively evaluated. ¹⁸F-FDG PET/CT findings were confirmed by either clinical/imaging follow-up or microbiological/histological findings. **RESULTS:** ¹⁸F-FDG PET/CT resulted positive in 27/38 patients and it correctly detected the localisation and the extent of disease, both in adjacent and in distant sites, in 22/27 (81%) positive studies. In particular, it could allow the diagnosis of infection at either axial or peripheral skeleton (n=6), at aortic prosthesis (n=4) or limited at soft tissues (n=5), thus determining an optimization of therapeutic strategy (antibiotic therapy or surgical intervention). In addition, ¹⁸F-FDG PET/CT findings could guide additional investigations (e.g. biopsy) or treatment planning in 7 patients with FUO, which had a final diagnosis of spondylodiscitis extended to psoas (n=1), spondylarthrititis (n=1), septic arthritis (n=1), thyroiditis (n=1), liver abscess (n=1), aortitis with a muscular abscess (n=1) and Hodgkin's lymphoma (n=1). In the remaining 5/27 (19%) cases, ¹⁸F-FDG PET/CT resulted false positive and showed a peculiar linear ¹⁸F-FDG uptake due to postoperative reparative tissue in a recent sternotomy and foreign body aseptic reaction in vascular grafts, even years after surgery. ¹⁸F-FDG PET/CT resulted negative in 11/38 cases and it could influence the therapeutic management in 8/11 (73%) patients with doubtful morphological imaging. In particular, it could exclude the presence of spondylodiscitis (n=3) or infectious pseudoaneurysm (n=4), allowing reconstructive surgery, and it suggested the diagnosis of neurotoxoplasmosis in one HIV positive patient with an intracranial mass lesion, suspected for lymphoma on magnetic resonance scan. The remaining 3/11 (27%) negative patients had FUO and in these cases ¹⁸F-FDG PET/CT did not contribute to a final diagnosis. In the whole population of 38 patients, ¹⁸F-FDG PET/CT could modify patient management in 23 (60%) cases. **CONCLUSION:** ¹⁸F-FDG PET/CT is a valuable tool in the diagnosis of well selected cases of bone or vascular infection, especially those with doubtful morphological imaging, and in patients

with FUD, allowing precise evaluation of both the localization and extension of disease foci, with a strong impact on patient management.

P0734

Prognostic evaluation of Cancer of Unknown Primary with cervical metastases based on ^{18}F -FDG PET/CT findings

Z. Wu, Y. Zhang, X. Lan, Q. Jia, X. Sun, H. Wei, X. Tan; The PET Center of Union Hospital, Tongji Medical College, Huazhong University of Science and Technology. Key lab of Molecular Imaging Research of Hubei Province, Wuhan, CHINA.

Aim: Cancer of unknown primary (CUP) remains a particular challenge in oncology. Cervical lymph node enlargement is the most frequent presentation of metastatic lesions of CUP. The aim of the study was to compare the overall survival of different group patients with CUP of cervical metastases according to ^{18}F -FDG PET/CT findings and to investigate the prognostic value of ^{18}F -FDG PET/CT in patients with cervical lymph node metastases from CUP syndrome. **Methods:** In a retrospective study, a total of 107 patients between March 2004 and April 2010 with proven cervical metastatic lesions of unknown primary sites were reviewed after unsuccessful conventional diagnostic work-up. PET/CT images were analyzed with visual and semiquantitative method. Cytology, histopathologic findings and/or clinical follow-up (lasting 1–85 months) were used to evaluate PET/CT results. Overall cumulative survival of PT+ group (PT positive/AM negative or PT positive/AM positive), PT+ group (PT positive/AM positive), PT+ group (PT positive/AM positive) and PET- group (PT negative/AM negative) was calculated by Kaplan-Meier method, and the log-rank test was used for comparisons. **Results:** In 59 of 107 patients ^{18}F -FDG PET/CT showed focal tracer accumulations corresponding to potential primary tumor sites. In 48 (44.9%, 48/107) of these 59 patients, FDG PET/CT results were true-positive, which were confirmed by biopsy, (n=27), surgery (n=13), and clinical follow-up (n=8, lasting 5–26 months). The sensitivity, specificity and accuracy of ^{18}F -FDG PET/CT to detect primary sites were 94.1%, 80.4% and 86.9%, respectively. The median overall survival of the 101 patients enrolled into the survival study was 20.0 months. The 43 patients with PT+ had a median overall survival of 13.0 months (95% CI 9.2–16.8 months) and mean survival of 18.4 months (95% CI 12.5–24.3 months), which was shorter than the mean survival of 60.8 months (95% CI 48.4–73.2 months) among 35 patients of PET- group ($\chi^2=22.9$, $P<0.0001$), so was the patients in AM+ group compared to that of patients in PET- group (17.2 vs. 60.8 months, 95% CI 11.8–22.6 vs. 48.4–73.2 months, $\chi^2=18.3$, $P<0.0001$). However there was no significantly difference in overall survival for patients between PT+ group and AM+ group (median survival 13.0 vs. 14.0 months, 95% CI 9.2–16.8 vs. 6.3–21.7 months, $\chi^2=0.080$, $P=0.778$). **Conclusions:** ^{18}F -FDG PET/CT is helpful in detecting the primary sites in patients with cervical metastases from CUP. In contrast to patients with no positive findings on FDG PET/CT, patients with primary tumor sites and/or additional metastatic lesions on FDG PET/CT has a shorter survival than negative findings, but patients with primary origin findings on FDG PET/CT shows no better survival than patients with only additional metastases findings, which indicates that the discovery of hypermetabolic lesions of primary sites and/or additional metastases mean a poorer prognosis, no matter whether the primary tumor sites be found or not on FDG PET/CT.

P0735

^{18}F FDG-PET/CT May Change the Stage and Treatment Planning for Volumetric Modulated Rapidarc™ Radiotherapy (RA-IMRT) in Cervical Cancer: the European Institute of Oncology Experience

L. L. Travaini, L. Gilardi, M. Colandrea, R. Lazzari, S. Vassallo, A. Ceconi, D. Familiari, R. Mei, C. De Cicco, G. Paganelli; European Institute of Oncology, Milano, ITALY.

Aim: To evaluate the role of ^{18}F FDG-PET/CT in the staging and target definition for Rapidarc™ modulated radiotherapy (RA-IMRT) in cervical cancer patients. **Materials and Methods:** From June 2010 to March 2011 41 patients (pts) affected by locally advanced cervical cancer were treated with RA-IMRT: group I (22 pts) received only that treatment integrated with boost and group II (19 pts) received it as adjuvant setting after surgery. At the baseline all pts underwent contrast enhanced computed tomography (ceCT), pelvic magnetic resonance (MR) and ^{18}F FDG-PET/CT. ^{18}F FDG-PET/CT and CT were also used for gross tumour volume (GTV) definition. Simultaneous integrated boost (SIB) was provided according to the baseline imaging results. Fifty minutes after the injection of 3 MBq/Kg of ^{18}F FDG a total body ^{18}F FDG-PET/CT was performed, in fasting conditions, with PET/CT D600 (GE Healthcare) in 3D mode, 2 minutes/bed and 256x256 matrix. Immediately after total body imaging, a ^{18}F FDG-PET/CT dedicated scan centred on pelvic/lombo-aortic region with the same flat tabletop and immobilization of the CT simulation, was carried out. PET-GTV was contoured manually on PET images on Advantage Windows 4.4 (GE Healthcare) by an experienced nuclear medicine physician. **Results:** Comparing MR and CT evaluation to ^{18}F FDG-PET/CT scan, we pointed out that PET/CT modified the stage in group I in 4/22 (18.2%) and in group

II in 2/19 (10.5%) pts. In detail, positive lymph nodes in external iliac (1 pt, IIB to IIIB upstaging) and para-aortic (4 pts, III to IVB upstaging) regions and persistence of disease in the T area (1 pt) were detected. PET imaging also changed radiotherapy treatment planning in group I in 5/22 (22.7%) and in group II in 1/19 (10.5%) pts. Three pts received SIB in the positive ^{18}F FDG area (1 in iliac-external lymph node, 1 in the T area and 1 in para-aortic area), 4 pts (one with positive ^{18}F FDG-PET/CT in common lymph nodes and 3 with positive para-aortic lymph nodes) received RA-IMRT in the pelvis and para-aortic area. **Conclusions:** our data indicate that ^{18}F FDG-PET/CT well integrates with ceCT and MR in the staging of cervical cancer, modifying the stage in 18.2% (in group I) and in 10.5% (in group II) of pts. Moreover ^{18}F FDG-PET/CT helps the radiotherapist in a better definition of the target, showing lymph-node metastases in areas not usually included in radiotherapy planning.

P0736

A comparison of ^{123}I -meta iodobenzylguanidine scintigraphy and ^{18}F -fluorodeoxyglucose positron emission tomography/computed tomography scans in the assessment of response to molecular radiotherapy with ^{131}I -meta iodobenzylguanidine therapy in neuroblastoma

J. Gains, O. Almukhailed, J. Bomanji, M. Gaze; University college London Hospitals NHS Foundation Trust, LONDON, UNITED KINGDOM.

Introduction: ^{123}I -mIBG scintigraphy with semi-quantitative scoring is the standard imaging modality for staging and response evaluation in metastatic neuroblastoma. Its main disadvantage is limited spatial resolution. This study evaluates the use of ^{18}F fluorodeoxyglucose (FDG) positron emission tomography/computed tomography (PET/CT) imaging in addition to ^{123}I -meta iodobenzylguanidine (mIBG) scintigraphy for response assessment in patients with metastatic neuroblastoma treated with ^{131}I -mIBG molecular radiotherapy. It aims to establish whether ^{18}F -FDG-PET/CT gives additional information to ^{123}I -mIBG scintigraphy to enhance response evaluation in neuroblastoma. **Materials and Methods:** Fifteen patients with relapsed or refractory metastatic neuroblastoma underwent molecular radiotherapy with ^{131}I -mIBG combined with topotecan as a radiosensitiser. Two patients were treated twice with the regime. Both ^{123}I -mIBG and ^{18}F -FDG PET/CT scans were performed before treatment to define disease extent, and again afterwards to assess response. Imaging was performed within the same institution with standardised protocols. Response on ^{123}I -mIBG scans was evaluated by semi-quantitative scoring (SIOPEN method). ^{18}F -FDG PET/CT scans were evaluated by both a semi-quantitative method and PET Response Criteria in Solid Tumours (PERCIST). **Results:** Ten patients were male, and 5 female, with a median age of 5 years (range 1–18 years). Seventeen pairs of scans were reviewed. Post therapy scans were performed a median of 8 weeks after treatment. Two patients with progressive disease on ^{123}I -mIBG evaluation, also had progressive disease on ^{18}F -FDG-PET/CT. Of two patients with complete response on ^{123}I -mIBG imaging, one had a complete response and one a partial response on ^{18}F -FDG-PET/CT. Six reassessment ^{123}I -mIBG scans showed stable disease. Of these, two had complete response by both semi-quantitative scoring and PERCIST using ^{18}F -FDG-PET. Two showed stable disease by semi-quantitative scoring and PERCIST; and two showed stable disease by semi-quantitative scoring but partial metabolic response by PERCIST using ^{18}F -FDG-PET. Seven reassessment ^{123}I -mIBG scans showed partial response. Semi-quantitative ^{18}F -FDG-PET showed 2 complete and 4 partial responses and 1 minor response. PERCIST using ^{18}F -FDG-PET showed 2 complete and 4 partial metabolic responses and 1 stable metabolic disease. **Conclusions:** For patients with stable disease on ^{123}I -mIBG scintigraphy following ^{131}I -mIBG therapy, ^{18}F -FDG PET/CT gave supplementary information on response assessment. It is uncertain what the clinical significance of these changes on ^{18}F -FDG PET/CT are and further clinical evaluation is required.

P0737

Underestimation of SUV in FDG PET of large (>2 cm) necrotic tumors with a narrow rim of viable tissue: possibly clinical implication, e.g. for interim PET evaluation of lymphoma.

T. V. Bogsrud, A. Skretting; Oslo University Hospital, Oslo, NORWAY.

Background: Underestimation of SUV caused by limited spatial resolution is well recognized for PET of small tumors (<1.2 cm depending on the scanner model and reconstruction parameters). Underestimated SUV also results from PET of tumors >2 cm with central necrosis surrounded by a narrow peripheral rim with viable tissue. Such errors may possibly lead to incorrect risk stratification and suboptimal treatment. The reduction of contrast recovery (CR) can be conceived as an ‘intensity diffusion’ (commonly erroneously called “partial volume effect”) and mathematically described as a 3D-convolution of an ideal image distribution with an effective point-spread function (PSF). **Aim:** To quantify CR by a computer simulation of intensity diffusion in a mathematical tumor models with a photopenic central necrosis surrounded by a narrow peripheral rim with viable tissue. **Methods:** Spherical tumor models with central necrosis of different diameters (d) and thicknesses of the peripheral rim (rT) were mathematically constructed on a

200 x 200 x 200 voxel array with voxel size 0.5 x 0.5 x 0.5 mm. Values were set to 1.0 in voxels fully covered by the tumor rim and equal to the fraction of the voxel covered by the rim for partially covered voxels. Four different effective 3D PSFs determined by fitting measurements to Gaussians were used in the convolutions: one resulting from a PSF-based reconstruction (Siemens TrueX), and three from OSEM using different widths (FWHM=2, 3.5 and 5mm) of the post-reconstruction filters. **Results:** For a tumor with a central necrotic sphere of d=3.0 cm and rT=3 mm, CR varied from 0.40 to 0.28 between the narrowest and the widest effective PSF. When the rT was increased to 6 mm the corresponding numbers were 0.71 and 0.53, respectively. With increasing rT, CR got closer for the two most extreme PSF widths and approached unity (CR=1.0). When the thickness of the rim was reduced CR decreased and the difference between CR obtained with different filter increased. **Conclusion:** FDG PET/CT imaging of larger tumors with central necroses surrounded by a narrow rim of residual viable tissue is associated with a significant loss of contrast and thus with underestimation of SUV. In the case of a rim thickness of 3mm the apparent SUV may be reduced by a factor of 0.28 for the most commonly used filter. The phenomenon may be of clinical relevance, e.g. for interim PET evaluation of lymphoma applying Deauville scores.

P0738

Evaluation of the influence of respiratory motion misalignment between PET and CT data on diagnosis of heart defects using 4D XCAT phantom and STIR reconstruction

M. Sedighpoor¹, P. Ghafarian², A. Emami³, M. Ay⁴, ¹Department of Medical Physics and Biomedical Engineering and Research Center for Science and Technology in Medicine, Tehran University of Medical Sciences, Tehran, IRAN, ISLAMIC REPUBLIC OF, ²Telemedicine Research Center and Chronic Respiratory Disease Research Center, NRITLD, Masih Daneshvari Hospital, Shahid Beheshti University of Medical Sciences, Tehran, IRAN, ISLAMIC REPUBLIC OF, ³Research Institute for Nuclear Medicine, Tehran University of Medical Sciences, Tehran, IRAN, ISLAMIC REPUBLIC OF, ⁴Department of Medical Physics and Biomedical Engineering and Research Center for Science and Technology in Medicine and Research Institute for Nuclear Medicine, Tehran University of Medical Sciences, Tehran, IRAN, ISLAMIC REPUBLIC OF.

In recent years, PET/CT scanners have been found very applicable for clinical diagnosis of cardiovascular diseases. In such systems, CT images are used for attenuation correction of PET data. But it can lead to misalignment artifacts and make error up to 60% in the critical regions of diagnostic PET images. Misalignment Artifacts are particularly disconcerting in cardiac imaging because they can present themselves as perfusion abnormalities or erroneous information on myocardial viability. This study is an attempt to quantify the influence of respiratory motion as a misalignment artifact cause between CT and PET data on the diagnosis accuracy of heart disease in cardiac PET/CT imaging. **Material and methods:** The 4D Extended Cardiac Torso (XCAT) software phantom was used to simulate the respiratory and cardiac motion and heart defect with predefined parameters. Two sets of data were generated: emission maps and attenuation maps (μmap). The sinograms of emission maps were attenuated by the corresponding attenuation maps. Thereafter, attenuation correction of the attenuated sinograms was performed with the matched and mismatched attenuation maps. PET images were then reconstructed using the mentioned two sets of corrected sinograms with OSEM algorithm. All of these steps were performed in STIR software. Polar map and profile analyses were used for evaluating the effect of misalignment in cardiac imaging. Also our result evaluated by nuclear medicine physician. **Results:** Depending on size and location of the defect, the uptake of the heart changed between 2.5% to 60% in some areas of the heart. This issue was more significant in inferior and lateral cardiac wall. **Conclusion:** The magnitude of errors depends on the size and the location of the defect and also the motion amplitude. For smaller defects, misalignment is more significant and so compensation techniques seem to be necessary. Mismatched attenuation correction can be compensated by using respiratory-averaged CT as the attenuation map partly. We suggest that it is critical to correct the respiratory motion in clinical studies to improve the accuracy of diagnosis and treatment using PET/CT imaging

P0739

Implications of false-negative ¹⁸F-FDG PET in staging oesophageal cancer

B. Al Suqri, L. Wing, M. Halim, K. Balan, J. Buscombe, N. Carroll, R. Hardwick, H. Ford, R. Fitzgerald; Addenbrookes Hospital, Cambridge, UNITED KINGDOM.

Background and aim: Staging of oesophageal cancer requires accurate assessment of regional lymph nodes and detection of disease at distant sites. Integrated ¹⁸F-Fluorodeoxyglucose (¹⁸F-FDG)-positron emission tomography (PET)-CT (PET CT) has been recommended to improve the accuracy of M staging and select potential candidates for curative surgery. A retrospective study was undertaken to assess the accuracy of PET CT in the staging of patients with oesophageal cancer. **Method:** Three hundred and twenty seven consecutive patients with biopsy proven

carcinoma of the oesophagus had undergone PET CT imaging over a 5-year period from 2006 to 2011. PET CT reports were compared with CT, EUS and pathological staging. Note was made of the time between the PET CT and surgery. **Results:** Of 327 patients (239 Males, 88 females; mean age 66 years) 322 (98%) were confirmed to have malignancy on PET CT. However, no metabolically active malignancy was present in five (2%) patients (table) with biopsy proven gastro oesophageal junctional (GOJ) carcinoma and higher staging on CT and EUS. Three PET CT negative patients who had curative surgery within 3 months of PET CT were found to have malignancy with or without regional lymph node involvement on histological examination. Two patients with a normal PET CT and poorly differentiated adenocarcinoma of signet ring type on histology underwent palliative treatment.

Conclusion: Our results confirm the pivotal role played by ¹⁸F- FDG PET CT in the pre-treatment staging of oesophageal cancer. However, false-negativity / underestimation of the extent of disease by PET CT in a small but significant number of patients would mean that this imaging, while being considered as the first-line investigation of choice, should be appropriately complimented / supported by other investigations like CT, EUS and laparoscopy.

P0740

Semi-automatic extraction of image-derived input functions using Temporal Shape Driven Filter (TSDF) for improved quantification of whole body dynamic FLT-PET images

M. Tamal¹, I. Trigonis¹, L. Horsley¹, B. Taylor², P. Manoharan², A. Jackson¹, M. Asselin¹; ¹The University of Manchester, Manchester, UNITED KINGDOM, ²The Christie Hospital NHS Trust, Manchester, UNITED KINGDOM.

Introduction: For pharmacokinetic analysis of dynamic PET data, precise and accurate estimation of the input function is important since errors propagate to the estimated kinetic parameters. Generation of input functions using invasive arterial blood sampling can be obviated by extracting the time-activity curve (TAC) from blood pools in PET images. Manual delineation of blood pools using either CT or sum of early PET frames is subject to intra- and inter-observer variability and requires good knowledge of anatomy. Semi-automatic and automatic segmentation using principle and independent component analysis based methods are dependent on the number of components chosen and similarly, clustering methods generally require the number of clusters to be defined before applying the algorithm. **Methods:** A temporal shape driven filter (TSDF) is presented here that takes advantage of the different shape of the blood TAC compared to other tissues and accounts for variations in its shape across subjects. The TSDF method creates a contrast enhanced distance map (CEDM) that is the inverse of weighted distance, measured between the shape of the sample voxel TAC and the fitted TAC generated with the blood TAC model. The enhanced contrast in the CEDM image allows the aorta to be semi-automatically segmented and the blood TAC extracted. Dynamic FLT data were acquired on the TrueV PET-CT camera for 60 minutes in twelve cancer patients of which six with paired baseline scans and used for the validation of the new method. The image-derived blood TAC was corrected for blood partition and peripheral metabolism using five venous blood samples. The lesions were manually delineated on CT by an experienced radiologist. The kinetic data were fitted to a two-tissue compartment three-rate constant model with a variable fractional blood volume. **Results:** The TSDF method yields reproducible aortic volume (10%) and area under the curve (5%). The blood TACs have lower noise and bias (compared to venous blood samples) than those from manual delineation of the aorta on CT and its eroded version. The TSDF method is also robust to motion during dynamic PET acquisition. These improvements translate into better reproducibility of the influx constant, Ki compared to manual delineation (32% vs 39%) and similar reproducibility for the forward transport rate constant, K1 (28% vs 25%). **Conclusion:** The TSDF method allows the assessment of whether changes in FLT uptake measured after treatment are related to alterations in transport and/or tyrosine kinase activity with minimal invasiveness and user intervention.

P0741

Therapeutic and Prognostic Impact Value of FDG PET/CT in Newly Diagnosed Head and Neck Malignancy

R. de Juan¹, S. Ruiz¹, P. Sarandeses¹, A. Hernández¹, A. Ruiz², J. Estenoz¹; ¹12 Octubre University Hospital, Nuclear Medicine Department, Madrid, SPAIN, ²12 Octubre University Hospital, Radiotherapy Department, Madrid, SPAIN.

Purpose: To prospectively assess the additional clinical value of PET/CT in newly diagnosed head and neck (H&N) malignancy for simultaneous baseline staging and radiotherapy planning (RTP) in terms of therapeutic impact, treatment response and prognostic impact. **Methods and materials:** 26 patients were prospectively included from 2009 to 2011. (88 %) 23 m, (12 %) 3 f; age range 48-74 y.o., median 57. Anatomic location of primary tumour was: oropharynx (n=6) tongue (n=6) larynx (n=6) nasopharynx (n=5) hypopharynx (n=3) All cases underwent baseline

low CT dose contrast-enhanced PET/CT with specific RTP patient positioning. Imaging findings were visually and quantitatively assessed both for diagnosis and therapeutic intent with latter volume delineation. Following primary therapy, all cases underwent PET/CT to assess response and further subsequent PET/CT investigations for follow-up purposes, which were compared to clinical follow-up [6 to 24 months (median 9)]. Results: Overall 64 PET/CT investigations were performed. PET/CT based RTP simulation was performed median 3 (1–13) weeks after biopsy diagnosis. Most patients (19/27) % presented with advanced disease (T3 or T4). On end-point follow-up 19 patients presented complete response: 12 had clinical and 7 had pathology confirmation; 4 patients died, 2 progressed and 1 had uncertain response. All patients who presented end-point complete response had already shown complete response on end of primary therapy PET/CT imaging. All deceased patients presented with T4 advanced disease and SUVmax > 15 at baseline diagnosis and 3/4 deceased patients did not respond to primary therapy as identified on 2nd PET/CT follow-up performed 6 months after baseline imaging. Conclusions: PET/CT allows for simultaneous baseline clinical staging and RTP within a single investigation, stratifying therapeutic approach and intent by altering clinical decision-making, while being a metabolic prognostic factor. Moreover, PET/CT imaging reassessment at the end of primary therapy may have prognostic impact in discriminating end-point patient outcome.

P0742

Correlation between 18F FDG Uptake with Pathological Prognostic Factors in Breast Carcinoma

O. Ekmekcioglu¹, A. Aliyev¹, M. E. Erkan², Z. R. Kaya¹, A. Caliskan¹, B. Baskir³, S. Ilvan³, M. Halac¹, K. Sonmezoglu¹; ¹Istanbul University Cerrahpasa Medical Faculty, Nuclear Medicine Dept., Istanbul, TURKEY, ²Duzce University Medical Faculty, Nuclear Medicine Dept., Istanbul, TURKEY, ³Istanbul University Cerrahpasa Medical Faculty, Pathology Dept., Istanbul, TURKEY.

Purpose ¹⁸F FDG Positron emission tomography (PET) has been used as a non-invasive imaging modality for the staging and follow-up in breast carcinoma. Several studies have reported that FDG uptake is correlated with the behavioral pattern and the aggressiveness of the tumor in various cancers. The aim of our study was to determine whether there is a relationship between FDG uptake and histopathological prognostic factors in patients with breast carcinoma.

Material&Method Twenty-nine women (age range 26–78 with a mean 56 ± 12) with a diagnosis of breast carcinoma, who was treated by surgery and underwent FDG PET/CT scan before any treatment were included in this study. As indices of tumor FDG uptake, SUV_{max} value, lesion/liver ratio and lesion/lung ratio were calculated from primary tumor and axillary lymph node, when FDG positive. The correlations between the tumor indices and histopathological prognostic parameters including tumor grade, hormone receptor status, CerbB2 status, microscopic lymphatic invasion, perineural and vascular invasion were assessed in all patients. **Results** Twenty-six patients had invasive ductal carcinomas and the remaining 3 had mixt type (ductal plus lobular) carcinomas. In all patients, primary lesions demonstrated FDG uptake in which mean SUV_{max} values, mean lesion/liver ratios, and mean lesion/lung ratios were 8.5±4.9 (2.2–23.8), 2.68±1.52 (0.58–6.43), and 10.05±6.06 (1.57–26.44), respectively. There was histologically proven axillary lymph node metastasis in 23 patients, 20 of whom showed discernible FDG uptake and included for analysis. For axillary lymph nodes included in the analysis (in 20 patients with FDG positive nodes), mean SUV_{max} values, mean lesion/liver ratios, and mean lesion/lung ratios were 7.4±5.3 (1.5–21.6), 2.3±1.4 (0.39–4.88), and 8.7±5.8 (1.67–22.5), respectively. There was a weak correlation (r=0.34) between primary tumor SUV_{max} value and histologic grade. Otherwise no significant correlation was found between FDG uptake indices and other histopathological parameters of primary tumors as well as all pathological parameters of metastatic axillary lymph nodes. Furthermore, there was no significant difference of primary tumor SUV_{max} values between in group with axillary involvement and in that of without axillary metastasis (p=0.132). **Conclusion** We have found a weak correlation between primary tumor SUV_{max} and histologic grade of the primary tumor. There was no correlation between FDG uptake indices of either primary tumor or axillary lymph node and histopathological prognostic parameters.

P0743

Recovering Iterative Thresholding Method (RITHM) for semi-automatic segmentation of PET images: preliminary results for validation in clinical settings.

C. Basile¹, M. Pacilio¹, F. Botta², A. Monaco¹, R. Belliato³, R. Linciano¹, L. Mango¹, C. De Cicco¹, G. Paganelli², M. Cremonesi²; ¹San Camillo Forlanini Hospital, Rome, ITALY, ²Istituto Europeo di Oncologia, Milan, ITALY, ³TBS Group, Trieste, ITALY.

Aim - Various methods are proposed for PET-based volume delineation: adaptive thresholding, region growing, Markov random field models, artificial neural networks, and many others, but performance in clinical settings remains the most challenging issue. The RITHM algorithm, proposed by Pacilio et al. for SPECT images

(Med Phys 2011), has been implemented for two PET scanners at the Istituto Europeo di Oncologia (Basile et al EJNMMI 2011;38;Suppl2:S270). In this work, further validation results on test objects and preliminary results on clinical images are presented. **Materials and Methods** - The RITHM is an iterative thresholding-based method, based on threshold-volume calibrations (volume range: 0.3–16 mL) at different source-to-background ratios (SBR, range: 2–8), with further inclusion of Recovery Coefficients curves for improving the segmentation accuracy. The algorithm, coded using MATLAB (R2009b), has a new Graphical User Interface and is implemented for two different PET/CT systems: Discovery-ST and Discovery-D600 (GE Healthcare). Spherical test objects (volume range: 0.5–98 mL; SBR range: 4–55) positioned in the NEMA IEC phantom were imaged and examined to further validate the method. Subsequently, images of 15 patients were analysed to test the performance in clinical settings. The volumes of interest (secondary spleens, lymph nodes, and urinary bladders) were segmented on the CT images. The agreement between CT volumetric estimates and RITHM results on PET images was statistically analysed, using linear regression fit and Bland-Altman plots with ±95% confidence interval (CI). **Results** - The accuracy of volume determination for the test objects was within ±10% for most volumes in the range 1–98 mL, except for 1 mL test object with SBR of 55, for which the percent difference estimated/true volume reached about 25%. This was probably due to the high SBR value of the test object (55) with respect to the SBR range experienced for calibrations. In patients' images, a good correlation (R²=0.928) was obtained between volumes segmented on CT and PET images by RITHM. Moreover, no significant bias was evidenced by the slope of linear regression (slope=1.04). This was also confirmed by the Bland-Altman plot: differences were within the ±95% CI, and the mean difference (bias line) was about 1 mL (close to zero). **Conclusion** - The analysis of the test objects and the preliminary results on clinical images demonstrate the robustness and accuracy of the method. A wider variety of cases is under analysis to confirm these results and further investigate the potential of the method.

P0744

Low 18F-FDG Uptake In Pleural Effusion Indicates a Malignant Etiology

S. Chen, H. Fu, R. Zou, S. Wu, F. Fang, Z. Wu, H. Wang; Xinhua Hospital Affiliated to Shanghai Jiaotong University School of Medicine, Shanghai, CHINA.

Objectives: The diagnosis of malignant serous effusion adversely affects the staging and prognosis of oncologic patients and may alter the therapeutic approach. The goal of the study was to define an accurate diagnostic approach for differentiating benign from malignant pleural/peritoneal effusion on positron emission tomography-computed tomography (PET/CT). **Materials and Methods:** The study population comprised 87 consecutive patients with serous cavity fluid including 48 patients with malignant effusions and 39 patients with benign effusions on PET/CT scanning. PET parameters including average standardized uptake values of effusions (SUV_{eff}), SUV difference (SUV_{dif}) between mediastinal blood pool (SUV_{bp}) with SUV_{eff}, ratio of SUV_{dif} to SUV_{bp} (SUV_{rt}), and CT parameters such as amount and density of effusion (HU) and pleural/peritoneal abnormalities were assessed and compared to results of fluid cytology, serous histology and/or clinical follow-up for at least 10 months. Analysis of variance test and receiver operating curve were used in statistical analysis. P<0.05 was considered statistically significant. **Results:** In patients with pleural effusion (n=52), all of the PET and CT parameters were significant in differentiation between malignant and benign effusion. SUV_{rt} was found to be the most accurate parameter. With a cutoff of 0.33, SUV_{rt} was true positive in 22 and true negative in 23 patients, with an sensitivity, specificity, positive predictive value (PPV), negative predictive value (NPV), and accuracy of 81.5%, 92%, 91.7%, 82.1% and 86.5%, respectively. In patients with ascites (n=35), 18F-FDG uptake in the effusion alone was not significantly correlated with the etiology of the effusion. The most accurate and reliable parameter for diagnosis of malignant ascites was found to be peritoneal abnormalities, with sensitivity, specificity, PPV, NPV, and accuracy of 90.4%, 78.6%, 86.4%, 84.6%, 85.7%. **Conclusions** PET/CT is a highly accurate and reliable noninvasive test to differentiate malignant from benign effusion in patients with primary extrapleural/extraperitoneal tumor. Relative to high uptake in pleural effusion, a low 18F-FDG uptake is more suggestive of a malignant etiology, even if there is no finding of pleural abnormality.

P0745

Comparison of PET images obtained in the PET-CT scanner and gamma camera with the function of the coincidence

A. Wyszomirski¹, S. Cichocka², K. Wypychowska¹, T. Sobota¹, A. Budzyńska³, M. Dziągiewski⁴, R. Czepczyński⁵, J. Sowiński⁶, M. Ruchala⁶, M. Dziuk²; ¹Dept. of PET/CT, Euromedic, Poznań, POLAND, ²Department of Computer Physics, Physics Department, Adam Mickiewicz University, Poznań, POLAND, ³Nuclear Medicine Dept. Military Institute of Medicine, Warsaw, POLAND, ⁴GE Healthcare, Warsaw, POLAND, ⁵Poznań University of Medical Sciences, Poznań, POLAND, ⁶Dept. of Endocrinology, Poznań University of Medical Sciences, Poznań, POLAND.

Introduction PET studies are usually performed on a dedicated PET-CT scanners. In some institutions, until recently, such studies were also performed on gamma cameras with the function of coincidence. [1,2] **Aim** Comparison of PET images obtained in the PET-CT scanner and gamma camera with the function of the coincidence was the aim of this study. **Materials and methods** PET-CT examination of water phantom NEMA IEC Body Phantom was done on the two devices: the PET-CT scanner Discovery STE and gamma camera Infinia VCHWK4 with the coincidence system. The phantom was prepared in accordance with the guidelines of NEMA NU 2007. This test allows to evaluate the image quality of PET examinations. The phantom simulates the cancer tissue (hot sphere) and healthy tissue (cold sphere). A comparison of the following parameters: total number of counts, the size of individual structures and semi-quantitative SUV parameter, characterizing the metabolism of FDG in the tissue was performed. The total number of counts for the regions of interest (spheres, background, and the whole phantom) were read on the NEMA phantom images. **Results** The total number of counts registered by the gammacamera with the function of the coincidence was lower than the number of counts registered by the PET-CT scanner. The analysis of ROI's diameter (sphere) in images obtained on both devices showed that the mean diameters are not comparable for the smallest hot sphere and cold areas. The values of spheres' diameters in the image received in gamma camera were significantly different from the diameters given by the manufacturer of the phantom. Diameters of hot spheres bigger than 13 mm were comparable for both devices. **Conclusions** Gamma cameras acquire lower number of coincidence photons than PET-CT scanner. A blur of structures' contours is observed in images obtained with a gamma camera. PET-CT scanner accurately detects and locates hot and cold spots.

P0746

Establishing a threshold SUVmax value on 18FDG-PET/CT for identifying metastatic lymph nodes in surgically resectable Non Small Cell Lung Cancer.

K. Boulougouri¹, I. Zerizer², N. DeSouza¹, I. Hunt³, C. Tan³, S. Chua², M. O'Brien², B. Sharma², ¹ICR/ RMH, London, UNITED KINGDOM, ²RMH, London, UNITED KINGDOM, ³St George's Hospital, London, UNITED KINGDOM.

Aim: To improve staging of NSCLC on ¹⁸FDG-PET/CT in patients considered for radical surgery by establishing a threshold SUV_{max} indicative of metastatic involvement of mediastinal lymph nodes (MLN). **Methods:** 56 eligible patients treated with radical surgery underwent ¹⁸FDG-PET/CT examinations between January 2010 and October 2011 using a Philips Gemini dual scanner. Images were reviewed retrospectively by two observers to measure SUV values of surgically sampled MLN visually assessed on a Hermes workstation (Hybrid1.1viewer). Receivers Operating Characteristic (ROC) analysis was applied to MLN with SUV_{max} higher than Blood Pool, (52/56 pts, n=104), to determine an optimal cut-off value indicative of metastatic involvement. Sensitivity and Specificity of visual assessment based on ¹⁸FDG-PET/CT reports of expert observers (n=6) was also performed. Bland-Altman plots were used to determine interobserver agreement. **Results:** A total of 132 MLN were surgically staged according to the 7th Edition TNM in Lung Cancer of the International Association for the Study of Lung Cancer (IASLC) Staging Committee (2009). A total of 104 lymphnodes in 52 patients were evaluated. 6 of these MLN were histologically verified as malignant, (median SUV_{max}:4.35, range 1.38-5.16) and 98 were not involved, (median SUV_{max}: 2.475, range 1.38-4.81). Area under the curve (AUC) was 0.927(p<0.01) for MLNSUV_{max}. A SUV_{max} threshold of 3.45 gave a sensitivity of 80%, specificity of 91.7% for identifying metastatic MLN. Bland Altman analysis demonstrated low interobserver variability. Visual assessment alone had 50% sensitivity and 94.9% specificity. **Conclusion:** The use of SUV_{max} threshold of 3.45 yielded high sensitivity and specificity for identifying MLN metastases, although sensitivity is relatively low in this select group of early stage NSCLC.

P0747

Imaging of Metastatic-Recurrent Paragangliomas and Pheochromocytomas with Ga-68 DOTATATE PET/CT

E. Demirci¹, M. Ocak², N. Yeyin¹, S. Asa¹, A. Aygun¹, M. Halac¹, L. Kabasakal¹, B. Kanmaz¹; ¹Department of Nuclear Medicine, Cerrahpasa Medical Faculty, Istanbul University, Istanbul, TURKEY, ²Department of Pharmaceutical Technology, Pharmacy Faculty, Istanbul University, Istanbul, TURKEY.

Introduction: Pheochromocytomas (Pheo) and extra-adrenal paragangliomas (PGL) are rare tumors arising from neural crest. Approximately %10-20 of PGL/PHEO are malignant. The only reliable criterion for malignancy is presence of metastasis. Currently I-123 MIBG is the most important nuclear medicine technique to detect metastatic lesions. However 73% of Pheo and 93% of PGL express somatostatin receptors and Ga-68 DOTATATE PET/CT may have a role in metastatic PHEO/PGLs for determination of extent of disease in MIBG negative tumors and for evaluation as candidates of peptide radionuclide therapy. **Aim:** The aim of the study was to evaluate the current role of 68Ga-DOTA-TATE PET/CT in the detection and follow-

up of patients with metastatic PGL and Pheo. **Materials and Methods:** Thirteen patients (F/M: 9/4, mean age 41,38± 13,33) who were referred to our department for Ga-68 DOTATATE PET/CT for diagnosis of recurrences and for staging were retrospectively evaluated. There were 7 patients with PGL and 6 patients with Pheo. All patients were injected 88-214 MBq 68Ga-DOTA-TATE (mean 170,2 ± 42,18 MBq). Whole body PET/CT images were acquired for 30-60 min. All images were evaluated visually and also SUVmax values were calculated for semiquantitative evaluation. CT and MRI results were also evaluated whenever available. **Results:** Pathological uptake of 68Ga-DOTA-TATE was seen in 12/13 patients. In one patient there was a discordant result, which was positive in MRI but negative in Ga68-DOTA-TATE PET imaging. Five patients had metastases to bone, 7 patients had metastases to lymph nodes and 2 patients had lung metastases. We observed abdominal lesions in 4 patients, cervical lesion in 1 patient and cranial lesion in 1 patient. Highest SUVmax values were ranged from 8,7 to 93,4 mean 47,2± 19,7. **Conclusion:** Conventional imaging is usually limited to the site where a paraganglioma is clinically suspected. Ga-68 DOTATATE PET/CT could provide additional information on evaluation of the recurrences for the determining the extent of the disease as an alternative diagnostic procedure. It can be used for selection of patient for possible of application for PRRT.

P0748

SPECT-CT Contribution in Assessing Osteochondral Lesions in the Astragalus Correlation of RMI, Preliminary Study

A. Gomez, I. Rodriguez, B. Rodriguez, J. Mucientes, A. Gonzalez, J. Huertas, M. Beresova, I. Castejon; Hospital Universitario Puerta De Hierro Majadahonda, MADRID, SPAIN.

AIM: The osteochondral lesion in the dome of the talus is one of the most frequent treatable causes of chronic inexplicable pain. SPECT-CT, whose impact in the treatment of this kind of lesion is not well known, can supply additional information to the MRI findings. The objective of the present research is to assess the utility of SPECT-CT in detecting and localizing osteochondral lesions in the talr dome analyzing the additional information to the MRI findings and its impact in the taking of therapeutic decisions. **MATERIALS AND METHODS:** From October 2011 to January 2012 we conducted three-phase scintigraphy Tc99m-DPD/MPD and SPET-CT studies to 10 patients with osteochondral talar dome lesion in the MRI. We analysed the matching between the focal uptake and degree of osteochondral lesion, its exact location and the correlation in the MRI image of the additional findings of SPECT-CT. We consulted to the responsible physician about the influence of SPECT-CT in the diagnosis and management (surgical / conservative). **RESULTS:** In 2 cases (20%) we found no osteoblastic activity in the osteochondral lesion on MRI (although we did find it on TC) suggesting conservative treatment. In 6 cases (60%) we observed multiple or isolated uptakes in a location other than that of the osteochondral lesion of the MRI (2 no osteoblastic activity with deposit at another location, 1 reflex sympathetic dystrophy, 2 patients with a similar lesion in contralateral ankle, 1 more intense uptake in 1 tibio-peroneo-astragalus joint) supporting a conservative attitude of the lesion, suggesting a different origin of the cause of the pain. In the 3 cases in which surgery was indicated, the scintigraphy with SPECT-CT showed inflammation and osteoblastic activity coincident with the MRI. **CONCLUSION:** SPECT-CT provides additional useful information to MRI, suggesting other possible causes of pain and helping to decide a conservative management when the osteochondral lesion of the talus shows no osteoblastic activity.

P0749

Metal artifact reduction in 18F-fluoride-PET/CT data of prosthetic hip patients

A. Karlberg, J. Sörensen, G. Ullmark, L. Lindsjö, T. Nyberg, M. Lubberink; Uppsala University Hospital, Uppsala, SWEDEN.

Aim: Under- and over estimation of activity concentration may occur due to artifacts from dense materials, such as metallic implants, in PET/CT images using low-dose CT for attenuation correction. For diagnostic evaluation of bone activity around hip prostheses in ¹⁸F-fluoride-PET patients the accuracy of the attenuation correction algorithm is of major importance to get reliable SUV values in bone tissue adjacent to the implant. The aim of the present work was to validate a metal artifact reduction (MAR) algorithm for low-dose CT images by comparison of PET/CT to dedicated PET images, attenuation-corrected using a ⁶⁸Ge-transmission scan, in patients with hip implants. **Materials and methods:** Five prosthetic hip patients were examined with ¹⁸F-fluoride-PET in a Discovery ST PET/CT using low dose CT for attenuation correction, immediately followed by a second scan in a dedicated PET scanner (ECAT Exact HR+) using a transmission scan with rotating ⁶⁸Ge rods for attenuation correction. The dedicated PET image was considered as reference. A virtual sinogram method was used to achieve MAR CT data for attenuation correction in PET images. Here, low dose CT data is forward projected into sinogram space. Projection bins affected by metallic objects are segmented from the sinogram and replaced with interpolated values from surrounding bins using cubic spline interpolation. Corrected low dose CT data is then produced by

back projection and used for attenuation correction of PET data. Spherical volumes of interest (VOIs) were drawn over and adjacent to implants in dedicated PET, uncorrected PET/CT and MAR-corrected PET/CT images. SUV_{max} values were compared. **Results:** Mean relative differences in SUV_{max} values between dedicated PET and PET/CT images in a VOI over the femoral collum area decreased from 22.1% (SD 10.2) to 5.6% (SD 3.7) after MAR. MAR did not affect SUV_{max} values over normal bone tissue and soft tissue outside the artifact area. **Conclusion:** Metal artifact reduction in low-dose CT images improved the quantitative accuracy of PET images in areas affected by the metallic implant. Further comparison with transmission based attenuation correction in a larger patient group is needed to confirm these results. Metal artifact reduction will then allow for quantitative ^{18}F -fluoride PET/CT imaging in patients with hip prostheses.

P0750

Follow-up of bone metastatic breast cancer patients treated by hormonal therapy : how to interpret 18F-FDG PET-CT ?

S. Hassler; Centre Paul Strauss, Strasbourg, FRANCE.

PET-CT with FDG could be useful in metastatic breast carcinoma patients, who are treated by hormonal therapy, in order to assess therapeutic response and to detect therapeutic escape, and so progressive disease. As well as modify general treatment, an early diagnosis of therapeutic failure is essential for local treatment. Whereas new metastatic lesion signs progressive disease, there are quite assessment criteria about increase of standardized uptake value to define progressive disease in pre-existent lesion. We have retrospectively included 7 patients with bone metastases of breast cancer and treated by the same hormonal therapy at time of successive follow-up PET-CT. Maximal SUV (SUV_{max}) have been measured for each metastatic bone lesion. The analysis was about 3 to 8 PET-CT during 13 to 44 months. If new lesion, definitely metastatic, in bone or another organ, was seen in PET-CT, the patient was considered as progressive. For others patients, clinical findings, including biologic markers, and follow-up, were used to classify patient as progressive or non progressive. PET/CT with FDG have detected 32 bone metastatic lesions in all. We have only considered lesions with increase SUV_{max} during follow-up. Seven of these bone metastases, that were previously gone down by treatment (that is to say without FDG accumulation discriminate from noise), have become discriminate from noise during follow-up. All these patients have been considered as progressive. Fourteen of bone metastases, have kept a FDG accumulation discriminate from noise despite treatment and have shown an increase SUV_{max} during follow-up. Twelve of these 14 lesions were considered as progressive. The SUV_{max} increase was up to 15%, but 9/12 lesions have a SUV_{max} increase up to 30%. Two of these 14 lesions, with a SUV_{max} increase of 14 and 30%, were considered as non progressive. These preliminary results reveal that apparition of FDG uptake (discriminate from noise) in bone metastatic lesion previously completely gone down by hormonal therapy, is highly correlated with progressive disease. It seems too that a SUV_{max} increase of more than 30% predicts a progressive disease.

P21-2 - Tuesday, October 30, 2012, 16:00 - 16:30, Poster Exhibition Area

Molecular & Multimodal Imaging: SPECT & SPECT/CT

P0751

Comparison of right-sided cardiac function measured by tomographic radionuclide ventriculography and cine MRI

O. Arkhipova, T. Martynuk, L. Samoilenko, M. Shariya, V. Mazaev, O. Stukalova, V. Sergienko, I. Chazova; Russian Cardiology Research-and-Production Complex, Moscow, RUSSIAN FEDERATION.

Aim: To compare volumes and ejection fraction of right ventricle using gated blood-pool SPECT and cine MRI in the patients with idiopathic pulmonary hypertension (IPAH). **Methods:** The study included 6 pts with IPAH: 5 f/1 m, mean age 38.0±10.5 yrs, mean disease duration 2.5 (1.3-6) yrs, mean 6-minute walking distances 385±56.3 m, WHO FC II-III. Total ratio of FC II-III was 50 %/50 %. All the patients were underwent gated blood-pool SPECT (gbp-SPECT). Imaging studies were performed according to standard protocols using gamma-camera 20 min after in vivo RBC labeling with 740 MBq ^{99m}Tc . All participants had breath-hold cine MRI performed according to standard protocol. **Results:** End Systolic and Diastolic Volumes (ESV and EDV), Stroke Volume (SV), Ejection Fraction (EF) of Right Ventricles (LV and RV comparison after application gbp-SPECT and MRT. Results had no significant differences. Results are presented in the table below as Me [25 %-75 %]. **Conclusions:** Preliminary results showed that the gbp-SPECT may be used for the noninvasive assessment of right-sided cardiac function in patients with IPAH. However further researches are necessary.

P0752

Quantification of the influence of misregistration between CT and SPECT images on the accuracy of CT-based attenuation correction of cardiac images in hybrid SPECT/CT systems

I. Saleki¹, A. Bitarafan-Rajabi², N. Yaghobi³, B. Falahi⁴, M. Ay⁵; ¹Department of Medical Physics and Biomedical Engineering and Research Center for Science and Technology in Medicine, Tehran University of Medical Sciences, tehran, IRAN, ISLAMIC REPUBLIC OF, ²Department of Nuclear Medicine and Rajaie Cardiovascular Medical and Research Center and Cardiovascular interventional research center, tehran University of Medical Sciences, tehran, IRAN, ISLAMIC REPUBLIC OF, ³Rajaie Cardiovascular Medical and Research Center, Tehran University of Medical Sciences, tehran, IRAN, ISLAMIC REPUBLIC OF, ⁴Research Institute for Nuclear Medicine, Tehran University of Medical Sciences, tehran, IRAN, ISLAMIC REPUBLIC OF, ⁵Department of Medical Physics and Biomedical Engineering and Research Center for Science and Technology in Medicine and Research Institute for Nuclear Medicine, Tehran University of Medical Sciences, tehran, IRAN, ISLAMIC REPUBLIC OF.

Integration of single photon emission computed tomography (SPECT) and computed tomography (CT) scanners into SPECT/CT hybrid systems, permit the acquisition of SPECT and CT data in a single patient study. Combining of acquisitions have a potential for misregistration of emission and transmission scans because CT and SPECT images are obtained sequentially. The present study aimed at quantifying the influence of misregistration on the accuracy of CT-based attenuation correction of cardiac images. **Methods:** The study carried out with patients underwent two days protocol stress-rest ECG gated myocardial perfusion SPECT with ^{99m}Tc -MIBI. Polar maps were divided into Seventeen segments for data analysis registration of the X-ray CT and SPECT images was done with Reregistration Quality Control software. To determinethe relative influence of misregistration, the CT images was shifted by ± 1 , ± 2 , ± 3 pixels in the X, Y, Z -axes (left/right, dorsal/ventral, cephalad/caudad) and differences between attenuation-corrected images before and after reregistration were for each shifting compared. Statistically P values < 0.05 were considered to determine the regions significantly were affected by shifting the CT image. The effect of manual registration with the Registration Quality Control software was evaluated by comparing of automatic processing results with manual registered results. **Result:** Influence of misregistration is non-uniform on each region of myocardial perfusion images. Regional radiotracer uptake was difference with shifting in the X, Y, Z -axes. A 3-pixel shift in x-axes caused most changes on polar map scoring (78.33%±4.51% change to 66%±8.48% in Mid Anterior region). In 6.2% cases, polar map scoring was unchanged. Quantitative analysis revealed an increase of the relative uptake after manual misregistration. Most changes occurred in basal inferolateral (-5.00%±1.41%) and mid inferolateral (-9.00%±8.48%) regions. **Conclusion:** Misalignment in the X, Y, Z-direction between SPECT and the CT data might lead to artifacts in the most regions. Performing of the manual registration with software can be useful in the correction of misregistration error. It is necessary for diagnostic accuracy of attenuation correction cardiac SPECT images to perform a manual realignment routinely for each patient.

P0753

Interobserver Variability of SPECT/CT, MRI, CT, Bone Scan and Plain Radiographs in Patients with Unspecific Wrist Pain

M. W. Huellner¹, M. Pérez-Lago¹, K. Strobel¹, B. Seifert², U. von Wartburg³, P. Veit-Haibach¹; ¹Department of Radiology and Nuclear Medicine, Lucerne Cantonal Hospital, Lucerne, SWITZERLAND, ²Division of Biostatistics, Institute for Social and Preventive Medicine, University of Zurich, Zurich, SWITZERLAND, ³Department of Hand and Plastic Surgery, Lucerne Cantonal Hospital, Lucerne, SWITZERLAND.

Materials and Methods: Thirty-two patients (median age 38 years, range 18 to 73 years; 19 female, 13 male) with unspecific pain of the hand or wrist were evaluated retrospectively. The diagnosis of unspecific wrist pain was made by the referring hand surgeon based on patient history, clinical examination, plain radiographs and clinical guidelines. All patients were imaged by plain radiographs, planar early-phase imaging (bone scan) and late-phase SPECT/CT imaging including high-resolution CT, and MRI. Two experienced readers analyzed the images based on a standardized read-out protocol. The interobserver variabilities were determined for detecting the relevant lesion, its location and type and etiology of the underlying pathology. Kappa values of the two readers for all analyzed imaging characteristics were calculated. The diagnostic accuracy of each modality was calculated according to the standard of reference (complete clinical examination and imaging) and a mean follow-up of 20 months. **Results:** Accuracy of plain radiographs, bone scan and CT was generally poor for both readers, but there was partly good agreement on lesion detection (plain radiographs 0.73, CT 0.87) and location (plain radiographs 0.69, bone scan 0.63, CT 0.87), and type of pathology (CT 0.74). The other modalities with higher diagnostic accuracy yielded generally high agreement, with SPECT/CT showing mostly superior results (lesion detection: SPECT/CT 0.93, MRI 0.72; lesion localisation: SPECT/CT 0.91, MRI 0.75; etiology of

pathology: SPECT/CT 0.85, MRI 0.74), while MRI yielded better results concerning determination of the type of the underlying pathology (MRI 0.75, SPECT/CT 0.69). **Conclusion:** SPECT/CT yields higher interobserver agreement than all other imaging modalities in all evaluation criteria except determination of lesion type. SPECT/CT may be a reliable diagnostic tool with consistent image reading in patients with unspecific pain of the wrist.

P0755

IV contrast-enhanced CT can be used for attenuation correction in clinical 111-In octreotide SPECT/CT

T. L. Klausen, F. L. Andersen, J. Mortensen, T. Beyer, L. Højgaard; Department of Clinical Physiology, Nuclear Medicine and PET, University Hospital Rigshospitalet, Copenhagen, DENMARK.

Aim: To assess the effect of CT contrast-enhancement (ceCT) on SPECT image quality and quantification following CT-based attenuation correction (CT-AC) using phantom and patient studies. **Methods:** A 20cm cylinder phantom (5.15L) was filled with In-111 in aqueous solution (20kBq/mL). Three scans were performed: (A) no IV contrast in the solution, (B) with 100mL IV contrast (Optiray, 350mg/mL iodine) and (C) with 200mL IV contrast added. Our clinical SPECT/CT (Philips Precedence-16) protocol included a to-pogram, a low-dose CT (140kVp, 38mA), a 'diagnostic' CT (120kVp, 469mA) and a single-bed SPECT emission scan (128 projections, scan time 1320s). 5 patients referred for octreotide scintigraphy were scanned using the clinical SPECT/CT protocol above with the 'diagnostic' CT being performed in arterial and venous phase following mono-phasic IV injection of 125mL Optiray (4.5mL/s). All SPECT data were reconstructed iteratively using the Astonish algorithm: 4 iter/8 sub following CT-AC using the low-dose and 'diagnostic' CT images. We report the average ROI value of a 10cm central circle placed on 11 central image planes. Patient images with low-dose CT and 'diagnostic' ceCT were examined for artifacts and quality (score 0-2). Reference circle ROIs were placed on healthy liver tissue. **Results:** Phantoms: In uncorrected emission data mean count density decreased with increasing IV concentration: (A) 181 ± 14 , (B) 173 ± 12 and (C) 167 ± 12 . After CT-AC using low-dose CT data the mean activity concentration increased by 2.1% (B) and 3.1% (C) when compared to no IV contrast in the phantom (A). When performing CT-AC with 'diagnostic' CT the mean activity concentration decreased slightly: -3.7% (A), -3.3% (B) and -2.7% (C) compared to low-dose CT. Patients: There were no visible artifacts in SPECT following CT-AC with ceCT. The average score of image quality was 2.0 ± 0.0 for both low-dose and 'diagnostic' ceCT. Across all 5 patients, reconstructed counts in the liver were reduced by (10±7%) when CT-AC was based on 'diagnostic' ceCT (arterial phase) compared to low-dose CT, possibly caused by the difference in kVp-levels. Using the same kVp level, the reconstructed counts in the liver following CT-AC with 'diagnostic' ceCT was (1.6±0.5)% higher in the venous than the in the arterial phase. **Conclusion:** In SPECT/CT imaging of phantoms and octreotide patients the use of IV CT contrast did neither degrade SPECT image quality nor the reconstructed counts significantly following CT-AC based on the ceCT images. Thus, no separate low-dose CT is required for CT-AC in SPECT/CT in these patients.

P0756

SPECT-CT Contribution in Assessing Osteochondral Lesions of the Talus Detected by RMI, Preliminary Study

A. Gomez-Grande, B. Rodriguez, I. Rodriguez, J. Mucientes, A. Gonzalez, T. Morales, J. Huertas, M. Beresova, I. Castejon; Hospital Universitario Puerta de Hierro, Majadahonda, Madrid, SPAIN.

AIM: The osteochondral lesion in the dome of the talus is one of the most frequent treatable causes of chronic inexplicable pain. SPECT-CT, whose impact in the treatment of this kind of lesion is not well known, can supply additional information to the MRI findings. The objective of the present research is to assess the utility of SPECT-CT in detecting and localizing osteochondral lesions in the talus dome analyzing the additional information to the MRI findings and its impact in the taking of therapeutic decisions. **MATERIALS AND METHODS:** From October 2011 to January 2012 we conducted three-phase scintigraphy Tc99m-DPD/MPD and SPECT-CT studies to 10 patients with osteochondral talus dome lesion in the MRI. We analysed the matching between the focal uptake and degree of osteochondral lesion, its exact location and the correlation in the MRI image of the additional findings of SPECT-CT. We consulted to the responsible physician about the influence of SPECT-CT in the diagnosis and management (surgical / conservative). **RESULTS:** In 2 cases (20%) we found no osteoblastic activity in the osteochondral lesion on MRI (although we did find it on TC) suggesting conservative treatment. In 6 cases (60%) we observed multiple or isolated uptakes in a location other than that of the osteochondral lesion of the MRI (2 no osteoblastic activity with deposit at another location, 1 reflex sympathetic dystrophy, 2 patients with a similar lesion in contralateral ankle, 1 more intense uptake in 1 tibio-peroneo-astragalus joint) supporting a conservative attitude of the lesion, suggesting a different origin of the cause of the pain. In the 3 cases in which surgery was indicated, the scintigraphy with SPECT-CT showed inflammation and osteoblastic activity coincident with the MRI. **CONCLUSION:** SPECT-CT provides additional useful information to MRI,

suggesting other possible causes of pain and helping to decide a conservative management when the osteochondral lesion of the talus shows no osteoblastic activity.

P23-2 - Tuesday, October 30, 2012, 16:00 - 16:30, Poster Exhibition Area

Molecular & Multimodal Imaging: Biology

P0757

Target affinity improvement of a PDGFRβ binding peptide through peptide array analysis

A. Marr¹, F. Nissen¹, A. Altmann¹, U. Haberkorn¹, J. Debus², V. Askoxylakis²; ¹Department of Nuclear Medicine, University Hospital Heidelberg, INF 400, Heidelberg, GERMANY, ²Department of Radiation Therapy, University Hospital Heidelberg, INF 400, Heidelberg, GERMANY.

Introduction Peptide arrays are a powerful method to identify peptide motifs that mediate protein-peptide interactions. This work focuses on the linear peptide PDGFR-P1 binding to the extracellular domain of PDGFRβ. Randomizing the whole peptide by amino acid exchange and additionally spotting of shortened versions of the original peptide should give information about the binding region and improve the affinity of PDGFR-P1 to its target. **Methods** A peptide array was constructed by spotting of truncated versions of the original peptide PDGFR-P1 and through randomizing the complete original peptide sequence by replacing every amino acid of the original peptide by all 20 naturally occurring amino acids. The peptide array was incubated with the target protein and evaluated with a target specific antibody. Results were validated in cell assays. Therefore peptides with different target affinity were radiolabeled with ¹²⁵I and characterized further in kinetic and competition experiments in comparison to the original peptide on human pancreatic BxPC-3 cells, known to overexpress the target. Stability studies were carried out in human serum to investigate half life *in vivo*. **Results** The pattern of the array showed that amino acids 1-4 are not important for binding to PDGFRβ, amino acid positions 5, 6 and 12 are tentatively crucial and amino acids 7 to 11 are indispensable. The spot G2 with a change from serine to arginine in position 7 of the original peptide was found to be the most prominent one and therefore used for further studies. *In vitro*, G2 showed a binding of 45 % binding/ [applied dose/ 1 mio. cells] to BxPC-3 cells compared to 12 % of the original peptide. Competition assay demonstrated an inhibition of radiolabeled peptide with cold peptide up to 96 %. Amino acid exchange also improved serum stability of yG2 in comparison to the original peptide from 5 to 120 minutes. **Conclusion** Using a peptide array the original peptide could be improved by amino acid exchange in position 7 from serine to arginine. The found peptide, G2, showed a significantly higher affinity to the target protein compared to the original peptide PDGFR-P1 and an increased half life.

P0758

Synthesis and evaluation of thioflavin-T analogues as amyloid imaging agents

S. Jung¹, J. Park¹, S. Kim², S. Yang¹, M. Hur¹, K. Yu³; ¹Korea Atomic Energy Research Institute, Jeongseup, KOREA, REPUBLIC OF, ²Department of Nano Material Chemistry, Dongguk University, Gyeongju, KOREA, REPUBLIC OF, ³Department of Chemistry, Dongguk University, Seoul, KOREA, REPUBLIC OF.

Aim: Alzheimer's disease (AD) is the most common form of dementia, and involves the accumulation of amyloid plaques. Amyloid beta (Aβ) is the main component of amyloid plaques, and thioflavin-T (ThT) is widely used to visualize and quantify the presence of Aβ. In this study, we synthesized the ThT analogues for the detection of Aβ40 fibrils *in vitro*. **Materials & Methods:** 2-(2'-Methoxy-4'-aminophenyl)benzoxazole (1) was synthesized through a condensation of 2-aminophenol and 4-amino-2-methoxybenzoic acid at 200°C in polyphosphoric acid. 2-(2'-Methoxy-4'-methylaminophenyl)benzoxazole (2) was monomethylated using the deprotonating agent, sodium methoxide; paraformaldehyde; and the reducing agent, sodium borohydride in methanol. 2-(2'-Methoxy-4'-dimethylaminophenyl)benzoxazole (3) was synthesized starting from compound 1, which was followed by dimethylation using methyl iodide and potassium carbonate. 2-(2'-Methoxy-4'-aminophenyl)benzothiazole (4) was the prepared conjugation of 2-aminothiophenol and 4-amino-2-methoxybenzoic acid in phosphorus oxychloride. 2-(2'-Methoxy-4'-methylaminophenyl)benzothiazole (5) was monomethylated using the deprotonating agent, sodium methoxide; paraformaldehyde; and the reducing agent, sodium borohydride in methanol. 2-(2'-Methoxy-4'-dimethylaminophenyl)benzothiazole (6) was synthesized starting from compound 4, which was followed by dimethylation using formaldehyde in the presence of sulfuric acid and powdered iron. **Results:** The synthesized 6 ThT analogues were tested with synthetic Aβ40 aggregates for their fluorescence response. Among the 6 tested compounds, compound 2 has two critical requirements for a fluorescence imaging probe; high fluorescence responsiveness

and strong binding affinity. **Conclusion:** Compound **2** demonstrated its excellent capability of imaging A β fibrils in AD mouse brain with good colocalization with ThT. Based on their delicately high binding affinity to A β 40 aggregates, this novel ThT analogue can be a good alternative candidate for a fluorescence imaging agent to study AD.

P0759

Antiproliferative effects of proteasome inhibition in rat Morris hepatoma

A. Altmann¹, A. Markert¹, T. Schoening², V. Askoxylakis³, M. Eisenhut⁴, U. Haberkorn¹; ¹Dept. of Nuclear Medicine, Heidelberg, GERMANY, ²Dept. of Pharmacy, Heidelberg, GERMANY, ³Dept. of Radiooncology, Heidelberg, GERMANY, ⁴Dept. of Radiopharmaceutical Chemistry, Heidelberg, GERMANY.

Aim: As a major component for the degradation of proteins involved in cell survival, proliferation and regulation of apoptosis and transcription, the ubiquitin/proteasome pathway has been identified as a potential molecular target for cancer therapy. Proteasome inhibitors have been shown to interfere with key steps of tumor cell regulation leading to inhibition of proliferation and death of neoplastic cells both *in vitro* and *in vivo*. Accordingly, the proteasome inhibitor Bortezomib provides strong antiproliferative effects in a variety of hematological and solid cancer cells and has marked clinical activity even in the setting of relapsed refractory multiple myeloma (MM). Here, we investigated the effect of a concentration range of Bortezomib on rat Morris hepatoma (MH3924A) cells *in vitro* and *in vivo*. **Methods:** MH3924A cells were exposed to different concentrations of Bortezomib (1nM–1 μ M) for 12, 24 or 48 hours. The effect on proliferation and metabolism was analyzed by uptake experiments employing ³H-thymidine (TdR), ³H-FDG, ¹⁴C-aminoisobutyric acid (AIB) and 3-O-Methyl-D-(³H)glucose. Using the Step one plus Real-time quantitative PCR (qPCR) system we quantified p21^{CIP/WAF1} transcription. Apoptosis measurement and the cell cycle analysis were performed by the Annexin V/Propidium Iodide Assay and FACS analysis. FDG metabolism was investigated in ACI rats bearing MH3924A tumors prior and 1 day after Bortezomib therapy employing PET and ¹⁸F-fluorodeoxyglucose (¹⁸FDG). **Results:** Bortezomib induced a dose-dependent reduction of proliferation in MH3924A cells with an increase of the apoptotic cell fraction. Furthermore, MH3924A cells exposed to 100nM Bortezomib for 12h and 24h accumulated in the G₂/M phase of the cell cycle. The cell cycle arrest was associated with increased p21^{CIP/WAF1} expression. Studies concerning metabolic changes revealed a significant dose-dependent decrease of the AIB uptake after Bortezomib treatment for 48h, but an increase of the uptake of FDG (up to 1.8fold) and of Glucose (up to 2.6fold). *In vivo*, a dose-dependent decrease of FDG uptake was observed 1 day after Bortezomib therapy. **Conclusions:** Based on the induction of apoptosis and cell cycle arrest and changes in metabolism Bortezomib mediates strong antiproliferative effects in rat Morris hepatoma cells.

P24-2 - Tuesday, October 30, 2012, 16:00 - 16:30, Poster Exhibition Area

Molecular & Multimodal Imaging: Optical Imaging

P0760

Multimodal hypoxia imaging in a preclinical glioma model

A. Lo Dico¹, C. Martelli¹, S. Belloli², A. Degrossi³, M. Russo³, S. Valtorta², U. Gianelli⁴, D. Tosi⁴, S. Todde², C. Monterisi², G. Lucignani¹, L. Ottobri¹, R. Moresco²; ¹university of milan, segrate (MI), ITALY, ²IBFM-CNR, Technomed Found. and Dept. of Surgical Sciences, University of Milan Bicocca, Nuclear Medicine Dept. San Raffaele Scientific Institute, Segrate (MI), ITALY, ³nerviano medical sciences, nerviano (MI), ITALY, ⁴Dept. of Medicine Surgery and Dentistry, University of Milan, Milan, ITALY.

Introduction: The aim of our study is to analyze the relationship between tumor growth and tumor hypoxia in an orthotopic glioma murine model by using a multimodal procedure, and to compare the features of the different imaging techniques in revealing hypoxia induction. **Materials and methods:** Engineered U251 cells were gently provided by Dr. Giovanni Melillo, National Cancer Institute, Frederick (MD). These cells express the luciferase reporter gene under control of a constitutive promoter (U251-LUC) or under control of three copies of a Hypoxic Responsive Element (U251-HRE). Cells have been analyzed by means of three different approaches: 1) *In vitro* evaluation of transcriptional activation of HIF-1 α at different times after deferoxamine (DFX) treatment by immunocytochemistry (ICC). 2) *In vivo* analysis of tumoral progression in orthotopic murine models obtained by stereotaxic injection of 10⁵ glioma cells; animals were monitored weekly with BLI (CCD camera), PET ([¹⁸F]FDG, [¹⁸F]FAZA, [¹⁸F]FLT) and MRI to evaluate tumoral progression and hypoxia activation. 3) *Ex vivo* analysis by H&E staining and hypoxia markers (HIF-1 α and CAIX) were performed. **Results:** *In vitro* studies showed no differences among the two cell lines as regards to HIF-1 α activation kinetic with a peak of activation between 3 and 6h and a decrease at 20h. *In vivo*, U251-HRE model showed a detectable and progressive luciferase activity induction starting at

18 days from injection demonstrating that luminescence expression is dependent on HRE-mediated activation. On the other hand, in U251-LUC model luciferase activity was detectable immediately after injection and remained proportional to tumor growth. Lesions were highly proliferative ([¹⁸F]FLT) but hypo-metabolic ([¹⁸F]FDG). In partial agreement with the results of U251-HRE, a hypoxia dependent [¹⁸F]FAZA uptake was observed at later times (30 days). MRI provided morphological characterization and diffusion studies showing hypoxic necrotic areas only at later days. *Ex vivo* H&E staining and immunohistochemistry (HIF-1 α and CAIX) performed after 30 days confirmed *in vivo* results including the presence of hypoxic regions. **Conclusions:** This study demonstrates that the U251-HRE orthotopic murine model may be proposed as a predictive and reliable tool to evaluate hypoxia dependent processes of human glioma in preclinical studies by BLI. Differences among the three imaging techniques may be related to methods sensitivity. Further *ex vivo* post mortem measurements of HIF-1 and CAIX at earlier times will be performed. Additional studies will be conducted to understand the clinical meaning of early or delayed hypoxia identification in terms of response to treatment.

P0761

Patterns on 99mTc-Mercaptoacetyltryglycine Scintigraphy in Children

M. Ait Idr, A. Guensi, S. Taleb, M. Kebbou; CHU IBN ROCHD CASABLANCA, MOROCCO.

Tc-99m-MAG3 dynamic renography is a functional procedure, indicated in several renal and urologic diseases. Better than Tc-99m-DTPA in image quality and functional value accuracy, particularly in newborn and patient with renal failure. Therefore, 99mTc-MAG3 dynamic renal scan is considered the first choice in routine practice. The aim of this study is to evaluate usefulness of this investigation in our experience. One hundred twenty seven consecutive patients (35F and 92M), aged 11 days to 13 years (mean 3.5 yrs), were studied between January 2010 and Mars 2012. The investigation was indicated to assess: obstruction and renal function in patients with pelvi-ureteric junction syndrome (73 cases), mega-ureter (20 cases) and uretero-hydronephrosis (18 cases), pyelo-ureteral duplication (2 cases), renal lithiasis (1case), neurologic bladder (3 cases) and post-surgical evaluation of a previously obstructed system (10 cases). F+20 protocol was used in 118 cases and F0 protocol in 9 cases. Static images, after micturition or sitting position, were acquired after Tc-99m-MAG3 dynamic scan. Qualitative and quantitative parameters were included for interpretation (dynamic display, relative renal function, time to maximum activity, clearance half time and residual renal activity). Interpretation criteria were those currently recommended by European associations of Nuclear medicine. The results showed: absence of urinary tracts drainage impairment (59 cases), drainage impairment without functional consequences (25 cases), drainage impairment with functional consequences (25 cases), improved drainage after surgery for obstruction (7cases) and absence of improved drainage (3 cases). The findings were unclear in 8 cases (6.3%), due to: an important distension (4cases), renal insufficiency (3 cases) and incomplete renal maturation (1case). The unclear response rate decrease with Tc-99m-MAG3 renography. Nevertheless, in a very few situations, it remains depending in clinical context including: age, importance of urinary tracts dilatation and renal function.

P25-2 - Tuesday, October 30, 2012, 16:00 - 16:30, Poster Exhibition Area

Molecular & Multimodal Imaging: New & Innovative

P0762

Procedural optimization of radioguided parathyroidectomy using a hand held portable gamma camera. Preliminary results.

S. Chondrogiannis¹, M. R. Pelizzo², A. Ferretti¹, S. Tadayyon¹, L. Rampin¹, L. Tamiso¹, E. Tommasi¹, A. Massaro¹, M. C. Marzola¹, D. Rubello¹; ¹Department of Nuclear Medicine, Rovigo, ITALY, ²Department of Surgical Pathology, Institution of Medical and Surgical Sciences, University of Padova, Padova, Rovigo, ITALY.

Aim: To assess the optimal protocol for the peri and intra-operative radioguided parathyroidectomy using a portable hand held gamma camera. **Materials and methods:** At the moment 9 consecutive patients affected by primary hyperparathyroidism and with a clear visualization of a solitary parathyroid adenoma (PA) at preoperative scintigraphy and ultrasound were enrolled in the study. A nuclear medicine physician in the operative room compared the results of traditional gamma probe with the results of a portable hand held im-aging γ -camera (IP Guardian 2, Li-Tech). Our main aim was to optimise the activity of sestaMIBI to be injected and to assess the optimal time for the injection of the tracer. Moreover we compared the performance of the hand held imaging gamma camera with the traditional gamma probe. **Results:** The protocol developed changed over time. In the first 2 patients 500 MBq of 99mTc-MIBI were injected 90 minutes before the

operation. In these cases we did not find any problem to identify the PA using the traditional gamma probe, whereas with the imaging gamma camera we obtained suboptimal imaging especially due to the very high background values. In the subsequent patients, the injected activity was progressively decreased down to 200 MBq and the tracer was injected close to the operation just during the induction of anaesthesia (therefore 15–20 minutes before surgery). These progressive changes allowed us to obtain good quality results with the imaging γ -camera in comparison to our first experience. The imaging hand held γ -camera appeared to be particularly useful in a case of a PA located deep in the neck. The portable γ -camera we used showed very high spatial resolution (2.4 mm) in the 4.4x4.4 cm² field of view, with a sensitivity of 180 cps/MBq (at a depth of 1cm) and its utilization did not prolonged the surgery time. Moreover it is interesting to report the appreciation by the surgeon of the possibility to record in the clinical file of the patient a “saved” image of the removed PA. Discussion: The preliminary data of our study indicate that is simple and no time consuming using a hand held imaging gamma camera in the operating room for radioguided parathyroidectomy. A relatively low activity of sestaMIBI (200 MBq) injected just before surgery is an adequate protocol. In our opinion imaging hand held gamma camera could be complementary to the traditional gamma probe in some challenging cases of PA but it couldn't substitute it.

P0763

Improve tracer selectivity for beta cell mass imaging using mini-pig pancreatic sections

H. Tsao¹, S. Wey², K. Lin³, J. Lin⁴, T. Yen⁵, M. Kung⁶; ¹Molecular Imaging Center, Chang Gung Memorial Hospital, Guishan Township, Taoyuan, TAIWAN, ²Medical Imaging and Radiological Sciences, Chang Gung University, Guishan Township, Taoyuan, TAIWAN, ³Nuclear Medicine, Chang Gung Memorial Hospital, Guishan Township, Taoyuan, TAIWAN, ⁴Animal Technology Institute, Miaoli, TAIWAN, ⁵Nuclear Medicine, Chang Gung Memorial Hospital, Taoyuan, TAIWAN, ⁶Radiology, University of Pennsylvania, Philadelphia, PA, UNITED STATES.

Objectives: The vesicular monoamine transporter type II (VMAT2) is highly expressed in pancreatic beta cells and thus has been proposed to be a potential target for beta cell mass (BCM) with molecular imaging. [18F]FP-(+)-DTBZ (AV133) showed promising results as a potential biomarker for BCM despite a relatively high background signal in the human pancreas. In the present study we used the mini-pig as a better human surrogate to confirm the selective binding characteristics of AV133 and its 2-hydroxymethyl congener, AV-300, in the pancreas. **Methods:** Mini-pig pancreatic tissues were dissected for in vitro autoradiography (ARG). AV133 and AV300 were respectively evaluated under normal and a selective masking/blocking condition [10 nM 1,3-di-o-tolylguanidine (DTG) to block sigma receptors]. IHC with anti-insulin was carried out to confirm the islets/beta cells. **Results:** AV133 showed avid signals in the mini-pig pancreatic sections under the optimized ARG conditions. The significant non-desirable background (36% of the total binding) can be clearly masked in the presence of DTG; whereas the specific signals matched well with the anti-insulin IHC. In contrast, AV300 (despite similar binding affinity toward VMAT2 in rodents) yielded poor islet labeling with a similar high background labeling. **Conclusions:** AV133 is a better BCM imaging agent as compared to AV300, but showing significant non-desirable background binding. In vitro ARG with mini-pig pancreatic sections could provide a more convenient screening for better and more selective VMAT2 imaging agents targeting BCM, which will ultimately facilitate diabetic prognosis.

P0764

Evaluating intensity and heterogeneity of primary tumour FDG uptake in breast cancer with a dedicated PET ring device. A correlation study with hanging breast PET/CT.

S. Vidal-Sicart¹, B. B. Koolen², J. M. Benlloch³, R. A. Valdés-Olmos²; ¹Hospital Clinic Barcelona and The Netherlands Cancer Institute-Antoni van Leeuwenhoek Hospital, Barcelona/Amsterdam, SPAIN, ²The Netherlands Cancer Institute-Antoni van Leeuwenhoek Hospital, Amsterdam, NETHERLANDS, ³Corpuscular Physics Institute (IFIC), Valencia, SPAIN.

Aim: The goal of the study was to compare the intensity and heterogeneity of primary tumour FDG uptake in breast cancer patients using a high-resolution dedicated breast PET ring device and a standard whole body PET/CT. **Method:** Patients with stage II-III breast cancer underwent a baseline FDG PET/CT before neoadjuvant chemotherapy. FDG-PET/CT was performed using a hybrid system (Gemini II, 16-slice CT), 60 minutes after intravenous administration of 180–240 MBq 18F-FDG. Subsequently, approximately 110 minutes after injection, a scan was performed with a dedicated high-resolution breast PET (MAMMI, Oncovision). Both scanning procedures were performed with the patient in prone position (hanging breast approach). The MAMMI device uses a ring of 12 LYSO crystal detectors, has a resolution of 1.6–2.7 mm at FWHM, and voxel size of 1 mm³. The images obtained by the dedicated PET were compared to the FDG PET/CT 2mm images concerning tumour visualization and uptake characteristics. A 4-point score was used to evaluate tumour FDG uptake in both series of images (0: non visualization;

1: light intensity; 2: moderate intensity; 3: high intensity). This assessment was done using orthogonal multiplanar projection (MPR) in axial, coronal, and sagittal views. A 4-point score was also used to evaluate the uptake heterogeneity (0= diffuse; 1= mild; 2= moderate; 3= high). For this purpose the evaluation was performed by generating maximum intensity projection (MIP) images with covering of the whole volume of the tumour. **Results:** We included thirty-five patients with evaluable tumour FDG uptake. The median size of the primary tumour was 30mm (range 10–75 mm). The uptake score was similar in both devices (average 2.4 for PET/CT and 2.3 for MAMMI), whereas heterogeneity score showed a slight difference (PET/CT 1.89 vs MAMMI 2.29). MAMMI showed a higher heterogeneity in 9 out of 35 patients (26%), especially when the tumour presented a higher uptake score (2–3). In 16 patients with heterogeneous FDG uptake on MAMMI (score 2–3), the highest heterogeneity scores were achieved in tumours with uptake score 3 (12 out of 16) and more than 2 cm in size (13 out of 16 cases). **Conclusion:** The MAMMI PET appears to be able to better depict heterogeneity in tumour FDG uptake especially in larger tumours. This aspect may enable FDG-guided biopsy for more accurate histopathological tumour profiles in breast cancer patients scheduled for neoadjuvant chemotherapy.

P26-2 - Tuesday, October 30, 2012, 16:00 - 16:30, Poster Exhibition Area

Radiopharmaceuticals & Radiochemistry: Radiopharmaceuticals - PET

P0765

Optimisation and Use of an Automated Manufacturing Process of Fluciclatide on FASTlab

J. Grigg¹, T. Engell², N. Osborn¹, J. Shales¹; ¹GE Healthcare, Amersham, UNITED KINGDOM, ²GE Healthcare, Oslo, NORWAY.

Aim Fluciclatide (¹⁸F) Injection is a diagnostic radiopharmaceutical intended for the imaging of $\alpha_3\beta_3$ and $\alpha_3\beta_5$ integrins. The active species is a RGD peptide-based molecule currently being used in clinical trials. Multiple patient doses of Fluciclatide (¹⁸F) Injection per batch were required after aseptic dispensing. In this work the radioactive yield and reliability of the automated manufacturing process has been significantly improved by incorporating novel chemistries in a two-step labelling approach and by the development of an automated purification method using disposable solid-phase extraction cartridges. **Methods** Multivariate data analysis and experimental design techniques were employed for the development of the automated chemistry process and the SPE-based purification method. In addition the built-in data-logging abilities of FASTlab were used during the development process and now this experience has been incorporated for diagnostic purposes during routine productions. **Results** All reagents and disposable hardware required for the manufacturing process are contained within a single-use cassette pack. The manufacturing process has now been transferred to internal and external manufacturing sites in US and EU. Average non decay-corrected yields of 35–40% have been observed in > 50 productions with no FASTlab synthesis failures being observed. Parameters that define the quality of the product and the reliability of the manufacturing process will be presented and discussed. **Conclusion** A reliable and robust automated manufacturing process has been achieved for Fluciclatide (¹⁸F) Injection on FASTlab that includes SPE purification. The manufacturing process is now available for transfer to additional manufacturing sites for further investigations of its utility and capabilities.

P0766

Preparation of [11C]Verapamil for Biological Studies

E. V. Németh, T. Miklovicz, J. P. Szabó, P. Mikecz, L. Galuska, T. Márián; Medical University of Debrecen, Debrecen, HUNGARY.

Verapamil is a calcium channel blocker and the substrate of the P-glycoprotein (Pgp) pump, causing multidrug resistance that may be responsible for the failure of chemotherapy of cancerous diseases. Its C-11 labeled variant has become the best PET ligand to study the blood-brain barrier, and the function of the Pgp pump in tumors. **Objective:** The aim of our study was the synthesis of 11C labeled verapamil with optimization of the production parameters in order to achieve high purity and specific activity, and the evaluation of its uptake in Pgp-negative and Pgp-positive cells. **Methods:** For the synthesis, a module was built with automatic process control and data acquisition. The module includes triflate- and reaction oven, and a HPLC separation unit with a column radiation detector. The produced [11C]CO₂ was converted to [11C]methyl iodide on a PETTrace MeI MicroLab module (GE Healthcare). The reaction took place between norverapamil and [11C]CH₃OTf in acetonitrile. The reaction mixture was loaded on a semi-preparative C18 HPLC column, and the eluted verapamil fraction was concentrated on a C18 SepPak column. The final product - collected in 0.2 ml ethanol - was diluted with saline for biological application. For the in vitro tests KB-3-1 Pgp-positive and CP-V1 Pgp-negative human epidermoid carcinoma cell lines were used. The Pgp pump efficiency was tested with fluorescent 123 rodamine dye by flow cytometer. **Results:**

[11C]verapamil was produced ($n=30$) with 200 ± 20 GBq/ μ mol specific activity, the radiochemical purity was $>98\%$. The decay-corrected reaction yield was $65\pm 4\%$. Since norverapamil significantly decreased the accumulation of [11C]verapamil in cancer cells, special attention had to be paid to its separation from the product. The precursor concentration was decreased by systematic optimization to 1.2 ± 0.5 nmol/mL. The *in vivo* experiments did not show [11C]verapamil accumulation in the brain of healthy mice. However, when the function of Pgp pump was inhibited by CSA, [11C]verapamil uptake was observed. There was little difference in the uptake of Pgp-positive and negative tumors of different types. Conclusion: From our measurements we concluded that [11C]verapamil can serve as a useful tool for the *in vivo* and *in vitro* demonstration of Pgp pump functions, and the effect of different drugs on the BBB.

P0767

New method for the preparation of O-¹¹C-methyl-L-tyrosine via [¹¹C]methylation on solid phase support

N. Gomzina¹, O. Kuznetsova¹, A. Gordon², ¹N.P. Bechtereva Institute of the Human Brain of Russian Academy of Sciences (IHB RAS), St.-Petersburg, RUSSIAN FEDERATION, ²St. Petersburg State University, St.-Petersburg, RUSSIAN FEDERATION.

Aim O-¹¹C-methyl-L-tyrosine ([¹¹C]MT), carbon-11 labeled analogue of tyrosine, is a promising PET imaging agent for brain tumors. The aim of this study was to investigate the feasibility of *on-line* [¹¹C]methylation for the synthesis of [¹¹C]MT, as this approach has proved to be efficient for routine automated production of N-[methyl-¹¹C]choline and L-[methyl-¹¹C]methionine. **Materials and methods** The synthesis of [¹¹C]MT was performed using fully automated home-made module for *on-line* ¹¹C-methylation. [¹¹C]methyl iodide ([¹¹C]MeI) was prepared by lithium aluminum hydride reduction of [¹¹C]CO₂ following treatment with 57% hydroiodic acid. The substrate solution (0.2 mL) containing di-potassium salt of L-tyrosine (2–15 mg), NaOH or tetrabutyl ammonium hydroxide (TBAH) as a base and DMSO as a solvent was loaded onto a tC18 Plus Sep-Pak cartridge. [¹¹C]MeI was passed through the cartridge by nitrogen flow (10 mL/min) over about 6 min. The cartridge was rinsed with 1 mL of ethanol. The eluate was diluted with water and assayed by reversed phase and chiral HPLC. **Results and discussion** The reported method for the synthesis of [¹¹C]MT based on the bubbling of [¹¹C]MeI through the solution of di-sodium salt of L-tyrosine in DMSO has provided ¹¹C-methylation yield of about 55–65 % (Y. Ishikawa, 2005). The attempted *on-line* ¹¹C-methylation of this substrate on the solid phase support resulted in very poor alkylation efficiency (less than 1% of [¹¹C]MT in reaction mixture). We supposed that the formation of a sufficiently stable anion from phenol precursor was essential to fulfill ¹¹C-methylation, because a trapping efficiency of [¹¹C]MeI on tC18 cartridge pre-loaded with labeling precursor was very high (80–90 %). Therefore we suggested the use of TBAH as a base for *on-line* methylations with addition of small amounts of methanol to increase the solubility of precursor. Under these conditions O-¹¹C-methylation of di-potassium salt of L-tyrosine resulted in formation of [¹¹C]MT with 50% yield that was comparable with the results obtained via “bubbling” technique. The optimal composition for *on-line* ¹¹C-methylation was found to be: 8–10 mg of precursor in 0.2 mL of solution containing 15 μ L of 0.5 M TBAH in MeOH and 185 μ L of DMSO. Under these conditions the L-isomer of [¹¹C]MT was the only detected by chiral HPLC. **Conclusion** The use of developed *on-line* ¹¹C-methylation method allows to obtain [¹¹C]MT with a high yield and suits well for the automation. Work is now in progress to further optimize synthesis and purification.

P0768

Stability of ⁶⁴Cu-ATSM solutions for clinical use

F. Lodi¹, C. Malizia¹, G. Ciorica², M. Marengo², S. Fanti¹, S. Boschi¹, ¹PET Radiopharmacy, Nuclear Medicine Dept., Azienda Ospedaliero Universitaria di Bologna Policlinico S. Orsola-Malpighi, Bologna, ITALY, ²Medical Physics, Azienda Ospedaliero Universitaria di Bologna Policlinico S. Orsola-Malpighi, Bologna, ITALY.

Aim Radiolysis is a process which leads the decomposition of radiolabelled molecules thus decreasing radiochemical purity and the quality of radiopharmaceuticals. The radiolysis could be suppressed by decreasing radioactive concentration and/or by adding appropriate additives at the proper stage of the purification or formulation. ⁶⁴Cu-ATSM is a useful radiopharmaceutical for hypoxia studies of solid tumors and low radiochemical purity due to radiolytic decomposition could be experienced. Aim of this paper is to study the stability on ⁶⁴Cu-ATSM solutions for clinical use and to examine the appropriate agent to prevent the radiolysis of this radiopharmaceutical. **Materials and methods** ⁶⁴Cu was produced by irradiation of ⁶⁴Ni target in a PETtrace cyclotron (GE Healthcare). ⁶⁴Cu purification and ⁶⁴Cu-ATSM synthesis were performed by means of an automated modular system (Eckert-Ziegler). ⁶⁴Cu was separated from target material by means of anion exchange column, concentrated into a cation exchanger columns and eluted into reactor with CH₃COONa 3M. The reactor was previously loaded with ATSM in DMSO. The synthesis was performed at room temperature. ⁶⁴Cu-ATSM was purified by solid phase extraction on C18 column, eluted with ethanol and diluted with saline. Stability was tested at different

radioactive concentration of ⁶⁴Cu-ATSM (mCi/mL) by analyzing the solutions with radio-HPLC at appropriate time intervals at room temperature up to 12 hours after EOS. Radiochemical purity was determined after dilution and after adding different additives such as ascorbic acid, ethanol, gentisic acid at different concentrations.

Results and conclusion ⁶⁴Cu-ATSM was prepared with high yield at different concentration by means of automated modular system. ⁶⁴Cu-ATSM showed instability depending on radioactive concentration of radiopharmaceutical. At concentration of 6–8 mCi/mL ⁶⁴Cu-ATSM was unstable after 2 hours EOS whereas at concentration ≤ 3 mCi/mL the radiopharmaceutical was found stable up to 12 hours after EOS without any precautions to prevent the radiolysis. Ascorbic acid was found to be ineffective in preventing ⁶⁴Cu-ATSM radiolysis. The use of other additives to reduce the radiolysis at 6–8 mCi/mL concentrations is under evaluation.

P0769

Development and pre-clinical evaluation of the new pan-somatostatin PET imaging probe Ga-68-DOTA-SOM230 (SOMscan®)

M. Fani¹, E. Gourni¹, A. Mann², A. Klierer², A. Dreykluft³, W. A. Weber¹, H. Bouterfa³, S. Schulz², H. R. Maecke¹, ¹University Hospital Freiburg, Freiburg, GERMANY, ²University Hospital Jena, Jena, GERMANY, ³OctreoPharm Sciences GmbH, Berlin, GERMANY.

Aim: Imaging of somatostatin receptor (sst)-positive tumors using ⁶⁸Ga-labeled somatostatin analogs is of high clinical interest, as somatostatin receptors (sst1–sst5) are expressed on many neuroendocrine tumors. Over the last years, many patients have been studied with ⁶⁸Ga-DOTA-TOC or ⁶⁸Ga-DOTA-TATE targeting sst2. However, a variety of somatostatin analogs have been developed with the aim to improve receptor subtype affinity profile, such as ⁶⁸Ga-DOTA-NOC targeting sst2, 3 and 5. Our aim is to develop and evaluate a new ⁶⁸Ga-labeled PET imaging probe for clinical application based on SOM230 (Pasireotide) with high affinity for sst1, 2, 3 and 5. **Materials and Methods:** The new radiotracer ⁶⁸Ga-DOTA-SOM230 was prepared within 10 min at 95°C, followed by purification. *In vitro* evaluation included stability studies in human serum, determination of logD, sst-subtype binding profile and internalization. *In vivo* studies were performed in tumor xenografts expressing the human receptors sst1, 2, 3 and 5, along with small animal PET imaging. The radiotracers ⁶⁸Ga-DOTA-TATE and ⁶⁸Ga-DOTA-NOC were used as reference tracers. **Results:** ⁶⁸Ga-DOTA-SOM230 was prepared in radiochemical purity $>95\%$ and specific activity ~ 50 MBq/nmol. ⁶⁸Ga-DOTA-SOM230 had logD = -0.93 ± 0.15 and exhibited very high stability in human serum up to 2 h, as no metabolites were determined. *In vitro* binding and internalization profiles were comparable to SOM230. ⁶⁸Ga-DOTA-SOM230 clearly visualized the hst-expressing tumors in PET images at 1 h p.i. Biodistribution studies exhibited relatively high blood pool activity ($\sim 4\%$ IA/g), kidney and liver uptake (~ 30 and 12% IA/g, respectively) at 1 h p.i. At 2 h p.i. tumor uptake remained high while tumor-to-background ratios and image contrast improved. The specificity of the radiotracer was confirmed with blocking experiments, in both biodistribution and PET imaging studies. ⁶⁸Ga-DOTA-SOM230 compares well with the clinically applied radiotracers. For example, the uptake in hst2 is somewhat higher for ⁶⁸Ga-DOTA-TATE than for ⁶⁸Ga-DOTA-SOM230 (17.8 ± 2.2 and $14.1\pm 4.5\%$ IA/g, respectively) but statistically not significant ($p > 0.05$), while the uptake in hst5 is statistically significantly higher for ⁶⁸Ga-DOTA-SOM230 than for ⁶⁸Ga-DOTA-NOC (11.4 ± 1.3 and $7.7\pm 1.5\%$ IA/g, respectively, $p < 0.05$), 1 h p.i. and the tumor-to-background contrast similar. **Conclusion:** The *in vitro* and *in vivo* pre-clinical evaluation of ⁶⁸Ga-DOTA-SOM230 (SOMscan®) reveals the good performance of this new radiotracer and supports its potential as PET imaging probe for a broad spectrum of somatostatin receptors.

P0770

New options in hepatocellular carcinoma therapy: the role of gossypol, quercetin and cytochalasin-B. Studies with 18F-FDG

A. F. Brito¹, F. Verissimo², M. Ribeiro³, A. M. Abrantes¹, F. Castro-Sousa⁴, J. G. Tralhão⁵, M. F. Botelho¹, ¹Biophysics Unit, IBILI, CIMAGO, Faculty of Medicine, University of Coimbra, Coimbra, PORTUGAL, ²Coimbra College of Agriculture, Coimbra; Biophysics Unit, IBILI, Faculty of Medicine, University of Coimbra, Coimbra, PORTUGAL, ³Biophysics Unit, IBILI, Faculty of Medicine, University of Coimbra, Coimbra, PORTUGAL, ⁴Surgical Department, Surgery A, HUC, Coimbra; CIMAGO, Faculty of Medicine, University of Coimbra, Coimbra, PORTUGAL, ⁵Surgical Department, Surgery A, HUC, Coimbra; Biophysics Unit, IBILI, CIMAGO, Faculty of Medicine, University of Coimbra, Coimbra, PORTUGAL.

Introduction: Hepatocellular Carcinoma (HCC) is the most common primary liver malignancy with a rising incidence worldwide. Therapies are very often palliative and have little effect on patient survival. Glucose transporter 1 (GLUT-1) is overexpressed in HCC and promotes tumorigenesis. Conversely, suppression of GLUT-1 significantly impaired growth and invasiveness of HCC cell lines. Consequently it was proposed that GLUT-1 could be an innovative therapeutic target for HCC. Some compounds as gossypol, flavonoids and cytochalasin-B have shown potential as GLUT-1 function inhibition and it can be useful therapeutical

weapons against HCC. A Positron Emission Tomography (PET) using the radiolabeled glucose analogue 18F-FDG ($[^{18}\text{F}]\text{fluorodeoxyglucose}$) enables the detection of increased glycolysis events in cancer cells. 18F-FDG is transported into the cell mainly through the GLUT-1 and 3. The aim of this study is to evaluate the potential anticancer effect of gossypol, quercetin (a flavonoid) and cytochalasin-B on two HCC cell lines which differ on p53 expression, HepG2(wp53) and HuH7(mp53), as well as check the effect of these compounds on 18F-FDG uptake in these cell lines. **Materials and methods:** The cell lines were propagated in the presence of gossypol, quercetin and cytochalasin-B in several concentrations. Cell proliferation was evaluated by the MTT test. 18F-FDG was incubated in a cell suspension with 2×10^6 cells/ml ($25 \mu\text{Ci}/\text{ml}$) in cells pre-incubated with gossypol, quercetin and cytochalasin-B and control cells. Samples were collected to eppendorf tubes for tracer uptake calculation. Eppendorfs were then centrifuged and radioactivity of cell pellets and supernatants was measured with a well-type gamma counter. **Results:** All compounds induced a decrease in cell proliferation on both cell lines, and was shown that their effect depends on the time, having gossypol the more expressive results. For example, the IC50 with gossypol incubation after 24 hours was $5.97 \mu\text{M}$ to HepG2 and $7.17 \mu\text{M}$ to HuH7. For quercetin, the value of IC50 after 24 hours was respectively $47.64 \mu\text{M}$ and $182.5 \mu\text{M}$, and for cytochalasin-B, the values were respectively $80.89 \mu\text{M}$ and $28.01 \mu\text{M}$. In addition, for the cell lines studied, gossypol, quercetin and cytochalasin-B was able to decrease the percentage of 18F-FDG uptake. **Conclusion:** These results shown that gossypol, quercetin and cytochalasin-B have anti-proliferative effect on HCC cell lines studied. These compounds also have shown ability to decrease the uptake of 18F-FDG. More studies must be done to clarify the role of p53 in the anti-proliferative effect of these compounds in HCC as well as the effect in the uptake of the 18F-FDG.

P0771

Gallium-NOTA -Aprotinin: a Potential PET Amyloid Seeker

F. E. Buroni, L. Lodola, C. Aprile; Fond. Policlinico S.Matteo, IRCCS, Pavia, ITALY.

Tc99m-Aprotinin has been reported to accumulate in extrarenal amyloid deposits with high sensitivity and specificity. **Aim** of this work was to find a rapid method to label Aprotinin with Gallium to obtain a radiopharmaceutical suitable for PET imaging. **Methods:** Recombinant Aprotinin (A) was conjugated with the intermediate chelator p-SCN-Bz-NOTA (N): a 6×10^{-4} M N solution with 2×10^{-4} M A solution (5 mL) was allowed to react in various synthesis reaction conditions (pH 2, 7, 9.5, 12 - temperatures of 5, 25 and 40°C) to obtain the conjugate (AN). AN was purified by filtration on Amicon Ultra-4 3kDa ultracel-PL membrane and labelled with Ga67 chloride (ANGa) after incubation at room temperature (RT) for 15 min. Quality control was performed using the HPLC method (Agilent HPLC 1200 series, C18 column, solvent A acetonitrile 99% - trifluoroacetic acid (TFA) 1%, solvent B water 99% - TFA 1%, gradient at 1 mL/min). ANGa was used to assess the fibrillar binding assay: equal amounts of synthetic amyloid insulin fibrils ($1 \text{ mg}/100 \mu\text{L}$), were incubated with different amounts of ANGa ($73\text{--}197 \text{ nmol}/\text{mg}$ fibrils) for 1 h at RT, washed and spinned 3 times at 12000 rpm for 30 min, counted in a well scintillator after subtraction of the non specific binding. For competition experiments, increasing amounts of cold A ($35\text{--}280 \text{ nmol}$) were added to 1 mg fibril samples labelled with ANGa (70 nmol). **Results:** The synthesis reaction gave a yield of approximately 80% with more favourable results at pH 9.6 ($0.1 \text{ M Na}_2\text{CO}_3$ buffer), 25°C , after 20h in the dark. Gallium labelling yield ranged from 73 to 86%, the compound is stable in vitro for at least 48 h. Scatchard analysis of the binding affinity revealed a K_d of 86.62 nmol . Competition binding tests showed a 50% displacement at 129 nmol. **Conclusion:** A stable Ga67-aprotinin-p-SCN-Bz-NOTA radiotracer was obtained rapidly (15 min) at RT with an acceptable yield, without affecting the aprotinin affinity for amyloid fibrils, with a K_d comparable to that we previously reported for Technetium labelled A. Therefore ANGa - 68 may be considered a potential radioligand for early PET detection of amyloid deposits.

P0772

Impact of an automated FDG infusion system in radiation exposure to PET technologists

S. Lima, S. Nogueira, L. Y. I. Yamaga, D. Wiecek, D. Magalhaes, J. Oliveira, G. Campos Nt, A. Osawa, M. Cunha, A. Thom, J. Wagner, M. Funari; Hospital Israelita Albert Einstein, São Paulo, BRAZIL.

The progressive growth in the number of PET-CT exams increases the radiation exposure of technologists in routine clinical practice with 18F-FDG. Effective radiation protection devices are required to reduce the radiation exposure of the staff handling with PET. **Objective:** The aim of this study was to compare the radiation exposure of PET technologists before and after the introduction of a commercially available automated PETdose preparation and infusion system. **Materials and methods:** Chest and limbs radiation doses of technologists working in a dedicated PET department were measured by thermoluminescence dosimeters (TLD) in two distinct periods: before and after the introduction of a commercially available shielded automated PET infusion system (MEDRAD Intego™). Before the

automated system, the radiation protection devices consisted of a hot laboratory with lead shield suitable for handling positron emitters, drawing up of FDG dose using a tungsten syringe shield, manual handling of the syringe for the infusion of FDG into the patient. In the second period of this study, the dose preparation and infusion to the patients were done automatically under supervision of the technologist. The ratios of mean technologist radiation dose / mean of PET exams were calculated in a period of 10 consecutive months before and in another period of 10 consecutive months after the introduction of the automated infusion system. The administered FDG doses to the patients didn't change in both periods. **Results:** The ratios of mean radiation dose/mean number of PET exams in the chest were 1,0 and 0,8 mSv and in the extremity were 6,3 and 1,9 mSv before and after the introduction of the automated infusion system, respectively with a reduction of the measured doses of 23% in the chest and 70% in the extremity. **Conclusion:** Technologists radiation dose decreased 70% after the implementation of a PET automated infusion system as it permits shorter exposure of the technologist s during FDG manipulation.

P0773

Automated Synthesis of $[^{18}\text{F}]\text{FLT}$ by Cartridges-Based Purification: Further Investigation on the Effects of the Phase-Transfer Agent Used

A. Bogni, C. Pascali, C. Cucchi, L. Laera, G. Parini, A. Coliva, E. Bombardieri; Fondazione IRCCS Istituto Nazionale dei Tumori, Milan, ITALY.

Aim. We recently showed (Pascali C. et al. *Nucl.Med.Biol.* in press) the feasibility to synthesize $[^{18}\text{F}]\text{FLT}$ in a solution suitable to human use - and with an EtOH content below the stated Ph.Eu.'s threshold - by means of a commercial $[^{18}\text{F}]\text{FDG}$ module, with no major changes in the original setup and program, i.e. by carrying out the purification step by means of disposable cartridges. Herein we set to further investigate the pro and cons of the two phase transfer agents employed, Kryptofix 2.2.2 and tetrabutylammonium. **Materials and methods.** The one-pot process was carried out on a GE TracerLab FX-FDG module. $[^{18}\text{F}]\text{Fluoride}$ was first trapped on either a carbonate- or bicarbonate-QMA cartridge and then eluted with $\text{K}_2.2.2/\text{KHCO}_3$ ($15\text{mg}/3.5\text{mg}$) or TBA-HCO_3 (30 mM), both in 1 mL $\text{CH}_3\text{CN}/\text{H}_2\text{O}$ 9:1. Drying was then accomplished by vacuum-assisted evaporation, followed by the SN_2 reaction on 3-N-Boc-5'-O-DMTr-3'-O-nosyl-lyxothymidine (15 or 20 mg in 1 mL dry CH_3CN ; 100°C x 5min). After partial evaporation of the solvent, the protective groups were removed with HCl (1.8 mL, 1N; 85°C x 4min). The reaction mixture was then reduced in volume to remove the CH_3CN , cooled down and passed through a cation-exchange cartridge (Maxi-Clean IC-H) and conveyed to a Millex-GS (vented) sterile filter joined to a tc18 SepPak Plus. WFI was then used to take away most of the impurities from the reversed-phase cartridges and send them to a waste. Finally, the product was eluted with WFI throughout an Alumina N Light SepPak and a further sterile filter. Both waste and product were analyzed for residual $\text{K}_2.2.2$ or TBA and percentage of $[^{18}\text{F}]\text{FLT}$. A commercial kit (Celltech) for the determination of $\text{K}_2.2.2$ in $[^{18}\text{F}]\text{FDG}$ solutions was validated also for $[^{18}\text{F}]\text{FLT}$ solutions. **Results.** Using 20 mg of precursor, the total decay-corrected $[^{18}\text{F}]\text{FLT}$ found in the product and waste when $\text{K}_2.2.2/\text{KHCO}_3$ or TBA-HCO_3 were used amounted to 49 and 43%, respectively. More data will be collected in the following months. Although both agents were not present in the product solution, variable amount of $\text{K}_2.2.2$ (from 2 to 6 mg) were found in the waste. **Conclusion.** $\text{K}_2.2.2/\text{KHCO}_3$ affords better yields than TBA-HCO_3 , whereas the latter is much better trapped by the cation-exchange cartridge, thus affording a better separation, especially when 20 mg of precursor are used. **Acknowledgements.** This research has been supported by AIRC Project Molecular and cellular Imaging of Cancer, by PIO Project PET Molecular Imaging and by 5 per mille Project.

P0774

Validation of an HPLC Method for the Analysis of $[^{18}\text{F}]\text{FLT}$

C. Cucchi, A. Bogni, C. Pascali, L. Laera, G. Maiocchi, E. Bombardieri; Fondazione IRCCS Istituto Nazionale dei Tumori, Milan, ITALY.

Aim. 3'-Deoxy 3'- $[^{18}\text{F}]\text{fluorothymidine}$ ($[^{18}\text{F}]\text{FLT}$) has shown a great potential as a proliferation tracer for studies with Positron Emission Tomography. Thus, a simplified synthesis applying a cartridge-based purification was recently developed in our laboratory. Presently, no official monograph is provided by the European Pharmacopoeia detailing the analytical conditions to follow for the HPLC analysis of this tracer. Aim of this work was to fill this gap by suggesting - and validating - an HPLC method for the qualitative and quantitative determination of the main possible side-products present in $[^{18}\text{F}]\text{FLT}$ solutions. **Materials and methods.** Standard solutions at different concentrations of thymine (THY), thymidine (TMD), stavudine (D4T), fluorothymidine (FLT) and chlorothymidine (CLT) were prepared in deionized water. CLT was included among the standards, even though not present in our $[^{18}\text{F}]\text{FLT}$ samples, because it is a side product of the synthesis. Analyses were done using an HPLC HP series 1050, associated to a UV/VIS PerkinElmer series 200 set at 267 nm and a Packard Flow One A500 radio-detector, while peak purity assessments were done using a Shimadzu photodiode array detector SPD-M10A VP

and its software Class VP7.2 The chromatographic condition used were: column Rocket Alltima C18 (53 x 7 mm; 3µm); mobile phase: H₂O/EtOH (90:10); flow rate: 1 mL/min; injection: 20 µL. **Results.** The observed retention times for THY, TMD, D4T, FLT and CLT were 2.2, 2.6, 3.5, 6.3 and 13.0 min, respectively, while the obtained resolutions using a mixture containing 1 ppm of each compound were 2.2, 2.2, 3.7, 7.3 and 12, respectively. Peak purity, expressed as “total purity”, TP, is designed to detect the presence of an impurity coeluting with the analyte. All samples showed a TP = 1.0 with the exception of D4T (TP = 0.99). Following the indications reported on the ICH “Validation of analytical procedures: text and methodology” Q2(R1), the chromatographic method was tested for both quantification and detection limits, specificity, linearity, accuracy and precision. The latter, assessed in terms of repeatability and reproducibility, was determined by alternating 3 different operators and carrying out the analyses in different days. The obtained values will be shown in detail on the poster. **Conclusion.** The validation has demonstrated the present method to fulfil all the requirements needed for the correct analysis of [¹⁸F]FLT solutions. **Acknowledgements.** This research has been supported by AIRC Project Molecular and cellular Imaging of Cancer, by PIO Project PET Molecular Imaging and by 5 per mille Project.

P0775

Radiation Dosimetry of (-)-[F-18]-Flubatine - Comparison of animal model data with first-in-man results

B. Sattler¹, M. Kranz¹, M. Patt¹, C. Donat², W. Deuther-Conrad², A. Hiller², S. Fischer², R. Smits³, A. Hoepping³, T. Sattler⁴, P. Brust², J. Steinbach⁵, O. Sabri¹; ¹University Hospital Leipzig, Dept. of Nuclear Medicine, Leipzig, GERMANY, ²Helmholtz Center Dresden-Rossendorf, Research Site Leipzig, Leipzig, GERMANY, ³ABX advanced biochemical compounds, Radeberg, GERMANY, ⁴University of Leipzig, Large Animal Clinic for Internal Medicine, Leipzig, GERMANY, ⁵Helmholtz Center Dresden-Rossendorf, Institute for Radiopharmacy, Dresden-Rossendorf, GERMANY.

Aim: (-)-[F-18]-Flubatine (former NCFHEB) is a new tracer for neuroimaging of alpha4beta2 nAChRs with PET. To assess the putative radiation risk after intravenous application of the radioligand, the biodistribution, organ doses (OD) and the effective dose (ED) were determined in pigs and compared to earlier results in mice and humans [SNM2011 No. 1454, 1459]. **Method:** Whole body dosimetry of (-)-[F-18]-Flubatine was performed in 5 female piglets (age: 44±3.0d, weight: 13.7±1.7kg). The animals were narcotized using 20 mg/kg Ketamine, 2mg/kg Azaperone; 1.5% Isoflurane in 70% N₂O/30% O₂ and sequentially PET-imaged up to 5h post i.v. injection of 186.6±7.4MBq (-)-[F-18]-Flubatine on a SIEMENS Biograph16 PET/CT-system with 7 bed positions (BP) per frame, 1.5 to 6 min/BP, CT-attenuation correction (AC) and iterative reconstruction (OSEM, 4 iterations, 8 subsets). All relevant organs were defined by volumes of interest using the structural information from the AC-CT. Exponential curves were fitted to the time-activity-data (%ID/g, and %ID/organ). Time and mass scales were adapted to the respective human scale. The ODs were calculated using the adult male model with OLINDA. The ED was calculated using tissue weighting factors as published in the ICRP103. **Results:** The highest OD was received by the urinary bladder (49.0±19.4µSv/MBq), the kidneys (39.9±6.14µSv/MBq) and the Pancreas (33.8±31.5µSv/MBq). The highest contribution to the ED was by the urinary bladder (2.0±0.8 µSv/MBq), the stomach (1.5±0.3µSv/MBq) and the lungs (1.5±0.2µSv/MBq). The ED to humans following an i.v. injection of (-)-Flubatine according to this data is 13.1±0.9 µSv/MBq. **Conclusion:** As true for other PET-Tracers too, preclinical incorporation radiation dosimetry underestimates the ED to humans. The ED by (-)-[F-18]-Flubatine yielded from pig- (this study) and mice- (14.2µSv/MBq) studies compared to human dosimetry data (22.6±0.68µSv/MBq) show that animal dosimetry underestimates the potential radiation exposure to humans by 35-37%. This fact needs to be considered in the assessment of the ED to humans in preparation prior to early phase clinical trials. **References:** The trial is granted by Strahlenschutzseminar in Thüringen e.V.

P0776

Novel PET probe derived from Resorufin for imaging neuritic and cerebrovascular Aβ Plaques selectively: [11C]-Methoxy-Res

V. K. Meena, S. Prakash, **P. P. Hazari**, A. K. Mishra; INMAS, Delhi, INDIA.

PET Imaging with [¹¹C]-Methoxy-Res can be used to quantify neural signaling related to neurodegeneration. The aim of this study is to evaluate the cerebrovascular amyloids with recently explored Resorufin. Resorufin is able to bind neuritic plaques as well as to cerebrovascular amyloid deposits in Alzheimer's disease (AD) patients. Early diagnosis and monitoring the amyloid deposits in Alzheimer's disease (AD) patients is crucial for the efficacy determination of newly developed anti-amyloid therapies. To date, precise diagnosis of cerebral amyloid angiopathy requires postmortem pathological brain tissues via brain autopsy. Resorufin as in vivo PET imaging tracer for amyloid show great promise for detecting both neuritic and cerebrovascular amyloid deposits. **Methods:** Synthesis of [¹¹C]-Methoxy-Res was done by the conversion of hydroxyl group to - [¹¹C]OCH₃

with [¹¹C]MeI. ¹¹C-methylation of resorufin was performed by using no carrier added [¹¹C] CH₃I, 3.0µmoles of resorufin, 8.0µmoles of K₂CO₃ in 500µL of DMSO at 65-70°C for 5-10 minutes. Chemical and radiochemical purities were determined by analytical HPLC. Fibrillar nature of amyloid was prepared synthetically using Aβ(1-40) and the aggregated peptide suspension were diluted to 5nM and kept at -80°C until use. Binding studies with synthetic Aβ(1-40) with [C-11] autofluorescence of bound resorufin was performed. In vivo brain uptake studies were done in Male Spargue-Dawley rats and %ID/g of body weight was calculated. **Results:** Radiochemical purity was > 95% and chemical purity was >98% with major chemical impurity was of unlabeled resorufin. Approximately 350-800 MBq of [¹¹C]-methylated resorufin was produced. [¹¹C] methylation of resorufin also changes the Log P_{oct} value of molecule from 0.31 to 0.80 which makes molecule more lipophilic and enhances its ability to cross blood-brain barrier easily. The specific binding of [¹¹C]-methoxy-Res was found to be 70-80% of the total binding in the synthetic aggregates. Microscopic results showed non-specific binding to both neuritic as well as cerebrovascular amyloid deposits at higher concentration and specific binding to cerebrovascular amyloid deposits at lower concentrations. **Conclusions:** Resorufin, the phenoxazine derivative showed a great deal of promise in binding to both neuritic and cerebrovascular amyloid deposits. This molecule showed a class of molecular tracers for PET imaging which specifically bind to amyloid plaques and provide discrimination as well as quantification of cerebrovascular deposits from neuritic plaques when used at lower concentrations. **References:** 1. Han H. B. et al (2011) *Molecular Neurodegeneration* 6:86. 2. Klunk et al (2002) *Journal of Neuropathology and Experimental Neurology*, 61(9), 797-805.

P0777

A versatile synthetic approach to develop a Biotin based PET Imaging agent Via Cu(I) Catalyzed Click Chemistry :68Ga-labeled DO3A-EA-Bis(Tz-Biotin)

S. Prakash¹, P. P. Hazari¹, V. K. Meena¹, A. Mishra²; ¹Institute of nuclear Medicine and Allied Sciences, Delhi, INDIA, ²INCIA, Bordeaux, FRANCE.

Biotin-avidin interaction has been very well known for the two step pre-targeting approach to image tumor sites and it gives high tumor/non-tumor ratios with potential signal amplification. Presenting here a target specific PET agent, 68Ga bound DO3A-EA-BP-Bis(Tz-biotin) which works on a two-step pre-targeting model based on Avidin. 68Ga is an emerging alternative to C-11, F-18 etc., due to its availability from an inhouse generator rendering 68Ga radiopharmacy independent of an onsite cyclotron. We aim to develop a “clickable” derivative of Biotin for its convenient conjugation to the macrocyclic ligand 1, 4, 7-tris(carboxymethyl)-10-(2-di-prop-2-ynyl-amino)-ethyl-1,4,7,10-tetraazacyclododecyl acetic acid (DO3AEA-BP) via incorporation of the highly stable triazole spacer. **Methods:** Synthesis of DO3A-EA-Bis(Tz-Biotin) was carried out by Cu(I) catalyzed click conjugation between biotinylated azide and N, N'-bis(propargylbromoethylamine) terminal alkynyl functionalised DO3A. Then 68Ga radiolabeling was performed using 68Ge/68Ga generator eluate. The pH was adjusted to 5.5 with 0.5 M sodium acetate buffer. The labeling mixture was heated for 30 minutes. Radiolabeled product was analysed and purified through Radio-HPLC. Cytotoxicity was determined using the MTT assay and cell uptake studies were performed using 68Ga-DO3A-EA-Bis(Tz-Biotin) compared with avidin treated cells for 2h. Tumor imaging was performed in U-87 cell line implanted tumor bearing nude mice and uptake of the imaging agent was estimated. **Results:** All compounds have been successfully characterized by NMR and Mass Spectroscopy. More than 96% radiolabeling efficiency was obtained and the radioconjugate exhibited sufficient stability under physiological condition. Preliminary studies in vivo suggested appreciable uptake of 68Ga-DOT3EA-Bis(Tz-Biotin) in U-87MG tumor bearing athymic mice. **Conclusion:** To summarize, a new clickable candidate for imaging containing two biotin units for avidin based two-step pretargeting of tumors has been synthesized and evaluated for diagnostic applications. The DOTA-Bis(Tz-Biotin) possesses high stability in biological environment, exhibits effective interaction with its avidin target giving high signal amplification in tumor area, excellent tumour/non-tumour ratio and low nonspecific retention in vivo.

P0778

68Ga DOTATATE accumulation in sarcoidosis

N. O. Kucuk, **C. Soydal**, E. Ozkan, O. Kumbasar, E. Ibis; Ankara University Medical Faculty, Ankara, TURKEY.

Aim: We aimed in this study to show Ga-68 DOTATATE uptake in relation with disease activity in sarcoidosis cases. **Material and method:** 8 patients with previous diagnosis of sarcoidosis were included to the study. A Ga-68 DOTATATE PET/CT was performed to evaluate of disease activity. PET/CT images were obtained 50 minutes after intravenous injection of at least 100MBq Ga-68 DOTATATE. Ga-68 DOTATATE PET/CT images were evaluated visually. Ga-68 DOTATATE accumulation higher than background mediastinal blood pool activity was considered to be pathological. Disease activity was described clinically by chest disease specialist by evaluation of lung function tests, serum ACE measurements and thorax CT. Correlation between Ga-68 DOTATATE uptake and disease activity was analyzed.

Results: In 3 out of 8 patients who had chronic inactive disease, Ga-68 DOTATATE PET/CT was normal. In the remaining 5 patients with active disease, different degree pathological Ga-68 DOTATATE accumulation was seen in the mediastinal lymph nodes. Additionally, in one patient Ga-68 DOTATATE accumulation was detected in the parotid glands, in one patient in jugular, iliac and inguinal lymph nodes and in one patient both lungs which were accepted disease involvement. **Conclusion:** Ga-68 DOTATATE accumulates in mediastinal, extra-mediastinal lymph nodes and lungs of sarcoidosis cases and Ga-68 DOTATATE accumulation is correlated with disease activity.

P0779

Synthesis of Radiogallium labelled bisphosphonate (68Ga-BPAMD): An agent for bone imaging

S. Lata¹, P. Nanda¹, S. Singla¹, R. Kumar¹, F. Rösch², A. Malhotra¹; ¹All India Institute of Medical Sciences, New Delhi, INDIA, ²Institute of Nuclear Chemistry, University of Mainz, Fritz-Strassmann-Weg 2, Mainz, GERMANY.

Aim : To synthesize 68Ga-DOTA (1,4,7,10-tetraazacyclododecane-1,4,7,10-tetraacetic acid) conjugated bisphosphonate and perform quality control procedures. **Materials and Methods:** 68Ge/68Ga generator (50mCi, itG) was eluted with 5-7ml of 0.05MHCl and the eluant was loaded onto a cation exchanger, Strata-X-C(Phenomenex), to remove the impurities and to preconcentrate. 68Ga was adsorbed onto the cartridge and rest has passed through into the waste. A solution containing 98% acetone / 0.02M HCl was used to desorb the concentrated and purified 68Ga from the Strata-X-C directly into the reaction vial. The reactor contained three concentrations respectively - 50,100 and 150 µg of BPAMD in ammonium acetate buffer to bring the pH between 5.0 and 6.0. Synthesis procedure was carried out at 95°C and at three time intervals 10, 20 and 30 minutes respectively. Once the heating is complete, reaction mixture was cooled and transferred to the product vial. Preparation was sterilized through 0.22µm filter and diluted by adding 2-3 ml saline. All the synthesis steps were carried out in automatic operated PC - controlled synthesis device Modular - Lab, Eckert & Ziegler, Germany. It was completed in 20-40 minutes depending upon the incubation time of the reaction. Quality control tests performed were clarity, pH, radiochemical purity, Rf using SG-TLC plates developed in acetylacetone alone or acetylacetone : acetone : HCl (1:1:0.1) and scanned by TLC scanner. Stability was checked by running chromatograms immediately after the preparation and later at 1, 2, 3 & 4 hrs. **Results:** The labeled preparation was clear having pH - 6.0. The best labeling took place at 95°C, pH 5.0-6.0 for a period of 20 minutes with the concentration of 150µg BPAMD. The 68Ga-bisphosphonate conjugate was prepared with very high radiochemical purity (≥ 99 %) and had Rf = 0.0. There was no free 68Ga. Final Preparation has shown stability upto four hours. **Conclusion:** It is possible to synthesize a novel PET tracer 68Ga-BPAMD with good stability, high radiochemical purity and might be a useful an potential tool for doing bone imaging in patients.

P0780

Comprehensive analysis of Radiochemical Purity of F-18-FDG synthesized by IBA-Synthera.

A. Rehman¹, W. Rafique¹, M. Mehmood¹, M. K. Nawaz¹, H. Bashir¹, Z. S. Faruqi²; ¹Nuclear Medicine Department, Shaukat Khanum Memorial Cancer Hospital & Research Centre., Lahore, PAKISTAN, ²Radiology Department, Shaukat Khanum Memorial Cancer Hospital & Research Centre., Lahore, PAKISTAN.

Introduction: Radiochemical Purity of a radiopharmaceutical is the fraction of total radioactivity in the desired chemical form in the radiopharmaceutical. F18-FDG is the most widely used radiopharmaceutical in the PET-imaging. IBA Synthera module follows Nucleophilic Substitution Reaction using Mannose Triflate as a precursor molecule. The importance of radiochemical purity in medical imaging can be well understood by knowing the fact that the presence of radiochemical impurities in the radiopharmaceutical results in poor-quality images due to high background from surrounding tissues & the blood. It also gives unnecessary radiation dose to the patients. In F18-FDG case European Pharmacopeia gives us some guidelines that radiochemical purity must be 95%. **Aim:** The aim of this study was to analyse radiochemical purity of F-18-FDG synthesised by IBA-Synthera module at Shaukat Khanum Hospital FDG Lab during five hundred productions. **Material & Method:** F18-FDG was synthesized on IBA Synthera module. Two IBA Synthera modules have been installed in PET-Hot Lab of our hospital. All these samples were analysed on Radio-HPLC (Raytest). **Result & Conclusion:** During all these five hundred F18-FDG productions, it was observed that 97.4% from total production-batches were successful. The radio-HPLC data obtained from this study reflected that 366 production-batches had 99% or more radiochemical purity of F18-FDG, 461 productions showed 98% or more, 477 productions showed 97% or more, 482 productions showed 96% or more whereas, 484 productions showed 95% or more radiochemical purity of F18-FDG. Hence, we may say out of five hundred batches on Synthera module, 96.8% batch productions were having the radiochemical purity of F18-FDG equal or more than 95%. **References:** 1. IBA

Synthera user manual FDG 000130/Sep 2007/4 2. Fundamental of Nuclear Pharmacy 4th Edition Gopal B.Saha, 1998. 3. Fluorodeoxyglucose (18F) injection; European Pharmacopeia 6.2.

P0781

Simple and fast procedure of labelling DOTATATE with 86Y and 44Sc.

S. Krajewski¹, I. Cydzik^{2,1}, K. Abbas², A. Bulgheroni², F. Simonelli², U. Holzwarth², A. Majkowska-Pilip¹, A. Bilewicz¹; ¹Institute of Nuclear Chemistry and Technology, Warsaw, POLAND, ²European Commission, Joint Research Centre, Institute for Health and Consumer Protection, Ispra, ITALY.

Aim: Two metallic β⁺-emitters, ⁴⁴Sc (τ_{1/2} = 3.92 h) and ⁸⁶Y (τ_{1/2} = 14.87 h), are prospective radionuclides for diagnostic imaging using PET technique. They can be produced in medical cyclotrons with (p,n) reaction on enriched ⁴⁴Ca/⁸⁶SrCO₃ targets and ⁴⁴Sc additionally from ⁴⁴Ti/⁴⁴Sc generator. The main advantages of these radionuclides are the relatively long half-life and the formation of the “matched pair” with therapeutic radioisotopes, ⁴⁷Sc and ⁹⁰Y, respectively. The proposed separation procedures of ⁴⁴Sc and ⁸⁶Y from target material are usually complicated and time-consuming. The aim of our study was to simplify the DOTATATE labelling procedure using the significant difference in the stability constants of Y/Sr[DOTA] and Sc/Ca[DOTA] complexes. **Materials and methods:** Highly enriched ⁴⁴CaCO₃ and ⁸⁶SrCO₃ (Isoflex, USA) were used as target materials. The irradiations were performed with the Scanditronix MC 40 cyclotron of the Joint Research Centre (Ispra, Italy). Targets of 45 µmol were irradiated for 1-2 h by proton current of 10-30 µA and proton energy of 9 and 16 MeV, respectively. The target materials were dissolved in HCl. ⁴⁴Sc/⁸⁶Y-DOTATATE were synthesised in pH = 6 and 4. The solutions were heated for 30 min at 95 °C and yield of reaction was checked by ITC. Afterwards, the SepPak® C18 column was used to separate labelled bioconjugate from the target material. Labelled DOTATATE was eluted by ethanol. **Results:** The obtained activity of ⁴⁴Sc was around 40 MBq and 22 MBq of ⁸⁶Y at the end of the bombardment. Reaction yield of DOTATATE labelling was ≥ 70% for ⁴⁴Sc and 98% for ⁸⁶Y, when using 31 nmol of the bioconjugate. The SepPak® separation was very efficient and radiochemical purity of obtained ⁴⁴Sc/⁸⁶Y-DOTATATE was ≥ 99%. The effluent containing enriched material can be used for target recovery using (NH₄)₂CO₃ to precipitate the respective carbonates. **Conclusions:** The proposed labelling method is very simple and fast. The best buffer for ⁴⁴Sc labelling is ammonium acetate buffer of pH = 6 and for ⁸⁶Y buffer of pH = 4. The higher labelling yield for ⁸⁶Y is caused by its higher concentration in the reaction mixture. DOTATATE was used as a model molecule and results can be transferred on labelling of other DOTA-bioconjugates. The proposed method can be applicable for PET imaging, but clinical investigation is necessary.

P0782

Radiosynthesis of [18F]Fluoroacetate: Comparison between on-column hydrolysis method and two-pot distillation procedure using a cassette-type multipurpose automatic synthesizer module

S. Kagawa^{1,2}, R. Nishii³, T. Higashi¹, H. Yamauchi¹, Y. Mizukawa⁴, K. Takemoto⁵, E. Hatano⁵, A. Tachibana⁶, K. Takahashi⁶, H. Mizuma⁶, H. Onoe⁶, S. Nagamachi³, K. Kawai², S. Tamura²; ¹Shiga Medical Center Research Institute, Morioka, JAPAN, ²Graduate School of Medical Science, Kanazawa University, Kanazawa, JAPAN, ³Department of Radiology, Faculty of Medicine, University of Miyazaki, Miyazaki, JAPAN, ⁴JFE Technos Corporation, Kanagawa, JAPAN, ⁵Department of Surgery, Graduate School of Medical Science, Kyoto University, Kyoto, JAPAN, ⁶RIKEN Center for Molecular Imaging Science, Kobe, JAPAN.

Objective [¹⁸F]Fluoroacetate ([¹⁸F]FACE) is an analog of [¹¹C]Acetate with a longer radioactive half-life (110 min). FACE is metabolized to fluoroacetyl-CoA and then fluorocitrate. A metabolite of fluorocitrate binds very tightly to aconitase, thereby halting the citric acid cycle. Therefore, it can be a potential tracer for the quantitative evaluation of TCA cycle/membrane metabolism of cancers, heart diseases, and brain. Recently, fully automated synthetic procedures of [¹⁸F]FACE have been developed using a cassette-type multipurpose automatic synthesizer module. The aim of this study was to assess and compare the two automated methods of [¹⁸F]FACE synthesis by on-column hydrolysis and by two-pot distillation procedure using a cassette-type multipurpose automatic synthesizer module. **Methods** Tracer synthesis of [¹⁸F]FACE was performed starting from Ethyl (p-tosyloxy) acetate as a precursor in two ways: on-column hydrolysis and two-pot distillation procedure. After labeling reaction, on the on-column hydrolysis procedure, the reaction mixture was passed through Oasis HLB cartridges. The trapped [¹⁸F]Ethyl Fluoroacetate ([¹⁸F]EFA) was hydrolyzed on-cartridge with sodium hydroxide. While on the two-pot distillation procedure, the reaction mixture was distilled under reduced pressure and trapped by sodium hydroxide, and then hydrolyzed. The crude product was passed through an ion exchange resin, rinsed with water, and then [¹⁸F]FACE was eluted by 0.9% NaCl. **Results** In both ways, [¹⁸F]FACE was successfully radiolabeled using Ethyl (p-tosyloxy) acetate in a

total synthesis time of less than 45 minutes. The radiochemical purity (>99%) and the specific activity (>74 GBq/μmol at EOS) were also satisfactory in both ways. The radiochemical purity (decay uncorrected) was higher in two-pot distillation procedure (62.4±5.0%, n=5) than that in on-column hydrolysis (42.7±0.1%, n=3). **Conclusions** Fully automated synthesis of [¹⁸F]FACE with disposable cassette by two-pot distillation procedure showed stable radiopharmaceutical production with higher radiochemical purity than that in on-column hydrolysis procedure.

P0783

Development of small interfering RNA labeling method using copper-62 and technetium-99m

Y. Nakagami, H. Kuno, T. Kobayashi, K. Shimada, R. Iwata, Y. Kojima, M. Satake; National Cancer Center Hospital East, Chiba, JAPAN.

Aim: Small interfering RNA (siRNA) was discovered as a promising gene silencing tool in research and in the clinic. The finding that exposure to siRNA duplexes shorter than 30 base pairs circumvent activation of the interferon pathway and overall suppression of gene expression enabled the successful use of this technique in mammalian cells. Pharmacokinetic study of siRNA is an important issue for the development of siRNAs for use as a medicine. For this purpose, a novel and favorable radiolabeled siRNA was prepared by Poly(A) Polymerase, ATP and cDTPA, and real-time analysis of siRNA trafficking was performed by using PET or SPECT. **Materials and Methods:** For RNA interference, the 3'-end of double strand 21-nucleotide oligoribonucleotides were added to poly adenines using E. coli Poly(A) Polymerase (E-PAP) and ATP, and was conjugated with cDTPA and subsequently labeled with copper-62 or technetium-99m under strict RNase-free conditions. A target gene is K-ras. The ability of copper-62 or technetium-99m was tested in cultured K-ras-overexpressing cells or non-overexpressing cells. The cellular delivery of copper-62 or technetium-99m-siRNAs could be quantified by gamma counting. The radiolabeled siRNAs were administered to mice with or without K-ras-overexpressing tumors, and differential biodistribution of the label was imaged by PET or SPECT. **Results:** The gene-silencing ability of siRNA does not change after radiolabeling. Radiolabeled siRNAs can be efficiently delivered into cells. Interestingly, the count of K-ras-overexpressing cells was about 20 times as much as non-overexpressing cells. And Radiolabeled siRNAs could acquire stability against RNase by our method. Radiolabeled siRNAs in normal mice were cleared quite rapidly from the bloodstream and excreted from the kidneys; but in contrast, radiolabeled siRNAs in mice with K-ras-overexpressing tumors tended to accumulate in the tumors. **Conclusions:** The instability of siRNA in vivo is serious problem when the siRNA is utilized for a clinical drug. Fortunately radiolabeled siRNAs could acquire stability in vivo by our method. The results of this study might confirm the distribution of siRNAs in target organs as targeted therapies, and could open up a new method of gene imaging in vivo by PET and SPECT.

P27-2 - Tuesday, October 30, 2012, 16:00 - 16:30, Poster Exhibition Area

Radiopharmaceuticals & Radiochemistry: Radiopharmaceuticals - SPECT

P0784

Design, Synthesis and Evaluation of ^{99m}Tc-DO3MP-EA as Bifunctional Bone Imaging Agent

P. Srivastava, K. Chuttani, A. K. Mishra; Institute of Nuclear Medicine and Allied Sciences, Delhi, INDIA.

INTRODUCTION: Malignant tumors form metastases on bone, especially in the advanced stages of prostate, breast and lung cancer. For the better management of bone metastases treatment, chelate should reach the target bone metastases. For that compounds containing phosphonate groups have shown significant potential. In literature 1,4,7,10-tetrakis(methylphosphonic acid)-1,4,7,10-tetraazacyclododecane (DOTMP) has shown good results as bone-seeking agent and exhibits good coordination with metal ions both for diagnostic as well as therapeutic applications.¹⁻⁴ **Aim** of the study was to make three phosphonate groups containing bifunctional tetraaza macrocyclic compound with amine at fourth pendant for loading cytotoxic drugs for therapy compare to its analog DOTMP which is used for bone palliation with Sm-153/ Lu-177. **MATERIALS AND METHODS:** 1,4,7-tris(phosphonomethyl)-10-(2-aminoethyl)-1,4,7,10-tetraazadodecane (DO3MP-EA) was synthesized starting from cyclen. DO3MP-EA was characterized by ¹H NMR, ¹³C NMR, ³¹P NMR and ESI-MS spectroscopy. The compound was coordinated with ^{99m}Tc and its blood kinetics, biodistribution and imaging were performed. **RESULTS:** DO3MP-EA was synthesized in quantitative yield and labeled with ^{99m}Tc with 98% of radiochemical purity. Blood clearance showed a quick washout from the circulation. Biodistribution of ^{99m}Tc-DO3MP-EA was examined in BALB/c mice. The compound accumulated rapidly in bone but no significant accumulation was observed in other non-osseous tissues. The compound was excreted mainly via kidney and accumulation of ^{99m}Tc-DO3MP-EA

in bone was 9.53±1.06 % of injected dose per gram of bone at 1h. Whole-body scintigraphy done on rabbit also showed significant uptake in bone. **CONCLUSION:** ^{99m}Tc-DO3MP-EA showed ideal biodistribution characteristics as a bone-imaging-agent. ^{99m}Tc-DO3MP-EA is better in terms of bone to blood ratio (17.65 at 1h) as compared to ^{99m}Tc-DOTMP (9.06 at 1h)². Amino group present in ^{99m}Tc-DO3MP-EA allows its conjugation with cytotoxic drugs for therapeutic application along with beta emitting radionuclides. **References:** 1) Z. Piskula et al./Inorganica Chimica Acta 360 (2007) 3748-3755 2) Datta et al./Cancer Biotherapy & Radiopharmaceuticals 24 (2009) 123-127 3) I.Svobodova et al./Journal of Alloys and Compounds 451 (2008) 42-45 4) Tu et al./Annals of Biomedical Engineering 39 (2011) 1335-1348

P0785

Preparation of ¹³¹I-Pyrimethamine and Evaluation for scintigraphy of experimentally Toxoplasma gondii infected rats

F. Yurt Lambrecht¹, Tonay Inceboz, Department of Parasitology, Dokuz Eylul University, School of Medicine, Inciralti, Iz, E. Sürücü², O. Yilmaz³, A. Yavasoglu⁴, K. Durkan¹, B. Baykara⁵, R. Bekiş², A. Uner⁶; ¹Institute of Nuclear Science, Izmir, TURKEY, ²Department of Nuclear Medicine, Faculty of Medicine, Dokuz Eylul University, Inciralti, Izmir, Turkey, Izmir, TURKEY, ³Department of Laboratory Animal Science, Dokuz Eylul University, Inciralti, Izmir, Turkey, Izmir, TURKEY, ⁴Department of Histology, Faculty of Medicine, Ege University, Bornova, Izmir, Turkey, Izmir, TURKEY, ⁵Department of Histology, Faculty of Medicine, Dokuz Eylul University, Inciralti, Izmir, Turkey, Izmir, TURKEY, ⁶Department of Parasitology, Ege University, Faculty of Medicine, Bornova, Izmir, Turkey, Izmir, TURKEY.

Aim: To assess the ability of ¹³¹I-Pyrimethamine scintigraphy to detect the lesions of *Toxoplasma gondii* (T. gondii) infection. **Materials and Methods:** An animal model of T. gondii infection was developed. The infected tissues taken from stock infection were implanted into the abdominal cavity of uninfected rats operatively. The success of implantation was controlled 60 days after implantation. Pyrimethamine was radioiodinated with ¹³¹I using the iodogen method. Three infected and two healthy Wistar rats (Rattus norvegicus) were studied. In visual evaluation, first normal ¹³¹I-Pyrimethamine uptake pattern was demonstrated in healthy and infected animals and then was evaluated visually. After injection of 3.7 MBq ¹³¹I-Pyrimethamine intravenously, static images from the whole body and some organs were obtained at 5 and 45 minutes, 2, 6 and 24 hours. Visual and semiquantitative analyses were performed. In semiquantitative analysis, an irregular region of interest (ROI) was drawn over the infected and normal rats' images (brain, neck, diaphragm, liver and total body) as a control. Infected/control ratios for organs were calculated using the mean counts. **Results:** ¹³¹I-Pyrimethamine was accumulated in the thyroid, stomach, liver, bladder and soft tissues of the infected and normal rats. In the visual evaluation, it was noticed that there was slightly increased ¹³¹I-Pyrimethamine uptake in the liver of the infected rats according to control. Although there is no statistically difference in mean counts between the infected and healthy rats, the ratio for mean counts of infected rats to the control rats in the liver and diaphragm were over 1 at the 2 hours images and later. **Conclusion:** In conclusion, ¹³¹I-Pyrimethamine might be useful as an agent for diagnosis of toxoplasmosis infection especially involvement of liver and diaphragm. Imaging at 2 and 6 hours seems to be more suitable imaging time for the diagnosis of toxoplasmosis.

P0786

Synthesis of [¹³¹I]iodo Tyrosin Conjugated Nanocomposites

J. Park¹, S. Park², M. Hur¹, S. Yang¹, H. Jung², K. Yu²; ¹Korea Atomic Energy Research Institute, Jeongseup-si, KOREA, REPUBLIC OF, ²Dongguk University, Seoul, KOREA, REPUBLIC OF.

Recently, the design and synthesis of surface modified nanoparticles have been of great interest because of their potential applications in nanobiotechnology. Among various nanoparticles, iron oxide is predicted to have important application in biosensing, drug delivery, and magnetic resonance imaging (MRI). More recently, tremendous effort has been expended in the application of surface modified magnetic nanoparticles as a multimodal imaging agents for positron emission tomography (PET) / computed tomography (CT) or PET / MRI systems. Specially, combined imaging system of single photon emission computed tomography (SPECT) / MRI provides more clearly diagnostic images. In this study, we have successfully developed 3-iodo-tyrosine conjugated Fe₃O₄@SiO₂ nanocomposites as a novel imaging agent for simultaneous detection of tumor in SPECT and MRI. Monodispersed Fe₃O₄ nanoparticles were synthesized through thermal decomposition of Fe(acac)₃ (acac=acetylacetonate) and Fe₃O₄@SiO₂ core shell structure was prepared by reverse microemulsion. After aminopropyl triethoxysilane modification on the surface of obtained nanocomposites, L-tyrosine molecules were introduced by simple amide coupling method. Finally, surface attached L-tyrosine molecules are labelled to 3-¹³¹I-iodo-L-tyrosine by aromatic iodination with Na¹³¹I. The physicochemical characterizations (XRD, TEM,

FT-IR, TG, Elemental analysis, γ -ray detection, and SQUID) on obtained nanocomposites have been carried out. This bifunctional imaging agent may allow for earlier tumor detection with a high degree of accuracy and provide further insight into the molecular mechanisms of cancer.

P0787

Synthesis, characterization and radiolabeling of DTPA-doxorubicin complex.

P. Kumar¹, **B. Singh**¹, **P. Acharya**², **R. Bansal**², **A. Ghai**¹, **D. Dhawan**³, **B. Mittal**¹; ¹Department of Nuclear Medicine, Postgraduate Institute of Medical Education and Research (PGIMER), Chandigarh, INDIA, ²University Institute of Pharmaceutical Sciences, Panjab University, Chandigarh, INDIA, ³Center for Nuclear Medicine, Panjab University, Chandigarh, INDIA.

Aim: To synthesize, characterize and radiolabel doxorubicin using cyclic diethylenetriaminepentaacetic acid anhydride as bifunctional ligand. **Materials and Methods:** The labeled anticancer drug (doxorubicin) can be used as a tool for the early detection of cancer. A new method is described for synthesis of the DTPA-doxorubicin conjugate complex. Cyclic diethylenetriaminepentaacetic acid (DTPA) anhydride was acylated with α,α -dichloromethyl methyl ether to conjugate with doxorubicin. 200 mg (0.56 mmol) of cyclic DTPA anhydride was dissolved in 2 ml of dichloromethane followed by addition of 100 μ l α,α -dichloromethyl methyl ether and mixture was stirred up to 40 min at room temperature. The excess of chlorinating agent was evaporated under vacuum. 50 mg of doxorubicin in 5ml of dichloromethane was added to the mixture and stirred at room temperature for overnight. The dichloromethane was vacuum evaporated and dark red precipitate was obtained. 2 mg of conjugate complex was dissolved in 1 ml Dimethylsulphoxide (DMSO) followed by addition of 100 μ g of stannous chloride. 500 μ Ci of ^{99m}Tc was added to the mixture and incubate at room temperature for 15 min. The formation of product was characterized by thin layer chromatography (TLC), melting point, ¹H-NMR. RadioTLC. The ^{99m}Tc-DTPA-doxorubicin was subjected to quality control tests and organ distribution was estimated by injecting 10.0-12.0 MBq radioactivity in to the penile vein in male Wistar (n=9) rats. The animals were sacrificed and the radioactivity biodistribution was estimated in different organs at different time (1h, 4h and 24h) intervals. **Results:** The melting point of the formed complex was 220-240 °C. Labeling efficiency of the radioligand was observed to be 95.0% and stable up to 24h. The protein binding was about 85%. The biodistribution studies showed that maximum uptake of the radiotracer in kidneys followed by spleen and liver at 4 h and activity washed out from lungs within 1 h. **Conclusions:** The use of bifunctional ligand like DTPA can be used effectively for radiolabeling of doxorubicin with ^{99m}Tc. The resultant radio-complex showed good labeling efficiency and stability. The localization of the radiolabeled doxorubicin in the tumor will indicate a good response to this agent and can be used in treatment response monitoring.

P0788

Radiolabeling, characterization and biodistribution studies of PAMAM dendrimers

A. Ghai¹, **B. Singh**¹, **P. Kumar**¹, **D. Dhawan**², **B. Mittal**¹; ¹Department of Nuclear Medicine, Postgraduate Institute of Medical Education and Research (PGIMER), Chandigarh, INDIA, ²Center for Nuclear Medicine, Panjab University, Chandigarh, INDIA.

Aim: To radiolabel and characterize the fourth generation of Poly(amido-amine) dendrimers (PAMAM-G4). **Materials & Methods:** The structure and tunable surface functionality of dendrimers allows for the encapsulation/conjugation of multiple entities. Their uptake increase at the site of tumor due to enhanced permeability and retention effect. Fourth generation PAMAM dendrimers (Sigma-Aldrich, USA) were labeled with pertechnetate (^{99m}TcO₄⁻) using a direct labeling technique. 50.0 μ l of dendrimers was diluted in 0.5 ml of normal saline. The concentration of stannous chloride was standardized by using various concentrations (20, 30, 40 & 100 μ g) of SnCl₂·2H₂O and chromatography was performed to analyze the labeling efficiency. Finally, 30 μ g of stannous chloride was found to be sufficient for adequate reduction of pertechnetate. The resultant radioligand (^{99m}Tc-PAMAM) was subjected to quality control tests like labeling efficiency, serum, and in vitro stability. The organ biodistribution was estimated by injecting 20.0 MBq radioactivity in to the penile vein of male Wistar (n=12) rats. The animals were sacrificed and the radioactivity biodistribution was estimated in different organs at different time (1h, 4h, 24h) intervals. **Results:** The dendrimers were labeled with efficiency of 97 \pm 1.5%. The labeled complex was stable up to 24h with a negligible degradation (2.5 \pm 0.5 %). Serum stability was estimated to be greater than 95%. The organ bio-distribution data showed maximum uptake in liver followed by spleen at 4 h. **Conclusion:** The dendrimers were conveniently labeled due to presence of amine group on the surface and form stable radio-complex. The radiolabeled dendrimers localized in the liver and therefore radiolabeled drug loaded dendrimers can be used to evaluate the retention time and biodistribution of the drug at the tumor site.

P28-2 - Tuesday, October 30, 2012, 16:00 - 16:30, Poster Exhibition Area

Radiopharmaceuticals & Radiochemistry: Radiopharmacy

P0789

Ion exchange processes in HCl-ethanol media for high-purified ⁶⁸Ga solutions

G. Kodina, **A. Larenkov**, **E. Lesik**; Burnasyan Federal Medical Biophysical Center, Moscow, RUSSIAN FEDERATION.

⁶⁸Ga obtained from ⁶⁸Ge/⁶⁸Ga generator is one of the most promising for the synthesis of radiopharmaceuticals (RP) for PET. The presence of metallic cations (e.g. Fe³⁺, Zn²⁺) in the eluate of generator prevents the formation of ⁶⁸Ga³⁺-complexes. Furthermore breakthrough of ⁶⁸Ge (~ 10⁻³%), large volume of eluate (5÷10 ml) and its acidity requires concentration of eluate for peptide labeling. Thus, purification and concentration of the ⁶⁸Ga-eluate before labelling is necessary. In most of the methods described in the literature, acetone and/or concentrated HCl are used, which can often be undesirable for ⁶⁸Ga-RP synthesis. **The aim** of the study was to investigate the ⁶⁸Ga ion exchange behavior in HCl-ethanol media for to design the method of purification and concentration of ⁶⁸Ga solutions. **Results:** ⁶⁸Ga from the ⁶⁸Ge/⁶⁸Ga generator (Cyclotron Ltd., Obninsk) eluate (0.1M HCl) quantitatively sorbed on cation exchange resin (Dowex 50W×8). Part of the non-isotopic carrier, and ⁶⁸Ge passes through the resin. The greater part of the non-isotopic carriers sorbed on the cation exchange resin, can be quantitatively eluted with the mixture of HCl/ethanol (0.5M HCl/70% ethanol) at which ⁶⁸Ga is not eluted. The ⁶⁸Ga-distribution coefficient K_d is ~ 8.6·10³. After washing, ⁶⁸Ga was completely and almost selectively eluted from the resin with a mixture of HCl/ethanol - 2.5M HCl/50-55%. In the subsequent interaction of the obtained eluate with strong anion exchange resin (Dowex 1×8) quantitative sorption of ⁶⁸Ga takes place (K_d ~ 9.3·10²). The resin was dried with air or inert gas. ⁶⁸Ga was eluted from the resin with 0.02-0.1M HCl (K_d ≤ 10⁻¹). The cleaning process takes 15 min. The process yield with decay correction is 90±5%. The minimum volume of final solution was 200-250 μ l. Production of purified and concentrated solution of ⁶⁸Ga chloride complexes in 0.02 - 0.1M hydrochloric acid significantly simplifies the process of synthesis of the RPs, as it becomes possible to use freeze-dried forms of precursor, without any subsequent purification. 1 ml concentrated and purified solution ⁶⁸Ga (293 MBq) was added to the freeze-dried composition (10 mg sodium acetate and 20 μ g of the DOTA-conjugated peptide). The vial was thermostated at 95°C for 10 min. The yield was more than 99% (radio-TLC and HPLC). **Conclusion:** Designed method is allows obtaining of concentrated ⁶⁸Ga-solutions with high chemical and radiochemical purity in 0.02 - 0.1M HCl medium without any organic solvents, that enables the use of standard procedures "lyophilizate-conditioned eluate" for any ⁶⁸Ga-RP synthesis.

P0790

"Hospital Radiopharmacy under new rules in Brazil: RDC-38"

M. F. de Barboza, **S. A. Nogueira**, **G. C. Campos Neto**, **L. Y. I. Yamaga**, **A. Osawa**, **J. C. S. Oliveira**, **M. L. da Cunha**, **A. F. Thom**, **J. Wagner**, **M. B. G. Furnari**; Hospital Albert Einstein, São Paulo, BRAZIL.

Introduction: the radiopharmaceuticals are considered a special group of medicine and its preparation and use are regulated by a number of recommendations or rules adopted in many countries. The development of ⁹⁹Mo/^{99m}Tc generators and lyophilized kits contributed for an easy and fast preparation of ^{99m}Tc compounds in hospital radiopharmacies. The evolution is attributable to the existence and chemical versatility of ^{99m}Tc and its ideal radionuclide characteristics: adequate for preparing the radiopharmaceutical, performing its quality control, and injecting into the patient. Radiopharmaceutical products must be of high routine radiochemical purity (RRP) just before clinical application, because the impurities result in poor quality of image leading to an erroneous interpretation or diagnosis. The operational level of the radiopharmacy and the dispensing area should be a separate, dedicated, secure and close to the imaging and injection areas. **Objective:** the aim of this work is to implement and validate the quality control assays of radiopharmaceuticals (lyophilized kits) labeled with Tc-99m, using different chromatographic systems, determining the most reproducible and faster assay for radiochemical quality control in routine, in accordance to the resolution (RDC-38) of Brazilian Health Authorities-ANVISA. **Material and methods:** radionuclide purity test of ⁹⁹Mo was performed on the first elution from ⁹⁹Mo/^{99m}Tc generator, as well the radiochemical assay, using Whatman3MM chromatography paper in 85% methanol, the pH and the aluminum ion contamination were determined before labeling process following manufacturer's instructions. Radiochemical purity tests of the different "kits" labeled with Tc-99m were performed, using different chromatographic systems: 1) solvent extraction or partition method, 2) solid extraction phase (Sep-Pak filter), 3) TLC and 4) paper Whatmann 3MM (10 x 1cm), in different mobile phases. Personnel involved in production, quality control tests and release of final products were trained in radiopharmaceutical specific aspects. Adverse events related to the radiopharmaceuticals have been carefully reported.

Results: since January to March of 2012, more than 160 ^{99m}Tc -IPEN generators and 347 “kits” (MDP; MIBI; DTPA; DMSA; MAA; ECD; Hynic-Toc, etc.) labeled with ^{99m}Tc were analysed. All the analyzed batches of each “kits”, showed an acceptable pH values and chemical, radionuclide and radiochemical purity higher than 90 %, before dose administration. Conclusion: the paper chromatography and solid extraction phase system were acceptable for RRP tests. The results provided a practice-oriented guidance to the group involved in the preparation and quality control of radiopharmaceuticals. A comprehensive RRP quality control program were developed and validated at “Albert Einstein Hospital Radiopharmacy”.

P0791

Large-scale Centralized Radiopharmacies: Is There Any Reason for Concern? An Insight into ^{99m}Tc -radiopharmaceuticals Adsorption and Stability

P. Costa¹, L. Cunha¹, T. Oliveira¹, A. Rebelo¹, A. Nunes², M. Milhães², E. Botelho², J. A. Silva³, R. Castro³, L. Pires⁴, M. Faria João⁴, L. F. Metello¹; ¹Nuclear Medicine Department, High Institute for Allied Health Technologies, Polytechnic Institute of Porto, ESTSP.IPP, Vila Nova Gaia, PORTUGAL, ²Nuclear Medicine Department, Instituto CUF, Porto, PORTUGAL, ³Nuclear Medicine Department, Hospital Geral de Santo António, Centro Hospitalar do Porto, Porto, PORTUGAL, ⁴Diaton, Centro de Tomografia Computorizada, SA, Coimbra, PORTUGAL.

Introduction: Worldwide, regulatory issues related to the field of radiopharmacy are switching and turning each day more rigid. Due to these legal constraints and all the related economical consequences, the concept of large-scale radiopharmacies, that label and distribute radiopharmaceuticals in a ready-to-use form, disseminate widely and seem more and more attractive, even in usually less receptive countries. In such a context, issues as the appropriate choice for recipient/methodology (vial or syringe? Multi- or Monodoses?) as well as the adoption of distinct behaviors should be considered relevant. Aim: It is aimed to disseminate the results obtained on a large study performed to evaluate whether there is any correlation between factors as syringe volume, residence time and type of radiopharmaceutical with adsorbed fraction and stability. Material and Methods: The most widely used radiopharmaceuticals (^{99m}Tc -Tetrofosmin/ ^{99m}Tc -Sestamibi, ^{99m}Tc -MAG3/ ^{99m}Tc -DTPA and ^{99m}Tc -MDP/ ^{99m}Tc -HDP) were labeled strictly according to manufacturer's instructions. After radiolabelling, single-doses of each radiopharmaceutical were collected into 1 ml and 2 ml plastic syringes, from the same commercial brand with increasing residence times on the syringes (0.5, 1, 2, 3 and 6 hours). The degree of adsorption to the syringes walls was determined after a real or simulated injection and the activity present at the empty syringes was recorded. Regarding radiochemical stability, the reference sample was the one withdrawn directly from the original vial and subsequent aliquots were tested for each time-point from the syringes immediately before radiopharmaceutical injection. Radiochemical purity was assessed by thin-layer chromatography, according to manufacturer's or EU Pharmacopeia instructions. Student's t-Test was used to evaluate differences between means from independent groups (stability on Syringe vs stability on Vial; adsorption on 1ml syringes vs adsorption of 2ml syringes) and Pearson's Test to measure the association between adsorption and time of retention inside the syringe. Results: Adsorption to plastic material of syringes varies significantly depending on the radiopharmaceutical. As an example, it is presented here the retention fraction for the most frequent situation: 1 ml syringe and 30 minute residence time: 0.65% for ^{99m}Tc -MDP, 2.15% for ^{99m}Tc -DTPA, 8.32% for ^{99m}Tc -MAG3 and 17.9% for ^{99m}Tc -tetrofosmin. Conclusion: Results demonstrate that adsorption of radiopharmaceuticals to plastic material of syringes should be a topic of concern on the daily practice as this can lead to misdiagnosis due to the administration of activities inferior to the ones needed to obtain good diagnostic information. This can have a major impact on Centralized Radiopharmacies, so special attention should be paid.

P0792

Sex Influence in the Cut-Off Age for the Indexed Glomerular Filtration Rate Values

R. Pérez Pascual, B. Martínez de Miguel, B. Santos Montero, M. de Gregorio Verdejo, E. Martínez Montalbán, L. Martín Curto; Hospital Universitario La Paz, Madrid, SPAIN.

AIM For patients under the age of 12, there is a dispersion in the values of Glomerular Filtration Rate (GFR) indexed to Body Surface Area (GFR_{BSA}) or Extracellular Fluid Volume (GFR_{ECFV}). The aim of this study is to evaluate the influence of sex variable on the cut-off age for the dispersion of GFR_{BSA} and GFR_{ECFV} . PATIENTS AND METHOD A retrospective analysis with 664 males and 284 females aged 0 to 85, with renal pathology was conducted. 1.11 MBq of ^{51}Cr -EDTA was administered in bolus injection to children under 16 years, 1.11 or 2.22 MBq (adjusted to weight) between 16 and 18 years, and 2.22 MBq for patients over 18 years. GFR measurements were obtained through the Ham and Piepsz's equation

(children) or Christensen and Groth's equation (adults). The results were indexed to GFR_{BSA} and GFR_{ECFV} . The difference between the GFR_{BSA} and GFR_{ECFV} values was used as dependent variable. RESULTS Results obtained from the analysis of ROC curve for the cut-off points in the dispersion of GFR values were as follows: in males, 11.38 years (12 years), sensitivity: 0.858 and specificity: 0.854. Area: 0.911 (95% Confidence Interval -CI-): 0.883-0.938). In females, 10.69 years (11 years), sensitivity: 0.744 and specificity: 0.866. Area: 0.880 (95% CI: 0.836-0.924). Nevertheless, in case of 11.98 years (12 years), sensitivity and specificity did not differ significantly (sensitivity: 0.811 and specificity: 0.773). The Pearson correlations for males were as follows: < 12 years, 0.958 (95% CI: 0.946-0.967), ≥ 12 years, 0.983 (95% CI: 0.979-0.986). And in the case of females, the results were: < 11 years, 0.966 (95% CI: 0.949-0.977), ≥ 11 years, 0.982 (95% CI: 0.976-0.986). These results were similar when taking 12 years as a cut-off point for females: < 12 years, 0.965 (95% CI: 0.948-0.976) and ≥ 12 years: 0.983 (95% CI: 0.977-0.987). CONCLUSION We can assume the same cut-off age point for males and females for the dispersion of the GFR_{BSA} and GFR_{ECFV} values.

P0793

Stability Study of Y-90 Labeled Resin Microspheres in Plasma, Pharmaceutical Vehicles and Contrast Media

M. Ben Reguiga¹, P. Fontaine¹, M. Abdel-Rehim², A. Sibert², A. Dieudonne³, D. Leguludec³, V. Vilgrain², R. Lebthah², N. Pons-Kerjean¹; ¹Radiopharmacy Unit, Beaulieu Hospital (APHP-HUPNVS), Clichy, FRANCE, ²Radiology Department, Beaulieu Hospital, Clichy, FRANCE, ³Nuclear Medicine Department, Beaulieu Hospital, Clichy, FRANCE.

Introduction Yttrium-90 labeled resins microspheres (RMS/Sir-Spheres[®], Sirtex) are used in inoperable liver cancer. They consist in a sulfonated ions exchange resin that bounds $^{90}\text{Y}^{3+}$ ions. Given the ionic nature for their chemical bonding, these ions may be displaced by competition. This may be due to the presence in the media of cations having greater affinity for sulfonate groups or to the presence of negative-charged ligands that show higher affinity to Y^{3+} ions than sulfonates. The aim of this study was to assess in presence of such competing conditions, the stability of RMS in human plasma, in different pharmaceutical vehicles and contrast media used in radiology. Materials and methods RMS were placed in contact with 5 pharmaceutical vehicles (Water-for-injection, NaCl-0.9%, Glucose-5%, Sodium-Bicarbonate-4.2%, Lactate-Ringer), 3 contrast agents (Xenetix[®] 350mg/mL, Iomeron[®] 250mg/mL, Visipaque[®] 320mg/mL) and human plasma. 20 μL aliquots of microspheres were incubated for 1hour in 1mL of each media, at room temperature or at 37°C for plasma. Samples were then centrifuged (3000rpm/10 min), the supernatant containing unbound Y-90 was collected. Spheres pellet was then completely dissolved in 1mL of $\text{H}_2\text{SO}_4/\text{DMSO}$ (50:50). Radioactivity present in each sample (dissolved pellet and supernatant) was then counted in a gamma counter [Perkin-Elmer-1470] previously calibrated for Yttrium-90. To increase *bremsstrahlung* emissions yield, samples were stored and counted in glass tubes. Results were expressed as a percentage of bound Y-90 (F%) persistent on spheres ($n=6/\text{media}$). Results and Discussion RMS were stable in water, saline, glucose and human plasma with a residual bound activity around 99%. Bound $^{90}\text{Y}^{3+}$ rates decreased significantly in sodium bicarbonate (F%=81.8 \pm 1.6%) and Ringer Lactate (F%=77.2 \pm 2.2%), suggesting a potential chelation and displacement of $^{90}\text{Y}^{3+}$ by bicarbonates and lactates. Results with contrast agents were different. Incubation with Iomeron[®] gave variable rates of bound Y-90 ranging from 70% to 95%. Interestingly, microspheres incubation with Xenetix[®] and Visipaque[®] showed an original chemical reaction taking place immediately after incubation and consisting in microspheres dissolution and the genesis of a new immiscible liquid layer. Dissolved RMS became non-extractable and their radioactivity non countable. This reaction evokes similar reported interactions of Lipiodol, another iodinated contrast agent, known to be incompatible with plastics and to induce their degradation. Conclusion Conventional vehicles (water, NaCl 0.9% and Glucose 5%) are compatible with RMS, unlike Ringer lactate and bicarbonate solutions. RMS remained also stable in human plasma. However, contrast media show incompatibility with RMS, and their co-administration may affect spheres integrity and change their biodistribution and efficacy.

P0794

Adsorption of radiopharmaceuticals to plastic syringes : measurement and consequences

M. Rannou¹, N. Lheureux¹, T. Prangere¹, J. Legrand¹, D. Huglo²; ¹CHRU de Lille - Radiopharmacy- Nuclear Medicine, Lille, FRANCE, ²CHRU de Lille - Hopital Huriez- Nuclear Medicine, Lille, FRANCE.

Aim: The aim of this study was to measure the residual activity after injection of the radiopharmaceuticals used in our department and to determine actions to be taken according to their importance. Materials and methods: For the 24 radiopharmaceuticals studied, a measure was made in the same conditions just before and just after injection for at least 10 samples. The time between the two measures was negligible, no correction of the results was necessary in terms of radioactive decay. Syringes having a significant residual volume, greater than 5% of

the initial volume, were excluded from the study. **Results:** The residual activity was lower than 5% corresponding to the dead space of the syringe for ^{18}F FDG, ^{18}F Na, ^{18}F -DOPA, ^{18}F -Choline, ^{18}F Flortetaben, Ibritumomab tiuxetan ^{90}Y , Norcholesterol- ^{131}I , ^{123}I -MIBG, ^{67}Ga citrate, ^{153}Sm -Quadramet, ^{111}In labelled platelets, ^{51}Cr -labelled red blood cells and $^{99\text{m}}\text{Tc}$ -HMPAO-labelled leucocytes. For these radiopharmaceuticals, no problem was identified, in particular for those used in therapeutic. The residual activity was between 5% and 10% for $^{99\text{m}}\text{Tc}$ -DPD, $^{99\text{m}}\text{Tc}$ -MIBI, $^{99\text{m}}\text{Tc}$ -mebrofenine, ^{123}I -Iodine, $^{99\text{m}}\text{Tc}$ -HMDP, $^{99\text{m}}\text{Tc}$ -DTPA, $^{99\text{m}}\text{TcO}_4^-$ and $^{99\text{m}}\text{Tc}$ -colloids, and the residual activity was 10% for $^{99\text{m}}\text{Tc}$ -DMSA. For these radiopharmaceuticals we used to prepare an activity a little bit higher than the prescribed dose. The residual activity was greater than 15% for $^{99\text{m}}\text{Tc}$ -MAA and ^{111}In -pentetate. This residual activity is important and can have consequences for the quality of the scintigraphy. To reduce this effect of adsorption, we tested a dilution of the initial volume with NaCl 0.9% from a volume of 1 mL. By this way, we obtained a residual activity around 10%. The lowest residual activities can be explained with PET tracers because of a systematic flushing after automatic or manual injection. In the literature, the adsorption of $^{99\text{m}}\text{Tc}$ -MAA was already reported but it wasn't reported for ^{111}In -pentetate. **Conclusion:** Most of the radiopharmaceuticals used in our department don't have significant residual activities. For $^{99\text{m}}\text{Tc}$ -MAA and ^{111}In -pentetate a dilution of the radiopharmaceutical with NaCl 0.9% could be recommended. For the others, the preparation of an activity slightly greater (5 to 10%) allows to inject the patient with the prescribed activity.

P0795

Preparation and radiochemical purity control of $^{99\text{m}}\text{Tc}$ - MAG3

R. Rebic, Slobodanka Beatovic, Vladimir Obradovic; Clinical Center of Serbia; Center for nuclear medicine, Belgrade, SERBIA.

Introduction: $^{99\text{m}}\text{Tc}$ - MAG3 used for renal scans, is prepared via a kit formulation and can contain a number of different radiochemical impurities. Especially when used for quantification of renal clearance high radiochemical purity (RCP) is recommended and can vary a boiling step is included in the preparation. HPLC analysis and SPE using SepPack C18 cartridges is recommended by the manufacturer to determine the RCP. **Aim:** The purpose of this study was to determine the RCP of $^{99\text{m}}\text{Tc}$ - MAG3 using an alternative method based on ITLC chromatography suitable for routine use in hospital setting and to compare different batches of MAG3, keeping in mind that recent batch variations have been reported. **Materials and methods:** Preparation of $^{99\text{m}}\text{Tc}$ - MAG3 were done in accordance with the instruction of the manufacturer (Mallinckrodt Medical) using $^{99\text{m}}\text{TcO}_4$ 1110MBq in the volume of 1 mL, diluted to a volume of 10mL and heat during 10 min in boiling water and cooled down in a water bath to room temperature. A simple alternative based on ITLC-SG, Gelman Sciences, strips 1,5 X 10cm, at a 1 cm mark was used for determination of RCP. The strips were developed in a mobile phase A of Butanone/Ethylacetate (2: 3) until the solvent front had reached the 7-8 cm marks. This mobile phase was used to determine the amount of free $^{99\text{m}}\text{TcO}_4$ (Rf=1) and $^{99\text{m}}\text{Tc}$ - MAG3 complex and $^{99\text{m}}\text{Tc}$ - colloid (Rf = 0,1-0,2). Second mobile phase B: 50% acetonitrile (ACN) was used to determine $^{99\text{m}}\text{Tc}$ - colloid (Rf = 0) Rf values for free $^{99\text{m}}\text{TcO}_4$ and $^{99\text{m}}\text{Tc}$ - MAG3 complex were at (Rf = 0,8- 1,0). Strips were cut and count, rates of the lower and upper parts (every 1cm), were determined in a Autogamma counter-LKB. **Result:** In total number of different kit batches (in total 37 preparations) were tested over 1 year. None of the preparations failed under the RCP values of 90% (range: 92 -95 %) with a mean RCP of 93%+- 1,8 (n=37). No significant differences between kit batches were observed. **Conclusion:** Recommended RCP methods based on HPLC or SPE cartridges, are not everywhere available in a clinical setting. The QC of RCP by ITLC as described above is a rapid procedure, generates an easy accessible profile and hence provides sufficient information for a fair estimate of labeling efficiency of the preparation. Generally for routine RCP testing ITLC method is very suitable method.

P0796

Comparison of Response of Radionuclide Calibrators to Yttrium-90 in 10-mL Dose Vial

J. T. Cessna; NIST, Gaithersburg, MD, MD, UNITED STATES.

The National Institute of Standards and Technology (NIST) conducted and participated in a comparison exercise with the assistance of the National Association of Nuclear Pharmacies and a commercial radionuclide supplier. Participants consisted of nuclear medicine facilities at both hospitals and commercial radiopharmacies. The aim was to compare the response of similar calibrator models to identical source geometries. **Methods:** The test-sample geometry for the exercise was chosen to represent one used in the preparation of ^{90}Y -ibritumomab tiuxetan. The geometry was 10-mL ^{90}Y solution in a 10 mL reaction vial. Sources were prepared and distributed by a commercial radioisotope manufacturer. Participants were requested to record the readout of their radionuclide calibrator over a range of calibration settings, covering settings giving a response both above and below their estimate of the source activity. Test

samples were returned to NIST for activity determination. **Results:** A total of 30 optional exercises were completed by 9 participants. The optional exercise was also completed at NIST for 4 radionuclide calibrators. Radionuclide calibrators from commercial manufacturers Capintec (8 models) and Biodex (1 model) are represented in the results. Instrument responses are compared graphically and calibration factors are derived from the results. Instrument response varied over a large range. A majority were within 10% of the average. However manufacturing tolerances are reported as $\pm 2-3$ percent. **Conclusions:** Although radionuclide calibrators are supplied with calibration settings, these settings should be individually validated by the user. Both variations in instrument response and use of incorrect or inappropriate calibration setting can lead to errors in activity measurement.

P0797

Nanotoxicology by Imaging Molecular Biodistribution of Radiolabelled Polymeric Nanoparticles

M. Sánchez-Martínez¹, P. Ojer², M. Collantes³, C. Caicedo⁴, G. Quincoces¹, J. A. Richter⁴, A. López de Cerain⁵, J. M. Irache⁶, I. Peñuelas⁷; ¹Radiopharmacy Unit, Department of Nuclear Medicine, Clínica Universidad de Navarra, Pamplona, SPAIN, ²Department of Pharmaceutics and Pharmaceutical Technology, University of Navarra and Toxicology Unit. Center for Applied Pharmacobiological Research, University of Navarra, Pamplona, SPAIN, ³Micro-PET Research Unit, CIMA-CUN, Pamplona, SPAIN, ⁴Department of Nuclear Medicine, Clínica Universidad de Navarra, Pamplona, SPAIN, ⁵Toxicology Unit. Center for Applied Pharmacobiological Research, University of Navarra, Pamplona, SPAIN, ⁶Department of Pharmaceutics and Pharmaceutical Technology, University of Navarra, Pamplona, SPAIN, ⁷Radiopharmacy Unit, Department of Nuclear Medicine, Clínica Universidad de Navarra and Micro-PET Research Unit, CIMA-CUN, Pamplona, SPAIN.

Toxicity studies (OCDE guides 407, 425) of conventional polymeric Gantrez® (NP), cyclodextrin (HPCD-NP) and pegylated (PEG-NP) nanoparticles have shown no toxicity (LD50>2000mg/kg) when they are administered orally but a slight toxicity after intravenous administration. Besides, the magnitude of this intravenous toxicity was different depending on the nanoparticles (HPCD-NP>PEG). **AIM:** In order to gather additional information in a nanotoxicity study after intravenous administration of the different nanoparticles (NP, HPCD-NP and PEG-NP), our purpose was to carry out the radiolabelling with $^{99\text{m}}\text{Tc}$ and perform *in vivo* gammagraphy/SPECT-CT biodistribution studies along with measurements of the radioactivity of the collected organs in a gamma counter. **MATERIAL & METHODS:** 1 mg of the different NP formulations was labelled with 56 MBq of $^{99\text{m}}\text{Tc}$ previously reduced with stannous chloride. Biodistribution studies were carried out in Wistar rats (n=13). The first group (n=4) received i.v. $^{99\text{m}}\text{Tc}$ -NP, $^{99\text{m}}\text{Tc}$ -HPCD-NP, $^{99\text{m}}\text{Tc}$ -PEG-NP or $^{99\text{m}}\text{TcO}_4$ and gammagraphic images were acquired continuously during 5 hours (1 dynamic study + 6 consecutive SPECT-CT). The dynamic study was analyzed drawing ROIs and uptake curves whereas SPECT-CT data were exported to PMOD program and VOIS were drawn on CT images for quantification. In the second group (n=9) 5 hours after intravenous administration of $^{99\text{m}}\text{Tc}$ -NP, $^{99\text{m}}\text{Tc}$ -HPCD-NP or $^{99\text{m}}\text{Tc}$ -PEG-NP animals were humanly killed and organs collected to measure their radioactivity in a gamma counter. **RESULTS:** Taking into account the quantitative analyses of the VOIS, the comparison of the uptake curves and data from *ex vivo* experiments it is possible to show the different biodistribution of the nanoparticle formulations. Imaging studies demonstrated that, at short acquisition times the highest activity is accumulated either in liver (NP), kidneys (HPCD-NP) or lungs (PEG-NP) but at long acquisition times the differences among formulations decrease significantly. *Ex vivo* biodistribution studies at 5 hours after intravenous administration show few differences among the formulations, thus supporting what we had previously seen by imaging. **CONCLUSION:** Differences showed at short acquisition times by *in vivo* biodistribution studies (due to the modifications of the different ligands loaded in the nanoparticles) demonstrated that this technique can add useful information to explain the different toxicity among the different nanoparticles after intravenous administration.

P29-2 - Tuesday, October 30, 2012, 16:00 - 16:30, Poster Exhibition Area

Radiopharmaceuticals & Radiochemistry: Radiometals

P0798

Development of an ethanol-based post-processing for generator-produced ^{68}Ga for medical application

E. Eppard, F. Roesch; Institute of Nuclear Chemistry, Johannes Gutenberg-University, Mainz, GERMANY.

OBJECTIVES Post-processing using a cation-exchanger in hydrochloric acid/acetone media represents an efficient strategy for concentration and purification of generator-derived ^{68}Ga eluates. It assures the removal of ^{68}Ge , and high labeling yields of injectable ^{68}Ga -labelled radiopharmaceuticals for routine medical

application. The aim of this work is to replace the acetone with ethanol to combine the very efficient strategy for concentration and purification based on cation-exchangers with the superior properties of ethanol. **METHODS** We developed a processing of generator-produced ^{68}Ga eluates including the labeling of DOTA-octreotide derivatives. A $^{68}\text{Ge}/^{68}\text{Ga}$ Obninsk generator was used with a ^{68}Ga yield of 100 MBq and 85 kBq breakthrough of ^{68}Ge . Preconcentration and purification of the initial generator eluate are performed using a cation exchange resin, Biorad (AG 50W-X8, -400 mesh) or Phenomenex (SCX), along the lines of the solutions N1 and N2 known from hydrochloric acid/acetone systems, but this time using hydrochloric acid/ethanol mixtures. Distribution of ^{68}Ga and metallic impurities like $^{68}\text{Ge(IV)}$, Fe(III) , Zn(II) , and Ti(IV) on the cation-exchange column was investigated. The purified fraction was used for labeling of nanomolar amounts of octreotide derivatives in pure aqueous solution and in different buffer systems. **RESULTS** We could obtain / develop a post-processing on cation-exchange resin hydrochloric acid/ethanol along the lines of the state-of-the-art post-processing based on hydrochloric acid/acetone media. Using this post-processing system up to 95% of the initially eluted ^{68}Ga activity was obtained in a 1 ml fraction of 90% ethanol / 0.9 N HCl as a hydrochloric acid/ethanol fraction within 4 min. The initial level of ^{68}Ge eluted from the generator is reduced. Due to the fact that the hydrochloric acid/ethanol systems have a lower pH than its acetone equivalent, buffer solutions are utilized for labeling octreotide derivatives. In pure aqueous solutions the labeling yields were very low (<15%). **CONCLUSIONS** Appropriate processing of generator-produced ^{68}Ga on the basis of cation-exchange chromatography is effective in hydrochloric acid/ethanol media. It successfully removes breakthrough of ^{68}Ge and allows the concentration of ^{68}Ga generator eluate with yields as good as with the established post-processing method. The whole process guarantees safe preparation of injectable ^{68}Ga -DOTATOC (or other ^{68}Ga -labeled radiopharmaceuticals) for routine applications and can be successfully used in clinical environment. However application of several generators in a cascade scheme can be used with this ethanol-based post-processing.

P0799

Novel ^{111}In -estradiol based complexes: preclinical evaluation for oestrogen positive tumour targeting

S. Cunha¹, F. Vultros¹, C. Fernandes¹, M. C. Oliveira¹, M. F. Botelho², I. Santos¹, L. Gano¹; ¹Instituto Tecnológico e Nuclear, Instituto Superior Técnico, Universidade Técnica de Lisboa, Sacavem, PORTUGAL, ²Biophysics, IBILI, CIMAGO, Faculty of Medicine, University of Coimbra, Coimbra, PORTUGAL.

Aim: The oestrogen receptor (ER) is an important tumour target for molecular imaging and radionuclide therapy due to its overexpression in many malignant cells (breast, ovarian, endometrial) as compared to normal cells. Furthermore ER status monitoring can predict the prognosis and the individual therapeutic responsiveness of tumours. Thus, our goal was to synthesise and evaluate two novel ^{111}In -estradiol based complexes to assess their feasibility for functional imaging of ER positive tumours. **Methods:** ^{111}In -complexes were obtained by reaction of estradiol substituted at the 16α - position with DTPA- or DOTA like bifunctional chelating ligands. Radiochemical purity and *in vitro* stability against apo-transferrin, DTPA and in human blood serum were assessed by ITLC and HPLC. Lipophilicity was determined through octanol/ PBS partition coefficient ($\log P_{o/w}$) obtained by the “shake-flask” method. Cellular uptake kinetics was studied in suitable human cancer cell lines, such as MCF-7 (human breast cancer positive ER) and MDA-MB-231 (human breast cancer negative ER). Biodistribution and *in vivo* stability studies in immature healthy female rats were also performed. **Results:** ^{111}In -complexes were obtained with labelling efficiencies higher than 95% at low ligand concentrations. The structure of the complexes was assessed by HPLC comparison with the analogous cold In-complexes, fully characterized by $^1\text{H-NMR}$, $^{13}\text{C-NMR}$, IV, and ESIMS. ITLC and HPLC analysis showed that radioactive complexes are stable in the presence of an excess of apo-transferrin and in human blood serum, up to 5 days. In the presence of an excess of DTPA solution a low degree of transchelation was observed after incubation at 37°C . A moderate cellular uptake was obtained in both cell lines probably due to the low lipophilicity of the complexes. In our animal model, ^{111}In -DOTA-estradiol complexes presented a rapid clearance from most organs and rapid excretion mainly by hepatobiliary pathway. High *in vivo* stability of the complexes was also confirmed by HPLC analysis of urine and blood samples. **Conclusion:** The ^{111}In -estradiol based complexes were prepared in high radiochemical yield and purity at low ligand concentrations. The complexes are stable *in vitro* in the presence of physiological concentrations of apo-transferrin and in human blood serum. Preliminary animal studies indicate high *in vivo* stability, a rapid clearance from main organs and fast excretion. Cellular uptake studies in breast cancer cells suggest that uptake may occur via an ER-mediated process.

P0800

Assessment of Cations Contamination Levels Released During Radiometallic Labelling Reactions

 Springer

M. Ben Reguiga¹, A. Chipan¹, B. Lages², D. Leguludec³, R. Lebtahi³, N. Pons-Kerjean¹, B. Do²; ¹Radiopharmacy Unit, Beaujon Hospital (APHP-HUPNVS), Clichy, FRANCE, ²AGEPS, Quality Controls Laboratory, Paris, FRANCE, ³Nuclear Medicine Department, Beaujon Hospital, Clichy, FRANCE.

Introduction The efficiency of metal radionuclides labeling reactions is affected by cationic impurities present in reactive media, as reported recently (Asti & coll., *Nuc.Med.Biol.*, 2011). Cations may be brought by raw material, accessories and glass vials used to host labeling reaction. Given the pH constraints necessary to avoid metal oxides formation, glass vials are often submitted to acidic pH, up to 5.5M of HCl in some Ga-68 labeling procedures. Hence, acidic pH, in addition to heating and stirring, may contribute to impurities release during labeling. The aim of this study was to assess the qualitative and quantitative profiles of impurities released from glass vials submitted to such aggressive conditions. **Material & Method** Three HCl solutions (*Metal-free* HCl, Sigma-Aldrich) were prepared (pH=4, pH=1 and 5.5M HCl). Glass vials provided by three suppliers were tested (IBA, GE, Covidien). Vials received 10mL of acidic solution and underwent 5min mechanical stirring followed 30min heating at 100°C . Vials contents were collected and analyzed by Inductively-Coupled-Plasma coupled to an Atomic-Emission-Spectrometry (ICP/OES, Varian). Analyses permitted to screen the contaminants released from vials and to quantify them in a second time. Results, expressed in ng of released element ($\text{mean} \pm \text{SD}; n=4$), were compared to negative and positive controls (One-way Anova test, $p < 0.05$). **Results & discussion** 11 chemical elements were found in significantly important amounts: Si, Mg, Zn, Al, B, K, Fe, Ni, Cr, V, Mn. Qualitative impurities profiles varied little according to the considered vials supplier. However, released amounts for all elements increased significantly with pH. For instance, Al(III) concentration increased from $41 \pm 3\text{ng}$ in control to $442 \pm 38\text{ng}$, $2194 \pm 71\text{ng}$ and $56491 \pm 23\text{ng}$ respectively at pH=1, pH=4 and 5.5M HCl. Zn increased too, from $1.0 \pm 0.3\text{ng}$ to $1803 \pm 178\text{ng}$, $12736 \pm 707\text{ng}$ and $19471 \pm 483\text{ng}$ respectively at pH=1, pH=4 and 5.5M HCl. When compared to radiometallic concentrations usually used, contaminants amounts are expected to affect labeling reactions, especially for ^{68}Ga -labelled-peptides, where high specific activities are needed. In fact, 1GBq of Ga-68 is $\approx 1\text{ng}$ of Gallium and Al(III) or Zn(III) released were in much higher levels. However, contaminations levels are not expected to affect Y-90 or Lu-177, where 7GBq-10GBq are usually used for PRRT, corresponding respectively to $\approx 370\text{ng}$ and 1800ng and where the higher molar ligands/radionuclides ratio limits contaminants interferences. **Conclusion** High levels of metallic and non-metallic contaminants were found in glass vials submitted to operating conditions used in radiometallic labeling. Contamination levels increased with acidity to reach micrograms. At these levels, metal cationic impurities may affect labeling yields, especially with Ga-68.

P30-2 - Tuesday, October 30, 2012, 16:00 - 16:30, Poster Exhibition Area

Radiopharmaceuticals & Radiochemistry: Radiopharmacokinetics & Drug Development

P0801

New Tc-99m-carbonyl based Octreotide analogues

T. M. Haslerud, M. Angelo, S. Kürpig, S. Gohlke; Uniklinikum Bonn, Bonn, GERMANY.

Objectives: Various radiolabeled octreotide analogues especially DOTA conjugates are being used for diagnostic and therapeutic purposes. The carbonyl approach is well known for use with Tc-99m and Re-186/188 and relative little has been published has been published to this subject lately. Therefore in this work we have followed the idea to combine the advantage of a tridentate carbonyl labeling approach including DOTA-conjugation to improve the biodistribution profile on a custom synthesized octreotate analogon with the sequence DOTA-D-Lys-D-Phe-Cys-Tyr-D-Trp-Lys(ivDde)-Thr-Cys-Thr-OH (Disulfide bond), thus a ivDde protected TATE derivative. **Methods:** The N-terminal extension by DOTA-D-Lys offers the possibility of a tridentate Tc-99m-carbonyl labelling approach with the $\text{Tc}(\text{CO})_3(\text{H}_2\text{O})_3$ aqua ion using PADA or DTPA. Radiolabeling was usually performed on the final deprotected peptide analogs. The various radiolabeled analogs were characterized by HPLC followed by biodistribution studies at 0.5, 1, 3 and 24 h p.i. using tumor free and tumour bearing mice. In addition to the radiolabeled the tc-carbonyl derivatives were complexed at the DOTA using stable Lu, Cu and Ga. In order to allow better comparison of the new analogs, Lu-177-DOTA-TATE was simultaneously co-injected. **Results:** Gradient HPLC studies (RP-18; 0.1% TFA vs. MeCN) revealed the following list of increasing lipophilicity: Lu-177-DOTA-Octreotate, Ga(Stabil)-DOTA-Lys(99mTc-DTPA)-Octreotate, DOTA-Lys(99mTc-DTPA)-Octreotate, Ga(Stabil)-DOTA-Lys(99mTc-PADA)-Octreotate, DOTA-Lys(99mTc-PADA)-Octreotate, Cu(Stabil)-DOTA-Lys(99mTc-PADA)-Octreotate, Lu(Stabil)-DOTA-Lys(99mTc-PADA)-Octreotate. Generally biodistributions were relative similar for the Tc-carbonyl-PADA labeled peptides including the metal complexed derivatives to the Lu-177 labeled peptide with the exception of a slightly lower tumor uptake. The DTPA-derivates showed higher activity levels in liver and

intestines. At 1 h p.i. the main biodistribution characteristics [%ID/g] of the Tc-carbonyl labeled analog were relative to the Lu-177 peptides similar blood retention [1,5% for Tc-PADA vs. 1.3% for Lu], heart uptake [1% for Tc-PADA vs 1% for Lu] and uptake in intestines [4% for Tc-PADA vs 5% for Lu] slightly higher liver and kidney uptake [13,5% for Tc-PADA vs 9,5% for Lu]. The Lutetium derivate showed higher tumor uptake in the early studies and a similar value to the Tc-PADA peptide 24h p.i. [5,5% for Tc-PADA vs 6% for Lu]. Conclusion: The biodistribution characteristics and tumor uptake of the Tc-carbonyl-PADA labeled analogs of this study seem to be relative similar to the compared Lu-177 analogue, whereas the DTPA-labelled analogues showed a less favourable distribution pattern. Complexing of the DOTA did not seem to have a relevant effect on the biodistribution.

P0802

Translational Oligosaccharide Nanoprobe for Imaging Infection

G. Bandopadhyaya¹, J. Shukla², G. Arora¹; ¹All India Institute of Medical Sciences, Delhi, INDIA, ²PGIMER, Chandigarh, INDIA.

Molecular interaction between host mucosal surfaces and outer membrane components of microbes is crucial for the establishment of infection. The subsequent inflammatory response to microbial infections can be utilized in elimination of invading microorganism. Breast milk oligosaccharides act as soluble receptors for different pathogens which protect new born child from infection. The differentiation between septic and aseptic loosening plays an important role in the patient management. ^{99m}Tc HPBCD was injected in human subjects with uninfected knee joint and clinically confirmed infected knee joint. Docking studies were done for ligand - protein interaction. ^{99m}Tc HPBCD was observed to form nanoassemblies of 60-180 μm. The ¹H NMR studies revealed the binding of Tc-99m at C-8/H-8 position of HPBCD. Docking studies demonstrated the interaction between HPBCD and bacterial maltose binding protein (MBP). We tried to exploit these properties of β-CD for imaging infection. HPCD was labelled with ^{99m}Tc by stannous chloride reduction method and evaluated by ITLC-SG. Transmission electron microscope (TEM) study and ¹H-NMR studies were done to evaluate the size and shape of nano-assemblies and to characterize ^{99m}Tc-HPCD, respectively. Docking studies were done for HPCD-MBP interaction and route of excretion was studied in Wistar albino rats. Normal and histologically proven infection subjects were imaged with ^{99m}Tc-HPCD at 0, 1 and 3hr p.i. with gamma camera, after getting approval from Drug Controller of India and Institutional Clinical Ethical Clearance Committee. SPECT/CT images were acquired at 3hr of the infection site. Informed consent was taken from all subjects. ^{99m}Tc-HPCD was labelled with >98% yield and was stable for 6hr at pH 4.0 & 6.5. ^{99m}Tc-HPCD self assemblies were spherical with 60-180nm size. Prominent shift at H-8 proton, on ¹H-NMR spectra, revealed the binding of ^{99m}Tc at C-8/H-8 position of HPCD. Docking studies demonstrated strong interaction of HPCD and MBP that stabilized HPCD in the cleft of MBP. ^{99m}Tc-HPCD had renal route of excretion. There was markedly increased uptake of ^{99m}Tc-HPCD in the patient having clinically proven infection. However, no uptake was seen in patient free of infection. Nano-assemblies facilitated accumulation ^{99m}Tc-HPCD in inflamed area and the retention in infection were due to ^{99m}Tc-HPCD-MBP interaction. ^{99m}Tc-HPCD nano-assemblies are a promising infection imaging agent showing infection specific localization and has the advantage of being cost effective, easy availability, easy method of preparation as compared to currently available infection imaging agents in nuclear medicine.

P0803

Antibody-functionalized gold nanoparticles to target tumor angiogenesis

S. Lucas¹, D. Bonifazi², V. Bouchat¹, O. Feron³, L. Karmani⁴, R. Marega², B. Masereel⁵, N. Moreau¹, V. Valembois¹, T. Vander Borgh⁶, C. Michiels⁷, B. Gallez⁴; ¹Namur Research Institute for Life Sciences (NARILIS), Research center for the Physics of Matter and Radiation (PMR), University of Namur (FUNDP), Namur, BELGIUM, ²Laboratoire de chimie organique des matériaux supramoléculaires, University of Namur (FUNDP), Namur, BELGIUM, ³Unité de Pharmacothérapie (FATH), Université catholique de Louvain (UCL), Bruxelles, BELGIUM, ⁴Laboratoire de résonance magnétique biomédicale (CMFA), Université catholique de Louvain (UCL), Bruxelles, BELGIUM, ⁵Namur Research Institute for Life Sciences (NARILIS), Namur Medicine & Drug Innovative Center (NAMEDIC), University of Namur (FUNDP), Namur, BELGIUM, ⁶Namur Research Institute for Life Sciences (NARILIS), Center for Molecular Imaging and Experimental Radiotherapy (IRME), Université Catholique de Louvain (UCL), Yvoir, BELGIUM, ⁷Namur Research Institute for Life Sciences (NARILIS), Unité de Recherche en Biologie Cellulaire (URBC), University of Namur (FUNDP), Namur, BELGIUM.

Introduction: In medicine, development of hybrid nanoparticles that target vascular, extra-cellular or cell-surface receptors is often considered as an attractive solution for cancer detection and treatment. Here, we propose a new method to produce small and biocompatible gold nanoparticles (AuNPs) that specifically target the epidermal growth factor receptor (EGFR), a membrane protein overexpressed

in several kinds of solid tumors. Since it is well-known that nanoparticle shape, size and surface coating may influence the biodistribution and pharmacokinetic profiles of nanoclusters, studies were performed with the antibody-functionalized AuNPs *in vitro* and *in vivo* studies in murine models xenografted with human cancer cells.

Methods and materials: The nanosized (2-10 nm) AuNPs are synthesized by plasma vapor deposition (PVD). The surface of these AuNPs is then functionalized by a PPAA coating (plasma-deposited polyallylamine), which enhances the AuNPs stability in an aqueous environment and affords primary amino functions for covalent antibody coupling. Indeed, EGFR was targeted by covalently bound cetuximab, a chimeric antibody, to the amino groups present in the polymeric shell of PPAA-coated AuNPs. Size, morphology, composition and dispersion of free and conjugated PPAA-coated AuNPs in solution were analyzed by Transmission Electron Microscope (TEM), CPS Disc Centrifuge, UV and Atomic Absorption analyses. For *in vivo* studies, the antibody was firstly labeled with ¹²⁵I or ⁸⁹Zr before being coupled to the PPAA-coated AuNPs. **Results:** *In vitro* cell surface ELISA assays showed that cetuximab linked to PPAA-coated AuNPs preferentially binds to the EGFR overexpressed by A431 cells compared to the non-expressing CHO and EAhy926 cell lines. Moreover, the conjugated PPAA-coated AuNPs was capable of inhibiting the EGF-induced phosphorylation of EGFR (at tyrosine 1173) as measured by phosphorylation assays and subsequent Western Blot analysis. *In vivo* studies also showed that tumor uptake of free and nanoconjugated cetuximab was similar, highlighting the fact that the antibody retains its recognition properties also *in vivo*. **Conclusion:** All these studies demonstrate the potential of using the antibody-functionalized AuNPs for *in vivo* human imaging and then therapy. **Acknowledgments:** This Targan project (Waleo-2 program) is supported by the Walloon Region

P0804

Evaluation of YTTRIUM-90 Urinary Elimination Following Resin Microspheres Selective Internal Radiotherapy

M. Ben Reguiga^{1,2}, P. Fontaine¹, G. Boirie², A. Dieudonne^{2,3}, D. Leguludec³, R. Lebtahi¹, N. Pons-Kerjan¹; ¹Radiopharmacy Unit, Beaulieu Hospital (APHP-HUPNVS), Clichy, FRANCE, ²Radiation Safety & Radiophysics Unit, Beaulieu Hospital, Clichy, FRANCE, ³Nuclear Medicine Department, Beaulieu Hospital, Clichy, FRANCE.

Introduction Yttrium-90 labeled resin microspheres (RMS) are medical devices used for non operable hepatic malignancies treatment. Placed into the targeted hepatic tissue via femoral arterial access, RMS are supposed to be trapped indefinitely into hepatic vessels. However, given the ionic nature of Yttrium-90 bounding to sulfonate resin, the radioelement is susceptible to move from spheres to the blood stream and to be cleared by kidneys. The aim of this study was therefore to evaluate urinary elimination of Yttrium-90 in patients treated with RMS. **Materials and methods** Urine was collected during 24 hours following RMS implantation in patients treated for advanced hepatocellular carcinoma (n=10 patients). Urine volume was evaluated and then sampled into glass tubes. Radioactivity (cpm or counts-per-minute) was counted immediately after collection in a Perkin-Elmer Wallac 1470 gamma counter previously calibrated for quantitative Yttrium-90 measurement. Samples were counted simultaneously with a negative (distilled water) and positive control (1MBq of liquid Y-90). Results were converted into Bq/L, taking in account the background correction (negative control) and counting efficiency (checked with the positive control). Results were expressed in Bq/24h and kBq/MBq of administrated RMS. **Results and Discussion** Patients received Y-90 activities ranging from 329 MBq to 1960 MBq. Urines analyses showed that patients eliminated between 101 kBq/24h and 1130 kBq/24h. Reported to the administered activity, patients eliminated 0.10kBq/MBq to 0.78 kBq/MBq of implanted Yttrium-90 [0.33±0.19 kBq/MBq, mean±RSD n=10]. These amounts of Y-90 evacuated in urine could be justified by spheres' chemistry: RMS are cationic ion exchange resin, where Y³⁺ ions are bound by a weak and non specific ionic bond, removable by competitive cations brought by biologic fluids or co-administrated pharmaceuticals. Y-90 levels in the urine still however lower than what met with other radiopharmaceuticals such as 90Y-Zealvin® or 90Y-DOTATATE where the major part of administrated Yttrium-90 is found in urine and need specific radioprotection rules for the patient, his relatives and for the environment. **Conclusion** Yttrium-90 brought by RMS is supposed to be trapped indefinitely in liver tumors vessels. However, our study shows that Y-90 confinement is not strict and a part is cleared in patients' urine. Even if rejected radioactivity levels are low, these data should be taken in account for patient information, to avoid radioactivity spilling in the environment and even for patient's dosimetry calculations.

P0805

Evaluation of affinity and lipophilicity of novel adenosine A3 receptor antagonists as potential PET-tracers

M. Zeilinger¹, D. Haeusler¹, K. Shanab¹, R. Dudczak¹, H. Spreitzer², W. Wadsak¹, M. Mitterhauser¹; ¹Medical University of Vienna, Vienna, AUSTRIA, ²University of Vienna, Vienna, AUSTRIA.

Aim: The adenosine A3 receptor (A3R) is involved in many of the body's cytoprotective functions; changes of its expression lead to a variety of pathologies. The evaluation and establishment of a selective PET-radioligand for the visualization of the A3R in-vivo would be pivotal for diagnosis and further treatment of A3R associated diseases (ischemia, inflammation, cancer, glaucoma). First A3R PET-tracers [^{18}F]FE@SUPPY and [^{18}F]FE@SUPPY:2 were presented and evaluated recently [1,2]. Since, in-vitro and in-vivo evaluation of both tracers revealed drawbacks in terms of high lipophilicity ($\log P \sim 4$) and appearance of metabolites [3,4], several novel structurally related derivatives were designed and synthesized to serve as additional potential PET-tracers. The aim of the present study was to determine the inhibitory constants (K_i 's) and the lipophilicity of those novel antagonists for the A3R. **Methods:** Cell-binding-studies were conducted on adherent Chinese hamster ovary (CHO) cells, expressing the human A3R and competition experiments were performed to determine the K_i 's of the investigated antagonists. For this purpose 1×10^6 cells were incubated on a petri dish under physiological conditions. Real-time competition experiments were performed on a Ligand Tracer[®] (Ridgeview Instruments, Uppsala, Sweden) with 0.7 nM of [^{125}I]AB-MECA (commercially available A3R receptor agonist, $K_D = 0.59$ nM). Novel compounds were added in various concentrations (1 nM - 10 μM). IC_{50} -values and correlated K_i 's were analyzed with GraphPad Prism 5. $\log D$ values were evaluated using a standard HPLC protocol. **Results:** Binding studies revealed K_i 's and $_{\text{HPLC}}\log D$ values as shown in table 1.

Table 1 Inhibitory constants and $\log D$ values of novel A3R receptor antagonists and parent compounds for comparison. **Conclusion:** $\log D$ -values of the four novel A3R antagonists revealed moderate levels ranging from 3.66–3.95. Real-time competition experiments were conducted in a reliable and feasible manner and revealed reasonable affinity for (FE)²@SUPPY and modest to low affinity for (Me)²@SUPPY, FEME@SUPPY:2 and FEME@SUPPY. We conclude that those four novel compounds do not comprise the good affinity of the parent compounds. Therefore, further A3R antagonists will have to be designed and synthesized on the basis of the structure activity relationships of the present and previously evaluated compounds [1–4].

P0806

Tc99m labeled resveratrol as an alternative renal imaging radiopharmaceutical.

D. K. Dhawan; Panjab university, Chandigarh, INDIA.

Labeling of resveratrol with 99mTc was performed using SnCl₂ reduction method. Labeling efficiency for the drug and radio-pharmaceutical stability for a period of two hrs was assessed by standard radio-chromatographic techniques. Blood kinetics and biodistribution pattern of the labeled radiopharmaceutical at time intervals of 15 min, 30 min, 60 min and 180 min was studied in normal male Sprague Dawley (S.D.) rats following i.v. injection of the radiopharmaceutical. Maximum labeling efficiency (>90%) was observed at 1:1 ligand to stannous ratio at pH 5–6. Maximum % specific uptake (30.5%) was observed in the kidneys 1 hr post injection which then decreased to 5.6 % at 3 hrs post injection. Increase in blood activity was observed at 15 sec and 10 min post injection. The results clearly depict Tc99m labeled resveratrol as a potential renal functional imaging agent owing to its quick uptake and excretion from the kidneys. Further studies to assess its diagnostic potential with regard to kidney diseases will be carried out.

P0807

In vivo evaluation of ^{18}F -Labelled Isatin and Azaisatin Derivatives as Potential Agents for the Specific Visualization of Activated Caspases in Apoptosis

C. Waldmann¹, A. Faust², S. Wagner¹, M. Schäfers², S. Hermann², O. Schöber¹, G. Haufe³, K. Kopka¹; ¹Dept. of Nuclear Medicine, University Hospital Muenster, Muenster, GERMANY, ²European Institute for Molecular Imaging (EIMI), Muenster, GERMANY, ³Organic Chemistry Institute, University Muenster, Muenster, GERMANY.

Introduction: Dysregulation of apoptosis has been implicated in numerous diseases, such as myocardial infarction, stroke, cancer and neurodegenerative disorders. Apoptosis is induced by complex regulated signaling pathways that trigger the intracellular activation of the enzyme class of the cysteinyl aspartate-specific proteases, in short caspases. The executioner caspases-3, -6 and -7, once activated, effect cellular death through cleavage of proteins which are responsible for DNA repair, signaling and maintaining cell shape. These enzymes therefore are suitable biological targets for the non-invasive molecular imaging of living apoptotic cells and tissues in vivo. To date there are two lead compounds for the selective inhibition of activated caspases-3 and -7 which are investigated in our group, namely (S)-5-[1-(2-methoxymethylpyrrolidinyl)sulfonyl]isatin and the recently developed (S)-5-[1-(2-(methoxymethylpyrrolidinyl)sulfonyl)-7-azaisatin (1), (2), (3). While showing similar inhibition potencies against activated caspases-3 and -7 in vitro, they differ considerably in their pharmacokinetic behavior in vivo. **Materials & Methods:** Aforementioned lead structures are tested for their

inhibition potency (expressed in IC_{50} values) for activated caspases-3 and -7. For imaging purposes both are functionalized with an alkyne at N1 giving a precursor compound ready for labeling with prominent ^{18}F -bearing azides via 1,2,3-triazole formation. The pharmacokinetic behavior of two putative radiotracer candidates is investigated in vivo. **Results:** The respective isatin and 7-azaisatin based caspase inhibitors showed efficient inhibition potencies in fluorimetric assays in vitro. In contrast to the isatin based inhibitors the resulting 7-azaisatin analogues are more hydrophilic as reflected by the negative $\log D$ values. As one main result an ^{18}F -labeled 7-azaisatin model tracer is preferentially excreted via the kidney after intravenous injection in wild-type mice. In general both radiotracer candidates, i.e. the ^{18}F -labeled isatin and 7-azaisatin, were efficiently cleared and showed no retention in any tissue. **Conclusion:** New potential PET-compatible radiotracers for the specific imaging of activated caspases in apoptosis were prepared. Initial biodistribution studies in wild-type mice demonstrated their potential for proof of principle studies in vivo in corresponding models of apoptosis. Therefore a mouse-model of increased levels of activated caspase-3 in the thymus was developed. Currently investigations with the putative apoptosis imaging agents based on isatin or 7-azaisatin are underway. References (1) Faust A. et al. [2007] Q. J. Nucl. Med. Mol. Imaging 51: 67–73 (2) Kopka K. et al. [2006] J. Med. Chem. 49: 6704–6715 (3) Podichetty A. K. et al. [2007] J. Med. Chem. 52: 3884–3895

P31-2 - Tuesday, October 30, 2012, 16:00 - 16:30, Poster Exhibition Area

Radiopharmaceuticals & Radiochemistry: Antibodies & Peptides

P0808

Development of ^{124}I -labelled anti-PSMA monoclonal antibody capromab for immunoPET staging of prostate cancer

J. Malmberg, R. Selvaraju, V. Tolmachev, A. Orlova; Uppsala University, Uppsala, SWEDEN.

Aim: Correct staging of prostate cancer is an unmet clinical need. Conventional anatomical imaging modalities (CT and MRI) tend to understage prostate cancer due to poor sensitivity to soft tissue metastases. A significant number of patients with extraprostatic disease nowadays undergo non-curative surgery due to false-negative diagnosis. Radionuclide targeting of prostate specific membrane antigen (PSMA) with ^{111}In -labelled capromab pentetide (ProstaScint) is a clinical option. A possible way to increase sensitivity is the use of PET which provides better resolution and better registration efficiency, which improves imaging quality. It is known that capromab targets intracellular domain of PSMA and tumor radioactivity accumulation should not depend on internalization of antigen/antibody complex. We proposed to use radioiodinated capromab with the aim to decrease retention of radioactivity in healthy organs due to non-residualising properties of radiolabel and further increase imaging contrast. **Methods:** Capromab was iodinated and its targeting properties were compared with indium labeled counterpart in LNCaP xenografted mice in dual isotope mode. PSMA negative xenografts (PC3) were used as a negative control. **Results:** Two iodination methods were applied: electrophilic iodination of tyrosines and use of para-iodo-benzoic prosthetic group. Both methods produced functional targeting agent, but direct iodination gave higher yields. Biodistribution of ^{125}I / ^{111}In -capromab in NMRI mice showed more rapid clearance of iodine radioactivity from liver, spleen, kidneys, bones, and colon tissue. ^{125}I -Capromab bound to PSMA specifically both in vitro and in vivo. Radioactivity uptake in PSMA expressing xenografts was 3-fold higher than in PSMA negative xenografts. In LNCaP xenografted mice radioactivity uptake from iodinated capromab was significantly lower in liver, spleen, pancreas, colon tissue, and kidneys, as well as in tumors than that from ^{111}In -capromab in dual isotope tumor targeting study. Maximum tumor uptake (19 ± 8 %IA/g for iodine and 29 ± 10 %IA/g for indium) and tumor-to-non-tumor ratios were found 5 d pi for both agents. High tumor accumulation and low uptake of radioactivity in normal organs anatomically relevant for prostate cancer metastases visualization was confirmed using microPET/CT 5 d pi of ^{124}I -capromab in LNCaP xenografted mice. **Conclusion:** ^{124}I -capromab can be used for visualization of prostate cancer metastases.

P0809

Toxicity after Combined Radioimmunotherapy with ^{177}Lu -mAb and ^{211}At -mAb in a Rat Model

S. E. Eriksson¹, T. Bäck², E. Elgström¹, H. Jensen³, R. Nilsson¹, S. Lindegren², J. Tennvall⁴; ¹Lund University, Lund, SWEDEN, ²University of Gothenburg, Gothenburg, SWEDEN, ³Rigshospitalet, Copenhagen, DENMARK, ⁴Skåne University Hospital, Lund, SWEDEN.

Radioimmunotherapy with beta-emitting radionuclides such as lutetium-177, ^{177}Lu , is considered suitable for treatment of small tumor lesions, while alpha-emitting radionuclides such as astatine, ^{211}At , are more effective in single cell and small cell cluster kill. In order to treat metastatic disease, consisting of both small metastatic lesions as well as minimal disease, a combination of the two different radionuclides

attached to monoclonal antibodies (mAbs) might be suitable. In our animal model, single administration of either 400 MBq/kg ^{177}Lu -BR96 (mAb) or 10 MBq/kg ^{211}At -BR96 resulted in tolerable, reversible myelotoxicity and complete response in 5 out of 6 rats bearing syngeneic colon carcinoma tumors. Both activities were below the maximal tolerable activity. However, metastases were detected in approximately half of the animals within 100 days after treatment. The aim of the present study was to investigate if administration of 400 MBq/kg ^{177}Lu -BR96 followed by administration of 10 MBq/kg ^{211}At -BR96 was tolerable. Materials and methods: 30 Brown Norway rats were allocated to two groups and either treated with 400 MBq/kg ^{177}Lu -BR96 and 10 MBq/kg ^{211}At -BR96 (combined group) or 400 MBq/kg ^{177}Lu -BR96 only. The second treatment was given 25 days after the first one, when white blood cells had started to recover. Cyclosporin A was co-administered to prevent formation of anti-antibodies. Body weight, blood cell counts, and general condition were monitored up to 100 days after the second administration. Results: The treatment resulted in temporal acute weight loss and reversible tolerable myelotoxicity. However, permanent weight loss was seen in half of the animals in the combined group starting 10–27 days after injection of ^{211}At -BR96 leading to earlier sacrifice of animals. Internal organs appeared normal at autopsy. The survival time of the combined group was significantly shorter (log-rank Mantel Cox test). The white blood cells decreased after both treatment, but nadir was lower after ^{211}At -BR96 compared to ^{177}Lu -BR96. Platelets decreased to the same levels after both administrations, but nadir was reached on day 10 after ^{211}At -BR96 compared to day 14 after ^{177}Lu -BR96. Conclusion: Although administered activities were tolerable as single treatments, the combination of ^{177}Lu -BR96 and ^{211}At -BR96 resulted in toxicity. This toxicity will be evaluated further.

P0810

Pharmaceutical development on DOTA-anti-CD20 monoclonal antibody for ^{177}Lu labelling

W. Wojdowska, U. Karczmarczyk, E. Byszewska, P. Garnuszek, R. Mikolajczak; National Centre for Nuclear Research Radioisotope Centre POLATOM, Otwock, POLAND.

Aim DTPA- or DOTA-chelated antibodies have been proved to be efficient in radioimmunotherapy of cancer after radiolabelling with beta-emitting radiometals. Recently, IAEA initiated coordinated research project on the development of radiopharmaceuticals labeled with ^{90}Y or ^{177}Lu aiming at the standardization of methodology for conjugation of suitable chelators to monoclonal antibodies and their further pharmaceutical development. Therefore, our study is focused on the development of dry kit based on DOTA-anti-CD20 for ^{177}Lu labeling as potential radiopharmaceutical for radionuclide therapy. Materials and methods Anti-CD-20 (rituximab, Mabthera, provided by Roche) in 2-ml aliquots (10 mg/ml) was concentrated by centrifugation using Amicon Ultra-2ml filter (Millipore, MWCO 10,000) to 20 mg/ml. This solution was washed three times with 0.2 M sodium carbonate buffer pH 9.5 to remove polysorbate 80, sodium citrate and other excipients. The antibody was then incubated with p-SCN-Bz-DOTA (Macrocyclics) in molar ratio 1:7 for 1.5 h at 37°C. To remove the excess of DOTA, reaction mixture was purified on PD-10 column. Final antibody concentration was quantified colorimetrically using BCA method, the number of conjugated DOTA molecules was determined by titration with the Cu(II)-arsenazo(III) complex. Radiolabelling conditions were investigated using various amounts of DOTA-anti-CD20 (480–1200 µg), varying volumes (100–550 µl) of buffer and pH (5.5 and 7.0). Radioactivities of ^{177}Lu LuCl₃ (specific activity 555 GBq/mg) (POLATOM) in the range 148–1480 MBq in 0.04 M HCl were added and incubation was carried out for 2 h at 22°C or 40°C. The labelling yield was determined by GF-HPLC using BioSep-SEC-S-2000 column (300x7.50 mm) with 0.1M phosphate buffer, pH 7.0, as mobile phase at 1 ml/min flow rate using UV at 280 nm and radioactivity detection. Results and Conclusion DOTA-anti-CD20 conjugates of 4 DOTA molecules substitution were obtained. The most essential parameter of the radiolabelling process was the volume of reaction mixture, which should be about 150 µl. GF-HPLC results revealed that high labeling yield (>95%) could be achieved within 15 min of incubation. No significant influence of temperature on radiolabelling yield was observed. Optimized conditions of radiolabelling at pH 7.0 (800 µg of DOTA-anti-CD20, ^{177}Lu of activity up to 1.4 GBq in 50 µl of 0.04M HCl, 30 min incubation at RT) resulted in ^{177}Lu -DOTA-anti-CD20 with specific activity of ca. 1.8 GBq/mg. ^{177}Lu -DOTA-anti-CD20 complexes were stable during 2h storage at RT (RCP >95%). Further works will be carried out in order to prepare antibody-chelate conjugates in the form of dry kit for ^{177}Lu labelling.

P0811

Upscaling of the in-house ^{177}Lu -DOTA-TATE-production with the ModularLab PharmTracer® for the treatment of neuroendocrine tumour patients at the Medical University of Vienna.

H. Eidherr¹, M. Hoffmann¹, C. Decristoforo², J. Ungersböck¹, F. Girschele¹, M. Mitterhauser¹, L. Nics¹, I. Leitinger¹, G. Karanikas¹, R. Dudczak¹, W. Wadsak¹; ¹Medical University of Vienna, Vienna, AUSTRIA, ²Medical University of Innsbruck, Innsbruck, AUSTRIA.

Aim: The demand of ^{177}Lu -DOTA-TATE for radiolabelled treatment of neuroendocrine tumour (NET) patients increased over last years at our department. Therefore our in-house- ^{177}Lu -DOTA-TATE-production had to be upscaled and both stringent radioprotection and European legal radiopharmaceutical regulations had to be observed. Materials and Methods: For the complete ^{177}Lu -radiolabelling process (40min, including conditioning and raw product purification and sterile filtration) a ModularLab PharmTracer® (Eckert&Ziegler) using one way synthesis cassettes was used: activities of 0.5–4.5–9.0–17.9GBq n.c.a. ^{177}Lu LuCl₃, in 0.5ml 0.04M HCl, (ITG), were reacted with DOTA-TATE-peptide (ABX) at 80°C/20min in 0.57M ascorbate buffer, pH 4.5 [1µg peptide/40MBq ^{177}Lu LuCl₃ +10–15%; the peptide was dissolved in 1µl deionized water]. For the complete procedure a dedicated synthesis cassette and the appropriate synthesis sequence was used. To each formulation 0.5–1.2ml DTPA (3mg/ml) solution was added. Quality control according to the pharmacopeia was performed for each lot (RCP by HPLC and TLC, pH, osmolality, sterility and bacterial endotoxins). Results: By now ^{177}Lu -DOTA-TATE could be produced in activities of ~0.5GBq (n=5), ~4.0GBq (n=8), ~8.5GBq (n=9), ~15.3GBq (n=3), corresponding to labelling yields of 80–96%. RCP always was ~99% with good stability (~98% even after 20h), pH ~5.0, osmolality 246–289mosmol/kg. All lots were sterile and endotoxins below 1EU/ml. The whole production (including preparation, actual radiolabelling process, quality control and radioactive waste management) takes about 7h. Conclusions: By upscaling ^{177}Lu -DOTA-TATE production the growing demand of the ^{177}Lu -radiopeptide can be sufficiently and reliably covered and this under both stringent radioprotection and proper radioactive waste management.

P0812

Comparison of serum stability and cellular binding properties of 8 DOTA-coupled Bombesin receptor targeting peptides

V. Rinaldi¹, A. Morisco¹, M. Aurilio¹, D. Tesaro², A. Accardo², L. Del Pozzo³, R. Mansi³, G. Morelli², S. Lastoria¹, L. Aloj¹; ¹SC Medicina Nucleare, Istituto Nazionale Tumori, Fondazione "G. Pascale", Napoli, ITALY, ²CIRPeB, Università "Federico II", Napoli, ITALY, ³Division of Radiological Chemistry, University Hospital, Basel, SWITZERLAND.

The bombesin receptor family consists of four receptor subtypes (BB1, GRP, BB3 and BB4) that are of interest as targets for diagnostic and therapeutic nuclear medicine applications. Overexpression of the first two members of this family has been documented in several human neoplasms such as breast, prostate and ovarian cancer. Peptide Receptor Radionuclide Therapy (PRRT) may be a viable therapeutic strategy in the management of these patients. Several Bombesin receptor targeted peptides have been described in recent years. Methods. In order to compare different bombesin analogues for their binding and stability properties, we have performed solid phase peptide synthesis of derivatives having the following general formula DOTA-Peg4-peptide in which the DOTA chelating agent has been introduced on the N-terminal end of each peptide and a Peg4 residue has been used as spacer. The peptide sequences are as follows: a DOTA-Peg4-Gln-Trp-Ala-Val-Gly-His-Leu-Nle-NH₂ MW 1595 b DOTA-Peg4-Gln-Trp-Ala-Val-Gly-His-Cha-Nle-NH₂ MW 1630 c DOTA-Peg4-Gln-Trp-Ala-Val-Gly-His-Sta-Leu-NH₂ MW 1636 d DOTA-Peg4-Gln-Trp-Ala-Val-NMeGly-His-Sta-Leu-NH₂ MW 1649 e DOTA-Peg4-DPhe-Gln-Trp-Ala-Val-Gly-His-Cha-Nle-NH₂ MW 1777 f DOTA-Peg4-DPhe-Gln-Trp-Ala-Val-Gly-His-Sta-Leu-NH₂ MW 1783 g DOTA-Peg4-D-Phe-Gln-Trp-Ala-Val-NMeGly-His-Sta-Leu-NH₂ MW 1796 h DOTA-Peg4-Gln-Trp-Ala-Val-Gly-His-Cha-Nle-Glu-NH₂ MW 1759 Serum stability experiments were based on HPLC analysis of Lu-177 labeled peptides incubated for different times in serum at 37°C in order to establish half life. The human prostate cancer cell line PC3 that is known to express high levels of GRP receptors was utilized to perform saturation binding experiments on whole cells at 4°C. Results. In serum stability experiments peptide g was the most stable with a half life of approximately 400 h whereas peptide a was the least stable with a half life of only 15 h. Dissociation constants were in the order of 1E–8M and Bmax values in the order of 1–400000 binding sites/cell for all peptides with the exception of peptide h which showed little specific binding. Conclusion. Our results indicate that the Sta13-Leu14 C-terminal sequence, and N-methyl-glycine (NMeGly) substitution for Gly yield elevated peptide stability in serum and conserve high binding affinity to GRP receptors. Issues pertaining to cellular internalization and in vivo distribution properties will be important in further development.

P0813

Comparison of DOTA-coupled minigastrin analogues and corresponding Nle congeners

M. Krošelj¹, R. Mansi², J. C. Reubi³, H. R. Maecke², P. Kolenc Peitl¹; ¹Department for Nuclear Medicine, University Medical Centre Ljubljana, Ljubljana, SLOVENIA, ²Department of Nuclear Medicine, University Hospital Freiburg, Freiburg, GERMANY, ³Division of Cell Biology and Experimental Cancer Research, Institute of Pathology, University of Berne, Berne, SWITZERLAND.

Aim In recent years development of radiolabeled minigastrin (MG) analogues has improved to a point of entering into clinic. Analogues with improved metabolic

stability and pharmacokinetics were developed. However, oxidation of methionin (to sulphoxides and sulphones) can have significant influence on binding affinities for receptor (Good et al., *Eur J Nucl Med Mol Imaging* 2008, 35). This led us to use isosteric methionin replacements in C-terminal part of minigastrin analogues. Since a possible enzymatic (ACE-like) hydrolysis of gastrin analogues occurring at the Met-Asp bond, releasing the C-terminal dipeptide amide Asp-Phe-NH₂ (as described in Dubreuil et al., *Biochim Biophys Acta* 1990, 1039, 171-6) we wanted to see if isosteric replacement also has any influence on enzymatic stability in human serum. We developed a series of DOTA-coupled minigastrin analogues with Nle instead of Met and compared their *in vitro* characteristics with Met minigastrin analogues to show if there is any influence on metabolic stability gastrin (CCK-2) receptor binding affinities and internalization rates. **Material and Methods** All DOTA-conjugated minigastrin analogues (DOTA-(D-Gln)₃-Ala-Tyr-Gly-Trp-Met/Nle-Asp-Phe-NH₂, DOTA-(D-Gln)₄-Ala-Tyr-Gly-Trp-Met/Nle-Asp-Phe-NH₂, DOTA-(D-Gln)₅-Ala-Tyr-Gly-Trp-Met/Nle-Asp-Phe-NH₂, DOTA-(D-Gln)₆-Ala-Tyr-Gly-Trp-Met/Nle-Asp-Phe-NH₂, DOTA-(D-Gln)₇-Ala-Tyr-Gly-Trp-Met/Nle-Asp-Phe-NH₂ and DOTA-(D-Gln)₈-Ala-Tyr-Gly-Trp-Met/Nle-Asp-Phe-NH₂) were synthesized manually on solid phase. Gastrin receptor affinities were determined by receptor autoradiography using ¹²⁵I-CCK as radioligand. ¹¹¹In-labeled peptides were evaluated *in vitro* in AR4-2J cell line and in human serum. **Results** All peptides showed high binding affinity to the CCK-2/gastrin receptor with IC₅₀ values in low nM range. All tested Nle conjugates showed receptor-specific internalization (9.8 to 15.1 %IA/10⁶ cells after 4h). Enzymatic stability in human serum ranged from (9.7 ± 1.6)h for ¹¹¹In-DOTA-(D-Gln)₃-Ala-Tyr-Gly-Trp-Nle-Asp-Phe-NH₂ to (123 ± 1.6)h for ¹¹¹In-DOTA-(D-Gln)₆-Ala-Tyr-Gly-Trp-Nle-Asp-Phe-NH₂. Methionin analogues show 2 to 4-fold higher enzymatic stability (T_{1/2}=(25.3 ± 3.8)h for ¹¹¹In-DOTA-(D-Gln)₃-Ala-Tyr-Gly-Trp-Met-Asp-Phe-NH₂ and T_{1/2}=(495 ± 104)h for ¹¹¹In-DOTA-(D-Gln)₆-Ala-Tyr-Gly-Trp-Met-Asp-Phe-NH₂ respectively). **Conclusion** We developed a series of DOTA-coupled minigastrin analogues with Met exchanged for Nle and compared their *in vitro* characteristics with methionin analogues. Changing amino acid sequence in C-terminal part had no influence on binding affinities of these molecules to CCK-2/gastrin receptors. This isosteric replacement also had no significant influence on internalization rates. We found no increase in enzymatic stability of these analogues, moreover, stability in human serum decreased 2 to 4-folds compared to Met analogues.

P0814

Towards a one pot formulation: To pre-concentrate or not to pre-concentrate? . A simplified preparation of 68 Ga-DOTATATE using 68 Ga obtained from a silica based column 68Ge/ 68Ga generator.

W. Oware, K. K. Solanki, C. Solanki, D. Gillett, A. Wong; Cambridge University Hospital NHS Foundation Trust, Cambridge, UNITED KINGDOM.

Aim Labelling of bio-molecules is thought to require a highly purified and concentrated form of 68Ga. Pre-concentration is necessary for the removal of residual parent radionuclide and any interfering trace metals that may be present in the eluate as well as constricting the volume. The procedure however is cumbersome, time-consuming and prone to high radiation doses for the operator. The purpose of this investigation was to compare the preparation of 68Ga-DOTATATE with and without pre-concentration and pre-purification of 68Ga obtained from a novel silica column based generator (ITG, Germany) Methods In the first study 68Ga-DOTATATE was prepared with 68Ga pre-concentrated and pre-purified on an anion exchange cartridge PS-HCO₃ (Macharay-Nagel). 400μL of pre-concentrated 68Ga was reacted with 40μg of DOTATATE in sodium acetate buffer at pH 3.8 at 90C for 15 minutes. In a series of separate experiments the pre-concentration of 68Ga was optimised with regards to column recovery, pH and volume of the pre-concentrate. The reaction parameters were then optimised with respect to temperature, reaction time and pH. In the second study 68Ga-DOTATATE was prepared by reacting 68Ga in varying volumes to a maximum of 6mL but without pre-concentration and using the same reaction conditions as the previous study. The RCP was examined with TLC and radio-HPLC. In both studies the final product purification was achieved using C-18 cartridge. The 68Ge breakthrough in eluate and products was measured using a Wallach automatic gamma sample counter Results Crude RCP yields for non-pre-concentration studies were significantly higher (93.7% ± 4.25, n=8) compared with the pre-concentration studies (44.2% ± 24.2 n=8. (P=99.0% RCP for each product. There was no relationship between volume and reaction yield in the second method. The 68Ge breakthrough in eluate was 0.003% but reduced to 0.001% with pre-concentration. However, 68Ge- content in final product in both studies was <0.001% indicating the non-reaction of the parent radionuclide. Conclusion Consistently higher yields were obtained by the non-pre-concentration method. The pre-concentration method was unreliable and yielded lower RCP values. We conclude it is not necessary to pre-concentrate 68Ga derived from a silica based column, thus allowing for a simple and quick preparation method.

P33-2 - Tuesday, October 30, 2012, 16:00 - 16:30, Poster Exhibition Area

Radiopharmaceuticals & Radiochemistry: New Targets

P0815

MC simulation for the assessment of the feasibility of the production of 99mTc with a 16.5 MeV biomedical cyclotron

G. Lucconi¹, G. Cicoria², D. Pancaldi², M. Marengo²; ¹Postgraduate School in Medical Physics, University of Bologna, Bologna, ITALY, ²Medical Physics Department, S.Orsola - Malpighi University Hospital, Bologna, ITALY.

Aim: the recent worldwide shortage of reactor-produced 99Mo has stimulated studies on the large-scale cyclotron production of 99mTc via the 100Mo(p,n)99mTc reaction, whose cross section starts at about 8 MeV, peaks at 16 MeV and drops around 24 MeV. In this work we investigated the feasibility of 99mTc production through a 16.5 MeV GE PETtrace cyclotron. Material and methods: MonteCarlo simulations using the well known and validated FLUKA code have been performed considering a 97.46% enriched 100Mo target material. In the model, an elliptically shaped proton beam is degraded by a 25 μm Havar foil before entering a 32-mm diameter disk with a thickness (target + backing) not exceeding 2 mm, according to the design of the solid target station previously developed and fully operational at our institution. Simulations of 2 h irradiations at a relatively low current of 50 μA have been performed with (100÷300) μm target thicknesses, corresponding to proton energy ranges from (16.03→14.26) MeV to (16.03→9.98) MeV. Russian Roulette biasing technique has used to reduce variance and improve simulation results for thin targets. The current FLUKA isomer patching method has been used, meaning a 50% splitting between ground state and isomer due to the spin-parity independence of evaporation model adopted in the code. Radionuclidic purity of the irradiated target was assessed at the End of Bombardment (EOB) and up to 12 hours later. Results: According to the preliminary results of this study, a 150 μm (16.03→13.3 MeV) enriched 100Mo target, practically achievable with current electrodeposition techniques, grants the production of clinically relevant amounts of 99mTc while keeping the impurities at a reasonably low level. Even at low irradiation currents, for which no target damage is expected, the saturation yield was (72.2±1.2) mCi/μA. The isotopic impurities produced were 100Tc (t_{1/2} = 15.8 s), 97mTc (t_{1/2} = 90.1 h) and minor quantities of 99Tc, 98Tc and 97Tc (half-lives longer than 10⁴ y); 99Mo, 97m+gNb and 96Nb were also found in the irradiated target. The radionuclidic purity referring to 99mTc resulted to be > 99.6 % at 2 hours after the EOB. Conclusion: the proposed approach allows to assess the optimal irradiation conditions for the production of 99mTc with a standard 16.5 MeV biomedical cyclotron. The encouraging results suggest that this may be a feasible, relatively low-cost and large scale alternative to the generator based production. Experimental tests and more accurate estimation of the 99mTc/99m+gTc ratio are currently on going.

P0816

Radiosynthesis & First Preclinical Evaluation of [18F]FE@SNAP - a Potential PET-Tracer for the Melanin Concentrating Hormone Receptor 1

C. Philippe¹, L. Nics¹, M. Zeilinger¹, J. Ungersboeck¹, D. Haeusler¹, M. Hendl¹, T. Heissenberger¹, E. Schirmer¹, H. Spreitzer², H. Viernstein¹, W. Wadsak¹, M. Mitterhauser¹; ¹Medical University of Vienna, Vienna, AUSTRIA, ²University of Vienna, Vienna, AUSTRIA.

Aim Changes in the expression of the Melanin Concentrating Hormone Receptor 1 (MCHR1) have been shown to be involved in a variety of pathologies, especially diabetes, obesity, deregulation of metabolic feedback mechanisms, depression and anxiety disorders. To monitor these pathologies in-vivo, there is an increasing interest in radiolabeled MCHR1-ligands. SNAP-7941 ((+)-methyl (4S)-3-(((3-(4-(acetylamino)phenyl)-1-piperidinyl)propyl)amino)carbonyl)-4-(3,4-difluorophenyl)-6-(methoxymethyl)-2-oxo-1,2,3,4-tetra-hydro-5H-pyrimidinecarboxylate) has been described as a very potent antagonist for the MCHR1. After the successful synthesis of [11C]SNAP-7941, we synthesised and evaluated a F-18 fluoroethylated analogue: [18F]FE@SNAP. MATERIALS & METHODS Radiosynthesis: Starting from the precursor Tos@SNAP (3mg/mL) the reaction was carried out in acetonitrile at 170°C using a NanoTek® microfluidic system. Azeotropic dried [18F]fluoride and the precursor solution were pushed through the reactor with an overall flow of 150mL/min. Purification and formulation of [18F]FE@SNAP was done via a Nuclear Interface synthesis module. Cell-binding studies: MCHR1-cell membranes were incubated (25°C) with [125I]MCH and different concentration of FE@SNAP (0.25nM - 2μM). After 2 hours, bound and free radio ligand were separated by centrifugation and analyzed in a Gamma Counter. Plasmastability (in vitro): Human plasma was incubated under physiological conditions with [18F]FE@SNAP over 120 min and analyzed via HPLC. Microsomes (in vitro): Human microsomes were incubated under physiological conditions with [18F]FE@SNAP over 60 min and analyzed via HPLC. Blood brain barrier penetration (in vitro): The passive blood brain barrier penetration of [18F]FE@SNAP was tested via an HPLC assay using an immobilized artificial membrane (IAM) column. RESULTS Radiosynthesis: Starting

from $25.6 \pm 0.6\text{GBq}$ [^{18}F]fluoride, $595 \pm 67\text{MBq}$ of formulated [^{18}F]FE@SNAP ($4.3 \pm 0.4\%$ EOB) were produced. Cell-binding studies: Ki of FE@SNAP was 22.48nM . Plasmastability (in vitro): A decomposition of 6% of [^{18}F]FE@SNAP was observed after 120 min. Microsomes (in vitro): A decomposition of 7% of [^{18}F]FE@SNAP was observed after 60 min. Blood brain barrier penetration (in vitro): The logK_{IAMw} of [^{18}F]FE@SNAP is 2.0, which is in the same range as for [^{11}C]DASB (logK_{IAMw}=1.8). **CONCLUSION** After the successful establishment of the radiosynthesis via microfluidics, we were able to produce sufficient amounts of [^{18}F]FE@SNAP for subsequent preclinical studies. [^{18}F]FE@SNAP evinced good binding affinity to the MCHR1 and formidable stability against microsomes and in plasma. As the logK_{IAMw} of [^{18}F]FE@SNAP and [^{11}C]DASB are comparable, the prediction of a blood brain barrier penetration of [^{18}F]FE@SNAP seems reasonable. Further preclinical evaluation steps will include autoradiography and small-animal PET. **ACKNOWLEDGEMENT** This research was funded by the Austrian Science Fund (FWF): P20977-B09

P0817

Radiolabeling of Magnetic Nanoparticles Conjugated Moxifloxacin (MOX) and Investigation of In Vitro Biological Affinities

P. Unak¹, O. K. Guldu¹, E. &. Medine, M¹, F. Z. B. Muftuler¹, S. Sakarya, M², S. Timur, F¹; ¹Ege University, Izmir, TURKEY, ²Adnan Menderes University, Aydin, TURKEY.

Introduction: Magnetic radioactive nanoparticles have the advantage of being able to deliver high concentrations of radioactivity to the target area, without damaging normal surrounding tissue. It's thought that these new complexes will find a wide spread field in creation of materials besides medicine. Moxifloxacin (MOX) is a fourth-generation synthetic fluoroquinolone antibacterial agent developed by Bayer AG (initially called BAY 12-8039). The aim of this study is to synthesize MOX conjugated magnetic nanoparticles radiolabeled with ^{131}I /125I and to evaluate its in vitro biological behavior. **Experimental:** Magnetic nanoparticles, Fe₃O₄, were prepared by the co-precipitation method from ferrous and ferric ion solutions with a molecular ratio of 1:2 and they coated with TEOS. The obtained silica-coated magnetic particles coated with aminosilane. Finally MOX, was conjugated to the NPs by the cross-linker of glutaraldehyde. Magnetic nanoparticles were characterized with Zeta potential, AFM, SEM, FTIR methods. Finally, Moxifloxacin conjugated magnetic nanoparticles (NP-MOX) were radiolabeled with ^{131}I by iodogen method. **Results:** Radiolabeling yield of ^{131}I -NP-MOX was found to be $99.9 \pm 0.22\%$ while radiolabeling yield of ^{131}I -MOX was $95.41 \pm 1.79\%$ according to TLRC method (n=6). In vitro bioaffinities of ^{125}I -NP-MOX and ^{131}I -MOX were performed on A549 (Human lung adenocarcinoma epithelial cell line). Cell uptake studies show that conjugation with magnetic nanoparticles was increased the uptake of radiolabeled compound by the cells. Also applying external magnetic field increase the cell uptake. **Conclusion:** ^{131}I -NP-MOX shows a potential for imaging of infections such as respiratory tract, cellulitis, anthrax, intraabdominal infections, endocarditis, meningitis, and tuberculosis. Also using this molecule under external magnetic field can increase its affinity for therapeutic purposes. **Keywords:** Moxifloxacin (MOX), magnetic nanoparticles, ^{131}I / ^{125}I radiolabeling, infections imaging and therapy.

P35-2 - Tuesday, October 30, 2012, 16:00 - 16:30, Poster Exhibition Area

Cardiovascular: Perfusion

P0818

Assessment of image quality for SPECT myocardial perfusion imaging with regard to reconstruction algorithms using visual grading regression

A. Davidsson¹, E. Olsson¹, J. Engvall², A. Gustafsson³; ¹Department of Medical and Health Sciences, Linköping University, Linköping, SWEDEN, ²Department of Clinical Physiology UHL, County Council of Östergötland, Linköping, SWEDEN, ³Department of Radiation Physics, UHL, Linköping, SWEDEN.

Background and Purpose: SPECT myocardial perfusion imaging (SPECT MPI) is a standard examination for patients with suspected or known ischemic heart disease. New reconstruction algorithms that include correction for the variable distance between the collimator and the imaged object, is expected to increase resolution and improve noise regularization. In this study, a software with these capabilities, "Evolution for Cardiac[®]", was used to reconstruct images acquired on an Infinia Hawkeye gamma camera (GE Healthcare). The reconstruction technique allows shorter time for image acquisition, which reduces the risk of motion artifacts. The purpose of this study was to assess whether image quality in SPECT MPI can be maintained or even improved with a reduced acquisition time (9 min) using the software Evolution compared with the standard FBP/OSEM using 15 minute acquisition time. All images were visually assessed with and without attenuation

correction (AC). **Material and methods:** The study included 21 clinical patients referred for a SPECT MPI investigation. All subjects were examined according to standard procedure using Myoview[®], adenosine provocation and a 2-day protocol. Imaging parameters were 30 projections/head (total 180°), 30 seconds per angle, 8 ECG-gating frames / cardiac cycle. All data were evaluated with the standard software QGS/QPS for filtered back projection (FBP) and with iterative reconstruction using Ordered Subsets Expectation Maximization (OSEM) with (IRAC) and without AC (IRNC). A shorter acquisition corresponding 9 minutes was created by using five instead of eight gated frames and was evaluated with Evolution, with (IRACRR) and without AC (IRNCRR). Four nuclear medicine specialists with long experience in myocardial SPECT visually assessed anonymized images according to eight criteria on a four point scale, using the Viewdex software. Criteria dealt with aspects on image quality as well as with diagnostic confidence. Statistical analysis was performed using Visual Grading Regression (VGR). **Results:** SPECT MPI, collected in 9 minutes and reconstructed with Evolution using AC (IRACRR) made physicians feel confident in their assessment of the presence or absence of ischemia or scar. Overall image quality was rated the best for the images that were reconstructed using Evolution. The physicians regarded the risk of a false positive diagnosis to be lowest for Evolution using attenuation correction. **Conclusion:** SPECT MPI collected in 9 minutes, reconstructed with Evolution and AC produced better image quality and a higher diagnostic confidence among physicians than the standard procedure.

P0819

Myocardial Viability Assessment by Gated Myocardial Perfusion SPECT in Patients with Coronary Artery Disease and Poor Ventricular Function

R. Ruano Perez¹, F. Gomez-Caminero Lopez¹, M. Diego Dominguez², A. Rosero Enriquez¹, A. Martin De Arriba¹, J. Garcia-Talavera Fernandez¹, C. Martin Luengo²; ¹University Hospital of Salamanca. Nuclear Medicine, SALAMANCA, SPAIN, ²University Hospital of Salamanca, Cardiology, SALAMANCA, SPAIN.

Aim: to assess the usefulness of the gated-Spect (gSpect) myocardial perfusion imaging to assess myocardial viability in patients with ischemic heart disease and ejection fraction <40%. **Method:** in the period 2001-2010 were referred to our unit for myocardial viability protocol 125 patients (103 men, 22 women). 68 underwent stress-rest study and 57 only rest with stimulation with nitrates. The radiopharmaceutical used was $^{99\text{m}}\text{Tc}$ -Tetrafosmin. Studies were analyzed in 17 segments, assigning as viable those with score 0-1-2 (normal, mild defect or moderate) and non-viable those with score 3-4 (severe, lack of perfusion). Viability was attributed to each coronary territory: at least 3/7 viable segments on LAD, 2/5 viable segments on RCA and 2/5 viable segments on LCX. 72% of cases had previous heart catheterization, correlating with the results of gSpect. The influence of gSpect in the decision not to revascularization and revascularization (percutaneous or surgical) was assessed. Follow-up was until December-2011, valued as overall mortality events and cardiac mortality. **Results:** gSpect decided after medical treatment in 73 cases (58.4%) and revascularization in 52 cases (41.6%) percutaneous in 27 and surgical in 25. Of the 68 patients with stress study, 26 had ischemia, residual area of necrosis in 15, at distance in 2, and residual and distance in 9. The presence of ischemia and multivessel disease was associated with a higher number of revascularization. In cases with non-viability and involvement of just one vessel predominated only medical treatment. At final follow-up were 21 deceased, 16 of cardiac causes of which 8 was decided not to revascularization. **Conclusions:** Gated SPECT perfusion adequately to estimate myocardial viability in order to establish the decision of revascularization treatment. Even in high risk patients the presence of extensive non-viability permitted to avoid catheterization and its morbidity risks.

P0820

Is Gated-SPECT cardiac scintigraphy early after Primary Percutaneous Transluminal Coronary Angioplasty (PTCA) able to predict myocardial salvage and LVEF increase?

A. Doumas¹, T. Christoforidis¹, I. Iakovou¹, V. Balaris¹, D. Boundas², V. Nikos¹, S. Georga¹, D. Lo Presti¹, N. Karatzas¹; ¹3d Nuclear Medicine Dept. of the Aristotle University, General Hospital "G. Papageorgiou", Thessaloniki, GREECE, ²"Hippocrates" Nuclear Medicine Center, Thessaloniki, GREECE.

Myocardial salvage is the main reason to perform primary PTCA in patients with acute myocardial infarction, in order to conserve left ventricular function as much as possible. The involvement of stunned myocardium in the discrepancy between the myocardial perfusion restoration and functional recovery has not yet fully investigated and assessed. The aim of this study was to evaluate if early performed gated-SPECT myocardial scintigraphy soon after successful primary PTCA can predict myocardial salvage and left ventricular recovery. **Method:** Dipyridamol stress/rest gated-SPECT using $^{99\text{m}}\text{Tc}$ Sestamibi was performed 3-4 days post successful primary PTCA in 72 (56 male) patients. Perfusion, wall motion score and LVEF from the rest images were automatically calculated, using a dedicated cardiac

processing program (QPS), utilizing the 20-segment model. A total number of 1440 segments were evaluated. Segments with 60% or more uptake at the end diastolic image were considered viable, whereas segments with more than one Standard Deviation wall motion score were judged as dysfunctional. Changes on both the myocardial uptake and function were assessed by a second gated-SPECT study, performed 6–8 months later. Results: Comparing the segments where revascularization took place (504 out of 1440), 338 segments appeared viable at the early study and increased uptake from 64% to 81% after 6 months, in contrary to the 166 segments with <60% uptake (non-viable), that only 12 increased the uptake. Concerning the LVEF, there was a significant improvement in LVEF in all patients when compared the late to the early studies (40 ± 8 to 52 ± 7 , $p<0.01$). Moreover, LVEF increased significantly at the segments with viable myocardium (from 39 ± 9 to 56 ± 11 , $p<0.01$), compared to the non-viable ones (from 41 ± 6 to 45 ± 7 , $p>0.05$). Conclusion: Assessment perfusion and function using gated-SPECT myocardial scintigraphy early after primary PTCA can predict LV functional recovery in patients with salvaged myocardium. An uptake value of >60% at the early images seems to be a suitable cut-off for predicting LVEF increase, after stunned myocardium has fully recovered

P0821

The incidence of severe bronchospasm in “asthmatic” patients, undergoing Dipyrindamol pharmacologic stress test.

A. Doulmas¹, T. Christiforidis¹, I. Iakovou¹, V. Balaris¹, D. Boundas², V. Nikos¹, D. Lo Presti¹, S. Georga¹, N. Karatzas¹; ¹3d Nuclear Medicine Dept. of the Aristotle University, General Hospital “G. Papageorgiou”, Thessaloniki, GREECE, ²“Hippocrates” Nuclear Medicine Center, Thessaloniki, GREECE.

Pharmacologic stress test using dipyrindamol enables coronary vasodilation and myocardial scintigraphic evaluation in patients unable to perform age-predicted maximum heart rate exercise. In real asthmatic patients thought, the administration of dipyrindamol or adenosine, may lead to severe bronchospasm, difficult to be resolved by aminophylline iv injection. On the other hand, many patients diagnosed as “asthmatics”, are candidates for pharmacologic stress test. The aim of this study was to investigate how often severe bronchospasm develops due to dipyrindamol administration, in patients who claimed that were diagnosed of having asthma on the past. Method: From a total number of 4162 patients who underwent dipyrindamol myocardial scintigraphy during the last 2 years, 183 were considered having at least one “asthmatic” attack in his/her medical history and 65 of them were currently inhaling anti-asthmatic medications. From the above 183 patients, 41 were excluded from the study due to inhaling or exhaling wheezing (39 of them belonged to the category of medically treated). The ordinary iv dipyrindamol administration protocol (0.56mg/Kg in 4 min) was performed at the remaining 144 individuals (96 men and 48 women). Findings: Severe bronchospasm was developed in only 3 patients, which was resolved by O2 mask, iv aminophylline injection and bronchodilator inhalation. The symptoms started declining 4–8 min after the antidote administration. All 3 patients finally performed their scintigraphy, since Tc-99m Sestamibi was given prior to aminophylline. Conclusion: We conclude that dipyrindamol administration is a safe pharmacologic intervention, even in those individuals characterized “asthmatics” in the past, since less than 3% of them develop severe bronchospasm. Only in patients presenting on auscultation with inhaling or exhaling wheezing is prudent not to administer dipyrindamol, but to alternate to other pharmacologic interventions.

P0822

The value of early myocardial scintigraphy in predicting restenosis after successful primary percutaneous coronary intervention.

T. Christiforidis, A. Doulmas, I. Iakovou, V. Nikos, V. Balaris, S. Georga, D. Lo Presti, N. Karatzas; 3d Nuclear Medicine Dept. of the Aristotle University, General Hospital “G. Papageorgiou”, Thessaloniki, GREECE.

AIM: The main complication of primary percutaneous coronary intervention (PPCI) still remains the in-stent restenosis, reaching in some cases a 6% of the total carried PPCI, occurring usually between the third and the ninth month after the revascularization. For this reason, Myocardial Perfusion Scintigraphy (MPS) is recommended at least six months after the PPCI. The purpose of this study was to investigate the potential role of an early performed MPS (5–7 days after the PPCI) in prediction of stent restenosis. METHODS: A total number of 86 patients, with proven one vessel disease and with a mean age of 59 ± 14 years (58 men) underwent MPS five to seven days after the PPCI (Early-MPS). Dipyrindamol stress test and Gated-SPECT using Tc-99m Sestamibi were applied. Six months later, the same protocol was repeated (Late-MPS). RESULTS: Twenty four of 86 patients (28%) presented a positive for ischemia scan at the Early-MPS study. Six months later, at the Late-MPS the percentage of positive for ischemia scans was reduced to 8% (7 of 86 patients). These seven patients underwent coronary angiography, which revealed an in-stent restenosis to all of them. Five individuals of this group were ischemic on the Early-MPS, meaning that the Positive Predictive Value (PPV) of the Early-MPS for restenosis was 20.8%. Only 2 of 62 patients with a negative for

ischemia Early-MPS turned to have an abnormal Late-MPS, giving the Early-MPS a Negative Predictive Value (NPV) of 96.7%. The Sensitivity of the Early-MPS was 71.5% and the Specificity 76%. CONCLUSION: Performing MPS early after a PPCI may be extremely useful in predicting stent restenosis, as it shows a very high NPV and an acceptable sensitivity and specificity.

P0823

Evaluation of Myocardial Perfusion and Function after Kidney Transplantation by Gated Myocardial Perfusion Scintigraphy

A. Fard-Esfahani¹, B. Fallahi¹, S. Mirpour¹, A. Gholamrezaezhad¹, M. Karimi¹, D. Beiki¹, E. Abdi², A. Emami-Ardekani¹, M. Ansari³, M. Eftekhari¹; ¹Research Institute for Nuclear Medicine, Tehran, IRAN, ISLAMIC REPUBLIC OF, ²Hasheminejad Kidney Center, Shahid Beheshti University of Medical Sciences, Tehran, IRAN, ISLAMIC REPUBLIC OF, ³Nuclear Medicine Department, Imam Hossein Hospital, Shahid Beheshti University of Medical Sciences, Tehran, IRAN, ISLAMIC REPUBLIC OF.

Introduction: The aim of this study was to evaluate the effect of successful kidney transplantation (KT) on myocardial perfusion and left ventricular function by both qualitative (visual) interpretation and quantitative parameters, using myocardial perfusion scintigraphy with gated-single photon emission computed tomography (gated-SPECT) in end-stage renal disease patients. Subject & Methods: From a total of 38 patients who were candidates of KT, twenty-six patients (16 female, 10 male, mean age: 47.5 yr, range: 24–64 yr) who had successful KT were included. Myocardial perfusion scintigraphy was performed by Gated-SPECT method, before and after surgery (mean: 24 months). Perfusion and function status was evaluated by qualitative and quantitative parameters. Results: Our data showed evidence of myocardial perfusion and function abnormality in pre-transplant scans as follows: Abnormal perfusion frequency was globally 61.5%, in left anterior descending (LAD), left circumflex (LCX) and right coronary artery (RCA) territories 42.3%, 53.8% and 34.6%, respectively; heterogeneity of perfusion was noted in 53.8% of cases and left ventricle dilation in 57.7%. However no statistically significant change was noted after transplantation neither qualitatively nor quantitatively, i.e. p values for summed stress score (SSS), summed rest score (SRS) and summed difference score (SDS), summed motion score (SMS), summed thickening score (STS), ejection fraction (EF), end diastolic value (EDV), end systolic value (ESV), and stroke volume (SV) were 0.9, 0.2, 0.3, 0.1, 0.3, 0.8, $p=0.5$, $p=0.4$ and $p=0.9$, respectively. Conclusion: Renal transplantation may not have considerable long term effect on myocardial perfusion and function in patients with chronic renal failure. This could be due to either non-reversible myocardial changes or continuing effect of degrading factors on myocardium.

P0824

Contributing factors of reverse perfusion pattern in myocardial SPECT with Technetium-99m MIBI

D. Beiki¹, B. Fallahi¹, Y. Salehi¹, M. Saghari¹, M. Eftekhari¹, A. Fard-Esfahani¹, J. Esmaili²; ¹Research Institute for Nuclear Medicine, Tehran University of Medical Sciences, Tehran, IRAN, ISLAMIC REPUBLIC OF, ²Department of Nuclear Medicine, Imam Khomeini Hospital, School of Medicine, Tehran University of Medical Sciences, Tehran, IRAN, ISLAMIC REPUBLIC OF.

Aim: Reverse perfusion pattern (RPP) on the stress/rest myocardial images using thallium-201 has been currently documented and recognized as “reverse redistribution”. The present study was conducted to evaluate the frequency and contributing factors of RPP in myocardial SPECT with technetium-99m methoxy-isobutyl-isonitrile (Tc-99m MIBI). Materials and Methods: One hundred and two patients including 41 male and 61 female cases, mean age of 56.51 ± 9.2 years, referred for myocardial perfusion imaging, were entered into the study. SPECT was performed on the basis of two-day protocol. A combination of multiple stress- and rest-phase images, acquired at 15, 60, 120 and 180 minutes of injection, was applied for the evaluation. RPP was referred to a new perfusion defect or a worsening of a pre-existing stress defect on the rest images. Results: The protocol with 180 min stress and 15 min rest images was associated with the highest frequency (42%) and the protocol with both stress and rest images at 120min of injection revealed the lowest frequency of RPP (20.6%). The most important factors causing RPP were incorrect normalization and the time of acquisition in stress/rest phases. Gender, diabetes mellitus and the presence of coronary artery disease (CAD) did not correlate with RPP. Conclusion: Our study did not show any association between RPP and CAD, diabetes and sex; however, the data revealed that incorrect normalization and inappropriate time of acquisition may be the most contributing factors for RPP occurrence.

P0825

The image quality and myocardial to visceral uptake ratio in myocardial perfusion scan using pharmacological stress with sub-maximal exercise in comparison with pharmacological stress alone

B. Fallahi¹, D. Beiki¹, F. Aghahosseini¹, M. Saghani¹, M. Eftekhari¹, A. Fard-Esfahani¹, F. Akhzari²: ¹Research Institute for Nuclear Medicine, Tehran University of Medical Sciences, Tehran, IRAN, ISLAMIC REPUBLIC OF, ²Department of Nuclear Medicine, Sina Hospital, School of Medicine, Tehran University of Medical Sciences, Tehran, IRAN, ISLAMIC REPUBLIC OF.

Aim: Myocardial perfusion imaging (MPI) is an important imaging modality in the management of patients with cardiovascular disease. MPI plays a key role in diagnosing cardiovascular disease, establishing prognosis, assessing the effectiveness of therapy, and evaluating viability. However, MPI is a complex process, subject to a variety of artifacts and pitfalls, which may limit its clinical utility. Combining vasodilator and exercise stress reduces noncardiac side effects, improves image quality, and enhances the detection of ischemia, compared with suboptimal exercise or vasodilator stress alone. However, prognostic data with combined protocols are limited. **Material and Methods:** 97 patients (62 male and 35 female), mean age of 57.1 ± 8.0 years referred for MPI with gated single-photon emission computed tomography (SPECT), were studied. Regarding the type of stress before radiotracer injection, the patients were randomly allocated into two groups: one with 49 cases underwent dipyridamole stress alone (Dip) and the second (48 cases) with a combination of dipyridamole injection and a concomitant submaximal exercise (Dip-Exe). All patients were imaged by 15^{th} , 60^{th} , 120^{th} , 180^{th} minutes after radiotracer injection. Region-of-interest (ROI) for different areas of the myocardium and viscera, i.e. right hepatic lobe and splenic curve of colon, were drawn and myocardial to visceral activity was analyzed in each patient. **Results:** Myocardial to visceral average count ratios in both groups significantly rise with time from 15^{th} to 180^{th} min of radiotracer injection. Significant differences of the mentioned ratios were noted between two groups up to the 120^{th} minute of radiotracer injection with the Dip-Exe group showing higher myocardial to visceral ratios as compared with Dip group. Between-group difference tends to be minimal for myocardial to hepatic ratio at 180^{th} min. **Conclusion:** A stress protocol that combines symptom-limited exercise and dipyridamole injection increases the average count ratios of myocardial to visceral activities, and potentially may improve the quality of stress-phase gated SPECT images.

P0826

Assessment of myocardial perfusion in patients with transposition of the great arteries corrected at childhood

A. García-Burillo, S. Aguadé-Bruix, E. Franquet Elía, M. Pizzi, G. Cuberas Borrós, J. Castell-Conesa, J. Casaldàliga-Ferrer, J. Candell-Riera; Hospital General Universitari Vall d'Hebron, Barcelona, SPAIN.

Transposition of the great arteries (TGA) is a congenital heart defect. The surgical correction of TGA (called arterial switch) is currently done during the first few weeks of life, and requires reimplantation of the coronary arteries. Objective. To assess the prevalence of myocardial perfusion defects by gated-SPECT in (mostly paediatric) patients with TGA surgically corrected during childhood. Materials/Methods. Prospective study in which 63 patients with surgical correction of their TGV were included (10.1 ± 4 years, 15 women) (2 Senning, 57 Jatene, 4 Jatene+IVC) in which 68 myocardial perfusion studies have been performed: 9 rest-only, 57 treadmill stress test and 2 stress test plus atropine. Clinical and electrocardiographic data from the stress test and gated-SPECT results have been analysed. Results. The maximum heart rate reached in the 59 stress studies was 150 ± 28 bpm (MTHR: $77.6 \pm 14\%$), with an average stress duration of 9.7 ± 2.5 minutes and a maximum estimated O₂ consumption of 9.5 ± 2.9 METs. One patient referred mild chest pain and two revealed dyspnea. There were no significant changes in the ST segment and only one patient negativized the T waves. Of the 68 studies, 1 rest study and 7 stress studies showed perfusion defects (4 reversible and 4 fixed). Both patients which Senning procedures showed perfusion abnormalities (1 reversible and 1 fixed). The ejection fraction was 69.3 ± 11 and end-diastolic and end-systolic volumes were 57.3 ± 16 ml/m² and 18.8 ± 10 ml/m², respectively. Conclusion. After 10 years of follow-up, most of TGA operated patients showed normal myocardial perfusion and left ventricular function. Perfusion abnormalities were observed in 8/68 patients (4 reversible patterns), suggesting the presence of myocardial ischemia or scarred tissue in 11.8% of this population.

P0827

Assessment of attenuation artifact in patients who underwent nuclear myocardial perfusion imaging (MPI).

A. B. Esfahane¹, J. H. Hankins¹, R. High¹, C. H. Morris¹, T. Dworak², J. Schubert², K. P. Holdeman¹, M. J. DeVries¹, S. Paknikar²: ¹University of Nebraska Medical Center, Omaha, NE, UNITED STATES, ²Creighton University Medical Center, Omaha, NE, UNITED STATES.

Aim: Evaluate correlation and effect of BMI, gender, wall motion abnormality and LVEF in patients with attenuation artifact and compare to patients with ischemia or infarction on nuclear cardiac stress test. **METHOD AND MATERIALS** 555 subjects (309 male, 246 female) with or without known coronary artery disease were retrospectively studied. The patients were selected by searching the radiology

database at University of Nebraska Medical Center and Creighton University Medical Center. Subjects were classified into 4 groups of ischemia, infarction, artifact and normal. LVEF of each patient was calculated by Emory Cardiac Toolbox (ECT), QGS or 4D-MSPECT. The heart was divided into 13 segments at 3 levels - base, mid and distal portion (excluding the apex) and each level divided into 4 segments - anterior, lateral, inferior and septal. Each scan was evaluated and segment numbers involved by ischemia, infarct, artifact or wall motion (WM) abnormality were recorded. Finally, correlation between gender, BMI, WM and segment(s) involved by ischemia, infarct, artifact and normal was calculated. Regression modeling with attenuation artifact as the dependent variable and subject BMI, gender, WM as independent variables was performed, and then comparison was made to infarction and ischemia groups. **RESULTS** Patient age range was 30-109 years old (mean age 66 ± 12), BMI from 17-64 (Mean BMI 32.3 ± 7.6) and LVEF from 10-89 (mean 54.2 ± 14). 39 subjects (7%) had ischemia, 134 (24%) had infarction, 283 (51%) had artifact and 99 (18%) had normal scans. There was significant correlation between gender (male) and artifact ($p < 0.001$). Effect of BMI on artifact represents p value of 0.06 compared to ischemia ($p = 0.52$) and infarct ($p = 0.81$). There were significant WM abnormalities in infarction in each wall ($p < 0.001$), ischemia except lateral wall ($p < 0.01$) and artifact in anterior and inferior walls ($p < 0.001$ & 0.002). Percentages of wall motion abnormalities in infarct, ischemia, artifact and normal were 89, 39, 22 and 4 respectively. There were significant decreased in LVEF in patients with WM abnormality in inferior and anterior walls ($p = 0.03$ or less). **CONCLUSION** Attenuation artifact has significant correlation with male gender. Although artifact is more common in patients with higher BMI it is not statistically significant. Wall motion abnormality in artifact is less common than ischemia and infarction but more than normal group. This quantitative approach on nuclear myocardial perfusion imaging may be useful to evaluate changes in attenuation artifact due to factors such as BMI, gender and wall motion abnormality.

P0828

Improvement of myocardial perfusion image quality by prone in Japanese (In institution without CT attenuation correction)

T. Morishima¹, M. Aiga¹, K. Takeishi¹, A. Yamazaki¹, T. Hatano², H. Kobayashi¹, K. Koizumi¹, K. Takazawa¹, A. Yamashina³: ¹Tokyo Medical University Hachioji Medical Center, Tokyo, JAPAN, ²Hatano Clinic, Tokyo, JAPAN, ³Tokyo Medical University, Tokyo, JAPAN.

Background: In the hospital without attenuation correction by CT, prone imaging is efficient measures for the uptake improvement of the infero-posterior wall. Previous report says that prone image reduces attenuation with the diaphragm, therefore decreases the false positive rate of the infero-posterior wall. But it is not clear effect of prone image and comparison of many patients is still obscure in Japanese. **Objective:** To evaluate the uptake improvement of the infero-posterior wall by prone image with myocardial perfusion imaging (MPI). To determine the factor that influences the improvement by prone. **Methods:** We studied 207 consecutive patients with ordered prone image who underwent stress myocardial perfusion imaging. All patients were imaged prone and supine during one session and measured body fat, chest and abdominal circumference, arm length in addition to the height, weight. Polarmaps generated from the American Heart Association (AHA) 17 segment model were used to calculate the %uptake. In RCA area (AHA Segment 3, 4, 9, 10, 15), it compared with a visual evaluation and we examined the enhanced factor. **Results:** One hundred fifty three men and 54 women with an age range 68.6 ± 10.0 years and weight range 62.7 ± 12.3 kg, height range 161.3 ± 9.2 cm. We used isotope ^{99m}Tc and was 201Tl, 80 patients and 127 patients respectively. In RCA area, the %uptake has significant difference between improvement and unchanged of the visual assessment (Stress 8.24 ± 14.9 vs 5.77 ± 11.04 , $P < 0.00001$; Rest 7.28 ± 7.8 vs 5.09 ± 12.5 , $P < 0.00001$). The factors in which uptake of the infero-posterior wall by prone improved were man, arm length and tall. No influence factors were body fat, chest circumference, weight and other factor. **Conclusion:** Prone image to decrease false positive of the infero-posterior wall has improved uptake in Japanese also. We believe that the benefit of prone is received to the man of a high height with a long arm.

P0829

Long-term effects of coronary angioplasty on myocardial perfusion in patients with chronic heart failure due to ischemic systolic dysfunction

L. Samoylenko, N. Shashkova, S. Tereshchenko; Russian Cardiology Research Center, Moscow, RUSSIAN FEDERATION.

Aim: Assessment of the myocardial perfusion during long-term follow-up after percutaneous transluminal coronary angioplasty in patients with chronic heart failure due to ischemic systolic dysfunction. **Materials and methods:** 27 pts (23 males; mean age 56.6 ± 8.8 yrs) with stable angina and chronic heart failure (NYHA II-III, LVEF < 40) were studied. All the patients were underwent rest/stress myocardial gated single photon emission computed tomography (G-SPECT) at baseline and after 6 and 12 months after PTCA. **Results:** Initial rest study

demonstrated mean perfusion defect volume of 43 (26;62) ml and extent of 21 (17;35)%. After 6 and 12 months these values were 49(25;63) ml and 27(15;39)%, and 42(25;60) ml and 21(14;30)% respectively (NS for all). Initial stress test showed mean perfusion defect volume of 56(38;77) ml and extent of 32(24;44)%. After 6 and 12 months values of perfusion defect volume were 49(33;71) ml and 50(33;72) ml, respectively (NS), values of perfusion defect extent were 28(20;39)% and 28(21;35)% respectively ($p<0,05$ vs baseline). Values of transitory myocardial ischemia were at baseline 13(9;17)%, and after 6 and 12 months 9(6;13)% and 11(5;16)% respectively ($p<0,05$ vs baseline). Conclusion: PTCA with coronary stents placement may improve myocardial perfusion in patients with chronic heart failure due to ischemic systolic dysfunction by decreasing extent of perfusion defect in the response to stress, and by diminishing transitory myocardial ischemia. These beneficial effects occurred by 6 months after intervention and maintained by 12 months. Patients with chronic heart failure due to ischemic systolic dysfunction have been not demonstrating any significant positive changes in the rest myocardial perfusion after PTCA with stents placement during the long-term follow-up.

P0830

Myocardial perfusion SPECT in Greece: qualitative characteristics from 4 academic departments

E. Moravidis¹, N. Papadimitriou¹, M. Stathaki², X. Xourgia³, T. Spyridonidis⁴, A. Fotopoulos³, D. Apostolopoulos⁴, N. Karkavitsas², A. Gotzamani-Psarrakou¹; ¹AHEPA Hospital, Thessaloniki, GREECE, ²Heraklion University Hospital, Heraklion-Crete, GREECE, ³Ioannina University Hospital, Ioannina, GREECE, ⁴Rio University Hospital, Patras, GREECE.

Introduction. Although myocardial perfusion scintigraphy in patients with suspected or known coronary artery disease (CAD) is widely performed in nuclear medicine departments, quantitative and qualitative data are sparse in Europe. In this study qualitative characteristics of such examinations are recorded from 4 high volume academic units in Greece. **Method.** Over a 9-month period (October 2010 - June 2011) data were collected from 4 academic units using a standardized questionnaire. In each center an experienced nuclear cardiologist gathered data from consecutive patients he examined, which were subsequently analyzed in the core department of the study. **Results.** Data from 3,032 patients (59% male), aged 66±11 years, were collected. Among them 44% had known CAD, 31% suffered from diabetes mellitus, 80% were hypertensive, 66% had dyslipidemia, 20% gave a family history of premature CAD and 19% were current smokers. Known CAD and current smoking were more frequent in men (57% and 25%, respectively), than in women (24% and 9%, respectively, $p<0.001$ for both). The most common reasons for testing were: assessment after invasive coronary revascularization (33%), symptoms in suspected CAD (32%) and asymptomatic patients without known disease (16%), followed by known CAD without intervention (6%), preoperative assessment (6%), evaluation after acute chest pain (6%) and myocardial viability evaluation (1%). Men were more frequently assessed after coronary revascularization than women (47% vs 18%, $p<0.001$), whereas females were mostly examined for symptoms without known CAD (47%), unlike their male counterparts (21%, $p<0.001$). There were no appreciable differences between sexes in other referral indications. Dynamic exercise was used in 29% of cases and pharmacological testing in the remaining 71% (adenosine 52%, dipyridamole 18%, dobutamine 1%). In 2 departments adenosine stressing was used exclusively, whereas in another unit dipyridamole was preferred. In 2 units with a treadmill exercise option, vasodilator stressing was more common in women (76%) than in men (68%, $p<0.05$). TI-201 was used more frequently than Tc99m-agents (63% vs 37%, $p<0.05$) and only in one department a Tc99m-agent was used almost invariably. Finally, normal studies were found in 47% of cases, but women had a higher proportion of normal perfusion than men (69% vs 32%, $p<0.05$). **Conclusion.** (1) Men after coronary revascularization and symptomatic women without known CAD consist the most common populations for myocardial perfusion SPECT referrals. (2) Vasodilator stressing (particularly in women) and TI-201 are employed quite often. (3) The markedly higher proportion of normal studies in women is of concern.

P0831

Diagnostic Relevance of Gated Myocardial Perfusion SPECT for the Assessment of Attenuation Artefacts

S. Czibor, I. Szilvási, M. Moravszki, K. Buga, M. Tóth; Military Hospital, Budapest, HUNGARY.

Aim: The purpose of the study was to assess the diagnostic efficacy of Gated Myocardial Perfusion SPECT (gMPS) in correctly interpreting attenuation artefacts in patients with fixed perfusion defects. **Materials and methods:** Of the 2839 consecutive patients referred for gMPS to our nuclear medicine department from August 2007 to January 2011, we studied a group of 120 patients (99 men and 21 women; mean age 61,99 years) who had fixed perfusion defects shown by the gMPS study and underwent coronary angiography (CAG) within 3 months after the SPECT study. All patients underwent a 1-day Tc-99m-tetrofosmin exercise

stress/rest myocardial perfusion imaging study, with gated SPECT acquisition at rest. Evaluation of myocardial perfusion defects included semi-quantitative visual assessment of perfusion images using the 17 segment model and quantitative analysis (perfusion scores, wall motion and thickening scores) using Cedars-Sinai QGS software package. No attenuation correction was used. MPS without and with gating were interpreted by two nuclear medicine physicians. Then we compared the two scintigraphic findings and angiography in each person, assigning myocardial segments to specific coronary artery territories. Diagnostic accuracy and predictive values were calculated. **Results:** In 83 of 120 cases the fixed perfusion defects were proven to be caused by previous occlusions of coronary arteries resulting in myocardial infarctions (65/83) or by the severe stenoses of the coronary arteries described by the CAG study (18/83). Of the 65 previous myocardial infarctions there were 25 anterior, 5 anteroapical, 7 extensive anterior, 5 lateral and 23 inferior infarctions. In the remaining 37 cases with fixed perfusion defects there were no significant coronary artery stenoses or a medical history of acute coronary syndrome. In 30 out of 37 patients normal wall motion and/or thickening were found by gMPS, so fixed perfusion defects were attenuation artifacts. Of these 30 artefacts, 23 were men's inferior defects, 5 were women's anterior defects and 2 were apically localized. False positivity rate of fixed perfusion defects was reduced from 37/120 to 7/120 by using functional data of gMPS. **Conclusion:** In our patient population ECG-gating is shown to be an effective tool for the assessment of attenuation artefacts, significantly reducing false positive findings of fixed perfusion defect on MPS.

P0832

Left Bundle Branch Block and Coronary Artery Disease in Tc-99m-MIBI SPECT Myocardial Perfusion Imaging

M. Kostkiewicz, W. Szot, K. Jonas; Dept of Nuclear Medicine, Hospital John Paul II, Krakow, POLAND.

Diagnosis of coronary artery disease (CAD) in patients with left bundle branch block (LBBB) is considered a challenge in cardiology due to the low accuracy the of noninvasive methods. Myocardial perfusion SPECT is considered as a valuable diagnostic procedure in CAD with concomitant Left Bundle Branch Block (LBBB), especially in conjunction with a dipyridamole stress test. The aim of our study was to assess 99mTc-MIBI myocardial uptake defects in coronary artery disease in groups with and without LBBB. **Methods:** 174 patients with LAD stenosis were included in the study: 55 (28 females, aged: 68±8) with LBBB and 119 (61 females, aged: 67±11 with no ECG block manifestations). All patients underwent a dipyridamole pharmacological stress myocardial perfusion SPECT protocol with 99mTc MIBI. Patients with previous history of coronary artery bypass grafts or myocardial infarctions were excluded. Patients were asked to withhold beta-blockers and calcium channel blockers for 24 hours testing. A semi-quantitative visual interpretation was performed, using a 17-segment representation of LV with a 5-point uptake scale in at rest and after dipyridamole stress study. **Results:** LBBB patients showed statistically greater LV perfusion defects than the control group. Radiotracer uptake was decreased in septal (S8; $p=0,00223$) and lateral (S12; $p=0,02845$) parts of the anterior wall. Perfusion changes were visible in apical segments (septal: $p=0,01496$, and lateral: $p=0,00298$). LBBB was, however, linked with perfusion improvement in the basal inferior segment (S4; $p=0,04339$). **Conclusion:** Our study showed significant differences in myocardial perfusion between LBBB patients and the control group. LV mechanical dyssynchrony during bundle block affects blood distribution in the left coronary artery territory. Right artery (RCA) supply was not affected. Analysis revealed even more efficient RCA blood distribution during blocks, possibly indicating a form of coronary steal syndrome.

P0833

The Role of the Attenuation Correction by ECG-GATED Myocardial Perfusion SPECT/CT

A. Radácsi¹, Z. Olbrich¹, I. Balogh², A. Rónaszéki³, A. Rónaszéki³; ¹Euromedic Peterfy Hospital, Budapest, HUNGARY, ²Euromedic, Budapest, HUNGARY, ³Peterfy Hospital, Budapest, HUNGARY.

Purpose: to examine the role of the diaphragmatic attenuation correction by SPECT/CT. **hods:** ECG-gated myocardial perfusion SPECT/CT was performed N=274 consecutive male patients, on suspicion of ischemia. Both corrected and uncorrected studies were evaluated with Corridor 4DM-software, using 17-segments model, 5-point segmental scoring scale from 0 (normal) to 4 (absent). We determined and compared corrected and uncorrected summed stress score (SSS), summed rest score (SRS), summed difference score (SDS) of the inferior left ventricle wall (inferoapical, inferomedial, inferobasal segments) and regional wall motion score as determined by uncorrected gated SPECT. **Results:** the value of the SSS, SRS, SDS for uncorrected and corrected studies were: 3.54±2.45, 3.15±2.25, 1.27±1.6 és 2.6±2.76, 2.12±2.38, 1.03±1.87. Differences were statistically significant ($p<0,005$) for SSS and SRS but not for SDS. In case of corrected studies SRS showed better correlation with regional summed wall motion score, $r^2=0.47$, in comparison to uncorrected SRS, $r^2=0.38$. **Conclusion:** Attenuation correction does not affect the

detection of ischemia, but it is essential in case of using only stress study. The corrected SRS correlated better with regional wall motion score, we can detect the size of ischemia more accurate by corrected SPECT/CT in case of diaphragmatic attenuation.

P0834

Regional myocardial mass estimation with SPECT perfusion scintigraphy

M. Zigman M. Stipic, D. Planing, Z. Kusic; University Hospital Centre "Sestre Milosrdnice", ZAGREB, CROATIA.

Aim: Quantification and regional characteristic values of viable regional myocardial mass of left ventricle (RLVM) performed in patients with different type of coronary artery disease (CAD) using SPECT myocardial perfusion scintigraphy. **Patients:** Study included a total number of 158 patients (98 male, 60 female) with suspected heart disease (68 with previous myocardial infarction) who were referred to scintigraphic evaluation of CAD. According to coronary angiography (CA) and scintigraphic finding patients were divided into the groups: A) negative CA and SPECT (n=29); B) negative CA but positive SPECT - patients with non-ischaemic hypertrophic cardiomyopathy (n=27); C) positive CA and SPECT hypoperfusion in LAD supply area (n=52); D) positive CA and SPECT hypoperfusion in RCA and LCX supply area (n=35); E) positive CA and SPECT with mixed hypoperfusion in LAD and RCA supply area (n=15). **Methods:** Patients underwent SPECT (Siemens Symbia SPECT/CT) after intravenous injection of 80MBq of thallium-201, mainly after stress but a few patients had only a rest study. Myocardial mass can be estimated by determining its volume from appropriate tomographic myocardial slices and also by knowing the specific weight of myocardium. The number of tomographic slices in which the myocardium was shown varied from 9 - 14 on VLA or HLA projection (slice width 6.9 mm, edges manually defined). Each slice reflects RLVM and global myocardial mass of LV (GLVM) is a sum of mass value of all slices in one projection. **Results:** Mean of GLVM was in group: A) 165g ± 13g; B) 240g ± 24g; C) 220g ± 28g; D) 185g ± 15g; E) 195g ± 28g. Mean value of slices with the highest RLVM were in group: A) 23g±3g; B) 38g±6g; C) 32g±6g; D) 28g±6g; E) 32g±11g. **Conclusion:** This scintigraphic method is simple, non-invasive and accurate diagnostic procedure for quantification preserved viable myocardial mass of LV. The presented results reveal differences in values of RLVM and GLVM regarding to presence and different type of CAD. Group A which included healthy patients had lower values of RLVM and GLVM compared with other groups. Higher RLVM values were shown in the group C compared to the group D due to regional hypertrophy caused by various degree of myocardial adaptation, depending on size and localization of affected area. Significantly higher RLVM and GLVM values were present in the group B compared with all other groups. Procedure enables follow-up and monitoring of quantitative changes in myocardial mass values during therapy.

P0835

SPECT MPI in evaluation of patients presenting with Atypical Chest Pain

S. Gayana, K. Manohar, R. Kumar, M. L. Abrar, A. Sood, A. Bhattacharya, B. R. Mittal; PGIMER, Chandigarh, INDIA.

Background: Atypical chest pain is a common symptom in middle aged people; the differential diagnosis of which included esophageal pain and cardiac pain and other causes. Differentiation of cause of pain is important for appropriate management. SPECT myocardial perfusion imaging (MPI) has been shown to be useful in evaluating patients with suspicion of coronary artery disease (CAD) in prognostication and directing the management. Importantly percentage of myocardium involved has crucial impact on management with patients with greater than 10% of ischemic myocardium benefiting from cardiac revascularization. However role of SPECT MPI is not much studied in patients with atypical chest pain. **Aim:** This retrospective study was carried to evaluate the utility of SPECT MPI in patients with atypical chest pain and its impact on management. **Methods:** A retrospective analysis of 103 patients with history of atypical chest pain who underwent stress SPECT MPI was made with an emphasis on incidence of perfusion defects and also on the size of the ischemic myocardium. **Results:** Of the total 103 patients included, 64 patients (62%) had normal study and 39 (38%) patients had perfusion defects. 18 (17%) patients had small defect (<5% of LV myocardium), 16 (16%) patients had medium sized defect (5-10% of LV myocardium), 5 (5%) patients had large defect (>10% of LV myocardium). Over all diagnosis of CAD as a cause of chest pain was suggested in 38% of the patients and thus having significant impact on management. SPECT MPI also influenced change in management from medical to revascularization (>10% of myocardium involvement with need for revascularization) in 5% of the patients. **Conclusion:** SPECT MPI helped in establishing the diagnosis of cardiac cause of atypical chest pain in around 38% of the patients. This needs to be addressed by further studies in patients with atypical chest pain and high pre-test probability of CAD.

P0836

The Effect of Soda in Reducing the Infracardiac Intestinal Activity in Tc-99m SESTAMIBI Myocardial Perfusion Scintigraphy

D. Kuşlu¹, E. Öztürk²; ¹Ufuk University Medical Faculty Nuclear Medicine, Ankara, TURKEY, ²Ufuk University Medical Faculty Nuclear Medicine Department, Ankara, TURKEY.

Aim: In the technetium labelled myocardial perfusion scintigraphies infracardiac intestinal activity makes difficulties to interpret especially the inferior wall of the myocardium. The aim of this study was to evaluate whether soda drinking before imaging facilitates the interpretation of the inferior wall. **Materials and Methods:** The images of 100 patients that drank soda before imaging (group 1, 45F, 55M, age 60.4±10.03, 66 physical exercise, 34 pharmacologic exercise), and 100 patients that did not drink soda (group 2, 50F, 50M, age 59.7±10.55, 77 physical exercise, 23 pharmacologic exercise) were evaluated retrospectively. All patients underwent One-Day rest-stress Tc-99m MIBI gated myocardial perfusion SPECT and milk or chocolate was given to accelerate the hepatobiliary excretion. Imaging started right after the patients drank 200 ml soda. The images of patient groups were compared visually (0: no infracardiac activity, 1: infracardiac activity ≤ myocardial activity, 2: infracardiac activity > myocardial activity). **Results:** Sex, age, exercise types of two groups did not show significant difference. In rest and stress images 50, 41, 9 and 78, 20, 2 patients scored as 0, 1, and 2 in group 1, respectively. In group 2; 32, 53, 15 and 61, 37, 2 patients scored as 0, 1, 2 respectively. The number of patients scored as 0 was higher in group 1 than in group 2. Whereas the number of patients scored as 1 and 2 was higher in group 2 than in group 1. Infracardiac abdominal activity was statistically significantly high in group 2 (p=0.03). Among patients underwent physical exercise; 84.8%, 13.6%, 1.55% of patients scored as 0, 1, and 2 in group 1 and 66.2%, 32.5%, 1.3% in group 2, respectively. Among patients underwent pharmacologic exercise; 67.7%, 32.4%, 2.9% of patients scored as 0, 1, and 2 in group 1 and 43.5%, 52.2%, 4.3% in group 2, respectively. Although the number of patients scored as 0 was higher in group 1 than in group 2 in both exercise types, there was significant difference in only physical exercise group (p=0.031). **Conclusion:** Drinking soda before imaging significantly reduces the infracardiac abdominal activity and facilitates the interpretation of the inferior wall.

P0837

Effect of acquisition time and reconstruction method on quantitative parameters in myocardial perfusion imaging

L. H. Enevoldsen¹, C. A. K. Menashi², L. T. Jensen¹, U. B. Andersen¹, O. M. Henriksen³; ¹Glostrup University Hospital, Glostrup, DENMARK, ²Næstved Sygehus, Næstved, DENMARK.

Aim: Use of iterative reconstruction algorithms applying resolution recovery (RR) and noise-reduction technology may allow reduction of acquisition time and/or administered dose without compromising image quality. Previous studies have reported that acquisition time may be halved without affecting automated perfusion and motion parameters when RR reconstruction algorithms are used. However, the relative effect of reduced acquisition time and reconstruction software has not previously been reported. This study investigates the effect of half time (HT) acquisition and RR reconstruction compared to standard full time (FT) acquisition and filtered back projection (FBP) reconstruction. **Methods:** 45 consecutive, non-selected patients (24 men, 21 women; mean age 61 ± 12 years; range 20 to 83 years) referred for routine 2-day stress (42 adenosine/3 dobutamine)/rest 600 MBq 99mTc-sestamibi myocardial perfusion SPECT because of known or suspected CAD were prospectively included in this study. All patients underwent a FT and a HT scan on a 90°-angled dual-head integrated SPECT/CT camera. Both FT and HT scans were processed with FBP reconstruction and HT scans, additionally, with the RR software (Evolution for Cardiac, GE Healthcare), producing three dataset for each patient (FT-FBP, HT-FBP and HT-RR). Subsequently, each data set was analyzed using commercially available software (QGS/QPS, Cedars-Sinai). From non-gated studies summed stressed score (SSS), summed rest score (SRS), summed difference score (SDS), stress and rest perfusion extent and non-gated volumes were obtained. From gated studies end-systolic volume (ESV), end-diastolic volume (EDV) and ejection fraction (LVEF) were obtained. To obtain normal distribution perfusions defect measures were log transformed and effects are reported as relative changes. **Results:** HT acquisition increased stress perfusion defect extent by a factor of 1.28 (p=0.02) whereas RR reconstruction increased rest perfusion defect extent by a factor of 1.4 (p=0.01). LVEF increased by 2% point and ESV and EDV was decreased by 5.5 and 4.2 ml, respectively, using RR reconstruction (p<0.01 for all). HT acquisition increased ESV by 2.2 ml (p=0.003) and tended to decrease LVEF (by 1.3%, p=0.052). Acquisition time and reconstruction method had no effect on SMS, SRS, SDS, non-gated volumes and TID ratio. **Conclusion:** Both HT acquisition and RR reconstruction have significant effects on automated motion and perfusion parameters obtained with standard software. In general, the changes induced by HT acquisition are not compensated for by RR reconstruction. However, the effects induced by both factors are relatively small and probably of limited clinical importance.

P0838

Effect of acquisition time and reconstruction method on image quality in myocardial perfusion imaging

L. H. Enevoldsen¹, C. A. K. Menashi², L. T. Jensen¹, U. B. Andersen¹, O. M. Henriksen¹; ¹Glostrup University Hospital, Glostrup, DENMARK, ²Næstved Sygehus, Næstved, DENMARK.

Aim: Shortening scan time and/or reducing radiation dose at maintained image quality using new iterative reconstruction algorithms with resolution recovery (RR) and noise-reduction technology seems promising compared to standard myocardial perfusion imaging (MPI) reconstruction protocols. Thus, the aim of the present study was to qualitatively evaluate myocardial perfusion SPECT obtained on an integrated SPECT/CT camera using short acquisition half time (HT) protocols with the use of the new Evolution for Cardiac (RR) Software package compared with standard acquisition full time (FT) acquisition. **Methods:** 45 consecutive, non-selected patients (24 men, 21 women; mean \pm -SD age 61 \pm 12 years; range 20 to 83 years) referred for routine 2-day stress (42 adenosine/3 dobutamine)/rest 600 MBq 99mTc-sestamibi myocardial perfusion SPECT because of known or suspected CAD were prospectively included in this study. All patients underwent a FT and a HT scan on a 90°-angled dual-head integrated SPECT/CT camera. Both FT and HT scans were processed with standard IR and additionally HT scans were processed with the new RR software, resulting in 3 dataset for each patient (FT-IR, HT-IR and HT-RR). Subsequently, all data sets were blinded and presented in randomized order to two experienced nuclear medicine physicians, who visually evaluated image quality using a 10 cm VAS-scale score and further classified the study as “normal”, “irreversible” or “reversible”. In case of observer disagreement, a consensus conclusion was reached. Effect of acquisition time and re-construction method on VAS scores were analyzed applying a variance component model. Inter-observer and method agreement was analyzed with kappa-statistics. **Results:** VAS score of overall image quality decreased by 1.2 from 6.8 when acquisition time was reduced and increased by 2.0 when RR reconstruction was used ($p < 0.0001$ for both). Similar effects were observed for other image quality parameters (background activity, myocardial homogeneity and quality of attenuation correction). Kappa value of inter-observer agreement decreased from 0.40 for FT-IR studies to 0.27 for HT-IR studies and 0.33 for FT-RR studies. Inter-method agreement with FT-IR was 0.35 for HT-IR and 0.36. **Conclusion:** Using standard processing methods, reducing the scan time by half compromises image quality in cardiac SPECT MPI studies. This image quality loss can be reversed using the new RR algorithm, resulting in image quality similar to or superior to standard FT imaging. However, loss of inter-observer agreement associated with decreased acquisition time is only partially compensated for by the RR reconstruction algorithm.

P0839


How reliable is a half time acquisition for gated myocardial perfusion imaging?

G. James¹, A. Jennings¹, J. O'Brien¹, J. Cullis², A. Notghi¹; ¹Sandwell and West Birmingham Hospitals NHS Trust, Birmingham, UNITED KINGDOM, ²University Hospitals Coventry and Warwickshire, Coventry, UNITED KINGDOM.

Aim: to assess the accuracy of low count gated half time myocardial perfusion image (MPI) acquisition compared to a full time gated acquisition. 19 consecutive patients (<90 kg) who agreed to enter the trial underwent two consecutive gated MPI scans using a half time imaging protocol. The patients received 400 MBq tetrofosmin during a standard adenosine infusion for stress. Patients came back the following day and rest images were acquired following 400 MBq tetrofosmin injection. Imaging (using GE Infinia with LEHR collimator) was commenced 30 minutes after each injection. On each visit two consecutive 180 degree acquisitions were performed (60 projections, 18 sec / frame with a zoom of 1.5). Eight bins were used for gating. Each acquisition was 9 minutes. Three sets of data were produced: half time acquisition 1, half time acquisition 2 and a full time acquisition by summing the two consecutive half time acquisitions (9+9=18 minutes). Cedar Sinai QGS software (Autoquant 7, Philips Medical Systems) was used to calculate the end diastolic volume (EDV), end systolic volume (ESV) and ejection fraction (EF) for each acquisition. Student's paired t-test was used for data analysis (Minitab statistical package, Minitab Inc). There were 19 patients, imaged twice (rest and stress). There were 38 paired half time and full time data for each parameter ($n=38$). There was no difference between half time and full time EDV (117.8 vs. 118.3, $p=0.639$, ESV 64.2 vs. 64.3, $p=0.946$), or calculated EF (52.9% vs. 52.8%, $p=0.963$), with near perfect correlation (EDV $r=0.996$, ESV $r=0.997$, EF $r=0.973$). There was also no difference between the first and second half time acquisitions (EDV $p=0.609$, ESV $p=0.356$, EF $p=0.304$). **Conclusion:** QGS software gives consistent EDV, ESV and EF regardless of the low count density of the short half time acquisition when compared to standard full time acquisition. Left ventricular gating parameters

P0841

Comparison of SPECT-CT and SPECT myocardial perfusion

 Springer

imaging in the low and intermediate pretest probability groups

B. Fallahi, A. HassanzadehRad, A. Fard-Esfahani, A. Emami-Ardekani, D. Beiki, M. Eftekhari, M. Saghari; Research Institute for Nuclear Medicine, Tehran, IRAN, ISLAMIC REPUBLIC OF.

Aim: The purpose of this study was to compare sensitivity, normalcy rate and Positive Predictive Value (PPV) of the SPECT-low dose CT and SPECT Myocardial Perfusion Imaging (MPI), both visually and by application of quantitative methods. We also wanted to quantify the possible shift in normal thresholds of Summed Stress Score (SSS) and Transient Ischemic Dilation (TID) ratio in the SPECT-CT MPI. **Materials and Methods:** 121 patients were classified into low (83 patients, Age: 48.41 ± 8.89 years, BMI = 29.46 ± 6.20 gr/cm²) and intermediate (38 patients, Age: 60.47 ± 1.04 years, BMI = 27.69 ± 3.78 gr/cm²) pretest probability groups for Coronary Artery Disease (CAD), based upon the Diamond-Forrester method and Duke University Medical Center nomogram. Each patient underwent both Attenuation Corrected (AC) SPECT-CT MPI and non Attenuation Corrected (non-AC) SPECT MPI (two day Tc-99m sestamibi stress-rest protocol) using Siemens SYMBIA-T2 SPECT-CT imaging system. Normalcy rate (in the low pretest group) and sensitivity and PPV (in the intermediate pretest group, using coronary angiography as the gold standard) were calculated and compared. The comparison was based on both visual interpretation and quantitative analysis (using Cedars-Sinai QPS-QGS and 4DM SPECT software packages). **Results:** In the low pretest probability group visual interpretations lead to a statistically significant improvement in normalcy rate in the SPECT-CT acquisition compared with the SPECT MPI (91.6 % versus 74.7 % respectively). This improvement was more prominent in the Right Coronary Artery (RCA) vascular territory. The SSS was also significantly lower in the attenuation corrected images in both QPS-QGS and 4DM-SPECT software analysis. In the intermediate pretest group the sensitivity and PPV of the SPECT-CT acquisition were significantly higher than SPECT MPI (Sensitivity: 86 % versus 66 % , PPV: 100% versus 92% respectively). Within each pretest probability group, no significant difference was noted in the TID ratios calculated by QPS-QGS and 4DM-SPECT. Quantitative analysis revealed a change in the normal threshold of the SSS in the SPECT-CT images compared with SPECT MPI. **Conclusion:** The preliminary data showed superiority of SPECT-CT MPI to SPECT MPI in terms of normalcy rate, sensitivity and PPV in the low and intermediate pretest groups. The quantitative software analysis confirmed the visual findings. Our study also suggests the need for redefining SSS normal threshold in the SPECT-CT MPI.

P0842

Prognostic value of stress myocardial perfusion imaging in low to intermediate risk patients for coronary artery disease

A. Peter¹, S. Lucic¹, R. Jung², M. A. Lucic¹, S. Tadic², S. Stojisic², M. Stefanovic²; ¹Institute of Oncology Vojvodina, Sremska Kamenica, SERBIA, ²Institute for Cardiovascular diseases of Vojvodina, Sremska Kamenica, SERBIA.

Introduction: Stress myocardial perfusion imaging (MPI) is one of the major diagnostic tools in the evaluation of the presence and severity of myocardial ischemia in patients with suspected coronary artery disease (CAD). **Aim of the study:** to determine the impact of stress MPI in the detection of perfusion abnormalities, their severity and to determine the prognostic value of this diagnostic modality. **Material and methods:** In the period from June 2007. to October 2011. a total number of 321 patients with suspected CAD and had a low to intermediate pre test likelihood (222 female or 65.16% and 99 male or 30.84%) underwent a two- day protocol, diprydamole stress/ rest Tc- 99m- MIBI myocardial perfusion imaging (MPI). After that they were followed up for the occurrence of cardiac death or myocardial infarction over a mean follow up period of 41.00 \pm -16.48 months. **Results:** Average age in the group of examined women was 61.93 \pm -8.83 years. In the group of women normal MPI had 85.14%, ischemia was found in 6.31%, discrete ischemia that was considered as nonsignificant had 6.75%, borderline perfusion defects had 1.80% and perfusion defects considered as normal for LBBB perfusion pattern had 3.60%. Average period of follow up was 41.09 \pm - 16.96, minimum 7 and maximum 58 months. Average age in the group of examined was 67.94 \pm - 8.85 years. In this group normal MPI had 81.81%, ischemia had 5.05%, discrete ischemia that was considered as nonsignificant had 8.08%, borderline perfusion defects had 2.02% and perfusion defects considered as normal for LBBB perfusion pattern had 3.03%. Average period of follow up was 40.96 \pm - 17.56, minimum 6 and maximum 58 months. In both groups the SDS was ≤ 3 in the group with normal MPI, in the group with ischemia ≥ 7 , in the group with discrete perfusion defects it was between 3 and 5, in the group with borderline perfusion defects between 5 and 7 and in the group with LBBB it was between 3 and 5. The results of stress MPI and consequent follow up showed us that the majority of the examined group was at low risk of nonfatal myocardial infarction and for cardiac death. **Conclusion:** Stress MPI identifies successfully patients with hemodynamically significant ischemia and gives important prognostic information toward the identification of patients under risk for major fatal cardiovascular incidents.

P0843**Myocardial SPECT after Revascularisation: Indications and Results**

A. Sallak^{1,2}, A. Guensi¹, A. Malika¹, M. Kebbou¹; ¹Ibn Rochd UH, Casablanca, MOROCCO, ²nuclear medicine department, Casablanca, MOROCCO.

Despite the development of myocardial revascularization techniques, the rate of restenosis remains significant. This work reports the indications and results of myocardial SPECT (MSPECT) after revascularization in 29 patients investigated between March 2009 and February 2012. Patients were aged 35 to 82 years with a male predominance (25 males/4females). In our patients 79 % have had bridged stents. The time between revascularization and the prescription of MSPECT ranged from 1 to 12 months. Twenty-four patients were referred for ischemia diagnosis (16 have had recurrent angina, 4 coronary stenosis affirmed by angiography, 3 asymptomatic, one patient have had myocardial infarction (MI) before MSPECT). Five patients were investigated for viability studies (3 patients with MI after revascularization and 2 with stent restenosis affirmed by coronary angiography). The one day stress-rest or rest-rest protocols were used in all patients. MSPECT rest study's (viability) tracers were thallium 201(3 patients) and tetrofosmin (2 patients). Analysis of the results was based on the indications (ischemia or Viability). In patients with suspected ischemia, 75% of patients (11 with residual angina and 3 asymptomatic) have had positive MSPECT in revascularized walls. MSPECT have shown ischemia in other left ventricular walls in 4 cases. The rest MSPECT done in 5 patients showed a lack of viability in known pathological territories. Outside these territories, other abnormalities were detected in 3/5 patients. The MSPECT is a non-invasive and efficient tool (predictive value superior to chest pain and EE) in screening coronary restenosis after revascularization with 93% of sensitivity and up to 80% specificity. MSPECT have a prognostic value in quantification of ischemia in known walls and detect other coronary lesion. In patients with MI a rest MSPECT screens patients who will need repeated revascularization. We emphasize the importance of a MSPECT reference before revascularization for better monitoring of patients.

P0844**Added Value of Nuclear Cardiac Perfusion Imaging in Patients with Diabetes type 2 who underwent Coronary Angiography**

A. Romeo¹, M. Rossi¹, M. Santoro¹, G. Corona², G. Nobile³, S. Bernardi¹, G. Fagioli¹; ¹Ausi di Bologna, Nuclear Medicine Unit, Bologna, ITALY, ²Ausi di Bologna, Endocrinology Unit, Bologna, ITALY, ³Ausi di Bologna, Cardiology Unit, Bologna, ITALY.

Background Coronary microvascular ischemia is quite a common clinical condition in diabetics and, thought coronary angiography is to be considered the gold standard method for the detection of coronary artery disease, myocardial perfusion imaging contributes to provide additional value supporting the physiopathological basis of diabetes microangiopathy. **Materials - Methods** A consecutive retrospective series of 72 diabetics with typical or atypical symptoms (51 men; 21 women; mean age 65 with Diabetes type 2), achieving balanced diabetes treatment and without known coronary artery disease underwent stress-rest two days protocol Myocardial Perfusion Single Photon Emission Computerized Tomography (SPECT). All the 72 subjects underwent coronary angiography within six months. **Results** SPECT studies showed that myocardial perfusion was abnormal in n. 65 (90%): 9 subjects had mild ischemia, 29 moderate ischemia and 27 severe induced ischemia. Coronary angiography revealed significant coronary stenosis in 63 patients (87%) while 9 of 72 subjects showed absent or non-hemodynamically stenosis. 58 of 63 subjects with positive coronary angiography (92%) were found to have a critical stenosis and 5 subjects to have a sub critical stenosis which was correlate anatomically with a perfusion abnormality. Correlation analysis between perfusion defects and critical coronary stenosis showed an overall agreement of 89% between the two methods (SPECT vs coronary angiography) and a mismatch in 11% of the cases, showing that plaque burden may partially explain the presence of myocardial perfusion defects in cases with angiographically non-obstructive coronary lesions but may be due to further mechanisms such as endothelial/microvascular dysfunction. **Conclusions** SPECT results suggest that sub-obstructive coronary artery disease noted on angiography could result in perfusion defects due to coronary microangiopathy, giving an additional diagnostic and prognostic value in early detection of coronary microvascular ischemia in symptomatic diabetic patients.

P0845**Hypertention and other Cardiocascular factors in diabetics type 2, assessed by Myocardial SPECT study**

I. Kotsalou¹, A. Kotsalos², N. Zakopoulos³, N. Dimakopoulos¹, M. Dimopoulos³; ¹NIMTS Hospital Nuclear Medicine Dept., Athens, GREECE, ²NIMTS Hospital Cardiovascular Dept., Athens, GREECE, ³University of Athens, Internal Therapy Dept., Alexandra Hospital, Athens, GREECE.

AIM : Diabetes is nowadays considered as a Coronary Artery Disease (CAD) risk equivalent with the evidence of an increased mortality rate in patients with Diabetes Mellitus type 2(DM 2). Aim of this study is to identify, using Myocardial Perfusion SPECT studies, in which degree Hypertension increases the Cardiovascular risk profile of diabetics. **METHOD** : We studied 96 individuals diabetics type 2, mean age 62 years, 78,6% male and 21,4% female. Inclusion criteria were: HbA_{1c} ≤ 7,0% and LDL < 206 mmol/L. 50 (52%) and Blood Pressure controlled (≤ 140/90 mmHg) using appropriate medication or not. Out of 96 diabetics had also history of Hypertension (Group A), whereas 46 (48%-Group B) had no additional risk factors, but Diabetes. All patients were subjected to a rest and stress Technetium-99m tetrofosmin myocardial perfusion SPECT study. The images were interpreted as fixed perfusion defects, reversible ischemia findings and normal perfusion studies. **RESULTS** : Significant perfusion abnormalities were found in 34 (74%) out of 46 diabetics (Group B) and in 41 (82%) out of the 50 Hypertensives diabetics (Group A). On the other hand, there were totally 21 (22%) normal myocardial perfusion SPECT studies. The correlation of MPS with the coronary angiogram which followed, showed similar incidence of CAD in both groups. **CONCLUSION** : Coronary Artery Disease (CAD) is a common complication of Diabetes Mellitus type 2. Hypertension moderately increases the cardiovascular risk profile of diabetics, which is anyway heavy. Patients with diabetes and hypertension should be screened routinely for CAD by SPECT MPI independently from other co-existing risk factors.

P36-2 - Tuesday, October 30, 2012, 16:00 - 16:30, Poster Exhibition Area

Cardiovascular: Metabolism**P0846****Investigation of ischemic myocardium using positron emission tomography (PET) by coincidence system with ¹⁸F-FDG comparing with perfusion image**

K. Koyama¹, T. Toyama¹, S. Kodaira², H. Tomonaga³, Y. Matsuda³, T. Higuchi⁴, Y. Arisaka⁴, H. Hoshizaki¹, S. Ooshima¹, Y. Tsushima³; ¹Gunma Prefectural cardiovascular center, Maebashi, JAPAN, ²Gunma Chuo General hospital, Maebashi, JAPAN, ³Gunma University Faculty of Medicine, Maebashi, JAPAN, ⁴Gunma University Faculty of Medicine, Maebashi, JAPAN.

Aim: ¹⁸F-FDG (FDG) image is useful method to evaluate myocardial glucose metabolism or myocardial viability. Perfusion image displays damaged myocardium. The purpose of this study was to investigate ischemic myocardium using PET by coincidence system with ¹⁸F-FDG comparing with perfusion image. **Materials and Methods:** Fifteen patients with ischemic heart disease, ten were with acute myocardial infarction (AMI) and five were with old myocardial infarction (OMI), were examined. Both FDG and perfusion image were performed. In perfusion study, delayed phase was added in protocol to obtain myocardial washout image. Defect score, segmental washout and FDG accumulation were assessed. The images were measured and localized according to the 17-segment model. **Results:** In 255 left ventricular segments were examined. Mean total defect scores of AMI patients and OMI patients were 21 and 18, respectively. Mean SUV of FDG in segment of abnormal perfusion and normal perfusion were 2.35 and 2.35 in AMI patients and 3.08 and 3.71 in OMI patients, respectively. Subtracted SUV of abnormal perfusion segment from normal perfusion segment in AMI patients and OMI patients were 1.44 and 0.63, respectively. The lowest FDG accumulation segment matched with severely reduced perfusion segment. Average number of washout segments in AMI and OMI were 3.28 and 0, respectively. In the segments with high washout showed reduced FDG accumulation. **Conclusions:** FDG images showed unique appearance in ischemic myocardium comparing with acute and chronic phase. PET by coincidence system made it possible to investigate myocardial glucose metabolism and perfusion in same instrument.

P0847**Length of Fasting Does Not Significantly Affect Myocardial Metabolism on Serial Tumor [¹⁸F]-FDG PET-CT scans.**

D. P. Thut, M. Djekidel; Yale University New Haven Hospital, New Haven, CT, UNITED STATES.

PURPOSE: Our study aims to evaluate the effect of fasting length on myocardial metabolism in selected oncologic patients using PET-CT scans. **METHODS AND MATERIALS:** We performed a retrospective review of 100 PET-CT scans from a total of 20 men and women with a history of lymphoma, who were being evaluated by at least 5 serial [¹⁸F]-FDG PET-CT scans. The number of fasting hours was obtained from patient questionnaire. Distribution of myocardial uptake was determined by visual assessment and the maximum standardized uptake value (SUV_m) was calculated using an AW-GE Workstation. **RESULTS:** Of the 20 patients, 13 were males, 7 were females and the mean age was 45. We found no statistically significant correlation between of the length of fasting and amount of cardiac

uptake (P-value: 0.4786). All patients had fasted for more than 5 hours. Some fasted up to 20 hours. Fourteen patients who fasted over 12 hours still had significant myocardial uptake. Even though fasting times varied, afternoon scans showed less myocardial uptake. **CONCLUSION:** Myocardial metabolism is extremely variable and the length of fasting does not appear to have a significant effect on [F18]-FDG uptake.

P0848

To study the effect of duration of fasting and diet on the myocardial uptake of F-18-2-fluoro-2-deoxyglucose (F-18 FDG) at rest

C. D. Patel, P. Kumar, S. Singla, A. Malhotra; Nuclear Medicine Department, All India Institute of Medical Sciences, New Delhi, INDIA.

Aim: We observed the effect of duration of fasting and diet on the myocardial uptake pattern of F-18 FDG in patients routinely referred for oncological evaluation and no previous history of CAD. **Methods:** A total of 153 patients (M: 81, F: 72; mean age: 47.43± 15.18 years; mean blood glucose level (mBG) 105.34± 23.26 mg/dl; were equally divided in three groups. Group A: 4-6 hrs fasting, Group B: Overnight fasting (12-14 hrs) and Group C: Patients on overnight fasting and a low carbohydrate and fat rich diet for 2 days prior to the PET scan. We classified the FDG uptake as: 1) Homogeneous uptake in the left ventricular (LV) myocardium, 2) Heterogeneous uptake (myocardial uptake more than the background) which was further assigned to conventional regional LV walls and 3) 'no uptake' or negligible uptake in the LV. **Results:** All the groups were matched for confounding factors like sex distribution, age, smoking, diabetes, hypertension and history of chemotherapy. Significant difference in mBG was noted between group A & B and Group A & C but the mBG between Group B & C was not significant (p=0.425). We observed the 'no uptake' pattern in 5 (10%), 28 (55%) & 39 (77%), 'Heterogeneous' pattern of FDG uptake in 20 (39%), 14 (28%) & 7 (14%) and 'Homogeneous' pattern in 26 (51%), 9 (18%) & 5 (10%) patients in Group A, B and C respectively. There was statistically significant difference of myocardial uptake pattern between group A and B (p<0.0001), between group A and C (p<0.0001) and between Group B and C (p=0.023). The mBG was 102, 105 and 111 mg/dl in 'no uptake', heterogeneous and homogeneous uptake pattern respectively (p = 0.103). Also, within each group the mBG was not related to the uptake pattern (p=0.103). Multivariate analysis showed that mBG levels did not affect the uptake pattern in different groups (p=0.805). Region wise distribution of 41 heterogeneous myocardial FDG uptake patterns were noted in lateral wall (90%), base of the heart (88%), inferior wall (56%) and distal antero-apical (46%). **Conclusion:** Both restricted diet and duration of fasting play an important role in determining the pattern and suppression of myocardial F-18 FDG uptake. Group C protocol of overnight fasting and restricted diet suppresses myocardial F-18 FDG uptake more than Group B protocol of overnight fasting alone which suppress uptake more than Group A protocol of 4 hr fasting.

P38-2 - Tuesday, October 30, 2012, 16:00 - 16:30, Poster Exhibition Area

Cardiovascular: New & Innovative

P0849

Reprojection of Tomographic Cardiac Blood Pool Images - Applicability to Clinical Studies

J. O' Doherty¹, J. Price², K. Wechalekar³; ¹Royal Surrey County Hospital, Guildford, UNITED KINGDOM, ²Institute of Cancer Research, Sutton, UNITED KINGDOM, ³Royal Brompton Hospital, London, UNITED KINGDOM.

Gated Radionuclide Ventriculography (RNV) is routinely used as a diagnostic test to assess parameters of ventricular function such as wall motion abnormalities, ventricular synchrony and overall left ventricular function. It is used for serial assessment in patients having cardiotoxic chemotherapy and for cardiac resynchronisation therapy. Recent developments in software have made it possible to perform tomographic imaging (SPECT RNV), which reduces effects of attenuation and improves cardiac chamber definition. The dependence on finding best septal separation angle and marking of representative background region is not required because of inherent tomographic nature of the study. However during this transition from planar to SPECT RNV, we must perform 2 serial but separate acquisitions for comparing and contrasting one against the other. This lead to an increased acquisition time per patient, potentially reducing patient compliance and throughput. To overcome these limitations, we propose a novel method of reprojecting gated planar data from gated tomographic acquisition. The tomographic acquisition was reprojected at the angle where septal separation is visualised as greatest, which thus simulates a planar acquisition. The original planar and reprojected planar images were processed using a planar quantification algorithm (HERMES FUGA Gated Blood Pool v 4.7). SPECT RNV data was processed using Cedars Sinai Quantitative Blood Pool SPECT (QBS) 2008. Left ventricular ejection fraction (LVEF) was determined for the randomised SPECT, planar and

reprojected planar dataset by a consultant nuclear medicine physician blinded to all patient data. On statistical analysis, results for the preliminary cases (n=10) show that LVEFs are comparable for all techniques (P>0.05). Student's t-tests performed between the reprojected planar and both planar and SPECT both show good correlation (P>0.05 in both cases). This small but novel study shows that the reprojected planar images can help with the transition from planar to SPECT RNV. This reduces the need for two separate acquisitions thereby increasing patient comfort and throughput. More studies are needed to identify the reproducibility, strengths and weaknesses of reprojection technique. If similar results can be proven in larger population, SPECT may supersede the need for planar imaging of cardiac blood pool assessment.

P0850

Thallium-201 Myocardium Scintigraphy Advocates for the 'Innocent' Character of the Parabolic ("Sagging") ST Depression during Dipyridamol Stress Test; Preliminary Results

A. Zafeiropoulos, G. S. Limouris; I Radiology Dept, Nucl Med Div 'Areteiaion' Hospital, University Medical Faculty, Athens, GREECE.

Aim: As early as 1992, Leo Schamroth in his historical 7th edition of the "Introduction to Electrocardiography" denoted that the parabolic depression of the ST-segment on a rest ECG was an 'innocent' finding. Furthermore it is not to ignore that according to guidelines to stress testing [Chang E 1997] ST depression on dipyridamol stress test is a highly specific marker of specific CAD. We first investigate the ST parabolic depression, during dipyridamol stress test, in correlation with ²⁰¹Tl concordant scintigraphy. **Materials and Methods:** Seven patients undergoing screening for CAD ²⁰¹Tl myocardium tomo- scintigraphy with normal initial (surface) ECG showed a >1.2mm parabolic ("sag-ging") ST depression, during dipyridamol stress test, with no disruption of the ECG line. In early recovery ECG a complete remission was observed. **Results:** In all 7 patients scintigraphy was normal, implying the 'innocent character' of the ST depression morphology. **Conclusion:** Parabolic ST depression, with no disruption of the ECG line, deemed innocent finding during dipyridamol stress test, and should be further assessed by a larger series. The aforementioned ST variant is due to the fusion of two factors: (a) the marked atrial repolarization wave and (b) the normal ST-segment.

P0851

Coronary Artery Calcium Scoring To Exclude Flow-limiting Coronary Artery Disease In Symptomatic Stable Patients At Low Or Intermediate Risk

M. Mouden, J. R. Timmer, S. Reiffers, A. H. J. Oostdijk, S. Knollem, J. P. Ottenvanger, P. L. Jager; Isala Kliniek Zwolle, Zwolle, NETHERLANDS.

Purpose: Recent guidelines recommend coronary artery calcium (CAC) scoring to exclude obstructive coronary artery disease (CAD) in symptomatic stable patients with a low or intermediate pre-test probability. However, this was recently debated because higher rates of obstructive CAD and ischemia were observed in more recent studies. Therefore, we assessed the frequency of flow-limiting CAD in a homogeneous population with stable anginal complaints, low to intermediate likelihood and a CAC score of zero. **Methods:** Between 2009 and 2011 a total of 3291 consecutive stable patients without known CAD underwent simultaneous myocardial perfusion imaging and CAC scoring on a hybrid SPECT/CT (64-slice) device. In 858 patients (26%) CAC score was zero, and they are the current study population. Additional CT coronary angiography (CTCA) was performed in those with abnormal SPECT findings when feasible. Clinical follow-up was recorded with regard to coronary revascularization, nonfatal myocardial infarction or death. **Results:** Of the 858 patients (mean age 54 ± 11 years, 69% female), SPECT was normal in 88% and abnormal in 12% (equivocal 5%, fixed defect 4% and ischemia 3%). In the group with abnormal SPECT, additional CTCA was performed in 90%, showing non-obstructive CAD in 8% and normal coronary arteries in 92%. In all patients not suited for CTCA, invasive coronary angiography excluded obstructive CAD. During a mean follow up of 16 ± 8 months, no ischemic events were recorded. **Conclusions:** Stable symptomatic patients at low to intermediate risk for CAD with a CAC score of zero never had flow-limiting CAD. Similar to recent guidelines, these findings support the application of CAC score testing as a reliable and safe selection tool to exclude relevant CAD.

P0852

Assessment of Ejection Fraction with DPD Gated SPECT in Cardiac Amyloidosis

D. R. Pencharz, A. Quigley, D. Hutt, T. Wagner, P. Hawkins, A. Wechalekar; Royal Free Hospital, London, UNITED KINGDOM.

Background 99mTc-3, 3-diphosphono-1, 2-propanodicarboxylic acid (DPD) localises to cardiac amyloid deposits, most notably those of transthyretin type, and correlates well with cardiac amyloid burden. Analogous to gated SPECT myocardial

perfusion scans with thallium, sestamibi or tetrofosmin, which are validated methods of assessing left ventricular size and function, we investigated the potential of DPD gated SPECT for estimating left ventricular ejection fraction (EF) in patients with cardiac amyloidosis, correlating the results with echocardiography. **Methods** EF was calculated from gated SPECT studies using commercially available software. We compared the EF obtained from DPD gated cardiac SPECT scans with values obtained from 2D echocardiograms in patients who had had both examinations and sufficient cardiac DPD uptake to use the software (Perugini grade 2 and 3). The EFs from DPD scans and echocardiograms were compared using a Bland Altman plot and by calculating the mean difference (echo EF - SPECT EF) and the 95% limits of agreement (interval between which 95% of differences would fall) in the EF between the two groups. **Results** Fifty-eight patients were studied. Uptake of DPD was heterogeneous in the majority of the scans, and was greater in the septum than in other parts of the myocardium. The range of the difference between the EF obtained from the two methods was -25% to +29%. The EF by DPD was $\leq 10\%$ or $\geq 10\%$ compared to echocardiography in 19 and 4 patients respectively. The 95% limits of agreement were -15.8%, 95%CI (-20.6 – -11.1) to 24.8% 95%CI (20.1 – 29.5). This variability in the agreement was confirmed by a Bland Altman plot. **Conclusion** There was poor concordance between EF measured by echocardiography and DPD scintigraphy. EF measurement by echocardiography has limitations in amyloidosis due to early loss of longitudinal cardiac function which results in overestimation. Limitations of this study include the software used to calculate EF not being designed for use with DPD and the heterogeneous nature of DPD uptake within the myocardium. Both these techniques evidently cannot be used interchangeably, and an alternative method is needed to validate the findings. We plan to correlate the EF from both methods with cardiac MRI and consider correlation with radionuclide ventriculography in a future prospective study.

P0853

The Potential Usefulness of the Myocardial Perfusion SPECT in the Identification of Pulmonary Hypertension: Evaluation in Patients with Normal Left Ventricular Ejection Fraction

T. Vieira, A. Oliveira, P. Oliveira, V. Alves, T. Faria, M. B. Pérez, J. G. Pereira; Centro Hospitalar de São João, Porto, PORTUGAL.

Aim: Pulmonary hypertension (PH) frequently causes symptoms similar to those observed in patients with coronary artery disease. The utility of myocardial SPECT (MPS) for the assessment of PH has not been extensively studied. Even so, it was previously reported that increased lung uptake of myocardial perfusion agents on MPS suggests increased pulmonary wedge pressure during stress and that the right ventricle to left ventricle uptake ratio (RV/LV UR) measured on MPS can be used to identify patients with high pulmonary artery pressure (PAP). We aimed to investigate the role of RV/LV UR obtained from MPS for the evaluation of PH in patients with normal left ventricular ejection fraction (LVEF) and without myocardial perfusion defects (MPD). **Materials and methods:** We studied 105 consecutive patients addressed for gated MPS with stress induced by the Bruce protocol and MPS was performed 30-60min after tetrofosmin-Tc-99m administration. LV perfusion and function were assessed. Subsequently, we summed coronal LV slices from SPECT acquisition for the purpose of lung/heart ratio (LHR) calculation. We manually generated LV and left lung ROIs in the resulting summed images. LHR was calculated as the ratio of the average pixel counts in the lung and LV ROIs. We conducted a Pearson's correlation analysis to evaluate the association of LHR with LVEF, and a visual analysis of the dispersion graphic to search for cases of greater variation around the line of best fit (LBF) in a range interval of normal LVEF obtained from the gated MPS. After identifying the cases with the greater variation, patients with MPD were excluded from the investigation. Seven patients with LHR below the LBF (group 1) and 8 patients with LHR above the LBF (group 2) were included for RV/LV UR calculation. From a midventricular tomographic slice, an investigator blinded for the LHR values placed 4x4 pixel ROIs in the RV and LV free walls. RV/LV UR was calculated as the ratio of total myocardial counts in each ROI. Statistical analysis was conducted to evaluate the association of RV/LV UR with LHR. **Results:** Mean EF was 64.9% ((group 1: EF - 64.6%; mean LHR - 0.23); (group 2: EF - 65.3%; mean LHR - 0.37)). Mean RV/LV UR was 0.27 in group 1 and 0.37 in group 2. RV/LV UR showed a positive correlation with LHR ($r=50.3$). **Conclusion:** RV/LV UR correlates with LHR as an indicator of PAP and may be a useful index of PH.

P0854

Correlation of Fractional Flow Reserve with stress perfusion scintigraphy for the detection of ischaemia due to intermediate coronary artery stenosis

V. P. Solomyanny; Russian Cardiology Research and Production Complex, Moscow, RUSSIAN FEDERATION.

Comparison of Fractional Flow Reserve with stress perfusion scintigraphy for the detection of ischaemia due to intermediate coronary artery stenosis Objectives. To compare ischaemia assessment by Fractional flow reserve (FFR) SPECT scanning by using cardiac gating testing in patients with intermediate coronary artery

stenosis. **Background.** FFR it is now frequently used to determine the management of intermediate coronary artery stenosis. A cut-off value of 0.75 is used in clinical practice to guide revascularisation supported by long-term outcome data, but a 'grey zone' of 0.75-0.8 with uncertain clinical significance exists. Advances in non-invasive imaging tests (gated SPECT) warrant a re-evaluation of FFR at intermediate stenosis severity against non-invasive imaging. **Methods and results.** In this study 50 patients (mean age, 60 +/- 9.1 years; 13 women) with coronary artery disease and a 50% to 70% coronary stenosis (target vessel). SPECT by using cardiac gating was performed as a single-day stress (veloergometers testing) /rest protocol by use of technetium 99m-MIBI. Within 4 (+/-9) days, coronary angiography was performed and FFR was calculated by use of a pressure wire (normal FFR, > 0.8). The mean FFR of all patients was 0.79 +/- 0.15. Overall sensitivity of SPECT was 77% whereas specificity reached 92%. **Conclusion.** SPECT cardiac gating showed reasonable combination of sensitivity and specificity in patients with intermediate coronary artery stenosis and may thus be the more useful additional test to determine the significance of 'grey' lesions on FFR.

P0855

Cardiovascular risk scintigraphic screening of diabetics type 2, with or without anginal symptoms

I. Kotsalou¹, A. Kotsalos², N. Zakopoulos³, N. Dimakopoulos¹, M. Dimopoulos³; ¹NIMTS Hospital Nuclear Medicine Dept., ATHENS, GREECE, ²NIMTS Hospital Cardiovascular Dept., ATHENS, GREECE, ³University of Athens, Internal Therapy Dept., Alexandra Hospital, ATHENS, GREECE.

Aim: Autonomic Dysfunction is common in patients with Diabetes causing Silent Coronary Disease. Aim of this study is to identify the prognostic role of anginal or atypical symptoms of diabetics undergoing myocardial perfusion (SPECT) studies. **METHODS:** This retrospective study included 78 patients, of both sexes, with known Diabetes and duration 1-15 years (64% Group 1) and 16-25years (36 Group 2). 22 (28%- Group A) of included diabetics claimed angina symptoms, 23 subjects (29%- Group B) mentioned atypical angina symptoms, whereas 33 (43%- Group C) were asymptomatic. Patients with known CAD were excluded. Gated- single photon emission tomography was performed using a one-day stress/rest protocol with Tc-99m tetrofosmin (n=65:physical exercise, n=13:adenosine). We also analyzed for statistical significance multiple risk and clinical prediction factors like the duration of DM, the presence of peripheral vascular disease, dyslipidemia, hypertension, smoking, family history of CAD and obesity. **RESULTS:** Using the 20- segments scoring model for SPECT analysis, we found that 77% of perfusion studies in Group A were positive for CAD (scar and/or ischemia) and 48% , 73% for Group B and Group C respectively. Incidence of Ischemia showed no significant difference in groups 1 and 2 (Duration of Diabetes Mellitus). **CONCLUSIONS:** Myocardial Perfusion Scintigraphy Study is a sensitive mean for screening of subclinical Coronary Heart Disease in patients with Diabetes type 2 and may help the Referring Clinical Cardiologist to handle properly and consider right controversial and confusing "angina" symptoms of diabetics. Finally, the presence or not of anginal symptoms doesn't increase more the definite high cardiovascular risk profile of diabetics type 2, because of high incidence of silent ischemia in those patients.

P39-2 - Tuesday, October 30, 2012, 16:00 - 16:30, Poster Exhibition Area

Cardiovascular: Miscellaneous

P0856

Influence of the method of renal replacement therapy on cardiac sympathetic nervous system, assessed by 123-iodine meta-iodobenzylguanidine imaging

B. E. Chrapko, A. Grzebalska, B. Stefaniak, A. Książek; Medical University of Lublin, Lublin, POLAND.

Cardiac sympathetic nervous system (CSNS) dysfunction has been suggested as an important mechanism involved in cardiovascular events in patients with end-stage renal disease (ESRD). The aim of the study was check if applied method of renal replacement therapy (RRT) has any influence on CSNS. We studied 35 patients in ESRD, receiving two different RRT: peritoneal dialysis (PD) and haemodialysis (HD). A group of 15 patients (F/M: 6/9), aged 31-70 years (mean 52,75±14,73) receiving PD (mean time 39,18±26,23 months). A group of 20 patients (F/M: 1/19) aged 34-76 years (mean 52.10±11.83) receiving HD (mean 56.20±40.51 months). Diabetic patients and patients with evident heart failure were excluded from the study. None of PD patients did not have peritonitis within 30 days before examination, neither signs of any other inflammatory process. The imaging procedures were performed in PD patients after drainage of peritoneal cavity (empty abdomen). Drugs that might affect cardiac sympathetic system function were eliminated. All patients were evaluated by myocardial perfusion imaging (MPI) at rest, with assessment of left ventricular ejection fraction at rest (rLVEF) and summed rest score (SRS). SPECT and planar 123-iodine meta-iodobenzylguanidine (123I-mIBG) myocardial scintigraphy were also performed in all the patients. Semiquantitative

analysis of 123I-mIBG myocardial uptake was expressed as routine heart to mediastinum ratio (HMR): 15 minutes (early HMR) and 4 hours (delayed HMR) post administration as well as washout rate (WR). Results: In group PD: rLVEF = 51.9 ± 9.12 ; SRS = 3.80 ± 2.44 ; eHMR = 1.87 ± 0.26 ; dHMR = 1.76 ± 0.54 ; WR = 37.15 ± 17.86 . In group HD: rLVEF = 57.5 ± 7.19 ; SRS = 3.50 ± 0.3 ; eHMR = 1.87 ± 0.27 ; dHMR = 1.74 ± 0.25 ; WR = 31.38 ± 9.49 . Conclusion: The lack of statistically significant differences within indices of SNS function assessed by 123I-mIBG cardiac uptake, between studies groups, suggests, that the methods of RRT do not affect the function of CSNS.

P0857

Value of the ejection fraction in patients with coronary artery disease in cardiac rehabilitation program

J. Freire, M. Pajares, E. Otero, L. Gheorghe, M. Alcantara, R. Vazquez; Hospital Universitario Puerta del Mar, Cádiz, SPAIN.

Aim To evaluate the ejection fraction after cardiac rehabilitation program in patients with ischemic heart disease by radionuclide ventriculography. **Materials and Methods** Retrospective study, 28 patients undergoing cardiac rehabilitation program. 75% men, 58 ± 8 years. Medical records, functional capacity by ergometry (METs) and ejection fraction were examined before and after intervention. Cardiac rehabilitation program included treadmill, recumbent cycle, upper body resistance training during 12-36 sessions of 90 minutes with remote telemetry. Statistical analysis was performed with nonparametric tests. **Results** An increase of 2% between initial and final ejection fraction ($n:28$, $52.4 \pm 11.4\%$ vs $54.32 \pm 11.06\%$, $p=0.2$) and 4% in the group with initial ejection fraction $<50\%$ ($n:11$, $40.6 \pm 6\%$ vs $44.1 \pm 9\%$, $p=0.1$) was observed. Functional capacity improved in 23 patients, did not change in 3 (> 7 METs before intervention) and decreased in 2 patients (these 5 patients presented initial ejection fraction $>55\%$). The group of patients with functional capacity improvement ($n:23$) have been increased 2,2% of ejection fraction, while the rest without functional capacity improvement ($n:5$) have been presented 0,5% increase. All of patients with initial ejection fraction $<50\%$ and 70% of those with initial ejection fraction $>50\%$ improved their functional capacity. **Conclusion** Those patients with reduced ejection fraction are more likely to improve the functional capacity at the end of the program and the biggest increase of ejection fraction occurs in those that improve the functional capacity after the same intervention

P0858

Left ventricular dysfunction in oncologic patients evaluated with Radionuclide Ventriculography

A. García-Burillo, S. Aguadé-Bruix, E. Franquet, G. Cuberas, R. Cárdenas, J. Monturiol Duran, F. Porta Biosca, J. Castell-Conesa; Hospital General Universitari Vall d'Hebron, Barcelona, SPAIN.

Radionuclide Ventriculography (RNV) is a reproducible methodology for calculating the ejection fraction and therefore is used to evaluate the follow-up of the left ventricular function in oncologic patients receiving potentially cardiotoxic treatments. Objective: To determine the prevalence and severity of left ventricular dysfunction in oncologic patients assessed by RNV. Materials and methods: This retrospective study analyzed 5,085 studies in 1,227 patients (mean age: 56.62 ± 12 , 6 years, 1152 women, 93,89%), with a predominance of breast cancer (83,1%), sarcoma (3,82%), ORL cancers (3,57%) and others. RNV was performed by in-vivo-vitro red blood cells labeling with 900 MBq of ^{99m}Tc , and planar detection of the best septal left anterior oblique, at a rate of 32 images per cycle and 250,000 counts per image, using a 1-head gamma camera with low-energy high-resolution collimator, a 642 matrix, and an acquisition zoom of 2. Quantification was performed using an automatic program of left ventricular edge delineation, supervised by the user, determining the left ventricular ejection fraction (LVEF). A LVEF ≥ 50 was considered normal. LVEF 45-49% was considered as minimal decrease, LVEF 40-44% as mild decrease, LVEF 35-39% as moderate decrease and LVEF ≤ 35 was scored as severe decrease. Results: FE $\geq 50\%$ Studies: 4.506 Patients: 873 St/Pac: 4.14 ± 3.04 FE 45-49,9% Studies: 334 Patients: 182 St/Pac: 1.64 ± 1.21 FE 40-44,9% Studies: 158 Patients: 105 St/Pac: 1.42 ± 1.08 FE 35-39,9% Studies: 52 Patients: 41 St/Pac: 1.30 ± 1.0 FE $<35\%$ Studies: 35 Patients: 26 St/Pac: 1.35 ± 0.74 Some degree of ventricular dysfunction was observed in 28,85% of patients (11.39% of the studies). Nevertheless, the majority of studies were scored as minimal or mild functional impairment (23,39% of the patients, 9,69% of the studies). Moderate or intense dysfunction was observed in only 5,46% of patients (1,71% of the studies). Conclusions: RNV detected left ventricular dysfunction in approximately one quarter of the studied patients, although this dysfunction was moderate or severe in only 5% of them.

P0859

Incidental Detection of Pericardial Effusion on Bone Scan

K. Unal¹, M. Unlu², L. Guner³, T. Cakir⁴; ¹Medical Park Hospital Nuclear Medicine Department, Izmir, TURKEY, ²Gazi University Nuclear Medicine Department, Ankara, TURKEY, ³Acibadem Maslak Hospital Nuclear

Medicine Department, Istanbul, TURKEY, ⁴Corlu State Hospital Nuclear Medicine Department, Tekirdag, TURKEY.

The patient was a 57-year-old male with lung cancer. He was referred to nuclear medicine department for the evaluation of bone metastases. Bone scintigraphy was performed with Tc-99m labeled HDP. A large photopenic area with sharp borders around the heart was seen on blood pool images. Delayed images of thorax showed no abnormal Tc-99m HDP uptake. Chest X-ray and echocardiography was performed to reveal the pathology. Asymptomatic pericardial effusion was diagnosed in the corresponding area. Atypical photopenic areas on scintigraphic images are usually caused by attenuation artifacts. Prosthetic implant, pacemaker or metallic items in clothes are the most common reasons of cold defects. But in our case, the photopenic area pattern surrounding the heart was thought to be related to a pericardial pathology. There is a couple of cases previously published about bone scan and pericardial effusion. In contrast to our case, increased uptake on delayed images due to malignant pericardial effusion was reported. This case documents a rare finding of blood pool images which was associated with asymptomatic pericardial effusion and exhibits the importance of following non-oncological signs on scintigraphic images.

P0860

Influence of different clinical and structural variables in the late aortic mediastinum ratio. Preliminary data

M. CozarR Santiago¹, R. Sanchez Jurado¹, A. Vicedo Gonzalez², P. Garcia Gonzalez³, J. Eestornell Erill⁴, F. Ridocci Soriano³, J. Ferrer Rebolledo¹; ¹Hospital General Universitario-Eresa, Servicio de Medicina Nuclear, VALENCIA, SPAIN, ²Hospital General Universitario-Eresa. Servicio de Radiofísica, VALENCIA, SPAIN, ³Hospital General Universitario, Servicio de Cardiología, VALENCIA, SPAIN, ⁴Hospital General Universitario-Eresa. Servicio de Cardiología, VALENCIA, SPAIN.

Aim: To assess the variability of the cutoff point in studies of cardiac adrenergic innervation in terms of clinical pathology (diabetes mellitus) and structural (cardiomyopathy), in relation to left ventricle ejection fraction (LVEF). **Material and methods:** We performed a cardiac innervation study at 20 minutes and 4 hours post-injection 185MBq of ^{123}I -MIBG. Planar images were performed to obtain the early and late heart/mediastinum uptake ratio and the washout rate. 27 patients (15 diabetic mellitus (DM) and 12 non-diabetics) were included in the study: (23 men and 4 women), all known cardiomyopathy (12 with ischemic cardiomyopathy (ICM) and 15 with dilated cardiomyopathy (DCM)). Excluded from the study those with necrotic mass percentage above 30%. All patients underwent an MRI study with calculation of the LVEF. We obtain a control group of 10 patients (four diabetic and six nondiabetic). We calculated the variability of both heart/mediastinum late cutoff ratio (H/M) and washout and LVEF in relation to the presence or absence of diabetic disease and ischemic or dilated cardiomyopathy. **Results:** We obtained a late heart/mediastinum uptake ratio of 1.63 in our control group with a washout of 20.85% (confidence interval 85%) and an LVEF of 42.5% which is modified in diabetic patients (ICM: 1.54, washout of 22.4 and 38.5% LVEF) with a linear correlation (R^2) of 0.75. We obtain a H/M: 1.43 ± 0.15 with a washout of $33\% \pm 9$ and an LVEF of $31\% \pm 4$, in diabetic patients with ICM and a H/M: 1.47 ± 0.3 in diabetic patients with DMC, washout of 39 ± 21 and LVEF: 24 ± 10 . In non-diabetic patients with ICM: H/M 1.3 ± 0.2 , 47 ± 22 and washout LVEF 32 ± 8 (with a linear correlation of 70%) and in nondiabetic DMC: H/M 1.5 ± 0.3 , ± 36 washout 23 and LVEF 22 ± 13 . **Conclusion:** The semiquantitative evaluation of cardiac innervation in patients with cardiomyopathy is conditioned by multiple factors, including the DM and the ICM. As preliminary data and not statistically significant, probably because of limited cohort of patients, the LVFE seems to have an inverse correlation.

P0861

Compliance with appropriate use criteria for cardiac radionuclide imaging - a case series report

A. Prata, A. I. Santos, I. Henriksson, H. Pereira; Hospital Garcia de Orta, Almada, PORTUGAL.

Aim: To evaluate referrals for myocardial perfusion scintigraphy (MPS) in terms of its compliance with 2009 Appropriate Use Criteria for Cardiac Radionuclide Imaging. **Patients and Methods:** We have retrospectively selected 107 patients, mean age 66.5 years (95%CI:64.5;68.6), referred to our institution for MPS between 1st January and 30th May 2011. In this sample population, we have characterized gender, medical speciality of referral (cardiologist versus non cardiologist), presence of previous history of coronary heart disease (CAD) and probability of CAD in patients without previous history. The 2009 Appropriate Use Criteria for Cardiac Radionuclide Imaging were used to classify appropriateness of referrals, score them and define clinical indication for the exam. We have used Mann-Whitney test to evaluate if there were statistically significant differences of appropriateness score between gender and medical speciality of referral. **Results:** Our data consisted on 60 male (56.1%) and 47 female (43.9%) patients, referred mainly by cardiologists (81/107=75.7%), with a majority of patients with previous

history of CAD (60/107=56.1%). Most of our 47 patients without previous history had an intermediate (20/47=42.6%) or high (11/47=23.4%) probability of CAD. We have found only one referral that was not possible to classify appropriateness, due to lack of information. We had a non appropriateness rate of 13.1% (14/107) and an appropriateness rate of 80.4% (86/107). Our average appropriateness score was 7.0 (95%CI:6.6;7.3). Our more frequent non appropriate clinical indication was low test probability of CAD and ECG interpretable (6 patients). We have not found statistically significant differences of appropriateness scores between males (average 6.9 - CI95%:6.4;7.4) and females (average 7.1 - CI95%:6.6;7.6) - $p=0.63$; neither between cardiologists (average 6.8 - CI95%: 6.4; 7.3) and non cardiologists referrals (average 7.5 - CI95%:7.0;8.0) - $p=0.41$. **Discussion:** Although this was a retrospective study, we were able to classify appropriateness in all but one of our selected patients, which indicates that we have complete clinical information to support our referrals. Our appropriateness rate is similar to what has been published by other authors; nevertheless our average score is on the lower level of appropriateness, which means that we have to improve our triage of referrals and our continuing dialogue with referring physicians. Finally, opposite to other published studies, we have not found significant differences in appropriateness scores between gender and type of medical speciality of referral, but maybe this is a bias introduced by our exclusive hospital referral.

P0862

Detection of vascular malformation mimicking lung mass in 18F-FDG PET/CT

E. Örsal, B. Seven, A. Ayan, A. Sahin, A. Maman; Department of Nuclear Medicine, Faculty of Medicine, Ataturk University, Erzurum, TURKEY.

The vascular abnormalities were classified into two categories as hemangiomas and vascular malformations (VM). VM are characterized with various dysplastic vessels without endothelial proliferation. Though VM are usually present at birth, it can be occurred at any age. Additionally VM can be seen anywhere in the body. Some of VM such as present superficially, can be determined easily, others especially deeper lesions are detected hardly. Besides VM discrimination from other lesion (mass like others) is very important for therapy design. Ultrasound, Computed tomography, Nuclear medicine imaging methods, Angiography, and Magnetic resonance imaging are essential to confirm the diagnosis, evaluate detailed morphology and planning treatment of VM. In this case study, we report a case of VM in a 55-year-old woman. A 55-year-old female patient visited a hospital due to dyspnea, chest pain and cough complains. An abnormal mass-like lesion in the left upper pulmonary lobe was detected in a chest radiograph at first health center. The patient referred to our hospital for further diagnosis and treatment. There was no significant abnormal change in patient's physical examination and laboratory tests. Patient was directed to our center for investigation of lung nodul with Positron emission tomography/ Computed tomography (PET/CT). At the result of PET/CT scanning, left lung upper lobe lesion fluoro-d-glucose (FDG) uptake pattern was at the level of blood pool and not typical for malignancy and, this lesion closed to vascular structures (aorta and pulmonary artery). After than, contrast-enhanced CT recommended for discrimination of VM and other mass like lesions. As a result of these findings, suspected lesion reported as VM. In conclusion, presence of the low-level FDG uptake detected with PET in lesions, vascular malformation should be thought.

P0863

Multigated Analysis in Patients with Hypertrophic Cardiomyopathy: Preliminary Report

A. O. - . Karacalioglu, E. Alagöz, S. Ince, Ö. Emer, B. Günalp, N. Arslan; GATA, Ankara, TURKEY.

OBJECTIVE: Hypertrophic cardiomyopathy (HCM) is a genetically transmitted cardiac disease in majority of cases which usually involves the apex and interventricular septum asymmetrically. It is an important cause of morbidity, arrhythmias and sudden cardiac death especially in young people. The aim of this study was to evaluate the diastolic functions derived by planar multigated analysis (MUGA) in patients with HCM diagnosed by echocardiography. **MATERIALS AND METHODS:** 6 patients (1 women, 5 men; 45±9 years) with HCM and randomly chosen 6 patients (1 women, 5 men; 47±6 years) without HCM diagnosed by echocardiography for comparison were included into the study. The diastolic functions of the left ventricle were derived from planar multigated analysis study in all patients. The results were compared by using the independent samples t-test. **RESULTS :** Although, the difference between the parameters of PFR and EF of the diastolic functions of the left ventricle of both groups was statistically significant ($p=0.020$, and $p=0.047$ respectively), the difference between the parameters of PER, TTPF, and TTPE of the diastolic functions of the left ventricle were not significant ($p=0.325$, $p=0.900$, $p=0.287$, respectively) (Table). Table: Results of the measurements

PFR: Peak filling rate, PER: Peak emptying rate, TTPF: Time to peak filling rate, TTPE: Time to peak emptying rate, EF: Ejection fraction, results: mean±SD

CONCLUSION: According to our results, the presence of HCM seems to reduce the

diastolic functions of the left ventricle and the early results of this study seems to be helpful in the management of these patients. Depressed diastolic functions of the left ventricle can lead to reduced diastolic filling of the left ventricle, increased congestion in the lungs and finally heart failure.

P0864

Comparison of Planar Muga and Gated Blood Pool SPECT in Determination of Diastolic Functions of the Left Ventricle

A. O. - . Karacalioglu, O. Emer, E. Alagoz, S. Ince, B. Günalp, N. Arslan; GATA, Ankara, TURKEY.

OBJECTIVE : There is growing recognition that congestive heart failure caused by a predominant abnormality in diastolic function. Diastolic dysfunction refers to a condition in which abnormalities in mechanical function are present during diastole. The aim of this study was to compare the parameters of the diastolic function of the left ventricle that were derived from planar multigated analysis (MUGA) and gated blood pool single photon emission tomography (gBPSPECT) **MATERIAL AND METHOD** 7 patients (all men; 52±8 years) were included in the study. After in vivo labeling of red blood cells, patients underwent MUGA and gBPSPECT analysis consecutively in the same day. The parameters of the diastolic functions were analyzed paired samples t-test. **RESULTS** The results of the EF, PFR and PER calculated by MUGA analysis were 36.71±9.16, 1.63±0.67, and 2.14±0.57, respectively. The results of the EF, PFR and PER calculated by gBPSPECT analysis were 41.57±14.62, 1.42±0.51 and 1.7±0.71, respectively. There were not statistically significant difference between the parameters of EF, PFR and PER that they were computed by MUGA and gBPSPECT ($p=0.215$, $p=0.379$, $p=0.082$, respectively). The correlations between the same parameters calculated by two different modalities were also good [$r(\text{EF}):0.789$, $r(\text{PFR}):0.536$, and $r(\text{PER}):0.621$]. **CONCLUSION** Although the modalities of planar MUGA and gBPSPECT are completely different, the results of the diastolic function parameters such as EF, PFR and PER are found to be similar and it seems to be a good correlation between these two different modalities.

P0865

Washout of technetium-99m-methoxyisobutyl isonitrile scintigraphy and cardiac function in patients with type 2 diabetes mellitus

H. Takase, T. Okado, T. Tanaka, T. Hashimoto, M. Sasaki, H. Ishikawa, K. Tsutsui, H. Kubono; Enshu Hospital, Hamamatsu, JAPAN.

Aim: Technetium-99m-methoxyisobutyl isonitrile (MIBI) is a myocardial perfusion tracer. Recently, an increased washout of MIBI has been reported to reflect mitochondrial dysfunction in the myocardium and its washout ratio (WR) is used for evaluation of the severity and prognosis of patients with congestive heart failure. On the other hand, mitochondrial dysfunction often occurs in the myocardium in patients with diabetic cardiomyopathy. Thus, the present study was designed to investigate the clinical significance of WR of MIBI in patients with type 2 diabetes mellitus. **Materials and Methods:** Consecutive 22 patients (men/women=11/11, age 68.5±8.6 years) with type 2 diabetes mellitus, who underwent MIBI scintigraphy for screening of ischemic heart disease, were enrolled in this study. Multistage ergometer exercise and/or adenosine stress were applied. For the stress and rest images, 185MBq and 555MBq of MIBI were injected, respectively. Two hours after the acquisition of the rest image, delayed image was further constructed and WR was calculated using the rest and delayed images. At the same time, echocardiogram was performed and blood was sampled for the measurement of brain natriuretic peptide (BNP). Same examinations were performed in age-matched 18 normal controls (men/women=10/10, age 69.9±7.0 years). **Results:** The WR of MIBI was not different between diabetic patients (29.6±5.7%) and normal controls (29.8±4.4%). In diabetic patients, the echocardiogram revealed that left atrial and left ventricular sizes and left ventricular systolic function were within normal limits. Among the parameters obtained from echocardiograms, only E/A (early transmitral flow velocity to late transmitral flow velocity) ratio was inversely correlated with the WR ($r=-0.457$, $p<0.05$). Although the WR was positively correlated with HbA1c ($r=0.473$, $p<0.05$) and end-diastolic volume of early image ($r=-0.446$, $p<0.05$), there was no relationship between the WR and age, body mass index, blood pressure, lipid profile, BNP or end-systolic volume, ejection fraction calculated by QGS program. In normal controls, neither E/A ratio nor HbA1c was correlated with the WR. **Conclusion:** In type 2 diabetic patients with preserved cardiac structure and systolic function, washout of MIBI is associated with E/A ratio and HbA1c. Washout of MIBI may reflect early stage of myocardial damage due to hyperglycemia prior to diabetic cardiomyopathy with reduced systolic function.

P41-2 - Tuesday, October 30, 2012, 16:00 - 16:30, Poster Exhibition Area

Neurosciences: Clinical Science Neurology**P0866****Physiological change of accumulation in I-123 IMZ brain SPECT appeared during childhood**

M. Uchiyama¹, M. Matsumoto², A. Tsujimura², E. Oguma², S. Hamano²; ¹The Jikei University School of Medicine, Tokyo, JAPAN, ²Saitama Children's Medical Center, Saitama, JAPAN.

Aim: Physiological regional accumulation shows change dramatically during childhood especially under 3 years old. The aim of this study was to compare regional accumulation in brain on anatomically standardized I-123 IMZ brain single-photon emission computed tomography (IMZ SPECT) images, which were obtained using 3DSRT, fully automated ROI analysis software. **Material and method:** One hundred patients with convulsive disease from 1 month to 15 years of age were examined with IMZ SPECT and did not show significant abnormal finding in Saitama Children's Medical Center, 35 patients under the age of 1 year, 14 patients at the age of 1 year, 11 patients at the age of 2 years, 6 patients at the age of 3 years, 11 patients 4 to 7 years of age, 9 patients 8 to 11 years of age, 14 patients 12 to 15 years of age. We assessed regional accumulation to leverage regional count ratio (RCR: regional count/dose administered/patient body surface area), and regional IMZ accumulation index (IAI: whole brain count on SPECT/[whole brain count on whole body scan/brain count in anterior projection image on SPECT]/[whole body count on whole body scan-liver count]). **Results:** In patients under the age of 3 months, both of RCR and regional IAI increased with advancing months in all cerebral and cerebellar cortex. In patients at the age of 3 months, mean RCR and regional IAI was 4.6 ± 0.8 and 33.2 ± 9.5 in superior frontal gyrus, 7.1 ± 1.1 and 53.5 ± 10.3 in cuneus, 6.4 ± 0.4 and 47.5 ± 9.4 in posterior lobe of cerebellum. In patients over the age of 17 months, both of RCR and regional IAI decreased with advancing months. In patients over the age of 8 years, both of RCR and regional IAI showed flat. In patients over the age of 8 years, mean RCR and regional IAI was 1.4 ± 0.2 and 22.3 ± 2.4 in superior frontal gyrus, 1.8 ± 0.4 and 32.0 ± 3.5 in cuneus, 1.4 ± 0.4 and 24.6 ± 2.5 in posterior lobe of cerebellum. **Conclusion:** In neonatal infant, physiological accumulation is low in whole brain and the lowest region is frontal lobe. With advancing months, accumulation in all regions increased, especially in occipital lobe, secondarily in cerebellum. The peak of accumulation was seen in patients in the age between 3 and 17 months. The change rate of physiological accumulation was smallest in frontal lobe.

P0867**Does Positron Emission Tomography really help in decision making for epilepsy surgery?**

J. C. Dickson¹, C. Rathore², P. J. Ell¹, J. S. Duncan²; ¹University College London Hospital, London, UNITED KINGDOM, ²National Hospital for Neurology and Neurosurgery, Queen Square, London, UNITED KINGDOM.

Purpose: To investigate the utility of Fluorodeoxyglucose Positron Emission Tomography (FDG-PET) in decision making for epilepsy surgery. **Methods:** All patients with medically refractory focal epilepsy and nonlocalizing or discordant information on non-invasive evaluation (clinical, electrophysiological and 3T-MRI) underwent FDG-PET at our centre. Thirty to forty minutes after the injection of 200MBq FDG, interictal PET/CT imaging was performed for 15 minutes in 3D mode on GE Discovery DST and DVCT scanners. Visual assessment of slice data and semiquantitative analysis with 3D-SSP Neurostat software was used to review PET images by two investigators blinded to clinical data. PET was considered useful if it led to surgery directly, helped in planning intracranial EEG (icEEG) or made surgery improbable. Final localization was based upon the noninvasive data supported by intracranial EEG (icEEG) and/or postoperative seizure freedom, when available. **Results:** 150 adult patients (median age, 32years) underwent FDG-PET; 120 had normal MRI and 30 had discordant noninvasive data. Final localization was medial temporal lobe epilepsy (MTLE, n=14), lateral TLE (n=36), frontal lobe epilepsy (n=46), temporal-plus epilepsy (n=22) and other extratemporal lobe epilepsies (n=32). The FDG PET scan was normal in 68 patients and showed unifocal hypometabolism in 70 patients. In the normal PET group, icEEG was planned in 29 patients while in patients with unifocal PET hypometabolism, direct surgery was planned in nine patients and icEEG in another 56 patients (p<0.0001). To date, 11 patients in the normal PET group and 23 patients in unifocal PET hypometabolism group have undergone icEEG or surgery (p=0.02) while others are awaiting icEEG or declined surgery. Ten of 17 postoperative patients with minimum one year postoperative follow-up became seizure free. Twelve patients had bilateral/diffuse hypometabolism making surgery improbable, and FDG-PET gave false localizing information in two patients compared to icEEG. In 40% patients, semi-quantitative analysis helped in detection and better delineation of hypometabolism. FDG PET provided equivalent information in all epilepsy localizations. **Conclusions:** In ~50% of presurgical patients with normal or discordant MRI undergoing presurgical evaluation, PET scan provided information that helped decision making. Presence

of focal PET hypometabolism significantly increases the chances of epilepsy surgery.

P0868**Brain SPECT demonstrates posture dependent rCBF differences in orthostatic hypotension**

L. R. Barnden¹, R. Kwiatek², B. Crouch¹; ¹The Queen Elizabeth Hospital, Woodville, AUSTRALIA, ²Lyell McEwin Hospital, Salisbury, AUSTRALIA.

AIM: Orthostatic hypotension (OH) is a condition of autonomic dysfunction in which a postural change from supine to upright causes an abnormally large decrease in blood pressure which, in severe cases, leads to fainting. Its cause is thought to be dysfunction in the peripheral vasculature - baroreceptor - brainstem - peripheral autonomic nervous system loop. A 33yo woman with debilitating OH, who was also diagnosed with chronic fatigue syndrome (CFS) - a commonly associated disorder - was referred for assessment with brain SPECT. Our aim was to identify postural differences in rCBF associated with OH. **METHODS:** 500 MBq HMPAO was administered with the patient upright (seated) and again, one day later, with the patient supine. At each injection, a dynamic acquisition with both heart and brain in the FOV was acquired for absolute cerebral bloodflow assessment. Blood pressure and heart rate were monitored during injection and SPECT. DDR corrected iterative reconstruction generated the SPECT rCBF sections. Using SPM5, the two SPECT scans were coregistered and then spatially normalised to standard anatomical space for access to brain atlases. The scans were then count-normalised using their median values and subtracted to highlight rCBF differences between supine and upright postures. **RESULTS:** Absolute CBF for both upright and supine was normal (48 and 49 ml/100g/min). Relative to supine rCBF, upright rCBF was reduced in the posterior cingulate cortex (PCC -22%), midbrain cerebral peduncles (-22%), anterior thalamus (-23%) and orbitofrontal gyrus (-14%). Upright rCBF was greater than supine rCBF in the right anterior insula (+22%), subgenual anterior cingulate cortex (ACC +27%), left inferior frontal gyrus (Broca's area +22%), and left cerebellum (+22%). **CONCLUSION:** The ability of Tc-99m HMPAO to label the rCBF distribution at injection permitted us to detect posture dependent rCBF differences in OH. We detected involvement of several elements of the central autonomic network (ACC, PCC, R insula and orbitofrontal cortex). A complex interaction within this network is associated with postural change and affects local CBF in multiple sites. It is not clear which site is the primary driver of this syndrome although rCBF changes in the cerebral peduncles suggest impaired midbrain neuro-conductivity may be a factor. Similarities were found with results from an MRI investigation of CFS. Formal statistical assessment of these results requires analysis of normal repeat scans in multiple subjects. Brain SPECT is a useful tool for research in OH.

P0869**Estimation of Mean Cerebral Blood Flow Reserve by Direct Integral Linear Least Square Regression Method in Acetazolamide-Augmented I-123 IMP Split-Dose CBF SPECT: Comparison with Nonlinear Regression Method**

N. Shuke, T. Onishi, A. Ando, K. Yamamoto, O. Saito, T. Inagaki, S. Irie, K. Saito; Kushiho Kojinkai Memorial Hospital, Kushiho, JAPAN.

Objective: In rest and acetazolamide (ACZ) split-dose I-123 IMP CBF SPECT, it is possible to estimate mean cerebral blood flow reserve by fitting whole brain time-activity curves (TACs) to 2-compartment model using nonlinear least square regression (NLS) method. For parameter estimation in 2-compartment model analysis, it is possible to use direct integral linear least square regression (DILS) method, which does not require initial estimates of parameters and iterative calculation, as a simple alternative to rigorous NLS method. The objective of this study was to investigate applicability of DILS method to estimation of mean cerebral blood flow reserve in comparison with NLS method. **Method:** Fifty-five patients (pts) with cerebrovascular disease (67 ± 11 y old, M/F=33/22) were studied with acetazolamide-augmented split dose I-123 IMP (IMP) dynamic SPECT. IMP (111MBq) was infused over 1min for each dosing, and immediately after starting each dosing, dynamic brain SPECT data acquisition (14 rotations/28 min) was performed. After the first data acquisition, ACZ (1000mg) was injected. After 4 min intermission, the second dosing and data acquisition were performed. Time-activity curves (TACs) of whole brain were obtained from two dynamic SPECT images and were fitted to 2-compartment model using uncalibrated standard arterial input function to obtain a product of influx rate constant (K1: ml/min) and coefficient (Cf) to individualize standard arterial input function (CfK1), and efflux rate constant (k2: 1/min) for both first and second dosing, using both NLS and DILS methods. The rest and ACZ influx rates (CfK1, CfK1A), and cerebral blood flow reserve (K1A/K1) were then compared between DILS and NLS methods. **Results:** By DILS and NLS methods, CfK1 values were 0.000904 ± 0.000354 and 0.000999 ± 0.000384 , CfK1A values were 0.00148 ± 0.00068 and 0.00130 ± 0.00052 , K1A/K1 values were 1.61 ± 0.30 and 1.31 ± 0.23 , respectively. Between DILS and NLS methods, these parameters showed significant correlations. Correlation coefficients (R2) of CfK1, CfK1A, and K1A/K1 were 0.989, 0.954, and 0.835, respectively (P<0.0001). **Conclusion:** DILS method

could be applicable for estimation of mean cerebral blood flow reserve as a simple alternative to NLS method in ACZ-augmented I-123 split dose CBF SPECT.

P0870

Depression Symptoms and Clinical Subtypes in Parkinson's Disease Patients: a ^{123}I -FP-CIT SPECT Study

D. Di Giuda¹, A. Fasano², G. Camardese³, I. Bruno¹, A. Guidubaldi², F. Coccioilillo¹, L. Pucci³, A. Collarino¹, A. Cinquino¹, D. Fortini¹, A. R. Bentivoglio², L. Janiri³, A. Giordano¹; ¹Nuclear Medicine Institute, Catholic University of the Sacred Heart, Rome, ITALY, ²Neurology Institute, Catholic University of the Sacred Heart, Rome, ITALY, ³Psychiatry and Psychology Institute, Catholic University of the Sacred Heart, Rome, ITALY.

AIM: Depression is one of the most common non-motor symptoms of Parkinson's disease (PD). Some studies reported an association between depression and different motor symptoms, such as tremor, postural instability-gait disturbance and hypokinesia-rigidity. Recent neuroimaging results suggest a relationship between striatal dopaminergic dysfunction and depression severity. We compared dopamine transporter (DAT) availability and depression symptoms in different clinical subtypes of PD, exploring the association between SPECT and psychometric findings. **MATERIALS & METHODS:** 63 idiopathic PD patients (43 M, mean age: 63±12 yrs; 44 drug-naïve) were enrolled. According to UPDRS III section, they were classified into three clinical subtypes: 28 tremor-dominant type, TDT (H&Y stage: 1.8±0.3; UPDRS III: 16.7±6.4), 20 akinetic-rigid type, ART (H&Y stage: 1.8±0.5; UPDRS III: 17.6±8.5) and 15 mixed type, MT (H&Y stage: 1.8±0.4; UPDRS III: 16.3±5.1) patients. Psychometric assessment included Hamilton Depression Rating Scale (HDRS) and Snaitn Hamilton Pleasure Scale (SHAPS). SPECT was carried out 3 hours after 111 MBq ^{123}I -FP-CIT intravenous injection. Specific to non-specific ^{123}I -FP-CIT binding ratios in the striatum, caudate and putamen were calculated, based on ROI analysis. **RESULTS:** PD subtypes were not significantly different concerning age, disease duration, H&Y stage and UPDRS III score. Clinically relevant depression symptoms (HDRS cut off score ≥ 18) were found in 16 TDT (57%), 14 ART (70%) and 8 MT (53%) patients. PD subtypes did not significantly differ in HDRS and SHAPS total scores. Although differences in ^{123}I -FP-CIT binding ratios did not reach statistical significance among the three groups, TDT patients showed a relative higher uptake than ART and MT subjects in all ROIs. In TDT patients, severity of depression symptoms (HDRS total score) inversely correlated with DAT availability in contralateral and ipsilateral caudate ($p<0.01$). Correlation remained significant in the contralateral caudate after controlling for age, H&Y stage and disease duration. DAT availability did not correlate significantly with psychometric measures in ART and MT patients. **CONCLUSION:** We found relevant depression symptoms in a high percentage of TDT, ART and MT patients. Despite the lack of significant differences in psychometric measures, our results provided evidence for a heterogeneous pathogenesis of depression symptoms in the different PD phenotypes, as symptom severity inversely correlated with DAT availability only in the TDT patients. This finding indirectly suggests that other neurotransmitters could be related to the manifestation of depression symptoms, probably in the context of a widespread neuronal degeneration detected in ART and MT patients. Further studies in this direction are required.

P0871

Alzheimer's disease and Progressive Non-Fluent Aphasia: Evaluation of perfusion differences using $^{99\text{m}}\text{Tc}$ -HMPAO SPECT and Brodmann Areas Mapping

V. Valotassiou¹, J. Papatriantafyllou², N. Sifakis³, C. Tzavara¹, I. Tsougos¹, D. Psimadas¹, K. Makrypoulas³, M. Kournouti¹, E. Kapsalaki⁴, G. Chadjigeorgiou⁵, P. Georgoulas¹; ¹Department of Nuclear Medicine, University Hospital of Larissa, Larissa, GREECE, ²Memory & Cognitive Disorders Clinic, Department of Neurology, "G.Gennimatas" Hospital, Athens, GREECE, ³Department of Nuclear Medicine, "Alexandra" University Hospital, Athens, GREECE, ⁴Department of Radiology, University Hospital of Larissa, Larissa, GREECE, ⁵Department of Neurology, University Hospital of Larissa, Larissa, GREECE.

AIM: Progressive non-fluent aphasia (PNFA) is characterized by apraxia of speech and/or expressive agrammatism. Verbal fluency is also impaired, but to a lesser degree, in Alzheimer's disease (AD). The aim of this study was the evaluation of perfusion in Brodmann areas (BA) in AD and PNFA, using an automated 3D-voxel based processing software, in order to improve brain areas definition that are specifically implicated in these disorders. **MATERIALS-METHODS:** We studied 50 consecutive patients from an outpatient Memory Clinic. We used the established criteria for the diagnosis of dementia and the specific established criteria for the diagnosis of AD and PNFA. All the patients underwent a neuropsychological evaluation with a battery of tests including the mini-mental state examination (MMSE), as well as a CT and/or MRI of the brain in order to exclude the presence of anatomical lesions. Thirty-nine patients received the clinical diagnosis of AD (age(±SD) 71±8 years, MMSE(±SD) 19±5, education(±SD) 9.3±4.7 years, duration of disease(±SD) 4±2 years), and 11 patients the clinical diagnosis of PNFA (age(±SD) 66.3±7.4 years, MMSE(±SD) 13±10, education(±SD) 13±4.9 years, duration of

disease(±SD) 3±1.37 years). All the patients underwent a brain SPECT 20 min after the intravenous administration of 740MBq $^{99\text{m}}\text{Tc}$ -HMPAO. We applied the NeuroGam™ software on the reconstructed data, for the semi-quantitative evaluation of perfusion in BA areas in the right(R) and left(L) hemispheres. Perfusion values are expressed as mean±SD percentage of mean perfusion of the cerebellum. **RESULTS:** Hypoperfusion in PNFA patients, compared to AD patients, was found in left premotor and supplementary motor cortex (BA 6), dorsolateral (BA 9, 46), ventromedial (BA 25), and inferior prefrontal (BA 47) cortices, orbitofrontal cortex (BA 11), left temporal lobe (BA 20, 21, 22), left anterior cingulate cortex (BA 32), BA 8, and Broca's area (BA 44, 45). Multiple logistic regression analyses showed that 25R could independently differentiate AD from PNFA ($p=0.003$). The optimal cut-off of 25R for the discrimination of AD from PNFA was 48.5 with sensitivity 76.9%, specificity 63.4%, positive and negative predictive values 88.2% and 43.8%, respectively. **CONCLUSION:** Perfusion SPECT studies exclusively in PNFA patients are limited and perfusion deficits consistent with neural substrate for the language disorder in PNFA have not clearly identified. Nevertheless, our findings are in good agreement with the pattern of neuropsychological impairment in these patients and brain perfusion SPECT with Brodmann areas mapping would contribute in a more accurate differential diagnosis of AD from PNFA patients.

P0872

Patterns of perfusion deficits in Semantic dementia and Progressive non-fluent aphasia: a $^{99\text{m}}\text{Tc}$ -HMPAO SPECT study with Brodmann Areas Mapping

V. Valotassiou¹, J. Papatriantafyllou², N. Sifakis³, C. Tzavara¹, I. Tsougos¹, D. Psimadas¹, A. Ziaka¹, K. Makrypoulas³, M. Kournouti¹, E. Kapsalaki⁴, G. Chadjigeorgiou⁵, P. Georgoulas¹; ¹Department of Nuclear Medicine, University Hospital of Larissa, Larissa, GREECE, ²Memory & Cognitive Disorders Clinic, Department of Neurology, "G.Gennimatas" Hospital, Athens, GREECE, ³Department of Nuclear Medicine, "Alexandra" University Hospital, Athens, GREECE, ⁴Department of Radiology, University Hospital of Larissa, Larissa, GREECE, ⁵Department of Neurology, University Hospital of Larissa, Larissa, GREECE.

AIM: Semantic dementia (SD) and Progressive non-fluent aphasia (PNFA) are the language variants of Frontotemporal Degeneration (FTLD). Although impaired fluency is used to distinguish major language variants of FTLD, significant overlapping exists since word-finding difficulty, caused by lexical semantic impairment, may slow speech in SD. The aim of this study was the evaluation of perfusion in Brodmann areas (BA) in SD and PNFA, using an automated 3D-voxel based processing software, in order to improve brain areas definition that are specifically implicated in impaired speech fluency of these disorders. **MATERIALS-METHODS:** We studied 32 consecutive patients from an outpatient Memory Clinic. We used the established criteria for the diagnosis of dementia and the specific established criteria for the diagnosis of SD and PNFA. All the patients underwent a neuropsychological evaluation with a battery of tests including the mini-mental state examination (MMSE), as well as a CT and/or MRI of the brain in order to exclude the presence of anatomical lesions. We studied 21 patients with SD (5 men, 16 women, age(±SD) 69±8 years, MMSE(±SD) 13±8, education(±SD) 9.5±5 years, duration of disease(±SD) 4.1±3.2 years), and 11 patients with PNFA (4 men, 7 women, age(±SD) 66.3±7.4 years, MMSE(±SD) 13±10, education(±SD) 13±4.9 years, duration of disease(±SD) 3±1.37 years). All the patients underwent a brain SPECT 20 min after the intravenous administration of 740MBq $^{99\text{m}}\text{Tc}$ -HMPAO. We applied the NeuroGam™ software on the reconstructed data, for the semi-quantitative evaluation of perfusion in BA areas in the right(R) and left(L) hemispheres. Perfusion values are expressed as mean±SD percentage of mean perfusion of the cerebellum. **RESULTS:** Hypoperfusion in PNFA patients, compared to SD patients, was found in left primary motor (BA 4L) and dorsolateral prefrontal (BA 9L) cortex, in premotor (BA 6L-6R) and anterior premotor (BA 8L-8R) cortex bilaterally, and in right orbitofrontal (BA 11R), ventral anterior premotor and ventrolateral prefrontal cortex (BA 44R, 45R, 46R, 47R). Multiple logistic regression analyses showed that BA 6L could discriminate PNFA from SD patients ($p=0.020$). **CONCLUSION:** Impaired speech fluency in language variants of FTLD is correlated with distinct hypoperfusion patterns. Brain perfusion SPECT with Brodmann areas mapping would contribute in a more accurate differential diagnosis of SD from PNFA patients.

P42-2 - Tuesday, October 30, 2012, 16:00 - 16:30, Poster Exhibition Area

Neurosciences: Neurotransmission - Clinical Science Psychiatry

P0873

Metabolic Brain Network of Anorexia Nervosa: A ^{18}F -FDG PET/CT study

H. Zhang¹, D. Li², P. Wu¹, Z. Huang¹, J. Zhao¹, Y. Guan¹, C. Zuo¹, B. Sun²; ¹PET Center, Department of Nuclear Medicine, Huashan Hospital, Fudan University, Shanghai, CHINA, ²Department of Neurosurgery, Ruijin Hospital, Shanghai Jiao Tong University of Medicine, Shanghai, CHINA.

Objectives: Anorexia nervosa (AN) has high mortality rate in psychiatric disorders. Drawing the brain metabolic pattern of AN may help to target the core biological and psychological features of the disorder and to perfect the diagnosis and recovery criteria. In this study we used ^{18}F -FDG PET to show brain metabolic network for AN. **Methods:** According to Diagnostic and Statistical Manual of Mental Disorders-Fourth Edition-Text Revision (DSM-IV-TR)¹, 6 female patients (17 (±0.8) years) were recruited in AN group. No patient had received any therapies including medication, behavioral interventions or surgery, etc. 12 females (24 (±3.3) years) were in Health Control (HC) group. All patients and HC underwent ^{18}F -FDG PET scans in a resting state with eyes open without medication. The PET images were corrected for head movement and transformed to the coordinate system developed and distributed by the Montreal Neurologic Institute (MNI) implemented in the SPM2 software package (Wellcome Department of Cognitive Neurology, London, UK) running on Matlab Version 2006a (Mathworks Inc., Sherborn, MA, USA). To quantify regionally-specific metabolic changes, we constructed a 4mm radius volume of interest (VOI) within the transaxial plane, surrounding the voxel of peak statistical significance in two-sample t-test results of decreased and increased glucose metabolism compared with HC, and calculated the relative glucose metabolism rates in HC and AN PET images respectively with ScAnVP (version 5.9.1, Center for Neurosciences, Feinstein Institute for Medical Research, Manhasset, NY). **Results:** Increased metabolism was found in the frontal lobe (bilateral superior, medial and inferior frontal gyrus), the limbic lobe (bilateral hippocampus and amygdala), bilateral lentiform nucleus, left insula (BA 13), left subcallosal Gyrus (BA25), right claustrum and brainstem (right pons). Hypometabolism was observed in bilateral parietal lobe (BA 7, BA 40). The relative glucose metabolism rates of ANs were significantly different from the HCs in right parietal lobule (36, -62, 50), left frontal gyrus (-16, 66, 10), left putamen (-16, 18, -2) and left hippocampus (-34, -14, -22). **Conclusions:** Our study showed significant metabolic changes in multiple brain regions in AN patients. These regions could be keystones in neurocircuits related to appetite. Accordingly, functional neuroimaging of brain glucose metabolism may indicate targets for AN treatment with neuromodulation like repetitive transcranial magnetic stimulation, deep brain stimulation or electrical cortical stimulation on a patient-based approach. Moreover, it could further contribute to assess the effects of existing and future treatment approaches in AN. Finally, functional neuroimaging serving as a diagnostic and prognostic tool and an aid in therapeutic decision-making could be expected.

P0875

Tc-99m Trodat Brain SPECT Changes in Adolescents with Attention Deficit Hyperactivity Disorder: After 2 Month-Methylphenidate Therapy

G. Capa Kaya*, A. P. Akay**, B. Baykara**, Y. Demir*, M. S. Eren*, N. Inal Emiroglu**, T. Ertay*, Y. Ozturk***, S. Miral**, H. Durak*, *Department of Nuclear Medicine, **Department of Child and Adolescent Psy, ***Department of Pediatrics; Dokuz Eylul University, School of Medicine, IZMIR, TURKEY.

The aim of this study was to assess Tc-99m Trodat-1 brain SPECT changes in adolescents with ADHD after 2 months methylphenidate (MPH) therapy. Eighteen adolescents with the diagnosis of ADHD participated in the study. None of them had comorbid neurological disease or psychiatric disorders other than oppositional defiant disorder. All patients were right handed and had never been medicated. ADHD diagnosis was made based on the ADHD criteria listed in DSM-IV-TR. Du Paul ADHD Questionnaire rating and clinical global impression (CGI) ratings were used. Tc-99m Trodat-1 SPECT was performed in all adolescents before (pre therapy) and after 2 months therapy (under treatment). MPH treatment was not discontinued during the second brain SPECT imaging. Radiochemical purity of Tc-99m Trodat-1 was exceeded 95% when tested by HPLC. Three hours after the injection of 444-814 MBq Tc-99m Trodat-1, brain images were obtained. A total of 128 frames were acquired in 128x128 matrices, 30sec/frame, 1.46 zoom and 360°. Transaxial slices were transformed into plane images. Regions of interest (ROIs) were drawn on the right basal ganglia (rbg), left basal ganglia (lbg) and the localization of cerebellum as the background. The two consecutive transverse slices showing the highest uptake in the basal ganglia were selected. Mean counts per pixel were used. Mean corrected activity in the basal ganglia was calculated as follows: (basal ganglia-

background)/background. Images were evaluated visually and semiquantitatively. There was a statistically significant decrease in pre-therapy availability of DAT assessed by brain SPECT under treatment (Wilcoxon statistical test, p=0.000). The mean score on the CGI was significantly decreased. There was also a statistically significant improvement in behavior under treatment, as indicated by the scores in Du Paul rating scales (p=0.000). Table shows clinical and Trodat-1 SPECT parameters.

P0876

Neuronal connectivity in Major Depressive Disorder. A SPECT CBF study

M. M. E. Pagani¹, D. Åstrand², H. Jacobsson², C. Jonsson², A. Danielsson², L. Engelin², A. Gardner³; ¹Institute of Cognitive Sciences and Technologies, Rome, ITALY, ²Department of Nuclear Medicine, Karolinska Hospital, Stockholm, SWEDEN, ³Järva psychiatric out-patient clinic, Praktikertjänst AB, Stockholm, SWEDEN.

Background. Major Depressive Disorder (MDD) has been extensively investigated by functional neuroimaging but a general consensus about cerebral blood flow (CBF) and metabolic changes occurring during the disease has not been reached yet. The aim of this study was to identify the CBF distribution differences between large groups of MDD patients and healthy controls and to investigate the neuronal connectivity underlying functional changes. **Methods.** CBF distribution at rest was investigated by 99mTc-HMPAO SPECT in 94 patients (54 females and 40 males, mean age 44±13) fulfilling DSM-IV criteria for MDD. Sixty-five healthy subjects (37 females and 28 males, mean age 49±15) were specifically recruited and served as controls (HC). CBF group differences were evaluated by statistical parametric mapping (SPM2) using age and sex as nuisance variables. The relative CBF value of the cluster in which significant group differences were found, normalized to thalamus uptake, was then used as covariate of interest and was correlated with 99mTc-HMPAO uptake in whole brain in: (i) whole patient group, (ii) HC, (iii) MDD females and MDD males separately. **Results.** Significantly increased rCBF distribution (p<0.05, False Discovery Rate corrected at voxel level) was found in MDD patients as compared to HC in a cluster covering large part of bilateral cerebellum. This cluster showed a highly significant negative correlation (p<0.001 Family-Wise Error corrected at voxel level) with bilateral caudatus in MDD patients, particularly in females. No correlation was found in HC between the CBF in the cluster and in any other brain region. **Conclusion.** A strong negative neuronal connectivity was found in MDD between cerebellum and "cognitive associative striatum" suggesting an important role for both structures in the neurobiology of the disorder. Disease-related resting-state network alterations may be associated in MDD to complex cognitive and emotional instability suggesting that whole brain functional connectivity might be considered as a potential biomarkers for clinical diagnosis.

P43-2 - Tuesday, October 30, 2012, 16:00 - 16:30, Poster Exhibition Area

Neurosciences: Neurodegeneration

P0877

C11-PIB and F18-FDG PET/CT in the Differential Diagnosis of Patients with Cognitive Impairment in the Clinical Setting

F. Ortega-Nava, I. Martínez-Rodríguez, J. Jiménez-Bonilla, R. Del Castillo Matos, S. Ibañez-Bravo, E. Rodríguez, J. Vázquez-Higuera, J. Berciano, J. Carril; Hospital Universitario Marqués de Valdecilla-Universidad de Cantabria, Santander, SPAIN.

Aim: To evaluate the contribution of C11-PIB and F18-FDG brain scans in the differential diagnosis between Alzheimer's Disease and other dementias. **Material and Methods:** 39 patients, mean age 64-year-old, with cognitive impairment were clinically classified by clinical neurologic criteria into the following groups: Subjective Memory Complaints (SMC): 6 patients, Non Amnesic Mild Cognitive Impairment (NA-MCI): 5 patients, Amnesic Mild Cognitive Impairment (A-MCI): 7 patients, Prodromic Alzheimer's Disease (AD): 7 patients, Fronto Temporal Dementia (FTD): 5 patients, Cortical Degeneration (CD): 2 patients, Dementia with Lewy Bodies (DLB): 2 patients, 5 patients were excluded due to technical problems. An C11-PIB PET/CT and an F18-FDG PET/CT exams were also requested for differential diagnosis. All of them had a 30-min PIB PET/CT, 60 minutes after injection of the radiotracer and a 15-min FDG PET/CT, 20 minutes after injection. Visual and semiquantitative (SUV ratio) analysis using cerebellar cortex as reference region were performed. An informed consent was obtained before examinations. **Results:** 5 of the 6 patients in the SMC group had negative FDG scans, 3 of them showed PIB retention and 2 of them negative PIB scans, the other one showed both FDG and PIB positive scans. In the NA-MCI all of the 5 patients had a negative PIB scan, and only one of them a positive FDG. 2 of the 7 patients in the A-MCI group had both scans negative, 3 of the 7 patients showed PIB retention with normal FDG, 1 showed a negative PIB with a positive FDG, and in another one

both scans were positive. 6 of the 7 patients in the AD group showed PIB retention, 5 of them with a positive FDG and 1 negative, another patient had a positive FDG and no PIB retention. All of the 5 patients in the FTD group had a positive FDG, and only one of them a positive PIB. The 2 patients in the CD group had positive FDG scans, one of them showed PIB retention. In the DLB group the two patients had both FDG and PIB positive scans. **Conclusions:** C11-PIB provided relevant contribution to the clinical management of these patients, specially when F18-FDG and C11-PIB are combined. The results obtained in this ongoing work are encouraging to continue this study including a larger number of patients.

P0878

Brain Perfusion with ^{99m}Tc -HMPAO SPECT in Differentiating Alzheimer's disease from Progressive Supranuclear Palsy and Corticobasal Degeneration: Analysis Using Brodmann Areas Mapping

V. Valotassiou¹, J. Papatrifiaylou², N. Sifakis³, C. Tzavara¹, I. Tsougos¹, D. Psimadas¹, A. Ziaka¹, E. Kapsalaki⁴, G. Chadigeorgiou⁵, P. Georgoulas¹; ¹Department of Nuclear Medicine, University Hospital of Larissa, Larissa, GREECE, ²Memory & Cognitive Disorders Clinic, Department of Neurology, "G. Gennimatas" Hospital, Athens, GREECE, ³Department of Nuclear Medicine, "Alexandra" University Hospital, Athens, GREECE, ⁴Department of Radiology, University Hospital of Larissa, Larissa, GREECE, ⁵Department of Neurology, University Hospital of Larissa, Larissa, GREECE.

AIM: Abnormal deposition of tau-protein in Alzheimer's disease (AD) is associated with cognitive impairment. Progressive supranuclear palsy (PSP) and corticobasal degeneration (CBD) are also characterized by tau pathology of neuronal cells and may be presented with dementia, making the differential diagnosis from AD difficult in many cases. The aim of this study was the evaluation of perfusion in Brodmann areas (BA) in AD and CBD/PSP, using an automated 3D-voxel based processing software, in order to improve brain areas definition that are specifically implicated in these disorders. **MATERIALS-METHODS:** We studied 60 consecutive patients from an outpatient Memory Clinic. We used the established criteria for the diagnosis of dementia and the specific established criteria for the diagnosis of AD and CBD/PSP. All the patients underwent a neuropsychological evaluation with a battery of tests including the mini-mental state examination (MMSE), as well as a CT and/or MRI of the brain in order to exclude the presence of anatomical lesions. Thirty-nine patients received the clinical diagnosis of AD (10 men, 29 women, age(\pm SD) 71 \pm 8 years, MMSE(\pm SD) 19 \pm 5, education(\pm SD) 9.3 \pm 4.7 years, duration of disease(\pm SD) 4 \pm 2 years), and 21 patients the clinical diagnosis of CBD/PSP (3 patients with PSP: 5 men, 16 women, age(\pm SD) 63 \pm 9 years, MMSE(\pm SD) 18 \pm 7, education(\pm SD) 11 \pm 4.3 years, duration of disease(\pm SD) 3 \pm 1.4 years). All the patients underwent a brain SPECT 20 min after the intravenous administration of 740MBq ^{99m}Tc -HMPAO. We applied the NeuroGamTM software on the reconstructed data, for the semi-quantitative evaluation of perfusion in BA areas in the right(R) and left(L) hemispheres. Perfusion values are expressed as mean \pm SD percentage of mean perfusion of the cerebellum. **RESULTS:** Compared with AD patients, CBD/PSP patients showed significantly lower perfusion in BA 10R (anterior prefrontal cortex), 17L-17R (primary visual cortex bilaterally), 18R (secondary visual cortex), 22R (superior temporal gyrus), 23L-23R (posterior cingulate cortex bilaterally), 46R and 47R (dorsolateral and inferior prefrontal cortex, respectively). Multiple logistic regression analysis demonstrated that 23R could independently differentiate AD from CBD/PSP ($p=0.012$). The optimal cut-off of 23R was 55.9 with sensitivity 76.9%, specificity 57.1%, positive and negative predictive values 76.9% and 57.1%, respectively. **CONCLUSION:** Our findings show involvement of frontal, temporal, parietal and occipital cortex, principally in the right hemisphere of CBD/PSP patients and are generally consistent with apraxia and impairment of frontal functions observed in CBD and PSP patients, respectively. Brain perfusion SPECT with Brodmann areas mapping would contribute in a more accurate differential diagnosis of AD from CBD/PSP patients.

P0879

Biokinetics of ^{65}Zn as an indicator for the assessment of Neurodegeneration

D. K. Dhawan, N. Singla; Panjab University, CHANDIGARH, INDIA.

Aim: Neurodegenerative disorders are heterogeneous in both their clinical and pathological features. Aluminium is linked to several neurological diseases including Alzheimer's and Parkinson's, while zinc is considered as an antioxidant and a neuromodulator. The present study was conducted to explore whether ^{65}Zn biokinetics in brain can be used as a marker of neurotoxicity. **Material and Methods:** Male sprague dawley rats weighing 140-160g were divided into four different groups viz: normal control, aluminium chloride, zinc sulphate and combined treatment of aluminium and zinc. Aluminium was given in drinking water at a dose of 100 mg/kg b.wt./day while zinc was given at a dose of 227mg/L in drinking water and all the treatments were carried out for a total duration of two months. In vivo uptake of ^{65}Zn in brain was recorded as a function of time following intraperitoneal injection of 40 μCi radioactivity by using suitably shielded gamma

ray spectrometer which allowed detection of gamma radiations coming only from brain. **Results:** ^{65}Zn biokinetics study showed two components: the fast component Tb_1 and the slow component Tb_2 . Aluminium treatment showed a significant increase in Tb_1 component and a significant decrease in Tb_2 component. However zinc supplementation to aluminium treated rats reversed the trend which indicated a significant decrease in Tb_1 component while the Tb_2 component was significantly increased. **Conclusion:** Therefore, the present study clearly demonstrates that ^{65}Zn biokinetics can be used a diagnostic marker in the assessment of neurotoxicity.

P0880

Review of Different Approaches in the Evaluation of Alzheimer's Patients including Amyloid Brain PET Scan

S. M. Akram¹, M. Vasanawala², M. Zeineh¹, N. Rasgon¹, M. L. Goris¹; ¹Stanford University, Palo Alto, CA, UNITED STATES, ²VA Palo Alto Health Care System/Stanford University, Palo Alto, CA, UNITED STATES.

Background: Practically all of the amyloid brain PET imaging analyses rely on quantitative and semi-quantitative methods to classify subjects into positive or negative. In this study we compared a consensus approach of pretest clinical diagnosis, amyloid brain PET scan visual analyses, and hippocampal atrophy with semi quantitative regional analyses of amyloid brain PET scans. **Methods:** We identified a cohort of 17 subjects with amyloid brain PET imaging as well as 3D T1 weighed MRI scan, who were participating under a research protocol for an amyloid brain imaging protocol. Regional semi quantitative analysis was performed on the PET scans at multiple locations in the cerebral including medial temporal and cerebellar cortices as well as in centrum semiovale. The ROIs were manually drawn based on fused PET MRI scans. The visual analysis was based on a simple criterion of presence or absence of tracer uptake outside of the central white matter deposition. MRI scans were visually and quantitatively evaluated for hippocampal atrophy. The consensus approach included pretest clinical diagnosis, visual interpretation of amyloid brain PET, and MRI analyses. The distribution of the average values in different regions were expressed as histograms separately for each of the consensus values. The positive versus negative histograms were compared by Chi-square goodness of fit. **Results:** The 17 subject cohort included 7 females and 10 males with ages ranging from 58 to 88 years old. The pretest clinical diagnoses in 12 of the 17 subjects were probable dementia of Alzheimer's. The visual analyses suggested Amyloid positivity in 9 subjects. Hippocampal atrophy was not seen in 6 subjects. Of the 17 subjects, 6 subjects were classified positive and 8 negative by the consensus approach, which included pretest clinical diagnosis, visual PET analyses, and hippocampal atrophy. The Chi-square values were significantly positive for all 3 criteria, but as expected, most for the visual versus quantitative PET. The values were: for visual PET 51.9, for clinical 40.7 and for MRI 39.1. **Conclusion:** In this limited and early analysis on a small cohort of scans, there was consensus between more than one relatively independent and useful criteria in the evaluation 13 of the 17 subjects. Secondly, visual interpretation of amyloid tracer distribution in the brain may seem as effective as more time consuming quantitative analysis. These need to be further evaluated in a larger clinical study. Table 1

P44-2 - Tuesday, October 30, 2012, 16:00 - 16:30, Poster Exhibition Area

Neurosciences: Dopamine Imaging

P0881

Effects of social exclusion on dopamine function in the human brain: A SPECT study in young adults with serious hearing impairment.

M. J. Gevonden¹, J. Selten², W. van den Brink¹, J. Booij¹; ¹AMC, Amsterdam, NETHERLANDS, ²Rivierduinen, Leiden, NETHERLANDS.

Background: According to the social defeat hypothesis the long-term experience of social exclusion or social defeat leads to enhanced baseline activity and/or sensitization of the mesolimbic dopamine (DA) system and puts the individual at increased risk for psychotic disorder and/or schizophrenia. Such increased risk has been found in migrants and in people with hearing impairment. This ongoing study tests the social defeat hypothesis by comparing dopaminergic function in two groups who differ greatly in the experience of social exclusion and are also expected to differ in DA release: (1) young adults (age 18-30) with a serious hearing impairment (HI); (2) normal hearing peers. **Subjects and methods:** Twelve subjects with HI (2 males; mean age 26, SD = 4.0) and 8 control subjects (2 males; mean age 25, SD = 3.3), were examined using SPECT imaging with the well-validated DA D2/3 receptor tracer [123I]iodobenzamide (IBZM) on a brain-dedicated system (Neurofocus; 12 detectors). In one session, baseline striatal D2/3 receptor binding and endogenous DA release after stimulation with D-amphetamine sulphate (0.3 mg/kg i.v.) were assessed (bolus/constant infusion technique). Statistical testing of DA release was done using two paired samples t-tests (one-tailed, $\alpha=0.05$) comparing binding at baseline and after stimulation within each group, and a t-test

(one-tailed) to compare DA release between the HI and control group. Results: [123I]BZM binding in the striatum decreased significantly after administration of D-amphetamine sulphate, reflecting DA release. Binding potential went down by 9.6%, $t(11)=2.89$, $p=.015$, in the HI group and 4.7%, $t(7) = 2.42$, $p=.046$, in the control group. The difference between groups was not statistically significant, $t(18) = 1.33$, $p=.20$, but has the expected directionality with greater DA release in the HI group. Discussion: In an ongoing study we have successfully measured DA release after a D-amphetamine challenge. The preliminary results show promise of demonstrating hyperdopaminergia in socially excluded individuals when scans have been acquired for a larger sample. Such a finding would add to the understanding of the biological mechanisms underlying unequal psychosis risk.

P0882

Comparison of Visual and Anatomically Co-registered Semi-quantitation of ^{99m}Tc SPECT in a Phantom Study

W. Huang¹, C. Cheng¹, M. Liao², C. Yeh¹, L. Shen², C. Chen², K. Ma³, ¹Tri-Service General Hospital, Taipei, TAIWAN, ²Institute of Nuclear Energy Research, Tao Yuan, TAIWAN, ³National Defense Medical Center, Taipei, TAIWAN.

Background: Semi-quantitative measurements of ^{99m}Tc -TRODAT-1 SPECT for evaluating striatal dopamine transporter (ST DAT) binding has been used in practice. Its reliability however remains concerned. The study was to undertake to evaluate potential usefulness of visually delineated regions of interest (ROIs) of ^{99m}Tc -99m striatal SPECT using an established brain phantom method. **Methods:** A simulated human brain volume and tissue-equivalent anthropomorphic phantom was used for brain ST DAT imaging. The added ^{99m}Tc radioactivity was adjusted similar to that of clinical use with original filling ratios ranged from 2:1 to 5:1 for ST and background that created imaging specific uptake ratios (SURs) ranged from 0.8 to 3. Semi-quantitative ROI analyses by either visual delineation or software assisted anatomic co-registration (PMOD) using a dual-headed camera equipped with ultrahigh resolution fan-beam collimators and Metz filter. The actual ST and background activity was measured by a gamma counter. Correlations of striatal SURs derived from both methods in reference to the actual counts were measured by the linear regression. **Results:** Both of the SPECT SURs measured by visual delineation and PMOD assisted anatomic co-registration well correlated with the corresponding actual radioactivity measured by the gamma-counter. The linear equations were: $y = 0.8094x - 1.1458$, $r^2 = 0.9581$ for visual delineation and $y = 0.8007x - 1.4546$, $r^2 = 0.9623$ for PMOD co-registration. Good correlations were also found between both kinds of SURs that were nearly parallel each other with respective slopes of 0.8090 and 0.8007. However, the PMOD data yielded a 0.3175 lower intersect than that of the visual delineation that could be adjusted accordingly. **Conclusions:** Using a specially designed brain phantom, good correlations between SURs obtained either by visual delineation or PMOD assisted anatomic co-registration and actual radioactivity measured by the gamma counter were achieved. Excellent correlations were also found between SURs derived from both methods. The phantom study might serve as a helpful means to fine-tune semi-quantitative analyses of striatal ^{99m}Tc TRODAT-1 DAT SPECT by visual delineation.

P0883

Accuracy of BasGan in the evaluation of doubtful 123FP-CIT SPECTs

A. Skanjeti¹, T. Angusti¹, M. Iudicello², F. Dazzara¹, G. M. Delgado Yabar¹, M. Margheron¹, V. Podio¹, ¹Nuclear Medicine Unit, San Luigi Hospital, Turin, ITALY, ²Neurology 1, San Luigi Hospital, Turin, ITALY.

BACKGROUND: Usually 123I-FP-CIT SPECT is qualitatively assessed. However, it has been shown that reproducibility of this kind of evaluation is not optimal: consequently accuracy can be affected. Recently, BasGan has been proposed as a semi-automated tool to analyze semi-quantitatively 123I-FP-CIT SPECTs. The aim of this study was to compare accuracy reached by BasGan analysis of 123I-FP-CIT SPECTs with accuracy of qualitative analysis in doubtful exams. **MATERIALS AND METHODS:** Seventy-eight consecutive exams were assessed separately by three nuclear medicine physicians and report them as normal, equivocal or pathological. In 25 cases (15M/10F mean age 69y) a full diagnostic agreement was not achieved, so these exams were considered doubtful: these composed our study population. Final diagnosis was established by the neurologist after at least 4 years of follow-up and in 6 of them (24%) neurodegenerative parkinsonian syndrome was detected. In order to determinate accuracy of 123I-FP-CIT SPECTs analyzed by BasGan, semi-quantitative values from the most deteriorated putamen were analyzed by Receiver Operating Characteristic (ROC) curves. **RESULTS:** ROC curves showed area under the curve=0.79 ($p=0.036$) with optimal cut-off for the most deteriorated putamen 3.3. Sensitivity, specificity and accuracy were 50%, 95% and 84% respectively. Each of the three nuclear physicians presented significantly lower accuracy in this population 32% ($p=0.0006$), 48% ($p=0.0169$) and 52% ($p=0.0338$) respectively. **CONCLUSIONS:** This study shows better performance of BasGan than qualitative assessment in the evaluation of doubtful 123I-FP-CIT SPECTs. In fact,

BasGan was mandatory to achieve a good accuracy in low prevalence population, due to high specificity of this cut-off.

P0884

Towards 123I-FP-CIT-SPECT standardized evaluation: BasGan accuracy in a two-center study

A. Skanjeti¹, G. Castellano², T. Angusti¹, M. Zotta², F. Dazzara¹, S. Cauda², M. Iudicello³, M. Zibetti⁴, P. Ferrero⁵, P. Filippi⁶, M. Margheron¹, G. Bisi², V. Podio¹, ¹Nuclear Medicine Unit, San Luigi Hospital, Turin, ITALY, ²Nuclear Medicine Unit, San Giovanni Battista Hospital, Turin, ITALY, ³Neurology 1, San Luigi Hospital, Turin, ITALY, ⁴Neurology 4, San Giovanni Battista Hospital, Turin, ITALY, ⁵Neurology 2, San Giovanni Battista Hospital, Turin, ITALY, ⁶Neurology, Maria Vittoria Hospital, Turin, ITALY.

BACKGROUND: Several methods have been suggested to evaluate semi-quantitatively 123I-FP-CIT-SPECTs; to the best of our knowledge no data from multicenter studies are available. Recently a new software, BasGan, has been proposed to perform a semi-quantitative semi-automated analysis of 123I-FP-CIT-SPECT exam. Aim of this study was to assess accuracy of 123I-FP-CIT-SPECTs performed in two centers and analyzed by BasGan. **MATERIALS AND METHODS:** One-hundred nineteen patients (51F, 68M, mean age \pm SD 66 \pm 10y) with movement disorders were enrolled. The diagnosis was established by the neurologists after a follow-up of at least 4 year: Neurodegenerative Parkinsonian Syndrome (NPS) in 76 and Essential Tremor (ET) in 43. 123I-FP-CIT-SPECTs from center A (n=59) were acquired with a Philips Axis and parallel hole collimators, while exams from center B (n=60) with a GE Millenium and fan beam collimators (voxel size of each reconstructed study showed small variability). All exams were analyzed with BasGan by a single operator. Semi-quantitative data from the most affected putamen and caudate (both raw and age-adjusted) were analyzed by Receiver Operating Characteristic (ROC) curve to estimate the accuracy. **RESULTS:** Area under the curve (AUC) was 0.911 ($p=0.0001$) for semi-quantitative values of the most affected putamen (best cut-off 2.52). AUC was 0.901 ($p=0.0001$) for age-adjusted data from the most affected putamen (best cut-off 0.635). AUC was 0.882 ($p=0.0001$) for semi-quantitative values of the most affected caudate (best cut-off 3.4). AUC was 0.876 ($p=0.0001$) for age-adjusted data from the most affected caudate (best cut-off 0.818). **CONCLUSION:** Both putamen and caudate analyzed by BasGan performed very well in accuracy analysis, despite exams were acquired in two different centers with different equipments. However, given the retrospective nature of this study, the obtained cut-off should be tested in other settings.

P45-2 - Tuesday, October 30, 2012, 16:00 - 16:30, Poster Exhibition Area

Neurosciences: Miscellaneous

P0885

Feasibility of Individualized Time Points in Isotope Baclofen Pump Imaging

J. Freden Lindqvist, A. Bergh; Sahlgrenska University Hospital, Göteborg, SWEDEN.

Aim: A retrospective follow-up of our experience of an individualized protocol in isotope baclofen pump investigations (IBPI). **Background:** Baclofen administered intrathecally by an implanted pump can treat spasticity. Decreased therapeutic effect can be due to baclofen tolerance or pump dysfunction. An IBPI with 111-Indium DTPA is a safe and reliable method for evaluating catheter failure (Le Breton 2001). A study of serial imaging with five fixed time points from 4 hrs to 7 days after radioisotope injection has been described (Pak 2007). We present an individualized approach with two image time points. **Materials and Methods:** In nine patients referred to our department for suspected baclofen pump dysfunction, we obtained a print-out of the current pump settings. Adding information from the manufacturer of the indwelling volume in the pump between the reservoir and the catheter, enabled calculation of the time at which the injected isotope should reach the intrathecal space - the catheter passage time (CPT). We timed our first image as close as possible after the CPT. A second image was taken 24 hrs later, to detect intrathecal propagation of the isotope. The patient journals have been reviewed to compare the radioisotope imaging result with the clinical outcome. **Results:** Four patients had normal findings, three were improved on increased baclofen dosage - in one case normal function was verified in surgery - and one is still under clinical evaluation. In two cases there was no isotope propagation at all, and a proximal catheter dysfunction was verified in surgery. In the remaining three cases, CPT was slow. In one of these cases intrathecal activity was seen and this patient improved on dose adjustment. In one case surgery showed distal leakage due to a catheter rift. The final patient received catheter replacement without improvement. IBPI was performed again with the same result - there is a suspicion of pump delivery dysfunction, but this has not been proven, since the patient has denied surgery. **Discussion:** Individualized IBPI decreases the number of images needed, and enables evaluation of the delivery status of the

pump. In evaluating our results, one must take into consideration the clinician's bias in knowing the result of the IBPI in the clinical decision making. There is also no side-by-side comparison with a fixed IBPI. Conclusion: Individualized time points in IBPI seems a reliable approach, possibly adding pump delivery information, and reducing camera time compared to fixed imaging times.

P0886

Sleep-dream Related Changes in Visual Cortex; Stages of Sleep and SPECT Findings

K. Unal¹, N. I. Karabacak², T. Cakir³. ¹Medical Park Hospital Nuclear Medicine Department, Izmir, TURKEY, ²Gazi University Nuclear Medicine Department, Ankara, TURKEY, ³Corlu State Hospital Nuclear Medicine Department, Tekirdag, TURKEY.

The patient was a 52-year-old male diagnosed with Familial Mediterranean Fever (FMF) and liver failure. He had generalized seizures. Diffuse electroencephalography (EEG) slowing was reported. Brain magnetic resonance imaging (MRI) showed minimal ischaemic gliosis in periventricular area and in centrum semiovale with no other abnormality in cortical gray matter. The patient was referred to the nuclear medicine department for brain perfusion single photon emission computed tomography (SPECT) study in order to rule out a focal area of an epileptic zone. The findings observed in the SPECT images were a relative flow increase in the occipital lobes, the bilateral posterior occipitoparietal cortex, and the left thalamus. The patient admitted that, he fell asleep after the injection during the uptake phase of the tracer. Due to the confounding sleep related changes, clinicians also ordered a fluorodeoxyglucose positron emission tomography/computed tomography (FDG PET/CT) study for the patient and the images revealed no abnormal hypo-hyper metabolic abnormality. The findings observed in this case in review of the sleep literature suggest that REM sleep seems to be associated with selective activation of extrastriate visual cortices. This pattern suggests a model for brain mechanisms subserving REM sleep where visual association cortices and their paralimbic projections may operate as a closed system dissociated from the regions at either end of the visual hierarchy that mediate interactions with the external world.

P0887

The Role of Oro-Pharyngo-Esophageal Scintigraphy in the Evaluation of Patients with Dysphagia: a Comparison with VFS and FEES

M. Meniconi¹, L. Locantore¹, M. Grosso¹, K. Massri¹, S. Mazzarri¹, B. Fattori², R. Raschilla¹, R. Cantini¹, V. Mancini², A. Nacci², M. Mihaese², L. Bastiani³, D. Volterrani¹, G. Mariani¹. ¹Regional Center of Nuclear Medicine, Pisa, ITALY, ²Department of Neuroscience, ENT Unit, University of Pisa, Pisa, Italy, Pisa, ITALY, ³CNR Institute of Clinical Physiology, Pisa, Italy, Pisa, ITALY.

Aim: Oro-pharyngo-esophageal scintigraphy (OPES) permits not only an overall functional evaluation of swallowing, but also a detailed semi-quantitative evaluation of the various stages of swallowing, especially data on transit time and retention of the bolus through the mouth, pharynx and esophagus. In this study, we evaluated sensitivity and specificity of OPES compared to Videofluoroscopy (VFS) and Fiberoptic Endoscopic Evaluation of Swallowing (FEES). Methods: We enrolled 33 patients (19 men and 14 women, mean age 66.2 years), 18 of whom with neurological disease (4 with Amyotrophic Lateral Sclerosis, 7 with stroke, 7 with Parkinson's disease or other parkinsonian syndromes), 6 post-surgery (partial laryngectomy, recurrent nerve paralysis, others), and 9 with either myopathy, gastro-esophageal reflux, chronic obstructive broncho-pneumopathy, or dermatomyositis. All patients underwent OPES with 99mTc-nanocolloid using a liquid bolus first, followed then by a semi-solid bolus. We evaluated the following parameters: Oral, Pharyngeal and Esophageal Transit Times, Oro-Pharyngeal and Esophageal Retention Index, Pre-swallow Falling, and presence of aspiration. These parameters were compared with VFS and FEES, that were considered as separate gold standards. Results: When compared to VFS, OPES had 93.1% sensitivity and 50% specificity with the liquid bolus, changing to 93.3% and 33.3%, respectively, with the semisolid bolus. Considering FEES as the reference standard, sensitivity and specificity of OPES were 96.2% and 42.9% for the liquid bolus, and finally 96.6% and 50% for the semisolid bolus. Regarding Pre-Swallow Falling, overall accuracy of OPES was 78.8% for the liquid and 72.7% for the semisolid bolus versus VFS, and 78.8% and 68.7%, respectively, versus FEES. Overall diagnostic accuracy of OPES was 75.8% for the liquid bolus and 63.6% for the semisolid bolus versus VFS, while it was 72.7% and 69.6%, respectively, versus FEES. The Spearman Correlation Index between all the above parameters assessed by OPES and the corresponding VFS and FEES parameters was statistically significant ($P < 0.01$). Conclusions: These results emphasize the value of OPES, which should be considered to characterize dysphagia and to better define the pathophysiological patterns of patients with swallowing problems. Furthermore, this procedure provides critical functional information which is complementary to those provided by commonly employed

invasive procedures that are either invasive (FEES) or entail a non-negligible radiation burden to patients (VFS).

P0888

High grade gliomas associated with abscess: description of two rare cases and role of 99mTc-Leukoscan

A. Campenni¹, M. Caffo², G. Caruso², N. Quartuccio¹, R. Gentile¹, M. P. Cucinotta¹, C. Alafaci², S. Baldari¹. ¹Department of Radiological Sciences, Nuclear Medicine Unit, University of Messina, Messina, ITALY, ²Department of Neurosurgery, University of Messina, Messina, ITALY.

Aim: Intracellar or parasellar tumors are among the most common neoplasms that develop abscess as complication due to direct extension of microbial flora from contiguous sinuses. Abscess formation within a brain tumor is uncommon. We describe two extremely rare cases of high grade gliomas associated with abscess formation. Material and Methods: The first patient was a 50 year old woman with a recent history of epileptic seizures, fever and headache. Hematologic examination demonstrated leukocytosis and elevated C-reactive protein. Magnetic Resonance (MR) obtained before and after contrast medium administration revealed a lesion (> 3 cm in size) in the right temporo-parietal consistent with brain abscess. Instead, MR spectroscopy (MRS) was conclusive for brain tumor. Patient underwent ^{99m}Tc-Leukoscan study of the brain obtained 4 and 24 hours after tracer administration (555 MBq) by dual-headed gamma camera equipped with low-energy high-resolution parallel-hole collimator (LEHRPAR). Scans were performed by planar (anterior, posterior and lateral views; magnification 1, matrix 256x256; 900 seconds per frame) and tomographic images (SPET; magnification 1, matrix 128x128; 180° rotation, a 3° step and shoot technique; 30s per frame). The study showed abnormal and non-homogeneous uptake of the tracer in the right temporo-parietal region corresponding to MR lesion and consistent with brain abscess. Craniotomy was performed and the lesion was totally removed. Histopathological examination permitted a diagnosis of glioblastoma with intralesion abscess. The second patient, a 47 years old woman, had fever, headache and jacksonian seizures. Hematologic examination demonstrated leukocytosis while C-reactive protein was normal. MR demonstrated a lesion in fronto-temporal area (>3 cm in size). Also in this patient, MR and MRS were not conclusive (brain abscess vs brain tumor). Patient underwent ^{99m}Tc-Leukoscan study with the same modalities employed for the first patient. Study showed an abnormal tracer uptake in the lesion observed with MR. Diagnosis of brain abscess was postulated. Craniotomy was performed and the lesion was totally removed. Histopathological examination revealed a glioblastoma with intralesion abscess Conclusion: These extremely rare cases demonstrated that the presence of brain abscess does not rule out cancer. The diagnosis of brain tumor associated with abscess is particularly difficult by conventional neuroradiological studies. Leukoscan can be useful in the diagnosis of brain abscesses and in differential diagnosis of cyst lesion and/or cystic brain tumor.

P46-2 - Tuesday, October 30, 2012, 16:00 - 16:30, Poster Exhibition Area

Neurosciences: Data Analysis & Quantification

P0889

Impact of automatized semiquantitative FDG brain biodistribution analysis in patients with neurodegenerative diseases: what can we expect from commercially available software tools?

H. Huber¹, W. Brandstätter¹, M. Hatzl¹, M. Klinger¹, J. Pilz², A. Sulzbacher¹, D. Pohn³, W. Struhala⁴, G. Ransmayr⁴, M. Gabriel¹. ¹AKH Linz, Institut für Nuklearmedizin und Endokrinologie, Linz, AUSTRIA, ²FH Gesundheitsberufe OÖ GmbH, Campus Gesundheit am AKH Linz, Linz, AUSTRIA, ³AKH Linz, Abteilung für Neurologie und Psychiatrie, Linz, AUSTRIA, ⁴AKH Linz, Abteilung für Neurologie und Psychiatrie, Linz, Austria, Linz, AUSTRIA.

Introduction: ¹⁸F-FDG-PET emerged as the method of choice for early diagnosis of dementias. Apart from visual assessment, algorithms for semiquantitative evaluation based on an integrated norm collective were developed. The aim of our evaluation was to define the value of automatized semiquantitative analysis of the biodistribution of ¹⁸F-FDG in patients suspected to suffer from neurodegenerative diseases. The analysis also included head-to-head evaluation of two different commercially available software packages. Materials and methods: Since 2009, 34 patients (14 m, 20 f; mean age 65 years; SD ± 13 years) were referred for ¹⁸F-FDG-evaluation of dementia. Each patient received 185 MBq ¹⁸F-FDG i.v.. Imaging was performed 30 min p.i. with a dedicated PET-CT (Siemens Biograph). Beside visual interpretation of the images by three readers data were semi-quantitatively analysed by two automated algorithms (HERMES BRASS® and SIEMENS SYNGO/SCENIC®). Clinical follow-up served as reference standard. PET-CT classification was based on biodistribution features described by Ishii et al. (2002). For numerical head-to-head comparison brain areas were comprised in a lobar map. Selected brain regions were defined pathological if Z-score ≤ -2 calculated

from the software database. If the patient study was classified as “abnormal”, the type of dementia was defined according to the distribution of decreased brain uptake. For visual assessment “hot iron” images were available for the blinded readers. They had to assess “pathological” images and the most probable type of dementia according to the pattern of ^{18}F -FDG biodistribution. **Results:** Both software tools showed high sensitivity, 92% for Hermes and 96% for Siemens, in definition of neurodegenerative diseases with low overall specificity of 60% to 67 %, respectively. Numerical data from BRASS and SYNGO were concordant in 77% of cases for definition of pathology. The prediction of individual diagnoses, however, as derived from the distribution pattern, significantly differed between the patient studies ($r = 0.30 - 0.59$; site specific evaluation). Visual reading showed a sensitivity of 87% and a specificity of 67 % for definition of brain disease. However, in those studies which were true-positive for neurodegenerative disease the type of dementia was correctly defined - in contrast to software analysis - in most cases. **Conclusion:** High correlation was found between both systems for numerical evaluation of different brain areas to provide convincing accuracy for predicting neurodegenerative diseases. The type of dementia, however, cannot be confidentially derived from the numerical distribution pattern. This finding requires additional visual interpretation in any case.

P0890

Differential diagnosis of fronto-temporal dementia using automated image classification

S. Young¹, V. Berti², F. Wenzel³, C. Polito², M. Bartolini², L. Settimo², S. Sorbi⁴, A. Pupic², ¹Philips Healthcare, Hamburg, GERMANY, ²Department of Clinical Pathophysiology, Nuclear Medicine Unit, University of Florence, Florence, ITALY, ³Philips Research, Hamburg, GERMANY, ⁴Department of Neurology and Psychiatry, University of Florence, Florence, ITALY.

Aim Fronto-temporal dementia (FTD) comprises of different syndromes with distinct clinical symptoms. FDG-PET has been shown to support clinical differential diagnosis, since alternative forms exhibit distinct patterns of hypo-metabolism. This study evaluates the utility of statistical classification of FDG-PET images to automatically distinguish between patients with different forms of suspected FTD. **Material and Methods** FDG-PET brain scans were acquired on 66 subjects (71 ± 9 y.o.), including frontal-variant FTD (fvFTD, $n=14$), progressive non-fluent aphasia (PNFA, $n=12$), temporal-variant FTD (tvFTD, $n=16$), and Alzheimer's disease (AD, $n=24$). Definitive clinical diagnoses were confirmed by a dementia-expert neurologist 1 year after FDG-PET. All images were acquired for 20 minutes 30 pi of 250 MBq ^{18}F -FDG on a Philips Gemini TF PET/CT scanner. 40 normal controls (NC, 70 ± 9 y.o.) imaged on another Gemini TF scanner with a similar protocol [1] were also included. After stereotactic registration and intensity normalization procedures, subsets of the database were used to train different classifiers, using a supervised learning approach based on the partial least squares (PLS) method. Each classifier defines a linear projection of image voxels to a vector with dimensionality equal to the number of training classes, and a maximum-likelihood decision rule is applied to assign class labels. The approach was evaluated using (i) a leave-one-out (LOO) cross-validation scheme, and (ii) a test cohort of patients not included in the training database (NC/AD/fvFTD/PNFA/tvFTD, $n=9/31/8/5/8$). Performance metrics included classification accuracy and mean-squared error (MSE) between the likelihood scores and idealized input vectors. Results For LOO analysis, two-class classification accuracy was 100% for NC/fvFTD, NC/PNFA, NC/tvFTD, and 97% for NC/AD. For differential diagnosis between fvFTD/PNFA, fvFTD/tvFTD, PNFA/tvFTD accuracy was 88/97/86 %, with corresponding MSE of 0.24/0.06/ 0.31. For the test cohort evaluation, two-class classification accuracy was 98/94/93/100% for NC/AD, NC/fvFTD, NC/PNFA, NC/tvFTD, respectively, and mean sensitivity and specificity was 92 and 97% respectively. The accuracy of five-class classification was comparable (79/84 %) in both evaluations. **Conclusion** The feasibility of automated classification of FDG-PET brain images to separate distinct sub-types of fronto-temporal dementia was demonstrated, showing excellent accuracy. The most evident labelling errors were seen for PNFA subjects, which may be expected due to the involvement of cortical regions (i.e. frontal and temporal lobes) that are common to other disorders (AD, fvFTD, tvFTD). [1] Young et al, “On template selection for spatial normalization of FDG-PET brain images”, EANM 2011

P0891

Impact of CT tube charge on FP-CIT quantification using attenuation corrected SPECT and comparison to Chang's uniform correction: an anthropomorphic phantom study

G. Petyt, P. Lenfant, F. Demailly, J. Legrand, C. Hossein-Foucher; Nuclear Medicine Department - CHRU Lille, Lille, FRANCE.

SPECT-CT is now widely available and is used in FP-CIT imaging for attenuation correction and MRI fitting. Our aim was to define the lowest irradiation achievable allowing precise quantification and accurate image fitting. **Material and methods:** 5 different CT protocols were performed on an anthropomorphic striatal phantom using a SymbiaT2 dual head gamma camera (Siemens). Target tube charge was set at 90, 70, 50, 30 and 15 mAs. Care Dose 2D software was used to avoid scout views

exposition. CT were reconstructed using a H08 smooth filter for attenuation correction purpose and a H30 filter for anatomical mapping and image fitting. SPECT was reconstructed using Flash3D iterative algorithm (Syngo, Siemens) with 8 iteration and 8 subsets without and with attenuation correction using the 5 acquired CT or Chang's uniform attenuation correction (with 0,14 and 0,11 cm-1 as linear attenuation coefficient as proposed in guidelines). Striatal Binding potentials (BP) were computed using anatomically based ROI for caudate nuclei, putamens and occipital cortex. CTDIw, DLP and effective mAs were recorded. To assess CT abilities to be fitted on a diagnostic CT, H30 series were modified using a rigid transformation including 15° rotation in both transverse and sagittal planes. Those modified CT were then fitted to the original 90 mAs CT using a mutual information based algorithm (Syngo). **Results:** As waited, decreasing tube charge linearly decreases DLP and CTDIw. Care Dose is useless at 15 mAs. At 15 mAs the CTDIw is 3.19 mGy and DLP for a whole brain CT is 58 mGy.cm corresponding to a effective dose of 0.12 mSv. All the modified CT were accurately fitted to the unmodified “diagnostic” CT leading to spatial errors lower than 1mm. ROI count variations are lower than 2% when decreasing mAs, whatever the ROI size. Reconstruction without attenuation correction overestimates striatal BP of 6% . Chang's attenuation corrected series underestimates BP of 12% to 10%. **Conclusion:** For FP-CIT SPECT-CT imaging on Symbia T2, tube charge can be decreased down to 15 mAs for attenuation correction purpose and diagnostic imaging realignment without any loss in accuracy.

P0892

Low Dose FDG Brain Imaging with a High Sensitivity PET Scanner

D. L. Bailey¹, E. A. Bailey², K. P. Willowson¹; ¹University of Sydney, Sydney, AUSTRALIA, ²Royal North Shore Hospital, Sydney, AUSTRALIA.

BACKGROUND: The brain is usually the organ demonstrating the highest uptake of [^{18}F]-FDG under euglycaemic conditions. We wanted to investigate the minimum dose of FDG that could be administered and still obtain brain images of sufficient quality for functional cerebral activation studies whilst remaining below the radiation dose guideline of 5 mSv for a volunteer. PET cerebral activation studies with FDG are useful for tasks that cannot be completed while the subject is in the scanner. **METHODS:** Subjects presenting for clinical FDG brain or whole body scans were imaged using a Siemens Biograph mCT extended axial field of view, high sensitivity Time-of-Flight (ToF) camera and an FDG activity of 150-300MBq. The acquisition was for 10 minutes in a single bed position in list mode with a simulated ECG gating signal (60 bpm). Scatter and attenuation correction were applied based on the CT scan. The data were rebinned prior to reconstruction using the gating signal into 10 frames, each corresponding to approx. 1/10th of the total FDG dose(D) administered. Reconstruction used 3D-OSEM with 4 iterations and 21 subsets. Images in increments of 0.1xD steps up to the total were produced and ROIs defined over brain corresponding to grey and white matter with known differential uptake of FDG and in the ventricles, and signal to noise ratios (SNR) obtained. **RESULTS:** Seven subjects have been studied to date. In a representative example the subject was administered 148 MBq of FDG and imaged 45 mins later, so that 0.1xD is equivalent to ≈ 15 MBq injected, 0.2xD ≈ 30 MBq, etc. Based on visual inspection and SNR analysis, 30-50 MBq of FDG gives useful brain images. **CONCLUSION:** The high uptake of FDG by the normal brain permits lower amounts of radioactivity to be administered compared with whole body imaging. On our scanner, around 30-50 MBq of FDG gives adequate image quality, especially if being used for neuroscience “activation” studies. The Effective Dose from 50 MBq of FDG is approx. 1 mSv, thus permitting multiple imaging studies in an individual while remaining below the 5 mSv limit.

P0893

Application of CT-based partial volume correction to 11C-PIB PET SUVR images with subtraction of nonspecific bindings in the white matter and comparison with MRI-based partial volume correction

E. Imabayashi¹, H. Matsuda¹, I. Kuji¹, A. Seto², Y. Shimano¹; ¹Saitama Medical University International Medical Center, HIDAKA, JAPAN, ²Saitama Medical University Hospital, MOROYAMA, JAPAN.

Aim: In amyloid imaging, partial volume correction (PVC) may be necessary for accurate assessment of accumulation in atrophied brain in Alzheimer's disease (AD). The visual evaluation of the slight 11C-PIB accumulation in grey matter (GM) may be difficult in the standardized uptake value ratios (SUVR) images because of the interference of its nonspecific accumulation in the white matter (WM). In the present study, we applied CT-based PVC to SUVR images with subtraction of WM accumulation to avoid spill-over to GM and to clarify cortical accumulations. Moreover CT-based PVC was compared with MRI-based PVC. **Materials and Methods:** Nine cognitively normal volunteers (CNV) with negative 11C-PIB accumulation and five AD patients with positive 11C-PIB accumulation were studied. Each subject received an intravenous injection of 600MBq of 11C-PIB and underwent 70 minutes list mode acquisition using PET/CT equipment (Biograph 6

Hi-Rez; Siemens Medical Systems, Inc.). The SUVR images were generated from 50 to 70 minutes acquisition. Attenuation correction was performed using CT data. Before intravenous injection of ^{11}C -PIB, CT scans with diagnostic quality were obtained using the same PET/CT equipment. Images were reconstructed at 3-mm thickness with filtered back projection. Both whole brain CT images and 3D T1 weighted structural MRI were segmented to GM, WM, and CSF spaces using statistical parametric mapping (SPM) 8. PVC procedure based on the assumption that WM uptake was homogenous was performed with PMOD software (<http://www.pmod.com>). Brain pixel counts were classified as WM or GM and sorted into respective segment. Based on these segments and the assumed PET resolution the spill-over from WM to GM could be estimated and subtracted. SUVR images with PVC based on CT, those with PVC based on MRI, and those without PVC were compared using VOI data obtained by applying automatic anatomical labeling templates. Results: Even without PVC, VOI values were significantly larger in AD than CNV. With PVC, both based on CT and MRI, VOI value differences between AD and CNV significantly increased more than those without PVC. There was no significant difference in VOI values between CT-based PVC and MRI-based PVC in AD. Conclusion: PVC may improve detectability of abnormal ^{11}C -PIB accumulation in SUVR images effectively in atrophied grey matter of the AD brain. CT-based PVC presented similar effect to MRI-based PVC. The availability of PET/CT scanner allows applying CT-based PVC in a single shot practical relevance.

P0894

Statistical voxel-based analysis of [^{18}F]FDG PET animal studies for the estimation of glucose metabolism in stress conditions

G. Di Grigoli^{1,2,3}, F. Gallivanone¹, L. Musazzi⁴, G. Gelsomino^{1,2,3}, G. Treccani⁴, S. Valtorta^{1,2,3}, E. Grosso⁵, I. Castiglioni¹, M. C. Gilardi^{1,2,3}, M. Popoli⁴, R. M. Moresco^{1,2,3}, F. Fazio^{1,2,3}, ¹IBFM-CNR, Segrate, ITALY, ²TECNOMED foundation of University of Milan-Bicocca, Monza, ITALY, ³San Raffaele Scientific Institute, Milano, ITALY, ⁴Center of Neuropharmacology, Dept. Pharmacol. Sci. – University of Milano, Milano, ITALY, ⁵University of Milan-Bicocca, Milano, ITALY.

Aim: Aim of this study was to evaluate the effect of acute stress on rat brain metabolism using PET [^{18}F]FDG and Foot-Shock (FS) paradigm. Regional stress effect was evaluated both by a statistical voxel-based analysis using a rat-model version of Statistical Parametric Mapping (SPM) optimized in our facility. **Materials & Methods:** 16 male CD rats, randomly assigned into two groups, 8 rats for Control Group (CG) and 8 rats for Stressed Group (SG), were injected with [^{18}F]FDG in a lateral tail vein. Following the FS protocol, the SG was exposed, immediately after radiotracer injection, to the shock session. One hour after [^{18}F]FDG injection, CG and SG were then subjected to a PET brain study for 30 minutes. All animals have been then sacrificed and corticosterone and circulating glucose were measured. A rat template was created using a control rat, outside of the two groups, who performed, in addition to the PET study, an and MRI study: the PET images for this rat, co-registered to his MRI, was used as [^{18}F]FDG/MRI template. Statistical analysis were performed setting $p < 0.05$, a threshold of 100 voxels and rescaling data to a mean glucose consumption value of 28mol/100g/min. In particular three SPM design were used: 1) a single subject design was used both to perform a Jack-Knife analysis on CG and to evaluate each SG rat with respect to CG; 2) a compare-populations model was used to evaluate differences in SG with respect to CG; 3) a simple regression model allowed to evaluate correlations between cerebral glucose metabolism and corticosterone levels in different brain regions. **Results:** Jack-Knife analysis on CG showed that one rat had a pattern of altered metabolism in comparison to the other control rats, suggesting a different susceptibility to experimental handling. This rat was excluded from analysis. Single-subject analysis on stressed rats revealed a similar pattern, except for one animal. Interestingly this rat escaped from box during stress paradigm. Group analysis showed a relative reduction of regional brain metabolism at the level of thalamus, hypothalamus, entorhinal and piriform cortex, and cerebellum, while an increase was observed in motor, somato-sensory cortex, olfactory bulb regions and hippocampal subregions. A negative correlation was observed between cerebral glucose metabolism and corticosterone levels in different brain regions. **Conclusion:** Results of the study indicated that acute stress modifies regional brain functions and these modifications are associated with circulating level of stress markers like corticosterone.

P0895

Interobserver variability of [^{123}I]FP-CIT striatal binding ratios assessment: a comparison between two different methods of analysis

D. Volterrani, V. Duce, M. Tredici, J. Bertoli, G. Manca, S. Mazzarri, I. Pagliani, K. Massri, F. Guidoccio, F. Betti, L. Antonacci, G. Mariani; Regional Center of Nuclear Medicine, University of Pisa, Pisa, ITALY.

Aim: [^{123}I]FP-CIT SPECT is employed to differentiate degenerative nigrostriatal parkinsonian syndromes (PD) from nondegenerative causes of parkinsonism. Its

potential usefulness to monitor PD progression and to assess putative neuroprotective drugs has also been reported. Thus, reproducibility is crucial to monitor nigrostriatal degeneration over time. We evaluated interobserver variability of two different methods of analysis, employing respectively a 2D ROI template and a template of anatomical VOIs automatically coregistered to SPECT data. Methods: Forty consecutive patients with suspected degenerative parkinsonism that had undergone [^{123}I]FP-CIT SPECT were included in the study. Images were acquired 3-4 hr after intravenous injection of 150-185 MBq [^{123}I]FP-CIT (DaTSCAN, GE Healthcare). A dual-head gamma camera (Infinia, GE Healthcare) was used to acquire 120 15-sec views over 360° on a 128×128 matrix (LEHR collimators). Images were reconstructed using FBP and corrected for attenuation. Three observers processed all the 40 [^{123}I]FP-CIT scans adopting two different semi-quantitative ROI uptake approaches: 1) After reorientation along the fronto-occipital line, each operator calculated the binding ratios with the DaTSCAN 3-2 software (GE Healthcare Xeleris workstation). In this software a 2D template of four ROIs of fixed shape and size is manually translated and rotated to match the nuclei in three reoriented transverse slices with the most intense striatal specific binding, previously chosen by the operators. A fifth ROI is then placed over the occipital lobe to evaluate nonspecific binding. 2) The free software Basal-Ganglia-Matching-Tool v.2 (BGV2) based on a high-definition 3D template of the striatum derived from Talairach and Tournoux's anatomical atlas was used, thereby SPECT data are manually reoriented parallel to the AP-AC line; the algorithm translates then the data in order to place the striata in a standard position. An optimization protocol automatically performs fine tuning of the position, orientates the 3D template on the reoriented slices, and locates an occipital ROI. Results: No significant differences in mean caudate and putamen binding ratios among the three observers were found by using both the 2D ROI and the anatomical VOI approach. However, a relevant interobserver variability was noted with the 2D ROI method (caudate 7.0%±6.3%, putamen 7.7%±5.3%), whereas almost perfect reproducibility was found with the BGV2 software. Conclusion: Besides the intrinsic limitations of reproducibility (6-8% on test-retest assessment) that characterize [^{123}I]FP-CIT SPECT, methods for semiquantitative analysis can significantly affect the measurement of binding ratios. Optimized automatic protocols such as BGV2 seem to overcome the above limitations in reproducibility of binding assessment.

P47-2 - Tuesday, October 30, 2012, 16:00 - 16:30, Poster Exhibition Area

Neurosciences: Movement Disorders**P0896****The severity of cardiac sympathetic denervation is not related to presynaptic nigrostriatal degeneration in Parkinson's disease.**

A. Chiaravalloti¹, A. Stefani², B. Di Pietro¹, M. Pierantozzi², M. Tavoletta¹, D. Di Biagio¹, A. Lacanfora¹, R. Catalano¹, P. Stanzione², O. Schillaci¹; ¹Nuclear Medicine University Tor Vergata, Rome, ITALY, ²Neurology University Tor Vergata, Rome, ITALY.

Aim: The aim of our study was to investigate the relationship between myocardial sympathetic and nigrostriatal degeneration in patients affected by Parkinson's disease (PD) by means of both 123I-MIBG scintigraphy and 123I-FP-CIT SPECT. **Patients and methods:** The study involved 37 patients with clinical diagnosis of PD (22 males and 15 females, mean age 62 years old(± 10); 15 Hoehn & Yahr (H&Y) stage 1, 8 stage 1.5, 7 stage 2 and 7 at stage 3. All of them were first evaluated by means of 123I-FP-CIT SPECT using standard technique and then by 123I-MIBG scintigraphy, performed after 20(± 3) days from the 123I-FP-CIT SPECT scan. For 123I-MIBG scintigraphy early (15 minutes) and delayed (4 hours) anterior chest images were acquired and the heart/mediastinum ratio (H/M ratio) was calculated. Linear regression and Spearman's correlation has been used in order to assess a relationship between striatal 123I-FP-CIT and cardiac 123I-MIBG uptake. **Results:** We didn't find statistical significant relationships between 123I-MIBG cardiac and 123I-FP-CIT striatal uptake in contralateral caudate to the clinically more affected side both in early ($r^2=0.03741$, $P=0.2514$; $r=0.2368$, $P=0.1582$) and delayed images ($r^2=0.03741$, $P=0.2514$; $r=0.2368$, $P=0.1582$), and contralateral putamen both in early ($r^2=0.003646$, $P=0.7226$; $r=0.1576$, $P=0.3517$) and delayed images ($r^2=0.001972$, $P=0.7941$; $r=0.2250$, $P=0.1806$), respectively. No statistically significant relationship has been found at any level also when considering omolateral striatum (both caudate and putamen). **Conclusion:** The results of our study suggest that cardiac sympathetic system and nigrostriatal system are differently affected in PD. In particular, in our series, the sympathetic neurodegeneration rate was not related to nigrostriatal degeneration rate as detectable by means of 123I-MIBG and 123I-FP-CIT scintigraphy, respectively.

P0897**Different patterns of cardiac sympathetic denervation in tremor type versus akinetic-rigid type of Parkinson's disease: molecular imaging with 123I-MIBG**

A. Chiaravalloti¹, A. Stefani², M. Tavoletta¹, M. Pierantozzi², D. Di Biagio¹, B. Di Pietro¹, R. Danieli¹, L. Travascio¹, P. Stanzione², O. Schillaci¹; ¹Nuclear Medicine University Tor Vergata, Rome, ITALY, ²Neurology University Tor Vergata, Rome, ITALY.

Aim: The aim of this study was to evaluate the relationship between the clinical motor phenotypes of Parkinson's Disease (PD) and 123I-MIBG myocardial uptake. **Patients and methods:** We examined 53 patients with PD, 31 males and 22 females, mean age 62 years old (± 10); 19 Hoehn & Yahr (H&Y) stage 1, 9 stage 1.5, 15 stage 2 and 10 at stage 3 and subdivided them in different clinical forms on the basis of dominance of resting tremor ($n=19$, TDT) and bradykinesia plus rigidity ($n=34$, ART). We correlated this status with the semi-quantitative analysis of 123I-MIBG myocardial uptake. Early (15 minutes) and delayed (4 hours) anterior chest images were acquired and the heart/mediastinum ratio (H/M ratio) was calculated. An age matched control group of 18 patients has been recruited; 8 males and 10 females, mean age 62.4 years old (± 16.3). **Results:** 123I-MIBG myocardial uptake significantly relates to disease duration in early ($r^2=0.1894$; $P=0.0028$) and delayed images ($r^2=0.1795$; $P=0.0037$) in PD patients while no relationship has been found when considering age at examination, UPDRS III and H&Y score. PD patients show a reduced 123I-MIBG myocardial uptake as compared to control group in early ($P=0.0026$) and delayed images ($P=0.0040$) and 123I-MIBG myocardial uptake resulted significantly lower in delayed images in TDT patients when compared with ART ones ($P=0.0167$). We found a decrease in H/M ratio between delayed images as compared to that of the early acquisition in TDT patients ($P=0.0040$) and in the whole PD population ($P=0.0012$), while no differences have been found in ART patients ($P=0.1043$). **Conclusion:** The results of our study show that cardiac sympathetic system is more severely impaired in TDT than in ART patients with PD, and that 123I-MIBG molecular imaging may help to improve therapeutic planning in these patients.

P0898**Parkinsonian Syndromes (PS) differential diagnosis: the usefulness of 123I-MetalodoBenzylGuanidine (123I-MIBG) cardiac scintigraphy**

S. Nuvoli¹, M. R. Piras², A. Nieddu³, F. Chessa¹, A. Spanu¹, G. Madeddu¹; ¹Unit of Nuclear Medicine, DPT of Clinical and Experimental Medicine, University of Sassari, Sassari, ITALY, ²Unit of Neurology, DPT of Clinical and Experimental Medicine, University of Sassari, Sassari, ITALY, ³Geriatrics DPT, Policlinico Sassarese, Sassari, ITALY.

Aim: To evaluate the usefulness of 123I-MIBG cardiac scintigraphy in PS differential diagnosis. **Methods:** We studied consecutively 80 pts clinically classified as affected by PS: all of them had movement disorders, vascular signs in basal ganglia at MR and pathological inconclusive 123I-iodoflupane SPECT. All pts underwent cardiac planar imaging (anterior and left anterior oblique views) after 111MBq of 123I-MIBG i.v. injection at 15 min (early) and 240 min (delayed) by a dual head gamma camera with a 128x128 matrix. Images were evaluated both qualitatively and quantitatively, the latter calculating the early and delayed heart/mediastinum ratios (H/M) by regions of interest (ROIs) manually drawn in anterior view. To better define ROIs areas a SPECT/CT was performed by hybrid dual head gamma camera integrated with a low-dose X-ray tube. SPECT images were reconstructed with iterative method (OSEM) and fused with CT. **Results:** 123I-MIBG uptake was slight to severe reduced in 59/80 (74%) cases (Group A) while normal/homogeneous uptake was observed in 22/80 (25%) cases (Group B). The early and delayed H/M mean values were in Group A 1.34 ± 0.14 (range: 1.08-1.51) and 1.28 ± 0.19 (range: 1.0-1.53), respectively and in Group B 1.72 ± 0.11 (range: 1.53-1.98) and 1.75 ± 0.16 (range: 1.56-2.1), respectively. During follow up, according to international clinical criteria, 53/58 Group A pts were finally classified as affected by Parkinson's disease (PD) and 5/58 as Lewy bodies dementia (LBD). Among Group B cases, 12/22 were considered as vascular tremor (VT), 5/22 as Progressive Supranuclear Palsy (PSP), 4/22 as Multiple System Atrophy (MSA) and 1/22 as Alzheimer dementia (AD). Mean early and delayed H/M values were significantly ($p < 0.00008$ and $p < 0.00002$, respectively) lower in Group A than in Group B. **Conclusions:** 123I-MIBG cardiac scintigraphy represents a useful diagnostic tool in PS differential diagnosis, especially in those cases with MR vascular lesions in basal ganglia and inconclusive at 123I-iodoflupane SPECT. Homogeneous 123I-MIBG cardiac uptake defining regular sympathetic post ganglionic assessment supported VT, MSA, AD and PSP diagnosis in our cases as well as a reduced 123I-MIBG uptake could suggest PD or LBD diseases, thus permitting adequate specific treatments. A longer clinical follow up and histopathological data are needed to confirm these results.

P0899**Cardiac Metaiodobenzylguanidine Scintigraphy in Patients With Spinocerebellar Ataxia Type 2**

S. De Luca¹, T. Pellegrino², S. Pappatà², A. De Rosa¹, M. De Leva¹, M. Tuccillo¹, A. Boemio¹, A. Filla¹, G. De Michele¹, A. Cuocolo¹; ¹University Federico II, Napoli, ITALY, ²National Council of Research, Napoli, ITALY.

Aim: Spinocerebellar ataxia type 2 (SCA2) is an autosomal dominant neurodegenerative disorder characterized by progressive cerebellar ataxia, slow saccadic eye movements, and peripheral neuropathy. Autonomic nervous system dysfunction represents also a significant component of SCA2 clinical picture. The aim of this study was to evaluate cardiac autonomic innervation in patients with SCA2 using cardiac I-123 metaiodobenzylguanidine (MIBG) scintigraphy, a marker of post-ganglionic sympathetic cardiac nerve terminals integrity, in comparison with patients with Parkinson's disease (PD), usually showing reduced myocardial MIBG uptake. **Material and Methods:** Cardiac autonomic innervation was assessed in 8 patients with SCA2 (5 men and 3 women, mean age 40 ± 12 years) and 5 patients with PD (3 men and 2 women, mean age 53 ± 7 years). None of these patients had diabetes mellitus, cardiac disease, or took drugs that may affect MIBG myocardial uptake. All patients underwent I-123 MIBG scintigraphy. Following thyroid gland blocking with potassium iodide, 111 MBq of I-123 MIBG was intravenously injected. Planar scintigraphic imaging in the anterior view was obtained 15 minutes (initial) and 4 hours (delayed) after the tracer injection using a dual-head gamma camera equipped with a low-energy, high-resolution collimator. A preset time of 10 min was used for image acquisition with a 159 ± 10 keV of energy window. Region of interest analysis was used to calculate the initial and delayed heart to mediastinum (H/M) ratios. The H/M ratio for both initial and delayed images and the background corrected myocardial washout rate were calculated. Two observers, blinded about patients' disease, performed data analysis. **Results:** Initial H/M ratio and delayed H/M ratio in patients with PD versus patients with SCA2 were 1.6 ± 0.3 versus 1.9 ± 0.2 and 1.4 ± 0.4 versus 1.8 ± 0.1 , respectively. In patients with PD, the initial H/M ratio and delayed H/M ratio were significantly lower compared to patients with SCA2 ($p < 0.05$). Washout rate in patients with PD versus patients with SCA2 were $63.3 \pm 24.5\%$ versus $33.9 \pm 7.4\%$, respectively. In patients with PD, washout rate was significantly higher than in patients with SCA2 ($p < 0.01$). **Conclusions:** Our preliminary findings show that myocardial I-123 MIBG uptake is reduced more markedly in PD than in SCA2 patients, suggesting a more severe and/or a different sympathetic autonomic dysfunction in patients with PD as compared to those with SCA2.

P0900

Comparison of the diagnostic performance of three methods of semiquantitative analysis for 123I-FP-CIT brain SPECT data in identifying Parkinson's disease

B. Palumbo¹, S. Nuvoli², M. L. Fravolini³, D. Pietroniro¹, A. Rossi⁴, A. Spanu², G. Madeddu², ¹Nuclear Medicine, University of Perugia, Perugia, ITALY, ²Nuclear Medicine, University of Sassari, Sassari, ITALY, ³Dept. of Electronic Engineering, University of Perugia, Perugia, ITALY, ⁴Dept. of Neurosciences, University of Perugia, Perugia, ITALY.

Aim: To investigate the different performance of 3 methods of semiquantitative analysis of ¹²³I-FP-CIT SPECT data, we compared ROI analysis and two different VOI methods, the Basal Ganglia V2 software (BasGan) and the Neurotrans3D (Segami Corp.) using a Classification Tree (CT); CT provides simple classification rules based on cut-off values derived from data set of the 3 semiquantitative methods to correctly diagnose Parkinson's disease (PD). **Materials and Methods:** ¹²³I-FP-CIT brain SPECT with semiquantitative analysis with the 3 mentioned methods was performed (according to EANM guidelines) in 30 patients with mild symptoms (bradykinesia-rigidity) to confirm or exclude PD. A clinical follow up of at least six months confirmed final diagnosis. Each patient was described by 4 descriptors (caudate-nucleus left/right - CL, CR- putamen left/right - PL, PR -) while '1' defined PD and '2' normal subjects. For each semiquantitative method, a CT tree was trained to predict the diagnostic categories in function of the 4 descriptors. The original CT was then pruned to have a classification based on a reduced number of rules. CT analysis was performed using the tools of the Matlab software (www.mathworks.com). **Results:** At follow up PD was confirmed in 17 patients, in 13 final diagnosis was depression and arthritis (they were considered as normal in our analysis). Considering BasGan software, the pruned CT correctly classified 29 out of 30 patients, while 1 normal subject was classified as PD. The classification rules were: if PL<2.57 then PD, if PL>2.57 and PR<2.69 then PD, otherwise Normal. Considering Neurotrans3D software, the pruned CT correctly classified 29 out of 30 patients, while 1 PD subject was classified as normal. The classification rules were: if PL<3.3 then PD, if PL>3.3 and PR<3.3 then PD, otherwise Normal. Considering ROI method, the pruned CT correctly classified 28 out of 30 patients, while 2 patients (1 PD and 1 normal) fall exactly on the borderline threshold, thus resulting unclassified. The classification rules were: if PL<3.33 then PD, if PL>3.33 and PR<3.57 then PD, otherwise Normal. **Conclusion:** These preliminary results showed that the CTs for the 3 methods were characterized by the same decision rules based only on PL and PR variables, with different values of classification thresholds. BasGan and Neurotrans3D softwares provided substantially the same performances, misunderstanding 1 patient, while the ROI analysis misunderstood 2 patients. Finally the CT method provided operative cut-off values capable to differentiate PD and non-PD patients for the 3 methods.

P0901

Apathy and poor emotional facial recognition correlation in Parkinson's Disease are supported by the posterior cingulate.

G. Robert¹, T. Dondaine², S. Drapier³, M. Vérin³, D. Drapier¹, **F. Le Jeune**⁴, ¹Psychiatry, Rennes, FRANCE, ²Host Team 4712 "Behavior and basal ganglia", Rennes, FRANCE, ³Neurology, Rennes, FRANCE, ⁴Nuclear Medicine, Rennes, FRANCE.

Apathy is frequently observed in a Parkinson's Disease (PD) and is associated with greater disease burden and poorer outcomes. Although it is accepted as a lack of motivation which expresses through behavioral, cognitive and emotional aspects that leads to reduced spontaneous and sustained goal and affective oriented activities, clear data concerning the emotional deficit in apathy in PD are lacking. To fill in this gap, we conducted behavioral and metabolic study within 36 non-depressed and non demented PD patients using 18-Fluoro Deoxy Glucose (18-FDG) Positron Emission Tomography (PET) scan at rest. PET data were treated as single covariates with three nuisance variables with Statistical Parametric Mapping 02 running on MathLab. Apathy was assessed with Marin's Apathy Evaluation Scale (AES), emotions were assessed with a performances on a facial affect recognition task (ART). PD patients were controlled for depressive symptoms using the Montgomery and Asberg Depression Scale (MADRS), cognitive performances using the Mattis Dementia Rating Scale (MDRS). Antiparkinsonian medications were controlled. PET results show positive correlations between the AES score and metabolic activity within the left posterior cingulate (BA 31) controlling for antiparkinsonian medications, the MDRS score and age. Concerning emotions recognition abilities, we find positive correlations between performances on the ART and metabolic activity within the right precuneus (BA 7) and left inferior occipital gyrus as well as negative correlations with metabolic activity within the bilateral posterior cingulate (BA 31), the right superior frontal gyrus (BA 6, 9 & 10), the left superior frontal gyrus (BA 10 & 11) controlling for the MADRS score, antiparkinsonian and antidepressant medications. Behavioral results find negative correlations between the AES score and performances on the ART across all emotions controlling for depressive symptoms. antiparkinsonian and antidepressant medications. Therefore, we create an inclusive mask between the apathy and the ART neural networks and found that posterior cingulate (BA 31)

supports the overlap between these two networks. These results suggest that apathy is correlated with impaired facial affect recognition across all emotions and that the posterior cingulum supports this overlap.

P48-2 - Tuesday, October 30, 2012, 16:00 - 16:30, Poster Exhibition Area

Oncology Basic Science: Preclinical Imaging

P0902

Molecular Theranostic Potential of Radiolabeled Glucosamine in Diffuse Large B-cell Lymphoma

E. E. Kim¹, D. J. Yang¹, F. Kong¹, J. Bryant¹, D. Rollo², ¹The University of Texas MD Anderson Cancer Center, Houston, TX, UNITED STATES, ²Cell>Point LLC, Centennial, CO, UNITED STATES.

Aim: D-glucosamine has been reported to inhibit proliferation of cancer cells in culture and in vivo. We have then synthesized Tc-99m-ethylenedicysteine-glucosamine (EC-G). We found Tc-99m-EC-G was involved in cell proliferation in lymphoma, lung, breast and head and neck cultures and could assess cancer treatment outcome in vivo by planar scintigraphy. Tc-99m-EC-G is a safe imaging agent in lung cancer patients. This study was aimed to assess a novel response to unlabeled rhenium-EC-G (Re-EC-G) and platinum-EC-G (Pt-EC-G) involving the translational regulation of O-glucosamine transferase (OGT) expression in lymphoma cells, and evaluate feasibility of using EC-G for theranostic approaches in cancers. **Material and Methods:** For theranostic assessment studies, we synthesized cold Re-EC-G and Pt-EC-G. Twelve types of DLBCL cells were incubated with Re-EC-G and Pt-EC-G at various concentrations and TUNEL assays were used to determine cell apoptosis. Immunoblotting was then performed on nuclear extracts with each 50 µg compound. For theranostic assessment studies, lymphoma-bearing SCID mice were imaged with Tc-99m-EC-G and tumor/muscle ratios were determined at 0.5-4 hrs. **Results:** There was a dose response relationship of Re-EC-G and Pt-EC-G inhibition in DLBCL cells. Extensive apoptosis was observed at 24 hrs in lymphoma cell cultures. Re-EC-G and Pt-EC-G caused decreased expression of OGT in DLBCL-LY10 cells. Tc-99m-EC-G could image lymphoma. **Conclusion:** EC-G is a useful molecular theranostic compound. Re-EC-G and Pt-EC-G inhibit OGT expression and are attractive anti-proliferation compounds.

P0903

Characterization of Thyroid and Non-Thyroid Tumors with a Novel PET Tracer [¹⁸F]tetrafluoroborate in a Rat Model

M. Balcerzyk¹, I. Fernandez-Gomez¹, L. Fernandez-Maza¹, A. Parrado-Gallego¹, J. Minguez-Molina², M. Illanes³, M. de Miguel³, J. Cobos-Sabate¹, ¹National Accelerators Center, Sevilla, SPAIN, ²Guadamar Servicios Veterinarios De Referencia, Sanlúcar la Mayor, SPAIN, ³Dpt. Cytology and Histology, Faculty of Medicine, Univ. Seville, Sevilla, SPAIN.

Aim: [¹⁸F]Tetrafluoroborate (TFB) is a new sodium-iodine symporter (NIS) PET tracer which mimics iodine behavior and may be used for thyroid tumor imaging (Jauregui-Osoro, Sunassee et al. 2010) as it is captured specifically by NIS at the site of iodine. Here we report the first preclinical study of this tracer in rat thyroid model complemented with [¹⁸F]Fludeoxyglucose (FDG), [¹⁸F]Fluorothymidine (FLT), CT, MRI and histopathology studies. The aim was to relate incorporation values (SUV) of various tracers tumors, establish optimum acquisition protocol and correlate in vivo studies with histopathology. We studied primary thyroid tumor, and a non-thyroid malignant tumor. **Material and Methods:** Wistar rats starting 8 weeks of age received 0.1 M a TSH stimulation treatment by water solution of potassium perchlorate solution as drinking water. After 12 months of treatment thyroid tumors started to appeared. The non-thyroid tumor was developed spontaneously under the skin in the neck region. MicroPET scans in Philips Mosaic and PET Siemens Biograph mCT systems were carried out with TFB, FDG, FLT and fused with CT. MRI scans were done on Vet-MR, ESAOTE. **Results:** In normal rat thyroid the maximum SUV for TFB is 17. In a rat with thyroid cancer the maximum SUV in one healthy thyroid was 3.35, while in the other tumor containing one the maximum was 3.6. The FDG uptake in healthy thyroid was 1.1 SUV, while in the center of the tumor was 2.4. The non-thyroid malignant tumor appeared in the other rat near the thyroid (MRI-T2 and PET-TBF). The final volume of the ellipsoidal tumor was 17 mL. MRI and PET-TFB showed more active area in the center of the tumor (2.73 SUV), which was very well vascularized. PET-FDG and PET-FLT showed very active region on the surface of the tumor (3.7 and 2.3 SUV respectively), where PET-TFB showed less activity (1.7 SUV). The histopathological study revealed a primary unilateral thyroid tumor in one of the rats, and that the big tumor developed in the neck near the thyroid of another rata presented features of malignancy but was not of thyroid nature. Moreover, it was observed that this non-thyroid tumor was necrotic in the center region. **Conclusion:** PET-TFB study showed maximum uptake 25 min after injection of the tracer. TFB is being captured in the thyroid tumors with high SUV of more than 5, in non-thyroid tumors with moderate SUV of about 2-5.

P0904

Novel Neurotensin-based Radio-tracers for Imaging and Therapy of Ductal Pancreatic Adenocarcinoma

F. Osterkamp¹, C. Haase¹, D. Riexinger, E. Weigt¹, J. Ungewiß¹, A. Burian¹, P. Schulz², C. Grötzinger², M. Stiebler³, A. Pethe³, J. Goldschmidt⁴, H. Amthauer⁵, H. Mäcke⁵, B. Waser, J.-C. Reubi⁶, U. Reineke¹, C. Smerling¹; ¹3B Pharmaceuticals GmbH, Berlin, GERMANY, ²Charité - Universitätsmedizin Berlin, Gastroenterology, Berlin, GERMANY, ³Universitätsklinikum Magdeburg A.Ö.R., Klinik für Radiologie und Nuklearmedizin, Magdeburg, GERMANY, ⁴Leibniz Institute for Neurobiology, Department Auditory Learning and Speech, Magdeburg, GERMANY, ⁵Universitätsklinikum Freiburg, Department of Nuclear Medicine, Freiburg, GERMANY, ⁶University of Bern, Institute of Pathology, Bern, SWITZERLAND.

BACKGROUND: Ductal pancreatic adenocarcinoma is a highly aggressive tumour type with a five year survival rate of less than 5%. The majority of patients presents with non-resectable metastatic disease and dies on average 2.5 months after diagnosis. There is a complete lack of effective therapies for non-resectable pancreatic tumours. We developed radiolabelled neurotensin analogues as tracers for the diagnosis and therapy of pancreatic cancer. Compared to its expression in normal organs, NTR1 is highly overexpressed on neoplastic ductal pancreatic adenocarcinoma cells in 75% of patients. The tumour-to-background ratio is excellent, since the normal pancreas does not express neurotensin receptors. **METHODS:** Peptides were synthesised using standard Fmoc solid phase peptide synthesis. Peptidomimetics were synthesised in solution phase using standard techniques. Peptides and peptidomimetics were characterised in vitro in Ca²⁺ mobilisation and radioligand binding assays and by autoradiography on human tissues. Stability against plasma proteases and plasma protein binding was tested in human and murine blood plasma. Substances were labelled with ¹¹¹In and in vivo SPECT imaging studies were performed in nude mice with HT29 and CAPAN-1 xenograft tumours. **RESULTS:** Based on the C-terminal part of natural neurotensin (NT8-13), we synthesised peptidic agonists and antagonists as well as antagonistic small molecule peptidomimetics. Peptidic agonists and peptidomimetic antagonists bound in vitro with high affinity to the receptor. The stability of selected compounds against human and murine plasma proteases was generally very good with some compounds having serum half lives of more than 24 h in human plasma. DOTA-coupled and ¹¹¹In-labelled high-affinity peptidomimetics showed good tumour uptake in NTR1-positive pancreatic adenocarcinoma and colon carcinoma xenograft tumours. **CONCLUSION:** The neurotensin receptor 1 is a well-suited target for diagnostic imaging and targeted radionuclide therapy of ductal pancreatic adenocarcinoma. Our novel neurotensin-derived radio-tracers have proved their adequacy for SPECT imaging of pancreatic and colon carcinoma tumours in xenograft mouse models, and the observed tumour accumulation makes the tracers good candidates for preclinical development. Using therapeutic radionuclides such as ¹⁷⁷Lu or ⁹⁰Y as well as diagnostic radionuclides such as ¹¹¹In for SPECT, these substances would be suitable for use as diagnostic and therapeutic tandem tracers. The tandem tracer concept for diagnostic imaging and targeted radionuclide therapy is a promising approach to provide personalised patient treatment with a great potential for improved efficacy while minimising side effects in indications with great unmet medical need.

P0905

Measurement of the Effect of Combined Treatment of Multidrug Resistant Gynaecological Tumors in Mouse Tumor Xenograft Using MiniPET-II

G. Trencsényi, P. Mikecz, L. Balkay, I. Lajtos, M. Emri, T. Miklovicz, E. Németh, K. Goda, I. Juhász, Z. Krasznai, T. Márián, Z. T. Krasznai; University of Debrecen, Medical and Health Science Centre, Debrecen, HUNGARY.

Objectives: P-glycoprotein (Pgp) is one of the active efflux pumps that are able to extract a large variety of chemotherapeutic drugs from the cells, causing multidrug resistance. It has been shown earlier that the combined application of a class of modulators used at low concentrations and UIC2 antibody is a novel, specific, and effective way of blocking P-glycoprotein (Pgp) function (JPET 320:81-88, 2007). In vivo study of this combined treatment was developed using multidrug resistant and sensitive human tumor xenograft models. The effect of this combined treatment by Pgp modulator and UIC2 antibody was monitored by the MiniPET-II camera and tumor diagnostic PET tracers. **Methods:** Pgp-positive and Pgp-negative ovarian and cervix carcinoma tumors were induced in 24 female SCID mice. Four days after the injection, mice were treated with doxorubicin (5 mg/kg, i.v.) combined with UIC2 monoclonal antibody (5 mg/kg, i.v.) and cyclosporine A (10 mg/kg, i.p.). The development of tumors and the efficiency of treatment was monitored using [¹⁸F]FDG, [¹¹C]methionine or [¹⁸F]FLT tracers. **Results:** The combined treatment resulted in significant regression of the tumor development, successfully demonstrated by the three applied PET tracers. At day 10, in contrast to the combined treated tumors, where the tumor volumes were 1±0.2 mm³ (Pgp⁻) and

0.5±0.3 mm³ (Pgp⁺), the volume of the untreated Pgp⁻ and Pgp⁺ tumors were 14.7±3 mm³ and 7.8±3.3 mm³ respectively. Glucose metabolism, protein synthesis and the proliferative activity were all significantly decreased (p<0.05) by the treatment. The untreated tumors showed 3-5 times higher relative tracer uptake than the treated ones. Immunohistochemical experiments showed high Pgp expression in the gynaecological tumors examined. **Conclusion:** Combined treatment with UIC2 antibody and low concentrations of Pgp modulators effectively blocked the function of the Pgp pump in human cervix and ovarian carcinoma tumors, and this effect could be followed *in vivo* by using [¹⁸F]FLT, [¹¹C]methionine and [¹⁸F]FDG tumor-diagnostic tracers and the MiniPET-II camera. This work was partially supported by the Szodoray grant (ZTK, KG).

P49-2 - Tuesday, October 30, 2012, 16:00 - 16:30, Poster Exhibition Area

Oncology Basic Science: Tumour Biology, Animal Models, New & Innovative

P0906

Targeting metabolic pathways in cancer cells using genistein derivatives

I. Tworowska¹, S. Zamanian¹, S. Thamake², E. S. Delpassand¹; ¹RadioMedix, Houston, TX, UNITED STATES, ²RITA Foundation, Houston, TX, UNITED STATES.

Cancer cells exhibit increased glucose metabolism amplified by overexpression glucose transporters, GLUT-1. Here we report our results on development of genistein-based agents for imaging of GLUT-1 transporters. Genistein have been shown high affinity toward multiple molecular targets, e.g. glucose transporters, tyrosine kinases, estrogen receptors and potential chemo-preventive and anticancer properties. Clinical application of genistein derivatives has been limited by their undesired pharmacokinetic properties, such as low blood concentration (after per os administration), rapid metabolism and low accumulations in target tissue. In vivo properties of genistein can be modified by its coupling to macrocyclic chelating agents labeled with gallium-68 (Ga68). We have tested bio-activity of 68Ga-labeled genistein conjugates in several cancer cell lines with high expression of GLUT1 transporters, such as A549, MCF-7 and SKBr3. Our studies have confirmed higher than > 5 %ID/mg uptake of genistein derivatives by GLUT1 transporters with increasing accumulation of agents during 2h. Specificity of binding of novel conjugates has been determined in competitions studies using cold GLUT-1 targeting agents (glucose, cytochalasin B, genistein and phloretin). Our preliminary results have confirmed that genistein-derivatives can be potentially used as metabolic imaging agents.

P0907

Assessment of Anxiety and Depression in Patients Undergoing Oncologic F-18 FDG PET/CT Imaging

U. Elboga¹, G. Elboga², H. Karaoglan¹, Y. Celen¹, M. Yilmaz¹, S. Goldsmith¹, C. Aktolun¹; ¹Gaziantep University, School of Medicine, Nuclear Medicine Department, Gaziantep, TURKEY, ²Gaziantep University, School of Medicine, Department of Psychiatry, Gaziantep, TURKEY, ³Weill Cornell Medical College, New York-Presbyterian Hospital, Nuclear Medicine and Molecular Imaging, New York, NY, UNITED STATES, ⁴Tirocenter Nükleer Tıp Merkezi, Istanbul, TURKEY.

Objective: Both the concern about malignant or possibly malignant disease to be investigated by F-18 fluorodeoxyglucose positron emission tomography-computed tomography (F-18 FDG PET-CT) and the procedure of PET-CT imaging itself may cause anxiety and other psychological reactions. The aim of this study was to study objectively the level of anxiety and depression in patients undergoing positron emission tomography-computed tomography. **Methods:** One hundred and forty four oncologic out-patients (76 males, 68 females) were included in this study. All patients were referred to Nuclear Medicine Department for F-18 FDG PET-CT imaging for the assessment of their malignant or possibly malignant diseases. The Hospital Anxiety Depression Scale and the State and Trait Anxiety Inventory I and II were used to evaluate the anxiety and depression levels in these patients. The Hospital Anxiety Depression Scale scores were evaluated between 0 and 21 points; patients with 8-10 points were classified as having 'tendency to anxiety', 10 or higher points as 'anxiety'. Similarly, depression scores were evaluated between 0 and 21 points; patients with 5-7 points were classified as having 'tendency to depression', 7 or higher points as 'depression'. Descriptive analyses and independent sample t-test were used for statistical assessment. **Results:** The mean anxiety and depression scores of The Hospital Anxiety Depression Scale prior to F-18 FDG PET-CT were 9.2 (±3.8) and 6.6 (± 3.4), respectively. The mean state and trait anxiety scores of the State and Trait Anxiety Inventory I and II prior to F-18 FDG PET-CT were 40.4 (±8.5) and 46.62 ± 7.8, respectively. The Hospital Anxiety Depression Scale and the State and Trait Anxiety Inventory I and II anxiety scores were found to be significantly higher in female patients, smokers and in patients

with higher stage disease. Other factors including previous surgery, chemotherapy and/or radiotherapy and perceived body image were not related to depression and anxiety scores. **Conclusion:** Our results suggest that F-18 FDG PET-CT imaging may at least contribute to patient's baseline anxiety which is already generated by being an oncology patient, and thus nuclear medicine physicians should handle the patients with extra care to minimize this affect.

P0908

Impact of blood glucose, diabetes, insulin, and obesity on standardized uptake values in tumors and healthy organs on 18F-FDG PET/CT

K. A. Büsing, S. O. Schoenberg, J. Brade, K. Wasser; University Medicine Mannheim, Mannheim, GERMANY.

Aim: Positron emission tomography (PET) with 18F-fluorodeoxyglucose (18F-FDG) is widely used in the assessment of many cancers. Acute hyperglycemia is known to reduce tumoral 18F-FDG uptake and may therefore lower the sensitivity of the technique. Still, the effect of chronic hyperglycemia on tumoral FDG uptake has been the subject of controversial discussion and little is known about the impact of altered glucose metabolism on 18F-FDG biodistribution in healthy organs although it may further affect tumor detection. The present study assesses the impact of blood glucose levels (BGL), diabetes, insulin treatment, and obesity on 18F-FDG uptake in tumors and biodistribution in normal organ tissues. **Materials and Methods:** 18F-FDG PET/CT was retrospectively analyzed in 90 patients with BGL ranging from 50 to 372 mg/dl. Here, 48 patients were hyperglycemic (BGL >110 mg/dl) at the time of 18F-FDG administration. Of those, 29 patients were diabetic and 21 patients had received insulin prior to PET/CT; 28 patients were obese with a body mass index >25. The maximum standardized uptake value (SUVmax) of normal organs, the main tumor site, and the mediastinal blood pool were measured. Differences in SUVmax in patients with and without elevated BGLs, diabetes, insulin treatment, and obesity were compared and analyzed for statistical significance. **Results:** Overall, increased BGLs were associated with decreased cerebral FDG uptake and increased uptake in skeletal muscle. Diabetes and insulin diminished this effect, whereas obesity slightly enhanced the impact of BGLs on cerebral and muscular tracer uptake. Diabetes, insulin, and obesity also influenced the average SUVmax in healthy tissues. Diabetes and insulin increased the average SUVmax in muscle cells and fat, whereas the mean cerebral SUVmax was reduced. Obesity decreased tracer uptake in several healthy organs by up to 30%. Tumoral uptake was not significantly influenced by BGL, diabetes, insulin, or obesity. **Conclusion:** Changes in BGLs, diabetes, insulin, and obesity affect the biodistribution of 18F-FDG mainly in muscular tissue and the brain by up to 30%. Although tumoral uptake is not significantly impaired, these findings may influence the tumor detection rate and are therefore essential for diagnosis and follow-up of malignant diseases.

P0909

Accuracy of Sentinel Lymph Node Biopsy in Breast Cancer After Neoadjuvant Treatment: Preliminary Results of Follow-up

D. Familiari, L. Gilardi, L. L. Travaini, M. Colandrea, S. Vassallo, A. Manika, M. Intra, S. Croce, C. De Cicco, G. Paganelli; European Institute of Oncology, Milano, ITALY.

Aim: Sentinel lymph node biopsy (SLNB) in breast cancer is widely used in order to stage axillary lymph nodes. The procedure is still controversial in patients (pts) with advanced disease who undergo neoadjuvant therapy. The aim of this study was to evaluate the accuracy of SLNB in this group of pts, looking for the presence of axillary lymph-node recurrences after surgery. **Materials and Methods:** This study retrospectively analyzed 77 patients with primary breast cancer clinically classified as cT2-T4b cN0-N2 who were submitted to surgery after a neoadjuvant treatment between 2007 and 2011. All the pts received SLNB after quadrantectomy or mastectomy. Sentinel nodes (SN) were identified using our standard method for lymphoscintigraphy. In case of positive SN an axillary lymph nodes dissection (ALND) followed. Patients received adequate treatment after surgery, according to biologic characteristics of the tumor and were followed-up for axillary events every 6 months by means of clinical exam and standard imaging. **Results:** The overall detection rate of SN was 100%. One SN was identified in 56% of pts, 2 in 21%. More than 2 lymph nodes were found in the remaining pts. Thirty-one pts had a positive SN (including 5 cases with micro-metastasis). In this group, only one patient with diagnosis of micro-metastases to SN did not receive ALND. In the others 46 cases, SN was found negative and in 44 pts ALND was not performed. However, two out of this 46 patients had in any case an ALND and were staged as pN1a (false negative) and pN0 (true negative), respectively. The median follow-up was 36 months (range: 1-61 months). Overall, among the 45 pts who did not received ALND, only one patient showed axillary disease three months after surgery (false negative). This patient underwent subsequently ALND with final diagnosis of pN3a disease. Three out of 77 patients died: two for distant metastases from breast cancer, one for a second neoplasia (glioblastoma) with a consequent short follow-

up (1 month). **Conclusion:** Our data indicate that lymphoscintigraphy was always successful in localize almost one SN and that SN was falsely negative only in two pts of this series. In our experience SNB after neoadjuvant treatment is a safe procedure and a reliable predictor of axillary lymph nodes status.

P0910

Assessment of zeolites for lesion simulation in PET-CT

F. Zito¹, E. De Bernardi², C. Soffientini³, C. Canzi¹, R. Casati¹, P. Gerundini¹, G. Baselli³; ¹FONDAZIONE IRCCS CA' GRANDA Ospedale Maggiore Policlinico, Milan, ITALY, ²Università degli Studi di Milano Bicocca, Monza, ITALY, ³Politecnico di Milano, Milan, ITALY.

Aim: Zeolites are porous aluminosilicates with adsorptive properties and regular internal structure that can be used to simulate no-border irregular shape lesions in PET/CT phantoms provided with a CT-derived ground truth, useful for the assessment of quantification and segmentation algorithms. The aims of this work are: 1) to propose a protocol for zeolite characterization and activation; 2) to present results obtained on samples of clinoptilolite and chabazite; 3) to present an anthropomorphic phantom with homogeneous lesions obtained with clinoptilolite; 4) to discuss the possibility to simulate heterogeneous lesions. **Materials and Methods:** Each family of zeolites is characterized by specific density and internal pore size. Water contained into pores can be simply removed by heating. Zeolite characterization involved: 1) assessment of zeolite uniformity and HU ranges by CT analysis; 2) weight measurement; 3) volume measurement, by means of Archimedes' principle; 4) assessment of zeolite absorbing properties (i.e. time necessary for saturation, percentage of adsorbing volume, dependence of adsorbing volume on zeolite dry weight). Zeolite preparation for phantom construction required: 1) use of the derived adsorbing law to define concentration of 18F-FDG solutions; 2) zeolite soaking for a time allowing saturation; 3) zeolite wrapping in Parafilm to avoid activity exchange with surrounding solutions; 4) zeolite positioning inside the phantom. Clinoptilolite samples fully characterized (volume ranging from 0.6 ml to 5.4 ml) and properly activated were inserted into an Alderson Thorax Abdomen phantom. The ground truth for zeolite borders on PET images was obtained by segmenting coregistered CT images, using the measured volume to set the segmentation threshold. **Results:** Two families of zeolites were characterized: 1) clinoptilolite (mean density = 1.6 g/ml; mean adsorbing volume = 28%; coefficient of the linear dependence of the adsorbing volume from zeolite dry weight = 0.18 ml/g, adsorbing time = 90min); 2) chabazite (mean density = 1.0 g/ml; mean adsorbing volume = 43%; coefficient of the linear dependence of the adsorbing volume from zeolite dry weight = 0.43 ml/g, adsorbing time = 90 min). **Conclusions:** The proposed methodology allowed obtaining an experimental phantom data set that can be used as a feasible tool to test and validate quantification and segmentation algorithms for PET/CT in oncology. Thanks to different density values and adsorbing properties, samples of chabazite and clinoptilolite can be coupled to simulate heterogeneous lesions with CT-derivable ground truth. The possibility to combine and activate zeolites of different families is under investigation.

P50-2 - Tuesday, October 30, 2012, 16:00 - 16:30, Poster Exhibition Area

Oncology Clinical Science: Brain

P0911

The utility of 18F-DOPA/18F-choline PET/CT in staging and restaging of brain tumours: initial experience

K. Siczek, M. Carletto, L. Roncoroni, G. Regolo, C. Songini, A. Assi, L. Maffioli; Ospedale Civile di Legnano, Legnano, ITALY.

Aim: Primary brain tumours, in particular gliomas, are rare tumours and they are difficult to diagnose and to treat. Current imaging modalities as FDG PET/CT, MRI and MR spectroscopy (MRS) have some limitations, particularly with regard to differentiating tumor from radiation induced necrosis (RIN) and from normal cerebral metabolic uptake. ¹⁸F-DOPA/¹⁸F-choline PET/CT (FDOPA/FCH) seem to be useful diagnostic tools. **Materials and methods:** 11 patients (5 females and 6 males; mean age 53 yrs, range 23-76) were studied with FDOPA/FCH, performed between March 2011 and March 2012: 9 pts with gliomas (3 in staging and 6 in restaging) and 2 with brain metastasis. In 6 pts in restaging MRI failed in differentiating tumour relapse from RIN: so they were studied with PET. Brain FDOPA/FCH was performed 10 minutes after iv injection of 3,5 MBq/Kg of ¹⁸F-FCH or 4 MBq/Kg of ¹⁸F-DOPA. FDOPA/FCH was compared with ^{99m}Tc-sestaMIBI SPECT/CT (SPECT/CT), MRI, CT and subsequent pathologic analysis. **Results:** FDOPA/FCH was considered pathological in 11/11 (100%) patients. In one case FDOPA evidenced three lesions (right frontal lobe lesion, left parasagittal frontal lesion and corpus callosum lesion), MRI evidenced only two (right frontal lobe lesion and corpus callosum lesion) and SPECT/CT only one (right frontal lobe lesion). This case was re-studied with radiologist. FDOPA/FCH and MRI in other cases had the same sensitivity. FDOPA/FCH had an overall sensitivity of 100% while MRI sensitivity was of 90.9%.

The diagnostic accuracy of FDOPA/FCH was of 100% vs. MRI of 90.9% [95% confidence interval (CI) 74–99%]. **Conclusions:** This study evidenced the utility of FDOPA/FCH in primary brain tumours, especially in patients with recurrent gliomas, where MRI cannot differentiate tumour from radiation induced necrosis. In our initial experience, PET scan seems to have higher sensitivity than MRI.

P0912

18F-FLT PET fused with MRI in primary and metastatic brain tumors. Prospective study- Preliminary results

A. Nikaki, D. Kechagias, F. Vlachou, I. Andreou, L. Gogou, V. Filippi, K. Gogos, R. Efthimiadou, V. Prassopoulos, P. Georgoulas; DTCA HYGEIA HOSPITAL, Aghios Stefanos, GREECE.

Purpose: 18F-FLT is a new tracer for PET imaging, not validated enough in brain tumors. MRI is the imaging method of choice in evaluating possible recurrence of brain tumors. However surgical removal of the tumor, as well as radiotherapy and chemotherapy can make the interpretation of the images quite difficult. The purpose of this study is to estimate the contribution of 18F-FLT-PET fused with MRI in the evaluation of possible recurrence in patients treated for primary or secondary brain malignancy. **Method- Material:** 9 patients, 5 female and 4 male, who underwent 10 PET/CT examinations are prospectively included in the study. 5 had metastatic brain disease (3 lung cancer, 2 breast cancer), 2 glioblastoma and 2 oligodendroglioma. All patients had previously undergone the appropriate treatment at least 6 months before PET examination and all were referred for 18F-FLT-PET examination for evaluation of possible recurrence. PET was performed at a Siemens Biograph LSO PET/CT tomographer. 60min dynamic acquisition and then standard one bed brain image was received. Tumor/Background/time curves were received from the dynamic acquisition. SUVmax and Tumor/Background ratio was measured at the last derived image. PET images were fused with MRI images. Results were analyzed in per examination (10 cases) and in per lesion (16 lesions) basis. **Results:** PET was positive in 8/10 cases and negative in 2/10. MRI was positive in 6/10 cases, equivocal in 2/10 and negative in 2/10. Uptake of 18F-FLT was apparent in 12/16 lesions. Average SUVmax was 2. Curves were ascending for 10 lesions and plateau for 2. Average T/B ratio was 3.5. Both PET and MRI were considered positive for 6 lesions. MRI was equivocal for 7 lesions, while PET was positive for 3/7, negative for 2 (osseous alteration, occipital lesion), while 2 lesions presented SUVmax 0.6 and 0.9 and T/B 1.2 and 1.8 accordingly but with plateau curves. One lesion was apparent in PET without MRI evidence, having SUVmax 2.4, ascending curve and T/B ratio 4. Both PET and MRI were negative in 2 lesions. **Conclusion:** Although our sample is small and inhomogeneous, there is evidence that 18F-FLT PET/fused MRI can provide additional information in characterizing tumor lesions regardless if they concern primary or secondary disease. T/B ratio showed higher values than SUVmax values. 18F-FLT-PET/fused MRI needs further to be validated in brain tumor imaging.

P51-2 - Tuesday, October 30, 2012, 16:00 - 16:30, Poster Exhibition Area

Oncology Clinical Science: Head & Neck

P0913

Comparison of SUVmax thresholds in benign and malignant lymph nodes in patients undergoing staging F-18 FDG PETCT for squamous cell carcinoma of the head and neck using iterative and high definition TruEx® reconstruction methods with histological correlation

E. Kauppila¹, A. Eccles², N. Patel², R. Sandhu², A. Al-Nahhas², Z. Win², ¹North Karelia Central Hospital, Joensuu, FINLAND, ²Imperial College Healthcare NHS Trust, London, UNITED KINGDOM.

Objective: Nodal spread of squamous cell carcinoma of the head and neck (SCCHN) is related to poor prognosis. We aimed to quantitatively define and compare the SUVmax thresholds of histologically proven malignant and benign (normal or reactive) lymph nodes (LN) in the neck using iterative and high definition TruEx® reconstruction methods in patients who had staging F-18 FDG PETCT for squamous cell carcinoma of the head and neck. **Methods:** We retrospectively investigated ten patients (mean age 57 ± 9, one female) who had staging F-18 FDG PETCT for squamous cell carcinoma of the head and neck and who subsequently underwent surgery with lymph node neck dissection. In total, we studied thirty-eight histologically examined LNs and calculated the SUVmax values. If a certain neck level was histopathologically negative, the highest SUVmax value was taken as true negative or false positive depending on the SUVmax threshold. In case of several malignant LNs, the number of malignant nodes from the highest SUVmax value was similarly taken as positive, and the next highest SUVmax value as negative. The shortest diameters (DM) of each LN on the CT were also measured. **Results:** Eighteen malign and twenty normal or reactive LNs were analysed. There were four nodes with DM > 10 mm (mean ± SD, 7.6 ± 5.7 mm). Using TruEx® reconstruction there were sixteen nodes with SUVmax values > 2.5, (mean ± SD, 3.7 ± 4.2). There

was a strong linear relationship between SUVmax values obtained with standard iterative and TruEx® methods ($R = 0.99$, $p < 0.01$). In comparison with standard iterative method TruEx® reconstruction gave systematically higher SUVmax values ($y = 1.4 \times x$). Sensitivity, specificity, positive, negative predictive values (PPV, NPV) and accuracy (AC) were 22/100/100/59/71 for CT (10 mm cut-off). With thresholds of 5.0, 4.0, 3.0 and 2.5 with TruEx® reconstruction sensitivity, specificity, PPV, NPV and ACC were 21/95/80/56/59, 27/95/83/59/63 and 64/85/75/77/76, and 61/75/69/68/68, respectively. **Conclusion:** With a sample of predominantly subcentimeter nodal disease of SCCHN our preliminary results showed that TruEx® reconstruction with SUVmax cut-off value of 3.0 (corresponding SUVmax of 2.1 with iterative method) was slightly superior in accuracy compared with other used thresholds and the standard CT assessment.

P0914

Metabolic Imaging Patterns of Complete Local Response to Chemoradiation in Patients with Nasopharyngeal Carcinoma: A Review

K. Keu, E. Mitra, A. Iagaru; Stanford University, Stanford, CA, UNITED STATES.

AIM Local response to chemo- and radiotherapy on FDG PET/CT imaging is difficult to assess in patients with nasopharyngeal carcinoma (NPC) because of underlying inflammation induced by radiation which is a major source of false-positive. Moreover, the physiological uptake in the Waldeyer ring often misleads the interpretation of the scan. This study evaluates the imaging findings of a post-therapy FDG PET/CT in patients who did not recur locally afterward. **METHOD AND MATERIALS** This is a retrospective descriptive review of patients diagnosed with nasopharyngeal carcinoma who were treated with chemo- and radiotherapy at our institution. All patients underwent FDG PET/CT initially for staging and within 3 months of completion of therapy for the evaluation of response. Only patients without any local recurrence on follow-up (minimum 12 months) and further imaging were analyzed. The variables evaluated were post-therapy SUV_{max}, the percentage of response [(initial SUV_{max} - post-therapy SUV_{max})/initial SUV_{max}], and the pattern of uptake on the post-therapy scan (diffuse vs asymmetrical). Descriptive statistics and frequencies were performed on these latter parameters. **RESULTS** This analysis included 28 patients treated from July 2003 to October 2009, who were followed for a median duration of 46 months (range: 13-78 months) without any local recurrence detected. In this cohort, the average age was 41.2 ± 12.7 year-old. 71% were men (n=20) and 82% were grade 3 on WHO classification (n=23). The median post-therapy SUV_{max} was 3.4 (IQR = 1.1) for the treated tumor and 3.1 (IQR = 1.0) for the contralateral side of nasopharynx. In three cases, the post-therapy SUV_{max} of treated tumor was above 5.0 and the uptake was focal. On average, the percentage decreased of SUV_{max} on post-therapy scan was 71 ± 13% (coefficient of variation of 18%). On post-therapy scan, the uptake in the nasopharyngeal area was diffuse in 57% (n=16) of cases and asymmetrical in 43% (n=12). **CONCLUSION** Post-therapy scans in patients with complete local response to chemoradiation show either diffuse or asymmetrical uptake without any predominant pattern observed. In general, the SUV_{max} tends to normalize except in three cases in which focal and relatively high residual uptake might mislead the interpretation of FDG PET/CT. Across all cases, the percentage decreased of SUV_{max} is the imaging parameter that might show the least variation. However, this prognostic value necessitates an initial and a post-treatment scans that are both not routinely done on every patient.

P0915

Unknown Primary Tumours in Patients with Verified Cervical Lymph Node Metastases: The Clinical Impact of FDG PET-CT

M. Fulop¹, M. Kasler², E. Remenar², Z. Lengyel³, K. Borbely²; ¹Ferenc Flór Regional Hospital ORL and Head & Neck Surgery Dept, Kistarcsa, HUNGARY, ²National Institute of Oncology, Budapest, HUNGARY, ³Pozitron LTD, Budapest, HUNGARY.

Aim 18F-FDG PET-CT is widely recommended in unknown primary tumours, however its definitive role and cost effectiveness are yet to be established. Our purpose was to test the additional value of FDG-PET-CT over conventional imaging techniques in unknown primary tumours with verified cervical metastases, possible distant metastases or synchronous tumours in order to plan the optimal treatment strategy. **Method** Four hundred and forty patients underwent 18F-FDG PET-CT examination between 1st January 2006 and 31st December 2010, including 77 patients with whom the examinations specified in the treatment protocol (physical examination, panendoscopy, CT/MRI, biopsy) failed to diagnose the primary tumour. **Results** PET-CT detected the primary tumour in 44% of patient's after all unsuccessful diagnostic tests. In 41% of patients PET-CT presented no additional information compared to all other diagnostic tests. In 24/77 (31%) patients the primary tumour was confirmed by histology. In 10/77 (13%) patients the results of CT/MRI were strengthened by PET-CT. In 10/77 (13%) patients the PET-CT findings were false positive. In 3/77 (4%) patients with false negative results the retrospective evaluation of PET-CT data proved the diagnostic failure. In 10/77

(13%) patients asymptomatic distant metastases and in 3/77 (4%) patients synchronous tumours were detected. The 18F-FDG PET-CT results modified the management of patients in 61% of cases by providing additional information over conventional imaging tests. **Conclusions** On the basis of our results 18F-FDG PET-CT is strongly recommended in the detection of unknown primary tumours in patients with verified cervical lymph node metastases. The whole body functional measurement has a high clinical impact on the management of patients due to the detection of possible asymptomatic synchronous tumours and/or distant metastases. These benefits make 18F-FDG PET-CT examination a reliable tool for the refinement of individually tailored treatment strategies leading to a better therapeutic results and a more favourable cost-benefit ratio.

P0916

FDG PET/CT in the Detection of Malignancy in Patients Treated for Squamous Cell Carcinoma of Head and Neck

S. A. Rogan¹, A. Balenovic¹, P. Anic¹, I. Luksic², M. Ivkic³, ¹Medikol Polyclinic, Zagreb, CROATIA, ²Dpt. of Maxillofacial Surgery, University of Zagreb School of Medicine, University Hospital Dubrava, Zagreb, CROATIA, ³Dpt. of Otolaryngology and Head and Neck Surgery, University Hospital Centre Sestre Milosrdnice, Zagreb, Croatia, Zagreb, CROATIA.

Aim: Retrospective comparison of the diagnostic accuracy of fluorodeoxyglucose positron emission tomography/computed tomography (FDG PET/CT) and CT in detecting local, regional and distant recurrence of head and neck squamous cell carcinoma after chemoradiotherapy (CRT). **Patients and methods:** Seventy five patients at a high risk of residual disease and regional or distant metastases after the completion of CRT were included in the study. All patients underwent CT followed by PET/CT after different period of time. Diagnoses were confirmed by histology or by follow-up imaging data. **Results:** Forty two patients (56,0%) out of 75 had malignancy. Mean time for PET/CT imaging from completion of CRT was 17,5 months (range 1-64 months) and for CT was 8,2 month (range 1-60 months). CT recognized malignancy in 30 (71,2%) patients and PET/CT in 38 (90,4%) patients. Additionally, two patients PET/CT revealed as false positive, but in three lymph nodes remains unrecognized to have malignancy as well in one patient with lung metastases. The lesion-based sensitivities for detection of local recurrence/residual disease of PET/CT was significantly higher than CT alone (95,0% vs. 71,4%, $p < 0,01$) and it was significantly higher for detection nodal malignancy and distant metastatic disease (88,8% vs. 42,8%, $p < 0,01$ and 94,4% vs. 83,3%, $p < 0,01$). The corresponding specificities of PET/CT and CT were 94,5 and 85,1% for local malignancy; 97,9 and 85,1% for nodal disease; 98,2 and 82,4% for distant metastases. Both, PET/CT and CT yielded false negative findings of lymph node recurrence, but PET/CT showed significantly better PPV and NPV compared to CT: 96,0% vs. 63,1% and 94,0% vs. 71,4%. Also for locally tumor recurrence PET/CT had better PPV but also NPV compared to CT alone (86,3 vs. 65,2% and 98,1 vs. 88,4% respectively). NPV was similar for both techniques for distant metastatic disease, but PET/CT had better PPV than CT (98,2 vs. 94,0%; 94,4 vs. 60,0%). In the early post-therapy period (up to 6 months) sensitivity and specificity of PET/CT imaging modality was also significantly better than CT alone to recognize the malignancy (92,9% vs. 57,7%; 92,6% vs. 79,3%). **Conclusions:** PET/CT as a whole-body combined imaging technique showed much better accuracy than CT in detecting recurrent tumor, nodal involvement and distant metastases in patients already treated for squamous cell carcinoma. Although, FDG PET/CT is not a specific marker for malignancy, it provides more reliable data for the local, lymph node and distant metastases than CT scanning in first six months post therapy period.

P0917

Synchronous tumors found by FDG-PET in patients with esophageal cancer

Y. Tseng, S. Chen, S. Chan, T. Yen, C. Huang, C. Liao, C. Kang; Chang Gung Memorial Hospital, Taoyuan, TAIWAN.

¹ Department of Nuclear Medicine and Molecular Imaging Center, Chang Gung Memorial Hospital, Chang Gung University College of Medicine, Taoyuan, Taiwan

²Department of Otolaryngology-Head & Neck Surgery, Chang Gung Memorial Hospital, Chang Gung University College of Medicine, Taoyuan, Taiwan **Aim:** To illustrate the ability of FDG-PET in identifying synchronous tumors in esophageal cancer patients **Materials and methods:** Medical records of patients with esophageal cancer who received FDG-PET scan for staging between December 2006 to August 2011 were reviewed. Synchronous tumors were identified by histopathologic proof or concordant conventional work-up results, which included CT, esophagram and panendoscopy. All tumors found within six months of the FDG-PET scan were regarded as synchronous. **Results:** Excluding 17 patients treated and followed at other hospitals, the charts of 420 patients were reviewed. Synchronous tumors were found in 70 patients (16.7%). The sites were esophagus (29), head and neck (28), stomach (4), colon (3), liver (2), kidney (1); three patients had double esophageal cancer and another head and neck. Among these, 5 head and neck, 3 esophageal, 3 colon, and another esophageal with head and neck tumors were revealed by the PET scan only (17.1%). PET missed 7 synchronous

lesions, three of which were gastric GIST, found only after surgical resection. The other three tumors were revealed by the panendoscopy, including 1 gastric cancer, 1 esophageal cancer, 1 hypopharyngeal cancer. They were Tis or T1 lesions. Another hepatocellular carcinoma was found by CT. FDG-PET had false-positive findings in 11 patients. 7 of them were in the esophagus, including 2 in the gastroesophageal junction. 3 were in the head and neck region, including squamous hyperplasia of the tongue, asymmetric laryngeal uptake due to vocal cord palsy, and tonsillar lymphoid hyperplasia. Another soft-tissue metastasis was mistaken as a second primary gastric cancer. **Conclusion:** FDG-PET scan could find synchronous tumors otherwise unknown to the conventional work-up. The existence of false-positive findings merit further confirmation for FDG-PET positive lesions.

P0918

Prognostic value of ¹⁸F-FDG PET/CT for head and neck squamous cell carcinoma

M. Nishio, M.D.¹, Y. Hasegawa, M.D.², T. Tamaki, M.D.³, Y. Shibamoto, M.D.⁴, ¹Nagoya PET Imaging Center, Nagoya, JAPAN, ²Department of Head and Neck Surgery, Aichi Cancer Center Hospital, Nagoya, JAPAN, ³East Nagoya Diagnosis Imaging Center, Nagoya, JAPAN, ⁴Department of Radiology, Nagoya City University Graduate School of Medical Sciences and Medical School, Nagoya, JAPAN.

Objectives: Eight years have passed since we have the approval of the PET / CT camera in our country. The purpose of this study was to investigate the prognostic value of maximum standard uptake value (SUV max) of the primary tumor and lymph nodes, and each staging, the PET / CT in head and neck squamous cell carcinoma before treatment. **Methods:** 230 patients a total of patients with squamous cell carcinoma of head and neck were performed PET / CT in March 2006 from March 2004 (case of 186 men and 44 women, aged 20 to 89) were reviewed retrospectively. Follow-up period were 5 years or more after treatment, or until death. The cases with double or triple cancers was observed to 21 cases in all cases, and applies only to difficult to affect the survival rate. We were evaluate the relationship between long-term follow-up study of patients and SUV max. **Results:** Patients with SUV max of the primary tumor is less than 7.78 5-year overall survival rate was significantly higher compared to patients with SUV max greater than 7.78 ($P < 0.0001$). Kaplan-Meier survival curves are shown in Figure. In SUV mean of the primary tumor, SUV max cervical lymph nodes and mean, there is no significant difference and they did not help to predict the prognosis. Significantly poor prognosis in gender differences and prognosis was worse than a high age. Patients with distant metastases at the time of diagnosis was significantly poor prognosis regardless of primary site ($P < 0.0001$). **Conclusions:** The SUV max of the primary tumor prior to surgery and/or treatment, it is possible to predict the prognosis of head and neck squamous cell carcinoma.

P52-2 - Tuesday, October 30, 2012, 16:00 - 16:30, Poster Exhibition Area

Oncology Clinical Science: Thyroid

P0919

Our experience with ^{99m}Tc (V)-DMSA scintigraphy in visualization of primary medullary thyroid carcinoma

M. P. Rajic, S. Jovic, M. Vlajkovic, S. Ilic, M. Stevic, M. Kojic, I. Misic, A. Karanikolic; Clinical Center of Nis, Nis, SERBIA.

The Aim: At time of diagnosis of medullary thyroid carcinoma (MTC) many of patients already have regional or distant metastases. Scintigraphy with tumor-avid radiopharmaceuticals enables visualization of primary MTC and its metastases. Based on it, therapy approach may be selected. In this study we evaluated our experience using ^{99m}Tc (V)-DMSA whole-body scintigraphy in visualization of primary MTC. **Methods:** ^{99m}Tc (V)-DMSA whole-body scintigraphy was performed in 17 patients (12 females, age range 26-83 yr., mean age 57.7 yr) with clinical (thyroid nodule) and biochemical (elevated serum calcitonin or carcinoembryonic antigen levels; calcitonin: 5.0-2630 pg/ml, carcinoembryonic antigen: 5.0-85.0 ng/ml) findings suggestive of primary MTC. In 16 patients diagnosis was established after thyroidectomy, biopsy or aspiration cytology of thyroid nodule, but in one patient upon the basis of repeated ^{99m}Tc (V)-DMSA scintigram, high calcitonin levels and signs of disease progression. **Results:** Eight of 17 patients had MTC. The sensitivity and specificity of ^{99m}Tc (V)-DMSA scintigraphy for primary tumor visualisation was 87.5% and 77.8%. False-positive findings were obtained in two patients with papillary thyroid carcinoma. False-negative finding was found in one patient with thyroid nodule smaller than 10 mm in diameter. Cervical lymph node metastases were visualized in two of four patients, and distant metastases (in bones) in one patient. **Conclusion:** The findings showed that ^{99m}Tc (V)-DMSA scintigraphy has high sensitivity for primary MTC visualization. Since the method can also show distant metastases, should be routinely used for treatment planning.

P0920

Is 99mTc (V)-dimercaptosuccinic acid scintigraphy still useful imaging method for follow-up of patients with medullary thyroid carcinoma?

M. P. Rajic, I. Radomirovic, M. Vlajkovic, S. Ilic, M. Stevic, M. Kojic, I. Mistic, T. Strahinjac; Clinical Center of Nis, Nis, SERBIA.

The Aim: Despite newer imaging methods, scintigraphy with pentavalent 99mTc-dimercaptosuccinic acid [99mTc (V)-DMSA] is often performed for postoperative localization of tumor foci in patients with medullary thyroid carcinoma (MTC) who have permanently elevated serum calcitonin (Ct) levels. Therefore, we evaluated 99mTc (V)-DMSA scintigrams in patients with medullary thyroid carcinoma who had hypercalcitoninemia after thyroidectomy. **Patients and methods:** Results of 22 follow-up 99mTc (V)-DMSA scintigrams of 11 patients with MTC and persistently elevated postoperative calcitonin levels (6 females, age range 27-65 yr, Ct range 21.0-20610 pg/ml) were compared with results of other scintigraphic or radiological imaging methods. **Results:** There were 10 true-positive, 10 false-negative and 2 true-negative 99mTc (V)-DMSA scintigrams resulting in sensitivity and specificity of 50.0% and 100% for metastatic diseases detection on patient base. 99mTc (V)-DMSA showed 47 (83.9%) out of 56 MTC lesions visible by all other imaging methods together. The best results were obtained in patients with bone and lymph node metastases. **Conclusion:** Findings of this study showed that 99mTc (V)-DMSA scintigraphy has satisfactory overall sensitivity for MTC postoperative metastases detection on lesion base and a high specificity for metastatic diseases detection on patient base. Based on these results, we believe that 99mTc (V)-DMSA scintigraphy is still very useful imaging method for follow-up of MTC patients with hypercalcitoninemia.

P0921

Clinical outcome and the value of diagnostic I-131 whole body scintigraphy and recombinant TSH in low-risk well differentiated thyroid cancer patients who have had I-131 radioablation and undetectable thyroglobulin levels

M. Argon, U. Yazarbaş, K. Kumanlioglu, H. Ozkiliç; Ege University Medical Faculty, Izmir, TURKEY.

Objective The aim of this study was to find out the recurrence rate of disease and to evaluate effectiveness of diagnostic I-131 whole body scintigraphy (WBS) and recombinant human (rh) TSH in low-risk well differentiated thyroid cancer (WDTC) patients who have had I-131 radioablation and undetectable stimulated serum Tg levels. **Material and Methods** Study groups (G) were consisted of 149 patients (G1) using endogen TSH stimulation and 50 patients (G2) using rhTSH. Mean follow-up period was 12 years for G1. and 3.5 years for G2. Postablative sixth, 18th month, 5th, 10th and 15th year endogen TSH stimulated diagnostic WBS and serum Tg levels in G1 and 6th endogen TSH stimulated and 18th month rhTSH stimulated diagnostic WBS and serum Tg levels in G2 patients were evaluated. **Results** The TSH stimulated Tg values were <1ng/ml after ablation. Only one patient was accepted recurrence, in this patients lymph node metastases was detected by thyroid ultrasonography and fine needle aspiration despite Tg levels and WBS were negative. The recurrence rate of tumor was 0.67%. Serum TSH levels were ≥ 30 μ U/ml in all patients. rhTSH was used successfully without causing hypothyroid state at I-131 WBS and serum Tg measurement. 13 of 149 patients (8.7%) had low activity uptake at thyroid bed at 6. month WBS. Ablation was accepted insufficient and 11 of these 13 patients were given second dose. At diagnostic 6. month WBS after second ablation no activity was detected and they were accepted successful ablation. The success rate of ablation was 91.3% in first dose and 100% in second dose. There was no significant difference between 6th months endogen TSH and 18th months rhTSH stimulated Tg levels and diagnostic WBS in G2 patients and the 6th, 18th months, 5th, 10th and 15th year endogen TSH stimulated diagnostic WBS and Tg levels in G1 patients. **Conclusion** In low-risk WDTC patients who have undergone total thyroidectomy and I-131 radioablation, the recurrence rate of tumor was extremely low. rhTSH was used successfully without hypothyroid state at I-131 WBS and serum Tg measurement. If 6th month WBS was negative and serum Tg level was undetectable, the 18th month, 5th, 10th and 15th years WBSs were also negative in almost all patients and yielded no additional information that could influence the following therapeutic strategy and therefore may be avoided. In the follow-up this group of patients, rhTSH stimulated Tg measurement may be considered as an alternative approach.

P0922

Prognostic value of vascular invasion in papillary thyroid carcinoma

M. Muckle¹, K. Biermann², A. Joe³, A. Sabet¹, S. Ezziddin¹, H. Biersack¹, H. Ahmadzadehfard¹; ¹University Hospital Bonn, Bonn, GERMANY, ²Clinic of Nuclear Medicine & Radiology, Trier, GERMANY, ³Clinic of Nuclear Medicine & Radiology, Bad Honnef, GERMANY.

Introduction: Vascular invasion is a well known prognostic factor in a variety of carcinomas. It has been considered as important for outcome in patients with follicular thyroid carcinoma but the prognostic role of vascular invasion is poorly investigated in papillary thyroid carcinoma (PTC). Thus, the aim of the present study was to investigate the prognostic value of histological vascular invasion for the course of disease of patients with PTC. **Methods:** The institutional database was retrospectively searched for patients with PTC. 388 patients (290 females), who were in aftercare at least between 1990 and 2002 at our institution, were included. Data of epidemiological, clinical and histological characteristics were obtained. All of the patients had undergone total or near-total thyroidectomy and subsequent ablative radioiodine therapy. The mean follow-up was 6.1 \pm 5.9 years. Sex, age, T-stage, N-stage, M-stage and angioinvasion were tested for significant relations with development of persistent or recurrent disease by the use of Fisher- and Pearson-test, as appropriate. Variables which were statistically significant in prior testing were further evaluated by discriminant analysis with regard to their independent prognostic value. **Results:** 43/388 patients (11%) showed vascular invasion. 10 of them (23%) had persistent or recurrent disease. Out of 345/388 patients without histological vascular invasion only 24 patients (7%) suffered from persistent or recurrent disease at the end of follow up, which was statistically significant ($p=0.002$). Besides angioinvasion, sex, T-stage, N-stage and M-stage were significantly associated with persistent or recurrent disease. Discriminant analysis revealed vascular invasion, T-stage, N-stage and M-stage as significant independent prognostic variables for PTC ($p<0.0001$, respectively). **Conclusion:** Our study showed, that angioinvasion is an independent prognostic factor for patients with PTC besides T-stage, N-stage and M-stage. Therefore angioinvasion should be considered for patient management in PTC.

P0923

Detection rate of recurrent medullary thyroid carcinoma using Fluorine-18 dihydroxyphenylalanine positron emission tomography: a meta-analysis.

G. Treglia¹, F. Cocciolillo¹, F. Di Nardo², A. Poscia², C. de Waure², A. Giordano¹, V. Rufini¹; ¹Institute of Nuclear Medicine, Catholic University of the Sacred Heart, Rome, ITALY, ²Institute of Hygiene, Catholic University of the Sacred Heart, Rome, ITALY.

Objective: to meta-analyze published data about the diagnostic performance of Fluorine-18 dihydroxyphenylalanine positron emission tomography or positron emission tomography/computed tomography (¹⁸F-DOPA PET or PET/CT) in detecting recurrent medullary thyroid carcinoma (MTC). **Methods:** A comprehensive literature search of studies published in PubMed/MEDLINE, Scopus and Embase databases through March 2012 and regarding ¹⁸F-DOPA PET or PET/CT in patients with suspected recurrent MTC was carried out. Pooled detection rate (DR) on a per patient- and a per lesion-based analysis was calculated. A sub-analysis considering serum levels of calcitonin, device used and carbidopa pretreatment was also performed. **Results:** Eight studies comprising 146 patients with suspected recurrent MTC were included. DR of ¹⁸F-DOPA PET and PET/CT on a per patient- and a per lesion-based analysis was 66% (95% confidence interval: 58-74%) and 71% (95% confidence interval: 67-75%), respectively. DR on a per patient-based analysis significantly increased in patients with serum calcitonin ≥ 150 ng/L (73%), calcitonin ≥ 1000 ng/L (86%) and calcitonin doubling time <24 months (86%). A significant advantage of hybrid PET/CT versus PET alone was not found. Furthermore, carbidopa pretreatment did not affect the DR. **Conclusions:** ¹⁸F-DOPA PET and PET/CT may be useful functional imaging methods in detecting recurrent MTC. DR of recurrent MTC using these imaging methods increases in patients with higher calcitonin levels and lower calcitonin doubling time.

P0924

Thyroid Cancer Metastases Treatment with Percutaneous Ethanol Injection

S. Kusacic Kuna, H. Tomic Brzac, G. Horvatic Herceg, M. Despot, D. Dodig; Clinical Hospital Centre Zagreb, Zagreb, CROATIA.

Aim: The aim of study was to evaluate the successfulness and side effects of percutaneous injection of 95 % ethanol (PEIT) for management of limited cervical neck metastases in selected group of thyroid cancer patients. **Patients and Methods:** PEIT was made in a group of patients with high risk of complications after repeated surgery and those who preferred not to have repeated surgery. All treated lymph nodes were previously citologically confirmed as malignant by ultrasound guided fine needle aspiration biopsy (US-FNAB) and by presence of thyroglobulin in the aspirate. 22 patients with solitary metastasis in the neck (16 women, mean age 61 years; range 26-81 years) were treated. All of them have undergone total thyroidectomy followed by radioiodine ablation. In majority of patients a lateral neck dissection had been performed, and most of them had been operated several times because of recurrent disease. Four patients had distant metastases, and two patients had a second malignancy that cannot permit another surgery. Ethanol was injected directly into each node without any premedication, and the volume of ethanol used in treated nodes depends on their size. All treated patients were

periodically followed by Color Doppler ultrasound. Result: In the majority of patients, after one or more treatments, a significant reduction of nodal size as well as decrease of thyroglobulin level were noticed. There were statistical differences in size between nodes before and after therapeutic sclerosation (in terms of longitudinal and anteroposterior diameter as well as in volume of treated nodes). Two nodes were completely disappeared. In four patients with a more widespread disease and metastases in the lungs and bones satisfactory results were not achieved. No serious adverse events were related to percutaneous ethanol administration. Some of patients experienced mild local pain at the site of injection. Conclusion: The PEIT is a safe, alternative treatment modality that can be helpful in reducing disease progression in selected group of patients with recurrent thyroid cancer neck metastases. The method is well received by patients, can be repeated several times with low rate of complications but surgery is always a choice if the disease progresses.

P0925

18F-FDG PET/CT in detection of iodine non-avid metastasis of well differentiated thyroid carcinoma

S. Lucic¹, A. Peter¹, D. Srbovan¹, D. Ilincic², D. Jovanovic¹, M. A. Lucic¹; ¹Institute of Oncology of Vojvodina, Sremska Kamenica, SERBIA, ²Institute of Pulmonary Diseases of Vojvodina, Sremska Kamenica, SERBIA.

Aim: The indicator of iodine-negative metastasis of well differentiated thyroid carcinoma presence is usually based on the elevated values of serum thyroglobuline level and represents a challenging diagnostic task with morphological diagnostic tools such as US, CT or MRI only. In this study we have tried to define the usefulness of 18F-FDG PET/CT scans in those patients (pts). **Material and methods:** Twenty-six pts (17 women (65%), 9 men (35%), average age 53,18±15,6 years) with elevated thyroglobulin level (ranging from 1,61 up to 5000 ng/mL; mean value: 426,98ng/mL) underwent 18F-FDG PET/CT diagnostic examination after 131-I therapy application and post-therapy whole body scan that showed no iodine-avid uptake. Five of 26 pts had follicular thyroid cancer (19%) and 21 papillary (81%) thyroid cancer, of which one had Hürthle-cell variant. Pts were also divided in subgroups according to their TNM classification (T1N1-4 pts, T2N1-5 pts, T3N1-2 pts, T4N1-10 pts and T1N0-1pts, T3N0-2 pts, T4N0-1 pts) and PET/CT results and were followed-up for 12 months after PET/CT scan. **Results:** Overall results showed 22 (85%) positive PET/CT scans that indicated the presence of nodal or distant metastasis and 4 (15%) negative scans. From 22 positive PET/CT results 7/22 pts had findings that indicated distant metastasis (6 lung and one bone). In 15/17 pts with positive scans cervical node metastasis in paratracheal and jugular nodes were found (in 9/15 pts histopathologically (pH) proven papillary lymph node metastasis after neck lymph node dissection, while the rest 6/15 pts are followed with US, CT or MR and clinically were stable). In a group of 5 pts with follicular carcinoma all five pts had positive scans (5/5) - one with nodal and four with distal metastasis (3 lung and 1 bone), out of them in one pts follicular lung metastasis has been pH proven. In a group of 21 pts of papillary thyroid carcinoma 4/21 scans were negative (two were T1N1, one T3N1 and one T4N1; 1/4 pts has been scanned after L-Thyroxin withdrawal and 3/4 while on L-thyroxin therapy), while 17/21 were positive on PET/CT. **Conclusion:** Since PET/CT scan demonstrated the presence of nodal or distant iodine-negative metastasis in 85% of all pts, enabling the change of the treatment modality and outcome in 38% of all pts, we may conclude that 18F-FDG PET/CT could be a diagnostic modality of choice in detection of iodine non-avid metastasis in well differentiated thyroid carcinoma patients.

P0926

Evaluation of focal thyroid lesions incidentally detected in F-18 fluorodeoxyglucose PET/CT images

O. Yaylali, F. S. Kirac, D. Yuksel, E. Marangoz; Pamukkale University Medical School, Denizli, TURKEY.

Aim: Increased uptake in the thyroid gland (TG) is often identified as an incidental finding on whole-body F-18 Fluorodeoxyglucose positron emission tomography/computed tomography (FDG-PET/CT) in the non-thyroid cancer (NTC) patients. Currently, there is no consensus on the appropriate approach for management of these cases. Thyroid ultrasound, scintigraphy and fine-needle aspiration biopsy (FNAB) are suggested to exclude malignant thyroid lesions. Our aim is to determine the importance of increased F-18 FDG uptake in TG on PET/CT in patients who are being screened for various NTC and to recommend a diagnostic strategy to identify patients with high risk of thyroid malignancy. **MATERIALS AND METHODS:** We evaluated 1086 cases undergoing whole-body PET/CT scan between April 2011 and April 2012. Images with incidental focal FDG uptake in TG were identified. Data of the age, sex, type of primary cancer, maximum standard uptake value (SUVmax), size of thyroid nodules and cervical lymph nodes (CLN) on F-18 FDG-PET/CT images, and if available, FNAB results were evaluated. **RESULTS:** 28 of 1086 patients (2.5%) showed a focal increased F-18 FDG uptake of lesions in TG (14 men, 14 women, mean age±SD, 60.29±13 years) and the SUVmax value ranged from 1.50 to 18.00 (average SUVmax: 4.19±3.41). Thyroid lesions ranged in

diameter from 7.0 to 55.0 millimeter (mean±SD:16.47±11.80mm). The CLN were detected in 11/28 patients (39%). The average SUVmax in CLN was 4.04±1.80, the mean CLN diameter was 10.13±2.95mm. Twelve of 28 patients (43%) were done FNAB, and the final histopathological diagnosis was malign thyroid nodules in five patient (average SUVmax 6.84±6.37 and nodule diameter 31.26±22.11mm), benign thyroid disease in five patient (average SUVmax 3.95±1.48 and nodule diameter 9.60±2.30mm) and limited and insufficient materials in two patients. Sixteen patients did not undergo any diagnostic test. **CONCLUSION:** Focal increased FDG uptake in TG incidentally identified on FDG-PET/CT occurred at a frequency of 2.5% and this finding may be associated with an increased risk of malignancy, but the clinical significance is unclear. More data are needed to elucidate the role of SUV in the differentiation of benign and malign thyroid lesions. Clinicians should take into consideration incidentally detected PET/CT findings. Thyroid scintigraphy and, if cold nodule is present, FNAB should be suggested to clinicians for definitive diagnosis.

P0927

Is it possible to overrule the 131I whole body scan performed previous to ablation therapy in patients with differentiated thyroid carcinoma? Our experience.

C. Isla Gallego, J. Miranda Ramos, M. Ochoa Figueroa, M. Canelas Subieta, A. Santana Borbones, J. Herrera Henriquez, F. Armas Serrano, S. Blanco Herrero, M. Hernández Briz; Nuclear Medicine Department. Complejo Hospitalario Universitario Insular Materno-Infantil de Gran Canaria, Las Palmas de Gran Canaria, SPAIN.

AIM: To evaluate the usefulness of 131I whole body scan (WBS) after total thyroidectomy in differentiated thyroid cancer (DTC) performed after ablation therapy and to consider the possibility of obviating it. **MATERIALS AND METHODS:** 85 DTC patients (women:67; men:18, ages:12-87) who had surgery between June/09 and February/12 were studied. There were 62 papillary carcinomas, 4 follicular variant of papillary, 1 papillary+Hürthle cell, 16 follicular and 2 Hürthle cell carcinomas. In 83 patients a WBS was obtained after the injection of 3 mCi of 131I, 1 to 3 months after surgery in a hypothyroidism situation and with TSH >30 mU/L. Depending on WBS findings ablation therapy was administered with a variable 131I dose: 100 mCi when post-surgery thyroid remnants were found (67 patients), 125 if there were also adenopathies (12), 150 if pulmonary metastasis were detected and 200 if they had bone metastasis (1). In one patient no thyroid remnants were found and thyroglobulin was undetectable, therefore, he didn't undergo ablation therapy. Post-ablation WBS was obtained 4-7 days after therapy, undergoing the same protocol that was used on the first scan. Both studies were compared. TSH levels were evaluated one month after surgery as an indirect measurement of the thyroidectomy. When TSH <30 mU/L, 99mTc scintigraphy and ecography were performed to evaluate the size of the thyroid remnants. **RESULTS:** Post surgery TSH levels >30 mU/L were found on 83 patients, 47 of them > 100mU/L and 79 > 50 mU/L. The minimum value was 31 mU/L. TSH values were 20 and 22 mU/L in two patients after repeated surgery and after 99mTc scintigraphy and ecography ablation with 100 and 125 mCi post rTSH stimulation was decided, without undergoing WBS. Both WBS were similar in 60 of the 83 patients (72,2%), in 12 (14%) less uptake intensity and/or less focal uptakes were seen after therapy (stunning) and in 11 (13,2%) the number of lesions was increased after ablation. **CONCLUSIONS:** 1. TSH, Tg and image techniques can help in the decision of obviating the WBS before ablation, which also avoids stunning. 2. WBS sensitivity is increased with a higher dose, making post ablation WBS necessary, also as base for future controls. 3. Pre-ablation WBS might only be used when incomplete surgery is suspected or to confirm distant metastasis. 4. An empiric ablative dose of 100-125 mCi might be used, considering that more than 94% of the patients receive those doses.

P0928

J-131 Treatment of Grave's Disease - Results of a 10 Year Follow Up Study

S. I. Mihajlovska, M. S. Mihajlovska, J. Tutevska; Clinical hospital, Bitola, MACEDONIA, THE FORMER YUGOSLAV REPUBLIC OF.

Aim: The aim of our prospective clinical study was to evaluate the results of J-131 treatment for Grave's disease. **Methods:** 40 patients (35 women and 5 men) with Grave's disease treated with J-131 between the years of 1995-2005 were included in the study. The age of patients ranged from 20-72yrs. 20 patients had an enlarge thyroid gland (50%). All patients were treated with antithyroid medications for a minimum of 18 months. The medications was suspended a week before and after treatment with J-131. The total 78 treatments with J-131 were done with dosages varying between 5 and 24 mCi. The dose was calculated using the Marinelli formula. **Results:** The treatments was successful in 20 patients (50%) after a single dose (mean administered activity of 6 mCi of J-131, in other 10 patients (50% of other remaining patients after a second dose mean administered activity was 10,5 mCi), in five patients after four dosages (mean dose 23mCi) and in 3 patients after five dosages (mean 25,1 mCi). In one year following up 20 patients (50% were

hypothyroid, increasing to 65% at 7 years. After therapy with J-131 in 5 of 25 patients with goiter there was reduction in the size of thyroid gland. 10 of total 40 patients had Grave's ophthalmopathy which was premedicated, observing improvement in 3 of them. There were no adverse secondary effects noted after treatment with J-131. Conclusion: Our results show that the patients with Grave's disease can be successful treated with one or two dosages of J-131. In our experience becoming euthyroid or hypothyroid after treatment with J-131 in our series of patients is mostly unrelated to the number of dosages and administered activity. The percentage of hypothyroidism observed after treatment with J-131 is determinate by individual radio sensitivity and the evolution of the autoimmune disorder in Grave's disease.

P0929

Detection of recurrent or persistence disease of Papillary thyroid microcarcinoma patients during the early postoperative time period

L. Iordanidou, I. Sevaslidou, D. Papadouli, S. Trekla, M. Erifillidou, E. Trivizaki; "Metaxa" Cancer Hospital, Piraeus, GREECE.

Aim The aim of this study was to investigate how early in the clinical course of the disease we can determine risk factors which could help identify papillary thyroid microcarcinoma (PTMC) patients with an aggressive biological behavior. **Patients - Methods** The clinical records of 181 PTMC patients 151 females and 30 males with median age 53 years (range 20-82 years) surgically treated by total thyroidectomy at our hospital were analyzed with respect to tumor clinicopathological features and postoperative TSH stimulated serum thyroglobulin (stTg). Among 181 PTMC pts 58.2% had a classic papillary histology and 41.8% display histologic variants with most common the follicular variant (30.3%, n=55). Multifocality, bilaterality, location close to resection margin, thyroid capsule and capsular tumor invasion, had a relative frequency of 18.4%, 7.8%, 7.1%, 10.5% and 5.2% respectively. Serum thyroglobulin (stTg) levels were determined just before ablative therapy and 6 months after RAI treatment of 131-I 2.59 -3.7 GBq (70-100 mCi) followed by WBS to confirm ablation of thyroid remnants. Response was assessed by comparing pre- and post-therapy stTg concentrations and by pre- and post therapy imaging, where available. Results Persistent/recurrent disease was found in 20 out of 181 (11%) PTMC patients with a mean stTg value 14.8 ng/ml (range 2.6-83.2 ng/ml) at the time of ablation. The increment of st-Tg in 13 of 20 (65%) pts was associated both with one or more of PTMC aggressive histological variants and thyroid and tumor capsule invasion in 3 out of 13 pts. The remained 7 pts (35%) had a classic papillary histology with the only pathological tumor feature the location of tumor at or within 2 mm from the resection margin. Multifocality (3/20) and bilaterality (1/20) alone was not predictive of relapse. Six months after RAI treatment complete ablation was seen in 16/20 (80%) patients with pre-ablative increased st-Tg value and in 152/161 (94.4%) with an undetectable stTg. Nine patients with pre-ablative undetectable st-Tg who showed remnant uptake on follow-up diagnostic WBS and 4 with persistent increased st-Tg values received a second ablation. **Conclusions** According to our first results the presence of a non classic PTMC in combination with an increment of pre-ablative stTg it seems an accurate predictor of persistence or recurrent disease. Additionally there is a tendency of a close resection margin to be a risk factor of residual disease.

P0930

The value of thyroglobulin levels in the fine needle biopsy aspirate of suspicious lymph nodes in patients with thyroid cancer

M. Tuncel, M. C. Tuncali; Hacettepe University, ankara, TURKEY.

Purpose: Accurate detection of lymph node(LN) metastases is crucial in patients with thyroid cancer. Determination of thyroglobulin levels in the fine needle aspirates of suspicious lymph nodes (FNAB Tg) helps for the appropriate diagnosis. Our study aimed to reveal the value of FNABTg in the detection of LN metastases compared with cytology. **Subjects and methods:** Seventeen patients (F/M:8/9 age:46±17years) who had, total thyroidectomy for thyroid cancer and suspicious LNs on neckUSG, underwent FNA biopsy. FNABTg levels were also determined by rinsing the biopsy syringe with saline solution. Cytological examinations were expressed as (1)positive: presence of epithelial cells with atypical characteristics, or with cytological features of papillary carcinoma; (2) negative: reactive lymphadenitis and absence of malignant cells; (3) inadequate or nondiagnostic: absence of cells or presence of blood cells. FNAB Tg/serum Tg >1 was accepted as positive for LN metastases. The cytology&pathology results, serum&FNABTg, imaging findings and follow-up data were used to achieve a final clinical decision **Results:** Nineteen LN from 17 patients with suspicious USG findings (2 cystic, 4 hyperechoic with microcalcifications, 13 hypoechoic without hyperechoic hilus) were biopsied. According to the results of cytology and FNABTg; 11 patients underwent surgery which confirmed LN metastases, 1 patient received additional radioiodine therapy, 1 patient although both positive with cytology and FNAB Tg did not undergo surgery because of his medical condition and 4 patients were accepted in remission with final clinical decision. In patients with LN

metastases the minimum shortest diameter of the positive LN was 4 mm (mean: 7.2 ±2.65) and the median serum Tg levels of LN metastases were significantly lower than FNAB Tg (20±132 vs 1962 ±16988 ng/ml. p:0.0001). In 2 patients with stimulated serum Tg levels of 0.2 ng/ml and positive anti-Tg antibodies, FNABTg levels were true positive (1119 and 73 ng/ml) as proved by surgery. In 3 patients with inadequate cytology FNABTg was true positive in 2 pts and true negative in 1 pts. The sensitivity, specificity, PPV, NPV and accuracy of FNABTg on patient bases were 92%, 100%, 100%, 80%, 94% whereas these values were 86%, 100%, 100%, 60%, 88% for cytology when the inadequate or nondiagnostic were accepted as negative. **Conclusion:** FNAB Tg is a validated tool for the detection of LN metastases in patients with thyroid cancer. The combined use of cytology and FNABTg must be the standard of care for optimal diagnosis.

P0931

Diagnostic value of FDG PET/CT in patients with differentiated thyroid cancer and negative I-131 WBS but high thyroglobulin levels

E. Cingi Ozdemir¹, N. Yildirim Poyraz¹, C. Aydin², D. Tuzun², S. Turkolomez¹, R. Ersoy², B. Cakir²; ¹Ankara Atatürk Training and Research Hospital, Department of Nuclear Medicine, ANKARA, TURKEY, ²Ankara Atatürk Training and Research Hospital, Department of Endocrinology and Metabolism, ANKARA, TURKEY.

Plasma thyroglobulin (TG) levels, ultrasonography and I-131 whole body scanning (WBS) are utilised periodically in the follow-up of patients with differentiated thyroid cancer (DTC) who have undergone surgery and RAI ablation. Current guidelines recommend F18-FDG PET/CT when negative I-131 WBS coexists with high TG levels. This study was designed to evaluate the diagnostic value of PET/CT and its relation with TG levels in the above mentioned patient population. **Material and method:** A total of 39 patients (30 female, mean age:41,6) who underwent surgery for DTC and received RAI ablation between 2007-2011 and also had negative I-131 WBS but high TG levels at follow-up were studied with PET/CT for the detection of recurrence or metastasis. L-thyroxine therapy was stopped for 2 weeks before PET/CT and serum TSH and TG levels were assessed on the day of scanning. The presence of either thyroid tissue or lymph node with pathological metabolic activity on PET/CT, that could possibly be causative for high TG levels, was considered positive. **Results:** PET/CT detected pathological activity that could possibly be causative for high TG levels in 17 out of 39 patients (43.5 %). Pathological metabolic activity was detected in the cervical or mediastinal lymph nodes in all patients except one who disclosed unablated ectopic thyroid tissue. The serum TG levels ranged from 4-569 ng/mL. The mean TG level was found to be higher in patients with positive PET/CT scans compared to those with negative scans (119,58 ± 41,7 vs 20,18 ± 3,70) respectively, P<0,01. PET/CT was negative in all 7 patients (100 %) with serum TG below 5 ng/mL and in 9 out of 12 patients (75 %) with serum TG below 10 ng/mL. **Conclusion:** F-18 FDG PET/CT is useful to detect the focus of pathological metabolic activity in patients with operated DTC and negative I-131 WBS and high serum TG at follow-up; its diagnostic value seems to be related with serum TG levels.

P0932

The Clinical Use of F-18 FDG PET in Patients with Thyroid Carcinoma

M. Urhan¹, A. Alavi²; ¹GATA Haydarpasa Training Hospital, Istanbul, TURKEY, ²Hospital of the University of the Pennsylvania, Philadelphia, PA, UNITED STATES.

Purpose: In up to 30% of the patients with thyroid carcinoma, the cancer cells lose the ability to concentrate radioiodine due to dedifferentiation process. In this study we assessed the clinical role of FDG PET in the management of patients with a clinical suspicion of iodine negative recurrent or metastatic thyroid carcinoma. **Subjects and Methods:** Eighty-one patients with a proven diagnosis of thyroid carcinoma (papillary; 76, follicular; 5, poorly differentiated subtype; 2) were included in the study. All patients underwent near-total or total thyroidectomy and radioablation previously. The patients were monitored by periodical serum thyroglobulin measurements, neck ultrasound and low dose diagnostic radioiodine whole-body scanning. Radioiodine scanning was negative in all patients both with detectable (68 patients, Tg >2 ng/ml, range; 2.2-4350) or undetectable (13 patients, <2 ng/ml, range 0.2-1.9) serum thyroglobulin levels. All patients underwent FDG PET whole-body imaging and positive findings were correlated with those of the cytology, histopathology and anatomical imaging. **Results:** The recurrent tumor was shown in the neck in 59 patients (70%), lung in 12 (14%), mediastinum in 6 (7%) and in the bone in 4 (5%). FDG PET was true-positive in 51 patients (63%). There were 3 false positive findings proved to be residual thymus with histology and radiological examination. PET was negative in 23 patients, however residual or metastatic thyroid carcinoma in the neck was detected with US-guided fine needle aspiration cytology. In 4 patients with inappropriately high serum thyroglobulin levels, small metastatic lesions were shown in the lungs on CT scans, however radioiodine and FDG PET scanning were both failed to show small pulmonary

lesions. **Conclusion:** FDG-PET is useful in detecting recurrent or metastatic iodine negative thyroid carcinoma. US-guided with fine-needle aspiration and computerized tomography complemented the PET findings in detecting minimal cervical adenopathy or tiny metastatic deposits in the lungs in patients with inappropriately high serum thyroglobulin levels respectively.

P0933

The Roles of Thyroglobulin Measurement, Neck Ultrasound, Radioiodine Scanning and 18-FDG PET in Patients with Locally Invasive Thyroid Carcinoma

M. Urhan¹, **A. Alavi**²; ¹GATA Haydarpasa Training Hospita, Istanbul, TURKEY, ²The Hospital of the University of the Pennsylvania, Philadelphia, PA, UNITED STATES.

Purpose: Local spread is common in patients with differentiated thyroid carcinoma (DTC). Surgical removal of the persistent disease is the only way for cure if the lesions lost the ability to take-up radioiodine. In this study we evaluated the pre-operative role of 18-F-Fluorodeoxy glucose positron emission tomography (18-FDG-PET), ultrasonography (US) and US-guided fine needle aspiration biopsy in patients with local persistent non-iodine avid thyroid carcinoma. **Subjects and Methods:** Forty patients (31 female, 9 male; age range 19-80 years) were enrolled. Histopathology was papillary in 36, hurtle in two, poorly-differentiated thyroid carcinoma in 2 of the patients examined. All patients underwent radio-iodine ablation following thyroid surgery 1 to 14 years previously. Thyroglobulin(Tg) levels were undetectable (≤ 2 ng/ml) in 6 patients, and 9 patients in whole group had a positive diagnostic 123-I whole-body scanning. The patients underwent PET study because of either detectable serum Tg levels or an anatomical lesion detected in the neck suspicious for malignancy. The patients with a proven distant metastasis were excluded. The patients underwent neck ultrasonography (US) and fine-needle aspiration cytology (FNAC) along with US-guidance. After cytologic verification of the tumor, all patients underwent cervical lymph node dissection. The findings obtained from all procedures were compared with those of operation notes and histopathology of the surgical specimens. **Results:** Sixty-five lymph node groups were removed and 48 of them represented DTC. Serum Tg was detectable in 31 patients (≥ 2 ng/ml) and had an overall sensitivity of 77%. Neck US has detected 40 tumor sites with a sensitivity and specificity of 84% (40/48) and 59% respectively when the lower limit is 5 mm in-size for the lymph node diameter. Along with fine needle aspiration, the sensitivity of US increased to 98%. FDG uptake was detected in 34 foci and 30 of them represented true-positive findings. In four; residual thymus, a lymph node with inflammatory changes and cervical muscle spasm in two was responsible for false-positive PET findings. The sensitivity and specificity of FDG PET were 63% and 77% respectively while I-123 scan presented a sensitivity of only 19% for cervical lymph node involvement. **Conclusion:** FDG PET improves the diagnostic investigation of local disease in thyroid cancer patients revealing metastasis in normal-sized lymph nodes as in enlarged nodes. It can give prognostic information which has an impact on planning the subsequent surgical strategy. US can complement the existing FDG findings as it offers a high sensitivity in detecting small cervical lesions.

P0934

¹⁸F-FDG-PET-CT in patients with differentiated thyroid carcinoma, elevated thyroglobulin and negative ¹³¹I scan

D. R. Mendez, S. Rodado, I. Santos, I. Hernandez, R. Couto, M. Marin, M. Coronado, L. Martin Curto; University Hospital La Paz, Madrid, SPAIN.

Aim: To evaluate the utility of the ¹⁸F-FDG- PET-CT in patients diagnosed of differentiated thyroid carcinoma (DTC) with elevated thyroglobulin (Tg) and negative results in ¹³¹I scan. **Material and methods:** We retrospectively studied 46 patients (49 PET-CT studies), 28 women and 18 males, with mean age of 57 years old, diagnosed of DTC (39p papillary carcinoma, 3p follicular carcinoma, 4p Hurtle's cells carcinoma), treated at least once with ¹³¹I. All patients underwent a ¹⁸F-FDG-PET-CT scan (under rTSH stimulation) because of elevated Tg and negative scan post therapeutic dose of ¹³¹I. PET-CT results were confirmed histologically and / or by means of clinical/radiological follow-up. The influence of PET/CT findings in the patient management was evaluated, as well as correlation of PET/CT findings with histology. The average time between ¹³¹I scan and PET-CT was 10.4 months. Average time of follow-up was 35.4 months. **Results:** 20 PET-CT studies were positive for malignancy (in 19 disease was confirmed and therapeutic approach was changed and in 1 case disease was not confirmed); 24 PET-CT studies were negative for malignancy (in 13 patients follow up confirmed absence of disease, in 4 patients disease was histologically confirmed, and 7 patients remain with elevated Tg but CTI without pathological findings). In 5 patients PET-CT was not conclusive for malignancy. Seven patients with confirmed disease, in whom PET-CT did not see or I did not conclude disease, had subcentimetric lymph nodes and milimetric lung nodules. The mean Tg value for positive PET-CT was 26.8 ng/ml and mean Tg value for negative PET-CT was 7.6 ng/ml. We did not find correlation between histology of the tumor and PET/CT findings. **Conclusion:** ¹⁸F-FDG-PET-CT is an useful and first-line technic for localization of DTC recurrence in patients with elevated Tg and

negative ¹³¹I scan, modifying in some cases the therapeutic approach. It has a more limited role when the tumour load is low (Tg< 10 ng/ml and/or small size lesions).

P0935

Diagnostic performance of 18FDG-PET/CT in recurrent differentiated Thyroid carcinoma. Do timing of imaging after radioactive iodine therapy (RAI) and TSH-stimulated levels influence imaging results?

C. Tranfaglia¹, **C. Degli Esposti**², **F. Monari**³, **G. Lucchi**¹, **M. Santoro**¹, **E. Cason**¹, **S. Zoboli**¹, **G. Fagioli**¹; ¹Nuclear Medicine Unit Maggiore Hospital, Bologna, ITALY, ²Radiotherapy Unit Bellaria Hospital, Bologna, ITALY, ³Radiotherapy Unit S.Orsola-Malpighi Hospital, Bologna, ITALY.

Aim The aim of this study was to assess the performance of 18FDG-PET/CT in diagnosing recurrent differentiated thyroid carcinoma (DTC), and to evaluate if it was affected in a subgroup of subjects imaged in a short interval after RAI in TSH-stimulated condition. Relationship between Thyreoglobuline on-T4 levels or TSH-stimulated levels and imaging findings was also analyzed. **Materials and methods** We performed 50 PET/CT in 37 patients with suspicion of recurrent DTC based on elevated Tg levels (on-T4 or under TSH stimulation) or clinical ground. All patients have had a previous RAI with ¹³¹I-posttreatment whole-body scan (131-I-WBS) resulted negative in all but two cases. Eighteen out of 50 examinations were done within 7 days after RAI (3700-5550 MBq) and TSH-stimulated values were collected. Results were verified by histology, ultrasound or clinical follow-up. Tg and TSH-stimulated values in positive and negative cases were compared (t-student test). Results We obtained 23 positive and 27 negative PET/CT (22 true positive-TP, 1 false positive-FP, 15 true negative-TN, 12 false negative-FN). Sensitivity, specificity, positive predictive value (PPV), negative predictive value (NPV) and accuracy were respectively 65%, 94%, 96%, 56% and 74%. In the "after-RAI" subgroup 9 PET/CT resulted positive (8TP, 1FP) and 9 negative (4TN, 5FN) with a decrease in specificity (80%), PPV (89%) and overall accuracy (67%), due both to the only FP finding of the study, and to the higher percentage of FN (28% vs 24% in the whole study population). Tgon-T4 resulted significantly higher (p=0.05) in PET positive (mean=32.3, median=18) than in PET negative cases (mean=7.5, median=3). In 5 TP (23%) cases it was ≤ 5 ng/ml. Conversely, TSH-stimulated values were not significantly different (p=0.27) between positive and negative "after-RAI" scans. In the two cases of positive 131-I-WBS and PET/CT, different lesions were detected from each imaging modality. **Conclusions** FDG-PET/CT confirms to be useful for the diagnosis of recurrent DTC in 131I-negative patients and to contribute to a better definition of disease extent in selected 131I-positive patients. We found a lower diagnostic accuracy when examination was performed in a small time interval after RAI. Larger studies are necessary to confirm this finding and to explore an eventually existing relationship between temporary radiation effects and PET findings. Our results confirm, finally, that the Tg cut-off of 10ng/ml for performing a PET/CT could be not adequate (Tg ≤ 5 ng/ml in 23% of TP), and that the relationship between TSH-stimulated levels and FDG uptake remains still unclear.

P0936

The Diagnostic Value of Stimulated Serum Thyroglobulin in the Follow-up of Low-Risk Patients with Differentiated Thyroid Cancer

V. Wagenhofer, I. Mihaljević, T. Kralj, D. Šnajder; Clinical Institute of Nuclear Medicine and Radiation Protection, University Hospital Centre Osijek, Osijek, CROATIA.

The aim of this study was to evaluate the diagnostic value of stimulated serum thyroglobulin (Tg-off) in the follow-up of low-risk patients with differentiated thyroid cancer (DTC). The study included 186 consecutive patients with DTC treated between 1992 and 2005 at our department (Osijek University Hospital). Initial therapy is assumed to be total thyroidectomy and radioiodine ablation. High-risk patients with DTC (patients with distant metastases, poorly differentiated histological types of cancer) and patients with positive anti-Tg antibodies were excluded from the study. The routine procedure in the follow-up of DTC was based on serum Tg measurements during thyroid hormone withdrawal (Tg-off), diagnostic (131) I - wholebody scan (WBS) and neck ultrasonography (US). Clinically persistent or recurrent disease was diagnosed in 23 of 186 patients (12.4 %). Serum thyroglobulin (Tg-off) was elevated (Tg > 2 ng/ ml) in 19/23 patients with recurrence (sensitivity: 82.6 %), and neck US identified (confirmed by fine-needle aspiration cytology) 17/23 patients with recurrent disease (sensitivity: 73.9 %). (131) I-WBS was positive (uptake outside the thyroid bed) in 6 patients with recurrence (sensitivity: 26 %). Neck US identified 4 patients that were not previously detected by serum Tg and (131) I-WBS. The negative predictive value (NPV) of stimulated thyroglobulin (Tg-off) was 97.5 %. The combined use of stimulated serum thyroglobulin and neck US detected all patients with recurrence of DTC. The present retrospective study confirmed high sensitivity and high negative predictive value (NPV) of stimulated serum thyroglobulin. We conclude that the serum thyroglobulin levels (Tg-off) with neck ultrasonography have the

highest diagnostic accuracy in detecting persistent or recurrent disease in the follow-up of low-risk patients with DTC.

P53-2 - Tuesday, October 30, 2012, 16:00 - 16:30, Poster Exhibition Area

Oncology Clinical Science: Breast

P0937

Axillary Lymphadenectomy Assessment in Breast Cancer and Positive Sentinel Lymph Node (SLN)

A. C. Rebollo, R. Sánchez, T. Aroui, M. Navarro-Pelayo, G. I. Guzmán, E. Pastor, J. García, S. Menjón, J. M. Llamas; HOSPITAL VIRGEN DE LAS NIEVES, GRANADA, SPAIN.

Aim Evaluate the axillary lymphadenectomy involvement in patients with sentinel node metastasis of breast cancer. **Methods** Retrospective analysis (January 2008 - March 2012). We studied 345 women with breast cancer (3 bilateral), without clinical axillary involvement including axillary ultrasonography: stage I (T1aN0M0: 15; T1bN0M0: 58; T1cN0M0: 171), stage IIA (T2N0M0: 95). Average age: 57 years (range 27 - 84), 59.1% post menopausal. 65.2% palpable lesions, average size of 17.6 mm (range 2 - 50) and 37 multiple (30 multifocal and 7 multicentric). 63.7% corresponded to invasive ductal carcinoma and 78% to the luminal-A molecular type. The day previous to surgery, 37 - 55 MBq albumin nanocolloid was injected periareolarly. 92.8% underwent breast cancer conservative surgery. Axillary lymphadenectomy was performed in patients with positive SLN or no migration. The SLN was analyzed by either frozen section, hematoxylin-eosin stain and immunohistochemistry (n:67) or OSNA, one-step nucleic acid amplification (n: 275). **Results** The SLN was identified in 97.9% cases, the non identification was associated with a BMI > 30 Kg/m² (P = 0.001) and histologically positive axilla (P = 0.009). The mean SLN identified was 1.76 (range 1 - 8). The mean lymph nodes resected in the axillary lymphadenectomy was of 14.97±5, 77 (range: 6-38). The SLN was positive in 97 (28.1%) patients, (1 SLN (+): 70; 2 SLN (+): 19; ≥3 SLN(+): 8): 34 micrometastasis and 63 macrometastasis. A positive SLN result was associated to T2 tumors (P = 0.009), clinical palpable lesions (P = 0.026) and multiple lesions (P = 0.012). In 71 patients (73.1%), the SLN was the only positive node. In 61/ 97 patients, all the SLN were affected (1/1: 40; 2/2:13; 3/3: 2; 4/4: 2; 5/5: 1; 6/6:2). The involvement of other axillary lymph nodes is more frequent in patients with SLN macrometastasis rather than in patients with micrometastasis (P=0.010). Only 11.7% (4/34) of patients with SLN micrometastasis showed axillary lymphadenectomy involvement: 1 SLN (+): 4/29; 2SLN: 0/4; 3 SLN(+): 0/1. 34.9% (22/63) patients with SLN macrometastasis showed axillary lymphadenectomy involvement (1 micrometastasis and 21 macrometastasis). **Conclusion** Axillary lymphadenectomy in patients with breast cancer and sentinel lymph node micrometastasis could be avoided.

P0938

Second Sentinel Lymph Node Biopsy after Neoadjuvant Chemotherapy in Patients with Positive Sentinel Lymph Node (SLN) of Breast Cancer Prior to Treatment. Preliminary Studies.

A. C. Rebollo, R. Sánchez, T. Aroui, M. Navarro-Pelayo, G. I. Guzman, E. Pastor, J. García, S. Menjón, J. M. Llamas; HOSPITAL VIRGEN DE LAS NIEVES, GRANADA, SPAIN.

Aim To evaluate accuracy of a second SLN biopsy in patients with operable breast cancer and clinically negative axilla, with SLN metastasis, treated with primary systemic chemotherapy in order to avoid unnecessary axillary lymphadenectomy in pathologic complete response cases or disease limited to the SLN. **Methods** Prospective study (September 2011-March 2012). 32 women, average age 50.7 years (range 29-73) with invasive ductal carcinoma (2 bilateral), stage II A (cT2N0M0). The axillary status was established clinically including ultrasonography or biopsy. Chemotherapy scheme: epirubicin/ cyclofosfamide x 4, and paclitaxel x 4. The day before surgery, 74-111 MBq albumin nanocolloid was injected periareolarly. The SLN was analyzed by OSNA. Axillary lymphadenectomy was performed in patients with positive SLN. **Results** The pre-chemotherapy SLN was identified in 94.1% (32/34) cases. SLN mean: 1.69±0.89 (range 1-4). In 15/32 (46.9%) the SLN was positive: 11 macrometastasis and 4 micrometastasis. At the moment, 14 patients (1 bilateral) have completed the chemotherapy and surgical treatments (13 lumpectomies, 2 mastectomies), 7 of them with positive pre-chemotherapy SLN (6 macrometastasis, 1 micrometastasis). Post-chemotherapy SLN was only identified in 4/7 (57.1%) cases. Non migration occurred in 3 patients: 1 patient with axillary lymphadenectomy involvement and 2 patients without axillary lymphadenectomy involvement. In 2 cases, the post-chemotherapy SLN was a true positive (1 macrometastasis, 1 micrometastasis), being the SLN the only affected (3/3 and 1/1 with axillary lymphadenectomy 0/13 and 0/10, respectively). In 2 patients, the post-chemotherapy SLN was a true negative (0/2 and 0/2 with axillary lymphadenectomy 0/6 and 0/7, respectively). **Conclusion** Though the post-

chemotherapy sentinel lymph node second biopsy migration percentage is very low, in cases with sentinel lymph node identification it maintains the predictive value of the axillary status.

P0939

Evidence-based appropriate use of SPECT/CT in breast sentinel lymph node

T. L. J. Wagner, S. Navalkisoor; Royal Free London NHS Foundation Trust, London, UNITED KINGDOM.

Introduction Axillary node status is the most important prognostic factor in patients with breast cancer and is assessed safely and accurately by the sentinel lymph node (SLN) biopsy. Hybrid imaging provides complementary anatomical and functional information. The aim of this study was to look for evidence guiding the use of SPECT/CT in breast lymphoscintigraphy prior to SLN biopsy. **Material and Methods** We reviewed the available peer-reviewed literature using Pubmed and keywords "SPECT/CT" and "breast" and "sentinel lymph node". **Results** Compared to planar imaging, SPECT/CT improved SLN detection rate and anatomical localisation. It also altered surgical approach and was found valuable by surgeons. SPECT/CT identified false positive findings on planar imaging and detected SLN in patients with negative planar findings. SPECT/CT seemed to have a role in overweight patients because of the high rate of nonvisualisation on planar images. SPECT/CT was superior to planar imaging due to improved spatial resolution, correlation of anatomical and functional information and attenuation correction. **Conclusion** Based on the available evidence we feel that SPECT/CT is indicated in patients with nonvisualisation on planar imaging, in overweight and obese patients, and in patients with unusual drainage pattern or difficult to interpret images.

P0940

ROLL by a portable gamma-camera

L. Camoni¹, P. Rossini¹, L. Dognini², F. Bertagna¹, E. Orlando³, R. Giubbini¹; ¹Nuclear Medicine, University of Brescia and Spedali Civili di Brescia, Brescia, ITALY, ²1st Division of Radiology, Spedali Civili di Brescia, Brescia, ITALY, ³1st Division of Radiology, University of Brescia and Spedali Civili di Brescia, Brescia, ITALY.

Objectives : Radioguided occult lesion localization (ROLL) is performed in breast cancer pts with non-palpable lesions. Limitations of ROLL are (a) the need of moving the pt from Radiology (where the injection is performed) to Nuclear Medicine to verify the absence of tracer diffusion and (b) the absence of methods for evaluating the distance between the center of the neoplasm (identified by ROLL) and the excision margins. Aim of this study was the evaluation of the clinical usefulness of a portable gamma-camera able to analyze the tracer distribution immediately after the injection and to measure the distance between the center of the neoplasm and the surgical margins. **Methods**: 37 MBq of 99mTc-MAA in 0.2-0.5 ml were injected intralesionally under stereotactic guidance. The tracer localization was checked by a portable lightweight, hand-held, battery-powered gamma camera (IP Guardian 2 -Li-tech Monterotondo, Rome, Italy). The same equipment was used to define location and size of the breast incision. After lesion excision, the specimen was immediately imaged by mammography to verify the location of microcalcifications. The portable gamma-camera was then placed over the mammograph upper plate and a scintigram was obtained. Radio-opaque markers defining the camera borders were added and the camera removed. A second mammogram with markers was obtained. The scintigram and the mammogram were than co-registered by dedicated software. Same procedure was obtained in a second orthogonal view. The distances between the hottest pixel and the margins of the specimen were measured. The entire procedure took less than 5 minutes and the images were available in the operation theatre by the hospital PACS. In this preliminary study 12 pts underwent this procedure. **Results** : The procedure was performed without difficulties in all pts. The distance between the lesion center and the surgical margins was 13.5 ± 6 mm (range 5-24 mm). In two pts reresection to obtain clear surgical margins was suggested. **Conclusions** : The use of the portable gamma-camera can improve the ROLL technique.

P0941

Value of 18F-FDG PET/CT for primary tumor visualization and staging in T1 breast cancer patients

B. B. Koolen, F. van der Leij, W. V. Vogel, E. J. T. Rutgers, M. T. F. D. Vrancken Peeters, P. H. M. Elkhuisen, R. A. Valdés Olmos; Netherlands Cancer Institute - Antoni van Leeuwenhoek Hospital, Amsterdam, NETHERLANDS.

Background: The use of 18F-FDG PET/CT in large and locally advanced breast cancer has been investigated extensively, but uncertainty remains regarding its value in early stage breast cancer. The aim of the present study was to assess the accuracy and yield of FDG PET/CT for primary tumor visualization and staging in T1 breast cancer patients. **Methods**: Sixty-two patients with invasive T1 breast cancer, who received baseline PET/CT within the scope of two clinical trials, were evaluated.

Image acquisition of the thorax was done in prone position (hanging breast technique), followed by whole body scanning in supine position. Primary tumor FDG uptake was qualitatively and quantitatively evaluated and compared with clinical and histopathological characteristics. Presence of locoregional and distant metastases and other events was assessed and compared with conventional imaging procedures. Results: The primary tumor was visible with PET/CT in 54 (87%) of 62 patients, increasing from 59% in tumors ≤ 10 mm to 98% in tumors over 10 mm. All triple negative and HER2-positive tumors and 40/48 (88%) of ER-positive/HER2-negative tumors were visualized. FDG uptake was significantly higher in triple negative, grade 3, and highly proliferative tumors. Sensitivity and specificity of PET/CT in the detection of axillary metastases were 73% and 100%, respectively. In two (3%) patients PET/CT depicted FDG-avid periclavicular nodes, which were detected with ultrasound as well. Of 12 distant lesions, one was confirmed to be a lung metastasis, three were false positive, and eight were new primary proliferative lesions. No metastases were missed. Conclusion: Using optimal imaging of the thorax and breasts, the majority of small invasive breast carcinomas (cT1) can be visualized with FDG PET/CT. Specificity in the detection of axillary metastases is excellent, allowing immediate axillary lymph node dissection in case of an FDG-avid axillary node. However, sensitivity was limited, requiring a sentinel lymph node biopsy in case of absence of FDG-avid nodes. Distant staging can be done relatively reliably, but the yield in T1 tumors is low.

P0942

Added Benefits of 18F-FDG PET/CT in the Primary Staging and Management of Patients with Breast Cancer

B. Gunalp, S. Ince, A. O. Karacalioglu, A. Ayan, O. Emer, E. Alagoz; Gulhane Medical Faculty, ANKARA, TURKEY.

Aim: The purpose of this study was to determine added benefits of 18F-FDG PET/CT (PET/CT) on initial staging, therapy planning, recurrence and metastases detection in patients with breast cancer. **Patients and Methods:** Total 424 consecutive breast cancer patients (141 biopsy proven pre-operative and 195 post-operative high risks patients for primary staging and 88 for recurrence and metastases detection) who referred to PET/CT were included in this retrospective study. Clinical evaluation for staging, recurrence and metastases detection had been made by conventional imaging modalities (CIM) before PET/CT scan. Clinical benefits of PET/CT were determined by taking into account the importance of additional PET/CT findings on patient management. **Results:** Of the 141 examined pre-operative patients, PET/CT modified staging for 5 (26%) of stage I patients, 15 (29%) of stage IIA patients, 23 (48%) of stage IIB patients, 7 (58%) of stage IIIA patients and 2 (100%) of stage IIIB patients. PET/CT detected extra-axillary regional lymph nodes in 14 (9.9%) patients and distant metastasis in 41 (29%) patients. PET/CT detected multifocal lesion in 30 (21%) patients, multicentric lesion in 21 (14%) patients and malign foci in the contralateral breast (bilateral breast cancer) confirmed by biopsy in 5 (3.5%) patients. Of the examined post-operative 195 patients PET/CT detected axillary lymph nodes in 22 (11%) patients, extra-axillary regional lymph nodes in 21 (10%) patients and distant metastasis in 24 (12%) patients. PET/CT findings changed radiotherapy planning in 22 (11%) patients and chemotherapy was adapted to the metastatic diseases in 24 (12%) patients. Recurrences and distant metastases were detected in 75 (85%) patients who referred to PET/CT due to elevated tumor markers or suspicious findings on CIM. PET/CT had an impact on the management of 48 (55%) patients. Of these, chemotherapy or radiotherapy was started in 36 patients and treatment was modified in 8 patients. **Conclusion:** PET/CT detected unexpected metastases that were missed or not imaged with CIM which were significantly affected therapeutic decisions and patient management. It is concluded that PET/CT should be considered as a first line imaging modality for the primary staging and recurrence/metastases detection in patients with invasive breast carcinoma.

P0943

Assessing neoadjuvant chemotherapy (NAC) response in patients with breast cancer using Positron Emission Mammography (PEM) and dynamic contrast enhanced breast MRI (DCE-MRI): Pilot data

K. M. Kulkarni¹, D. Appelbaum², C. Sennett², Y. Pu², G. Newstead²; ¹University of Chicago, Chicago, IL, UNITED STATES, ²University of Chicago, Chicago, IL, UNITED STATES.

Clinical relevance/Application: PEM can be a promising functional based tool to assess final tumor burden after NAC which is a pivotal prognostic factor Purpose: To predict "true" functional/metabolic response of breast cancer to NAC using PEM. PEM relies on metabolic differences between cancerous and normal tissue rather than tumor angiogenesis as seen in DCE-MRI. **Methods and Material:** IRB approved prospective study (n=2) at University of Chicago from 12/15/09 to 3/20/10 to assess NAC response in patients with breast cancer using PEM. PEM (Naviscan Inc.) is a high resolution dedicated breast PET scanner. Patients underwent 1st/baseline PEM and MRI before starting NAC, 2nd PEM and MRI within 2 cycles and 3rd/pre-operative PEM and MRI at the end of NAC. PEM was

performed by injecting 10 mCi of 18F-2fluorodeoxyglucose in a foot vein. Bilateral CC, MLO, axillary PEM views were obtained 60-90 minutes post injection. Standard DCE-MRI was obtained using 1.5 T Philips scanner, 16 channel dedicated breast coil, injecting 20 cc of gadolinium intravenously within 1 week of PEM. 2 patients (mean age 55 yrs) with infiltrating ductal carcinoma grade 3, triple receptor negative with biopsy proven metastatic ipsilateral axillary lymph node (ALN) were included. Index cancer size mean = 2 cm. PEM and MRI studies were interpreted by consensus of two radiologists (fellowship- trained in Mammography and the other also board certified in Nuclear Medicine). Subjective assessment of PEM based on intensity of uptake, categorized as: none, minimal and significant. Quantitative PEM analysis included size and max PEM uptake value. Gold standard chosen was pathological response on mastectomy or lumpectomy categorized as: underestimation (<70% of longest dimension), equal estimation, overestimation (>130%). **Results:** Significant uptake on PEM and heterogeneous enhancement with rapid uptake and wash out kinetics on MRI were observed in the index cancer and ALN on subjective analysis. No additional lesions identified on PEM or MRI. In 2 patients, average reduction in size of the index cancer and ALN was 96% by PEM and 91% by MRI with equal estimate of pathological response in PEM and MRI. **Conclusion:** Preliminary PEM data from 2 patients shows promising results in more accurate assessment of final tumor burden than MRI after NAC. Further progress in this ongoing research can help demonstrate role of PEM as a more accurate predictor of tumor response to NAC.

P0944

Predictors of Sentinel Node Metastatic Involvement in patients with Breast Cancer and Follow up

A. Andres, A. Santapau, L. Tardin, A. Parra, P. Razola, E. Rambalde, E. Prats, S. Ayala, J. Banzo; Hospital Clinico Universitario, Zaragoza, SPAIN.

Aim: To evaluate the factors that can predict the status of sentinel node (SN) and its follow up. **MATERIALS AND METHODS:** We evaluated 221 cases of breast cancer (217 women, three bilateral, and one man), 27 to 88 years old. We performed preoperative detection of SN, planar imaging and SPECT / CT, and intraoperative detection with hand held gamma probe. SN analysis was made using hematoxylin-eosin and immunohistochemical techniques. We reviewed estrogen and progesterone receptors status, breast lymphovascular invasion, levels of Ki67, multifocality, Her2 status and lymphoscintigraphic degree of uptake of SN. The cancer histology was infiltrating ductal (76'9%), intraductal high grade (9'1%), invasive lobular (6'7%) and other histologies (7'3%). The 67.2% were T1 and 32'8% T2. **RESULTS:** The status of SN was negative in 154/221(69'7%) cases, positive in 63/221 (28.5%) [metastases (17'6%), micrometastases (5'9%) and isolated cells metastases (5%)] and SN was not detected in 4/221(1'8%) and underwent an axillar lymphadenectomy (ALDN). When the SN was negative for metastasis the pathological characteristics of tumor were: 74'1% infiltrating ductal carcinoma and 13% intraductal (the SN of all intraductal carcinoma were negative), 74% T1, 87% unifocal and 14'3% had lymphovascular invasion. The immunohistochemical characteristics were: 70'7% positive estrogen receptors, 59'7% positive progesterone receptors, 33'8% Ki 67 was low and 8.4% intermediate and 76'1% Her2 negative. The lymphoscintigraphic radiotracer uptake was high or moderate in 74%. There was one false negative SN. In the follow up 11% had high level tumor markers (CA 15.3 and / or CEA) and 0.2% clinical disease progression. When the SN was positive for macrometastases the pathological characteristics of tumor were: 84'1% infiltrating ductal carcinoma, 49'2% T2, 81% unifocal and 49'2% had lymphovascular invasion. The immunohistochemical characteristics were: 76.2% positive estrogen receptors, 74'2% positive progesterone receptor, 36.5% low Ki 67 and 76.2% Her2 negative. The lymphoscintigraphic radiotracer uptake degree was mild in 34.5%. The 46'1% of patients with macrometastases and 7'6% with micrometastases in SN had lymph node metastases in ALDN. The follow up of these patients showed that 14'3% had high level tumor markers and 9'5% clinical disease progression. When the SN was not detected intraoperatively, the ALDN showed metastatic involvement in two patients. **CONCLUSION:** Patients with SN involvement are associated in greater proportion with ductal carcinoma, lymphoscintigraphic lower degree of uptake, lymphovascular invasion, multifocality and positive hormone receptors was higher. In the follow-up, progression was observed in higher proportion when the SN was positive.

P0945

Breast scintigraphy with breast-specific γ -camera (BSGC) and SPECT/CT in the preoperative identification of residual disease following neoadjuvant therapy

A. Spanu, G. Sarobba, G. Sanna, F. Chessa, I. Gelo, S. Nuvoli, G. Madeddu; Unit of Nuclear Medicine. University of Sassari, Sassari, ITALY.

Aim. Both BSGC scintigraphy and SPECT/CT have proved effective diagnostic tools in the detection of primary breast cancer (BC). In the present study we compared the two procedures in the preoperative identification of residual disease in BC patients following neoadjuvant therapy. **Methods.** Thirty-five consecutive BC patients, aged 26 to 82 yrs, scheduled to surgery following neoadjuvant chemo (28 cases) or

hormone (7 cases) therapy were studied. Ten min. after the i.v. injection of 740 MBq of ^{99m}Tc -tetrofosmin, all patients underwent breast scintigraphy in both cranio-caudal and medio-lateral oblique views (600 sec./view) using a high resolution BSGC. A SPECT/CT study was then acquired using a dual head gamma camera integrated with a x-ray tube for low-dose CT, including both breasts in the field of view. Scintigraphic data were correlated with surgical histopathological findings in all cases. Results. At surgery, 28/35 (80%) patients had breast residues (microscopic in 4/28 cases and macroscopic in 24/28 cases), while the remaining 7/35 (20%) patients had a complete remission without any evidence of residual disease. BSGC scintigraphy resulted positive in 27/28 patients with residual disease, while SPECT/CT in 24/28 (sensitivity: 96.4% and 85.7%, respectively; $p>0.05$) cases. A precise definition of breast quadrant localization was also given with both procedures in all positive cases in association with a correct tumor extension. BSGC scintigraphy was false negative, concordantly with SPECT/CT, in one patient who had microscopic tumor foci scattered in a fibrotic area. SPECT/CT was false negative in 3 further patients (one with a microscopic invasive ductal carcinoma, one with a macroscopic mucinous carcinoma and one with a macroscopic invasive lobular carcinoma). Both procedures were true negative in all 7 patients with complete remission (specificity: 100%). Conclusion. In our series, both BSGC scintigraphy and SPECT/CT proved highly sensitive diagnostic tools in the preoperative identification of residual breast carcinomas following neoadjuvant therapy, and without false positive findings. However, BSGC scintigraphy proved more sensitive than SPECT/CT, especially in cases with minimal residual disease and with tumor characterized by low metabolism and slow growth rate. Thus, BSGC scintigraphy should be preferred, but SPECT/CT remains a useful alternative when BSGC is not available.

P0946

Prognostic Value of 18F-FDG-PET/CT and Correlation between 18F-FDG Uptake and Hormone Receptors for a Suspect of First Breast-Cancer Recurrence in Women Treated with Curative Intention

A. Ortiz de Tena, I. Borrego Dorado, R. Fernandez Lopez, I. Acevedo Banez, R. Álvarez Perez, P. Gomez Camareno, M. Ruiz Borrego, R. Vazquez Albertino; Hospital Universitario Virgen del Rocío, Sevilla, SPAIN.

OBJECTIVE: To establish the prognostic value of 18F-FDG-PET/CT and to evaluate the correlation between 18F-FDG uptake and the hormone receptors (estrogen and progesterone), for unidentified/unconfirmed suspect of first breast-cancer recurrence in women treated with curative intention **MATERIALS AND METHODS:** Retrospective study of 107 consecutive women (mean age 62 years - range 34-87) with breast cancer treated with curative intent, who had an unidentified/unconfirmed suspect for first recurrence. Exclusion criteria: Previously known metastatic disease. All patients underwent 18F-FDG-PET/CT scan. Results were confirmed by histology ($n=13$) or by clinical-radiological follow-up ($n=94$). The maximum SUV cut off level with predictive value was calculated by ROC Curve. The survival was analyzed by Kaplan-Meier's test. In a subgroup of 82 patients, Maximum standardized uptake values (SUVmax) were compared with estrogen (ER) and progesterone receptors (PR). For the evaluation of relationship between tumor SUVmax values and hormone receptors, statistical analysis were performed using Mann-Whitney U Test and Pearson correlation coefficient and "p" values of less than 0.05 were considered to indicate statistically significant differences. **RESULTS:** 18F-FDG-PET/CT scan was negative in 41 and positive in 66 patients, with 2 false positive and no false negative results. Fifty-seven patients (53.2%) were classified as stage IV (according to the TNM staging classification) by 18F-FDG-PET/CT scan. Mortality rate (2 years) was 14.95%. Disease-free survival was 92.7% (38/41) in 18F-FDG-PET/CT scan-negative patients and 13.6% (9/66) in positive cases. Overall survival was 97.6% (40/41) and 80.3% (51/66) in 18F-FDG-PET/CT scan negative and positive patients respectively. A SUV cut-off value of > 5.55 was considered as predictive for mortality (area under the curve 0.77; Confidence interval 0.659-0.897). Tumors with negative ER [($n=33/82$); SUVmax median (min-max): 7.3 (0.7-18.7)] and negative PR [($n=36/82$); SUVmax median (min-max): 6.9 (0.7-18.7)] were associated with higher SUVmax values ($p = 0.01$) In addition 18F-FDG-PET/CT scan detected 4 second primary tumors (2 lung, 1 thyroid, 1 colon cancers). 18F-FDG-PET/CT scan modified therapeutic approach in 87 patients (81.3%). **CONCLUSIONS:** 18F-FDG-PET/CT can predict, in patients with suspect for first breast-cancer recurrence without previously known metastases, which ones among them have a poor prognosis, thus modifying management in a high percentage of patients. In addition, strong relationships were detected between the negativity of ER and PR and SUVmax values.

P0947

Lymphoscintigraphy for sentinel node detection in breast cancer reveals that removal of all positive nodes is useful

I. Sabalich¹, G. Fazzi¹, P. Giovenali², E. Francesconi¹, P. Gerli³, A. Rulli⁴, H. Sinzinger⁵, B. Palumbo¹; ¹Nuclear Medicine, Perugia, ITALY, ²Pathological Anatomy, Perugia, ITALY, ³Surgery, Perugia, ITALY, ⁴Breast Unit, Perugia, ITALY, ⁵Nuclear Medicine, Vienna, AUSTRIA.

AIM. Lymphoscintigraphy for sentinel node detection in breast cancer patients can evidence multiple radioactive nodes. To evaluate whether the hottest node is the sentinel node, we retrospectively investigated patients undergoing lymphoscintigraphy for sentinel node biopsy surgically treated. **MATERIALS AND METHODS.** We retrospectively investigated 329 breast cancer women undergoing lymphoscintigraphy and sentinel node biopsy at our institution during the period January 2009-March 2012. Fifty-seven (17.3%) out of the 329 patients showed multiple nodes. Each patient presented 1-4 radioactive nodes (mean 2.2 nodes) and all were surgically removed and evaluated by standard pathological analysis. To each patient filtered ^{99m}Tc nanocolloid was administered. The activity (37 MBq) was divided into four syringes and injected into the breast parenchyma around the tumor site. Lymphoscintigraphy was performed by a dual-headed gamma camera (MillenniumVG, G.E.). Images were acquired in anterior and lateral projections immediately as well as, 15 and 30 minutes after injection. If no sentinel node was identified, an additional image was obtained at 60 minutes. Lymphoscintigraphic mapping was considered successful if a focal area of radiotracer uptake was observed separate from the injection site. An intraoperative gamma probe (Gamma Detection System, Neo 2000) was used to measure counts in background, liver, breast injection site and axilla. The region in the axilla with the highest counts was marked on the patient's skin. Intraoperatively, 5 mL of isosulfan blue dye (Lymphazurin; Zenith Parenterals, Rosemont, IL) were injected around the tumor site. At 5 min, an axillary incision was made and sentinel node biopsy was performed. A node was considered a sentinel node if it exhibited blue staining at surgery or if after its removal no significant residual axillary radioactivity was measured, or both. All sentinel nodes were excised. **RESULTS.** In 78.3% of the 329 patients, nodes identified by lymphoscintigraphy were negative, while in 21.7% they were neoplastic. In 8 (14%) out of the 57 patients with multiple radioactive nodes (2 hot nodes), metastases were not found in the hottest one but in the other less active, while in 49 (86%) the hottest lymph node was neoplastic. Seven patients with metastases in the second node had grading 2, one had grading 3. **CONCLUSION.** Removal of multiple radioactive nodes is useful to avoid false negative judgement, although - due to the early screening programs for breast cancer - the number of patients with metastasis in the less active node is low.

P0948

Influence of the location of breast cancer in upper-outer quadrant in the detection of axillary sentinel lymph node (SLN) with intratumoral administration of tracer

R. Díaz-Expósito¹, I. Casáns-Tormo¹, A. Orozco-Molano¹, C. Rocafuerte-Ávila¹, S. Prado-Wohlwend¹, Á. Martínez-Agulló², A. Julve-Parreño³; ¹Nuclear Medicine. Hospital Clínico Universitario de Valencia, Valencia, SPAIN, ²General Surgery. Hospital Clínico Universitario de Valencia, Valencia, SPAIN, ³Radiology. Hospital Clínico Universitario de Valencia, Valencia, SPAIN.

Aim. The location of breast cancer in upper outer quadrant (UOQ) might difficult the detection of axillary SLN because of its proximity, when we use intratumoral administration (IA) of tracer, the one that guarantees access to true SLN that communicates the lymphatic channel directly with the tumor. **Material and methods.** We analyzed 160 consecutive patients, 68 (42.5%) with tumor located in UOQ. The group of study were 48 of them with IA of tracer (27 right - 21 left UOQ), mean age 58 ± 10 (35-84) years, 40/48 (83.3%) with infiltrative ductal cancer, all with IA of ^{99m}Tc albumin nanocolloid (1-3mCi) the same day of surgery (previous 24h in 8 patients) by palpation (24 patients) and guided by ultrasound or stereotaxy in the non palpable lesions (24 patients). We performed planar lymphoscintigraphy (PL) in different projections, with external mark of SLN in surgical position and intraoperative detection always with hand held gammaprobe and with portable gammacamera (PG) in 14 patients. The results were compared with surgical findings, SLN intraoperative pathologic analysis and delayed immunohistochemical analysis. **Results.** We have detected SLN in 47/48 (97.9%) patients (44 with PL and 3 at the operation room with hand held gammaprobe), all in homolateral axilla, being necessary periareolar reinjection in 3 of them. In 40/48 (83.3%) patients we could remove the SLN, but in 7/44 (15.9%) patients with SLN detected with PL, we did not identify significant activity at surgery. There was SLN involvement in 11/40 (27.5%) patients, performing lymphadenectomy, that showed 7 patients without pathological findings and 4 with more nodes involved. In the 8 patients without any SLN removal, lymphadenectomy showed only 1 with node metastasis. 7 patients had non-palpable tumor. We found 4 factors that could have conditioned some difficulty to detect SLN in these 8 patients: faint uptake in PL (4 patients), age above the mean (7), previous 24h injection (3) and proximity of the SLN to the injection point in 3 of the patients. Some of these factors were coincident at the same patient. **Conclusions.** The results of the detection of axillary SLN with intratumoral administration in breast cancer located in upper outer quadrant are similar to the described in other locations. Only in 3 patients the lesion proximity could have been the cause of no detection of the SLN, therefore we consider intratumoral administration also the first choice to detect SLN in upper outer quadrant located lesions.

P0949**Recurrent Breast Cancer Involving the Brachial Plexus Identified by FDG PET/CT**

P. J. Peller, A. Crush, R. Murphy; Mayo Clinic, Rochester, MN, UNITED STATES.

Purpose: Identifying malignant involvement of the brachial plexus in breast cancer patients is challenging from both a clinical and an imaging perspective. We evaluated the ability of PET/CT to detect malignant involvement of the brachial plexus in patients with a prior history of breast cancer. **Methods:** A retrospective analysis of a prospective database of patients presenting with neuropathy and a prior history who underwent a FDG PET/CT scan from 9/01/05 to 9/01/09 was undertaken. Patients were included if the neurologic examination documented a regional pain syndrome, motor abnormalities or sensory deficits and PET/CT was ordered within 1 month of presentation. Brachial plexus involvement was confirmed by biopsy and/or resolved with cancer treatment. The location of brachial plexus involvement and other sites of disease identified on PET/CT were correlated to the pathologic results and clinical outcome. **Results:** Arm pain or peripheral neuropathy led to PET/CT evaluation in 81 patients (mean age 67.3±9.6) who had subsequently biopsy or clinical follow-up. FDG uptake indicative of recurrent malignancy was identified in the brachial plexus on PET/CT scans in 66 patients (81.5%). Forty-three patients had biopsy confirmation and the rest demonstrated resolution on PET/CT following treatment. The linear FDG uptake within the thickened plexus ranged from mild to intense (SUVmax= 2.1-12.3; mean 5.6). In 3 patients discontinuous plexus involvement was seen and confirmed by biopsy as skip lesions. In all but 5 patients, the brachial plexus was the only site of breast cancer recurrence identified on PET/CT. In the 15 PET/CT negative patients, 12 had positive MR. Biopsy or clinical follow-up determined that these 12 patients did not have brachial plexus disease but MR signal abnormalities were due to from post-treatment radiation or surgical changes. **Conclusions:** PET/CT readily detects breast cancer involvement in the brachial plexus in presenting with upper extremity symptoms. FDG PET/CT was able to differentiate an active tumor from post-treatment changes.

P0950**The role of FDG PET/CT in initial staging of patients with newly diagnosed breast cancer with an emphasis on distant metastasis**

A. Aliyev¹, M. Halac¹, S. Yilmaz¹, M. Erkan², S. Asa¹, M. Ozhan¹, S. Sager¹, F. Aydogan³, K. Sonmezoglu¹; ¹Department of Nuclear Medicine, Cerrahpasa Faculty of Medicine, Istanbul University, Istanbul, TURKEY, ²Department of Nuclear Medicine, Duzce University Medical Faculty, Duzce, TURKEY, ³Department of General Surgery, Cerrahpasa Faculty of Medicine, Istanbul University, Istanbul, TURKEY.

It is accepted that axillary or regional lymph node involvement with metastatic tumor and the presence of distant metastasis are the two most important prognostic factors in patients with breast cancer. The literature on the performance of FDG PET for detecting regional lymph node and distant metastasis in newly diagnosed breast cancer is limited. In this retrospective study, we aimed to evaluate the role of FDG PET/CT in the detection of extraaxillary regional nodal and distant metastasis. A total of 154 patients with breast cancer (149 female, 5 male) who underwent FDG PET/CT for primary staging were enrolled in this study. All the patients were diagnosed by tru-cut/core or FNAB. Twenty-nine patients were in T1 stage, 81 in T2, 14 in T3 and 30 were in T4 stage. Distant metastases were seen in 41.6% out of 154 patients with breast cancer who underwent FDG PET/CT for primary staging. Of these 29.9% had bone/bone marrow metastasis, 11% lung metastasis, 18.8% mediastinal lymph node metastasis, 5.8% liver metastasis, 13.6% other organ/system metastasis and 9% contra-lateral axillary-supraclavicular-internal mammary lymphadenopathies. According to the T staging percentage the distant metastasis are as follows: 27.5% of 29 T1 stage patients, 45.6% of 81 T2 stage patients, 50% of 14 T3 stage patients and 40% of 30 T4 stage patients had distant metastasis. T stage of the disease is positively correlated with presence of distant metastasis until T3. As a conclusion, FDG PET/CT is a useful imaging modality to identify extra-axillary regional nodal and especially distant metastasis in the initial staging of breast cancer and can replace conventional imaging modalities. Therefore, accurate staging of breast cancer at the time of the initial diagnosis has a major impact on the choice of therapeutic modalities that are selected for optimal management of these group patients.

P54-2 - Tuesday, October 30, 2012, 16:00 - 16:30, Poster Exhibition Area

Oncology Clinical Science: Lung**P0951****Pet/Ct in the Evaluation of Early Treatment Response and Its****Contribution to Patient Management in Advanced Stage Non Small Cell Lung Cancer**

U. Ogur¹, F. Sen¹, A. T. Akpınar¹, G. Ozkaya², D. Kumtepe Aygun¹, B. Sevilimis¹; ¹Uludağ University Faculty of Medicine, Dept. of Nuclear Medicine, Bursa, TURKEY, ²Uludağ University Faculty of Medicine, Dept. of Biostatistics, Bursa, TURKEY.

Aim: Advanced stage non small cell lung cancer (NSCLC) is a leading cause of cancer-related deaths. Currently, as a molecular imaging modality, PET/CT has been accepted to have an essential role in the evaluation of treatment response. The aim of this retrospective study was to evaluate the early treatment response after 2 or 3 cycles of chemotherapy by PET/CT and to investigate the potential contribution of PET/CT to treatment strategies. **Materials and Methods:** A total of 94 patients with histopathologically proven NSCLC, were included in this study in whom the early treatment response evaluation was made by PET/CT after 2 cycles (group 1; n=27), or 3 cycles of chemotherapy (group 2; n=67). Patients were followed-up for 12 to 44 months. Groups were classified into four metabolic response categories such as progressive metabolic disease (PMD), stable metabolic disease (SMD), disease with partial metabolic response (DPMR) and disease with marked metabolic response (DMMR). Both groups and metabolic response subgroups were analyzed with Kaplan-Meier method for progression-free survival and overall survival, statistically. Regression analysis was used for independent variables. In patients that still survived and had no change in chemotherapeutic regimen after interim PET/CT and in patients that had an alteration in treatment, a third PET/CT scan were undertaken afterwards to evaluate the final metabolic responses. **Results:** No statistically significant difference was found between groups for PFS. In group 2, with a great number of stage 4 patients, shorter OS was determined. There was a statistically significant relationship between metabolic non-responders with PMD and SMD and metabolic responders with DPMR and DMMR for PFS and OS (P<0.001). When metabolic progression, that was not apparent on interim PET/CT, was detected on final PET/CT in patients in whom the chemotherapy finished without a change in regimen, it led to a change in metabolic response categories and necessary treatment modifications were made thereafter. A third PET/CT imaging was performed to reevaluate the metabolic response in patients receiving second-line chemotherapy after interim PET/CT and a third-line chemotherapy was planned. **Conclusion:** According to the data of this study, it appears that PET/CT can accurately predict the metabolic responses, be useful to detect which patient will benefit from surgery, and change patient management significantly. It is obvious that interim PET/CT is a valuable method with its potential predictive value of metabolic response on the third PET/CT performed at the end of the treatment or after alteration in treatment.

P0952**18F-FDG PET-CT evaluation of ground-glass opacities and part-solid lesions regarding the new IASLC/ATS/ERS 2011 adenocarcinoma classification**

E. Franquet, M. Simo Perdigo, G. Cuberas Borros, E. Pallisa, M. Montero, M. Boronat Ferrater, M. Sabater, J. Castell-Conesa; Hospital Universitari Vall D'Hebron, BARCELONA, SPAIN.

Clinical Statement IASLC/ATS/ERS in 2011 has changed the adenocarcinoma classification, and it might have imaging diagnostic implications regarding to 18F-FDG PET-CT role. **PURPOSE** To evaluate the clinical usefulness of the FDG PET-CT in the assessment of patients with lung ground-glass opacities (GGO) in order to differentiate between pre-invasive (including *in situ* adenocarcinomas) and invasive adenocarcinomas (ADK), according to the new classification of lung adenocarcinoma (IASLC/ATS/ERS 2011); to establish a correlation between SUV, the GGO and solid volumes of the lesions and histopathology, and to lay down its role in the TNM staging. **MATERIAL AND METHODS** This retrospective study included 17 patients (10 men, mean age 70±8.3) with 19 GGO nodules, who underwent FDG PET-CT and HRCT before surgery (12 atypical resections, 7 lobectomies). Both GGO and solid volumes were measured in the HRCT, creating ROIs in each transaxial slice. SUVmax and solid percentage were obtained for each lesion. **RESULTS** Total histology results were 9 pre-invasive lesions (6 nonmucinous ADK *in situ*, 1 mucinous ADK *in situ* and 2 atypical adenomatous hyperplasia) and 10 invasive ADK (4 well-differentiated G1, 4 moderate-differentiated G2, 2 poor-differentiated G3). There were no significant differences (p=0.18) in SUVmax (mean SUVmax 1.2±0.58) between pre-invasive (1.01±0.57) and invasive lesions (1.37±0.56). All the pre-invasive lesions had SUVmax less than 1.56. However, there were significant differences in SUVmax, if we grouped pre-invasive lesions with G1 (p=0.007). SUVmax was significant positively correlated with GGO volume (r=0.477, p=0.039), but it was not neither with volume of solid nor solid percentage. There was not a correlation between solid percentage and pathology. PET-CT correctly staged the mediastinal lymph nodes involvement (N) according to the surgical mediastinal verification. **CONCLUSION** In this preliminary study, in similar radiological lesions (GGO) PET-CT could differentiate those with bad prognostic factors (moderate-to-poor differentiated lesions). However, it could not separate pre-invasive from invasive lesions, although there is a tendency for pre-invasive lesions to have a lower SUV than invasive. There is a correlation between

SUVmax and GGO volume. PET-CT and postsurgical N staging were concordant. Authors: E. Franquet, M. Simó Perdigó, G. Cúberas Borrós, E. Pallisa, M.A. Montero, M. Boronat, M. Sabaté, J. Castell

P0953

Prediction of occult lymph node metastasis in clinically N0 squamous cell lung carcinoma

D. Kim, B. Song, C. Hong, S. Lee, B. Ahn, J. Lee; Kyungpook National University, Daegu, KOREA, REPUBLIC OF.

Objectives: The aim of this study is to investigate preoperative predictors of occult lymph node metastasis (OLM) in squamous cell lung carcinoma (SqCC) patients who are clinically node-negative (cN0) before surgery. **Methods:** Forty-two clinically node-negative SqCC patients (M/F=41/1, mean age, 64.4±7.8), diagnosed by preoperative workups (biopsy, conventional chest CT and PET/CT) were enrolled. All patients had undergone surgical resection of primary tumor with lymph nodes dissection. SUVmax, metabolic tumor volumes and metabolic diameter were obtained with a transaxial image with highest FDG uptake. Metabolic index (MI) was calculated as SUVmax × metabolic diameter. Total lesion glycolysis (TLG) was calculated by multiplication of MTV and its SUVmean. Primary tumor size on enhanced CT was measured. Pretreatment PET or CT variables were analyzed for predictability of OLM. **Results:** Eight (19.0%) of 42 patients were found to have OLM by pathologic evaluation of specimens. Among the metabolic tumor parameters, only SUVmax and metabolic diameter was significantly higher in patient with OLM (P=0.029, 0.034 respectively). Meanwhile, MI showed only trends toward significance (P=0.057). However, MTV-2.5 (P=0.116), MTV-25% (P=0.124), MTV-50% (P=0.122), MTV-75% (P=0.264), TLG-2.5 (P=0.127), TLG-25% (P=0.124), TLG-50% (P=0.120) and TLG-75% (P=0.222) were not associated with OLM. More than 3cm in tumor size was higher in pathologic positive group. (P=0.028). The cut-off value of 8.8 for SUVmax was determined using a receiver operating characteristic (ROC) curve. And The cut-off value of 31mm for metabolic diameter was determined using a receiver operating characteristic (ROC) curve. **Conclusions:** SUVmax and metabolic diameter were determined by F-18 PET/CT demonstrated a statistically significant relationship with OLM in patients with cN0 squamous cell lung carcinoma. Therefore patients with high SUVmax and metabolic diameter should be cautiously evaluated for LN metastasis.

P0954

Role of 18F-FDG PET/CT in preoperative staging of non-small-cell lung cancer

K. Nikoletic¹, D. Srbovan¹, J. Mihailovic¹, E. Matovina¹, D. Kozic¹, V. Kolarov², N. Prvulovic¹, I. Miucin-Vukadinovic¹; ¹Institute of oncology of Vojvodina, Sremska Kamenica, SERBIA, ²Institute for Pulmonary Diseases of Vojvodina, Sremska Kamenica, SERBIA.

Aim: Therapeutic choice of non-small-cell lung cancer in stage I, II or IIIA is surgery, while advanced lung cancer (stage IIIB and IV) has to be treated with chemo/radiotherapeutic approach. Since proper staging of NSCLC is crucial for further therapy, aim of this study was to determine role of 18F-FDG PET/CT in preoperative staging. **Materials and methods:** From January 2010 to March 2012 we analyzed 34 patients (17 female, 17 male; aged 46-73, mean 56.16±7) who were referred to our Institute because of preoperative lung cancer staging. Histology type of cancer included: adenocarcinoma (16), squamous cell carcinoma (14) and large cell carcinoma (4). Diagnosis was obtained by bronchoscopy or TTP (trans-thoracic needle biopsy). Before PET/CT examination, most of the patients were considered stage II or IIIA based on CT results. Patients were examined with whole-body 18F-FDG PET/CT approximately 60-90 minutes following iv. injection of 18F-FDG. Images were interpreted independently by 2 nuclear medicine physicians and 1 radiologist. Impact of the images result on therapeutic management of patients was evaluated on the basis of clinical decision obtained from patient files. **Results:** All patients were positive on PET/CT scan. All 34 patients had intense foci in primary tumor with SUV values ranging from 5.42-29.75 (mean 10.17). Other than in primary tumor, focal uptake of 18F-FDG was noted in 22 patients (47%): ipsilateral lung tissue (6), contralateral lung tissue (4), ipsilateral lymph nodes (6), contralateral mediastinal lymph nodes (4), distant metastases (7) that were localized in bones, suprarenal gland or contralateral axillar lymph nodes. In further follow up, 8 patients were lost for data analysis. Out of remaining 26 patients, 17 (65.4%) were operated: in 16 pathohistology confirmed lung cancer and in 1 patient lung tumor turned out to be breast cancer metastases (preoperative bronchoscopy: Ca squamocellulare). In 9 (34.6%) patients PET/CT finding prevented unnecessary surgery and they were treated with chemo/radiotherapy. **Conclusion:** 18F-FDG PET/CT is a useful imaging modality in preoperative staging of NSCLC (in our study stage II and IIIA) with impact on future therapeutic management on patients in 34.6% cases.

P0955

Diagnostic Value of FDG PET/CT in a Low Dose CT Lung Cancer Screening Program

 Springer

M. J. Garcia-Velloso, G. Bastarrika, J. Zulueta, M. D. Lozano, C. Caicedo, J. M. Marti-Climent, U. Montes, J. A. Richter; Clinica Universidad de Navarra, Pamplona, SPAIN.

Objective: To evaluate the diagnostic accuracy of FDG PET/CT in predicting the malignancy of radiologically indeterminate pulmonary nodules detected in a low-dose spiral computed tomography (LDCT) based lung cancer screening program. **Methods:** Asymptomatic smokers were prospectively studied in an early lung cancer detection protocol conducted following the I-ELCAP program. FDG PET/CT was done in 60 non-calcified solid lung nodules (NCLN) larger than 10 mm in diameter with non-cicatricial aspect on LDCT and 30 smaller nodules showing growth in follow-up. FDG PET/CT was called positive if the NCLN showed focal uptake and SUVmax was calculated. Histology or follow-up by means of LDCT were used for final diagnosis. **Results:** FDG PET/CT was carried out in 89 patients with 90 NCLN. The median nodule diameter was 12 mm (IQR 8 - 18 mm). FDG PET/CT imaging correctly identified 83 NCLN with an accuracy of 92%. The values of sensitivity, specificity, PPV and NPV were 84%, 97%, 93% and 92% respectively. PET/CT was positive in 29 NCLN, of which 27 were diagnosed with lung cancer and had a median SUV of 5.4 (IQR 2.2-8.1). The lowest SUV was 0.6 and the highest 15.6, belonging to 25 mm and 48 mm nodules respectively. There were 2 false positive PET scans, granuloma and silico-anthraxis. Sixty-one nodules did not show focal FDG uptake, 5 of which were diagnosed stage IA adenocarcinoma after growth was observed on 3-month follow-up LDCT scans, and 4 of them had bronchoalveolar features in part of the tumour. In 17 patients lung cancer was diagnosed at baseline screening, and 15 lung cancer were diagnosed among the annual repeat LDCT. Nineteen (59%) patients were stage I, 3 (9%) patients stage II, 5 (16%) patients stage III and FDG PET/CT detected distant metastases in 5 (16%) patients. Establishing a cut-off SUVmax<2.5 to rule out neoplasm, sensitivity and NPV would have decreased to 63% and 83%, respectively, but specificity and PPV would have increased to 98% and 95%, respectively. **Conclusions:** FDG PET/CT may improve screening for lung cancer in high-risk patients. FDG PET/CT improved the diagnostic yield of LDCT and reduced the number of invasive procedures performed for histologically benign nodules. The SUVmax did not contribute to improve the sensitivity of the qualitative visual analysis. Although FDG PET/CT rendered FN results, when combined with short-term follow-up with LDCT, 68% lung cancers were diagnosed in early stages.

P0956

Stage I Non-Small Cell Lung Cancer: adenocarcinoma vs squamous cell carcinoma. Evaluation of morphologic characteristics (CT) and functional activity (18FDG PET-CT)

M. L. Calcagni¹, G. Treglia¹, A. Del Ciello², M. T. Congedo³, S. Taralli¹, A. Mulè⁴, D. Di Franco¹, L. Bonomo², A. Giordano¹; ¹Institute of Nuclear Medicine. Department of Bioimaging and Radiological Sciences. Università Cattolica del Sacro Cuore, Rome, ITALY, ²Institute of Radiology. Department of Bioimaging and Radiological Sciences. Università Cattolica del Sacro Cuore, Rome, ITALY, ³Department of Thoracic Surgery. Università Cattolica del Sacro Cuore, Rome, ITALY, ⁴Department of Pathology. Università Cattolica del Sacro Cuore, Rome, ITALY.

Aim. Adenocarcinoma and squamous cell carcinomas are the main histological types of non-small cell lung cancer (NSCLC). They are characterised by many genetic and epigenetic differences, which determine different biological and prognostic behaviours. Moreover, the prognosis is also related to the stage of the disease: patients in early stages have a favourable prognosis compared with those in advanced stages. Integrated 18F-fluoro-deoxyglucose positron emission tomography-computed tomography (18F-FDG PET-CT) is a functional technique used for staging in patients with NSCLC. Aim of our study was to evaluate whether adenocarcinomas and squamous cell carcinomas of the lung are also different in morphological characteristics and/or in functional activity. **Materials and Methods.** This retrospective study included sixty-one patients (42 males, mean age 67.5 ± 8.7 years) with stage I NSCLC, surgically treated. All patients underwent clinical and cardio-respiratory evaluation, diagnostic CT, and 18F-FDG PET-CT. According to the histology, all lung cancers were divided in two groups: adenocarcinomas and squamous cell carcinomas. For each tumour, the evaluated morphological and functional parameters were the following: size (cm), margins (regular or spiculated), density (solid or non-solid), and SUV maximum. For statistical analysis, un-paired T test was used for comparison. **Results.** The histology proved 41 adenocarcinomas and 20 squamous cell carcinomas. The majority of adenocarcinomas were moderately differentiated (66%), and the remaining were almost equally distributed between well and poorly differentiated tumours. On the contrary, the majority of squamous cell carcinomas were poorly differentiated (55%), only one was well differentiated, and the remaining were moderately differentiated. Significant difference (p=0.03) in the SUV max values between adenocarcinomas (4.89 ± 3.88) and squamous cell carcinomas (7.17 ± 4.45) was found. No significant differences in mean size (adenocarcinomas: 2.13cm ± 1.06cm; squamous cell carcinomas: 2.34cm ± 1.1cm), margins, and density of the lesions between the two groups were found. **Conclusion.** From our data, squamous cell carcinomas differed from adenocarcinomas only for the functional activity, and not

for the morphologic characteristics. The higher values of SUV max in squamous cell carcinomas further confirm that this histological type is more aggressive than adenocarcinoma. This finding could be partially attributed to the highest amount of poorly differentiated tumours in squamous type. The highest 18F-FDG uptake, which well reflects the biological aggressiveness of lung cancer, could suggest a worst prognosis also in early stages. Relationship between histological grading and the morphologic and functional characteristics is under investigation.

P0957

Role of F18-FDG PET-CT Imaging in 188 Patients in an Asbestosis Endemic Area for the Differential Diagnosis of Pleural Pathologies: Early Imaging versus Delayed Imaging

U. Elboga¹, M. Yilmaz¹, M. Uyar², Y. Celen¹, K. Bakir³, O. Dikensoy², C. Aktolun⁴, ¹Gaziantep University, School of Medicine, Nuclear Medicine Department, Gaziantep, TURKEY, ²Gaziantep University, School of Medicine, Pulmonary Disease Department, Gaziantep, TURKEY, ³Gaziantep University, School of Medicine, Pathology Department, Gaziantep, TURKEY, ⁴Tirocenter Nuclear Medicine Clinic, Istanbul, TURKEY.

OBJECTIVE: We previously presented our preliminary results in a small number patients of an ongoing clinical trial examining the role of F18-FDG PET-CT in the diagnostic work-up of pleural lesions in an asbestosis-endemic area in southeastern part of Turkey. In this report, we now aim to present the findings in a larger group of patients evaluating the role of F18 fluorodeoxyglucose positron emission tomography-computed tomography (F18-FDG PET-CT) in the differential diagnosis of pleural lesions including malignant pleural mesothelioma (MPM). **MATERIAL AND METHODS:** One hundred eighty eight patients (120 females, 68 males; age range 23-87 years) with pleural thickening, fluid, plaques or calcification on CT scan were examined with F18-FDG PET-CT. F18-FDG PET-CT was performed 1 hour after injection, but in 57 patients, delayed imaging of the thoracic region was also performed 2h after injection. F18-FDG uptake was evaluated visually and semiquantitatively using standardized uptake value (SUV). F18-FDG PET-CT findings were compared with histopathologic diagnosis. **RESULTS:** One hundred forty-five patients had increased F18-FDG uptake in pleural lesions but PET-CT results were negative in 43 patients. When compared with histopathological results in F18-FDG positive group, 127 patients had MPM, 18 had benign pathology. In FDG negative group, 12 patients had MPM, 31 had benign pathology. Of the 57 patients in whom delayed imaging was performed, 43 showed increased SUV but 14 had a decreased SUV on delayed images; in the increased SUV group, 26 patients had MPM, and 17 benign pathology (10 chronic granulomatous inflammation, 7 benign asbestotic plaque), and in the decreased SUV group, all patients had benign pathology (fibrosis, chronic inflammation, myofibrosis). **DISCUSSION:** FDG PET-CT is a useful imaging modality in differential diagnosis of malignant and benign pleural lesions. Decreased SUV in delayed imaging seems to be useful in differentiating benign from malignant pleural lesions.

P0958

The Optimality of Different Strategies for Staging of Non-Small-Cell Lung Cancer: A Health Economic Decision Analysis

R. Sogaard¹, B. M. Fischer², J. Mortensen², T. R. Rasmussen³, U. Lassen², ¹Centre for Health Services Research and Technology Assessment, University of Southern Denmark, Odense, DENMARK, ²Rigshospitalet, Copenhagen, DENMARK, ³Aarhus University Hospital, Aarhus, DENMARK.

Objectives To assess the expected costs and outcomes of alternative strategies for staging of lung cancer in order to inform a Danish National Health Service perspective about the most cost-effective strategy. **Methods** A decision tree was specified for patients with a confirmed diagnosis of non-small cell lung cancer. Six strategies were defined from relevant combinations of mediastinoscopy, endoscopic or endobronchial ultrasound with needle aspiration, and combined PET-CT with F18-fluorodeoxyglucose. Patients without distant metastases and central or contralateral nodal involvement (N2/N3) were considered to be candidates for surgical resection. Diagnostic accuracies were informed from literature reviews, prevalence and survival from the Danish Lung Cancer Registry and procedure costs from national average tariffs. All parameters were specified probabilistically in order to determine the joint decision uncertainty. The cost effectiveness analysis was based on the net present value of expected costs and life years accrued over a time horizon of 5 years. **Results** At threshold values for cost effectiveness around €30,000, it was found to be cost effective to send all patients to PET-CT with confirmation of positive findings on contralateral nodal involvement by endobronchial ultrasound. The result appeared robust in deterministic sensitivity analysis. The expected value of perfect information was estimated at €59 per patient, indicating that further research might be worthwhile. **Conclusion** The policy recommendation is to make combined PET-CT and endobronchial ultrasound available for supplemental staging of patients with non-small-cell lung cancer. However, the impacts of these strategies on patients' quality of life should be examined in future studies.

P0959

Characterization of Solitary Pulmonary Nodule using Fluorine 18-Deoxyglucose (¹⁸F-FDG) PET/CT: Study of 137 Patients

A. Martinez Lorca, M. Marin Ferrer, C. Escabias del Pozo, M. Coronado Poggio, D. Mendez Mareque, S. Rodado Marina, I. Santos Gomez, L. Martin Curto; Hospital Universitario La Paz, Madrid, SPAIN.

AIM: Characterization of indeterminate solitary pulmonary nodules (SPN) is an established indication of ¹⁸F-FDG-PET/CT. The aim of the study is to evaluate the diagnostic accuracy of PET/CT using ¹⁸F-FDG for the characterization of SPN in our clinical setting. **MATERIALS AND METHODS:** Retrospective study of 137 patients (p), 100 male and 37 female; mean age 68,9 ±12,47 with a range between 23-89 years, that underwent low doses PET/CT scan without intravenous contrast, between 2008 and 2011 for the evaluation of SPN. PET-CT images were interpreted using a visual analysis for pulmonary nodule uptake: (0+) no uptake; (1+, 2+, 3+) uptake more intense than lung parenchyma SPN was considered malignant when it showed an uptake higher than lung parenchyma. Final diagnosis was determined by pathologic analysis or radiological follow-up for at least 24 months. **RESULTS:** The definitive diagnosis was established through histopathology in 106p and through radiological follow-up in 31p. The mean SPN diameter was: 1,65±1,7(<1cm:39p, 1-2cm:52p, 3cm:46) and the SPN location: RUL 54, ML 8, RLL 19, LUL 39, LLL 10, Lingula 7. PET/CT findings: 51p 0+ uptake: (4p Carcinoid Tumor, 6p No malignant findings, 3p Fibrose Tumors, 4p Hamartomas, 2p Tuberculosis, 2p Pulmonary Fibrosis, 1p Pneumonia, 2p Adenocarcinoma, 27p no changes in CT control); 23p 1+ uptake (1p Benign Alveolar Tumor, 1p Hamartoma, 1p Tuberculosis, 1p Necrotic Granuloma, 1p Carcinoid Tumor, 9p Adenocarcinoma, 2p Squamous cell carcinoma, 2p Bronchioalveolar carcinoma, 1p Lymphoma, 4p no changes in CT control); 22p 2+ uptake (10 Adenocarcinoma, 1 Large cell carcinoma, 7p Squamous cell carcinoma, 1p Sarcoma, 1p Hemangioma, 1p Small cell carcinoma, 1p Carcinoid Tumor); 41p 3+ uptake (1p Tuberculosis, 2p Inflammatory Pseudotumor, 11p Adenocarcinoma, 5p Small cell carcinoma, 8p Large cell carcinoma, 14p Squamous cell carcinoma). PET/CT found 74p true positive, 45p true negative, 12p false positive and 6p false negative. PET/CT was found to have a sensitivity of 92% and specificity of 78%, a positive predictive value of 86% and negative predictive value of 88%. **CONCLUSIONS:** ¹⁸F-FDG PET/CT demonstrates to be good predictor of malignancy in the study of SPN with a NPV of 88%.

P0960

Lymphangitic Carcinomatosis in the Nonsmall Cell Lung Cancer Detected on FDG-PET/CT

M. Serdengecti¹, E. Varoglu¹, B. Kaya¹, O. Sarı², T. Guler¹, O. Ozbek¹, S. Keskin¹, D. M. Yavsan¹, K. Odevi¹, ¹Necmettin Erbakan University Medical Faculty, Konya, TURKEY, ²Selcuk University Medical Faculty, Konya, TURKEY.

OBJECTIVES: FDG PET/CT is widely used for staging of non small cell lung cancer (NSCLC). Lymphangitic carcinomatosis (LC) has poor prognosis and response to chemotherapy is rare. Although it has very typical appearance on the PET/CT, the diagnosis of LC sometimes may be difficult. The aim of this study is to diagnose LC using FDG PET/CT and evaluate the prognostic importance of LC in NSCLC. **MATERIALS AND METHODS:** A retrospective study was performed. 9 patients (8 M, 1 F, mean age: 54 ± 13.9) with histological diagnosis of NSCLC who had undergone thin-sliced contrast enhanced CT (ceCT) and whole body FDG PET/CT scans were identified. All patients had the signs of LC. We analyzed localizations of tumor and LC, their patterns and SUVmax measurements. **RESULTS:** The location of primary tumor was the right lung in 7 patients and the left in 2 patients. Coexisting LC lesions were shown ipsilateral in all patients. FDG PET/CT and ceCT results were well-matching for LC lesions. In 7/9 patients, there were also pathological mediastinal lymph nodes. Distant metastases was positive only 1 patient in adrenal gland. LC patterns were classified as lobar in 2, segmental in 1 and focal linear in 6 patients. Mean SUVmax was calculated as 3.1±1.4. **CONCLUSIONS:** It is very well known that LC is poor prognostic indicator but is not included in TNM classification. Most of the patterns of LC on FDG PET/CT are focal or linear and it shows hazy FDG uptake. The CT findings of LC sometimes may be difficult alone for diagnosis. Differential diagnosis of other causes of this type of appearance should be noticed. Our calculated mean SUVmax measurements are above from cut-off point. This parameter may be helpful to make accurate diagnosis. The limited number of patients of this study is not enough to determine prognostic significance of this finding. Follow up studies are necessary for this purpose.

P0961

2Years-survival analysis of patients with Non-Small Cell Lung Cancer by means of 2deoxy-2-[18F]fluoro-D-glucose Positron Emission Tomography: implications of Maximum Standardized Uptake Value (SUVmax)

N. Quartuccio¹, A. Cistaro², A. Campenni¹, E. Amato¹, P. Fania², P. L. Filosso³, F. Ceraudo⁴, M. Cucinotta¹, U. Ficola⁵, S. Baldari¹; ¹Department of

Radiological Sciences, Nuclear Medicine Unit, University of Messina, Messina, ITALY, ²Positron Emission Tomography Centre IRMET S.p.A., Turin, ITALY, ³Department of Thoracic Surgery, S. Giovanni Battista Hospital, Turin, ITALY, ⁴Department of Biological Sciences, University of Calabria, Cosenza, ITALY, ⁵Department of Nuclear Medicine, La Maddalena Hospital, Palermo, ITALY.

Aim: to evaluate the correlation between Maximum Standardized Uptake Value (SUVmax), % Δ SUVmax, diameter of primary lung lesion, 2years-disease-free survival (2y-DFS) and overall survival (OS) in patients with NSCLC in different stages (I-IV). **Materials & Methods:** 135 patients were divided in two groups (A and B). In group A (stage I-II) a pre-surgical FDG-PET/CT study was performed. Group B patients (stage III-IV) underwent 2 FDG-PET/CT scans, before and after cisplatin-based chemotherapy, and were classified in different classes of response (EORTC criteria). The relationship between SUVmax, tumor size and clinical outcome was evaluated by Student-t test. Then we calculated the cut-off for SUVmax and tumor size with the best prognostic significance (chi-square test). Probability of DFS was investigated through the univariate analysis of Kaplan Meier. Furthermore, in group B we evaluated the possible correlation between SUVmax and response to therapy (Student-t test) and the relationship between % Δ SUVmax and OS (chi-square test). **Results:** In Group A we found a significant correlation between SUVmax and DFS ($p=0.038$), but not between tumor size and DFS. The optimal cut-offs were 9.00 for SUVmax ($p=0.004$) and 30mm for tumor size ($p=0.005$). In fact patients with SUVmax<9 and diameter <30mm had an expected 2y-DFS of 88%, while it decreased to 40% if SUVmax was>9 and tumor was>30 mm. In Group B no significant correlation between SUVmax, tumor size and prognosis was found. Patients with Δ SUVmax<+25% showed a better OS than patients with Δ SUVmax>+25% ($p=0.0235$). **Conclusions:** At a follow up time of 24 months it is possible to correlate both SUVmax and size of the primary lung lesion with DFS and OS in patients affected by early stage (I-II) NSCLC. The most relevant evidence in stage I-II is that the combination of a dimensional cut-off (30 mm) and of a SUVmax cut-off (9) could identify a subgroup of patients that will have a higher risk of recurrence of disease (60%) within 2 years from surgery. On the contrary, no useful correlation between SUVmax, tumor size and clinical outcome of NSCLC patients in stage III-IV can be proved. In patients with advanced disease, only % Δ SUVmax could be considered a useful prognostic factor.

P0962

The Correlation of F-18 Fluorodeoxyglucose (FDG) uptake and Epidermal Growth Factor Receptor Mutation (EGFR) in Non-small Cell Lung Cancer

B. Degirmenci Polack¹, I. Oztop², N. P. Karahan¹, Y. Baskin³, O. U. Unal², G. Calibasi³, ¹Dokuzeyul University Faculty of Medicine Nuclear Medicine Department, IZMIR, TURKEY, ²Dokuzeyul University Faculty of Medicine Oncology Department, IZMIR, TURKEY, ³Dokuzeyul University, Institute of Oncology, IZMIR, TURKEY.

Defining somatic mutations in the tyrosine kinase (TK) domain of the epidermal growth factor receptor gene (*EGFR*) is important to select patients with non-small cell lung cancer (NSCLC) who can be treated with EGFR-specific TK inhibitors (TKIs). F-18 FDG PET/CT is widely used imaging method for evaluating staging, therapy response and prognosis in the patients with NSCLC. In this study we aimed to investigate F-18 FDG uptake patterns between mutation-positive *EGFR* and wild-type *EGFR* patients. **Methods:** A total of 25 NSCLC (21 male, 4 female; mean age :63.32 \pm 9.51) patients were included in the study. EGFR mutation analyses were performed with RT-PCR method for all the patients. F-18 FDG PET/CT imaging was obtained before the any treatment of the patients. F-18 FDG uptake was analyzed and SUVmax values were obtained for the primary tumors, mediastinal lymph node and distant organ metastases in both mutation-positive *EGFR* and wild-type *EGFR* patients. **Results:** EGFR mutations were found in five patients. Twenty patients had wild-type *EGFR*. The average size and SUVmax of the primary tumor in the patients with mutation- positive *EGFR* patients was 5.1 \pm 2.04 cm and 14.60 \pm 12.42, respectively. In EGFR mutation positive group, one patient is in stage 1, three patients in stage 3 and one patient in stage 4. In wild-type *EGFR* patients, the average size and SUVmax of the primary tumor were 4.2 \pm 2 cm and 10.57 \pm 5.60, respectively. In the wild-type *EGFR* group, 10 patients were in stage 3, two patients in stage 2, and eight patients in stage 4. The average SUVmax of mediastinal lymph node metastases were 4.86 \pm 3.44 and 7.90 \pm 4.47 in EGFR mutation positive and wild-type *EGFR* patients, respectively. All distant organ (adrenal gland, liver and bone) metastases in wild-type *EGFR* patients showed increased F-18 FDG uptake with the mean SUVmax of 7.97 \pm 5.20. There were bone and adrenal metastases with high FDG uptake in one patient with EGFR mutation positive. SUVmax values of the bone and adrenal metastases were 22.2 and 11.3, respectively. There was no statistically significant difference between two groups of patients in terms of SUVmax in neither primary tumors nor lymph node metastases. **Conclusion:** The primary tumor and metastases showed increased F-18 FDG uptake in both mutation-positive *EGFR* and wild-type *EGFR* group of patients. In this small sample group of NSCLC patients, F-18 FDG uptake and SUVmax do not seem to be

predictive for EGFR mutation. Further studies with large group of patients are needed.

P0963

Lung Cancer: The Value of PET and CT in the Tumor Size Measurement

E. Sürer Budak¹, F. Aydın¹, L. Dertsiz², F. Güngör¹, G. Özbilim³, S. Demirelli¹, A. Öner¹, G. Kaplan¹, M. Sipahi¹, A. Yıldız¹, ¹Akdeniz University Medical School, Department of Nuclear Medicine, Antalya, TURKEY, ²Akdeniz University Medical School, Department of Thoracic Surgery, Antalya, TURKEY, ³Akdeniz University Medical School, Department of Pathology, Antalya, TURKEY.

Objective: In this study, we compared the maximum morphological (CT) and functional (PET) tumor size with the histopathological (HP) size in order to determine which is the most compatible method correlating with HP size in lung carcinoma patients. **Materials and methods:** Forty lung carcinoma patients (39 men, 1 woman) diagnosed histopathologically from surgical resection materials were included in this retrospective study. The median age of the patients was 67.8 \pm 10.3 with a range of 44 to 81 years. While 20 CT scans were performed in our institute, other 20 were performed in other institutes. PET/CT scan was performed within the same week as the CT scan. In CT scans, morphological tumor sizes were measured three dimensionally by the longest transaxial section in the parenchymal and mediastinal screening window. Functional tumor sizes were also measured three dimensionally in PET scans. These two measurement values were compared with HP size by using Bland-Altman plotting. Bland-Altman plotting was also performed to define the 95% limits of agreement, which was presented as bias \pm 1.96 SD. **Results:** HP sizes were measured in a range of 1.2 to 7.5 cm. In Bland-Altman analyze, it was calculated as 0.2 \pm 2.9 cm and 0.2 \pm 2.2 cm (95% confidence interval Bias \pm 1.96 SD) for CT and PET respectively. Also when it was evaluated as % Bias, it was found 10.1 \pm 84 for CT and 11 \pm 64.6 for PET. **Conclusion:** According to the findings, PET measurements were more compatible with the HP sizes than the CT measurements. Also, it was found that both PET and CT had a tendency to measure larger than HP sizes. In our opinion, PET and CT are inappropriate techniques for determining the tumor size.

P0964

The Role of 18F FDG PET-CT in Staging and Outcome Prediction for Small Cell Lung Cancer (SCLC)

S. McKay¹, S. Han², N. Mohammed¹, **L. M. Tho¹**, ¹Beatson West of Scotland Cancer Centre, Glasgow, UNITED KINGDOM, ²West of Scotland PET-CT Centre, Glasgow, UNITED KINGDOM.

Aims Whilst the role for 18F FDG PET-CT is established in the management of non-small cell lung cancer, its role in staging and prognosis for small cell lung cancer (SCLC) remains uncertain. We set out to analyse outcomes for SCLC patients who underwent a baseline PET-CT in a large, tertiary oncology referral centre. **Materials and Methods** A retrospective review was performed on 42 SCLC patients (36 with potentially radically treatable disease on conventional workup [CW] ie. clinical assessment and CT) who underwent further assessment with PET-CT between 2008 and 2010. Univariate and multivariate analysis of variables potentially influencing overall survival was performed using cox regression analysis. **Results** Median age was 68.5 (50 to 84) years. 30 patients had died, median follow up for 12 survivors was 29.5 (17 to 47) months. According to TNM criteria, PET-CT upstaged nodal disease in 11/42 (26.2%) of patients. PET-CT uncovered occult metastases in 6/42 (14.3%) of patients, which was confirmed by MRI and/or serial CT imaging. In one patient (1/42), a false positive distant metastasis was disproven on MRI. In 2/42 patients CW positive nodes were PET-CT negative, and in 2/42 CW positive distant metastases were PET-CT negative. Overall PET-CT changed TNM stage in 20/42 (47.6%) patients, upstaging 15 (35.7%) and down-staging 5 (11.9%). PET-CT upstaged 7/42 (16.7%) from limited stage to extensive stage disease and downstaged 2/42 (4.8%) from extensive stage to limited stage disease, thereby altering radical versus palliative treatment intent in 9/42 (21.4%) of patients. Univariate analysis showed that CW (TNM) stage, PET-CT (TNM) stage and primary tumour (PT) SUVmax, but not age, significantly correlated with overall survival. On multivariate analysis, only PET-CT stage ($p=0.002$) and PT SUVmax ($p=0.023$) significantly correlated with overall survival. Average PT SUVmax for stage III/IV patients was significantly higher than stage I/II patients (13.6 versus 10.6, $p=0.030$). Median overall survival for PET-CT stage I/II patients was significantly longer than stage III/IV patients (24.0 versus 9.6 months, $p=0.002$). **Conclusion** Our data suggests that 18F FDG PET-CT plays a crucial role in staging and prognosis of SCLC patients. In nearly half of patients, PET-CT altered conventional workup TNM stage. Importantly, PET-CT influenced radical versus palliative treatment intent in 21.4% of patients. On multivariate analysis, primary tumour SUVmax significantly predicted for overall survival, and was significantly higher in patients with advanced stage III/IV disease. SUVmax may represent a potential biomarker in SCLC.

P0965

Ratio of SUVmax of N2 lymph nodes to primary tumor for preoperative staging of clinical stage IIIA non-small-cell lung cancer; a promising parameter to improve specificity of mediastinal node staging in a tuberculosis-endemic country

S. Oh¹, K. Kim¹, S. Park¹, H. Moon¹, D. Lee², J. Chung², ¹Seoul National University Boramae Hospital, Seoul, KOREA, REPUBLIC OF, ²Seoul National University Hospital, Seoul, KOREA, REPUBLIC OF.

Purpose: Precise lymph node (LN) staging is very important to determine treatment plan in patients with clinical stage IIIA non-small-cell lung cancer (NSCLC), but it is difficult to correctly diagnose nodal malignancy, especially in a region with a high prevalence of granulomatous disease. We investigated diagnostic accuracies of a ratio of maximum standardized uptake value (SUV_{max}) of N2 LN to primary tumor to predict positive LN. **Methods:** Among 186 patients who underwent FDG PET/CT for preoperative staging during the year of 2010, 20 patients (M:F=16:4, 69.5 ± 8.6 y) with clinical stage IIIA NSCLC were retrospectively enrolled. SUV_{max} of primary tumor (n=20) and N2 LNs (n=30) were measured, and ratios of SUV_{max} of N2 LNs to primary tumor (SUVr) were calculated. Pathology of N2 LN was confirmed via surgery (n=12) or endobronchial ultrasound guided biopsy (n=8). **Results:** Primary tumor was 9 adenocarcinomas, 9 squamous cell carcinomas, 1 large cell carcinoma, and 1 sarcomatoid carcinoma. Among 30 N2 LNs pathologically confirmed, 24 were positive and 6 were negative for cancer. SUVr (0.57 ± 0.47 vs. 0.27 ± 0.10 p=0.004) as well as SUV_{max} (3.5 ± 1.8 vs. 2.3 ± 1.1 p=0.043) of positive LNs was significantly higher than negative LNs, with stronger statistical significance than SUV_{max}. The receiver operating characteristics analysis revealed that area under curve was 0.77 for SUVr and 0.73 for SUV_{max}, and it was predictive of malignancy with SUVr of 0.43 (sensitivity 50.0%, specificity 100.0%, p=0.039), and SUV_{max} of 2.6 (sensitivity 83.3%, specificity 79.2%, p=0.125). **Conclusion:** We demonstrated that SUVr successfully predicted N2 LN malignancy in patients with clinical stage IIIA NSCLC. SUVr could be a promising parameter to improve specificity of mediastinal node staging in a tuberculosis-endemic country.

P0966

F-18 FDG PET/CT metabolic tumor volume correlates with epidermal growth factor receptor expression in patients with NSCLC

A. Nappi¹, S. Giacomobono¹, G. Improta¹, A. Nardelli², R. Gallicchio³, E. Soscia⁴, F. Leggiadro¹, A. Zupa¹, G. Giudice¹, D. Capacchione¹, G. Vita¹, C. Lequaglie¹, G. Storto¹, ¹IRCCS CROB, Rionero in Vulture (Pz), ITALY, ²IBB CNR, Rionero in Vulture (Pz), ITALY, ³Department of Biomorphological and Functional Sciences, University "Federico II", Napoli, ITALY, ⁴IBB CNR, Napoli, ITALY.

Aim: epidermal growth factor receptor (EGFR) mutations may be encountered in Non-small cell lung carcinoma (NSCLC) and represent a therapeutic option for implementing new target drugs. Its presence has not been related to the quantitative PET/CT lesions' assessment so far. We evaluated whether EGFR over-expression may correlate with metabolic tumor volume (MTV) and standardized uptake value (SUVmax) on PET in patients complaining with NSCLC. **Material and Methods:** 20 patients (mean age, 72±7 years) presenting NSCLC without loco-regional lymph-node involvement underwent surgery resection and specimens were assessed for EGFR mutations. F-18 FDG PET/CT was performed 3 ± 1 months before intervention and SUVmax as well as MTV (cm³; 42% threshold) of lesions were computed on reconstructed images. SUVmax and MTV values were correlated to the presence of EGFR mutation. **Results:** Twelve patients were found positive whereas eight did not show mutations and served as control. Mean SUVmax of lesions in patients presenting EGFR mutation was 7.1±1 and it was 9.2±3 in those who did not (p=0.8). MTV(cm³) of lesions was 47.8±30 and 13.0±3 (p=0.003) in patients with and without EGFR mutation, respectively. A significant correlation (r=0.76; p=0.008) was found between MTV and the presence of EGFR mutations whereas SUVmax did not correlate with EGFR overexpression (r=0.04; p=0.8). **Conclusion:** the quantitative assessment by MTV rather than SUVmax on F-18 FDG PET/CT correlates with EGFR mutation expression which represents a parameter to be considered on whether a neo-adjuvant therapeutic regimen by target drugs may be helpful in selected cases (individualized therapy).

P0967

Assessment of Adrenal Metastasis in Patients with Lung Cancer using F-18 FDG PET/CT

S. Aksoy, B. Dirlik Serim, F. Üstün, G. Durmus Altun; Trakya University, EDIRNE, TURKEY.

BACKGROUND: Lung cancer is the most common cancer leading to death in men and increasingly more common in women. An accurate preoperative staging approach is important for the appropriate treatment regime. Autopsy series have shown a high occurrence of adrenal metastases in patients with lung cancer,

-ranging from 35% to 59%. Therefore, characterizing the adrenal masses accurately is important when they are discovered in patients with lung cancer. Diagnostic histopathological approaches with biopsy is the gold standart however those are associated with complications. Adrenal gland metastasis, the sensitivity, specificity, and accuracy of PET/CT were 80%, 89%, and 84%, respectively. **PURPOSE:** The aim of this study was to assess whether the metabolic activity of primary lung tumor would predict the adrenal metastasis, and to investigate that relation within the histopathological groups. **MATERIALS and METHODS:** This retrospective study analyzed F-18 FDG PET/CT scans of 85 patients with lung cancer. Primary tumor size and SUVmax values of primary tumor and metastatic adrenal mass were calculated. The relation between pathological diagnosis, size and SUVmax values of primary lung tumor and the metastasis of adrenal gland were evaluated. **RESULTS:** Adrenal metastasis were detected in 17 of 85 patients on PET /CT. 23 (27%) patients with small cell lung cancer (SCLC) and 62 (73%) patients with non-small cell lung cancer (non-SCLC). SUVmax was calculated in primary tumor without adrenal mass (SUVmin: 5.7, SUVmax: 32.6 and SUVmean: 13.7) and with adrenal mass (SUVmin: 2.7, SUVmax: 17.7 and SUVmean: 9.7). A reverse correlation between SUVmax values of primary tumor and adrenal mass was detected (p=0.008). Primary lung tumors with low SUVmax group include more adrenal metastasis, statistically. There was no correlation between tumor size and adrenal metastasis (p=0.442). **CONCLUSIONS:** F-18 FDG PET/CT is an accurate, noninvasive technique for detecting metastatic adrenal lesions in patients with lung cancer. Besides PET/CT has the advantage of evaluating the primary cancer sites and detecting other metastases. A reverse correlation between SUVmax values of primary tumor and adrenal metastasis was detected. Previous studies were reported that metabolic activity of primary tumor related with staging of diseases, however, in our study surrenal metastasis reversely correlate SUVmax of primary tumor, for this reason it's need to be clarified with further investigation.

P0968

PET-CT performed for radiotherapy planning in lung cancer. Impacts on staging and subsequent treatment decision.

L. Geraldo, V. Camacho, A. Fernández, N. Farré, A. Ruiz, T. Eudaldo, A. Domènech, R. Jaller, I. Carrió; Hospital Santa Creu i Sant Pau, Barcelona, SPAIN.

Objective: To assess the impact of 18F-fluorodeoxyglucose positron emission tomography (18F-FDG PET-CT) on planning radiation therapy (RT) in patients with lung carcinoma, in order to confirm/modify tumor staging. **Methods:** Thirty three consecutive patients (mean age 66y; range 48-87y) with lung cancer were studied: 26 with NSCLC and 7 with SCLC. All of them had a lung CT with intravenous contrast. We performed a 18F-FDG PET-CT scan (Philips Gemini TF PET-CT) for radiotherapy planning (RT). An average dose of 245 MBq of 18F-FDG was administered. PET-CT was performed in the same RT-position, with a flat carbon stretcher and internal lasers centering. Staging with stand alone CT and PET-CT were compared. **Results:** PET-CT changed T staging in 6/33 patients (18%), N in 10/33 (30%) and M in 8/33 (24%). These findings led to a change in staging in 18 out of 33 patients (54%). Twelve patients (36%) were not candidates for curative intent with radiation therapy, 9 of them because of up-staging (unknown metastases) and 3 because of down-staging (whom were treated with surgery). Six out of the 7 patients with SCLC were up-staged after PET-CT. Three of these patients were excluded for radiation therapy. In one patient a synchronous pulmonary tumor was found. **Conclusion:** 18F-FDG PET-CT improved staging of patients candidates to RT. Patients found to have non suspected metastases were excluded from RT. Patients who were down-staged after PET-CT were selected for surgery.

P0969

Stage I Non-Small Cell Lung Cancer patients: are the different histological grading characterised by different morphologic and metabolic features?

S. Taralli¹, M. L. Calcagni¹, A. Del Ciello², L. Leccisotti¹, G. Petrone³, L. Petraccia Ciavarella⁴, A. Stefanelli¹, L. Bonomo², A. Giordano¹; ¹Institute of Nuclear Medicine. Department of Bioimaging and Radiological Sciences. Università Cattolica del Sacro Cuore, Rome, ITALY, ²Institute of Radiology. Department of Bioimaging and Radiological Sciences. Università Cattolica del Sacro Cuore, Rome, ITALY, ³Department of Pathology. Università Cattolica del Sacro Cuore, Rome, ITALY, ⁴Department of Thoracic Surgery. Università Cattolica del Sacro Cuore, Rome, ITALY.

Aim. Pathological stage and histological grading are important prognostic factors in patients with non-small cell lung cancer (NSCLC). Advanced stages (III-IV) and poorly differentiated cancers (G3) are associated to higher risk of recurrence and shorter survival. Nevertheless, a significant number of early stage (I-II) NSCLC have poor prognosis. Therefore, the histological grading is an important prognostic factor, independently of the pathological stage. Integrated ¹⁸F-fluoro-deoxyglucose (¹⁸F-FDG) Positron Emission Tomography-Computed Tomography (PET-CT) is a useful technique for NSCLC staging. It has been reported that ¹⁸F-FDG uptake is

related to the tumour aggressiveness. Aim of our study was to evaluate whether stage I NSCLC patients with different histological grading have different morphologic and metabolic features. **Materials and Methods.** We retrospectively evaluated sixty-one patients (42 males, mean age 67.5 ± 8.7 years) with stage I NSCLC, surgically treated. Before surgery, all patients underwent clinical and cardio-respiratory evaluation, diagnostic CT, and ^{18}F -FDG PET-CT with standard protocol. According to the histological grading, all NSCLC were divided in three groups: well differentiated (G1), moderately differentiated (G2), and poorly differentiated (G3) tumours. For each lesion, the evaluated parameters were: size (cm), margins (regular/spiculated), density (solid/non-solid), and SUV maximum. For statistical analysis, Anova test was used for multiple comparisons. **Results.** According to the histological grading, the 61 NSCLC were classified as follows: 9/61 (15%) well differentiated (G1), 35/61 (57%) moderately differentiated (G2), and 17/61 (28%) poorly differentiated (G3) tumours. Significant difference ($p=0.03$) in the mean size of the lesions between G1 ($1.59\text{cm} \pm 0.83\text{cm}$) and G3 ($2.52\text{cm} \pm 1.05\text{cm}$) NSCLC was found. Significant differences in the SUV max value between G1 (2.22 ± 0.92) and G2 (5.56 ± 3.34) NSCLC, as well as between G2 (5.56 ± 3.34) and G3 (8.89 ± 5.22), and between G1 and G3 were found: $p=0.005$, $p=0.007$, $p=0.0001$, respectively. In the three groups, the tumour's margins were mainly spiculated; the non-solid density was present in G1 and G2 NSCLC, while it was never observed in G3 tumours. **Conclusion.** From our data, we found that ^{18}F -FDG uptake well reflects the biological aggressiveness of NSCLC, also in stage I patients. SUV max gradually increased with the increase of tumour grading: lower values in well differentiated, and higher values in poorly differentiated tumours. Conversely, the lesion's size was significantly bigger only in poorly differentiated tumours. From a clinical point of view, the evaluation of the potential correlations between functional activity and prognosis in stage I NSCLC patients is still under investigation.

P0970

The value of ^{18}F FDG PET-CT staging in Lung Cancers for Bone Metastasis

S. Duffy¹, A. Livie¹, S. Han²; ¹Glasgow University School of Medicine, Glasgow, UNITED KINGDOM, ²West of Scotland PET-CT Centre, Gartnavel General Hospital, Glasgow, UNITED KINGDOM.

INTRODUCTION & AIM: Early detection of distant metastasis in lung cancer patients is crucial to optimise their management potentially improving the quality and longevity of life. Diagnosis of metastatic bone lesion(s) is based on clinical findings, laboratory results and various imaging modalities. ^{18}F FDG PET-CT has become a standard imaging test in lung cancer staging. Our aim was to investigate the value of FDG PET-CT in diagnosing bone metastases in patients with primary lung cancers in the West of Scotland. **METHODS:** Clinical and imaging records of patients with confirmed or suspected lung cancers who had FDG PET-CT between 01/05/2008 to 30/10/2009 at our centre were evaluated retrospectively. Information collected included the clinical indications, PET-CT findings, and influence it had on patient management. Overall outcome was noted and follow up investigation results were recorded where possible. In majority of cases final clinical diagnosis and follow up imaging such as CT, MR, and bone scintigraphy were taken as the gold standard to validate PET-CT results, with very few bone biopsy undertaken. **RESULTS:** 1183 patients with known or suspected lung cancers had FDG PET-CT imaging. The indications for PET-CT were for initial cancer diagnosis (10), and staging of pathologically proven lung cancers (66) and post neo-adjuvant therapy (1). Almost all cases were non small cell lung cancers (NSCLC). 166/1183 patients (14%) had PET-CT suggesting distant metastases. 77/166 patients had PET-CT reports mentioning bone metastases (42 male, 35 female, age from 51 to 85yrs, mean 72yrs). PET-CT identified true positive bone metastasis in 73/77 patients (95%) including 69 patients with previously unsuspected bone disease. PET-CT was false positive in 4 patients (5%). PET-CT diagnosis of bone metastasis led to a change in patient management in majority; largely excluding radical surgery or radiotherapy, and diverting to palliative management including 47 patients having palliative radiotherapy. **CONCLUSIONS:** ^{18}F FDG PET-CT is a valuable non-invasive staging modality for patients with lung cancers and can reliably detect previously unsuspected bone metastases resulting in more appropriate patient management.

P0971

Radiotherapy Planning with ^{18}F -FDG PET/CT in Lung Cancer: Assessment of the Impact on Management

M. P. Fierro Alanis, R. Delgado Bolton, M. Fernández Sáez, P. Alcántara Carrió, A. Prieto Soriano, J. Corona Sánchez, A. González Maté, L. Lapeña Gutierrez, M. de las Heras González, J. Carreras; Hospital Clinico San Carlos, Universidad Complutense de Madrid, Madrid, SPAIN.

Aims: The aim of this study was to assess the impact on management when using ^{18}F -FDG PET/CT in radiotherapy planning in lung cancer patients. **Materials and methods:** Fifty-two patients with lung cancer (non-small cell lung cancer $n=44$; small cell lung cancer $n=8$) were analysed retrospectively (39 male, average age 66) in whom 54 PET/CT studies had been carried out for radiotherapy planning. The impact on management was assessed by a nuclear medicine physician together

with a radiotherapy oncologist. Four categories were defined: (a) high impact when PET/CT modified the intention or mode of treatment or if a negative PET/CT contraindicated a treatment; (b) moderate impact when it modified the treatment partially (dose, area to be treated, etc.); (c) low impact when it did not determine any change on the treatment; and (d) no impact when the information supplied by PET/CT was considered inadequate by the referring physician. **Results:** The impact on management was high (category a) in 16 of 54 studies (29.6% of the total); of these, in three it generated changes in the type of treatment planned, in 7 it contraindicated radiotherapy and in 6 it modified the intention of treatment (palliative to radical or inversely). In 26 studies (48.2%) the impact was moderate (category b): in 24 of them it modified the radiotherapy treated volume and in 2 it modified the dose of radiotherapy. The impact was low (category c) in 12 studies (22.2%), although in 6 of these cases they had a previous PET/CT performed for staging which had had an impact on management. No studies were categorized as no impact (category d). Therefore, the impact on management was high or moderate in 42 of 54 studies (77.8%). **Conclusions:** These results indicate that ^{18}F -FDG PET/CT has a high or moderate impact on management in radiotherapy planning in lung cancer patients.

P0972

Evaluation of standard uptake value (SUV) 2.5 as a threshold for detection of malignant pulmonary lesions on FDG PET-CT examinations using PET and CT segmentation

Z. Tóth¹, L. Papp², N. Zsótér², V. Tóth¹, P. Szabó¹, P. Szabó³, I. Garai⁴; ¹ScanoMed Ltd., Budapest, HUNGARY, ²Mediso Medical Imaging Systems Ltd., Budapest, HUNGARY, ³Jósa András Hospital, Nyíregyháza, HUNGARY, ⁴ScanoMed Ltd., Debrecen, HUNGARY.

Aim: Solitary pulmonary nodule characterisation and diagnostics of lung cancer are widely accepted FDG PET-CT indications. Our aim was to assess the accuracy of the commonly adopted 2.5 SUVmax value for malignant pulmonary lesion delineation in our patient population using a semi-automatic PET lesion detection algorithm. **Methods and Materials:** 87 histologically verified pulmonary lesions (69 malignant, 18 benign, size: 0.7-3.5 cm, SUVmax:0.6-11.2) of 83 patients were retrospectively evaluated. The PET-CT images were semi-automatically processed by the PET lesion detection algorithm of InterView Fusion evaluation application (Mediso) with SUVmax 2.5 as a threshold; 1.4 as lesion/background ratio and 100-36000mm3 as size interval for main parameters. The algorithm detected the local maxima positions on the PET images within the given parameters, tissue information (including lung, fat, soft tissue and bone) was generated by automated fuzzy segmentation methods operating on the CT images and lesions were automatically classified based on this material information. The results were compared with histological data. **Results:** All the pulmonary lesions with SUVmax above 2.5 were successfully found by the algorithm (68), although 2/68 lesions were misclassified as soft tissue focuses and 6 additional non pulmonary focuses were also found and misclassified as lung disorders. Among our histologically confirmed pulmonary lesions considering SUVmax 2.5 as a threshold for malignancy, the sensitivity, specificity, PPV and NPV were 87%, 56%, 88% and 53% respectively. **Conclusion:** Despite the high sensitivity and PPV, the low specificity and NPV restricts the use of 2.5 SUVmax value for automatic delineation of malignant pulmonary lesions. With the use of more detailed CT data (e.g. shape, consistency) and modification of SUV value, the algorithm may be further improved and optimised.

P0973

Analysis of Pet/Ct Imaging Findings at the Time of Diagnosis and Initial Staging of Lung Cancer in Women

F. Sen, A. T. Akpinar, D. Kumtepe, B. Sevilimis, E. Alper; Uludag University, Faculty of Medicine, Dept. of Nuclear Medicine, Bursa, TURKEY.

Aim: Numerous studies show that lung cancer behaves differently in women. Gender-based differences in clinical and histological characteristics and treatment outcomes have so far been documented in the literature. Women with lung cancer tend to be younger at the time of diagnosis, have higher incidence of adenocarcinoma, more likely to be never-smokers and have a favourable prognosis and survival relative to men. The aim of this study was to evaluate PET/CT imaging findings at the time of diagnosis and initial staging of lung cancer in women. **Materials and methods:** Between January 2009 and December 2011, medical records of the female patients who underwent PET/CT imaging for suspected or newly diagnosed lung cancer at our institution were retrospectively analyzed. Only patients with histopathologically confirmed lung cancer were included in the study. Patients with a history of any other malignancy or incidentally detected synchronous tumor were excluded from the study. Disease staging was performed using PET/CT and available chest CT data. Patient characteristics and treatment types were also abstracted from medical records. Follow-up PET/CT reports, if any, were also collected to evaluate treatment outcomes and survival. **Results:** Of 98 female patients evaluated for lung cancer, 59 patients (aged 35-82 yrs, mean±std:59.8±10.5) met the inclusion criteria and underwent a total of 95 PET/CT examinations. Among main histological categories of lung cancer, NSCLC

accounted for 84.7% (n:50), SCLC 8.5% (n:5) and NET 6.8% (n:4) of cases. Adenocarcinoma was found as the most common (n:30, 50.8%) and LCC as the least common (n:3, 5.1%) subtypes of NSCLC. 67.8% of patients had stage 4 disease (n:40), of these 59.3% of cases (n:35) presented with distant metastasis. At moment of the last analysis 15 (25%) were exitus. 10 patients (16.9%) were found resectable, others received chemotherapy or radiotherapy alone or in combination. Conclusion: According to the results of the study it appears that women with newly diagnosed lung cancer tend to present with stage 4 disease more frequently on PET/CT imaging.

P55-2 - Tuesday, October 30, 2012, 16:00 - 16:30, Poster Exhibition Area

Oncology Clinical Science: Oesophageal

P0974

18F-FDG PET-CT Plays a Crucial Role in Staging and Outcome Prediction for Radically Treatable Oesophageal Cancer

L. M. Tho¹, I. Sanders¹, J. Hu¹, S. McKay¹, S. Y. Foo², V. MacLaren¹, S. Han²; ¹Beatson West of Scotland Cancer Centre, Glasgow, UNITED KINGDOM, ²West of Scotland PET-CT Centre, Glasgow, UNITED KINGDOM.

Aim 18F-FDG PET-CT is indicated in patients with oesophageal carcinoma to facilitate accurate staging and selection of appropriate candidates for radical therapy. Some studies suggest a role in prognosis but there is no consensus. We undertook analysis of outcome data for oesophageal PET-CT from a large tertiary referral centre. **Materials and Methods** A retrospective review of 132 patients with newly diagnosed oesophageal carcinoma (n=121) or suspected recurrence (n=11) undergoing PET-CT between 2008 to 2009 at our centre was undertaken. Conventional workup (CW) - clinical assessment, EUS and CT, had staged these patients as radically treatable or having equivocal metastases requiring further assessment. Results 91 patients had died. Median follow up for 41 survivors was 35 months (30 to 51 months). In 38/56 (67.9%) of CW N1 patients, PET-CT confirmed avid nodal uptake. In 32/76 (42.1%) of CW N0 patients, PET-CT upstaged disease to N1. Occult metastases were detected by PET-CT in 20/105 (19.1%) of CW M0 patients, upstaging to M1. Of these, 16 patients had confirmatory biopsy and/or further imaging. In 4 patients, pre-surgical laparoscopy revealed peritoneal disease which was not detected by PET-CT. PET-CT downstaged 15/27 (55.6%) of CW M1 patients to M0. Over all, PET-CT changed intention to treat radically in 35/132 cases (26.5%). Univariate and multivariate analysis was performed for age, tumour grade, primary tumour (PT) SUVmax, presence or absence of CW nodal disease (CW N), PET-CT nodal disease (PET-CT N), CW metastases (CW M) and PET-CT metastases (PET-CT M) with different outcome measures. Univariate analysis revealed PT SUVmax, CW N, PET-CT N, CW M and PET-CT M were significantly correlated with overall survival (OS), disease-free survival (DFS) and metastases-free survival (MFS). However on multivariate analysis only PET-CT M remained significantly correlated, and this was with all outcome measures OS, DFS and MFS (p<0.001). Median OS for patients with PET-CT M1 was significantly lower than PET-CT M0 (9.5 versus 27.0 months, p<0.001). Average PT SUVmax for patients with PET-CT M1 was significantly higher than PET-CT M0 (15.5 versus 11.2, p=0.012). Conclusion PET-CT is a critical staging investigation for patients with potentially radically treatable oesophageal carcinoma. It improves accuracy of N and M staging and changes clinical decision making in up to 26.5% of cases. Multivariate analysis revealed that PET-CT M stage significantly influenced outcome prediction with poorer overall survival, disease-free survival and metastases-free survival demonstrated. PT SUVmax in patients with PET-CT M1 was significantly higher than M0.

P0975

18F-FDG PET-CT for detection of suspected recurrence in patients with esophageal carcinoma: single institutional experience

S. Jain, P. Sharma, T. Jain, A. Mishra, C. S. Bal, R. Kumar, A. Malhotra; All India Institute of Medical Sciences, Delhi, INDIA.

Objective: To evaluate the role of 18F-Fluorodeoxyglucose (18F-FDG) positron emission tomography-computed tomography (PET-CT) in patients with esophageal carcinoma for detection of recurrence, suspected clinically or on conventional imaging (CIM). **Methods:** This was a retrospective study. Data of 78 patients (Age: 55.2±10.1 years; male/female: 54/24) with histopathologically proven esophageal carcinoma (squamous cell-59; adenocarcinoma-17; small cell-1; neuroendocrine carcinoma-1) who underwent 84 18F-FDG PET-CT studies for suspected recurrence was analyzed. Recurrence was suspected clinically (n=29) or on CIM (n=55). Pre PET-CT treatment included combined chemo-radiotherapy (n=37), chemotherapy (n=15), surgery (n=8), surgery with chemotherapy (n=8), surgery with chemo-radiotherapy (n=7), radiotherapy (n=6) and surgery with radiotherapy (n=3). 18F-FDG PET-CT images were reevaluated by two nuclear medicine physicians in consensus who were blinded to all details except for primary diagnosis. Findings

were grouped into local, nodal and distant recurrence. Results were compared to CIM (CT/Ultrasound/Bone scintigraphy) when available (n=55). Clinical/imaging follow up (minimum-6 months) with histopathology (when available) were taken as reference standard. Results: Fifty seven 18F-FDG PET-CT were positive and 27 were negative for recurrent disease. 18F-FDG PET-CT showed local recurrence in 43, nodal recurrence in 37 and distant recurrence in 11 (lung-7; liver-2; bone -2; spleen-1), with more than one site of recurrence in 34. Fifty four PET-CT were true positive, 23 were true negative, 3 were false positive and 4 were false negative. The sensitivity of 18F-FDG PET-CT was 93% [95% CI: 83-98], specificity 88% [95% CI: 70-97], PPV was 95% [95% CI: 85-99], NPV was 85% [95% CI: 66-96%] and accuracy was 92%. In 55 cases where comparable CIM was available, 18F-FDG PET-CT was significantly superior to CIM (P=0.012). Conclusion: 18F-FDG PET-CT shows high accuracy for detection of suspected recurrence in post therapy patients with esophageal carcinoma, suspected clinically or on imaging. Moreover, it is superior to CIM for this purpose.

P56-2 - Tuesday, October 30, 2012, 16:00 - 16:30, Poster Exhibition Area

Oncology Clinical Science: Liver

P0976

Is there any Additional Value of Delayed FDG-PET/CT Scan in Detection of Hepatocellular Carcinoma?

F. A. Caliskan¹, Z. Kaya, O. Ekmekcioglu¹, O. Vural Topuz², A. Kurt¹, S. Asa¹, M. Halac¹, M. Sager¹, K. Sonmezoglu¹; ¹Istanbul University Cerrahpasa Medical Faculty, Nuclear Medicine Department, ISTANBUL, TURKEY, ²Okmeydanı Research and Training Hospital Department of Nuclear Medicine, ISTANBUL, TURKEY.

Aim Hepatocellular carcinomas (HCC) demonstrate variable FDG uptake on PET/CT images, often leads unsatisfactory diagnostic accuracy due to low FDG uptake in standard 60-90 min imaging. Since delayed FDG-PET imaging has been reported to have additional value in various solid carcinomas, we aimed to evaluate any possible additional role of 3-hr delayed PET/CT scanning in lesion detection in patients with known HCC in this retrospective study. **Materials and Methods** 18 patients with diagnosis of HCC were included in the study (16 male, 2 female; mean age 66 yrs with a range 48-85). The patients were referred to PET/CT scan for either primary staging (n=12) or restaging (n=6). In all patients, a standard whole body PET/CT scanning was performed from skull base to upper thighs, approximately 90 min after an IV injection of 370-555 MBq FDG, using a dedicated PET/CT scanner. A delayed abdominal PET/CT examination was also obtained approximately three hours after the injection. The body weight normalized SUVmax values of the tumor region (TM) and SUVmean values of the non-tumorous liver area (N) were calculated on early and delayed PET/CT images by using the vendor software. **Results** Acquisition times were not well consistent for both early and delayed PET/CT imaging due to heavy work load of the laboratory. Early PET/CT imaging was performed from 60 min to 122 min (93 ± 19), and late imaging between 113 min and 264 min (195 ± 44). SUVmax values of the tumor areas varied from 2.7 to 10.2 (mean 5.55 ± 2.44) in early images versus from 2.5 to 10.3 (mean 5.53 ± 2.57) in delayed scans and there was no significant difference (T test; p=0.82). Only in one patient, the delayed SUVmax was increased over 10%, comparing to early SUVmax value. Liver SUVmean values were consistently decreased from early scan (2.36 ± 0.50) to delayed imaging (2.14 ± 0.47) (p=0.007). TM/N ratios were increased over 10% in 10 patients and found to be 2.44 ± 1.18 and 2.70 ± 1.41 in the early and late PET images, respectively (p=0.055). **Conclusion** It seems that the body weight normalized SUVmax values at 3hr-delayed PET/CT imaging do not contribute to the lesion detection in patients with HCC. However, 3-hr delayed imaging has a better TM/N ratio than 90-min imaging, implying that this index might be useful to increase diagnostic sensitivity of FDG-PET imaging in HCCs.

P0977

Prediction of ICG blood clearance from 99mTc-mebrofenine scintigraphy in normal volunteers and in patients.

C. Saelens, S. Walrand, R. Lhomel, S. Pauwels, F. Jamar; Université Catholique de Louvain, Brussels, BELGIUM.

Aim: ICG blood clearance is increasingly used to assess the liver function in view of therapeutic hepatic lobectomy. Our aim is to evaluate whether ICG blood clearance can be predicted using the less invasive ^{99m}Tc-mebrofenine scintigraphy technique that can visualize other additional informations. **Method:** ten normal volunteers (38±11y, 6 females) and ten patients (62±11y, 4 females, 4 cholangiocarcinoma, 1 hepatocarcinoma, 5 CRC metastases) were injected with 85 MBq of ^{99m}Tc-mebrofenine. A dynamic acquisition of 1 hour (successively sixty 10 sec and fifty 1 min frames) in anterior-posterior direction was performed with blood samples took 150, 250, 350, 600 and 900 sec post-injection. Three ROIs were drawn: on the heart, on the bowels+macroscopic intra liver biliary ducts and on the remainder of the liver. The ^{99m}Tc-mebrofenine blood clearance was assessed assuming a two

way blood-liver compartmental model by fitting the parameters of the corresponding equations to the ROIs counts on all the frames acquired after 3 min post-injection. The blood clearance was also assessed by fitting the ^{99m}Tc -mebrofenine in the blood samples by a mono-exponential function and by using the Ekman's method on the scintigraphy. ICG clearance was assessed using the 3 time-points standard method from blood samples took one hour before the scintigraphy for the volunteers, and within 3 days before, up to 5 days after the scintigraphy for the patients. Results: Both, mono-exponential blood fit and the Ekman method provided a low correlation versus the ICG blood clearance: ($y = -0.02 + 1.05 \times \text{ICG} [\text{min}^{-1}]$ $R^2 = 0.57$) and ($y = 0.08 + 0.44 \times \text{ICG} [\text{min}^{-1}]$ $R^2 = 0.44$), respectively. Correlation between clearances estimated from mono-exponential fit of the blood samples between 2-4 and 4-6 min gave a fit slope of 0.35, showing that ^{99m}Tc -mebrofenine was not cleared following a mono-exponential. The compartmental model provided a good correlation with the ICG blood clearance for the volunteers ($y = -0.02 + 0.85 \times \text{ICG} [\text{min}^{-1}]$ $R^2 = 0.87$). The correlation was lower for the patients ($y = 0.03 + 0.77 \times \text{ICG} [\text{min}^{-1}]$ $R^2 = 0.64$). Conclusion: ICG blood clearance can be predicted from ^{99m}Tc -mebrofenine scintigraphy using an appropriate compartmental model that doesn't made the assumption that the compartments follow mono or multi-exponential functions. The slope of the linear regression was close to 1 with a small offset origin. The lower correlation obtained for the patients could be due to the delay between the ICG assessment and the scintigraphy.

P0978

Comparison of Y-90 PET and Bremsstrahlung SPECT images after Radioembolization with Y-90 Microspheres

L. Uslu, S. Sager, M. Halac, L. Kabasakal, I. Uslu, M. Demir, B. Kanmaz; Istanbul University Cerrahpasa Medical Faculty, Istanbul, TURKEY.

Introduction: Radioembolization with Y-90 microspheres is advancing treatment modality in patients with primary or metastatic liver tumors. In current practice, bremsstrahlung SPECT images are used to detect biodistribution of Y-90 posttherapy. However due to scattering of X-rays, only low quality images could be obtained. Recently, PET imaging option using seldom internal pair production of Y-90 was introduced. The aim of our study was to compare imaging quality of bremsstrahlung SPECT images with Y-90 PET images in patients who had undergone Y-90 microsphere therapy. **Methods:** 10 patients, 3 with primary tumor and 7 with liver metastasis, mean age: 64.8±12.5, female/male ratio: 1/1.5 underwent Y-90 microsphere therapy with glass microspheres with a mean activity of 2.41±0.7 GBq. 4 patients had single lesion, 6 had multipl lesions. Y-90 PET images were acquired for 2 positions with liver at the center, 20 min/bed with a non-TOF PET/CT (Siemens Biograph 6) on same day with radioembolization. SPECT images (Mediso, DHV Sprint) were taken on the next day with 120 images, 15 sec/image. Maximum count for SPECT and mean SUV level for PET was calculated by region of interest (ROI) drawn around the lesions and same sized ROI taken on liver for background activity. Lesion/background (L/B) ratio was calculated for each patient using formula $[\text{ROI}(\text{lesion}) - \text{ROI}(\text{background})] / \text{ROI}(\text{background})$. Wilcoxon statistical analysis was performed using L/B ratio. **Results:** Mean L/B value was 4.15±2.9 for SPECT and 2.7±2.3 for PET. Contrast increase from PET to SPECT was 65%. Statistical analysis revealed that SPECT acquisition has better contrast ratio in comparison to PET images ($p = 0.022$). **Conclusion:** Bremsstrahlung SPECT images were found to be superior to Y-90 PET to evaluate radiopharmaceutical uptake by the lesions, despite its scattering artifacts.

P57-2 - Tuesday, October 30, 2012, 16:00 - 16:30, Poster Exhibition Area

Oncology Clinical Science: Urogenital

P0979

Significant glomerular filtration rate (Tc99mDTPA GFR) deterioration in 20 % of patients after nephron sparing surgery (NSS) for renal tumors

M. Benke, R. Sosnowski, A. Garszel, J. Niewiadomska, I. Kozłowicz-Gudzińska; Maria Skłodowska-Curie Memorial Cancer Center and Institute of Oncology, Warszawa, POLAND.

NSS is method of choice in surgical treatment of renal tumors up to 7 cm in diameter. This surgical technique seem to render comparable results of long-term tumor-related survival. Aim of this study was to assess kidney function pre- and postoperatively in patients treated with NSS for renal tumors. Material and methods 20 patients, aged 32-73y (mean 59) was included in the study. The pre-operative and post-operative Tc99mDTPA GFR measurement were carried out under the same conditions in each patient. The following risk factors potentially affecting kidney function were identified in patients' medical history: nicotineism – in 2 patients, hypertension – 9 patients, diabetes – 1 patient, and prior chemotherapy – 1 patient. Results Mean GFR before surgery was 84 ml/min/1.73 m² and after NSS was 79 ml/min/1.73 m². Mean decrease of GFR value after the surgical treatment was 5.1 ml/min/1.73 m² ($p > 0.058$ NS). The relative percentage

share of operated kidney decreased by mean value of 3,8% ($\pm 5,325$) ($p < 0,005$). Significant deterioration of renal function after NSS (GFR decrease by a mean value of 17.1 ml/min/1,73 m² and change in the renographic curve from type 1 or 2 to type 4) was observed in 4 patients (20%) and improvement of renal function of operated kidney was found in one patient. No cases of kidney failure as specified by KDOQI criteria were diagnosed after NSS. Due to a relatively small study group statistical analysis of potential influence of risk factors on kidney function was not undertaken. Conclusions Dynamic renal scintigraphy is a valuable method for assessment the changes of renal function in patients with renal tumors treated by NSS. The results of this study show that significant renal function impairment after this type of surgical procedure is a relatively infrequent event.

P0980

Determination of the physiological metabolic activity in adrenal glands on F-18 FDG PET/CT imaging

A. Öner, F. Aydın, S. Demirelli, E. Sürer Budak, G. Kaplan, M. Sipahi, F. Güngör; AKDENİZ UNIVERSITY MEDICAL SCHOOL, DEPARTMENT OF NUCLEAR MEDICINE, Antalya, TURKEY.

AIM: In this study, it is aimed to determine whether increased metabolic activity is a physiological condition without morphological changes in adrenal glands and the rate of the physiological average metabolic activity (SUVmax) in F-18 FDG PET/CT imaging performed due to oncological reasons. **MATERIAL AND METHOD:** Our clinic performed staging, re-staging and treatment response assessment by using FDG PET / CT scan on 2750 patients in oncology between September 2010 and September 2011. The morphological images of adrenal glands in these cases and the involvement of FDG were evaluated. It was not observed morphological changes in abdominal window, transaxial sections, adrenal glands with PET/CT, but, only with reference to the liver, the areas of increased metabolic activity than the liver (SUVmax) were evaluated in interpretation of visual. The diagnosis result was found with clinical follow-up and other imaging methods. **RESULTS:** A retrospective screening of 81 patients with ages ranging from 42 to 82 years (44 males, 37 females) showed that there were no morphological change in adrenal glands but it was observed increased FDG uptake than the liver. The values of adrenal gland SUVmax of the cases were seen that ranged between 2.1 to 5.4 and were calculated the average SUVmax as 3.7 ± 1.5 . There was no pathology of the adrenal glands at clinical follow-up and other imaging modalities of these cases. **CONCLUSION:** In oncology, the patients undergoing PET/CT scanning can be physiologically observed increased FDG uptake in adrenal glands. It is physiologically acceptable the involvement of increased FDG (between 2.2-5.2) being not accompanied by morphological changes in adrenal glands.

P0981

The Role of F-18 FDG PET/CT in the Assessment of Bladder Carcinoma

S. Demirelli, E. Sürer, A. Öner, G. Kaplan, M. Sipahi, B. Karayalçın; Akdeniz University Faculty of Medicine, Department of Nuclear Medicine, Antalya, TURKEY.

OBJECTIVE: In this study, it was aimed to evaluate the role of F-18 FDG PET/CT in the assessment of bladder cancer. **MATERIALS AND METHODS:** Between February 2010 and April 2012, 76 PET/CT scans of 43 bladder carcinoma patients were evaluated retrospectively. The median age of the patients was 61.6 with a range of 26 to 92 years. The diagnosis of all patients were verified by histopathologically. In the follow-up, patients were evaluated clinically and by other imaging techniques. **RESULTS:** PET/CT scans were grouped according to the indications such staging (24 scans), therapy response (31 scans) and restaging (21 scans). In 24 scans performed for staging, while in 5 (20%) of them there were no pathological findings, in 15 (63%) patients PET/CT upgraded the stage by detecting metastatic sites. In 31 scans performed for therapy response, complete response, partial response, stable disease and progression was reported in 9 (29%), 8 (26%), 10 (32%) and 4 (13%) cases respectively. In 21 scans performed for restaging, while 13 (62%) of them were reported as recurrent disease, in 8 (38%) cases no pathology was detected. **CONCLUSION:** PET/CT is an useful method in staging, restaging and in the assessment of the therapy response in bladder cancer.

P58-2 - Tuesday, October 30, 2012, 16:00 - 16:30, Poster Exhibition Area

Oncology Clinical Science: Prostate

P0982

Sequential PET/CT with 11C-Choline in Monitoring Treatment Response to Androgen Deprivation in Patients with Biochemical Recurrence of Prostate Cancer

P. Medina-Quiroz, R. Quirce, I. Banzo, M. De Arcocha-Torres, A. Rubio-Vassallo, F. Ortega-Nava, F. Gutierrez-Baños, F. Campos-Juanatey, E.

Acuña, J. Carril; University Hospital Marques de Valdecilla. University of Cantabria Nuclear Medicine department, Santander, SPAIN.

Although the role of 11C-Choline PET/CT (CHO) in the diagnosis of prostate cancer recurrence (PC) in patients with increase PSA serums levels is well established, its contribution of monitoring the response to androgen deprivation (AD) remain to be proved. AIM: To assess the role of 11C-Choline PET/CT (CHO) in monitoring treatment response to androgen deprivation (AD) in patients with biochemical recurrence of prostate cancer (PC). MATERIALS AND METHODS: These prospective study included 6 patients, mean age 73-year-old, with biochemical suspicious recurrence confirmed by imaging. All of them were treated with radiotherapy; 4 with both radiotherapy and prostatectomy and 2 received hormone therapy until five years before. PSA serums levels range between 2.70-32 ng/dl. Gleason score at initial diagnosis between 6 and 7. To monitoring the treatment response, we performed two PET/CT after IV administration of 720 MBq of 11C-Choline. The first as a baseline scan previous to hormone therapy and the second one a month after starting treatment. A visual and semi-quantitative analysis by SUVm was performed. The follow-up was based on PSA monitoring. RESULTS: In the baseline scan abnormal uptake was detected in all patients: Prostate in 1 patient, lymph nodes in 3 and multiple localizations in 2 (lymph node and bone in 1 and prostatic bed, lymph node and bone in the other one). One month later the visual analysis showed decrease in uptake in all patients. In one of them the decrease was very low. Semi-quantitative response was heterogeneous among the different lesions detected in each patient. The level of response in all patients was estimated by the decrease of SUVm. This decrease was in a range between 4.41% - 50.67%. With regard to the PSA follow-up the levels of the concentration decreased by 99.1% to 88.49%. There was not correlation between the decrease of SUVm and PSA. CONCLUSION: The preliminary results of this ongoing work, show that 11C-Choline PET/CT is a useful tool for monitoring the treatment response in patients with recurrent prostate cancer with androgen deprivation therapy. The results are encouraging to include a larger number of patients.

P0983

PET/TC with 18F-fluoromethylcholine in patients with biochemical relapse of prostate cancer: a single centre experience.

V. Pirro¹, A. Douroukas², F. Buttar¹, P. Scapoli¹, T. Varetto¹; ¹IRCC Candiolo, Candiolo, ITALY, ²Nuclear Medicine Department, San Giovanni Battista Hospital, Turin, ITALY.

Background. An increase of PSA level is the earliest and most sensitive indicator for residual or recurrent disease in patients treated for prostate cancer (biochemical failure), preceding clinical relapse. Furthermore, the knowledge of the exact site of recurrence is crucial for the treatment planning in these patients. Conventional imaging (TRUS, MRI, CT) is often inconclusive showing a low detection rate in some districts. The aim of our study was to evaluate the accuracy of PET/CT using ¹⁸F-fluoromethylcholine for the correct detection of recurrence site after biochemical failure in patients treated for prostate tumour. **Materials and methods.** Eighty-two patients with biochemical relapse, previously treated for prostate cancer (both surgical and/or radiotherapeutic) were retrospectively studied. Mean age was 72 years (50-88 years) and PSA mean level at PET/TC was 5,95 ng/mL (0,51-236 ng/mL). All PET findings were confirmed by histology or conventional imaging when available, and/or clinical follow-up. **Results.** In 64 patients (80%) PET revealed pathological uptakes (mean PSA 12,1±32,6 ng/mL): 15 local, 13 lymph node, 15 bone, 20 multiple sites, 1 only lung findings. In 18 cases (20%) PET was negative (mean PSA 1,93±1,44 ng/mL). Global sensitivity, specificity, PPV, NPV and accuracy of PET were 85,4%, 100%, 100% and 85,4% respectively. Lesion-by-lesion analysis showed a sensitivity, specificity, PPV and accuracy of 59,4%, 81,9%, 90,5% and 65,1% respectively for local relapse; 95,8% sensitivity, 100% and 96,5% accuracy in the lymph node districts; at bone level 93,1% sensitivity, 96,4% PPV, 81,8% NPV and 92,3% accuracy. The R.O.C. analysis showed an optimal cutoff point for trigger PSA of 2.36 ng/mL (A.U.C.=0.78). Using this cut-off, 21/35 patients (58,3%) with PSA <2,36 ng/mL had true positive result (sensitivity of 70% and accuracy of 75%), while in patients with PSA>2,36 ng/mL, 44/47 (89,5%) resulted true positive (sensitivity and accuracy of 93,6%). Finally, in 24/82 cases (29%) PET depicted not expected sites of disease and resulted crucial in changing the management of these patients who underwent a targeted treatment (surgery or radiotherapy). **Conclusions** PET/CT with ¹⁸F-fluorocholine shows a high diagnostic value in revealing recurrence sites in patients with biochemical relapse of prostate cancer, often exceeding conventional diagnostic methods overall in nodal and distant districts. In one third of cases, PET was able to modify the therapeutic strategy becoming an instrument of high importance for treatment planning.

P0984

Influence of Gleason score on Fluorocholine PET/CT findings: our experience in 800 consecutive patients

M. Hodolic¹, M. Cimitan², T. Barešić², E. Borsatti², M. Nader³, J. Fettich¹; ¹University Medical Center Ljubljana, Nucl. Med. Dept., Ljubljana, SLOVENIA, ²National Cancer Institute (IRCCS) - CRO Aviano, Nuclear Medicine Unit, Aviano, ITALY, ³IASON GmbH, Zyklotron, Linz, AUSTRIA.

Introduction 18F-choline (FCH) PET/CT is a nuclear medicine procedure that has greater sensitivity and accuracy than 18F-FDG PET/CT to detect prostate malignancy: 73% vs. 31% and 67% vs. 53%, respectively. The efficiency of FCH to detect prostate cancer disease before and after treatment is related to the PSA levels. Purpose To investigate the role of Gleason score (GS) on FCH PET/CT findings in patients with prostate cancer disease, before and after the treatment, versus prostate specific antigen (PSA). Material and Methods FCH findings of 841 prostate cancer patients were retrospectively evaluated. 175 patients were investigated before radical prostatectomy (RP) for exclusion of distant metastases. Further 666 patients underwent for FCH PET/CT after the treatment (radical prostatectomy, radiotherapy, hormonal therapy alone or combined treatment). FCH was provided by IASON GmbH, Graz, Austria for all PET/CT studies. Results In 175 patients studied before radical prostatectomy, FCH PET/CT detected prostate malignancy in 152 of patients (87%) with GS > 7, and showed distant metastases in 60% of cases. In 666 patients with biochemical relapse (PSA>0.2 ng/ml) FCH PET/CT detected prostate cancer recurrence in 75% of patients with GS>7 (95% of patients with PSA>3 ng/ml, 68% of patients with PSA level within 1.5-3 ng/ml, 47% of patients with PSA3 ng/ml, 29% of patients with PSA level within 1.5-3 ng/ml, 18% of patients with PSA<1.5 ng/ml), as well as in 53% of patients with GS 3 ng/ml; 29% of patients with PSA level within 1.5-3 ng/ml; 7% of patients with PSA <1.5 ng/ml). Conclusion Gleason score can predict FCH PET/CT findings (before and after the treatment) especially in patients with GS > 7 at any PSA levels.

P0985

Intraindividual comparison of Ga-68 DOTATATE and C-11 Choline uptake in patients with recurrent prostate cancer lesions

G. Dos Santos¹, R. Castro², E. Savio³, A. Paolino², A. Quagliata³, H. Balter², V. Trindade², J. Giglio², J. P. Gambini¹, H. Engler², O. Alonso³; ¹University of Uruguay, Montevideo, URUGUAY, ²CUDIM, Montevideo, URUGUAY, ³CUDIM, University of Uruguay, Montevideo, URUGUAY.

Objectives: In the framework of an ongoing trial aiming to assess the value of Ga-68-DOTATATE PET-CT (GALPET) in patients with prostate cancer, the objective of this study was to perform an intraindividual comparison of this technique with C-11 Choline PET-CT (CHOLPET) in a sample of prostate cancer patients. **Methods:** We studied seven patients with prostate cancer during follow-up: two with known bone metastases confirmed by a previous bone scan (PSA: 79-480 ng/mL) and five with biochemical recurrence after treatment (PSA: 0.7-10 ng/mL). Within 1-2 weeks, a PET-CT study was performed with Ga-68-DOTATATE and C-11 Choline with a dose of 110 MBq and 420 MBq, respectively, using a 64-slice PET-CT with time-of-flight correction. The maximum SUV (SUVm) was measured in all abnormal foci. **Results:** Both techniques were negative in three patients with biochemical recurrence. GALPET and CHOLPET were positive in 63/64 bone lesions corresponding to both patients with known bone disease and to one patient with biochemical recurrence. Two discordant bone abnormal foci were found (positive for GALPET or CHOLPET only). Additionally, in one patient with bone metastases and in other with biochemical recurrence, 3 normal-sized pelvic lymph nodes were positive by means of GALPET whereas CHOLPET detected two of them. CHOLPET SUVm were higher than those from GALPET (7.8±3.8 vs. 3.9±1.4, n=67, p<0.0001). However, a significant correlation was found among both tracers SUVm (r=0.732, n=67, p<0.0001). **Conclusions:** In advanced prostate cancer patients, Ga-68-DOTATATE uptake in lesions expressing somatostatin receptors seemed to correlate with C-11 Choline uptake. More studies are needed in order to test for the possible complementary value of these techniques and for the potential of receptor-mediated therapies with appropriate ligands labeled with Y-90 and/or Lu-177.

P0986

The role of serum osteoprotegerin and osteocalcin in bone pain palliation with Samarium -153- EDTMP in patients with metastatic prostate cancer

M. T. Siabanopoulou¹, S. El Mantani Ordoulidis², I. Iakovou³, A. Doumas³, G. Galaktidou⁴, N. Dimasis⁵, A. Sioundas⁵, A. Gotzamani-Psarrakou¹; ¹2nd Nuclear Medicine Dpt., AHEPA University Hospital, Aristotle University of Thessaloniki, Thessaloniki, GREECE, ²Nuclear Medicine Dpt, Bioiatriki S.A., Thessaloniki, GREECE, ³3rd Nuclear Medicine Dpt., Papageorgiou General Hospital, Aristotle University of Thessaloniki, Thessaloniki, GREECE, ⁴Theagenio Cancer Hospital, Thessaloniki, GREECE, ⁵Medical Physics Laboratory, Medical School, Aristotle University of Thessaloniki, Thessaloniki, GREECE.

Introduction: While initially thought to be primarily osteoblastic, it is now recognized that prostate cancer (CaP) bone metastases have an extensive bone resorptive component that is caused primarily by osteoclasts. Recently, a novel

cytokine system consisting of receptor activator of NF- κ B ligand (RANKL), its receptor RANK and the protein osteoprotegerin (OPG) was identified and characterized for its role in bone remodelling. OPG is a glycoprotein that acts as a decoy soluble receptor for the receptor activator of nuclear factor κ B ligand (RANKL), neutralizing its interaction with RANK and thereby inhibit osteoclastogenesis. This study assesses the efficacy of palliative treatment using 153-Samarium Lexidronam ($^{153}\text{Sm-EDTMP}$) regarding pain symptoms and quality of life in bone metastatic CaP patients and investigates the role of serum OPG and osteocalcin as prognostic factors of disease progression. **Method:** Overall 43 CaP patients (mean age 73 ± 5 , 5 years) were recruited (20 patients with localized CaP - M0- and 23 with bone metastatic cancer -M1). We examined whether serum OPG and osteocalcin (OC) could serve as predictors for appearance and expansion of CaP. Control sera were obtained from 32 healthy men. All metastatic patients had pain palliative therapy using 153Sm-Lexidronate. All patients were undergoing hormone treatment before entering this study. Pain palliation was evaluated on the basis of the Wisconsin pain test improvement and response was graded as complete, partial or absent. **Results:** The mean serum levels of OPG and OC in CaP patients were significantly higher than the control group ($p=0.003$ and $p=0.042$ respectively). Furthermore, serum levels of OPG and OC in metastatic PCa patients were highly elevated compared with those without metastases (OPG: $p<0.001$ and OC: $p=0.048$). Treatment efficacy was complete in 50% of patients, partial in 34% and absent in 16% of patients. A mild hematological toxicity was apparent in 3 patients. The patients who did not respond to palliative therapy had higher OPG levels than the responders ($p<0.001$). In that case, PSA values were high as well ($p<0.031$). A month after radiopharmaceutical therapy a statistically significant difference in OPG's serum levels was observed between responders and non-responders (OPG: $p=0.002$) while this difference was not evident in osteocalcin levels ($p>0.05$). **Conclusion:** Serum OPG could play a role in monitoring therapy and evaluating malignant progression in CaP. Elevated levels of OPG are associated with disease progression, but its role in predicting pain palliative treatment response remains to be established.

P0987

The role of IGF-1 and IGFBP-3 in predicting disease progression in Prostate Cancer patients

M. T. Siabanopoulou¹, I. Iakovou², E. Zaromitidou³, S. El Mantani Ordoulidis⁴, G. Galaktidou⁵, N. Dimasis⁶, A. Sioundas⁶, A. Gotzamani-Psarrakou¹, ¹2nd Nuclear Medicine Dpt., AHEPA University Hospital, Aristotle University of Thessaloniki, Thessaloniki, GREECE, ²3rd Nuclear Medicine Dpt., Papageorgiou General Hospital, Aristotle University of Thessaloniki, Thessaloniki, GREECE, ³Nuclear Medicine Dpt., Kavala General Hospital, Kavala, GREECE, ⁴Nuclear Medicine Dpt., Bioiatriki S.A., Thessaloniki, GREECE, ⁵Theagenio Cancer Hospital, Thessaloniki, GREECE, ⁶Medical Physics Laboratory, Medical School, Aristotle University of Thessaloniki, Thessaloniki, GREECE.

Introduction: Prostate cancer (PCa) is one of the most common among men malignant tumors. Recently, IGF-I and IGFBP-3 have been implicated in PCa risk among Western populations. IGFs are potent mitogens for a variety of cancer cells since they stimulate cancer cell growth and suppress programmed cell death. Through modulation of IGF bioactivity and other mechanisms, IGF-binding proteins (IGFBPs) have growth-regulatory effects on prostate cells also. We examined whether serum IGF-I and IGFBP-3 could serve as predictors for appearance and expansion of prostate cancer. **Method:** 72 patients with histologically confirmed PCa were recruited (30 patients with localized -M0- and 42 with bone metastatic cancer PCa -M1-). Control sera were obtained from 30 healthy and 33 men with benign prostate hyperplasia (BPH). Serum concentrations IGF-I and IGFBP-3 were analyzed using specific radioimmunoassays (Immunotech, Marseille, France). PSA levels, served as a tumor marker, were determined as well. Whole-body bone scan revealed the presence of metastatic bone lesions. All patients received endocrine therapy as initial treatment. Results: Serum IGF-I levels were higher in PCa patients than the control groups (PCa: 169.8 ± 79.5 ng/ml, control: 138 ± 51.8 ng/ml, $p=0.001$), while there was not observed statistically significant difference between healthy non metastatic and men with BPH ($p>0.05$). Moreover, serum PSA levels were higher in the group of patients with elevated IGF-I compared to those with normal levels ($p<0.05$). On the other hand, IGFBP-3 levels were lower in the metastatic patients -M1- compared to M0 group ($p=0.005$). There seems to be an inverse association between IGF-I, IGFBP-3 and disease progression. In patients with advanced disease IGF-I levels were higher and IGFBP-3 levels were significantly lower, compared with patients without progression ($p=0.05$). **Conclusion:** Our findings, with respect to PSA, provide evidence that IGF-I and IGFBP-3 are determinants of prostate cancer and emphasize the need to further explore their full potential in the setting of early diagnosis and treatment of prostate cancer.

P0988

Intraindividual comparison of Ga-68 DOTATATE and C-11 Choline uptake in patients with recurrent prostate cancer lesions.

O. Alonso¹, G. Dos Santos², R. Castro³, E. Savio¹, A. Paolino³, A. Quagliata¹, H. Balter³, V. Trindade³, J. Giglio³, J. P. Gambini², H. Engler³, ¹CUDIM, University of Uruguay, Montevideo, URUGUAY, ²University of Uruguay, Montevideo, URUGUAY, ³CUDIM, Montevideo, URUGUAY.

Objectives: In the framework of an ongoing trial aiming to assess the value of Ga-68-DOTATATE PET-CT (GALPET) in patients with prostate cancer, the objective of this study was to perform an intraindividual comparison of this technique with C-11 Choline PET-CT (CHOLPET) in a sample of prostate cancer patients. **Methods:** We studied seven patients with prostate cancer during follow-up: two with known bone metastases confirmed by a previous bone scan (PSA: 79-480 ng/mL) and five with biochemical recurrence after treatment (PSA: 0.7-10 ng/mL). Within 1-2 weeks, a PET-CT study was performed with Ga-68-DOTATATE and C-11 Choline with a dose of 110 MBq and 420 MBq, respectively, using a 64-slice PET-CT with time-of-flight correction. The maximum SUV (SUVm) was measured in all abnormal foci. **Results:** Both techniques were negative in three patients with biochemical recurrence. GALPET and CHOLPET were positive in 63/64 bone lesions corresponding to both patients with known bone disease and to one patient with biochemical recurrence. Two discordant bone abnormal foci were found (positive for GALPET or CHOLPET only). Additionally, in two patients with bone metastases and in other with biochemical recurrence, 6 pelvic lymph nodes were positive by means of GALPET whereas CHOLPET detected 4 of them. CHOLPET SUVm were higher than those from GALPET (7.7 ± 3.9 vs. 3.8 ± 1.4 , $n=70$, $p<0.0001$). However, a significant correlation was found among both tracers' SUVm ($r=0.74$, $n=70$, $p<0.0001$). **Conclusions:** In advanced prostate cancer patients, Ga-68-DOTATATE uptake in lesions expressing somatostatin receptors seemed to correlate with C-11 Choline uptake. More studies are needed in order to test for the possible complementary value of these techniques and for the potential of receptor-mediated therapies with appropriate ligands labeled with Y-90 and/or Lu-177.

P0989

Evaluation of Samarium-153-lexidronam in the palliative treatment of prostate adenocarcinoma

W. El Ajmi, L. Zaabar, Y. Mahjoub, A. Sellem, H. Hammami; Military hospital of instruction of Tunis, tunis, TUNISIA.

Objectives: A retrospective study evaluating the efficacy of samarium-153 (^{153}Sm)-lexidronam (Quadrament *) on bone metastases of prostatic adenocarcinoma. **Material and Methods:** 24 treatments were administered to 18 patients with a median age of 71 years (minimum: 64 years, maximum 84 years). Each patient received 1 mCi/kg of ^{153}Sm -lexidronam, the median dose is 73.5 mCi, after rehydration of 1 liter of saline serum. Planar scans were performed 24 hours after injection. The pain is evaluated by visual analogue scale (VAS), and monitoring of hematological toxicity by a formula and blood counts at the second and fourth weeks. Results: ^{153}Sm -lexidronam had significative positive effects on measures of pain relief at weeks 4 ($p<0.001$) and 52.2% have no pain (VAS = 0). Reductions in opioid and second level of painkillers were noted. The evolution of median Karnofsky Performance Status Scale at week 0, week 2 and week 4 was respectively 75%, 70% and 80% with a statistically significant improvement between week 0 and week 4 ($p=0.03$). Bone marrow toxicity was observed with thrombocytopenia in 40.9% and anemia in 27.3% of cases in the second week. **Conclusions:** Our results demonstrate that 1 mCi/kg of ^{153}Sm -lexidronam is an effective treatment for the palliation of painful bone metastases in prostatic adenocarcinoma patients with risk of reversible thrombocytopenia.

P0990

The first experience with 18F-Choline PET-CT in (re-)staging prostate cancer.

B. van der Hiel, W. V. Vogel, M. P. M. Stokkel; Netherlands Cancer Institute - Antoni van Leeuwenhoek hospital, Amsterdam, NETHERLANDS.

Purpose: The aim of our study was to assess the value of 18F-Choline PET-CT in patients with prostate cancer and to investigate the value of 18F-Choline PET-CT compared to bone scintigraphy in detecting bone metastases. **Materials and Methods:** Retrospectively, patients with prostate cancer who have had a bone scintigraphy as well as an 18F-Choline PET-CT in the period from March 2009 until November 2011 were included. Age, TNM stage, Gleason-score, therapy in history related to prostate cancer and biochemical parameters as PSA and PSA doubling time were collected. The results of bone scintigraphy were defined as positive, negative or inconclusive for bone metastases. The results of 18F-Choline PET-CT were defined as positive, negative or inconclusive for local recurrence, lymph node metastases or bone metastases. Patient's follow-up was registered in time, histology, PSA or by imaging. **Results:** Fifty patients were included in this study with a mean age of 62 years (range 48-79). TNM stage was T3 or higher in 31 patients, 12 patients were diagnosed with lymph node or distant metastases. Gleason-score was 6 or higher in all patients except one. 43 Patients have had previous therapy, predominantly radiotherapy, surgery, hormonal therapy or a combination of those. The indication for performing bone scintigraphy was restaging in 40 patients and staging in ten patients. In as well as the restaging group as in the staging group,

most patients had a negative bone scintigraphy (26/40 restaging group, 7/10 staging group). Of these patients, in the restaging group 19/26 patients had a positive PET. In 16/19 patients this was due to local recurrence and/or lymph node involvement, and three patients had also distant metastases, amongst others bone metastases. In the staging group all patients had a positive PET, 6/7 patients PET showed lymph node metastases and one patient revealed bone metastases. In all patients with an inconclusive bone scintigraphy, additional PET was helpful in 9/10 patients. Conclusion: The results of this study seem consistent with literature, that 18F-Choline PET has an additional value in (re-)staging prostate cancer when bone scintigraphy is negative or inconclusive. Furthermore, it has an additional value in imaging local recurrence and lymph node metastases.

P0991

Molecular imaging of prostate cancer with Fluorocholine PET/CT (FCH-PET): effect of imaging protocol standardization on diagnostic accuracy.

A. Belletti, L. Maccanelli, M. Scarlattei, G. Baldari, C. Cidda, R. Mazza, L. Ruffini; Azienda Ospedaliero-Universitaria di Parma, Parma, ITALY.

Prostate cancer evaluation by FCH-PET has increased its importance in clinical practice. FCH-PET is performed using different protocols: dynamic, static early, late or combined acquisitions. Standardization of imaging procedures is needed to improve PET study quality, measurement of treatment response, data useful for multicenter studies. Therefore, FCH-PET requirement for dynamic scanning restrains its routine use in many clinical settings, generally requires more patient compliance and impacts workflow; in addition, dynamic studies cover a field of view of only up to 20 cm. **Aim.** To measure staff and patient compliance in performing double time FCH-PET (dynamic/late whole-body acquisition) and precision in following the standardized protocol. To verify impact of the selected protocol on diagnostic results. **Methods** -Literature research -Prospective observational study -Standardization of FCH-PET acquisition protocol: CT scout view, low-dose CT scan over the pelvis. Dynamic PET scan starting with injection (1 min/frame for 8 min; one bed position, 2D). Delayed-whole-body imaging after definition of axial extension by CT scout (10 mA, 120 Kv) and low-dose CT scan (120 kV, FOV 70, thickness 3.75, speed 0.8 sec); 3D-PET study (GE Discovery ST) 60 min after tracer administration from mid-thighs to skull base (overlap 7, acquisition time 2.5 min/bed; 6/7 bed positions). **Results** The study was approved by local Ethical Committee. From April 2010 to April 2012 we performed 214 FCH-PET for prostate cancer. Pts mean age 70±7 yrs, range 47-87; injected tracer activity 280±20 MBq. Dynamic acquisition 174 (81%); whole-body only 29; PET-guided radiotherapy planning 16 (5 dynamic acquisition). Staging PET was performed in 42 pts before surgery or radiotherapy (Gleason Score 6-9, PSA >10 ng/ml). Local disease resulted in 21 pts (11 dynamic imaging); locoregional/distant disease was revealed in 9 pts (6 dynamic imaging). In 172 pts FCH-PET was performed in the suspicion of recurrence after radical prostatectomy (119), radiotherapy (21), hormonal therapy (22), radiotherapy+hormone therapy (10). Local disease was revealed in 10 pts (7 dynamic imaging); locoregional/distant lesions were detected in 58 pts (58 dynamic imaging). Dynamic acquisition was not performed for tracer decay or delayed acquisition for radiotherapy planning. **Conclusion** Dynamic acquisition of FCH-PET imaging is routinely feasible not inducing staff or patients discomfort. It adds extra-information in few cases, but impacts diagnostic accuracy (i.e. radiotherapy planning, clinical decision). Protocol standardization and adhesion guarantee PET data reliability and site reputation for complex procedures and/or scientific investigations.

P0992

Staging of patients affected by high risk prostate cancer with 18F-Choline PET/CT: preliminary results.

V. Pirro¹, M. Racca¹, E. Garibaldi², T. Varetto¹; ¹Nuclear Medicine Department, IRCC, Candiolo, ITALY, ²Radiotherapy Department, IRCC, Candiolo, ITALY.

Background. An accurate staging protocol is crucial in patients with prostate cancer, particularly in high risk group of patients (PSA serum level greater than 20ng/mL and/or Gleason Score >7 and/or with T3 tumor) where the exclusion of nodal or distant metastases is mandatory to properly plan the therapeutic strategy. Even if not yet widely used, early results are encouraging and suggest a potential role of Choline PET/CT in regional and distant assessment, in addition to MRI for T evaluation. **Aim.** To prospectively explore the role of 18F-choline PET/CT in the staging of N and M parameters in patients with high risk prostate cancer. **Patients and methods.** Thirty untreated patients with high risk prostate cancer underwent 18F-Choline PET/CT at our Nuclear Medicine Department for disease staging in addition to conventional imaging modalities (at least 14 days after prostate biopsy). Mean PSA was 48.1 ng/mL (range 5.05-671 ng/mL); 7 patients had T2 stage, 7 with T3a, 3 with T3b, 1 with T4; Gleason score was 6 for three patients, 7 for eleven patients, 8 for eleven patients, 9 for three patients and 10 in two patients. PET/CT findings were confirmed by MRI, CT, bone scan and, when possible, by histology. A dual-phase imaging protocol was used: precocious pelvic images starting 2 minutes

after radiotracer injection and delayed whole-body images at 60 minutes from injection. Informed consent was obtained. Per-patient and per-district sensitivity, specificity and accuracy of 18F-choline PET/CT were calculated. **Results.** PET/CT was positive for N or M lesions in 19/30 patients. In 13 of them it revealed a total of 29 lymph-nodal lesions (27 true positive, 2 false positive), while in 1 patient 2 lymph node metastases histologically proved at surgery were missed. Eight patients had a total of 18 bone lesions (17 confirmed; 1 false positive). Other extra-prostatic lesions were observed: 5 patients with seminal vesicles involvement, 1 with rectal involvement and 2 with multiple lung metastases, all confirmed as true positive findings. On the per-patient analysis, The sensitivity, specificity and accuracy resulted: 94%, 83%, 90% (per-patient evaluation); 93%, 100% and 96% (lymph nodal district); 89%, 95%, 93% (distant metastases) respectively. **Conclusions.** On the basis of our preliminary results, 18F-Choline PET/CT gained high sensitivity and specificity in staging high risk prostate cancer patients, allowing an accurate evaluation of disease extension (N and M). Useless radical approaches were avoided in 8/30 patients (26%), since PET identified unexpected distant metastases.

P0993

Influence of hormonal therapy in 18Fluoromethylcholine (18FCH) PET/CT imaging in prostate cancer: preliminary data

S. Sivoletta¹, T. Buresta², I. Palumbo³, V. Radicchia³, R. Bellavita³, C. Aristei³, G. Pelliccia¹, B. Palumbo²; ¹Nuclear Medicine and PET Centre, Osp.Foligno, Foligno, ITALY, ²Nuclear Medicine, University of Perugia, Perugia, ITALY, ³Radiotherapy, University of Perugia, Perugia, ITALY.

Aim: The influence of hormonal therapy (HT) in patients with prostate cancer undergoing ¹⁸Fluorocholine PET/CT is still an open question. Some authors described no decrease in labeled choline uptake in subjects under HT, while other showed an interference of anti-androgenic therapy in radiopharmaceutical uptake. To contribute to this knowledge we retrospectively evaluated patients surgically treated for prostate cancer with suspected recurrence with and without HT undergoing ¹⁸Fluoromethylcholine (¹⁸FCH) PET/CT. **Materials and Methods:** ¹⁸FCH PET/CT was performed in 71 patients surgically treated for prostate cancer with suspected recurrence or progression; thirty-seven out of the 71 patients (PSA range 0.3-7.53 ng/dl) were under hormonal therapy (HT) at the time of PET/CT scan, while 33 (PSA range 0.68-16.8 ng/dl) were not (never treated or without therapy for the last 3 months). PET/CT was carried out by an integrated system (Biograph 6, Siemens), intravenously administering 3,2MBq/kg of ¹⁸FCH (ACOM S.p.A.) to each patient; image acquisition was performed 45-60 minutes after. PET/CT scans were interpreted by two expert nuclear medicine physicians and neoplastic disease was diagnosed when areas of tracer uptake were greater than background activity. **Results:** In the 71 patients studied 262 lesions were considered as neoplastic at PET/CT scan, being the majority localized in bone and lymph nodes (particularly pelvic). In the 71 patients 47 were true positive cases (TP), 6 false positive (FP), 4 false negative (FN) and 14 true negative (TN). Sensitivity of ¹⁸FCH PET/CT in the 71 patients studied was 92%, specificity 70%, accuracy 86%, Positive Predictive Value (PPV) 89%, Negative predictive value (NPV) 78%. Among the 37 patients under HT 27 subjects were TP, 3 FP, 2 FN and 5 TN. Sensitivity in patients under HT was 93%, specificity 62%, accuracy 86%, PPV 93% and NPV was 71%. In the group of patients (n.33) without HT 20 subjects were TP, 2 FP, 2 FN and 9 TN. Sensitivity in patients without HT was 90%, specificity 82%, accuracy 88%, PPV 90% and NPV 82%. **Conclusion:** In our preliminary data specificity and NPV of ¹⁸FCH PET/CT were decreased in patients in HT, while sensitivity was similar in the 3 groups, substantially in agreement with recent literature (Giovacchini Eur J Nucl Med Mol Imaging 2010); this could be explained for the presence of inflammatory lesions (particularly in lymph nodes) of difficult interpretation. Further data are necessary to confirm these results.

P0994

Follow-Up of Prostate Cancer: Clinical Data, Bone Scans and Prostate-Specific Antigen Levels

B. A. L. Abreu¹, A. M. Santos², A. R. Santos¹, L. A. Soares¹, L. A. Macedo², R. M. Santos¹, J. B. Abreu¹, D. F. Leal³, P. E. B. Santos⁴, J. L. S. Junior⁴; ¹Centro Bionuclear de Diagnostico, Teresina, BRAZIL, ²Faculdade Novafapi, Teresina, BRAZIL, ³Universidade Federal do Piauí, Teresina, BRAZIL, ⁴Universidade Estadual do Piauí, Teresina, BRAZIL.

AIMS: Prostate Cancer (PC) is a slow-growing tumor with non-linear progression whose most common site of hematogenous spread is the bone. Bone scans are the most common and useful investigation method for the detection of bone metastases in PC. ^{99m}Tc methylene diphosphonate (MDP) remains the most widely used bone agent, in the detection and monitoring of skeletal metastases. This work aims to correlate the bone scintigraphic findings with age, pain, gleason and PSA values in follow-up of PC patients. **MATERIALS AND METHODS:** We retrospectively evaluated 123 patients in followed up for CP that underwent bone scintigraphy in Bionuclear Diagnostic Center, from May 2010 to May 2011. The scintigraphies were held in the anterior and posterior incidences in Génesys Epic gamma camera, 4 hours after a 600 MBq intravenous injection of ^{99m}Tc-MDP. Upon examination, all

patients were asked about pain and if they had suffered some kind of trauma. In addition, patient identity (age), gleason and PSA values were collected. This information was correlated with presence or absence of bone metastases. For data analysis, the chi-square test with statistical significance set at 5% ($p < 0.05$) was used. Data analysis was performed using the Statistical Package program for Social Sciences (SPSS) 17.0. RESULTS: The age ranged from 46 to 90 years with a mean of 70.42 years; the final gleason score ranged from 5-9; PSA values ranged from 0.01 to 1809.4 ng/ml with a mean of 68.04 ng/ml. Skeletal Scintigraphy was normal in 69.1% of cases, slightly positive (1 to 3 sites of metastases) in 11.4%, moderately positive (4 to 6 sites of metastases) in 4.1% and strongly positive (disseminated lesions or superscan) in 15.4% of cases. There was a statistically significant correlation between the variables gleason and bone scintigraphy ($p = 0.047$), showing that the higher the final score of gleason, the greater the likelihood of presenting positive scintigraphy. However, there was no correlation between the abnormal scintigraphic findings and age ($p = 0.237$), presence of bone pain ($p = 0.759$), nor with PSA levels ($p = 0.902$). CONCLUSION: The variables age and pain were not correlated with the positive findings of bone scintigraphy. In addition, PSA also did not show significant correlation with abnormal findings on bone scans. However there was a statistically significant correlation between Gleason and abnormal bone scintigraphy.

P59-2 - Tuesday, October 30, 2012, 16:00 - 16:30, Poster Exhibition Area

Oncology Clinical Science: Gynaecological

P0995

Evaluation of dual-time-point FDG PET/CT for differentiation between ovarian cancer, low potential malignancy, and benign ovarian tumor

T. Okamura¹, H. Seura¹, Y. Hamazawa², M. Hamuro², A. Moriyama³, T. Murata³, K. Koyama⁴; ¹Department of PET center, Saiseikai Nakatsu Hospital Osaka, Osaka, JAPAN, ²Department of Radiology, Saiseikai Nakatsu Hospital Osaka, Osaka, JAPAN, ³Department of Gynecology, Saiseikai Nakatsu Hospital Osaka, Osaka, JAPAN, ⁴Department of Radiology, Osaka City University Graduate School of Medicine, Osaka, JAPAN.

[Aim] Ovarian tumors are often difficult to differentiate between ovarian cancer, low potential malignancy (LPM) and benign tumors with solid portion on MRI. It is important to differentiate these ovarian tumors for planning the operation procedure. Adnexectomy and/or simple hysterectomy are adequate for LPMs, with peritoneal lymph node resection and omentectomy not being required, unlike cancer surgery. We evaluated the usefulness of the dual-time-point FDG PET/CT for differentiating these ovarian tumors referring to MRI. [Patients•Methods] Forty-three women with ovarian tumors (age range 24-84 years, mean 55 years) who were performed MRI and dual-time-point FDG PET/CT before surgical resection were studied. All tumors were histologically proven: eighteen ovarian cancers (6 endometrioid adenocarcinomas, 5 clear cell adenocarcinomas, 4 papillary serous adenocarcinomas, 1 mucinous adenocarcinoma, 1 malignant mesodermal mixed tumor and 1 malignant Brenner tumor), nine LPMs (4 serous cystic tumors, 2 mucinous cystic tumors, 2 immature teratomas and 1 granulosa cell tumor), and sixteen benign tumors (6 mucinous cystadenomas, 5 dermoid cysts, 2 fibromas, 2 serous cystadenomas and 1 fibrothecoma). For dual-time-point FDG PET/CT scanning, the early and delayed scans were performed at 1 and 2 hours after FDG administration. Quantitative evaluation was done using SUVmax. [Results] SUVmax of the early scan (SUVe) and that of the delayed scan (SUVd) of ovarian cancers were 6.37 ± 2.82 (mean \pm S.D.) and 8.51 ± 4.06 , respectively, while SUVe and SUVd of LPMs were 3.34 ± 3.33 and 3.8 ± 4.71 , respectively. Seven of 16 benign tumors had solid areas on MRI and those SUVe and SUVd were 2.67 ± 0.96 and 3.0 ± 1.12 , respectively. The other nine benign tumors showed no FDG uptakes. The SUVd were significantly higher than SUVe for both cancers and benign tumors, while there was no significant difference between SUVe and SUVd for LPMs. SUVe and SUVd of ovarian cancers were significantly higher than those of LPMs and benign tumors. However, 3 ovarian cancers showed low SUVmax and 1 LPM showed high SUVmax on early and delayed scans. There was no significant difference between SUVe of LPMs and that of benign tumors, also between SUVd of LPMs and that of benign tumors. [Conclusion] The SUVmax of LPMs was lower than that of cancers on early and delayed scan. SUVmax of ovarian cancers increased significantly in delayed scan, but that of LPMs did not increase. Consequently, FDG PET/CT was useful for differentiating LPM from cancer.

P0996

Sentinel lymph node detection in surgical treatment of cervical cancer

V. V. I. Chernov¹, I. G. Sinilkina², L. A. Kolomiets², A. L. Chernyshova², A. A. Titskaya², R. V. Zelchan²; ¹Institute of Cardiology, Tomsk, RUSSIAN FEDERATION, ²Institute of Oncology, Tomsk, RUSSIAN FEDERATION.

The purpose of the study. To evaluate the feasibility of radionuclide imaging modalities in the assessment of regional lymph node status in cervical cancer. Materials and methods: The study included 11 cervical cancer patients. On the day before surgery, all patients were injected with the 80 MBq 99mTc-labelled - nanocolloid in four points into the submucosal space of the uterine cervix. Single Photon Emission Tomography (SPECT) of the pelvis was performed 20 minutes and 3 hours later (E.CAM 180, Siemens). SPECT scans were visually assessed. Sentinel lymph nodes (SLN) were detected intraoperatively using gamma probe (Gamma Finder II®, Germany). After pelvic-iliac lymphodissection, the removed lymph nodes were re-examined by the gamma probe and these results were compared with intraoperative findings. The nodes were considered as sentinel lymph nodes if their radioactivity was minimum 3 times higher compared to other lymph nodes. Results. 17 sentinel lymph nodes were detected by pelvic SPECT in 8 patients and 21 were founded intraoperatively by gamma probe in 10 patients. By SPECT the most frequent locations of SLNs were external iliac - 9 (52.9%), obturator - 5 (29.4%), internal iliac - 2 (11.8%), common iliac - 1 (5.9%) arteries. In XX of cases (41.9%) lymphoscintigraphy showed unilateral drainage. By radioguided study the most frequent locations of SLNs were external iliac - 11 (52.4%), obturator - 5 (23.8%), internal iliac - 2 (9.5%), common iliac - 2 (9.5%) arteries and in the cardinal ligament area in one case (4.8%). In 6 of cases (60%) lymphoscintigraphy showed unilateral drainage. The sensitivity of intraoperative SLN detection with the gamma probe was found to be higher than the sensitivity of SPECT SLN detection (90.9% versus 72.7%). Thus, the technique of radioguided detection of sentinel lymph nodes is more effective compared to SPECT. Conclusion. SPECT is useful method for preliminary SLN detection before surgery. The use of intraoperative radioguided detection allows to detect sentinel lymph nodes with 90.9% sensitivity.

P0997

Utility of 18F-FDG-PET-CT in retroperitoneal staging of locally advanced cervical cancer. Preliminary results in correlation with histopathology.

J. Mucientes, B. Rodríguez, T. Perez Medina, M. J. García-Espantaleón, J. Cardona, A. Gomez, A. González, M. Beresova; Hospital Universitario Puerta de Hierro Majadahonda, Madrid, SPAIN.

AIM To analyse the usefulness of 18F-FDG-PET-CT for the detection and characterization of retroperitoneal lymphadenopathies in patients with locally advanced cervical cancer. MATERIALS AND METHODS All patients diagnosed with locally advanced cervical cancer and no evidence of distant disease (M0) between June/09 and September/11 were prospectively selected and underwent a 18F-FDG-PET-CT study for presurgical staging. 18F-FDG-PET-CT was performed 50 minutes after the intravenous injection of 370 MBq of 18F-FDG and then evaluated by two experienced nuclear physicians who assessed the presence or not of retroperitoneal lymphadenopathies as well as the metabolic activity for each of them. All the patients were then referred to retroperitoneal lymphadenectomy for definitive staging. A thorough inspection of the abdomen and pelvis in search of metastatic spread is performed. Excision of the nodes is performed from laterocava, to interaorto-cava, infra and supramesenteric paraaortic and precaval in a standardized systematic form. Lymph nodes were formalin fixed and embedded in paraffin blocks after macroscopic dissection by an experienced pathologist who was blinded to the FDG-PET results. Each lymph node was examined microscopically to determine whether it harbored a metastasis and measure the size of the metastatic lesion. Serial sectioning and immunohistochemical analysis were performed when a micrometastasis was suspected. RESULTS Fourteen patients were included. The mean size of the primary tumour assessed by 18F-FDG-PET-CT was 5.5cm (range: 2.3-8.0 cm) and the maximum SUV was 14.0 (3.5-28.1). Six patients showed positive pelvic adenopathies according with PET criteria (SUVmax 11.4; range 4.2-19.1). None of the patients showed retroperitoneal lymphadenopathies suspicious by 18F-FDG-PET-CT. Retroperitoneal lymphadenectomy for definitive staging was performed 8-58 days after the 18F-FDG-PET-CT study (mean or the interval 25 days). The number of lymphadenopathies resected per patient varied between 5 and 22 (mean 9.3). There was no evidence of histopathological metastases in 13 of the 14 patients (92.9%). In the group of patient without pelvic adenopathies according to 18F-FDG-PET-CT results, the histopathological analysis of the retroperitoneal lymph nodes was negative in 8 of 8 patients (negative predictive value of PET 100%). In the six patients with pelvic involvement in 18F-FDG-PET-CT studies, the results of the retroperitoneal lymph node dissection was positive in one patient (negative predictive value of 18F-FDG-PET-CT 83.3%). CONCLUSIONS 18F-FDG-PET-CT is a useful tool for the evaluation of retroperitoneal involvement in patients with locally advanced cervical cancer. It has a high negative predictive value (92.9%), especially in patients without pelvic lymph node detected in 18F-FDG-PET-CT (100%).

P0998**Initial Nodal Staging of Locally Advanced Cervical Cancer with FDG-PET/CT**

A. P. Caresia Aroztegui¹, M. Barahona Orpinell², E. Sabrià Bach², C. Gámez Cenzano³, M. Cortés Romera¹, A. Sánchez Márquez⁴, J. Robles Barba¹, L. Rodríguez Bel¹, S. Rossi Seoane¹, L. Martí Cardona², J. Ponce i Sebastia², ¹PET UNIT Institut de diagnòstic per la Imatge (IDI). Hospital Universitari de Bellvitge- IDIBELL, Barcelona, SPAIN, ²Gynecology. Hospital Universitari de Bellvitge, Barcelona, SPAIN, ³PET UNIT Institut de diagnòstic per la Imatge (IDI). Hospital Universitari de Bellvitge, L'Hospitalet de Llobregat, Barcelona, SPAIN, ⁴Radiology Institut de diagnòstic per la Imatge (IDI). Hospital Universitari de Bellvitge- IDIBELL, Barcelona, SPAIN.

Objective: To evaluate the contribution of FDG-PET/CT for primary para-aortic nodal staging of locally advanced cervical cancer (LACC). **Material and methods:** This prospective study included 22 women (25–78 years old; mean age = 53.3) diagnosed with LACC. All cases were squamous cell carcinoma (100%) and distribution according to International Federation of Gynecology and Obstetrics (FIGO) stage was as follows: IB2 (4), II (14), III (3) and IV (1). All patients underwent a whole-body FDG-PET/CT for primary staging. PET positive findings were described (site, maximum diameter and SUVmax) and correlated with MRI results, follow-up and histopathologic confirmation was possible, including surgical exploration for para-aortic lymphadenectomy (PAL). Values of true positive (TP), true negative (TN), false positive (FP), false negative (FN) and negative predictive value (NPV) were estimated. **Results:** All the primary tumors showed FDG uptake (SUVmax=8–36; mean 15.5). MRI was performed in 20/22 (2 refused by claustrophobia) and parametrial involvement was found in 18/20. FDG-PET/CT showed positive para-aortic nodes in 4 patients: 3 TP (1 with a positive PAL and 2 with confirmed extraabdominal metastasis) and 1 FP with a negative PAL. PAL was technically feasible in 13/22 women: positive in 2 (1 TP and 1 FN by PET) and negative in 11 (10 TN and 1 FP by PET). NPV was 90%. The treatment was modified in 3/22 (13%) women that received chemotherapy because of detection of unsuspected distant metastasis. **Conclusions:** This pilot study suggests that PET/CT is an effective imaging technique in the initial staging of LACC. It may help to evaluate para-aortic nodal metastasis and to plan the management, especially when unsuspected distant metastasis are detected. Combined use of MRI and PET is complementary.

P0999**Clinical utility of 18F-FDG PET in ovarian cancer patients with normal levels of CA-125**

J. Deportos, A. Domenech, J. Duch, C. Artigas, L. M. Quintero, R. E. Jaller, C. A. Achury, A. Flotats, I. Carrio; Hospital de la Santa Creu i Sant Pau. Servei de Medicina Nuclear., Barcelona, SPAIN.

Aims: The purpose of the study was to evaluate 18F-FDG-PET clinical utility for recurrence detection and therapy response evaluation in ovarian cancer patients with normal levels of CA-125 (<35 U/dL). **Materials and methods:** From June 2010 to February 2012, 71 18F-FDG-PET/CT scans (18F-FDG scans) were performed on 40 patients with ovarian cancer. We analyzed retrospectively clinical and imaging data of 16 ovarian cancer patients (mean age 53.6y, range 18–80y) with normal levels of CA-125 who had one or more (3 patients) 18F-FDG scans at variable stages of the disease. Recurrence detection and therapy response were analyzed in 22 scans. **Results:** 7 out of 22 scans were performed to confirm disease visualized on a previous CT scan as well as to evaluate extent of disease. All the scans were positive for disease in the same localization as the CT scans. The 15 remaining scans were performed to determine therapy response to chemotherapy and/or radiotherapy, 10 being positive for disease persistence. Out of the 17 positive scans, 3 showed distant metastases in one or more viscera (spleen, liver and lung), 4 showed peritoneal implants, 4 showed peritoneal implants and adenopathy, 4 showed adenopathy in one or more localizations, 1 showed peritoneal implants, lung metastases and adenopathy, and the last one showed local recurrence of the disease. These findings were confirmed either by pathological analysis or imaging follow up after treatment. Overall, the presence of disease was detected by 18F-FDG scans in 16 out of 22 scans (73%), representing 23% (16/71 scans) of all the scans performed in ovarian cancer. **Conclusion:** 18F-FDG PET appears to be a valuable imaging modality in detecting recurrence and evaluating therapy response in patients with ovarian cancer and normal levels of CA-125.

P1000**18F-FDG PET/CT in the assessment of suspected ovarian cancer recurrence**

A. Annovazzi, R. Sciuto, R. Pasqualoni, S. Bergomi, S. Rea, C. Mazzone, L. Romano, C. Di Russo, C. L. Maini; "Regina Elena", National Cancer Institute, Rome, ITALY.

Aim: the study evaluates diagnostic performance of 18F-FDG PET/CT in the early detection of ovarian carcinoma relapse. **Methods:** 18F-FDG PET/CT scans performed in 73 ovarian carcinoma patients with suspect of recurrence on the basis of rising

CA-125 values with/without radiological evidence of disease were retrospectively evaluated. A recent contrast-enhanced CT scan was available in 60/73 cases. Results of 18F-FDG PET/CT scan were validated by patient follow-up (n = 60) or by histological confirmation (n = 13). **Results:** a positive 18F-FDG PET/CT scan was reported in 64 out of 73 studies. In 19 patients, despite a negative CT scan, at least one disease localisation was detected at 18F-FDG PET/CT in the pelvis (n=7), abdominal/pelvic (n=9) or supra-diaphragmatic (n=4) lymph nodes, peritoneum (n=9), liver (n=2) and spleen (n= 2). When compared to CT imaging PET/CT exactly matched radiological findings in 16 cases while additional localisations were found in 15 and a lower number of sites in 2. Finally, in 7 cases of equivocal CT findings PET/CT resulted negative. Six of them showed no evidence of disease at follow up. Two false negative 18F-FDG PET/CT scans reported were related, respectively, to microscopic peritoneal colonisation and to a subcentimetric lung nodule, while the only false positive result was due to an inflamed pelvic lymph node. PET/CT was able to change patient management in 60% of patients, in many cases by disease upstaging. The overall accuracy of 18F-FDG PET/CT was 87.7%, with a sensitivity of 96.9% and a specificity of 87.5%. **Conclusions:** 18F-FDG PET/CT is very useful in the evaluation of suspected relapses of ovarian carcinoma strongly impacting on clinical management.

P1001**The role of 18F-FDG PET/CT in pelvic and paraaortic lymph node staging of uterine cervical cancer**

C. Soyda, E. Ibis, F. Ortac, E. Ozkan, N. O. Kucuk, K. M. Kir; Ankara University Medical Faculty, Ankara, TURKEY.

Aim: We aimed to evaluate the sensitivity of 18F-FDG PET/CT in the detection of pelvic and paraaortic lymph node metastases of cervix cancer in the comparison of surgical staging as gold standard. **Material and Methods:** 20 patients (mean age: 56.1±12.6) who had histopathologically proved cervix cancer diagnosis and underwent 18F-FDG PET/CT in Ankara University Medical School Department of Nuclear Medicine for preoperative staging of disease were included to the study. 18F-FDG PET/CT findings were compared with pathology reports in patients who underwent surgery after PET/CT. In 7 patients, findings could not be compared with pathology reports because they were taken under radiation therapy rather than surgery due to extended disease. In this patient group, PET/CT findings were confirmed by other imaging findings and radiation therapy response. Sensitivity, specificity, PPV, NPV and accuracy of 18F-FDG PET/CT in the detection of lymph node metastases were calculated both patient and lesion based. **Results:** 18F-FDG uptake were seen all patients' primary cervical lesions. Mean SUVmax of cervical lesions were calculated as 14.3±6.6 (6.7–25). In 9 patients, pathological 18F-FDG uptake was not detected in pelvic or paraaortic lymph nodes. In the remaining patients, while 18F-FDG uptake was seen in pelvic lymph nodes in all of them and in pelvic lymph nodes in 4. Totally 18F-FDG uptake was detected in 37 lymph node stations. Mean SUVmax of lymph nodes was calculated as 5.9±4.3 (2.6–21.9). According to PET/CT findings, disease was upstaged 1 to 4 in 1, 2 to 3 in 2, 3 to 4 in 1 and 1 to 3 in 2 patients. Treatment management was changed radiotherapy in 5 patients. Sensitivity, specificity, accuracy, PPV and NPV of 18F-FDG PET/CT in patients based analysis were calculated as 81%, 77%, 80%, 81% ve 77%, respectively. In the lesion based analysis, sensitivity, specificity, accuracy, PPV and NPV of 18F-FDG PET/CT were calculated as 85%, 84%, 84%, 81% ve 88%, respectively. Mean SUVmax of metastatic lymph nodes were calculated as 8.96±3.3 and of reactive ones were 4.33±1.05. (p<0.05). **Conclusion:** 18F-FDG PET/CT is a reliable imaging tool in the evaluation of pelvic and paraaortic lymph node metastases of cervical cancer with its high sensitivity and specificity and it change treatment management in about quarter of patients.

P1002**FDG PET-CT in the Preoperative Assessment and Stating of Ovarian Tumors**

B. Gonzalez, M. Bellon, A. Palomar, J. P. Pilkington, V. Poblete, M. P. Talvera, A. Garcia, A. Soriano; HGCR, CIUDAD REAL, SPAIN.

OBJECTIVES To determine the utility of 18F-FDG PET-CT in the clasification of ovarian lesions and the preoperative staging of ovarian neoplasm. **MATERIAL AND METHODS** We performed a prospective study (PI-2009/39) that included patients who had ovarian lesion suspicious for malignancy by laboratory criteria (elevated Ca125) and/or conventional image. All of them underwent PET-CT study with 18F-FDG according to standard protocol. All ovarian lesions with SUVmax≥2.5 were considered highly suspicious for malignancy. Additionally, staging was performed based on qualitative criteria. The final diagnosis of all the ovarian lesions was established by histopathological examination as all the patients underwent surgery (excisional biopsy with/without protocolized intervention). The PET-CT findings that could not be evaluated with the surgery, because of their location, were classified according to clinical-radiological follow-up (≥ 6months). **RESULTS** Our study included 27 ovarian lesions belonging to 26 patients. Regarding histology, 16

lesions were benign and 11 malignant. 14/27 lesions had a PET-CT study consistent with malignancy, 11 of them being true positives. No false negative results were found. The statistical parameters obtained for the PET-CT were: sensitivity 100%, specificity 81.3%, positive predictive value 78.6% and negative predictive value 100%. The average SUVmax in malignant lesions was of 10.1 (range: 3.5–27), while in benign lesions it was 1.73 (range: 0.66–3.9). In the group of patients with histologically confirmed ovarian carcinoma, PET-CT was able to detect extraovarian disease in 63.6% of them (deividir adenopatías y meetastasis a distancia.30% lymph node, 10% metastatic disease and 23.6% both). These findings were confirmed by histopathological analysis (4/7 patients) or clinical-radiological follow-up (3/7 patients). **CONCLUSION:** The PET-CT with 18F-FDG achieves a correct classification of ovarian lesions with a high sensitivity and specificity (100% and 81.3% respectively). In patients with ovarian carcinoma PET-TC detects extraovarian disease in 63.6% of cases, allowing better planning of therapeutic strategy.

P1003

Increasing Level of Ca 125 in Post-Treatment Observation in Ovarian Carcinoma: When PET- CT is Needed ?

M. Bryszewska, MD, G. Lapinska, MD, A. Fijolek-Warszewska, MD, I. Kozłowicz-Gudzinska, MD, A. Sackiewicz-Slaby, P. Ochman; Maria Skłodowska-Curie Memorial Cancer Center and Institute of Oncology, Warsaw, POLAND.

Purpose: Detecting co-dependence between Ca-125 level and speed of increasing of cancer marker and findings in PET-CT. The aim of this study is to attempt to answer the question when exactly PET-CT should be performed: when the level of Ca-125 becomes abnormal, or maybe earlier, when the level of the marker is still proper but reveals tendency to increasing. **Methods:** 54 women after treatment of ovarian cancer (surgery, surgery and chemotherapy or surgery, chemotherapy and radiotherapy), who were examined using PET-CT during post-therapy monitoring as regards to Ca-125 level or CT scan, were evaluated. It has been taken into consideration not only single Ca-125 level, but increasing marker level as well. The results were confirmed or not using histopathology results or response to chemotherapy, measured by Ca-125 level. **Results:** In 22 patients with high Ca-125 level (above 35 IU/mL) PET-CT results were positive, and in 12 patients with low Ca-125 level results were negative. In 6 patients with low Ca-125 level PET-CT results were positive, and in 5 patients with high Ca-125 level PET-CT results were negative (1 woman suffered from endometriosis). In remaining patients the results of PET-CT were not certain. In 30 patients (75 % patients with high level of marker) with PET-CT findings (PET-CT positive or not certain) speed of increasing Ca-125 level before performed PET-CT was above 200% during 5 months (average time). **Conclusion:** The outcome of this study proved well known value of PET-CT scan in post-treatment monitoring of patients with ovarian cancer. Therefore performing PET-CT scan depending on tendency of Ca-125 level to increase, even if it is still under 35 IU/mL, should be considered.

P60-2 - Tuesday, October 30, 2012, 16:00 - 16:30, Poster Exhibition Area

Oncology Clinical Science: Colorectal Cancer

P1004

Influence of physiological FDG uptake on lesion detection in the large intestine

S. Yasuda¹, M. Takechi¹, K. Kobayashi², Y. Miyatake², M. Ono², T. Katoh², N. Yamamoto², M. Akeboshi², T. Kojima², W. Ko²; ¹Tokai University School of Medicine, Kanagawa, JAPAN, ²Yotsuya Medical Cube, Tokyo, JAPAN.

Objective: Physiological FDG uptake in the large intestine is frequently noted on PET images and can be problematic for the interpretation of PET images. The purpose of the study is to determine the frequency of high physiological FDG uptake and its influence on lesion detection in the large intestine. **Methods:** Between November 2010 and January 2012, 152 asymptomatic subjects (117 men and 35 women), aged 57.5±10.0 years, underwent both PET/CT and total colonoscopy under our cancer screening program. All subjects underwent colonoscopy within one to 24 days (5.5±3.5 days) following PET/CT, regardless of the PET/CT results. Interpretation of PET images had been recorded on the perspective of screening of colorectal lesions. Retrospectively, gray-scale projection PET images were visually evaluated and all 152 subjects were classified into three groups according to the intestinal FDG uptake: L (localized uptake), D (diffuse uptake), or N (no apparent uptake) group. Intestinal FDG uptake was considered positive if the activity is higher than that of the liver. Images of coronal sections were also available. Lesions less than 1 cm detected with colonoscopy were excluded from the study. **Results:** Colonoscopy revealed 9 small lesions in 8 men: localized colitis or ulcer (4) and polyps 10 to 13mm in size (5). Remaining 144 subjects had no lesions. By excluding the 8 subjects, physiological intestinal uptake was determined to be positive in 27 of the 144 subjects (18.8%): 6 in the L group and 21 in the D group. No significant difference was observed in the frequency

between both genders. PET result had been false positively recorded in 2 of 8 subjects (25%) in the L group. Two lesions in the L group, an adenoma (13mm in size) and a caecal ulcer, were proven to be true positive. The other 7 lesions were found in 6 men in the N group and, consequently, the PET results were false negative. As a whole, false positive interpretation was found in 2 of 152 subjects (1.3%), and 2 of 29 (6.9%) subjects with positive intestinal uptake. True positive result was found in 2 of 8 subjects (25%) with localized FDG accumulation. **Conclusion:** Although physiological FDG uptake is frequently observed at an overall rate of 18.8%, careful interpretation can lead to minimize misinterpretation of PET images and detect even small lesions.

P1005

The use of combined FDG PET and MRI liver with Primovist in the restaging of colorectal carcinoma prior to hepatic resection

D. C. Wong; The Wesley Hospital, Brisbane, AUSTRALIA.

Introduction: The aim of the study is to assess the combined role of FDG PET and MRI liver with Primovist in the restaging of colorectal carcinoma prior to hepatic resection by comparison with surgical findings. **Methods & Materials:** This is a prospective study over a 3.5year period involving combined FDG PET and MRI liver with Primovist studies in 24 patients. There were 14 males and 10 females with ages from 47 to 79 yrs and median age of 61 yrs. All available imaging including CT and ultrasound were correlated with, and cases were discussed at the Wesley Liver Multidisciplinary meetings. **Results:** 20 patients proceeded to laparoscopic surgeries. 12 patients (60%) had concordant MRI and PET studies, with two patients having undetected extra hepatic metastases - left pelvic brim and bladder. Three patients had more MRI lesions than PET with lesions measuring 7mm to 14mm. There were two patients with PET negative studies compared to MRI that were suspected to be related to chemotherapy, with lesions measuring 5mm to 19mm. There were two patients with lesions that were both MRI and PET negative, measuring 4mm to 12mm. Four patients did not proceed to surgery due to extensive disease involving both hepatic lobes. Two of these patients had concordant PET and MRI studies, two patients showed more lesions with MRI compared to PET, with lesions measuring 3.5mm to 5mm. **Conclusion:** Combined FDG PET and MRI liver with Primovist have an important role in the restaging of colorectal carcinoma prior to hepatic resection. MRI liver with Primovist has shown more hepatic metastases when compared to FDG PET, with some explained by recent chemotherapy. A few hepatic metastases can be both MRI and PET negative.

P1006

Comparison of Gross Tumor Volume (GTV) Determined by 18F-FDG PET/CT and MRI in Radiotherapy Planning in Rectal Cancer

G. Salazar Andía¹, L. F. León Ramírez¹, J. Corona Sánchez², A. Prieto Soriano¹, A. Ortega Candil¹, R. C. Delgado-Bolton¹, C. Rodríguez Rey¹, C. González Roiz¹, M. De Las Heras González², J. L. Carreras Delgado¹; ¹Nuclear Medicine Department, Hospital Clínico San Carlos, Universidad Complutense, Madrid, SPAIN, ²Department of Radiotherapy. Hospital Clínico San Carlos, Madrid, SPAIN.

Objective: To evaluate if radiotherapy planning with 18F-FDG PET/CT in rectal cancer (RC) can modify the gross tumor volume (GTV) to be irradiated compared to pelvic MRI. In addition, if PET/CT provides additional information on initial staging of RC. **Materials and Methods:** We retrospectively analysed 39 patients (23 male, mean age 68 years) with RC, who had a PET/CT scan performed for radiotherapy planning and an MRI with an interval of time not exceeding 30 days. GTV in both studies (PET/CT and MRI) included: (a) primary rectal tumor; and (b) pelvic lymph nodes or perirectal soft tissue injuries increased in size, usually larger than 1 cm. The GTV determined by PET/CT measure also included subcentimetric lymph nodes with pathological 18F-FDG uptake (SUVmax >2.5). **Results:** In 23/39 patients (59%) PET/CT did not induce changes in the GTV. In 7/39 (18%) PET/CT underestimated the GTV (MRI showed millimetric lymphadenopathies in mesorectum suggestive of malignancy, while PET/CT did not reveal pathological uptake of 18F-FDG in this location, probably due to the small size of these lymph nodes). In 7/39 (18%) PET/CT modified the GTV (GTV increased in 6 patients and decreased only in one). In the two remaining patients (5%) GTV was not defined as PET/CT detected liver metastases and neoadjuvant chemotherapy was initiated. PET/CT also identified distant metastases in 14 patients, unknown in 8 of them (21%), inducing a different therapeutic management (in 4 patients surgical liver metastases resection was performed, in one patient the lung disease was totally resected and in three patients the chemoradiotherapeutic treatment was modified). **Conclusions:** The combination of the information supplied by PET/CT and MRI is useful in the precise definition of GTV in rectal cancer, minimizing normal tissues radiation. Unknown metastases detected in PET/CT can modify patient management in these cases.

P1007**Usefulness of 18F-FDG PET-CT in the initial staging of locally advanced rectum carcinoma.**

D. R. Mendez Mareque, M. Coronado, R. Couto, A. Martinez, S. Rodado, M. Marin, I. Santos, L. M. Martin Curto; University Hospital La Paz, Madrid, SPAIN.

Aim: To assess the usefulness of ¹⁸F-FDG-PET/CT in the initial staging of locally advanced rectum carcinoma (LARC). **Materials and methods:** Prospective study that includes 26 patients diagnosed of locally advanced adenocarcinoma of the rectum (T3/T4 or N1), before starting treatment. All patients have histologic diagnosis by colonoscopy and biopsy, and staging studies by conventional image techniques (CIT): pelvic MR that defines tumor and lymph node extension (TN) and total body CT that defines distant disease (M). All patients undergo PET-CT (low-dose CT) for N and M definition. All patients are presented in the Committee of colorectal tumors in our hospital, in order to consensuate therapeutic approach. Findings in each imaging technique are classified as positive (+), negative (-) or indeterminate (x) for malignancy. NM stadification following the 7th AJCC classification is determined for each imaging modality. Correlation between stages of each modality is analyzed with the Chi-Square test. Change of therapeutic attitude based on PET-CT results is evaluated in relation to CIT. **Results:** PET/CT changed stadification in 8/26 patients (31%) in comparison with CIT: it classified as M0 4 patients Mx by CIT; as M1 2 patients Mx by ICT, as M1b 1 patient M1a by ICT, and as M0 1 patient M1a by CIT. A weak correlation between MR and PET/CT for N staging was found ($\kappa = 0.3$, $p=0.04$); MR defined N0/1 a high percentage of cases Nx in PET/CT. A good correlation between PET-CT and CT was found for M staging ($\kappa = 0.8$, $p=0.00$); PET-CT classified M0/1 a high percentage of cases Mx by CT. In 5/26 patients (19%) PET/CT modified therapeutic approach: indicating the need of adjuvant treatment in 2 patients with M1 disease, modifying tumour volumes for RT planning in 2 patients, and planning treatment for a synchronous primary in one patient. **Conclusion:** In the initial staging of LARC, PET/CT provides additional information to CIT in the detection of distant disease. Although it is necessary to enlarge the serie, change in the therapeutic approach based on PET/CT seems to justify its use in these patients.

P1008**Clinical utility of FDG PET-CT in surveillance of patients with colorectal malignancy when serum CEA level is within normal range - A prospective study**

S. Dash, A. Gupta; Action Cancer Hospital, NEW DELHI, INDIA.

Aim: To evaluate the diagnostic capability and impact of FDG PET-CT scan in surveillance of patients with colorectal malignancy when serum CEA level is within normal range. **Material and Methods:** A prospective study of 31 consecutive patients of colorectal malignancy with normal serum CEA was carried out using whole body FDG PET-CT scan. All patients were biopsy proven cases of CEA secreting colorectal adenocarcinoma, appropriately treated for the primary malignancy, were in remission for at least three months and on surveillance. They presented with or without any suspicious sign(s) / symptom(s) with normal serum CEA level (less than 4 ng/ml). FDG avid lesions were subjected to cyto / histopathology or interval FDG PET-CT scan within 8-20 weeks with serial serum CEA determination to confirm / refute recurrence. Negative PET-CT studies also had interval PET-CT scans 8-20 weeks later with serial serum CEA measurement to confirm absence of recurrent disease. **Result:** FDG PET-CT detected metabolically active lesions in 13 patients (Mean serum CEA - 3.2 ng/ml), out of which 11 were true positive (Mean SUVmax - 5.6) and 2 were false positive (Mean SUVmax - 2.7) for recurrence. False positive lesions had histological evidence of granuloma, possibly tubercular etiology which is quite common in Indian population. All FDG negative patients (total number 18, mean serum CEA - 2.6 ng/ml) had interval FDG PET-CT scan performed along with measurement of serum CEA. 15 patients showed no significant interval change (True Negative). 2 patients had new FDG avid lesions in the second scan with rising CEA values (True Negative). One patient had normal serum CEA with FDG avid solitary serosal deposit along anastomotic site in second scan, which though present in the first scan, was missed probably due to its subcentimeter size and intense physiological FDG uptake along adjacent bowel mucosa (False Negative). Overall FDG PET-CT showed 91.7 % sensitivity, 89.5 % specificity, 84.6 % positive predictive value and 94.5 % negative predictive value in detecting recurrence in suspicious colorectal malignancy patients with normal serum CEA. **Conclusion:** Serum CEA is widely used as the only colorectal tumor marker in the post treatment surveillance. Early detection of recurrence improves chance of survival. However normal CEA value does not completely rule out recurrent disease. FDG PET-CT as an isotropic metabolic imaging modality shows promise to be an useful modality in the surveillance of colorectal malignancy. **Key Words:** FDG PET-CT, CEA, Recurrence, Colorectal Malignancy

P1009**F-18 FDG PET/CT in the assessment of patients with****unexplained CEA rise after surgical curative resection for colorectal cancer**

S. Giacomobono¹, D. Capacchione¹, M. Lancellotti¹, A. Nardelli², R. Gallicchio³, G. Improta¹, A. Nappi¹, A. Cammarota¹, A. Di Leo¹, L. Pace⁴, G. Storto¹; ¹IRCCS CROB, Rionero in Vulture (Pz), ITALY, ²IBB CNR, Napoli, ITALY, ³Department of Biomorphological and Functional Sciences, University "Federico II", Napoli, ITALY, ⁴Department of Biomorphological and Functional Sciences, University "Federico II", Napoli, ITALY.

Aim: Postoperative follow-up for asymptomatic patients with rising serum CEA levels after curative colorectal cancer resection represents a clinical challenge. We evaluated the role of the quantitative assessment by maximum standardized uptake value (SUVmax) on F-18 FDG PET/CT for stratifying patients with unexplained CEA rise after surgical curative resection. **Material and Methods:** forty-one asymptomatic patients (mean age, 63±14 years) with previous colorectal cancer presenting serum CEA levels >10 ng/ml underwent F-18 FDG PET/CT 13±3 months after the complete surgical intervention. All patients had adjuvant chemotherapy, none received radiotherapy recently. The SUVmax was registered on anastomosis and peri-anastomotic tissue lesions, if any (i. e. pericolic fat thickening and/or n. 1 lymph nodes >1cm or n. 3 in cluster). Patients were followed up 24±13 months thereafter. Main events such as re-intervention, evidence of newly discovered distant metastases or death constituted surrogate end-points. Receiver-operator-curve (ROC) analysis was performed to estimate the optimal cut-off of SUVmax for differentiating patients at high risk events. PET/CT results were then compared to the disease outcome (overall survival; OS). **Results:** Mean SUVmax at the anastomotic site was 6.2±3 (range 2.5-15). 15/41 patients (36%) had evidence of peri-anastomotic involvement at F-18 FDG PET/CT as per pericolic fat thickening or lymph nodes showing increased uptake (SUVmax 6.2±4). 7/41 patients (17%) had biopsy confirmation of recurrence and further underwent re-intervention whereas 6/41 (15%) showed newly discovered distant metastases and 5/41 (12%) died. The remaining 23 patients (56%) were fully active without signs of relapse. The mean SUVmax of patients with main events was 7.9±3 as compared to those without relapse 5.1±2 ($p=0.002$). At logistic regression analysis the presence of loco-regional involvement (i.e. fat thickening or nodal) was not independently associated with a poor outcome. ROC analysis recognized that the optimal threshold of SUVmax for differentiating patients at high risk of main events was 7.01. The sensitivity of SUVmax cut-off at PET/CT for predicting outcome was 88% whereas specificity was 80%; PPV was 74% and PNV 91%. A worse OS was observed for patients with a SUVmax greater than 7.01 as compared to those with SUVmax values lesser (median survival: 13 vs 29 months; $p<0.001$). **Conclusion:** the quantitative assessment by SUVmax on F-18 FDG PET/CT may be helpful for stratifying patients presenting unexplained CEA rise after curative resection at risk of main events. A better OS was observed in patients with SUVmax values less than 7.01 at the anastomotic site.

P1010**The role of FDG PET-CT in the evaluation of patients with colorectal cancer. Interobserver study**

M. Tuncel, S. E. Vargöl, N. Bariskanat, E. Topbaş; Hacettepe University, ankara, TURKEY.

Purpose: FDG PET-CT is a validated tool in the staging and restaging of patients with colorectal cancer. Our study aimed to asses the interobserver variability in the interpretation of the images and to define lesion types which lead to interobserver discordance. **Subjects and methods:**Forty patients with diagnosis of colorectal cancer (M/F:34/6, mean age: 58±14) underwent FDG-PET-CT 60 minutes after i.v. injection of 370 MBq FDG for staging (n:15) and restaging (n:25) purposes . The images were interpreted by 3 nuclear medicine physicians(P) who were unaware of patients' clinical data.The lesions were characterized as benign:0,probable benign:1,equivocal,probable malign:3 and malign:4 for analyses. Lesion size and SUV max values were also noted for further evaluation. Finally clinical decision of the lesions were made by follow-up data, histopathology and imaging results. **Results:** On patient bases, the sensitivity specificity, PPV, NPV and accuracy for P1 were found as 100%,88%,92%,100% and 95%, for P2 91%,88%,91%,88% and 90% and for P3 92%,81%,88%,87% and %88 respectively.The discordant lesions among the authors were further analyzed. There were 12 equivocal lesions that were interpereted as malign in 5 (all, lung metastases) and benign in 7 (1 hilar lymph node, 2 bowel, 2 increased density of the mesentery, 1 lung, 1 abdominal lymph node) by final clinical decision. There were 7 lesions which are interpreted as malign but accepted as benign by final decision (3, hilar lymph node , 2 increased density of the mesentery, 2 abdominal lymph node) only 1 lesion interpereted as benign and accepted as malign (lung). There were 18 malign lesions missed by at least one interpreter (11 lung, 3 abdominal lymph node, 3 liver and 1 bone) which have low FDG uptake (mean SUV max: 1.3±1.7), and small size (shortest size:6.2±2. and ,longest diameter 7.6±4 mm) **Conclusion:** FDG PET-CT is an accurate imaging tool for the patients with colorectal cancer patients. Knowledge of lesion types which leads to discordance is helpful for accurate diagnosis

P1011

Evaluation of F18-FDG PET/CT accuracy in detection of local recurrence and distant metastases in colorectal cancer

A. Fijolek-Warszewska, Z. I. Nowecki, G. Łapińska, M. Bryszewska, I. Kozłowiec-Gudzinska; Oncology Institute, Warsaw, POLAND.

Objective The purpose of the study was to evaluate diagnostic accuracy of F18-FDG PET/CT in detection of local recurrence and distant colorectal cancer metastases. We have evaluated PET/CT sensitivity, specificity and accuracy in local recurrence, liver metastases and extrahepatic metastases. Subjects and Methods Retrospective study was undertaken. We have reviewed PET/CT results of 158 patients, with suspected recurrence of CRC, referred for a PET/CT. Referral was based on CT results, elevated CEA level or clinical examination. All patients included in the study had a follow up information: histopathology and/or further imaging diagnostic examination. Results In case of local recurrence sensitivity of PET/CT was 88% (95% CI: 73-96%), specificity 93% (86%-96%), accuracy 92% (86%-95%), positive and negative predictive values respectively 77% (61%-88%) and 97% (91%-99%). In case of intrahepatic recurrence FDG PET/CT sensitivity was 81% (95% CI 66%-90%), specificity 100% (88%-100%), accuracy 95% (90%-98%), positive and negative predictive values 100% (CI 88%-100%) and 93% (87%-97%). In case of extrahepatic metastases sensitivity of FDG PET/CT was 94% (95% CI 86%-98%), specificity 82% (71%-89%), accuracy 88% (82%-92%), positive predictive value 83% (CI 73-90%), negative predictive value 94% (85%-98%). Conclusion F18 FDG PET/CT is a highly accurate modality to detect recurrent colorectal cancer regardless of recurrence location. For local, hepatic and extrahepatic metastases modality has a very high 88-95% accuracy. The sensitivity of the method is in all cases very high (81%-94%). In case of hepatic recurrence lower sensitivity is related to resolution of PET images (lower in lesions smaller than 10mm) and due to histopathology type (lower in mucinous adenocarcinoma)

P61-2 - Tuesday, October 30, 2012, 16:00 - 16:30, Poster Exhibition Area

Oncology Clinical Science: Gastrointestine & Pancreas

P1012

Prospective comparison of ^{18}F -FDG and $3'$ -deoxy- $3'$ -[^{18}F]fluorothymidine PET/CT in the differentiation and characterization of periampullary tumors

M. Cheng¹, H. Wang¹, K. Liu¹, R. Yen¹, K. Tzen¹, Y. Wu²; ¹National Taiwan University Hospital and National Taiwan University College of Medicine, TAIPEI CITY, TAIWAN, ²Far Eastern Memorial Hospital, NEW TAIPEI CITY, TAIWAN.

Purpose: This study aims to assess the clinical usefulness of [^{18}F]fluorodeoxyglucose (FDG) compared with $3'$ -deoxy- $3'$ -[^{18}F]fluorothymidine (FLT) positron emission and computed tomography (PET/CT) in characterizing and clarifying the indetermined periampullary tumors seen in endoscopic retrograde cholangiopancreatography (ERCP) or endoscopic ultrasound (EUS). **Material and Methods:** Forty-seven consecutive referred patients aged 27-86 years with indetermined periampullary tumors in ERCP or EUS and scheduled for surgery were included in this study. Subjects with obvious pathology seen in ERCP or EUS were excluded. Dual-phase whole-body FDG PET/CT was performed in all patients. An additional FLT PET/CT was performed in 21 of the 47 patients (44.7%). Visual interpretation, tumor maximized standardized uptake value (SUVmax), and tumor SUVmax normalized to venous FDG activity (tumor to background ratio, TBR) were correlated with the final diagnoses based on histopathology of the surgical specimens. **Results:** Malignancies were diagnosed in 29 patients (61.7%): 15 ampulla vater cancer, 8 pancreatic cancer, 3 distal CBD cancer, and 3 neuroendocrine carcinoma. Benign tumors were found in 18 cases (38.3%), including 7 adenomas of ampulla vater. Using visual analysis, the sensitivity, specificity, and diagnostic accuracy of FDG PET/CT were 96.6%, 40.0%, and 76.6%, respectively. Significant statistical differences in SUVmax (mean, malignancy=7.3, benign=3.8, $P=0.0003$) and TBR (mean, malignancy=4.63, benign=2.42, $P=0.0005$) were observed between periampullary malignancies and benign tumors in FDG PET/CT. A SUVmax of 3.2 or TBR of 1.74 discriminated malignancies from benign tumors with a sensitivity, specificity, and accuracy of 93.1%, 50.0%, and 76.6%, respectively. In the subgroup of patients who also underwent FLT PET/CT ($n = 21$, 13 malignant, 8 benign), sensitivity was 84.6% for FLT and 92.3% for FDG; specificity was 62.5% for FLT, better than the 37.5% of FDG. Mean FLT SUVmax and TBR in the malignant tumors were 3.91 ($P=0.07$) and 3.85 ($P=0.05$), respectively. ROC analysis revealed FLT TBR was the better semi-quantitative method in differentiating indetermined periampullary tumors when both FDG and FLT PET/CT were performed (AUC=0.7500). **Conclusions:** These preliminary data suggest FDG PET/CT has a good diagnostic performance in the differential diagnosis of indeterminate periampullary tumors seen on EUS or ERCP. Superior sensitivity was found with FDG PET/CT. In contrast, FLT PET/CT offers a higher specificity and TBR may help in the identification of patients with periampullary malignancies.

P1013

Prospective evaluation of dual time 18F-FDG PET-CT for differentiating benign and malignant pancreatic masses: comparison with contrast enhanced CT and endoscopic ultrasound

R. Kumar, P. Sharma, P. Garg, R. Sharma, S. Singla, S. Thulkar, A. Malhotra; All India Institute of Medical Sciences, New Delhi, INDIA.

Aim: To evaluate dual time 18F-Fluorodeoxyglucose (^{18}F -FDG) positron emission tomography-computed tomography (PET-CT) for differentiating benign and malignant pancreatic masses and compare the same with contrast enhanced CT (CECT) and endoscopic ultrasound (EUS). **Material and methods:** This prospective study was approved by institutional ethics committee. Total 75 consecutive patients (Age: 51.9 ± 13.3 years; male/female: 54/21; CA $19.9-2239.94 \pm 7407.62$ U/mL) with ($n=25$) or without ($n=50$) underlying chronic pancreatitis (CP), presenting with pancreatic mass lesions suspicious of pancreatic cancer were enrolled in this study. All patients underwent whole body PET-CT 1 hr post ^{18}F -FDG injection followed by limited field PET-CT of pancreas at 3 hr (dual time). Images were evaluated qualitatively as well as quantitatively [Standardized uptake value (SUVmax)]. PET-CT findings were interpreted as positive for malignancy, if the ^{18}F -FDG uptake in pancreatic lesion was focal and/or SUVmax of ≥ 2.5 . Retention index (RI) of the lesions was calculated by dividing the change in the early and delayed SUVmax by the early SUVmax. In addition to PET-CT, 73 patients underwent CECT (triple phase pancreatic protocol) and 54 underwent EUS. Results of PET-CT were compared to CECT and EUS. Histology ($n=51$), cytology ($n=17$) and clinical/imaging follow up ($n=7$; minimum 6 months) were taken as reference standard. **Results:** Based on reference standard 56 masses were malignant and 19 were benign. The sensitivity, specificity and accuracy of ^{18}F -FDG PET-CT were 91%, 79% and 88% respectively. Specificity increased marginally to 93% if a rising RI was added to PET-CT interpretation criteria for malignancy ($P=0.880$). PET-CT detected distant metastasis in 16 patients. There was significant difference in early SUVmax (3.2 ± 2.6 vs. 5.85 ± 4.2 ; $P=0.002$), late SUVmax (3.53 ± 3.56 vs. 7.2 ± 4.87 ; $P=0.007$) and RI (-6.32 ± 21.18 vs. 18.72 ± 27.38 ; $P=0.009$) between benign and malignant pancreatic masses. The accuracy of PET-CT was lower in patients with CP as compared to those without CP (80% vs. 92%). PET-CT and CECT were concordant in 51 patients (benign-11; malignant-50) and discordant in 12 ($\kappa=0.544$). Specificity of CECT was much lower compared to PET-CT (79% vs. 59%; $P=0.014$). PET-CT and EUS were concordant in 42 patients (benign-8; malignant-34) and discordant in 12 ($\kappa=0.5$). Specificity of EUS was similar to PET-CT (76% vs. 79%; $P=0.849$). **Conclusion:** ^{18}F -FDG PET-CT appears useful for differentiating benign and malignant pancreatic masses. However, dual point imaging doesn't add much. PET-CT is more specific than CECT, but not EUS for this purpose.

P1014

Is dual-time point imaging helpful in the characterisation of pancreatic mass lesions?

B. R. Mittal, S. Santhosh, D. Bhasin, R. Nada, R. Srinivasan, A. Bhattacharya, S. S. Rana, R. Gupta; PGIMER, Chandigarh, INDIA.

Purpose: To prospectively assess the utility dual-phase imaging of 18F-FDG-PET/CT in characterisation of mass forming lesions of pancreas **Materials and methods:** 18F-FDG-PET/CT was performed in 51 patients (31 males; age range: 28 to 86 years) with pancreatic mass presumed to be malignant and detected by conventional imaging modalities. Focally increased FDG uptake was considered malignant and diffuse or no FDG uptake was considered benign. Semi quantitative measurement was measured by calculating maximum standardised uptake value (SUVmax) of the lesions. Delayed imaging was done at 2 to 3 hours after FDG administration. Retention index (RI) was calculated according to the equation: $(\text{SUV}_{\text{delayed}} - \text{SUV}_{\text{early}}) \times 100 / \text{SUV}_{\text{early}}$. The diagnosis was confirmed by histopathological examination of the resected specimen or by image guided cytological analysis. **Results:** Thirty patients showed focal FDG uptake, with all (100%) of them being true positive. Fifteen patients showed no increased FDG uptake, with 13 of them being true negative. Six patients showed diffusely increased FDG uptake, with all of them being true negative. Sensitivity, specificity, positive predictive value (PPV), negative predictive value (NPV) and accuracy of PET/CT in characterising the pancreatic masses in to benign and malignant lesions were 94%, 100%, 100%, 90% and 96% respectively. The mean SUVmax of the malignant pancreatic masses was 6.3 ± 2.9 (range: 1.3 - 27.7). For a SUVmax cut-off of 2.8, the sensitivity was 94% & specificity was 53%. RI range of benign lesions was -18.75 to 37.5 and malignant lesions was -12.76 to 129.4. There was statistically significant difference in the RI of malignant and benign lesions ($p=0.006$). For a cut-off RI value of -8.6, sensitivity and specificity were 97% & 21% respectively. RI of two pancreatic tubercular lesions was 3.1 & 25 respectively and caused false positive interpretation. **Conclusion:** FDG uptake pattern in PET/CT can differentiate malignant from benign mass-forming lesions of the pancreas with high accuracy. Most of the benign lesions were due to chronic pancreatitis. Inflammatory benign lesions of the pancreas also tend to show increase in SUVmax during delayed imaging. Hence, RI and a discrete cut-off value of SUVmax may not be useful in

differentiating benign from malignant conditions with certainty in pancreatic mass-forming lesions.

P1015

The Usefulness of 18F-FDG PET/CT with Intravenous Contrast Enhancement in the Evaluation of Flat Gallbladder Wall Thickening

H. Kim, M. Yun, J. Choi, A. Cho, Y. Choi, H. Yong, J. Lee; Yonsei university health system, seoul, KOREA, REPUBLIC OF.

Gallbladder cancer is the fifth most common malignancy of the gastrointestinal tract, and is often detected at a late stage of the disease, due to lack of early or specific symptoms. Early gallbladder cancer can manifest as wall thickening, although a thick-walled gallbladder is a non-specific findings that may occur in a variety of conditions. Accurate preoperative evaluation of gallbladder wall thickening is essential for diagnosis of gallbladder cancer. The purpose of this study was to evaluate the usefulness of positron emission tomography (PET) with 18F-FDG CT with intravenous contrast enhancement in differential diagnosis of flat gallbladder wall thickening. Methods: The patient population consisted of 43 patients with flat gallbladder wall thickening, who underwent PET/CT with intravenous contrast enhancement. The findings of CT images was scored using a 5 grade scale (1=definitely benign, 2=probably benign, 3=indeterminate, 4=probably malignant 5=definitely malignant). Semiquantitative and qualitative (visual) analyses of each gallbladder lesion were performed. The maximal standardized uptake value in the gallbladder wall thickening (SUVmax) and the ratio of SUVmax to mean SUV of the liver (GB/L ratio) were obtained. Results: The SUVmax of the gallbladder wall thickening on PET/CT ranged from 0.9 to 24, with a mean of 3.6. When used for the diagnosis of gallbladder cancer, Cut off value (SUVmax>2.5) had a sensitivity of 93%, a specificity of 86%, and an accuracy of 88%. CT achieved a NPV of 100% with higher than score 2 being malignant. The combining of FDG uptake and CT grade of gallbladder flat wall thickening can suggests meaningful view of differential diagnosis and surgical plan. Conclusion: FDG PET/contrast enhanced CT may play an important role in evaluating patients with flat gallbladder wall thickening and significantly impact on subsequent surgical decision making.

P1016

Usefulness of 18F-FDG PET/CT in the evaluation of malignant suspected pancreatic lesions: Diagnostic accuracy and clinical impact.

H. Palacios-Gerona¹, R. Sánchez-Sánchez², M. Navarro-Pelayo Laínez², A. Rodríguez-Fernández², D. Garrote-Lara², M. Gómez-Río², M. Moreno-Caballero², G. Guzmán-Caro², T. Aroui-Luquin², J. Llamas-Elvira²; ¹General Hospital, Jaen, SPAIN, ²Virgen de las Nieves University Hospital, Granada, SPAIN.

AIM: To analyze the usefulness of 18F-FDG PET/CT in management of patients with pancreatic lesions suspicious for malignancy, in terms of diagnostic accuracy and clinical impact. MATERIAL AND METHODS: The design of the study have been a prospective cohort of patients with pancreatic lesions under suspicion for malignancy by conventional imaging techniques, studied by FDG-PET/CT (Siemens Biograph 16). The images evaluation was performed using visual and semiquantitative analysis (SUVmax). The results were confirmed by histological specimen (50) or by clinical follow-up (6).RESULTS: Fifty six patients were included (32 males and 24 females; mean age 60.24±13.49 years). FDG-PET/CT was positive for malignancy in 38 patients and all of them were histologically confirmed (37 true positive: 29 ductal carcinoma, 1 acinar cell carcinoma, 1 mucinous carcinoma, 1 papillary mucinous carcinoma, 1 mucinous cystadenocarcinoma, 1 microcystic cystadenoma, 3 pancreatic endocrine tumors; and 1 false positive was in a case of acute pancreatitis). Thirteen studies were considered true negative (8 confirmed histologically and 5 under clinical follow-up) and 5 false negative. The diagnostic accuracy parameters were: sensitivity: 88.1%, specificity: 92.9%, PPV: 97.4% and NPV: 72.2%. SUVmax analysis (ROC curves) showed an area under the curve of 93.1; cutoff value for malignancy of 2.82 (S: 92.7, E: 89.9). Fifteen cases (15/56; 27%) had distant metastases, identified in FDG-PET/CT in eleven cases, and unsuspected in three of them (3/11, 20%). In two patients FDG-PET/CT provided conclusive information in respect to discrepant structural techniques. In other two patients showed more disease spread (metastases in unknown location) and finally in the remaining four patients FDG-PET/CT was in agreement with the other techniques. COMMENTS: The incorporation of FDG-PET/CT in the study of pancreatic lesions suspicious for malignancy is useful in terms of diagnostic accuracy and providing additional information in respect to conventional imaging techniques, with an impact on therapeutic management in a significant proportion of patients (>12.5%).

P1017

Is there any Clinical Benefit to Obtain Delayed FDG-PET/CT Scan in Patients with Signet Ring Cell Gastric Carcinoma?

Z. R. Kaya¹, F. A. Caliskan¹, O. Ekmekcioglu¹, O. Vural Topuz², M. S. Sager¹, M. Halac¹, K. Sonmezoglu¹; ¹Istanbul University Cerrahpasa Medical Faculty Department of Nuclear Medicine, ISTANBUL, TURKEY, ²Okmeydani Research and Training Hospital Nuclear Medicine Department, ISTANBUL, TURKEY.

Introduction It is well known that signet ring cell (SRC) type of gastric carcinomas have low FDG affinity, most probably due to their low GLUT1 expression comparing to other histological types. As delayed FDG-PET imaging has additional value in various of solid carcinomas, we aimed to evaluate the clinical impact of 3-hr delayed PET/CT scanning in terms of better lesion detectability in patients with known SRC gastric carcinoma in this retrospective study. **Material and Methods** A total of 28 patients with a diagnosis of SRC gastric carcinoma, who have both early and late PET/CT imaging were recruited from our archive and were included in the study (20 male, 8 female; mean age 51 yrs with a range 32-68). The patients were referred to PET/CT scan for either primary staging (n=10) or restaging (n=18). In all patients, a standard whole body PET/CT scanning was performed from the skull base to the upper thighs, 60-90 min after of an IV injection of 370-555 MBq FDG, by using a dedicated PET/CT scanner (Siemens Biograph 6 HI-REZ LSO). 3-hr delayed PET/CT examination including the upper abdomen and also other areas with FDG positive lesions, if available was also obtained approximately three hours after of the injection. In patients with FDG positive lesions (n=15), body weight normalized SUVmax values are calculated using the vendor software by drawing regions of interest from the identified FDG positive lesion on both early and delayed PET/CT images. **Results** Among 28 patients, only 15 (54 %) had a total of 23 FDG positive lesions (6 primary; 17 metastatic) in early PET/CT scans. SUVmax values varied from 0.8 to 15 (mean 6.11 ± 3.55) in early images versus from 2.5 to 14.9 (mean 6.32 ± 3.48) in delayed scans (p=0.61). Although 6 out of 23 FDG positive lesions showed an increased SUVmax value over 10% on delayed PET/CT images, there was no significant difference between early and delayed groups (p=0.61). There were also no significant differences between primary and metastatic lesion in neither early nor delayed scans. 13 out of 28 (46%) patients showed no discernible FDG uptake in neither early nor delayed images. **Conclusion** FDG-PET/CT imaging does not seem as an effective modality in primary staging of SRC gastric cancers. Furthermore, 3-hr delayed FDG-PET/CT scanning does not contribute enough to strength lesion detectability in this particular group of patients.

P1018

Quantitative FDG-PET/CT Imaging of Pancreatic Cancer: Increased Diagnostic Potential using a Ratio-Based Method.

M. Scarlattei, A. Belletti, G. Baldari, C. Cidda, L. Ruffini; Azienda Ospedaliero- Universitaria di Parma, Parma, ITALY.

18F-fluorodeoxyglucose positron emission tomography/computed tomography (FDG-PET/CT) imaging is useful for diagnosis, staging, and treatment response in patients with pancreatic cancer. Preliminary data suggest a significant influence of FDG-PET/CT in influencing treatment strategies. **Aim** To evaluate diagnostic potential of FDG-PET/CT in pancreatic cancer. To assess utility of a standardized ratio-based method in characterizing neoplastic lesions. **Methods** From January 2009 to March 2012 we performed 102 FDG-PET whole-body studies for 85 consecutive patients (mean age 67 ± 10 yrs, range 43-84, M 41, F 44). Pancreatic localization: head 34%, tail 10%, body 3%, uncinate process 10%, two or more sites of lesions 43%. PET scan was performed 60 min after tracer injection. The 18F-FDG uptake within lesions was quantified by determining the maximum activity within a fixed sized spherical region of interest (ROI) placed around the tumor area (T/N/M) with the highest uptake. For background control, the mean SUV was measured in a standardized region of interest in the liver. The SUVratio between lesion and background (SUVr) was used to differentiate uncertain findings with low rate of metabolic activity. **Results** Staging (CA19-9>100) was performed in 22 pts: 5 negative, 17 positive (5T, 2T+N, 6T+M, 4T+N+M) Restaging (recurrence suspicion by imaging and/or CA19-9 increasing): FDG-PET was performed in 32 pts (9 with previous surgery + ChT, 12 with previous surgery only, 2 with ChT only, 4 with surgery+ChT+RT, 1 treated with Y-90, 4 with other therapy). PET scan was negative in 16 pts, positive in 16 (2T, 5N, 6M, 1T+M, 1N+M, 1T+N+M). FDG-PET for tissue characterization was performed in 31 pts: 21 negative, 10 positive (7T, 1T+N, 2T+N+M). The mean value of SUVmax was 7.3±2.8, 7±5 and 4.8±2.7 in staging, restaging and characterization PET studies, respectively. Uncertain lesions (6T, 1N, 1T+N) were detected in 8 pts (5 of them studied for tissue characterization), all with SUVmax < 2.7. The SUVr in the uncertain lesions showed a reduced value in comparison with SUVmax of the target lesion in 7 pts; in 1 patient SUVr was unchanged. All the lesion were defined as benign. **Conclusion** FDG-PET allows metabolic characterization of pancreatic cancer and detection of disease recurrence. Quantitative analysis of tracer uptake allows to define uncertain neoplastic lesions/recurrence with low rate of metabolic activity.

P1019

18F-FDG PET/CT in Initial Staging of Gastric Cancer

M. Filik, K. M. Kir, B. Aksel, E. Ozkan, N. O. Kucuk, E. Ibis, H. Akgul; Ankara University Medical Faculty, Ankara, TURKEY.

Aim: To evaluate the role of 18F-FDG PET/CT in the primary staging of gastric adenocarcinoma. **Material and method:** 32 patients (25M, 7F; mean age; 57.1; range;24-77) who underwent 18F-FDG PET/CT for primary staging of gastric adenocarcinoma were included to the study. All the patients had been performed endoscopic biopsy and diagnosed as adenocarcinoma within 4 weeks period before 18F-FDG PET/CT. 18F-FDG findings were confirmed with histopathological examination results in 25 patients who were suitable for surgery and results of conventional imaging tools and clinical follow-up in 7 patients who were inoperable. Overall sensitivity, specificity, accuracy, positive predictive value and negative predictive value of 18F-FDG PET/CT in the primary staging of gastric adenocarcinoma were calculated in patients based method. **Results:** Primary lesions of 5 patients were not 18F-FDG avid (1 signet-ring cell, 3 grade 3 adenocarcinoma, 1 intramucosal adenocarcinoma). Mean SUVmax of primary lesions were calculated as 10.6±9.65 (range;2.56-44.6). 18F-FDG uptake was detected in local lymph nodes in 16 patients, mean SUVmax of local lymph nodes was calculated as 10.01±7.48 (range;2.8-29.1). 18F-FDG uptake was seen in distant lymph nodes (mean SUVmax: 10.9±4.96), lungs (mean SUVmax: 6.73±0.19), liver (mean SUVmax: 6.77±1.88), bones (mean SUVmax: 4.9±0.42), soft tissue (SUVmax: 5.6) and adrenal gland (SUVmax: 7.7) in 6, 3, 3, 1 and 1 patients, respectively. In the comparison of histopathological examination results 18F-FDG PET/CT could not show metastases in local lymph nodes, peritoneum, ascites fluid and liver in 5, 2, 1 and 1 patient, respectively. Postoperative histopathological subtype of 4 out of 5 patients whose local lymph nodes were not FDG avid was signet-ring cell variant. Overall sensitivity, specificity, accuracy, positive predictive value and negative predictive value of 18F-FDG PET/CT in the primary staging of gastric adenocarcinoma were found 65%, 88%, 71%, 93% and 50%, respectively. **Conclusion:** 18F-FDG PET/CT can be performed in the primary staging of gastric adenocarcinoma in addition to conventional imaging tools with high positive predictive value. However false negative results especially in local lymph nodes and peritoneum should be considered in the preoperative evaluation of patients.

P62-2 - Tuesday, October 30, 2012, 16:00 - 16:30, Poster Exhibition Area

Oncology Clinical Science: Lymphoma

P1020

18F-FDG PET/CT diagnostic value in the temporal follow-up of lymphoma patients

S. Lucic, A. Peter, D. Jovanovic, L. Popovic, D. Petrovic, M. A. Lucic; Institute of Oncology of Vojvodina, Sremska Kamenica, SERBIA.

Introduction: The uprising paradigm in development of the Hodgkin and non-Hodgkin lymphoma patients personalized treatment includes the PET/CT in the deciding on initial treatment modality, fast estimation of the treatment response and immediate treatment changes based on the attractive possibility to prompt the poor therapy response estimation. Having in mind that the expected increase of answer-adaptive and risk-adaptive approaches in the treatment of these patients and that the integrated imaging of the exact effects of targeted treatment of different tumor types should result in more appropriate and more individualized outcome than the prediction of outcome based on morphoanatomical prognostic information, the aim of this investigation was to establish the 18F-FDG PET/CT diagnostic value in correlation to clinical disease course in a follow-up of lymphoma patients. **Methods and material:** Eightyseven lymphoma patients (average age 43,78±14,91 years), divided in group of 39/87 patients with Hodgkin lymphoma and the group of 48/87 with Non-Hodgkin lymphoma (15 patients with diffuse large B cell, 10 with follicular, 14 mixed cells, 3 B-cells, 2 T-cells and 4 MALT lymphoma) underwent PET/CT exam in order to stage the disease, estimate the early treatment effects and estimate the treatment response. All of them were clinically followed-up in a period of up to two years after initial PET/CT scan. **Results:** Overall sensitivity and specificity values of 18F-FDG PET/CT findings were 93% and 87% and positive and negative predictive values were 81% and 96%, respectively. Sensitivity and specificity values in the group of Hodgkin lymphoma patients were 92% and 96%, while positive and negative predictive values were 92% and 96%, respectively. In the Non-Hodgkin lymphoma group we found sensitivity and specificity values of 94% and 73%, while positive and negative predictive values were 68% and 96%, respectively. **Conclusion:** 18F-FDG PET/CT demonstrates superior position in the diagnostic algorithm in the follow-up of lymphoma patients, especially in cases where it is not possible at all to establish the early treatment effect/response and post-treatment status on the basis of morphoanatomical imaging methods and by use of RECIST criteria only, which in our opinion creates a realistic urge for full introduction of PERCIST criteria.

P1021

Assessment of Bulky Mediastinal Lymphoma with Chest Radiography, Computed Tomography and Positron Emission Tomography: Comparisons Across Modalities, Pathology, and Treatment.

S. M. Akram, E. S. Mittra; Stanford University, Palo Alto, CA, UNITED STATES.

INTRODUCTION: Accurate evaluation of mediastinal lymphadenopathy is important for staging and prognosis in lymphoma. This was done with radiography but now more frequently with CT and PET/CT. The association between the findings across these modalities is not well known. Our goal is to better understand the correlation between these modalities, both pre and post-therapy, and in treatment naïve patients and those with recurrence. **METHODS:** In this retrospective study, 28 patients (17 male, 11 female), age 43.6 ± 20.1 years) were identified who had both a chest radiograph (CXR) and PET/CT before and after therapy at Stanford University between 2008 and 2010. Sixteen patients had HD and 12 had NHL. Seventeen patients were evaluated for staging and 11 for recurrence. Measurements of the widest mediastinal diameter and internal thoracic diameter were made on both CXR and CT. Additional CT measurements included the longest dimension of the mediastinal mass in the transaxial plane and its volume. Metabolic data measured include SUV max and mean. We analyzed the data using descriptive and correlative statistics. Pearson's correlation and Student's t-tests comparisons were done. A p-value of <0.05 is considered significant. **RESULTS:** There was good correlation in all measurements of mediastinal width and tumor volume across all patients (p-values <0.0001) but not with the metabolic measurements (p > 0.05). Indeed, the anatomical measurements either from CXR or CT largely did not correlate with any of the PET parameters, except for longest dimension and volume of the primary mass. Almost all the anatomic measurements by CXR and CT as well as the PET data were significantly different before and after therapy in patients referred for staging and patients with HD or NHL. The only exception was that the CXR measurements were not significantly different before and after therapy in patients who had recurrence. **CONCLUSION:** This retrospective study provides two main findings. First, there was good correlation between the anatomic measures of bulk between CXR and CT, although the CXR findings were not reliable in patients with recurrent disease since post therapy mediastinal ratio of these patients were within normal limits (<0.33). Secondly, there was poor correlation between the anatomic and metabolic data except for the longest dimension and volume of the tumor. This suggests that anatomic and metabolic information is complementary in this cohort. Also, the key findings from the PET/CT were often outside of the mediastinum. **TABLE:**

P1022

Castleman's Disease - Our Experience with 18F-FDG PET and PET/CT Examination. A Set of 18 Examinations with 6 Patients.

Z. Rehak¹, P. Szturcz², Z. Adam², R. Koukalova¹, J. Bartl¹, K. Bolcak¹; ¹Dpt. of Nuclear Medicine, Masaryk Memorial Cancer Institute, Brno, CZECH REPUBLIC, ²Department of Internal Medicine – Hematooncology, Faculty of Medicine of Masaryk University and University Hospital Brno, Brno, CZECH REPUBLIC.

Castleman's disease (CD) is a rare non-clonal lymphoproliferative disorder. Clinically, either unicentric (UC, localized) or multicentric (MC, generalized) forms are recognized while, histopathologically, hyaline-vascular (HV), plasma-cell (PC) and mixed variants of the disease exist. Although there is only a little literature data so far, it can be said that lymphadenopathy caused by CD may show up in high 18F-FDG (FDG) uptake. **Aim:** To verify whether various forms and variants show up in a higher FDG uptake and whether a PET/CT examination can be used for monitoring of the therapy. **Patients and method:** 6 patients with histologically verified CD (3 males and 3 females) at the age of 47-67. HV represented 3x (2x MC and 1x UC form), 1x mixed variant in MC form and 2x PC variants (1x in UC and 1x in MC form). Our 6 patients have undergone an 18 (3 PET a 15 PET/CT) examination during 2008-2012(January). There were 5 initial, staging examinations and the other examinations were done within the monitoring of the disease. The extent of FDG uptake was expressed as SUVmax and the lymph node size was measured on Computed Tomography. **Results:** All 3 variations of CD initially showed up in lymphadenopathy with higher 18F-FDG uptake. The lowest values of SUVmax were with HV UC - 2.2, on the contrary the highest value was with the mixed variant of MC - 6.15. All nodes accumulating FDG were enlarged, but on the contrary not all enlarged nodes showed up a higher accumulation of FDG. In the monitoring of the therapy (various forms and modes of chemotherapy) we detected a correlation between a metabolic activity with a change in size of the lymph node and clinical state (both from the progression and regression point of view). **Conclusion:** In our set of patients we have verified that various forms of CD can show up in lymphadenopathy with a higher accumulation of FDG, but the PET/CT image is not specific and for establishing the diagnosis the histological examination is

determinative. A PET/CT examination can be used within the monitoring of the treatment of the disease especially of multicentric forms.

P1023

No more indeterminate findings - ^{18}F FDG-PET/CT provides a reliable new tool to assess primary bone lymphoma response to treatment

Y. Du¹, J. Bomanji², A. Ramsay³, T. Illidge⁴; ¹Royal Marsden Hospital, Sutton, UNITED KINGDOM, ²Institute of Nuclear Medicine, UCLH, London, UNITED KINGDOM, ³Department of Histopathology, UCLH, London, UNITED KINGDOM, ⁴School of Cancer and Imaging Sciences, University of Manchester, Manchester, UNITED KINGDOM.

Aim: The optimal treatment for primary bone lymphoma (PBL) has not been determined and there is no established imaging technique to be able to assess PBL response to therapy in a timely manner. ^{18}F FDG-PET functional imaging has demonstrated its advantages over conventional imaging modalities in assessing lymphoma, however few data is available in PBL. Correlating serial ^{18}F FDG-PET/CT with clinical follow-up, this study investigates the value of this hybrid imaging technology in the assessment of PBL. **Method:** 18 consecutive patients are included. 17 of them had sequential staging and restaging ^{18}F FDG-PET/CT scans (10 patients had additional interim scans). One patient had restaging ^{18}F FDG-PET/CT scan only. 11 patients had sequential MRI scans. The temporal changes of ^{18}F FDG uptake, corresponding CT morphology appearances and MRI features of disease identified in these patients are followed-up and correlated with treatment information retrospectively. With an average follow-up time of 32-month/patient, all patients are in remission. **Results:** Before treatment, the 25 bony lesions and associated soft tissue disease detected by conventional imaging all showed high grade ^{18}F FDG uptake. ^{18}F FDG-PET/CT detected more lesions in 3 patients and upstaged 2 of them. All patients received combined chemotherapy, 9 patients received radiotherapy and 2 patients had autologous bone marrow transplantation. Re-staging scans demonstrated complete remission on PET in 14 patients (no increased ^{18}F FDG uptake), whilst all the bony lesions remain abnormal on CT and MRI with heterogeneous morphological appearances. Three bony lesions (in three patients) showed persistent low grade ^{18}F FDG uptake after treatment but biopsy revealed necrosis only. One patient developed new extra-osseous lesions during first-line chemotherapy and was diagnosed correctly by interim ^{18}F FDG-PET/CT as primary refractory lymphoma. For the 10 patients who had additional interim ^{18}F FDG-PET/CT scans performed after 2 to 4 cycles of chemotherapy, the interim scans provided similar diagnostic information as the standard re-staging scans. **Conclusion:** ^{18}F FDG uptake reflects the prompt tumour activity change in PBL and is a reliable tool to assess PBL response to treatment. Persistent low grade ^{18}F FDG uptake following treatment could present in a minority of patients with post-therapy necrosis.

P1024

Role of PET/CT in patients with follicular lymphoma

X. Setoain¹, E. Gainza¹, S. Rodríguez¹, C. Trampal², I. Navales¹, D. Fuster¹, E. Giné¹, A. Salazar³, A. López-Guillermo¹, F. Pons¹; ¹Hospital Clinic, Barcelona, SPAIN, ²CRC Mar, Barcelona, SPAIN, ³Hospital del Mar, Barcelona, SPAIN.

Aim: The aim of this study was to determine the role of ^{18}F -FDG PET/CT in initial staging, treatment response and as a prognostic factor in patients with follicular lymphoma (FL). **Material and methods:** The study included 116 patients (62M/54F; median age 59 years) consecutively diagnosed with FL in two hospitals. ^{18}F -FDG PET-CT was performed at the staging of all patients and in 90 cases after treatment. Cheson criteria were used to assess treatment response with CT and visual analysis following Juweid criteria was used to assess treatment response with PET/CT. Progression free survival (PFS) and (OS) were performed according to Kaplan Meier curves. Median follow-up after treatment was 4.2 years. **Results:** When comparing PET/CT with CT in the initial staging, in most patients (78/105; 74%) CT scan and PET showed the same number of lesions. In 27 cases (26%) PET/CT identified more involved sites than CT. In 13 patients (12%) PET modified the Ann Arbor stage as assessed by CT scan. However, this information did not change treatment in any patient. In the assessment of response to therapy in the 90 patients with ^{18}F -FDG PET/CT after treatment, CT showed no residual image in 45 patients (50%) and all these patients were also PET negative. The remaining 45 cases showed some residual mass on CT, with no uptake on PET in 21 (23%) and with pathological uptake in 24 (27%) (median SUV 3.5; range 2-23). The number of patients who eventually relapsed in these three groups was 7/45 (15%) for CT and PET negative patients, 3/21 (14%) for CT positive PET negative patients, and 8/24 (33%) for CT positive and PET positive cases. No differences in PFS were found in negative PET/CT patients irrespective of the presence or absence of a residual mass (4-year PFS 76% vs. 85%, respectively), whereas a significant difference was observed in positive PET/CT cases (4-year PFS 57%; $p=0.016$). Negative PET/CT patients had longer PFS than those with positive PET ($p=0.005$). Patients with negative PET/CT after treatment had longer OS than those with positive PET/CT (4-year OS 91%

(95%CI: 83-99) vs. 77% (95%CI: 59-95), respectively; $p=0.01$). **Conclusion:** PET/CT increases the Ann Arbor staging in the initial staging of follicular lymphoma, although rarely changes treatment strategy. Positive PET/CT at the end of treatment indicates reduced progression free survival and overall survival compared with negative PET/CT, so can be used as a prognostic factor in follicular lymphoma.

P1025

Post chemotherapy mesenteric panniculitis: a new entity of false positives in ^{18}F FDG-PET/CT imaging for lymphoma

Y. Du¹, I. Kayani², T. Illidge³, J. Bomanji², P. Ell²; ¹Royal Marsden Hospital, Sutton, UNITED KINGDOM, ²Institute of Nuclear Medicine, London, UNITED KINGDOM, ³School of Cancer and Imaging Sciences, University of Manchester, Manchester, UNITED KINGDOM.

Aim: ^{18}F FDG-PET has demonstrated its advantages over conventional imaging techniques in the post therapy assessment of lymphoma and the recently revised response criteria for malignant lymphoma has thus recommended ^{18}F FDG-PET for routine use in post-therapy assessment of patients with Hodgkin's lymphoma and diffuse large B-cell lymphoma, the most common and potentially curable form of malignant lymphoma. However, the high false-positive rate of ^{18}F FDG-PET is an ongoing clinical challenge and it is of paramount importance to enrich our knowledge to recognize non-malignant ^{18}F FDG uptakes. **Materials and Methods:** We present three consecutive patients who exhibited a distinctive feature of showing adverse response to systemic chemotherapy with the presentation of new ^{18}F FDG positive mesenteric soft tissue or nodal lesions whilst the original diseases (Stage IV diffuse large B cell lymphoma) had responded to the treatment. Under the current International Harmonization Project (HIP) criteria, these new ^{18}F FDG positive mesenteric lesions should be classified as progressive disease with the appearances of being metabolically active abnormal soft tissue or nodal lesions. **Results:** Excisional biopsies demonstrated the common microscopic features of these lesions - a mixture of benign proliferation of histiocytes and areas of fat necrosis, in keeping with mesenteric panniculitis. On follow-up imaging, these lesions remained ^{18}F FDG positive and persisted for a protracted time up to 12 months before becoming ^{18}F FDG negative without anti-cancer treatment. **Conclusion:** The three cases represent a new entity of false positives in ^{18}F FDG-PET/CT imaging for lymphoma with the common features of: post chemotherapy presentation (detected at routine end of treatment ^{18}F FDG-PET/CT assessment); asymptomatic; new, usually but not always ill-defined ^{18}F FDG positive mesenteric soft tissue lesions whilst other diseases had responded to treatment.

P1026

^{18}F -fluorodeoxyglucose (FDG) positron emission tomography (PET) as a predictor of therapy response and long-term prognosis in follicular lymphoma (FL) patients.

D. Lamonica¹, Y. Zhang¹, T. Hahn¹, R. Sultana², D. Drumsta³, M. Achakzai¹, M. Czuczman¹, F. Hernandez-Illizaliturri¹; ¹Roswell Park Cancer Institute, Buffalo, NY, NY, UNITED STATES, ²State University of New York at Buffalo, Buffalo, NY, Buffalo, NY, NY, UNITED STATES, ³School of Medicine and Biomedical Sciences, State University of New York at Buffalo, Buffalo, NY, NY, UNITED STATES.

Background: We have updated our prior experience with pre-treatment FDG PET and the association of maximum Standardized Uptake Value (SUV) with complete response rate (CRR) post-induction therapy, and long-term progression-free and overall survival (PFS, OS) in follicular lymphoma patients (FL). **Methods:** This retrospective cohort includes 118 FL patients grade 1 (n=35), 2 (n=39), 3 (n=33), or unknown (n=11). Patient characteristics include: median (range) age 65 (28-90) years; 58% male; 82% stage III-IV disease; FLIPI risk category low (n=29), intermediate (n=52), high (n=35); diagnostic SUV <5 (n=98) or ≥ 5 (n=20). Induction (front-line) therapy included: chemotherapy (1%), immunotherapy (19%), or combined chemo-immunotherapy using CD20-directed monoclonal antibodies (80%). SUV was categorized as <5 vs. ≥ 5 ; <7 vs. ≥ 7 ; or <9 vs. ≥ 9 , and ranged from 3 to 45.6. **Results:** CRR was higher in FL patients with diagnostic PET SUV <5 vs. ≥ 5 (89% vs. 71%, $p=0.09$). CRR was also associated with FLIPI risk group (Low 88%, Intermediate 77%, High 62%, $p=0.06$). At median follow-up of 4 years (range 0.2-8.1), the prognostic value of FLIPI score at diagnosis with PFS was validated in our cohort (Table 1). SUV >5 also demonstrates a significant inverse association and PFS. However, since SUV is significantly correlated with FLIPI score ($p=0.004$), a multivariate analysis was performed which demonstrated that SUV ≥ 5 had a hazard ratio (HR) of 2.61 (95% CI 0.93-7.34, $p=0.07$) after adjusting for FLIPI risk category. **Conclusions:** Pretreatment SUV can predict response to front-line chemo-immunotherapy, as well as long-term PFS in FL. Given demonstrated associations between SUV and FLIPI and its bearing on CRR and PFS, baseline FDG PET may serve to direct more effective initial therapy of FL. Table 1.

P64-2 - Tuesday, October 30, 2012, 16:00 - 16:30, Poster Exhibition Area

Oncology Clinical Science: NET (Neuroendocrine Tumours)

P1027

18F-DOPA PET/CT in different neuroendocrine settings: staging, restaging and increase in tumor markers

L. Evangelista¹, G. Valentini², P. Panichelli², D. Martini², V. De Francesco³, M. Gregianin¹, A. R. Cervino¹, C. Villano³, A. D. Di Nicola³, ¹Radiotherapy and Nuclear Medicine Unit, Istituto Oncologico Veneto, Padova, ITALY, ²ACOM S.p.A., Montecosaro (MC), Località Cavallino, Italy, Macerata, ITALY, ³U.O.C. Medicina Nucleare e Terapia Radiometabolica Ospedale Civile "Spirito Santo", Pescara, ITALY.

Background. Fluorine-18-labeled dihydroxyphenylalanine (18F-DOPA) positron emission tomography (PET)/computed tomography (CT), reflects amine uptake mechanisms in tumor lesion, particular in neuroendocrine phenotype. The aim of the present study was to describe the use of 18F-DOPA PET in patients with endocrine tumors. **Materials and methods.** From bi-institutional databases, we retrospectively reviewed 18F-DOPA PET/CT images of 60 patients (male 31, female 29; mean age: 57±15 years). Twenty-six patients (43.3%) underwent PET/CT for neuroendocrine tumor, 10 (16.7%) for paragangliomas, 3 (5%) for familial neuroendocrine syndromes, 13 (21.7%) for pheochromocytomas, 7 (11.7%) for medullary thyroid cancer and 1 (1.7%) for glioblastoma. The main indication for DOPA PET/CT were suspicious of disease or initial staging in 33 (55%) patients, restaging in 16 (26.7%) and increase in tumor markers in the remaining 11 (18.3%). The acquisition was performed after 60-min from tracer injection acquiring a whole-body PET scan (from vertex to mid-thigh). Maximum standardized uptake value (SUVmax) was calculated in the lesions by drawing an isocounter region of interest. **Results.** DOPA PET/CT resulted positive in 25 patients and negative in 35 subjects (41.7 vs. 58.3%, respectively). In the subset of patients at initial evaluation (n=33), PET/CT was positive in 16 and negative in 17 (48.4 vs. 51.6%) while in restaging group it showed a positive finding in 5 patients (31.3%). Among patients with increase in tumor markers (chromogranin or calcitonin), DOPA PET/CT was positive in 4 patients and negative in 7 (36.4 vs. 63.6%). PET/CT demonstrated a high rate of positivity for patients with suspicious of pheochromocytomas (64%) and in patients with suspicious of paragangliomas relapse (66%), while it resulted negative in 100% of patients with familial neuroendocrine syndromes. In patients with a positive PET/CT scan, the mean values of SUVmax were 7.58±5.64, 11.6±10.93 and 5.73±4.42, respectively for the three subsets of patients (ANOVA test p=0.524), demonstrating a slightly higher value in the group of restaging. **Conclusions.** DOPA PET/CT is a new imaging metabolic tool that can contribute in the staging and restaging of neuroendocrine tumor. In particular, it seems of a great utility for patients with pheochromocytomas, with paragangliomas and perhaps it can be easily used in the screening of familial neuroendocrine syndromes.

P1028

BONE METASTASES IN NEUROENDOCRINE TUMOURS - A pilot study comparing PET/CT assessment using F-18 NaF and Ga-68 labelled somatostatin receptor analogues

I. Heinle, H. Kulkarni, F. Heinle, G. Schalch, C. Carreras, R. P. Baum; Zentralklinik Bad Berka, Bad Berka, GERMANY.

Aim: The presence of metastatic bone disease in neuroendocrine tumours (NETs) has a considerable impact on the long-term prognosis, making early detection crucial. The aim of our study was to compare the findings of PET/CT using F-18 sodium fluoride (NaF) and Ga-68 somatostatin receptor (SSTR) analogues DOTATOC or DOTATATE in patients of well-differentiated NETs with metastatic bone disease. **Material and Method:** This retrospective study between Sept. 2009 and Sept. 2011 included 62 patients of histologically verified well-differentiated NETs (29 female, 33 male; mean age 62.3 years), who had been investigated by both F-18 NaF PET/CT and Ga-68 SSTR (DOTATOC/DOTATATE) PET/CT within an interval of 30 days. Each patient underwent PET/CT using 250-300 MBq F-18 NaF and 100-150 MBq Ga-68 SSTR analogues on a dedicated PET/CT scanner (Biograph duo; Siemens) and following EANM guidelines. **Results:** Extensive metastatic bone involvement with innumerable discernible lesions was identified in 9 (14.5%) patients on both F-18 NaF and Ga-68 SSTR PET/CT. Concordant results between the two imaging modalities were found in only 13 (21.0%) patients. A mismatched pattern was found in 33 (53.2%) patients. In 7 (11.3%) patients, there was a gross discrepancy - none of the bone metastases detected by Ga-68 SSTR PET/CT was visualized on F-18 NaF PET/CT and vice-versa, or only one common lesion was detected on both scans, all the others being mismatched lesions. Overall, F-18 NaF PET/CT detected more osteoblastic metastases in both the axial and the appendicular skeleton. **Conclusions:** A large discrepancy was observed between the findings of F-18 NaF PET/CT and Ga-68 SSTR PET/CT in the detection of bone metastases of well-differentiated NETs, the imaging modalities being performed within a short time interval of each other. The "mismatch pattern" of bone lesions is probably related

to different pathophysiological mechanisms that co-exist in NETs - increased blood flow and osteoblastic activity making the metastases F-18 NaF avid, and increased SSTR expression, a prerequisite for binding of Ga-68 SSTR analogues. Further studies will concentrate on the consequences of the dual-imaging on prognosis and therapeutic management.

P1029

Comparison of I-123 MIBG Scintigraphy with Somatostatin Receptor Scintigraphy Using Tc-99m HYNIC TATE in Neuroblastoma Patients

L. Uslu¹, L. Kabasakal¹, M. Ocak², G. Tuysuz¹, T. Celkan¹, H. Apak¹, B. Kanmaz¹, ¹Istanbul University Cerrahpasa Medical Faculty, Istanbul, TURKEY, ²Istanbul University Pharmacy Faculty, Istanbul, TURKEY.

Introduction: Neuroblastoma is one of the most common and aggressive malignancies in childhood with long term survival under 40%. Besides morphological imaging, functional scintigraphical imaging using I-123 MIBG (MIBG) is critical in its staging and follow-up. Recently, few studies related to neuroblastoma imaging using FDG-18 or octreotide analogues and molecular radiotherapy based on octreotide receptors has been introduced. Tc-99m HYNIC TATE (HYNIC) is another octreotide analogue with strong affinity to Sst-2. It is advantageous in its high imaging quality, low radiation burden, availability, in-house production option and cost-effectiveness. The aim of this study was to evaluate the value of HYNIC and compare it with MIBG in diagnosis and staging of neuroblastoma patients. **Methods:** The study group was composed of 11 neuroblastoma patients (8 female, 3 male, median age: 4 years, range: 1-13 years), who were evaluated with both MIBG and HYNIC scans performed on different days. Median interval between two scans was 21 days (range: 8-416). Whole body planar images and SPECT images from suspicious lesions were taken and compared with 2 different nuclear medicine specialists. Conventional MRI, whole body bone scan and tumor markers were also available in patients. **Results:** A total number of 42 lesions were detected in 11 patients using both MIBG and HYNIC scans. Of these 42 lesions, 32 (76.2%) were MIBG positive and 39 (92.6%) were HYNIC positive. HYNIC revealed 10 extra lesions, which could not be detected with MIBG, on contrary, MIBG revealed 3 extra lesions. Statistically no difference was observed between two scans (p=0.092). When both tracers were compared on patient basis, 5 patients were found to be lesion free in both scans and 6 patients had at least one lesion positive with both scans. **Conclusion:** Tc-99m HYNIC TATE scan is found to be a comparable and useful diagnostic modality in neuroblastoma patients. It can be used as a complementary approach, and it is especially crucial for subgroup of patients who are refractory to conventional treatment modalities and therefore referred to somatostatin receptor therapy.

P1030

Pathologic versus Physiologic Pancreatic Uptake of ^{99m}Tc-HYNIC-TOC in Patients with Neuroendocrine Tumours using SPECT/CT and Quantification

R. Silva¹, A. Morão¹, G. Costa¹, J. Pedroso de Lima², ¹Serviço de Medicina Nuclear - Centro Hospitalar e Universitário de Coimbra, Coimbra, PORTUGAL, ²ICNAS-Universidade de Coimbra, Coimbra, PORTUGAL.

AIM: Neuroendocrine Tumours (NET) are a heterogeneous group of neoplasms characterized by their ability to over express somatostatin receptors (SSTR) in most cells. Somatostatin receptor scintigraphy has, therefore, gained widespread acceptance in NET patients. False positives are known to occur in the pancreatic head, due to physiologic expression of SSTR2 to a highly variable extent. The aim of this study was to distinguish pathologic versus physiologic uptake of ^{99m}Tc-HYNIC-TOC (SPECT/CT) in the pancreas using a quantification method. **MATERIAL AND METHODS:** A total of 53 ^{99m}Tc-HYNIC-TOC SPECT/CT scans performed since 2010, involving 43 patients (23 males, 20 females, mean age: 62 years, SD: 16, 25-88) with diagnosis or suspected NET, with any noticeable uptake in the pancreas were retrospectively reviewed. SPECT/CT studies were divided into two groups (Group 1: physiologic uptake, 37 patients and Group 2: pathologic uptake, 16 patients) according to clinical and radiological follow-up data, including specific tumour markers, CT, MRI, PET, and histological confirmation, when available. The mean post-imaging follow-up was 10.4 months. Tracer uptake in the pancreas and in the spleen was measured using the maximum pixel activity (MPA) value and a ratio was obtained by dividing the values in the pancreas (MPAp) by those in the spleen (MPAS). Because of previous splenectomy it wasn't possible to calculate the MPAp/MPAS ratio in 5 patients (3 from Group 1 and 2 from Group 2). These patients were excluded from analysis. A nonparametric Mann Whitney U test was used for comparisons between groups. **RESULTS:** The MPAp/MPAS ratio in Group 1 (n=34) ranged from 0.103 to 0.451 (mean: 0.197, SD: 0.080) and in Group 2 (n=14) ranged from 0.193 to 9.667 (mean: 2.363, SD: 3.211). A statistically significant difference between group ratios (p<0.05) was obtained. Considering the studies with pathological uptake in the pancreatic head only (n=4), the MPAp/MPAS ratio ranged from 0.230 to 2.057 (mean: 0.767, SD: 0.868). Despite the considerable reduction of the second group's sample size the statistically significant difference

between ratios remained. **CONCLUSION:** SPECT/CT associated to a quantification method appears to be a useful tool for the evaluation process of somatostatin receptor scintigraphy images, allowing a better separation between physiologic and pathologic pancreatic uptake than visual assessment alone.

P1031

The Correlation of ^{18}F -FDG-PET SUV and ki-67 proliferation index in metastatic neuroendocrine tumors

D. Waitz, D. Putzer, A. Kroiss, S. Buxbaum, O. Bechter, R. Prommegger, C. Ensinger, A. Loizides, D. Kendler, I. Virgolini; Medical University, Innsbruck, AUSTRIA.

Background: The Ki-67 proliferation index is a well established biomarker in predicting the prognosis of patients with neuroendocrine tumors (NET). The correlation of the proliferation index and ^{18}F -FDG-PET SUV uptake values is barely investigated. Since ESMO and WHO guidelines base their treatment recommendations in part on the proliferative activity of the tumor, non invasive diagnostic assessments are keenly needed to get an estimate of the tumor grading. We therefore initiated a retrospective analysis in order to correlate ^{18}F -FDG-PET SUVs with Ki-67 immunohistochemistry in NET patients. **Material & Methods:** Eight patients (5 male, 3 female) with well differentiated (grade 1 and 2), metastatic NET (primary site: 5 pancreas, 3 unknown) who showed a disease progression based on Recist 1.1. criteria on ^{68}Ga -DOTA-TOC PET/CT were evaluated with a ^{18}F -FDG-PET scan. In Patients where tumor lesions showed an increased glucose uptake subsequent histological assessment was pursued either with a biopsy or in selected cases with the surgical removal of tumor material when indicated. The immunohistochemical analysis included a staining for the Ki-67 antigen. **Results:** The metastatic sites for tissue collection were liver (n=6, tumor biopsies), lymph nodes (n=2, surgical resections) and bone (n=1, tumor biopsy). SUVmax (tumor)/SUVmean (tumor)/SUVmean (healthy liver)/Ki-67 were analyzed on a per-lesion-basis. The values were: 11.3/7.4/3.0/40%, 15.7/9.2/2.8/10%, 10.1/7.0/1.8/60%, 11.9/7.5/3.2/40% (liver, pancreas); 11.0/6.7/2.5/30%, 17.2/10.9/2.5/20% (liver, unknown primary); 10.2/7.3/3.6/30% (lymph node, pancreas); 7.7/5.3/2.6/15% (bone, unknown primary). In 6/7 patients (86%) a NET lesion with a SUVmax >10 was associated with a Ki-67 $\geq 20\%$. By comparing the proliferative activity of the glucose hypermetabolic metastatic sites with the proliferative activity at initial diagnosis we saw an increase in the proliferative activity during the course of the progressing disease in 6/7 patients (86%). Four grade 1 tumors dedifferentiated to one grade 2 and three grade 3 tumors, one tumor remained grade 2, two grade 2 tumors dedifferentiated to grade 3 tumors. **Conclusion:** Glucose hypermetabolic NET lesions are associated with a Ki-67 index corresponding to grade 2 or grade 3 NET. Metastatic lesions of progressing NET which show an increased ^{18}F -FDG uptake were more dedifferentiated than the tumor cells at first diagnosis. Based on our results we conclude that studies need to be conducted including more patients in order to establish the role of ^{18}F -FDG PET scans in detecting patients with dedifferentiated, progressing neuroendocrine tumors.

P1032

Gallium-68-DOTATOC-PET/CT: Can we be impartial about the extent of partial volume effects?

J. Ruf¹, J. Schiefer¹, C. Furth¹, O. Kosiek¹, S. Kropf², T. Denecke³, M. Pavel⁴, A. Pascher⁵, B. Wiedenmann⁴, H. Amthauer¹; ¹Klinik für Radiologie und Nuklearmedizin, Universitätsklinikum Magdeburg AöR, Magdeburg, GERMANY, ²Institut für Biometrie und Medizinische Informatik, Medizinische Fakultät der Otto-von-Guericke-Universität, Magdeburg, GERMANY, ³Klinik für Strahlenheilkunde, Campus Virchow-Klinikum, Charité-Universitätsmedizin Berlin, Berlin, GERMANY, ⁴Medizinische Klinik m. S. Hepatologie und Gastroenterologie, Campus Virchow-Klinikum, Charité-Universitätsmedizin Berlin, Berlin, GERMANY, ⁵Klinik für Allgemein-, Viszeral- und Transplantationschirurgie, Campus Virchow-Klinikum, Charité-Universitätsmedizin Berlin, Berlin, GERMANY.

Aim: Combined positron-emission-tomography / computed tomography (PET/CT) using Gallium-68 labelled DOTA(0)-Phe(1)-Tyr(3)-octreotide (Ga-68-DOTATOC) is well established for imaging of neuroendocrine neoplasms (NEN). However, although PET offers the possibility of tracer uptake quantification, the presence of partial volume effects (PVE) and blurring has to be heeded. This study determined the minimal size at which PET-foci will not suffer from PVE in a clinical setting. **Materials and Methods:** Within the bounds of a retrospective blinded read, the Gallium-68-DOTATOC-PET/CT, whole-body imaging data of 51 patients with known or suspected NEN (25 m, 26 w; age, 57+/-13; range, 31-79 y) had been assessed by two independent specialists. For all examinations a 16-row PET/CT-device had been used (Biograph 16, Siemens AG, Erlangen, Germany). In all PET-Foci, the maximal standardized uptake value (SUVmax) and maximal lesional diameter on axial CT had been recorded. Follow-up (mean 21.2; range, 12-36 months) and an interdisciplinary truth panel served as a reference. In a first data filtering, only PET-findings classified as definitely malignant by the reference standard were taken into account. A second filtering step excluded PET-lesions that had no measurable correlate on CT. Using Loess-regression, the SUVmax was correlated to the lesional

size and the start of the horizontal plateau of the resulting curve was determined as the cut-off for independence of the SUVmax from lesional size. **Results:** A total of 413 PET-foci were found in 45 patients. 371/413 foci (90%) were of malignant origin. 313/371 NEN-lesions (84%) had a measurable correlate on CT (n=205 liver, n=60 lymph-node, n=22 bone, n=14 pancreatic, n=5 lung and n=7 other lesions). The SUVmax in these lesions ranged from 2.45 to 103.27 (mean 20.5±15.18) and maximal lesional diameters on axial CT ranged from 5.3 to 103.3 mm (mean 21.8±13.1 mm). After correlation of SUVmax to the lesional size in a Loess-regression, the cut-off for the independence of the SUVmax measured from the lesional diameter was 25 mm. **Conclusion:** In our model analysis using the aforementioned PET/CT-system, the correlation of lesional Gallium-68-DOTATOC-uptake and diameter showed a dependency of the determined SUVmax from the diameter in tumor lesions smaller than 25 mm. Despite the methodological shortcomings of this clinical analysis of PVE-effects, this signifies that a reliable quantification of tracer uptake (e.g. for the assessment of changes in SUVmax after therapy or the determination of physiological tracer distribution for the use in atlases) is only acceptable if the target structure possesses a sufficient size.

P1033

Short-term Haematological and Biochemical Safety of Lu-177 DOTATATE Therapy

E. Kaupila³, R. Allen², K. Ifigeneia², R. Meades², T. Tan², T. Barwick², N. Soneji², A. Al-Nahas², Z. Win²; ¹North-Karelia Central Hospital, Joensuu, FINLAND, ²Imperial Healthcare NHS Trust, London, UNITED KINGDOM, ³University of Eastern Finland, Kuopio, FINLAND.

Objective: Lu-177-DOTATATE treatment has proven to be effective and safe compared with alternative therapies for neuroendocrine tumours (NETs). The aim of this study was to explore and share our experiences of possible short-term toxicity effects of Lu-177-DOTATATE therapy. **Material and Methods:** Thirteen patients (mean age 56 ± 16 years, four females) with NET (eleven metastatic carcinoids, one gastrinoma and one paraganglioma) were enrolled in this retrospective analysis. Haematological and biochemical variables (haemoglobin, platelets, white cells, creatinine, bilirubin, and albumin), measured after each therapy, were compared with pre-therapy levels. Significant group level changes (Paired Samples T-test, p<0.05) and all individual changes were explored. **Results:** At the time of analysis total number of Lu-177 DOTATATE treatments was forty (mean dose 7.1 ± 1.4 GBq; range 5.3-8.0 GBq). Maximal four treatments had been given for seven patients; three patients had three treatments, one patient two, and one patient one treatment. Statistically significant changes (mean post-therapy value / pre-therapy value) were observed in haemoglobin, platelets and white cells from 12.8 to 12.0 g/dL, 275 to 216 x10⁹/L and 7.6 to 5.1 x10⁹/L, respectively, (for all p < 0.001). There were no significant changes in biochemical parameters. Five patients developed leucopenia (<3.5 x10⁹/L), which resolved during or soon after the treatment in all without intervention (the lowest measured leukocyte level was 2.6 x10⁹/L). Two incidences of thrombocytopenia (<150x10⁹/L) were observed, one with a patient who also had chemotherapy (the lowest measured platelet count was 57x10⁹/L). The most significant individual change in haemoglobin was from 12 to 10.8 g/dL, in a male patient who also developed thrombocytopenia and leucopenia. **Conclusion:** In line with previous studies our results demonstrate that Lu-177-DOTATATE therapy is relatively safe treatment for malignancy (NET) with mild reversible short term haematological toxicity effects.

P1034

Characterization of neuroendocrine neoplasms of the lung by 111In-pentetreotide SPECT and 18F-FDG PET: correlation with the pathological grading

V. Berti¹, V. Briganti², P. Ferri², A. Pupi¹; ¹University of Florence, Florence, ITALY, ²Azienda Ospedaliero-Universitaria Careggi, Florence, ITALY.

AIM Our purpose is to study the performance of two functional imaging techniques, 111In-pentetreotide single photon emission computed tomography (SPECT) and 18F-fluorodeoxyglucose (18F-FDG) positron emission tomography (PET), in the characterization of pulmonary neuroendocrine tumors (NETs), with correlation of tracer uptake and tumor grade on histology. **MATERIALS AND METHODS** Fifty-four patients with histologically-verified pulmonary NET underwent 111In-pentetreotide SPECT and/or 18F-FDG PET. Imaging results were compared to histopathological grading. **RESULTS** Final histological diagnosis confirmed 31 low-grade (G1), 11 intermediate-grade (G2) and 12 high-grade (G3) pulmonary NETs. The overall sensitivity of 111In-pentetreotide SPECT and 18F-FDG PET was 82% and 57%, respectively. At 111In-pentetreotide SPECT, more than 90% pulmonary NETs showed high tracer uptake. However, these tumors demonstrated high glucose at 18F-FDG PET only in 10% of cases (typically the most aggressive ones). G2 and G3 pulmonary NETs showed high 18F-FDG uptake in 100% of cases and positive 111In-pentetreotide SPECT in 80% and 55% of cases, respectively. **CONCLUSIONS** The overall sensitivity of 18F-FDG PET was low as compared to 111In-pentetreotide SPECT in the diagnosis of pulmonary NETs. G1 NETs of the lung showed higher and more selective uptake of 111In-pentetreotide than of 18F-FDG. In higher-grade (G2

and G3) NETs 18F-FDG PET demonstrated the highest sensitivity, with less ^{111}In -pentetreotide avidity. In conclusion, ^{111}In -pentetreotide SPECT and 18F-FDG PET provide complementary diagnostic information on the characterization of pulmonary NETs, reflecting differences in clinical behavior and prognosis.

P1035

The diagnostic role of ^{68}Ga -DOTATATE PET/CT in the detection of gastroenteropancreatic neuroendocrine tumors: comparison with ^{111}In -octreotide scintigraphy and CT scan

S. Sobhani, N. O. Kucuk, E. Ozkan, E. Ibis, K. M. Kir; Ankara University Medical Faculty, Ankara, TURKEY.

AIM: To evaluate the diagnostic and additional effective value of ^{68}Ga -DOTATATE PET/CT, in comparison with ^{111}In -octreotide scintigraphy and CT scan in gastroenteropancreatic (GEP) NET's. **METHODS:** Between November 2010 and December 2011, 27 patients who pathologically confirmed GEP NET had been referred to our nuclear medicine department for ^{68}Ga -DOTATATE PET/CT imaging. The primary tumor localisation were: 7 in stomach, 7 in liver, 4 in pancreas, 4 in abdominal lymph nodes or masses, 2 in intestine, 2 in choledoc and 1 in appendix. 25/27 patients had underwent abdomen CT and 18 of them had ^{111}In -octreotide scintigraphy as well. PET/CT acquisitions were performed using standard techniques, 45-60 minutes after the intravenous injection of 2.5-5 mCi (95-190 MBq) ^{68}Ga -DOTATATE. Results has compared with CT and ^{111}In -octreotide scintigraphy imaging. **RESULTS:** ^{68}Ga -DOTATATE PET/CT was positive in 22 of the 27 patients. 5 patients had normal PET/CT. We could find 10/27 liver NET lesions, were seen with ^{68}Ga -DOTATATE PET/CT, whereas CT scan detected 14/25 liver lesions. About intestinal, abdominal lymph nodes and masses, gastric and bone lesions PET/CT detected more pathologic uptakes. ^{68}Ga -DOTATATE PET/CT and CT results almost were equal in splenic and pancreatic lesions. ^{111}In -octreotide scintigraphy detected only 5 liver, 4 abdominal masses, 2 thoracic and 1 splenic lesions. 6/18 ^{111}In -OCT scintigraphy were found normal. **CONCLUSIONS:** ^{68}Ga -DOTATATE PET/CT, CT scan and ^{111}In -OCT scintigraphy showed comparable overall detection rates for organ involvement in GEP NET's. Although CT detected more liver lesions than PET/CT, most of these lesions were nondiagnostic. In organ-based detection rates we showed superiority of ^{68}Ga -DOTATATE PET/CT for gastric, intestinal, abdominal LN's and masses, bone and also liver lesions due to whole body scan and small lesion detection capability of ^{68}Ga -DOTATATE PET/CT.

P1036

Comparison of positron emission tomography with ^{68}Ga - DOTA-TATE and 18F FDG in neuroendocrine tumours

S. Yilmaz, E. Demirci, M. Ocak, A. Aygun, M. Halac, S. Sager, L. Kabasakal, B. Kanmaz; Istanbul University, Istanbul, TURKEY.

Purpose/introduction: Neuroendocrine tumours (NETs) are rare tumours originating from the neural crest. Most frequently, NET arise in the gastrointestinal tract, the pancreas, the lung and rarely in other organs. The diagnosis of NET relies on radiological-scintigraphic imaging methods and tumour marker levels. It's difficult to detect NET by positron emission tomography (PET) with 18F FDG because of low metabolic activity. However, PET using ^{68}Ga DOTA peptides is a promising imaging method in diagnosis and follow-up of NET because NET typically express somatostatin receptor. The aim of this study is to compare the diagnostic efficacy of ^{68}Ga -DOTA-TATE and 18F-FDG PET scintigraphy. **Subjects & methods:** 39 patients (20 men, 19 women, range: 11-79 mean age: 48 y) with diagnosis of NET who underwent ^{68}Ga -DOTA-TATE and 18F-FDG PET /CT at our institution were enrolled in this study. Maximum interval between the two study was 2 months (median interval: 23 d). The imaging findings were recorded per region in 7 regions (thyroid bed, lymphatic stations, lungs, liver, bones, pancreas and other) for every patient. PET images were evaluated visually. **Results:** Of 39 patients with NET. 15 patients had no uptake; 22 patients had uptake by either modality. On a lesion basis, ^{68}Ga -DOTA-TATE PET detected more lesion than 18F-FDG PET. In 5 patients (12.8%), ^{68}Ga -DOTA-TATE PET was positive but 18F-FDG PET was negative. On the other hand, 3 patients (7.6%) had 18F-FDG positive but ^{68}Ga -DOTA-TATE negative lesions. ^{68}Ga -DOTA-TATE PET is found to be superior to 18F-FDG PET for detection of NET ($P=0,001$). There was significant correlation with FDG SUV and Ki-67 index ($r=0,514$; $p=0,004$) The correlation with ^{68}Ga SUV and Ki-67 index was statistically significant ($r=0,181$; $p=0,338$). **Discussion/conclusion:** ^{68}Ga -DOTA-TATE PET/CT is a valuable imaging modality for diagnosis and follow-up of NETs and is superior to 18F-FDG PET /CT.

P1037

Comparison of I-123 MIBG Scintigraphy with Ga-68 Octreotide PET/CT Imaging in Neuroblastoma Patients

L. Uslu, S. Sager, L. Kabasakal, G. Tuysuz, T. Celkan, H. Apak, I. Uslu, B. Kanmaz; Istanbul University Cerrahpasa Medical Faculty, Istanbul, TURKEY.

Introduction: Neuroblastoma is a common solid tumor of childhood with poor prognosis. In current practice, I-123 MIBG scintigraphy is essential in staging and follow up of neuroblastoma patients. Neuroblastoma was shown to express somatostatin receptors, mainly subtype-2, therefore somatostatin receptor scintigraphy is another promising tool for neuroblastoma imaging and also may lead to somatostatin receptor therapy. Studies comparing somatostatin receptor and MIBG scintigraphies showed that I-123 MIBG scintigraphy is superior to In-111 octreotide. The aim of our study is to compare accuracy of Ga-68 DOTATATE PET/CT with I-123 MIBG scintigraphy in neuroblastoma patients and to search if better imaging qualities of Ga-68 octreotide makes a change in tumor detection. **Material and Methods:** 7 patients (6 neuroblastoma and 1 paraganglioma, mean age: 68,2 months \pm 64,9) underwent both Ga-68 DOTATATE PET/CT and I-123 MIBG scintigraphy on different days with a mean interval of 61,3 \pm 73,7 days (mean interval 21,6 d for 5 patients and 160,5 d for 2 patients). SPECT images were taken from suspicious lesions and all the images were compared by two nuclear medicine specialists. MRI or CT were also available for all patients. **Results:** A total number of 19 lesions were detected in 7 patients using both modalities, 18 of them (94,7%) were positive with Ga-68 DOTATATE, 8 (42,1%) were positive with I-123 MIBG, 7 lesions (36,8%) were positive with both radiopharmaceuticals. Ga-68 DOTATATE revealed 11 (57,9%) extra lesions and I-123 MIBG showed 1 extra (5,3%). Statistical analysis showed that Ga-68 DOTATATE is superior in lesion detection ($p=0,004$). Out of 7 patients, 4 (57,1%) were positive with both agents, 1 (14,3%) was positive with only Ga-68 DOTATATE, 1 (14,3%) was positive with only I-123 MIBG and 1 (14,3%) patient showed no pathological uptake. **Conclusion:** In neuroblastoma imaging Ga-68 DOTATATE is a useful diagnostic tool and it may be helpful for patients in somatostatin receptor radionuclide therapy planning.

P1038

The Influence of Proliferation Index on Somatostatin Receptor Scan in Patients with Carcinoid Tumors

M. Vlakovic¹, M. Rajic¹, M. Stevic¹, M. Matovic², D. Macut³, ¹Clinical Center Nis, Nis, SERBIA, ²Clinical Center Kragujevac, Kragujevac, SERBIA, ³Clinical Center of Serbia, Belgrade, SERBIA.

Aim of the study: Since somatostatin receptors tend to be overexpressed in patients with carcinoid tumors, the purpose of this study was to assess the role of the somatostatin analogue $^{99\text{mTc}}$ -EDDA-HYNIC-TOC ($^{99\text{mTc}}$ -Tektrotyd) scintigraphy in carcinoid tumor diagnosing and staging. The scan results obtained in this study were compared with the final diagnosis, taking into consideration the value of proliferation index of the tumor. **Material and methods:** Fifty-five patients (26 female, 29 male; age range: 33-76 years; mean age: 57,8 \pm 11,5 years) were examined: 11 patients highly suspected of having a carcinoid and 44 patients who had undergone the surgical removal of the tumor. Whole body scintigrams at 4h postinjection, spot scintigrams, and SPECT of the selected regions were obtained for all patients using "ROTA" and e.cam Siemens gamma cameras, equipped with ICON and an e.soft computers, respectively. After the reconstruction of the radiopharmaceutical according to the manufacturer's instruction manual, the patients were administered 740 MBq activities and 8 μg of octreotide. **Results:** Fifty-tree out of 55 patients were diagnosed with carcinoid tumor, 36 of which were well differentiated (Ki67<2%), 11 were found to have well-differentiated neuroendocrine carcinoma (Ki67 2-15%), and 6 patients were diagnosed with poorly differentiated neuroendocrine carcinoma with proliferation index above 15%. Positive scan results, defined as detection of either primary tumor or/and metastatic spreading were found in 28 patients, and negative scan results in 27. On a per patient basis, overall sensitivity was 79%, specificity 80%, and positive and negative predictive value 79% and 78%, respectively. In 21 patients, the negative scan findings correlated with results obtained by means of other methods, and 24 patients with positive scintigraphy findings had their results confirmed. Six patients had false negative scan results, and 4 false positive results. The greatest incidence of positive scan results (71%) was found in patients with low proliferation index (below 2%), whereas 4 out of 6 false negative patients had proliferation index above 15 %. **Conclusion:** The results of this study point to the fact that somatostatin receptor scintigraphy with $^{99\text{mTc}}$ -Tektrotyd represents a sensitive and specific method for diagnosing and staging patients with well-differentiated carcinoid tumors. However, in poorly differentiated tumors with high Ki67 proliferation index, additional analyses are necessary for precise staging.

P65-2 - Tuesday, October 30, 2012, 16:00 - 16:30, Poster Exhibition Area

Oncology Clinical Science: Bone

P1039

Risk Stratification at the Time of Diagnosis Using Bone Scan Index

R. Kaboteh¹, J. Damber¹, P. Gjerdtsson¹, P. Höglund², M. Lomsky¹, M. Ohlsson¹, L. Edenbrandt¹, ¹Sahlgrenska Academy at Gothenburg University, GÖTEBORG, SWEDEN, ²Competence Centre for Clinical Research, Lund

University Hospital, Lund, SWEDEN, ³Dept. of Theoretical Physics, Lund University, Lund, SWEDEN.

Purpose Bone Scan Index (BSI) is a method of expressing the tumor burden in bone as a percent of the total skeletal mass. BSI has been proposed as a response biomarker in castration-resistant metastatic prostate cancer. The purpose of this study was to explore BSI as a prognostic biomarker in a group of high risk prostate cancer patients at the time of diagnosis. **Patients and Methods** This retrospective study was based on 183 consecutive prostate cancer patients, who had undergone whole-body bone scans at the time of diagnosis and who were classified as high risk patients, i.e. at least one of the following criteria were fulfilled: T stage (T2c/T3/T4) or Gleason score (8-10) or PSA >20 ng/mL. BSI was calculated using an automated method. **Results** The 5-year probability of survival for all patients was 54% and when this group was subdivided into the groups BSI=0, 0<BSI<1 and BSI>1, the corresponding 5-year probabilities of survival were 79%, 64%, and 12%, respectively. The Kaplan-Meier curves for patients with BSI=0 and 0<BSI<1 were close to that of an age and sex matched control cohort. The curve for patients with 0<BSI<1 was closer to the BSI=0 curve than the corresponding BSI>1 curve, indicating that the tumor burden is important and not only the presence of metastases. In a multivariate survival analysis BSI was associated with survival (Hazard Ratio, 1.25; P<0.001). The Concordance index increased from 0.66 to 0.73 when adding BSI to a model containing Clinical stage, PSA and Gleason score. **Conclusions** These data show that BSI can be used as a complement to PSA to risk stratify prostate cancer patients at the time of diagnosis. BSI may play a role for the decision when to start hormonal therapy in advanced asymptomatic prostate cancer patients. The risk or expected median survival time based also on BSI analysis may be of value, for example, to advice patients with a strong wish to avoid treatment-related side-effects.

P1040

What does the single skeletal lesion mean in 99mTc-MDP bone scintigrams of children with known malignancy?

L. I. Sonoda¹, K. Sonoda¹, K. K. Balan²; ¹Paul Strickland Scanner Centre, Mount Vernon Hospital, Northwood, UNITED KINGDOM, ²Department of Nuclear Medicine, Addenbrooke's Hospital, Cambridge, UNITED KINGDOM.

Introduction 99mTc-MDP bone scintigraphy plays an important role in the management of children with known or suspected malignancy. While the presence of multiple lesions on bone scans of children in the context of known or suspected malignancy is generally considered to be due to multiple skeletal metastases, the exact significance of solitary hot spots remains unknown. An accurate diagnosis and staging is critical in order to determine the optimal management and eventual outcome. This study was undertaken to evaluate the significance of solitary abnormalities on bone scintigrams of children with known or suspected malignancy. **Materials & Methods** A retrospective review of 215 sequential paediatric bone scintigrams over a 10-year-period was performed. Further evaluation of the solitary lesions demonstrated on bone scintigrams was carried out by either imaging or biopsy studies. Spontaneous resolution of a lesion on subsequent bone scintigram without a change in therapy was considered benign while progression of the solitary abnormality was considered malignant. Results 49 scans (22.8%) were found to have single lesions, of which 18 were due to uptake at the primary site and were excluded from further consideration. Of the remaining 31 lesions 13 (41.9%) were confirmed as metastases, 18 lesions were proven to be benign (by imaging in 14, biopsy in 2 and clinical follow-up in 2). No statistically significant difference was observed between patients with benign and malignant conditions and the sites of occurrence of solitary lesions. **Conclusion** Solitary skeletal abnormalities on 99mTc-MDP bone scintigraphy in children with known or suspected malignancy are common, and they carry higher risk of metastasis than in adults.

P1041

Bone Imaging in Cancer Patients. The Diagnostic Advantages of ¹⁸F-NaF PET/CT

J. Correia¹, P. Lapa¹, A. Albuquerque¹, P. Gil¹, J. Isidoro¹, I. Ferreira¹, G. Costa¹, J. Pedroso de Lima²; ¹Serviço de Medicina Nuclear - Centro Hospitalar e Universitário de Coimbra, Coimbra, PORTUGAL, ²ICNAS - Universidade de Coimbra, Coimbra, PORTUGAL.

Aim: Bone scintigraphy is a widely used imaging modality for assessment of skeletal metastases, due to its sensitivity, availability and reasonable cost. However, published studies have demonstrated that ¹⁸F-Sodium Fluoride (¹⁸F-NaF) PET/CT is able to detect bone metastatic disease with even better sensitivity than conventional bone scanning. ¹⁸F-NaF has approximately two-fold increased bone avidity, with faster blood clearance. Therefore, images can be available in a short time and with a better quality. The aim of this study was to evaluate the clinical value of ¹⁸F-NaF PET/CT in distinguishing malignant from benign bone lesions. **Material and Methods:** Seventy eight ¹⁸F-NaF PET/CT scans were performed in 56 oncologic patients (24 males, 32 females; mean age 63.07 years; range 42-82 years) to detect the presence of bone metastases, between August 2009 and March 2012.

Sixteen patients (29.82%) had combined ¹⁸F-Fluoride/¹⁸F-FDG scans. Nineteen patients were also evaluated by ^{99m}Tc-MDP planar scintigraphy, 11 of them with SPECT/CT. Twenty seven patients (48.21%) had breast cancer, 23 (41.07%) prostate cancer, 3 (5.36%) lung cancer, 1 (1.79%) colon cancer and 2 (3.57%) had bone lesions of unknown primary cancer. PET/CT acquisition was performed 30 minutes after intravenous administration of ¹⁸F-NaF (370 MBq). Lesions showing increased ¹⁸F-NaF uptake were classified as malignant, benign or inconclusive and compared to a clinical diagnosis based on diagnostic CT, MRI, histopathology or clinical follow-up. Results: ¹⁸F-NaF PET/CT identified bone metastases in 30 (53.57%) patients and benign lesions in 23 (41.07%). The CT component of PET/CT enabled the characterization of the benign lesions into degenerative changes, fractures and vertebral hemangioma. In 3 patients (5.36%) ¹⁸F-NaF PET/CT was inconclusive, although in 1 of these patients MRI was also equivocal. Among the 19 patients who underwent both studies (¹⁸F-NaF PET/CT and ^{99m}Tc-MDP bone scan), PET/CT detected metastatic disease in 12, whereas ^{99m}Tc-MDP (planar and SPECT/CT) characterized the lesions as malignant in 7 patients. Compared with ¹⁸F-NaF PET/CT, ^{99m}Tc-MDP scan underestimated the extent of disease in 3 patients and did not identify any additional metastatic lesion. **Conclusions:** This study shows that ¹⁸F-NaF PET/CT is a useful tool to identify and distinguish benign lesions from skeletal metastases due to the good quality of the functional image and the morphologic characterization from the CT component. ¹⁸F-NaF PET/CT has demonstrated a significantly higher diagnostic value compared to bone scintigraphy, even when a complementary SPECT/CT is performed.

P1042

Prognostic value of Bone Scan Index for survival in patients with prostate cancer

M. Reza¹, L. Edenbrandt¹, M. Ohlsson², E. Trägårdh¹, A. Bjartell³, P. Wollmer¹; ¹Department of Clinical Physiology, Clinical Sciences, Malmö, SWEDEN, ²Department of Astronomy and Theoretical physics, Lund University, Lund, SWEDEN, ³Department of Urology, Clinical Sciences, Malmö, SWEDEN.

Objectives: Bone scintigraphy is a commonly used method to assess metastatic spread to the skeleton. Bone Scan Index (BSI) is a measurement that reflects the tumor burden in bone as a percent of the total skeletal mass. BSI has been proposed both as a prognostic biomarker and as a response biomarker in prostate cancer patients. Recently, an automated method to calculate BSI was developed, which makes it feasible to use in clinical routine. The purpose of this study was to build on earlier work and evaluate the prognostic value of BSI in a large group of prostate cancer patients. **Patients and Methods:** In this study, we retrospectively studied 950 prostate cancer patients who had undergone whole-body bone scintigraphy (750 MBq Tc-99m Methylene Diphosphonate) during the period 2004-2010. BSI were calculated using the automated software EXINI Bone™ (EXINI Diagnostics AB, Lund Sweden). Survival data were collected from computerised medical records. A univariate Cox proportional hazards model was built using the BSI measurement. **Results:** A total of 144 patients had a BSI greater than 1% and 806 had a BSI lower than 1%. In the group with high BSI, 49 patients were alive two years after the bone scan. In the group with low BSI, 707 patients were alive after two years. This corresponds to 2-year survival rates of 34% and 88%, respectively (p<0.0001). In the univariate Cox model BSI was significantly associated with survival (p<0.0001) with hazard ratio of 1.25 (CI 1.22 - 1.29). **Conclusions:** The results obtained in this study confirm earlier findings that BSI contains prognostic information in prostate cancer patients. BSI is significantly associated with survival and patients with BSI greater than 1% have a worse prognosis. BSI may be a valuable imaging biomarker that could be used for risk stratification in the management of prostate cancer patients.

P1043

Evaluation of bone metastases in prostate cancer patients - bone scan compared to 18F - FCH PET/CT - with emphasis on doubtful BS results

A. Tabain¹, A. Balenović¹, S. A. Rogan¹, K. Kovačić², Z. Kusić²; ¹Policlinic Medikal PET/CT Centre, Zagreb, CROATIA, ²University Hospital Centre "Sestre Milosrdnice", Zagreb, CROATIA.

Aim The aim of this study was to compare bone scintigraphy (BS) and 18F FCH PET/CT as more differentiated imaging method in prostate cancer patients, with special attention to patients that had equivocal findings on BS. Equivocal finding on BS is the accumulation of the radiopharmaceutical which could be benign (degenerative changes or trauma) but could also be metastasis too. Such cases must be resolved as soon as possible because of the therapy. Sometimes, the months are needed, specially when other imaging methods didn't give us explanation for BS finding. Therefore the result of FCH PET/CT scan could be crucial because of the specificity of the method. If the PET/CT scan was positive equivocal result on BS is considered positive, if it was negative some benign reason exist. **Methods** 27 patients with prostate cancer in various stages of disease who underwent BS and PET/CT in period not exceeding three months, from October

2008 to December 2011, were retrospectively analysed. There were no significant clinical events or treatments in the interim and afterwards patients were followed up either with BS or PET/CT. BS and PET/CT images were visually analysed by two experienced specialists of nuclear medicine. BS was performed with 99mTc-MDP on Siemens Symbia TruePoint SPECT/CT two-headed gamma camera (dose range from 592 - 740 MBq), only planar projections were obtained and PET/low-dose CT study with 18F - FCH on Philips Gemini TF 64 hybrid scanner (dose range from 211-259 MBq), according to the standard oncologic protocol. Results Bone scintigraphy was positive in 5, negative in 16 and equivocal in 6 of 27 patients, while PET/CT was positive in 12, negative in 15 with no equivocal results. Concordant results occurred in 17 (63.0%) patients: 5 with positive and 12 with negative results with both methods. In 4 (14.8%) patients results were discordant; negative on BS but positive on PET/CT. Our interest were 6 (22.2%) patients with equivocal BS findings. In that group PET/CT provided further information for all examined patients - metastatic disease was confirmed in 3/6 patients, while negative PET/CT excluded metastatic disease in 3/6 patients. In total, PET/CT revealed more positive patients 12/27 (44.4%). Conclusion Number of patients in our study is not sufficient for statistical analysis, but thanks to higher specificity of FCH-PET/CT in prostate cancer patients it would be reasonable to compare these two methods in cases with equivocal BS results, if available.

P1044

The Impact of SPECT/CT for Excluding Bone Metastases in Patients with Equivocal Bone Scintigraphy

B. B. Nascimento, A. O. Santos, B. J. Amorim, M. C. Lima, E. C. Etchebehere, J. P. Souza, G. F. Martins, M. L. Baracat, J. M. Altamari, C. D. Ramos; State University of Campinas - UNICAMP, Campinas, BRAZIL.

INTRODUCTION: Detection of bone metastases has usually been performed with conventional technetium 99m methylenediphosphonatescintigraphy (MDP-99mTc), because is widely available, relatively inexpensive, and highly sensitive. However, this method presents a low specificity and a significant rate of equivocal lesions, because many benign conditions exhibit increased radiotracer uptake. This limitation is greater in patients with single lesions. SPECT/CT images enables a better characterization of focal areas of radiotracer uptake, but the literature is not clear about the clinical impact of these images in the evaluation of patients with single lesions on conventional bone scintigraphy. **AIM:** The objective of the study was to evaluate the impact of SPECT/CT images in the evaluation of cancer patients with inconclusive solitary bone lesions on conventional bone scintigraphy. **MATERIALS AND METHODS:** We prospectively analyzed 32 patients (24 women, 30-77 years-old, mean age 61 +/- 13.8 years) with an equivocal single lesion on conventional bone scintigraphy performed for metastases detection of with various cancers (breast: 23, prostate: 3, lung: 1, liver:3 and kidney: 1). Whole-body scan and static images were performed 3 hours after an intravenous injection of 740 MBq of 99mTc-MDP. SPECT/CT images using a scintillation camera coupled with multislice computed tomography were also obtained, only of the segment with the solitary inconclusive lesion identified on the conventional images. Utilizing a consensus of two nuclear medicine physicians and one experienced radiologist, the lesions were reclassified as: benign (uptake around joints, osteophytes, joint damage, trauma or benign bone tumor), malignant (cortical destruction, localization in the posterior aspect of the vertebral body and pedicle and other characteristic morphological changes on CT image) or still indeterminate. **RESULTS:** SPECT/CT images reclassified 69% of the bone lesions as definitely benign (14/32) or definitely metastatic (8/32). Ten/32 (31%) remained undetermined. **CONCLUSION:** SPECT/CT significantly reduces the number of inconclusive bone scintigraphies performed for the diagnosis of bone metastasis in oncologic patients.

P66-2 - Tuesday, October 30, 2012, 16:00 - 16:30, Poster Exhibition Area

Oncology Clinical Science: CUP (Cancer of Unknown Primary)

P1045

Usefulness of 18-F-FDG-PET/CT on the study of unknown primary tumors. Preliminary results.

L. Castillejos Rodriguez, M. A. Balsa Breton, M. P. Garcia Alonso, A. Ortega Valle, E. Rodriguez Pelayo, I. S. Vasquez Tineo, A. Mendoza Paulini, F. J. Penin Gonzalez. UNIVERSITARIO DE GETAFE, Madrid, SPAIN.

Unknown primary tumors (CUP) represent approximately 2-5% of all cancers. They are generally aggressive tumors showing survival between 2-10 months. The choice of appropriate therapy according to primary tumor improves survival, hence the importance of typify them. **Aim:** The aim of our study was to assess the effectiveness of PET/CT in location the primary lesion in patients suspected of CUP.

Material and method: Retrospective review from July 2009 to November 2011. We studied 32 patients, 13 women and 19 men aged between 43 and 79 years old. Group 1: 27/32 patients had histological diagnosis of neoplastic disease. Group 2:

2/32 patients with neurological symptoms and suspected paraneoplastic syndrome. Group 3: 3/32 patients with single brain lesion unable to differentiate between metastasis and primary central nervous system tumors (CNS). PET/CT results were confirmed by histological study and/or clinical course. **Results:** - GROUP 1: PET/CT located primary tumor in 15 of 27 patients (55.5%): in 7 patients lung was the origin, in 1 cervix, 2 pancreas, 1 cavum, 1 mesothelioma, 1 esophagus, 1 breast and 1 ovary. In 12/27 patients tumor was not located by PET/CT: 7 continue with diagnosis of CUP, in 3 the origin was lung, in 1 carcinoid in sigma and in 1 breast cancer. - GROUP 2: PET/CT did not locate tumor lesions and were considered as demyelinating polyneuropathy and transverse myelitis retrospectively in the clinical course. - GROUP 3: PET/CT confirmed single CNS lesions in the 3 patients and were subsequently operated by neurosurgery, resulting glioblastomas. **Conclusions:** In our study PET/CT has proved to be very useful in locating primary tumor in patients with CUP. In patients with paraneoplastic syndromes and single central nervous system lesions, PET/CT can avoid performing multiple diagnostic tests.

P1046

18F-fluorodeoxyglucose Positron Emission Tomography/Computed Tomography in Carcinoma of Unknown Primary: 6-Year Single Institution Experience

U. Elboga¹, **Z. Kurt¹**, **Y. Celen¹**, **C. Aktolun²**; ¹Gaziantep University, School of Medicine, Nuclear Medicine Department, Gaziantep, TURKEY, ²Tirocenter Tiroid ve Nükleer Tıp Merkezi, İstanbul, TURKEY.

Objective: Carcinoma of unknown primary (CUP) is a heterogeneous group of tumors with various clinical features causing diagnostic and therapeutic challenges. The aim of this study was to evaluate the ability of F-18 FDG PET/CT for localizing the primary tumor, disclosing additional metastases, and changing the treatment in patients with CUP. **Materials and Methods:** One hundred and twelve metastatic patients (female=40, male=72, median age=60.5 years) in whom conventional diagnostic work-up failed to disclose the primary tumor were included in the study. F-18 FDG PET/CT imaging was performed in a standard protocol (patient supine, arms on patient's side, vertex to thigh, 369.3 MBq (296-444 MBq) F-18 FDG, a 60-minute uptake period, 6-7 bed position). Histopathology was taken as the only reference standard. **Results:** F-18 FDG PET/CT correctly detected primary tumor in 37 of 112 (33.03%) patients. The most common site of primary tumor detected by F-18 FDG PET/CT was lung (n=18), which was followed by nasopharynx (n=7), pancreas (n=5), tonsil (n=2), breast (n=2), thyroid (n=1), uterus (n=1) and colon/rectum (n=1). F-18 FDG PET/CT imaging disclosed additional previously undetected metastases in 32 (28.5 %) and changed the treatment in 33 (29.4%) of 112 patients. **Conclusions:** F-18 FDG PET/CT is able to disclose the primary tumor, disclose new metastases and change the treatment in about one third of patients with CUP.

P1047

PET scans in Tumours of Unknown Primary Origin - What to Expect

P. M. B. C. Ratão; Instituto Português de Oncologia de Lisboa, Lisbon, PORTUGAL.

Introduction: Metastatic neoplasia of unknown primary origin is characterized by an average survival after diagnosis of less than one year. Recent studies indicate that PET scans with 18F-FDG (FDG-PET) are able to identify the original location of the tumour in 24-40% of the cases. **Objective:** Assess the relevance of FDG-PET in the diagnostic approach of tumours of unknown primary origin (TUPO). **Materials and Methods:** Three thousand two hundred and sixty eight (3268) PET studies performed between 01/01/2009 and 31/12/2010, at the Department of Nuclear Medicine of our institution, were analysed. Patients (pts) with a diagnostic of TUPO were included in the study. The tomographic images were obtained about 60 minutes after the intravenous administration of 3.7MBq/Kg of 18F-FDG in a PET scanner ECAT ACCEL-LSO. The results of PET, were considered positive or negative for the location of primary tumour. These results were compared with other diagnostic tests (CT). **Results:** Of the 3268 PET studies analyzed, 118 pts (3.6%) met the criteria for inclusion in the study. Of these, 68.6% (n = 81) were male and 31.4% (n = 37) were female, with an average age of 61 years. The initial presentation was lymph node involvement in 67.8% of the patients (n = 80). The primary tumour could not be identified in 71.2% of the patients (n = 84), by any method. Of the 34 pts (28.8%) in which it was possible to locate the primary tumour, FDG-PET identified 58.8% of the cases (n = 20). FDG-PET scan was the only test that located the primary tumour site in 8 of the 34 pts (23.5%). In the other cases identified by FDG-PET (n = 12), there was full agreement with the results of the CT scans. In 41.1% of the patients (n = 14), FDG-PET failed to identify the primary tumour. In the follow-up, 43 of the 118 pts (36,4%) have died. Pts in which we located the primary tumour had an average survival of 17 months. In the group of pts in which the primary tumour could not be identified, average survival was 12 months. **Conclusions:** PET had an impact in the diagnostic approach of TUPO, identifying the primary tumour in 20 of 34 patients (58.8%), in which it was possible to locate the

primary tumour site. The average survival after diagnosis was higher in pts in which definitive localization of primary tumour was possible.

P67-2 - Tuesday, October 30, 2012, 16:00 - 16:30, Poster Exhibition Area

Oncology Clinical Science: Melanoma

P1048

The Role of FDG PET/CT in Detecting Malignant Transformation of Giant Congenital Melanocytic Nevus : Double Density Sign

F. Novruzov, M. Aras, S. Gungor, F. Dede, T. Ones, S. Inanir, T. Y. Erdil, H. T. Turoglu; Marmara University Hospital, Istanbul, TURKEY.

Aim: Giant Congenital Melanocytic Nevus (GCMN) is a rare premalignant lesion which must be followed up due to its high malignancy potential. The risk for transformation to malignant melanoma (MM) is increased by the age of the patient and size of the lesion. Herein we report the FDG PET/CT findings of GCMN which is accompanied by MM and covered the dorso-lumbar region. **Case Presentation:** A 44-year-old female patient presented to the chest medicine out-patient clinic with cough complaint. Multiple enlarged mediastinal lymph nodes were seen on thorax CT. Bronchoscopic biopsy from the LAP's revealed MM involvement. Then shave biopsy was performed from the GCMN and the pathology confirmed the diagnosis of MM lesion which measured 2 mm. in thickness and 0.5mm. in diameter. The baseline FDG PET/CT requested for staging showed intense hypermetabolic lesions in the right parietal cortex of the brain and in both lungs. Mild to moderate hypermetabolism involving the axillary and inguinal lymph nodes bilaterally was depicted on FDG PET/C images. The giant GCMN lesion had diffuse, homogeneous mild FDG uptake. Morpho-metabolic progression was seen in the follow-up PET/CT scan which was performed after 3 cycles of chemotherapy. Although the FDG uptake of the GCMN was similar to the baseline study, a focus of intense hypermetabolism was detected within the giant lesion. We suggest to call this finding which is highly suggestive of malignant transformation as a "double density sign". **Conclusion:** The dark pigmentation of the GCMN makes it difficult to detect the focus of malignant transformation. In our case, the diffuse mild FDG uptake on both baseline and follow-up PET/CT scans indicates baseline metabolism of the lesion. The distinct hypermetabolic focus within the GCMN with relatively less FDG uptake i.e. "double density sign" that was detected on the follow-up scan suggests that FDG PET/CT may be useful in detecting malignant transformation of GCMN.

P1049

Ultrasound and US-guided FNAC can reduce the number of sentinel lymph node biopsies in cutaneous melanoma

G. Horvatic Herceg¹, I. Bracic¹, S. Kusacic-Kuna¹, D. Herceg², A. Mutvar¹, D. Dodig¹; ¹University Hospital Zagreb, Clinical Department of Nuclear Medicine and Radiation Protection, Zagreb, CROATIA, ²University Hospital Zagreb, Clinic of Oncology, Zagreb, CROATIA.

The involvement of regional lymph nodes is the most important prognostic factor for overall survival of patients with stage I/II melanoma. Sentinel lymph node biopsy (SLNB) is considered to be reliable tool in detection of lymph node metastases, enabling planning of complete lymph node dissection (CLND). The aim of this study was to analyze the usefulness of additional ultrasound (US) with power Doppler sonography and fine needle aspiration cytology (FNAC) of sentinel nodes (SN) prior to SLNB. **Methods:** In a prospective study 59 consecutive patients with cutaneous melanoma (31 females and 28 males, mean age 58 years; median tumor Breslow depth 2.2 mm), in whom dissection of SLNs was indicated, were examined by ultrasound before the preoperative lymphoscintigraphy. FNAC was performed in suspicious lymph nodes (round or broad oval shaped lymph node, asymmetric cortical thickening, a cap like structure and a loss of normal hilar vascularization, with multiple peripheral, capsular vessels penetrating the nodal cortex). In the case of malignant finding, patients were referred to CLND. **Results:** Suspicious echographic finding was concordant with findings of FNAC in 8 out of 9 patients. All FNAC findings were confirmed by pathohistology. In 6 out of 50 echographically negative patients pathohistology revealed metastases, although in 4 out of these 6 cases only a very small number of melanoma cells was found. The sensitivity, specificity, positive predictive value, and negative predictive values of ultrasound combined with FNAC were 57.1%, 100%, 100% and 88.2%. **Conclusion:** Performing ultrasound combined with power Doppler sonography and FNAC prior to lymphoscintigraphy in the detection of possible melanoma lymph node metastases, unnecessary surgical sentinel node staging can be avoided. In our study 14% (8/59) of patients were directly referred to complete lymph node dissection, sparing them additional unnecessary surgery. For patients with a negative ultrasound finding, sentinel lymph node biopsy remains the best diagnostic option. Ultrasound examination should be included in the preoperative algorithm in patient with cutaneous melanoma.

P1050

Evidence-based appropriate use of SPECT/CT in sentinel lymph node studies of melanoma

S. Navalkisoor¹, T. L. J. Wagner²; ¹Royal Free London NHS Foundation Trust, London, UNITED KINGDOM, ²Royal Free London NHS Foundation Trust, London, FRANCE.

Introduction Sentinel Lymph node (SLN) biopsy has become the standard of care for patients with malignant melanoma and is now routine practice in the lymphatic staging of early melanoma. SPECT/CT is a new tool in lymphatic staging of melanoma. We reviewed the literature to determine the appropriate usage of SPECT-CT in melanoma. **Material and Methods** A Pubmed search was performed using keywords "SPECT/CT" and "melanoma" and "sentinel lymph node". **Results** Several SLN studies showed that SPECT/CT provides significant advantages over planar imaging particularly in patients with head and neck and posterior truncal melanomas. The advantages include a higher detection rate of SLN, the ability to detect SLNs in difficult to interpret planar studies, better detection of SLNs near an injection site, better anatomical localisation, resulting in altering the surgical approach. SPECT-CT should not be used as a substitute for dynamic imaging as it would not be possible to differentiate SLNs from second tier nodes. **Conclusion** Based on the available evidence we feel that SPECT/CT is indicated in all patients with head and neck and posterior truncal melanomas, in patients with nonvisualisation on planar imaging, with unusual drainage pattern or difficult to interpret planar images

P69-2 - Tuesday, October 30, 2012, 16:00 - 16:30, Poster Exhibition Area

Oncology Clinical Science: Miscellaneous

P1051

Radiometabolism, whole-body distribution and radiation dosimetry of Ga-68-bombesin antagonist BAY86-7548 in healthy men

A. Roivainen¹, E. Kähkönen², S. Borkowski³, B. Hofmann³, K. Lehtiö¹, P. Luoto¹, T. Rantala¹, A. Rottmann³, H. Sipilä¹, R. Sparks⁴, S. Suilamo¹, T. Tolvanen¹, R. Valencia³, H. Minn¹; ¹Turku PET Centre, Turku University Hospital, Turku, FINLAND, ²Turku University Hospital, Turku, FINLAND, ³Bayer Pharma AG, Berlin, GERMANY, ⁴CDE Dosimetry Services, Knoxville, TN, UNITED STATES.

Aim: Gallium-68 labelled DOTA-4-amino-1-carboxymethylpiperidine-D-Phe-Gln-Trp-Ala-Val-Gly-His-Sta-Leu-NH₂ (BAY 86-7548) is a bombesin antagonist and a ligand for gastrin-releasing peptide receptor which holds promise as a novel PET tracer for imaging of prostate cancer. This study investigated the radiometabolism, whole-body distribution and radiation dosimetry of BAY 86-7548 in healthy humans.

Materials and methods: Five healthy male volunteers (aged 52 ± 2 years, mean ± SD) underwent 250-min dynamic whole-body PET/CT imaging. Serial venous blood samples were drawn during 1-150 min after 138 ± 5 MBq intravenous bolus injection of BAY 86-7548. Plasma samples were analyzed by radio-HPLC for intact tracer and radioactive metabolites. Following PET imaging, the radioactivity in voided urine was measured. Radiation dosimetry was calculated according to the MIRD protocol, with OLINDA/EXM software. **Results:** Three radioactive metabolites of BAY 86-7548 were detected in human venous plasma. The proportion of unchanged BAY 86-7548 decreased from 92 ± 9% of total radioactivity at 1 min after tracer injection to 19 ± 2% at 65 min. The whole-body distribution of BAY 86-7548 showed the highest uptake in urinary bladder contents with approximately 36%, and liver with 14% of the injected radioactivity. The organs with the highest absorbed doses were the pancreas at 0.51 mSv/MBq followed by the urinary bladder wall at 0.24 mSv/MBq. The mean effective dose (ICRP 103) was 0.028 mSv/MBq (range 0.024-0.032 mSv/MBq). No adverse events related to injection of BAY 86-7548 were detected. **Conclusion:** Intravenous injection of BAY 86-7548 was safe and rapid metabolism was demonstrated in human subjects. The effective radiation dose of BAY 86-7548 is in the same range as the effective dose derived from somatostatin receptor ligands [⁶⁸Ga]DOTATOC (0.023 mSv/MBq) and [⁶⁸Ga]DOTANOC (0.025 mSv/MBq). An injection of 150 MBq of BAY 86-7548 would expose a subject to 4.2 mSv of radiation. This supports the use of BAY 86-7548 in up to 4 repeated PET scans, for example in trials clarifying treatment efficacy of novel drug candidates.

P1052

Incidentalomas Detected by 18F-FDG PET-CT: a Study of Prevalence and Risk of Malignancy.

I. L. Hernandez Perez, M. Coronado, D. Mendez, C. Escabias, D. Marin, R. Couto, A. Martínez Lorca, L. Martín Curto; La Paz University Hospital, Madrid, SPAIN.

AIM Incidentalomas in PET studies are defined as FDG accumulations unexpectedly detected in a PET-CT study not attributable neither to 18F-FDG physiological distribution nor to the patient's basal pathology. The aim of this study was to determinate the incidence of incidentalomas in oncological PET-CT studies and to elucidate their risk of malignancy. **MATERIAL AND METHODS:** We performed a systematic retrospective review of 2234 consecutive PET/TC examinations carried out in the Nuclear Medicine Department of our hospital between January 2009 and March 2010 for staging or therapeutic monitoring of various neoplasms, or for characterization of underminate lesions with conventional diagnostic methods. We looked for incidentalomas in this group of studies. Follow up of the patients was done in order to confirm their nature. **RESULTS:** From the total PET/TC studies that were revised, 196/2234 (8,7%) presented incidentaloma/s. A total of 204 incidentalomas were found (corresponding to 196 patients). Location of incidentalomas was: large bowel-rectum (100), small bowel (16), thyroid (41), gynaecological (9), pituitary gland (4), parotid gland (6), prostate (5), pancreas (4), kidney (3) and others (16). Follow up was possible in 153/196 patients (78%), corresponding to 160 incidentalomas, from which 96/160 (60%) were confirmed and 64/160 were not confirmed. A total of 58/96 incidentalomas (60%) were histologically confirmed and 38/96 (40%) were clinically-radiologically confirmed during a 1-36 months follow up period (x=15,8 months). Histology revealed 45 malignant and 13 benign lesions, and clinical-radiological follow up 12 malignant and 26 benign findings. Malignancy was found in 59% (57/96) of the incidentalomas and benignancy in 41% (39/96). Malignancy confirmation (57): premalignant polyp (26), second primary tumour (25), metastasis from basal tumour (6). Benignancy confirmation (39): thyroid (5 colloid goiter, 2 multinodular goiter, 2 adenoma, 1 lymphocytic thyroiditis and 5 single benign node); pituitary gland (1 macroadenoma); nasal mucosa (1 inflammatory); amygdala (1 inflammatory); parotid gland (1 Warthin tumour); heart (1 physiologic/inflammatory); spleen (1 physiologic); large bowel-rectum (4 inflammatory and 7 inflammatory/physiologic); small intestine (1 inflammatory); prostate (1 hyperplasia); uterus (2 physiologic and 2 miomas) and ovary (1 functional). **CONCLUSION** The incidence of incidentalomas in oncological PET-CT studies is low. However, due to their high risk of malignancy, follow up of these patients is crucial in order to confirm their nature.

P1053

Lipomatous Hypertrophy of the Interatrial Septum: 18F-FDG PET-CT imaging findings.

J. Mucientes, B. Rodríguez, J. Cardona, I. Rodríguez, A. Gómez, T. Morales, A. González, J. Huertas, M. Beresova; Hospital Universitario Puerta de Hierro Majadahonda, Madrid, SPAIN.

AIM To assess the incidence and the 18F-FDG PET-CT imaging findings of lipomatous hypertrophy of the interatrial septum (LHIA). **MATERIAL AND METHODS** All patients with imaging findings suggesting LHIA in PET-CT studies performed between September/2011 and March/2012 were prospectively selected for the study. 18F-FDG-PET-CT were carried out 50 minutes after the intravenous injection of 370 MBq of 18F-FDG and then evaluated by two experienced nuclear physicians who assessed the presence of characteristic image findings of LHIA. **RESULTS** From September/2011 to March/2012, 1036 PET-CT were performed in oncological patients at our institution. Seven (0.7%) met the inclusion criteria (five females and two males; ages ranged from 53 to 79 years). All of them showed a mediastinal focal uptake. The CT image characteristics, its shape (bilobed or dumbbell) and its location at the interatrial septum suggested the diagnosis of lipomatous hypertrophy in FDG PET-CT studies. **CONCLUSION** Lipomatous hypertrophy of the interatrial septum is a relatively infrequent cause of FDG uptake in mediastinum (7 of 1036 studies in our institution; 0.7%). It is a usually clinically innocuous abnormality of the heart and the correlation with CT and possibly MRI can avoid the false positive diagnosis of malignancy.

P1055

Diagnostic value of ¹⁸F-FDG PET/CT in patients with carcinoma of unknown primary

Ü. Abdülrezzak, Y. Sarıkaya, M. Kula, A. Tutus; Erciyes University School of Medicine, Nuclear Medicine Department, Kayseri, TURKEY.

Aim: Carcinoma of unknown primary is defined as a biopsy-proven malignancy whose anatomical origin remains unidentified after a thorough diagnostic evaluation. The aim of this study was to evaluate the effectiveness of whole body FDG PET/CT scan in the detection primary site in patients with metastatic carcinoma of unknown primary. **Material and Methods:** A total of 119 patients with unknown primary tumor underwent FDG PET-CT imaging; 49 patients with histologically proven metastases and 70 patients with clinical suspicion of the presence of a malignancy. For all patients, the results of conventional diagnostic examinations were negative. The criterion for malignancy was FDG hypermetabolism at the site of pathological changes on CT or marked focal hypermetabolism at site suggestive of malignancy despite absence signs of pathology at those sites on CT. Histopathological findings and/or follow-up data

were used as the gold standard. The sensitivity, specificity, positive predictive value, negative predictive value and accuracy were determined. **Results:** The primary tumor discovered in 91 patients (77%) histologically; 28 patients (23%) remained primary unknown. FDG PET/CT was able to determine the primary tumor site in 77 of 91 patients. In the whole study population, the sensitivity, specificity, positive predictive value, negative predictive value and accuracy were 85%, 65%, 86%, 63%, 79%, respectively. In the patients with histologically proven metastases, the sensitivity, specificity and accuracy values were 84%, 63% and 80% respectively. **Conclusion:** FDG PET/CT imaging is a valuable method in detection of primary tumors in patients with metastatic cancer from unknown primary origin. It should be performed early in the workup of the patients for accurate staging and optimizing treatment planning.

P1056

The Role of F-18 FDG PET-CT for Detecting Second Primary Neoplasms

Ü. Abdülrezzak, E. Orhan, A. Tutus, M. Kula, V. Berk, H. Karaca, M. Gundog, C. Eroglu; Erciyes University School of Medicine, Kayseri, TURKEY.

Aim: F-18 FDG PET-CT is very powerful imaging tool for initial staging and subsequent treatment planning of malignancies. With the increased utilization of PET-CT, there has been increased awareness of the possibility of detecting an unsuspected synchronous malignancy. Detection of unsuspected malignancy can have significant impact on a patient's treatment plan and prognosis. The aim of this study was to determine the rate and clinical relevance of additional primary malignancies on F-18 FDG PET-CT. **Material and Methods:** Between September 2009 and January 2012, total of 796 patients had unexpected FDG foci with biopsy-proven primary tumor underwent F-18 FDG PET/CT for staging, re-staging and response to therapy examinations. F-18 FDG accumulation in regions not likely to be sites of metastatic spread from primary tumor was reported as suggestive of second primary neoplasm. All PET-CT reports were retrospectively analyzed. Suspected second primary tumors were identified in 148 patients. **Results:** The 49 patients of suspected second primary tumor with histopathologic correlation are included in this study. The 25 of these 49 suspected lesions were second primary tumor, 13 lesions were metastasis and 11 lesions were benign origin. The most common organ detected as second primary neoplasm was lung (14/25; %56). Two neoplasms were in the stomach, two in the colon, one in the endometrium, one in the nasopharynx, one in the pancreas, one in the breast, one in the thyroid, one in the kidney and one in the vulva. **Conclusion:** Because of the detection of unsuspected second primary tumor will often affect both patient treatment and prognosis, evaluation of these patients with advanced imaging modalities is very important. Routine interpretation of F-18 FDG PET/CT may reveal incidental hypermetabolic foci and these sites of foci should be confirmed by dedicated additional investigations before treatment.

P1057

Comparison of Cerebellar 18F-FDG Uptake between Oncological and Brain 18F-FDG PET Specific Conditions

L. Guner¹, E. Vardareli¹, T. Cakir², K. Unal³; ¹Acibadem University, Istanbul, TURKEY, ²Istanbul Gulhane Military Medical School, Istanbul, TURKEY, ³Izmir Medical Park University, Izmir, TURKEY.

Aim Brain 18F-FDG scans should be obtained in certain strict conditions, usually not followed in routine oncological PET scans. These conditions include placement of the patient into a quite and dimly lit room several minutes before radiopharmaceutical administration; during uptake phase, not to speak and read. In addition, an iv cannula should be inserted at least 10 minutes before FDG administration. Cerebellar FDG uptake is one of the recommended SUV reference regions in oncological PET scans. Our aim was to evaluate the effect of applying brain FDG PET conditions on the cerebellar 18F-FDG uptake. **Material** We included 76 patients referred to our department for oncological PETCT scans. We applied strict brain FDG scan conditions in 38 patients and the remaining 38 patients had conditions without adherence to these conditions. For each cerebellar lobe we calculated the cerebellar SUVmax (Cb_max_L and _R) and SUVmean (Cb_mean_L and _R) values along with SUVmean values of liver. We then calculated cerebellar SUVmax/liver SUVmean and cerebellar SUVmean/liver SUVmean ratios and compared these ratios in the two groups. **Results** In the oncological group Cb_max_L was 10.50±2.49, Cb_max_R 10.51±2.58, Cb_mean_L 6.41±1.36, Cb_mean_R 6.37±1.37 and liver SUVmean was 2.11±0.35. In the brain PET group Cb_max_L 9.92±2.55, Cb_max_R 9.96±2.56, Cb_mean_L 6.27±1.63, Cb_mean_R 6.14±1.62 and liver SUVmean 2.06±0.43. In the oncological group; The cerebellum to liver ratios were Cb_max_L/liver_mean 4.99±1.09, Cb_mean_L/liver_mean 3.05±0.61, Cb_max_R/liver_mean 4.98±1.05, Cb_mean_R/liver_mean 3.03±0.58. Cb_max/liver_mean 5.15±1.06. In the brain PET group; Cb_max_L/liver_mean 4.97±1.42, Cb_mean_L/liver_mean 3.12±0.85, Cb_max_R/liver_mean 4.99±1.43, Cb_mean_R/liver_mean 3.06±0.82. Cb_max/liver_mean 5.11±1.43. None of the SUV values or ratios was significantly different between groups. **Conclusion** Brain

18F-FDG scan conditions do not seem to have any significant effect on cerebellar FDG uptake. Cerebellum may safely be used as a reference region in oncological 18F-FDG PETCT studies.

P1058

⁶⁸Ga-DOTA-TATE PET/CT in detection of the tumor causing osteomalacia

J. Zhang¹, Z. Zhu¹, X. Xing¹, H. Jing¹, Y. Jiang¹, D. Zhong¹, J. Shi², Y. Du¹, F. Li¹; ¹Peking Union Medical College Hospital, Beijing, CHINA, ²Medical Isotopes center, Peking University, Beijing, CHINA.

Purpose Tumor-induced osteomalacia (TIO), also called oncogenic osteomalacia, is a rare disease characterized by hyperphosphaturia, hypophosphatemia, low serum vitamin D3 levels, and osteomalacia. The causative tumor is usually benign and surgical removal can reach a cure. However, localization of the tumor is often challenging via routine imaging techniques. Somatostatin receptor imaging might be one of the best ways to locate the hidden lesions in the body. In this study, a novel diagnostic approach, ⁶⁸Ga-DOTA-TATE PET/CT, was evaluated for detection of the causative tumor and it was compared with ^{99m}Tc-HYNIC-TOC scintigraphy and ¹⁸F-FDG PET/CT. **Methods** Seventeen patients (M7, F10, 41.3 ± 11.7 y) in suspicion of TIO were recruited. They complained of bone pain, multiple fractures, and muscle weakness from 1 year to more than 4 years and were treated with calcium, vitamin D, and phosphate supplementation. 15 patients had negative finding in prior imaging examinations such as ultrasonography, CT and MRI, also including ^{99m}Tc-HYNIC-TOC scintigraphy and ¹⁸F-FDG PET/CT in some patients. The patients underwent PET/CT scans from head to toe with a Siemens Biograph64 TrueV system 1 hour after injection of nearly 111 MBq ⁶⁸Ga-DOTA-TATE. ^{99m}Tc-HYNIC-TOC scintigraphy and ¹⁸F-FDG PET/CT were also performed in the positive patient within 2 weeks for comparison. **Results** Fourteen of the patients (82%) were found with ⁶⁸Ga-DOTA-TATE positive lesions in the mandible, scapular spine, base of pelvic cavity, femur, knee, tibia, fibula, ankle joint, and plantar soft tissues. The tumor sizes were 0.5-4.0 cm and the standardized uptake values (SUV) were 0.9-8.4 (3.0±2.1). Whereas, the lesions had remarkably low ¹⁸F-FDG uptake or were negative on the images, with the SUVs ranged from 0.5 to 2.8 (1.1±1.7). Only 3 patients showed mild ^{99m}Tc-HYNIC-TOC uptake in the lesions. Until now, 6 patients have accepted surgery and all were confirmed histopathologically and clinically as the causative tumor. **Conclusions** ⁶⁸Ga-DOTA-TATE PET/CT is a powerful approach for detection of the causative tumors of TIO and suited for patients with negative somatostatin receptor SPECT imaging.

P70-2 - Tuesday, October 30, 2012, 16:00 - 16:30, Poster Exhibition Area

Oncology Clinical Science: Paediatric

P1059

¹²³I-MIBG Scintigraphy in patients with known or suspected Neuroblastoma : Added value of SPECT-CT imaging

I. Slim, Y. Mahjoub, I. Yeddes, T. Ben Ghachem, B. Letaief, A. Mhiri, M. F. Ben Slimene; Nuclear Medicine Department, Salah Azaiez Institute, Faculty of Medicine, University of Tunis El Manar, Tunis, TUNISIA.

Introduction: Neuroblastoma is one of the most common childhood solid tumors. Iodine-123 metaiodobenzylguanidine (¹²³I-MIBG) remain the first-choice investigation for the diagnosis, staging and follow-up of children with neuroblastoma. The aim of this study was to investigate the utility of ¹²³I-MIBG scan in the diagnosis and follow-up of children with neuroblastoma and to evaluate the additional contribution of SPECT-CT imaging. **Patients and Methods:** In this retrospective study we included 20 children with known or suspected neuroblastoma: 12 males and 08 females aged 7 months to 11 years (mean age 3.76 year). All patients underwent whole-body planar imaging 18-24 hr following IV administration of 2-5 mCi (74-185 MBq) ¹²³I-MIBG. SPECT-CT imaging was performed in 13 patients. **Results:** A total of 26 studies (with SPECT-CT acquisition in 14 cases) were performed in different clinical phases (20 for diagnosing and staging and 6 for monitoring response to therapy). Uptake of ¹²³I-MIBG by the primary tumour occurred in 18 of 20 patients (90%). In the two negative patients SPECT-CT was not performed. Planar imaging showed bone and/or bone marrow involvement 7 patients with hepatic metastases in 2 of them. Among the 6 children studied for evaluating the response to therapy 2 patients were in remission (good responders) and 4 were bad responders and they benefit of a change of treatment. Overall, SPECT-CT provided additional information over planar imaging in eight of the 14 studies (57%) : in 5 cases SPECT-CT showed more lesions and more precise anatomical localisation of foci, in 2 studies SPECT-CT allowed accurate local extension of primary lesions and in the last case, SPECT-CT acquisition prevented false positive interpretation of planar scan by characterisation a suspicious site of residual disease as a physiologic renal uptake. **Conclusion:** Our results confirmed the high accuracy of ¹²³I-MIBG scintigraphy in the diagnosis, staging and follow-up

of neuroblastoma and highlight the diagnostic advantages of SPECT-CT in comparison with planar imaging.

P1060

Diagnostic and prognostic value of ¹²³I-MIBG scintigraphy in paediatric patients with neuroblastoma since initial diagnosis

I. Casás-Tormo¹, R. Díaz-Expósito¹, C. Rocafuerte-Ávila¹, A. Orozco-Molano¹, S. Prado-Wohlwend¹, J. Donat-Colomer², R. Fernández-Delgado²; ¹Nuclear Medicine. Hospital Clínico Universitario de Valencia, Valencia, SPAIN, ²Pediatrics. Hospital Clínico Universitario de Valencia, Valencia, SPAIN.

Aim. Early diagnosis, prognostic assessment and adequate follow-up are essential in neuroblastoma (NB) paediatric patients to evaluate the therapeutic response. We present a retrospective study of the results obtained with ¹²³I-MIBG scintigraphy since the initial diagnosis and during follow up. **Material and methods.** We have performed 69 studies (1999-2012) with ¹²³I-MIBG in 37 children (17 women) age range 17 days -12 years (mean 29±34 months), obtaining 24h whole body scan and SPECT (21 cases). We assessed uptake in primary tumor (PT) and possible metastases, comparing with CT-MRI images (fusion when possible), since the initial diagnosis, during chemotherapy and surgical treatment, with histological diagnostic confirmation. Follow up during 1-13 years (4.5 ± 3.6), by clinical, radiological and radioisotopic assessment, evaluating persistent disease (PD), progression (P) death (D) or if the patients were disease-free (DF). **Results.** All patients were referred with suspicion of NB, that was confirmed in 29/37. There was no uptake of ¹²³I-MIBG in the 8 patients without NB. In 5 of the patients with NB, the first study was performed after initial diagnostic surgery and before chemotherapy. In the remaining 24 patients, before any other therapy or surgery. The sensitivity and specificity in the initial detection of NB were 95.8 % and 100%, without false positives. The only false negative was one case of mature ganglioneuroblastoma. The location of PT was adrenal (17 patients), mediastinum (7), paravertebral (3) and pelvic (2). There was uptake by hepatic metastases at the initial diagnosis in 4 patients, pulmonary in 2 and bone marrow in 8. SPECT and CT/MRI comparison always improved the lesions location. The group of 16/18 (88.8%) patients that were disease-free after follow up, showed only uptake in PT without metastases in the early study or decrease/disappearance of uptake in successive studies during follow-up. In 8/8 (100%) patients with persistent disease (4), death (3), metastases (1) after follow up, there was initial uptake in other locations besides de PT, that decreased in 7/8 patients, but without disappearing in consecutive studies. **Conclusions.** Our study in children with NB followed since initial diagnosis shows excellent results with ¹²³I-MIBG in the early initial diagnosis, allowing evaluation of PT and detection of possible metastasis, with high prognostic value. Provides whole body images and SPECT, strongly recommended, and also SPECT-CT or CT-MRI fusion, when possible. Follow up studies during the treatment allows us effective assessment of therapeutic response and prognostic evolution.

P71-2 - Tuesday, October 30, 2012, 16:00 - 16:30, Poster Exhibition Area

Conventional & Specialised Nuclear Medicine: Endocrinology

P1061

Incremental diagnostic accuracy of ^{99m}Tc-Sestamibi SPECT/CT over conventional SPECT and dual-phase planar imaging in the preoperative localization of parathyroid adenoma

B. Shafiei¹, S. Hoseinzadeh¹, F. Fotouhi², H. Malek³, F. Azizi⁴, M. Naderifar⁵, A. Jahed⁶, M. Salehian⁷, H. Parsa⁸; ¹Nuclear Medicine Department, Taleghani Hospital, Shahid Beheshti University of Medical Sciences, Tehran, IRAN, ISLAMIC REPUBLIC OF, ²Nuclear Medicine Department, Erfan Hospital, Tehran, IRAN, ISLAMIC REPUBLIC OF, ³Nuclear Medicine Department, Shaheed Rajaei Heart Center, Tehran University of Medical Sciences, Tehran, IRAN, ISLAMIC REPUBLIC OF, ⁴Research Institute for Endocrine Sciences (RIES), Shahid Beheshti University of Medical Sciences, Tehran, IRAN, ISLAMIC REPUBLIC OF, ⁵Shahed University of Medical Sciences, Tehran, IRAN, ISLAMIC REPUBLIC OF, ⁶Booali General Hospital, Islamic Azad University, Tehran Medical branch, Tehran, IRAN, ISLAMIC REPUBLIC OF, ⁷Surgery Department, Taleghani Hospital, Shahid Beheshti University of Medical Sciences, Tehran, IRAN, ISLAMIC REPUBLIC OF, ⁸Surgery Department, Shahid Rajaei Hospital, Qazvin University of Medical Sciences, Qazvin, IRAN, ISLAMIC REPUBLIC OF.

Optimal minimally invasive parathyroidectomy requires precise preoperative localization of parathyroid lesions in patients with primary hyperparathyroidism. The purpose of this study was to directly compare the diagnostic accuracy of hybrid

SPECT/CT, SPECT, and dual-phase planar imaging for the localization of parathyroid lesions in patients with primary hyperparathyroidism. **Patients & Methods:** Scintigraphy was performed on 107 patients (80 female, 27 male; age range: 26–85 years, mean age: 57.28 ± 12.05 years), with a clinical diagnosis of primary hyperparathyroidism, who were referred to the nuclear medicine department of Erfan hospital, Tehran, Iran, between May 2009 and October 2011. The patients underwent an early set of planar ^{99m}Tc -MIBI scanning, followed by SPECT and CT scans, and finally, 2 hours delayed set of planar ^{99m}Tc -MIBI scans. Scintigraphic data were interpreted by three experienced nuclear medicine physicians without knowledge of other test results or of the final diagnoses. Imaging data were correlated with the site and histopathology of removed parathyroid glands/lesions as the standard. **Results:** Totally, 140 lesions were identified by imaging in 107 patients. One hundred and one parathyroid adenomas were removed at surgery in 98 patients (double parathyroid adenomas in 3 patients). Other mentioned 39 lesions in imaging techniques were considered as false positive, 32 (82.05%) of these sites were associated with thyroid nodules and one site was associated with papillary thyroid carcinoma. The incidence of nodular or multinodular goiter in our population was 51%. The sensitivity and specificity for SPECT-CT were 90% and 94%, respectively, versus 85% and 60%, for SPECT. Dual-phase planar scintigraphy only identified 65 adenomas with a sensitivity of 68% and a specificity of 44%. Overall accuracy of SPECT-CT to exact localization of parathyroid adenoma (91%) was significantly greater than that of SPECT (77%, $p=0.002$), and of the dual-phase planar study (61%, $p=0.0001$). SPECT-CT hybrid imaging provided better localization of 15 lesions relative to SPECT images. Twenty-six adenomas were identified in aberrant locations at surgery, which SPECT/CT was able to predict the exact position of all abnormal glands, however dual-phase planar and SPECT could detect only 12 and 17 aberrant lesions, respectively. **Conclusion:** Our present study suggests that the SPECT-CT modality is significantly more accurate than dual-phase planar and SPECT techniques for parathyroid lesion localization, and it seems to be essential for surgical planning and selection of patients who are candidates for minimally invasive parathyroidectomy. **Key words:** primary hyperparathyroidism, SPECT-CT, minimally invasive parathyroidectomy.

P1062

What are the differences in Tc-99m MIBI ECT/CT findings between primary and secondary hyperparathyroidism as compared to ultrasound examination and fine needle aspiration biopsy?

Z. Jurasinovic, H. Tomic-Brzac, R. Petrovic, G. Horvatic-Herceg, I. Bracic, M. Medvedec, S. Tezak; Clinical Hospital Centre Zagreb, Zagreb, CROATIA.

The aim of our study was to investigate differences in ECT/CT findings between patients with primary and secondary hyperparathyroidism using ultrasound examination and fine needle aspiration biopsy (US/FNAB) as reference method. We examined data from 105 consecutive studies retrospectively over the last two years in patients with hyperparathyroidism (primary 74 patients, male 8, female 66; secondary 30 patients, male 16, female 14; tertiary 1 male patient) in whom parathyroid adenomas were discovered with ultrasound examination and proven using fine needle aspiration biopsy. Nodules were considered to be hyperfunctional parathyroid glands if the argyrophil reaction with the Grimelius silver nitrate stain was positive and/or if the parathormone concentration in the aspiration material was at least three-fold as compared to the parathormone serum level. Neck and thoracic region emission computed tomography was performed 30 minutes after the administration of 740 MBq of Tc-99m MIBI while ECT/CT study was acquired 2 hours post injection. Low-dose CT was limited to the neck region and guided by the ECT study. In 74 patients with primary hyperparathyroidism US discovered 79 nodules that proved to be parathyroid tissue on FNAB while ECT/CT detected 68 lesions (86%). Ninety-nine hyperfunctional parathyroid glands were detected in 30 patients with secondary hyperparathyroidism by means of US/FNAB, out of which number 51 lesions (51,5 %) were detectable by ECT/CT. Both enlarged parathyroid glands in one patient with tertiary hyperparathyroidism were visible on US/FNAB and ECT/CT. Using χ^2 test we found significantly ($p=0,031$) higher sensitivity of the ECT/CT in group of patients with primary as compared to the group with secondary hyperparathyroidism. We concluded that Tc-99m MIBI ECT/CT has sensitivity higher enough to be performed in patients with primary hyperthyroidism as the first imaging method while in patients with secondary hyperparathyroidism ultrasound examination and fine needle aspiration biopsy is still the method of choice.

P1063

Subtraction and dual phase scintigraphy in combination with ultrasound scanning for detecting and locating parathyroid adenomas

D. Hrastnik; General Hospital Celje, Celje, SLOVENIA.

Materials and methods: In 42 patients with biochemical evidence of hyperparathyroidism the same physician performed high-resolution ultrasound scanning of the neck immediately followed by subtraction scintigraphy (in 30 patients) or dual phase scintigraphy (in 12 patients). Whenever possible the

subtraction scintigraphy with $^{99m}\text{TcO}_4$ 60 MBq and ^{99m}Tc -sestamibi 600 MBq was performed (planar images of the neck and mediastinum, subtraction images and SPECT). In patients with hypothyroidism on substitution therapy and patients on amiodaron therapy dual phase scintigraphy with ^{99m}Tc -sestamibi 600–900 MBq was performed (planar image of the neck after 10 minutes and 2 hours, early planar images of mediastinum and SPECT after 2 hours). Findings of ultrasound scanning and scintigraphy were interpreted together. **Results:** In first group of 30 patients subtraction scintigraphy revealed 35 and ultrasound 45 adenomas. In second group of 12 patients dual phase scintigraphy found 19 and ultrasound 18 adenomas. Ultrasound scanning found 16 adenomas that scintigraphy overlooked (adenomas of small size less than 1 cm on normal locations). Scintigraphy found 14 adenomas that were not detected with ultrasound (ectopically located in mediastinum, adenomas in presence of multinodular goiter, some adenomas on normal locations). In 42 patients ultrasound scanning found 63 adenomas, scintigraphy 54 adenomas, both imaging modalities together 79 adenomas. No adenomas were found in 2 patients, 1 adenoma in 25 patients, 2 adenomas in 4 patients, 3 adenomas in 2 patients, 4 adenomas in 6 patients and 5 adenomas in 3 patients. Parathyroid adenomas were found and located in 40 out of 42 patients (95,2%). **Conclusion:** Both imaging modalities in combination proved very successful detecting and locating parathyroid adenomas. Both methods are widely available and suitable for routine use in daily practice. This combination of methods demands very good skills in ultrasound scanning of the neck.

P1064

Nuclear Medicine methods and prognostic significance of calcitonin and pentagastrin test at diagnosis of sporadic MTC

K. Zaplatnikov¹, V. Soukhov²; ¹Clinic for Nuclearmedicine, Nürnberg, GERMANY, ²Medical Military Academy, St. Petersburg, RUSSIAN FEDERATION.

Aim: We evaluated the usefulness of routine Calcitonin test in these patients with presence of hypoechogenic nodes. **Methods:** Routine radio immunological measurements of serum calcitonin concentrations were performed in 1,548 patients (415male; 1,133 female) with ultrasonography (US) revealed nodular thyroid diseases and pentagastrin stimulation in some of them. The average age was 44 years (range 8–86 years). Additional examination included thyroid Tc-99m-pertechnetate scan, measurements of thyroid hormones, TSH and thyroid autoantibodies. **Results:** 44 (2,8%) of all patients with diagnosis of nodular thyroid diseases had serum calcitonin level by RIA above 10 pg/mL. 10 of these patients (22,7%) presented histologically confirmed MTC. 6 of 10 patients with MTC had basal serum calcitonin level above 80 pg/mL. Serum calcitonin levels raised > 120–150 pg/mL after administration of pentagastrin in all of these pts. This group show statistically bad prognosis with LN-metastases revealed during follow up. The remaining 4 patients had low level basal serum calcitonin and moderate elevation after pentagastrin administration (12–66 pg/mL). 4 of 34 pts with Calcitonin levels from 10–33 pg/ml and negative pentagastrin stimulation had C-cell hyperplasia; the rest had renal failure or other disorders. **Conclusions:** These results suggested that routine RIA measurement of serum calcitonin is useful for early detection of MTC among patients with nodular thyroid diseases, especially in presence of hypoechogenic nodes. Pentagastrin stimulation test may also be a reliable way for evaluating thyroid nodular patients with mild or moderate elevation of serum Calcitonin concentrations and statistically correlated with prognosis of the MTC.

P1065

Primary hiperparathyroidism. Added value of the combined study ^{99m}Tc -MIBI- neck ultrasound versus both techniques separately.

J. G. Rojas Camacho, A. Benitez Segura, R. Ortega Martinez, A. Rodriguez-Gasen, M. A. Vidal Gonzalez, J. Mora Salvado, M. T. Bajen Lazaro, Y. Ricart Brulles, A. Sabate Llobera, J. Matin Comin; HOSPITAL UNIVERSITARIO BELLVITGE, BARCELONA, SPAIN.

Objective: To assess the diagnostic performance of parathyroid scintigraphy with ^{99m}Tc -MIBI (PS-MIBI) and neck ultrasonography (NU) in primary hyperparathyroidism (PHPT), together and each one separately. **Material and methods:** 97 patients with PHPT operated between 2006–2010 who underwent GP-MIBI were studied. PS-MIBI: planar scintigraphy (15 minutes and 2 hours post injection of 20 mCi ^{99m}Tc -MIBI) and SPECT or SPECT / CT (from september 2010) after early acquisition. Thyroid Scintigraphy was performed with 6 mCi ^{99m}Tc -pertechnetate to rule out coexisting thyroid pathology. NU was performed in all patients. The following were analyzed: 1) The result of the PS-MIBI (positive, negative or doubtful) with respect to histology. 2) a retrospective assessment of false negative PS-MIBI (second look) and NU result in these patients; 3) The sensitivity (S) and positive predictive value (PPV) of the PS-MIBI and the NU separately and together. **Results:** 1. PS-MIBI was positive in 80 p (72%); histology confirmed adenoma in 55p, hyperplasia in 14p, and carcinoma in 1p; PS-MIBI was doubtful in 1p (1%); histology confirmed hyperplasia; and negative in 26 p (27%);

histology confirmed 18p adenoma and hyperplasia in 8p. 2. Second look analysis of 26 p with false negative PS-MIBI: reminded negative in 22 p, was doubtful in 1 p, and modified the diagnosis in 3 p (2p showed rapid washout from parathyroid adenoma (6,6%), and 1p showed positive SPECT). NU was positive in 14p out of 26p (54%). 3. The S and PPV of both techniques separately were 68% and 96,5% respectively for PS-MIBI, 65%, 94,5% for NU and 84% and 93,2% for NU + PS-MIBI. Conclusion: The diagnosis performance of PHPT improves with the combination of both techniques (PS-MIBI + NU).

P1066

Could the Addition of Spect or Spect-CT avoid the Acquisition of Late Imaging in the Localization Diagnosis of Hyperparathyroidism?

P. García-Talavera¹, C. Gamazo¹, A. Sainz-Esteban¹, G. Diaz-Soto², M. L. González¹, R. Olmos¹, M. A. Ruiz¹, A. Gómez¹; ¹Department of Nuclear Medicine. Hospital Clínico Universitario de Valladolid, Valladolid, SPAIN, ²Department of Endocrinology. Hospital Clínico Universitario de Valladolid, Valladolid, SPAIN.

Aim: To assess the contribution of early SPECT or SPECT-CT to ^{99m}Tc-MIBI double-phase planar scintigraphy in the localization diagnosis of primary hyperparathyroidism and to evaluate if these techniques would allow doing without late phase. **Material and methods:** We include 29 patients (24 women; mean age: 56, 9 +/- 15, 8 years old) who underwent parathyroidectomy for primary hyperparathyroidism, between April 2010 and November 2011. A ^{99m}Tc-MIBI double-phase planar scintigraphy (10 minutes and 2 hours post-injection) had been performed to all patients, prior surgery. SPECT was acquired in 16 patients and SPECT-CT in 13 out of 29 (both 20 minutes post-injection). In all cases a histological confirmation and a decrease of intraoperative PTHi levels greater than 50%, 10-15 minutes after gland/s extirpation, were obtained. **Results:** In 17 cases tomography did not significantly improve planar imaging results (59%). In 4 out of 16 patients, in whom SPECT was performed, it improved planar scintigraphy results, increasing sensitivity. In 6 out of 13 patients in whom a SPECT-CT was acquired, it improved pathological gland detection. In total, tomography (SPECT + SPECT-CT) showed 6 new foci and resolved 6 doubtful cases of planar imaging (planar scintigraphy sensitivity of 79% vs 96% if a tomography is added). Moreover, SPECT-CT specified the localization of 4 ectopic glands. On the other hand, when planar scintigraphy and early tomography were performed, late planar imaging was essential to help to pathological gland detection only in three patients. In none of them, a hybrid imaging had been performed. **Conclusion:** The addition of early tomography to planar scintigraphy increases sensitivity and diagnostic confidence in the detection of parathyroid pathological gland/s localization. Moreover, the use of hybrid imaging significantly improves ectopic glands localization, and our experience suggests that SPECT-CT could avoid late imaging acquisition if the early imaging is assessed by the physician prior to the decision of performing or not late imaging.

P1067

Role of the Preoperative Parathyroid Subtraction Scintigraphy in the Surgical Management of Secondary Hyperparathyroidism about 33 Cases

M. Noura, T. Kamoun, M. Guezguez, A. Hachani, I. Jardak, R. Sfar, M. Ben Fredj, K. Chatti, O. Tounsi, N. Ayachi, H. Zanzouri, H. Essabbah; Sahloul University Hospital, Sousse, TUNISIA.

Aim: ^{99m}Tc-MIBI is used in the imaging of hyperparathyroidism in order to guide the surgical procedure and to propose methods of less invasive surgery. The aim of our study was to evaluate the efficiency of preoperative subtraction parathyroid scintigraphy (MIBI-^{99m}Tc/Pertechnétate) in the management of secondary hyperparathyroidism. **Materials and methods:** The records of 33 patients with renal impairment (15 women and 18 men) consecutively operated from 2009 to 2011 for secondary hyperparathyroidism were retrospectively reviewed. We collected data on parathyroid function, the results of parathyroid scintigraphy performed preoperatively, intraoperative findings and pathological findings. **Results:** Scintigraphy was positive in 32 patients by objectifying a total of 75 hyperplastic parathyroid glands. The surgical exploration of all parathyroid glands revealed 99 hyperplastic glands confirmed by histological analysis. The sensitivity of parathyroid scintigraphy was 70.7% with a specificity of 85%. Its positive predictive value was 93.3%, while its negative predictive value was 50%. No correlation was found between the values of parathyroid hormone measured preoperatively and scintigraphic results, as well between the size of gland and scintigraphic results. **Conclusion:** Although parathyroid scintigraphy has a high specificity and a high positive predictive value, it has a poor interest in the surgical management of secondary hyperparathyroidism. In fact, the consensus is to achieve the removal of 7/8 glands. However, this examination is indicated for detecting an ectopic or supernumerary gland and in cases of recurrence.

P1068

Incidence and Impact of Concomitant non-Medullary Thyroid

Cancer to Parathyroid Scan

M. E. Altinyay, M. O. Aldakker, M. A. Ali, S. Shehri, G. M. S. Syed; King Fahad Hospital, KAIMRC/KSAU, Riyadh, SAUDI ARABIA.

Objective: Aim of this study is to evaluate for concomitant non-medullary thyroid cancer and its impact to dual phase sestamibi parathyroid scan reading in patients with hyperparathyroidism. **Method:** A retrospective review was performed of patients referred for dual phase sestamibi parathyroid scan between September 1, 2007 and March 31, 2012 in National Guard Health Affair King Abdulaziz Medical City. The prevalence of non medullary thyroid carcinoma was compared with parathyroid scan findings. **Results:** There were 352 dual phase sestamibi parathyroid scans for 305 patients. Of these, 50 patients had surgery for hyperparathyroidism. Thyroid carcinoma was diagnosed in 18% of the patients (7/38) with primary hyperparathyroidism and 8% of the patients (1/12) with secondary or tertiary hyperparathyroidism. Seven of the patients had papillary carcinoma and 1 had follicular carcinoma. Parathyroid scan was positive for 62% of patients (5/8) with concomitant non medullary thyroid carcinoma and 92% of patients (39/42) with hyperparathyroidism. One patient with primary hyperparathyroidism and positive dual phase parathyroid scan was diagnosed with parathyroid carcinoma.

Conclusion: Significant percent of patients with hyperparathyroidism have concomitant thyroid cancer. Parathyroid scan specificity may be affected in the presence of non medullary thyroid cancer.

P1069

Thyroid Sestamibi-Tc-99m Uptake Quantification: A New and Accurate Method for the Differential Diagnosis of Amiodarone-Induced Thyrotoxicosis - Preliminary Results

T. Vieira, S. B. Souto, T. Faria, P. Oliveira, A. Oliveira, D. Carvalho, J. G. Pereira; Centro Hospitalar de São João, Porto, PORTUGAL.

Aim: Amiodarone, an iodine-rich compound, is a potent antiarrhythmic drug used to treat cardiac tachyarrhythmias. Amiodarone-induced thyrotoxicosis (AIT) may be classified as: type 1 (T1), caused by iodine-induced excess thyroid hormone synthesis and release; type 2 (T2), caused by a destructive thyroiditis that leads to the release of preformed thyroid hormones; and type 3 (T3), indefinite mixed form. The recognition of the correct type of AIT, important for therapeutic purposes, remains a diagnostic challenge. Recently, it has been reported that sestamibi-Tc-99m thyroid scintigraphy (STS), using a qualitative evaluation method, proved to be superior to a variety of diagnostic tools in the differential diagnosis (DD) of AIT. Our aim was to study the usefulness of a new quantitative analysis method for the DD of AIT with STS. **Materials and methods:** Our study included 9 AIT patients with enough follow-up time to conclude the AIT type. All patients were evaluated by biochemical blood analysis (fT4, fT3, TSH, AbTg, AbTPO and TRAb), thyroid colour flow Doppler sonography and STS. STS was performed after the i.v. injection of 185MBq of sestamibi-Tc-99m. Anterior projection images (5 min) were acquired at 2, 10, 15 and 60min after the radiotracer administration. Initially, STS was interpreted by visual qualitative analysis, in accordance with previously published criteria, as: T1, when there was apparent clear diffuse retention; T2, when no significant uptake was found; and T3, for the other patterns of uptake and washout. Subsequently, a blinded investigator (for the qualitative STS results and final diagnosis) manually generated thyroid and cervical background ROIs. Mean counts in each ROI were used to calculate the simple thyroid to background activity ratio (TBR) at 2, 10, 15 and 60min. Finally, TBR values obtained were compared with qualitative STS results and final AIT type diagnosis. **Results:** AIT final diagnosis was T1 in 4 patients, T2 in 3 patients and T3 in 2 patients. Qualitative analysis correctly diagnosed 6/9 (67%) patients. In quantitative analysis, 10min TBR interval values were the most useful: values of 0-1.35 (for T2), 1.35-1.6 (for T3) and 1.6-2 (for T1) were able to identify the correct diagnosis of 8/9 (89%) patients (only 1 patient with T1 AIT would be classified as T3). **Conclusion:** These preliminary results suggest that a new sestamibi-Tc-99m quantitative method of TBR calculation at 10min can be more accurate than the qualitative method for the diagnosis of AIT. Our ongoing research is expected to reveal more definite results.

P1070

Assessing the Relative Contribution of Free and Bound Radioiodine to Thyroid Visualization in I-123-MIBG Imaging

A. F. Jacobson¹, N. C. Friedman², D. T. Matsuoka¹; ¹GE Healthcare, Princeton, NJ, UNITED STATES, ²Edward Hines Jr. VA Hospital, Hines, IL, UNITED STATES.

Aim: Although iodinated radiopharmaceuticals usually contain a small quantity of unbound iodine, it is difficult to establish the degree to which thyroid activity on scintigraphic images reflects uptake of free radioiodine. The present study examined the effect of thyroid blockade on planar ¹²³I-MIBG images of the chest to determine if change in thyroid activity over time could be used to assess the relative contribution of the two forms of iodine to thyroid imaging findings. **Materials and Methods:** 669 adult subjects whose planar myocardial images at 15

minutes (early) and 4 hours (late) post-injection of 370 MBq ^{123}I -mIBG included the entire thyroid region were studied. Of these subjects, 442 (66%) had been pretreated with thyroid blocking medications and 227 (34%) had no pretreatment. An experienced nuclear medicine technologist examined each image for presence of thyroid uptake, and drew rectangular regions of interest (ROIs) for the entire thyroid (or the expected location if the gland was not visualized) and the adjacent upper mediastinum (representing background). Net thyroid counts (T_n =thyroid counts-thyroid ROI pixels*mediastinum counts/pixel) at the two time points (decay-corrected for late image) and change from early to late (as % of activity on early image) were then calculated. Results were compared between blocked and unblocked subjects, assuming that findings for the former only reflected changes in ^{123}I -mIBG uptake, while those for the latter included a component of free ^{123}I uptake. Results: On early images, mean T_n was not different between subjects with and without blockade (9045 vs 7974 counts, $p=0.11$). On late images, mean T_n was significantly lower for subjects with blockade (4507 vs 11473 counts for unblocked, $p<0.0001$). Mean T_n change between early and late images was also significantly different between blocked and unblocked subjects (40% decrease vs 149% increase respectively, $p<0.0001$). Overall, 87% of blocked subjects ($n=383$) showed decreased or unchanged T_n , while 75% of unblocked subjects ($n=171$) showed increased T_n . At 4 hours, approximately 61% of T_n in unblocked subjects could be attributed to thyroid uptake of unbound ^{123}I . Conclusions: This analysis suggests that increasing thyroid activity over time following ^{123}I -mIBG administration reflects progressive uptake of unbound ^{123}I . Although 13% of subjects who received thyroid blockade showed increased net thyroid activity between early and late images, it is not possible to determine whether this reflected inadequate amounts of blockade medication or an effect of in vivo deiodination of ^{123}I -mIBG.

P72-2 - Tuesday, October 30, 2012, 16:00 - 16:30, Poster Exhibition Area

Conventional & Specialised Nuclear Medicine: Thyroid

P1071

Influences on thyroid function in euthyroid patients with Hashimoto's thyroiditis and in healthy subjects

M. Žitko-Krhin¹, K. Zalete¹, S. Gaberšček¹, I. Grabnar², S. Hojker¹; ¹University Medical Centre Ljubljana, Ljubljana, SLOVENIA, ²University of Ljubljana, Faculty of Pharmacy, Ljubljana, SLOVENIA.

Aim It is believed that thyroid function in patients with euthyroid Hashimoto's thyroiditis (EuHT) is not significantly different than in healthy subjects (HS) and only a few reports have demonstrated the demographic influences on thyroid function. The aim of our study was to compare thyroid function tests and serum fT_4/fT_3 ratio between EuHT and HS and to evaluate the association of age, smoking and body mass index (BMI) with serum fT_4/fT_3 ratio in both groups. Methods We included 509 EuHT patients and 564 HS, examined at our thyroid department in the period between March 2009 and February 2010. Among EuHT 52 were males and 457 females, aged between 15 and 88 (mean, 47.5 ± 16.9 years). HS group included 137 males and 427 females and their age was between 15 and 85 (mean, 42.5 ± 17.7 years). EuHT was diagnosed in patients with positive thyroid peroxidase and/or thyroglobulin antibodies and with characteristic hypoechoic thyroid ultrasound pattern. HS were negative for thyroid antibodies and on ultrasound thyroid appeared isoechoic. In all subjects we measured TSH, fT_4 , fT_3 and all values were within normal ranges (0.35-5.5 mU/L, 11.5-22.7 pmol/L and 3.5-6.5 pmol/L, respectively). The fT_4/fT_3 ratio was calculated. The influence of age, smoking and BMI on fT_4/fT_3 ratio in EuHT and HS was evaluated with a multiple regression analysis. Results In EuHT, TSH level was significantly higher than in HS (median, 3.158 and 2.110, respectively, $p<0.01$). The fT_4 level was significantly lower in EuHT compared with HS (median, 13.8 and 14.8, respectively, $p<0.01$). Only in subjects with TSH below 0.7 mU/L the fT_4 level did not differ between EuHT and HS. There was no significant difference in fT_3 level between the two groups. The fT_4/fT_3 ratio was significantly lower in EuHT than in HS (median, 2.73 and 2.89, respectively, $p<0.01$). Only when TSH was below 1.4 mU/L, the fT_4/fT_3 ratio did not differ significantly between EuHT and HS. Multiple regression analysis revealed only age as an independent predictor of fT_4/fT_3 ratio in EuHT and HS (beta, 0.181, $p<0.02$ and beta, 0.256, $p<0.01$, respectively), whereas no association with smoking and BMI was confirmed. BMI was significantly higher in EuHT compared with HS (median, 25.71 and 24.69, respectively, $p<0.01$). Conclusion Although considered euthyroid, patients with EuHT differ significantly from HS with respect to TSH, fT_4 and fT_4/fT_3 ratio. In both, EuHT and HS, only age significantly influences the fT_4/fT_3 ratio.

P1072

An Audit of Adolescent Differentiated Thyroid Carcinoma -Its Presentation & Management Perspective

M. Sarma, B. C. R, S. G, S. Babu, P. S, S. S. P; Amrita Institute of Medical Sciences, COCHIN, INDIA.

INTRODUCTION Paediatric differentiated thyroid carcinoma (DTC) is a rare disease but with excellent prognosis. Striking differences in juvenile DTC have been reported when compared to adult onset types like: (1) larger primary tumor at diagnosis; (2) multifocality pattern, with capsular/vascular invasion (3) metastases at presentation: greater prevalence of neck lymph nodes & distant metastases at diagnosis. OBJECTIVE: We aimed to analyse the variance of presentation in adolescent age group, identify predictive factors for thyroid bed recurrence (TBR) or lymph node recurrence and, recommend right therapeutic options i.e. surgical & I-131 therapy to have a recurrence free survival (RFS). MATERIALS & METHODS: A retrospective analysis of 31 DTC patients treated between 2004 to 2011 (M:F = 4 : 27, age range 11 - 18 yrs, mean 13.5 ± 1.5 yrs) was performed. Presentation pattern, duration of disease, clinical features, histopathology, radioiodine diagnostic and post therapy scan patterns, disease behaviour on follow up were analysed in each of them. RESULTS: All patients were found to have papillary type or its variants (Classical: Follicular: Insular = 22:8:1). 13/31 (42%) patients underwent neck dissection along with total thyroidectomy as they presented with cervical nodal metastases. All 31 patients underwent high dose I131 therapy (range 925-4699MBq mean 2741 MBq) . 74.1 % pts (23/31) had high risk features on biopsy like capsular invasion, extra thyroidal extension & lymph nodal metastases. They were followed up for a maximum of 84 months. No DTC-related deaths occurred, 51.1 % patients (16/31) had successful ablation and remained disease free. Histologically proven persisting nodal disease/ recurrence was seen in 8/31 patients (25.8 %), and distant metastases in 2/31 (6%). Among patients treated with radical intent, the most recent thyroglobulin level was $<1 \text{ ng/mL}$ in all but 42 % of cases. For neck recurrence, classic papillary histology, incomplete primary lymph node dissection (i.e., lack of modified lymphadenectomy of affected lymph nodes or lack of confirmation of disease-free nodes by intraoperative staging) were independent significant predictive factors that increased the recurrence. Age or sex did not correlate with local recurrence risk. CONCLUSION In DTC patients less than 18 years of age, extensive initial therapy-consisting of total thyroidectomy combined with modified lymphadenectomy performed in case of lymph node metastases and followed by radioiodine therapy is associated with a substantial decrease of locoregional recurrence risk.

P1073

I-131 Thyroid Uptake in Congestive Heart Failure

G. Daglloz Gorur¹, G. Kozdag², M. A. Oc¹, S. Isgoren¹, H. Demir¹, F. Berk³; ¹Department of Nuclear Medicine Kocaeli University, Kocaeli, TURKEY, ²Department of Cardiology Kocaeli University, Kocaeli, TURKEY, ³Department of Nuclear Medicine Oregon Health & Science University, Portland, OR, UNITED STATES.

Aim: Abnormalities in thyroid function are frequent in patients with congestive heart failure (CHF) and are associated with increased mortality. In this study, we aimed to compare I-131 thyroid uptake (TU) of CHF patients with control group and investigate if I-131 TU test has a prognostic value. Material-method: 32 CHF patients and 15 healthy controls with normal thyroid function tests (TSH, FT_3 , FT_4) are included in the study. Exclusion criteria were history of interfering medications, exposure to iodine-rich contrast in two months, ingestion of iodine-rich foods, pregnancy/breastfeeding for females and nodules or abnormal echogenicity of thyroid defined by ultrasonography. TU test was done at 4th and 24th hours after 50μCi I-131 administration using thyroid uptake probe. Thyroid volumes were calculated by ultrasonography. The patients were followed up for a mean time period of 32, 09 ± 8 months. Results: The patient group consisted 30 male and 2 female with a mean age of 67.91 ± 11.89 (range 32-85). The mean LVEF and BNP (brain natriuretic peptide) of the patients were 23.75 ± 11.14 and 1617 ± 816.48 respectively. The mean 4th hour uptake ratio was 6.28 ± 5.51 and 24th hour mean uptake ratio was 14.43 ± 9.49 in the patient group. The control group 4th and 24th hour mean uptake ratios were 11.91 ± 3.85 and 24.17 ± 4.62 which were statistically higher than patient group ($p=0.002$; 0.006). Thyroid volumes were statistically higher in the patient group than controls (32.34 ± 22.54 ; 16.27 ± 9.42 ; $p=0.04$). There was no difference between patient and the control group by means of FT_3 , FT_4 and TSH. Cardiac death occurred in 9 patients (28%) during follow up. The 4th and 24th hour uptake ratios were statistically significantly lower in the cardiac death group than no death group (3 ± 2.01 versus 7.57 ± 5.93 and 7.39 ± 7.34 versus 17.18 ± 8.9 respectively; $p=0.003$ and $p=0.007$). There was no statistically significant difference between these groups by means of age, gender, previous myocardial infarction, coronary artery by-pass grafting, diabetes mellitus, dilated cardiomyopathy type (ischemic, non-ischemic), stroke, FT_3 , FT_4 , TSH, thyroid volumes, LVEF, BNP levels and follow-up time. Conclusion: CHF patients with normal thyroid hormone levels have lower I-131 TU and larger thyroid volume. This is explained by expanded iodine pool. But lower I-131 TU values in the patients who died during follow-up suggest it has a prognostic value and different mechanisms may account for this consequence. However, studies with larger patient groups are definitely needed.

P1074

The unusual variant of papillary carcinoma: a case report

S. Gracan, S. Tomić, R. Beljan, A. Punda, V. Markovic, D. Eterovic, D. Brdar, Z. Colovic; KBC Split, Split, CROATIA.

Thyroid carcinoma is the most common of all endocrine tumors in human. Most common one is the papillary thyroid carcinoma. Among them, according their pathohistological and clinical characteristics we distinguish few unusual variants, including cribriform-morular type. CASE REPORT: 45-year old female patient first came for the examination because of palpitations and weakness. Hormone blood levels were normal. Neck ultrasonography revealed two hypoechoic nodules in the right lobe and isthmus. The fine needle aspiration of the isthmus nodule revealed distinctive proliferation of thyroid epithelium with few nuclear inclusions. The patient underwent total thyroidectomy with exploration of the region VI of the neck. Final pathohistological result showed not clearly bordered nodule, 1x0,7 centimeters in size, formed of complex branching papillary structures lined by cuboidal cells. The nuclei were, optically clear with longitudinal grooves as in classic. There are cribriform areas formed of back-to-back follicles with anastomosing bars and arches of cells in the absence of intervening fibrovascular stroma. The solid areas consisted of whorls of cells that form squamoid morules. Immunohistologically cells were positive to TTF-1 and CK-19 antigen, and negative to calcitonin. During two hospitalizations on Clinical Department for Nuclear medicine patient received radioiodine and in both cases no evidence of tumor's dissemination was found. Because the form of papillary carcinoma was cribriform-morular type, patient was recommended to do colonoscopy, what was negative for polyps. The cribriform-morular variant of papillary carcinoma is very rare. First cases were reported in the 90-s, when it was noticed that one kind of papillary carcinoma was found more often in patients with familial adenomatous polyposis and congenital hypertrophy of retinal epithelia. This kind of papillary carcinoma was characterized with cribriform structure and squamous morules. Among them APC gene mutation was found. This mutation can be congenital or somatic. Immunohistologically they were stained positive with antibody to p-53 and β -catenin. The clinical course is similar to classical type of papillary carcinoma. This morphologic variant should be borne in mind by pathologists because of its characteristic pattern. The clinician should be alerted to exclude FAP along with appropriate family screening. In 25-30% of cases, this might provide the first indicator of an underlying FAP syndrome.

P1075

Remission of Graves Disease with ^{131}I Treatment, using Standard Dosis (Changed by Grade of Goiter and Data Uptake Percentage)

T. Morales Avellaneda, A. I. González Ramírez, B. Rodríguez Alfonso, J. Mucientes Rasilla, I. Rodríguez Lizarbe, A. Gómez Grande, J. Huertas Cuaserna, M. Beresova; PUERTA DE HIERRO HOSPITAL, MADRID, SPAIN.

Aim: To determine the effectiveness of ^{131}I treatment based on goiter degree and uptake probe at six and twelve months. **Materials and methods:** A retrospective and descriptive study of patients treated with ^{131}I for hyperthyroidism in Graves-Basedow disease in association with our hospital's endocrinology service. Patients were selected to receive the first ^{131}I dose during the period of 01/03/2009-31/03/2011. All patients had a twenty days diet low in iodine and antithyroid medications were discontinued at least five days prior to treatment with ^{131}I . They were divided into four groups according to clinical goiter size to give the dose in Grade 0 (296MBq), 1 (296-333MBq), 2 (333-370MBq), 3 (370-407MBq), 4 (484MBq). Each subgroup was chosen based on the dose uptake data at four and twenty-four hours. **Results:** Six medical records out of 80 were excluded for not being followed at least the first six months post-treatment. Of the 74 patients with an average age around 47.5 (23-84 years), 55 women (74.3%) and 19 men (25.7%); 77% of them showed a remission of the disease six months after receiving treatment (75 % of grade 1, 57.9% grade 2, 100% grade 3-4 and 86.4% grade 0), and an 83.8% had shown remission of the disease after one year. **Conclusions:** The ^{131}I treatment in patients with Graves' disease with fixed doses depending on goiter's grade and adjusted uptake probe, showed results at six months post-doses higher than those observed in other studies, and a 100% effective goiter in patients with grade 3 and 4 with a relatively low dose, compared with similar studies.

P1076

Modification of the Common Technique used for Individualized Treatment Hyperthyroidism

N. Del Rio Torres, F. Martín, M. Cardoso Rodríguez, Y. Santaella Guardiola; Hospital Punta de Europa, ALGECIRAS, SPAIN.

INTRODUCTION: We observed that after treatment with ^{131}I , are detected both hyperthyroid patients as hypothyroid which show that failure to meet the ALARA principle, on the use of ionizing radiation in patients, workers and general public in the treatment of hyperthyroidism. The calculation of the activity administered to

each patient, allow us to reduce subjectivity and individual dose and information before treatment. **OBJECTIVE:** Offering a simple method to provide some parameters about the calculation to obtain a personal dose of ^{131}I , that allow us to get the most accuracy on treatment with radioiodine to prevent patients from suffering the fewest side effects to treatment to achieve meet the ALARA principles. **MATERIAL AND METHOD:** After performing this technique to 3 times (4, 24 and 120 hours, reflected in the poster presented at national congress 2010), and we having studied for three years the optimization and organization of waiting times in nuclear medicine unit of the Hospital Punta Europa, it has been evaluated that the changes in time intervals of 120 to 96 hours, give results which are not significant differences. - **1st Step:** The patient is injected with 3 mCi of ^{123}I . After 15 minutes post injection, the patient goes to the gamma camera: • E CAM Siemens® DUAL LEHR collimator for Spect Tomography Thyroid. • Circular Rotation. • Matrix: 128 x 128. • Window: 123-I • Images: 60 • Time Images: 20 seconds. - **2nd Step:** After 4 hours, we will perform the scan with LEHR planar collimator. • Projection: anteroposterior position. • Matrix: 256 x 256 • Window: 123-I • Time: 5 minutes per projection • Neck distance from detector surface: 10 - 15 centimeters. - **3rd Step:** We will target all the data in the spreadsheet. - **4th Step:** We will perform the thyroid scintigraphy with pinhole collimator. • Anterior position • Right Anterior Oblique position • Left Anterior Oblique position. - **5th Step:** We repeat the second step at 24 and 96 hours. **CONCLUSION:** We consider that although this technique is uncomfortable for the patient because he has to go several times a nuclear medicine unit of the Hospital Punta Europa, it compensates for obtaining an individualized radiation dose, because in the common technique (^{131}I 99mTc, ^{131}I), we have found in many cases high irradiated patients, therefore not meet the ALARA principle.

P1078

Congenital hypothyroidism - Should Ultrasound scan be used in all abnormal Isotope thyroid Scans?

A. Sreedasyam, A. Tarbuck, A. O'Brien, H. Shannon; Raigmore General Hospital NHS Highland, INVERNESS, UNITED KINGDOM.

Introduction: Congenital hypothyroidism is one of the common but serious conditions seen in paediatric clinical practice. Early diagnosis and appropriate treatment effectively prevents serious complications such as mental retardation and stunted growth. The use of Isotope thyroid uptake scan, in addition to lab tests and ultrasound scan provides additional information to pinpoint aetiology of the neonatal hypothyroidism, aid genetic counselling, assess likelihood of lifelong treatment if proven permanent and provides useful guide to the dose of levothyroxine. The current evidence advises the use of ultrasound scan of thyroid along with isotope thyroid Scintigraphy in all cases of congenital hypothyroidism. **Purpose:** To assess the need for ultrasound scan of thyroid in patients with congenital hypothyroidism and abnormal isotope ($^{99\text{Tc}}$ pertechnetate) thyroid Scintigraphy. **Materials and methods:** The current study reviewed 4 cases of patients with various causes of congenital hypothyroidism. Isotope thyroid uptake scans were performed in neonates with established hypothyroidism. The isotope activity is calculated as per patient body weight and administered using i.v. cannula. Anterior +/- lateral neck views were obtained 20 minutes post injection using low energy all purpose collimator. The ultrasound scan was performed subsequent to the thyroid uptake scan. **Results:** Example 1, demonstrates absent tracer uptake by thyroid. The subsequent US scan showed normal volume thyroid gland. Example 2, demonstrates absent tracer uptake by thyroid. The subsequent US scan showed thyroid aplasia. Example 3, demonstrates tracer uptake in the ectopic thyroid situated at the floor of mouth. The US scan showed lingual thyroid. Example 4, demonstrates increased tracer uptake in a normally situated thyroid indicating possible dysmorphogenesis or excessive iodine exposure. **Conclusion:** From the above results, it is clear that in the absence or reduced isotope uptake (first 3 examples), the additional use of ultrasound scan helps identify exact cause of hypothyroidism. However, in the case of increased tracer uptake (either due to dysmorphogenesis or excessive iodine exposure) in a normal thyroid shape and location, the subsequent ultrasound scan did not provide any additional information. Therefore, its use in these circumstances appear not only inappropriate use of resources but also potentially distressful for the patient.

P73-2 - Tuesday, October 30, 2012, 16:00 - 16:30, Poster Exhibition Area

Conventional & Specialised Nuclear Medicine: Pulmonology

P1079

The role of SPECT lung scan on the diagnosis of pulmonary embolism

J. Cordero García, A. García Vicente, Á. Soriano Castrejón, G. Jiménez Londoño, A. Núñez García, V. M. Poblete García; Hospital General de Ciudad Real, Ciudad Real, SPAIN.

Aim To investigate the possible usefulness of SPECT technique in the evaluation of lung scans in the diagnosis of pulmonary embolism (PE), as compared with planar images. **Material and methods** We prospectively studied 35 consecutive patients with suspicion of PE. The pretest likelihood of PE was calculated according to the Wells pre-test probability scoring algorithm, and all patients had a score value above 2 (intermediate or high risk). A planar perfusion study was carried out in all of them, including 6 projections, followed by a SPECT acquisition. In 15 patients, a planar and tomographic ventilation study was also performed. The images were evaluated according to the EANM guideline by two experienced nuclear medicine physicians, or the PISAPED criteria, when only the perfusion study was available. The number of embolic lesions detected with each technique was also registered. The concordance between the result of the evaluation of planar and SPECT images was analyzed. **Results** A total of 7 patients were diagnosed of PE, 2 of them only with a perfusion study. In 34 patients, the final result of planar and SPECT images was coincident (97%), allowing the SPECT technique the correct classification as a negative study in one case of planar positive study. On the other hand, we found that, in those positive cases, the number of embolic lesions was higher in the SPECT study (a total of 45 lesions in the SPECT study, 36 on planar images, 25% of increase), with a more precise location of them in the tomographic study. **Conclusions** The SPECT images allow obtaining a higher definition of the location and extent of the perfusion defects, as compared with planar images, improving, thus, the diagnostic accuracy of the study.

P1080

The role of Tc-99m DTPA aerosol scintigraphy in the differential diagnosis of asthma and COPD

S. Karacavus, Y. Intepe; Bozok University, Yozgat, TURKEY.

Aim: Chronic obstructive lung disease (COPD) and asthma are characterized as similar to another by airway obstruction and an inflammatory process. Spirometric tests have a limited value in differentiating bronchial asthma from COPD. The purpose of study was to evaluate the capacity of inhalation scintigraphy in distinguishing between these two diseases. **Material and Methods:** Eighty four patients (M/F: 32/52; mean age 52±13 years) with obstructive lung disease were enrolled in the study. The patients were divided into two groups as COPD and asthma and also active and passive smoking subgroups. Alveolar clearance study was performed by using a radiolabeled aerosol of 15 mCi Tc-99m diethylenetriametaacetic acid (DTPA). Mucociliary clearance were evaluated with $T_{1/2}$, cap value and penetration index parameters. Also, FEV1, FVC ve FEV1/FEVC parameters were obtained by doing pulmonary function tests. **Results:** The means of $T_{1/2}$ ($p=0.02$), cap value ($p=0.03$) and FEV1/FEVC ($p=0.04$) were statistically significant difference between nonsmoker COPD and asthma groups. In the active and passive smoker groups, only FEV1/FEVC parameter ($p=0.04$) was observed significantly different between COPD and asthma groups. **Conclusion:** Assessment of mucociliary permeability with Tc-99m DTPA aerosol scintigraphy is a reliable, easy to apply and noninvasive technique in the differential diagnosis of nonsmoker COPD and asthma.

P1081

Lung tissue density measured by low-dose CT in patients with suspected pulmonary embolism

O. Lang, H. Balon, R. Pichova, H. Krizova, H. Trojanova, I. Kunikova; Charles Univ., 3rd Medical Faculty, Prague 10, CZECH REPUBLIC.

Introduction: Interpretation of lung perfusion scintigraphy in patients with suspected pulmonary embolism (PE) is difficult, especially in the presence of chronic obstructive pulmonary disease (COPD) and most often has to be combined with pulmonary ventilation scintigraphy. We investigated the data from the CT portion of pulmonary perfusion SPECT/CT to try to solve this problem. **Methods:** We retrospectively assessed data from 12 patients (4 male, 8 female, mean age 68y), 6 with PE (group A), 6 with COPD (group B). The final diagnosis was based on ventilation/perfusion scintigraphy. Perfusion scintigraphy was performed with a hybrid gamma camera with non-diagnostic CT (GE Infinia Hawkeye). Lung tissue density in the areas of perfusion defects on SPECT was evaluated from the CT data in Hounsfield units (HU), radioactivity in counts. We analyzed 32 areas with a perfusion defect in patients with PE and 25 areas in patients with COPD. Data from both groups were compared with non-parametric Kolmogorov-Smirnov test (not-normal distribution) for two independent samples, $p<0.05$ was considered statistically significant. **Results:** The mean lung tissue density in perfusion defects caused by PE was -695 HU (SD 77, range from -829 to -516), in defects caused by COPD -900 HU (SD 48, range from -973 to -802). The mean radioactivity in perfusion defects caused by PE was 51 counts (SD 29, range from 13 to 127), in defects caused by COPD 32 counts (SD 22, range from 10 to 80). Both the density and radioactivity differed significantly (p for density = 0.000, p for radioactivity = 0.041). **Conclusion:** Lung tissue density measured by CT is significantly lower in perfusion defects caused by COPD than in those caused by PE and the overlap of values is minimal. We believe this data could be used as an adjunct in

interpretation of pulmonary perfusion studies and potentially help avoid the performance of ventilation scintigraphy in patients with COPD.

P1082

Usefulness of SPECT/CT scintigraphy in the diagnosis of pulmonary embolism

A. Mazurek, S. Piszczek, Z. Stembrowicz-Nowakowska, A. Gizewska-Krasowska, M. Dziuk; Military Institute of Medicine, Warsaw, POLAND.

Aim SPECT lung scintigraphy is a method for diagnosis of pulmonary embolism (PE), however usefulness of the hybrid method (SPECT/CT) has not been determined. The aim of this study is to evaluate the accuracy of SPECT/CT scintigraphy in the diagnosis of PE. **Material and methods** In 54 consecutive patients suspected of PE, perfusion SPECT scintigraphy with non-diagnostic low-dose CT (SPECT/CT) was performed. Ventilation scintigraphy was done only if lung perfusion abnormalities were equivocal. PE was diagnosed when: there was at least 1 segmental or 2 subsegmental perfusion defects with the absence of abnormalities in the lungs parenchyma (visualized in CT). PE was excluded when there was: normal perfusion pattern, perfusion defects that were not located according to the lungs vascularity, perfusion defects caused by abnormalities in the lungs parenchyma (visualized in CT). Final clinical diagnosis was established by physician responsible for patient care (based on clinical symptoms, laboratory tests, other imaging studies, the treatment). To establish the performance of SPECT/CT all patients were followed up for 6 months. **Results** All reports were conclusive. Data for follow-up were available in 42 patients (men-16, women-26, mean age-67,8 y). PE (SPECT/CT) was reported in 18 (43%) and excluded in 24 (57 %) patients. One patient was classified as false positive and one as a false negative. The sensitivity, specificity, accuracy, positive predictive value, negative predictive value was 94 %, 96 %, 95 %, 94 %, 96 % respectively. Normal perfusion pattern was described in 7 patients. Non-diagnostic low-dose CT allowed to classify for correct interpretation of perfusion defects in 22 (62,9%) patients. Lung ventilation scintigraphy was performed in 13 (37,1%) patients. The most frequently observed abnormalities in CT were: focal emphysema or fibrosis, fluid in the fissures, thickening of the fissures and tumor. **Conclusions** Combined interpretation of SPECT perfusion scintigraphy and low-dose non-diagnostic CT may be a highly sensitive and specific method for PE imaging. The CT may obviate the need of ventilation in more than half of scanned population.

P74-2 - Tuesday, October 30, 2012, 16:00 - 16:30, Poster Exhibition Area

Conventional & Specialised Nuclear Medicine: Gastroenterology

P1083

Scintigraphic evaluation of esophageal transit and gastroesophageal reflux in adult patients presenting with upper respiratory tract symptoms

J. Amalachandran, S. Simon, I. Elangovan, A. Pawaskar; Apollo Hospitals, Chennai, INDIA.

Aim: To evaluate the findings and assess utility of esophageal transit and gastroesophageal reflux scintigraphy (GES) in adult patients presenting with upper respiratory symptoms suspected to be due to gastroesophageal and non acid reflux disease. **Materials and methods:** 30 patients with upper respiratory tract/non GI symptoms like chronic cough, hoarseness of voice etc were evaluated. All patients underwent nasopharyngolaryngoscopic examination, esophageal transit and GES. Correlation between the three variables were evaluated. **Results:** Overall, 28 patients had positive GES findings for reflux, 18 of these had grade III reflux; 5 had grade II reflux and the remaining 5 had grade I reflux. Interestingly the esophageal transit time was abnormal in all the patients irrespective of grade of reflux. However the severity of posterior laryngitis documented by nasopharyngolaryngoscopy was higher as the grade of GER increased. Two symptomatic patients in whom GER was absent showed delayed esophageal motility. **Conclusion:** Our study suggests that esophageal transit and gastroesophageal scintigraphy objectively showed the presence of esophageal dysmotility along with associated gastroesophageal reflux in almost all patients presenting with upper respiratory tract symptoms pointing to the possibility of esophageal motility disorder as a primary disorder causing the symptoms. This procedure is highly sensitive and specific for detecting esophageal motility disorder and reflux disease, hence can be included in routine workup of all patients with recurrent upper respiratory symptoms. It helps in deciding treatment options and following up patients.

P1084**Clinical Usefulness of Sequential Subtraction Technique in Gastrointestinal Bleeding****A. F. Apostol**; Philippine Heart Center, Quezon City, PHILIPPINES.

Methods: Twenty-two patients referred for ^{99m}Tc -labeled RBC scintigraphy were included in this study. Sequential conventional scintigraphy and subtraction images at 5-minute per frame were processed. Sequential subtraction technique was done wherein each 5-minute frame were subtracted from its precedent frame. Three independent nuclear physicians blinded to the history, clinical set-up of the patients and processing technique interpreted the images in terms of time of bleed, localization and detection confidence. **Results:** Although there was a decrease in the mean detection time in between conventional scintigraphy with sequential subtraction technique and conventional scintigraphy alone, there was no statistically significant difference in between the mean time to bleed detection between the two techniques. There was also an increased mean detection confidence observed with conventional scintigraphy plus sequential subtraction technique than conventional scintigraphy alone, however, no statistically significant difference was noted between both techniques. **Conclusion:** Sequential subtraction technique is a useful adjunct with conventional scintigraphy in gastrointestinal bleeding.

P1085**Isotopic Investigation of Gastro Esophageal Reflux: About 43 cases****D. Ben Sellem**, L. Zaabar, Y. Mahjoub, W. Ajmi, A. Sellem, H. Hammami; Military Hospital, TUNIS, TUNISIA.

Aim: Gastro-esophageal reflux (GER) is a multifaceted disease presenting with both esophageal and extra-esophageal clinical manifestations. Tools for the diagnosis lack sensitivity and reproducibility. The aim of this study is to report cases of GER and to determine the reliability of the isotopic tool in the diagnosis of this pathological condition. **Materials and Methods:** We retrospectively studied 43 patients, with age ranging from 04 months to 77 years (average of 20 years), referred to investigate a clinical suspicion of GER. Their principal complaints were: respiratory symptoms in 35 cases (81.40 %), typical gastric symptoms (including heartburn, regurgitation) in 2 patients (4.65 %), suspicion of GER in 5 infants (11.63 %). The indication for the last case was to control the GER after treatment. We administered orally 37 to 111 MBq of ^{99m}Tc -sulphur colloid after a fasting of 12 hours (infants: only 3-4 hours). The exam is performed with 20 minute-dynamic acquisition, gamma camera focused on the chest and the upper abdomen, patient in supine position. We noted number, duration and rising level of each reflux episode; a time activity curve was drawn to evaluate quantitatively the reflux. **Results:** Sixteen patients (37.21 %) yielded abnormal findings on scintigraphy. ^{99m}Tc -sulphur colloid scintigraphy confirmed the diagnosis of GER in three infants and in adult patient presenting dyspepsia. In the others twelve patients, it helped to attribute respiratory symptoms to reflux. Reflux was multiple in 5 cases. It reached the mouth in 2 cases (12.5 %), the upper third of the esophagi in 8 cases (50 %), the middle third in 3 cases (18.75 %) and the lower third of the esophagi in 3 cases (18.75 %). **Conclusion:** Gastro-esophageal reflux is a very common and chronic condition. Unfortunately, detecting such reflux is only just becoming available. The scintigraphy is an additional noninvasive, reproducible and less irradiating tool that can help in the clinical management.

P1086**Role of ^{99m}Tc -colloid Scintigraphy in Diagnosis of Splenosis and Accessory Spleen****V. Valenza**, F. Cocciolillo, P. Basile, M. V. Mattoli, A. Giordano; Institute of Nuclear Medicine, Catholic University of Sacred Heart, Rome, ITALY.

Aim. About 10% of the population is born with one or more accessory spleens and it has estimated that persistence of splenic tissue after surgery occurs in 5-20% of splenectomised patients. Hyperplastic splenic tissue after splenectomy may result in incidentally discovered masses and undergoes to differential diagnosis from other incidentalomas. Splenosis is the auto transplantation of splenic tissue after splenectomy for traumatic or iatrogenic spleen injuries. Splenic implants derive their blood supply from surrounding tissue and grow into mature splenic tissue. They can cause abdominal pain, due to intraperitoneal nodule infarction, bowel obstruction, compression and hydronephrosis or haematoma from pre-existing splenic implant trauma. Although there are many imaging methods to detect splenosis and accessory spleen, the origin of such tissue is not easy to determine. **Aim** of this study is to emphasize the role of ^{99m}Tc -colloid scintigraphy in characterizing focal lesions observed at routine imaging in patients with suspect of splenosis and/or accessory spleen. **Material and methods.** Sixteen patients (11 male, mean age 63 ± 12) underwent colloid scintigraphy after radiological imaging: 9/16 for suspect accessory spleen (2/9 patients previously splenectomised for malignant lymphoma); 7/16 patients, splenectomised for abdominal trauma, for

differential diagnosis between splenosis and multiple intra-abdominal nodules (5/7 with radiological imaging suspects for metastatic cancer; 2/7 for liver transplantation work-up). Four static images (anterior, posterior, right and left lateral views) were performed 20 minutes after intravenous injection of 148 MBq ^{99m}Tc -colloid. **Results.** In all patients areas of intense ^{99m}Tc -colloid uptake corresponding to the radiologically detected lesions were observed, revealing the presence of reticulo-endothelial tissue. This finding confirm the clinical suspect of spleen tissue. **Conclusions.** Our study suggest a pivot role of radiocolloid imaging to clarify the nature of suspect lesions. ^{99m}Tc -colloid imaging is a simple and less time-saving method to detect splenic tissue.

P1087**Bile Acid Malabsorption in Patients with Chronic Diarrhea: Diagnosis and Evaluation of Treatment Response****O. Puig Calvo**, S. Maisterra, J. Mora Salvado, Y. Ricart Brulles, A. Sabaté i Llobera, L. Camacho Berne, R. Puchal, J. Guardiola Capo, J. Martin-Comin; Hospital Universitari de Bellvitge, L'hospitalet de Llobregat (Barcelona), SPAIN.

AIM To assess the prevalence of bile acid malabsorption (BAM) in patients with chronic diarrhea and evaluate the dose of treatment and response to treatment in these patients depending on the bile acid abdominal retention determined by ^{75}Se -SeHCAT test at the moment of diagnosis. **MATERIAL AND METHODS** Seventy five patients with chronic diarrhea were studied. A 37 KBq ^{75}Se -SeHCAT capsule was administrated and the abdominal activity was assessed using a collimated gammacamera 3h and 7d post-administration. Abdominal retention index (ARI) was calculated and, depending on its result, patients were included in 3 groups: <5% (G1); = or > 5% but < 10% (G2); = or > than 10% (G3). BAM was diagnosed when ARI was < 10%. Specific treatment was administered to those patients diagnosed of BAM and the response grade and dose needed were evaluated. **RESULTS** BAM was diagnosed in 45% of the patients (28% G1 and 17% G2), there was one false negative (ARI 10.5%). 57% of the patients with G1 index needed high doses of treatment and 53% needed low doses while only 38% of patients with G2 retention needed high doses and 62% needed low treatment doses. 76% of the patients with G1 retention reached a complete response to treatment, 20% partial and 4% had no response to treatment. 85% of the patients with G2 retention reached complete response and 15% partial response to treatment. **CONCLUSIONS** ARI is a reliable test to diagnose BAM in patients with chronic diarrhea. Patients with BAM and low ARI needed higher doses of treatment and showed less response than patients with BAM but higher ARI.

P76-2 - Tuesday, October 30, 2012, 16:00 - 16:30, Poster Exhibition Area

Conventional & Specialised Nuclear Medicine: Paediatrics**P1088****Serum Levels of 25-Hydroxyvitamin D (25OHD) as Prognostic Factor in Children with Bronchial Asthma****A. S. Zissimopoulos**¹, M. Iordanidou², P. Giasari², E. Parashakis², N. Boussios³, M. Giannouloudi², E. Karathanos³, A. Giamoustaris³, A. Hatzimihaili²; ¹Demokritos University of Thrace University Hospital of Alexandroupolis, Alexandroupolis, GREECE, ²Paediatric Clinic Demokritos University of Thrace University Hospital of Alexandroupolis, Alexandroupolis, GREECE, ³Dpt of Nuclear Medicine Demokritos University of Thrace University Hospital of Alexandroupolis, Alexandroupolis, GREECE.

Introduction: Asthma is a chronic inflammatory lung disease characterized by reversible airway obstruction and hyperactivity. Vitamin D may be involved in bronchial asthma pathogenesis and especially in oxidative stress process. **Aim:** The aim of this study was to evaluate the serum levels of 25-hydroxyvitamin D (25OHD), as prognostic factor in bronchial asthma pathogenesis, in children with bronchial asthma. **Patients and Methods:** 54 children (20 males) mean age 9.6 ± 2.5 years, from the pediatric department have been studied to our laboratory, ($p=0.8$), while 20 children (4 males) mean age 9.6 ± 2.5 years, have been used as a control group. Measurement of serum total IgE and 25-hydroxyvitamin D (25OHD) levels was carried out through the radioimmunochemical method (RIA) using Diasorin[®] and ImmunoTech[®] kit equipment respectively. **Results:** Children with diagnosed asthma, treated with fluticazone on a mean dose (\pm SD) of 158 ± 60 mcg/day (Group A), had a mean FEV1%(\pm SD) value of 85.42 ± 8.7 and a mean (\pm SD) IgE value of 287 ± 164 IU/ml. Control group children (Group B) had mean FEV1%(\pm SD) 97.9 ± 9 and mean (\pm SD) IgE 45.4 ± 24 IU/ml. In 44 patients of Group A, levels of (25OHD) found to be lower compared to Group B patients levels. (Mean (\pm SD) Group A values = 37.21 ± 5.4 ng/ml, Mean (\pm SD) Group B values = 62.33 ± 5.1 ng/ml $p=0.004$). **Conclusions:** The results of this study show clear that even in countries with high sunlight coverage, children with asthma have lower vitamin D levels, a fact that suggests the contribution of vitamin D in the pathogenesis of asthma.

P1089

The essential role of ^{18}F -DOPA PET/CT study in the diagnosis of congenital focal form of hyperinsulinism - 2 case reports

D. Chroustova¹, J. Kubinyi¹, J. Trnka¹, A. Pudlac², J. Kytarova³,
¹Department of Nuclear Medicine, General Teaching Hospital and First Faculty of Medicine, Charles University, Prague, CZECH REPUBLIC,
²Department of Radiology, General Teaching Hospital and First Faculty of Medicine, Charles University, Prague, CZECH REPUBLIC, ³Clinic of Pediatrics and Adolescent Medicine, General Teaching Hospital and First Faculty of Medicine, Charles University, Prague, CZECH REPUBLIC.

Aim: Congenital hyperinsulinism (CHI) is a neuroendocrine disease secondary to either adenomatous hyperplasia or a diffuse abnormal pancreatic insulin secretion. While diffuse forms CHI require near-total pancreatectomy when are resistant to medical treatment, focal CHI may be reversed by selective surgical resection followed by patient's recovery. We present 2 cases where ^{18}F -DOPA PET/CT identified focal lesion in two children with CHI. **Material and methods:** ^{18}F -DOPA-PET/CT were performed in two male children aged 2 and 4.5 months with recurrent hypoglycemia and specific CHI treatment (diazoxide and octreotide) using PET/CT Discovery 690 GE. Paternally inherited mutation of the sulfonylurea receptor ABCC8 gene was found in both patients, which is associated with focal islet-cell hyperplasia. After i.v. ^{18}F -DOPA application (4MBq/kg) early and late dynamic thoraco-abdominal emission studies were performed. The first PET acquisition was done 5 minutes after injection - 1bed 15cm, 1 frame/min, 10 frames, total time 10minutes, matrix 256x256. The second PET/CT dynamic acquisition (1bed 15cm, 1frame/min, matrix 256x256) was acquired 60 min after radiotracer injection (and immediately after i.v. 12 ml iomeron 400) during 20 minutes. Children were sedated using midazolam. CT parameters: Helical, 80kV, 100mA, Pitch 0,948:1 (39,47mm/rot), detector coverage 40mm. The PET images were reconstructed using CT transmission correction for attenuation of the gamma radiation. All frames of dynamic study were evaluated visually and those good qualities (no movement, no artefacts) were summed to one static image. The evaluation was completed using calculation of standardized uptake value (SUV) with comparison of the ratios between SUV max and mean of the pancreatic regions. For focal form SUV ratio was >1.2. **Results:** The saturated pancreatic cauda with focus of the increased ^{18}F -DOPA accumulation were detected in the first child. SUV ratio cauda/surrounding pancreatic tissue was 2.6. After this examination selective surgery of the pancreatic cauda was performed followed by normalization of glycemia levels. Pathologic finding of increased ^{18}F -DOPA accumulation in pancreatic corpus and head were found in the second child. SUV ratio corpus/cauda was 1.48. SUV ratio head/cauda was 1.29. Due to the localization of foci and uncomplicated medical treatment, this child has not yet indicated for surgery. **Conclusion:** In our experience ^{18}F -DOPA PET/CT is very good tool for the localisation of focal CHI. Dynamic PET studies are very useful for children, because allow to exclude the targeted frame with motion of child during the acquisition.

P1090

Assesment of Diagnostic Efficacy of Parametric Clearance Images in Detection of Renal Scars in Children with Recurrent Urinary Tract Infections (UTI)

E. Pietrzak-Stelmasiak¹, M. Biełkiewicz², W. Woźnicki¹, M. Surma¹, K. Bubińska³, M. Kowalewska-Pietrzak⁴, A. Plachcińska², J. Kuśmerek¹,
¹Department of Nuclear Medicine, Medical University, Lodz, POLAND,
²Department of Quality Control and Radiological Protection, Medical University, Lodz, POLAND, ³Children Hospital of J. Korczak Paediatrics Center, N.Copernicus Hospital, Lodz, POLAND, ⁴Department of Paediatrics, Oncology, Haematology and Diabetology, Medical University, Lodz, POLAND.

The aim of the study was: 1.To assess diagnostic efficacy of parametric clearance images (PAR) in comparison with conventional renoscintigraphic summation images (SUM) and a reference SPECT study in detection of renal scars as well as to analyse reproducibility of results of the studies. 2.To analyse relationships between incidence of renal scars in children with UTI and with or without history of acute pyelonephritis (APN) as well as prevalence and severity of vesico-ureteral reflux (VUR). **Material and methods:** Studies were conducted in 91 children at the age between 4 to 18 years, with recurrent UTI. 32 patients had a documented history of one or more incidents of APN. In 44 patients VUR has been diagnosed (I°-II° in 30, III°-V° in 14). $^{99\text{m}}\text{Tc}$ -EC renoscintigraphy and $^{99\text{m}}\text{Tc}$ -DMSA SPECT study were performed in every patient, not earlier than 6 months after the last incident of UTI. Images were assessed by 2 independent observers, using a Howard's scale. Altogether images of 171 kidneys were analysed. **Results:** Sensitivity, specificity and accuracy of PAR and SUM in detection of renal scars amounted to 90%, 87%, 88% and 48%, 94% and 73%, respectively. Sensitivity and accuracy of PAR images were statistically significantly higher ($p<0,05$) than of SUM images. Inter-observer reproducibility of PAR and SUM results were equal to 90% and 89%, respectively and similar to reproducibility of a reference SPECT method - 89%. Both PAR and SPECT methods revealed statistically significantly higher incidence of scars in

children with UTI and APN than without APN: PAR-67% vs 46%, $p=0,036$ and SPECT-72% vs 46%, $p=0,017$. PAR and SPECT studies also revealed a higher incidence of scars in patients with high than with low or lack of VUR: PAR-79% vs 49%, $p=0,04$ and SPECT-79% vs 50%, $p=0,048$, respectively. This relationship could not be observed in results of SUM study (APN vs UTI without documented APN: 38% vs 27%, $p=NS$, and high vs low or lack of VUR: 36% vs 30%, $p=NS$). **Conclusions:** 1.PAR images provide a high diagnostics efficacy in detection of renal scars in children with UTI and are a source of reproducible results. 2.SUM images also provide reproducible results, but sensitivity of this study is unacceptably low. 3.PAR images, similarly to a reference SPECT study, revealed a significantly higher incidence of renal scars in children with UTI and history of APN, as well as high VUR. This relationship could not be found with SUM method.

P1091

Lung Scintigraphy in the Assessment of Respiratory Disease in Children

D. Ben Sellem, I. El Bez, L. Zaabar, Y. Mahjoub, T. Ben Ghachem, B. Letaief, M. F. Ben Slimene; SALAH AZAIEZ INSTITUTE, TUNIS, TUNISIA.

Aim: Lung scintigraphy provides a regional, functional test of pulmonary ventilation and perfusion. It allows an early detection of pulmonary damage or dysfunction, in particular in detection of pulmonary infraction, cystic fibrosis, chronic obstructive pulmonary disease and congenital anomalies in childhood. **Materials and methods:** This is a single centre retrospective study. Fifty three children were sent to our department for lung perfusion scintigraphy. The main indication was chronic obstructive pulmonary disease observed in 15 patients (28.3 %). Twelve patients (22.64 %) had congenital anomalies. Eight children (15.09 %) had inhaled a foreign body. Pulmonary infraction was suspected in 6 cases (11.32 %). Four children (7.55 %) had hepatic disease. Four other children (7.55 %) had chronic cough and hemoptysis and two patients (3.77 %) had tuberculosis. The last two patients had connectivities. Lung perfusion scan was performed after intravenous injection of 74 MBq of radioactive technetium macro aggregated albumin (99m Tc-MAA) in 0.5 ml in volume. Multiple static images in the anterior, posterior, right anterior oblique, left anterior oblique, right posterior oblique, left posterior oblique, positions were acquired under a large field of view dual head gamma camera, coupled with low-energy general purpose collimator. One experienced nuclear medicine physician interpreted the static images for the presence or absence of perfusion defects or shunt. **Results:** Children were aged from 1 month to 18 years (mean age 6.3 years, median 3 years). The sex ratio was 1.52 (32 males, 21 females). The lung perfusion scintigraphy was normal in 17 children (32 %) and abnormal in 36 patients (68 %). Perfusion defects were objectified in 29 patients (80.6 %). Global hypoperfusion and nonperfused lung were noted in 6 children (16.7 %). In the last case, an important right-to-left shunt was described. **Conclusion:** Lung scintigraphy allows early detection of local pulmonary abnormalities, sometimes undetectable with a chest X-ray or even with a chest tomodensitometry. It can reveal bronchial obstructive plugs, avoiding thus the development of bronchiectasies thanks to a quick suitable treatment.

P1092

SPECT/CT of the Lumbar Spine Compared to Conventional Radiographs and MRI in School Age Patients with Low Back Pain.

M. J. Gelfand, S. E. Sharp, C. G. Anton; Cincinnati Children's Hospital, Cincinnati, OH, UNITED STATES.

SPECT/CT of the lumbar spine was compared retrospectively to conventional radiographs (XR) and MRI in school age patients with low back pain with particular reference to spondylolysis. 104 pairs of SPECT/CT and XR studies were compared, and also 42 paired SPECT/CT and MRI studies. CT was performed with a very low dose, limited field technique. For XR studies, 29 of 104 studies had spondylolysis on the CT of the SPECT/CT. XR was positive or questionably positive for spondylolysis in 17/29 (59%) and negative in 12/29 (41%) for a sensitivity of 59%, specificity of 80% and a positive predictive value of 53%. 10 studies had positive SPECT; 7/10 had pedicle sclerosis on CT consistent with a localized stress reaction and 3/10 had normal CT. When SPECT and XR were normal, CT has a very low diagnostic yield; 1/30 were positive (3%) for spondylolysis. For MRI, 10/42 paired SPECT/CT-MRI studies had spondylolysis on the CT of the SPECT/CT. MRI identified clefts in the pars interarticularis (pars) in 5/10. There was increased signal in the pars without a cleft in 4/10 and other findings in one. These 4 studies and 5 additional studies had pars signal abnormalities, in each case with positive SPECT. Conventional radiographs have low sensitivity for detection of spondylolysis even when questionably normal studies are included. In a limited number of patients, MRI is sensitive for the detection of pars abnormalities, but does not accurately differentiate pars fractures from pars stress reactions.

P1093**Is the Motion Correction of Renal Pinhole SPECT by Paediatric Patients Beneficial?**

G. Demonceau¹, M. Hesse¹, S. Walrand², ¹St Elisabeth Hospital, Zottegem, BELGIUM, ²Univ. Catholique de Louvain, Brussels, BELGIUM.

The majority of the ^{99m}Tc-DMSA imaging is performed in pediatric patients, which means a long acquisition time and a high probability of motion. Renal motion correction is particularly challenging in pinhole SPECT, due to the presence of two volumes of interest, jointly with the pinhole magnification that is strongly spatially dependent. We visually evaluated the results of a motion correction by comparing them with the non-corrected SPECT data and the planar data. Six hours after a weight-dependent injection of ^{99m}Tc-DMSA, four 5min-planar views and one 25min-pinhole SPECT were performed in 70 patients (pts) less than 15 years old. Firstly, the maximal set of acquired projections free of motion is determined, based on the variation of the kidney centers of mass from one incidence to the next. Secondly, a reconstruction of that largest motion-free sequence of incidences is created and reprojected for each view. Thirdly, the acquired projections are shifted to match as well as possible those reprojections. This entire process can be repeated to improve the size of the sequence. The final reconstruction quality, with and without correction, was visually assessed, based on the presence of high background, cortical defects, double contours and the convergence with the planar data. A (mostly mild) motion was detected in almost all patients. The method globally improved the quality of the reconstruction in 48pts (68%). No degradation was observed. The improvement was correlated with the intensity and the amount of movements. After motion correction, some defects, mainly located on the poles of the non-corrected kidneys, disappeared, modifying the final diagnosis in 11pts (15.7%). No additional defect appeared but the existing defects were more clearly seen than before correction. Only 1 motion corrected SPECT didn't bring at least the same amount of clinical information as the planar views. We strongly recommend the use of a motion correction method in pinhole SPECT with ^{99m}Tc-DMSA in paediatric patients. A significant amount of false positive would then be avoided. Moreover, sedation would be necessary in less than 2% of the patients.

P77-2 - Tuesday, October 30, 2012, 16:00 - 16:30, Poster Exhibition Area

Conventional & Specialised Nuclear Medicine: Urology

P1094**Fractional rate as unjustly neglected approach to gamma-camera measurement of renal and plasma clearance**

M. Samal¹, V. Ptacnik², D. Skibova², H. Jiskrova², J. Kubinyi², ¹Charles University Prague, Prague, CZECH REPUBLIC, ²General University Hospital, Prague, CZECH REPUBLIC.

Presenting plasma and renal clearance as fraction of plasma volume cleared per unit time is subject of controversy. Volume is more physiological norm than body surface area (BSA) and measurement is technically simple. Critics argue that relation between kidney function and plasma volume is complex and that fractional clearance may reflect changes in plasma volume rather than the changes of renal function. The aim of this contribution was to validate 3 methods for measurement of fractional plasma and renal clearance in dynamic renal scintigraphy (DRS). Methods: ^{99m}Tc-MAG3 DRS was performed in 45 men and 62 women at age of 15-86 years with a wide range of GFR. MAG3 fractional clearance was calculated from the curves generated by the heart and kidney ROIs and compared with BSA-normalized plasma clearance measured using 1 and 2 blood samples. Fractions of plasma volume per minute [1/min] were scaled to standard clearance units [ml/min] using plasma volume estimate by Dissmann et al (Klin Wochenschr 1975). The validated methods were (A) $ZA = P(0)/\int P(t)dt$ where ZA is fractional plasma clearance and P(t) is the curve from the heart ROI, (B) $ZB = q/h$ where q is the slope of the second one and h the intercept of the first linear segment of the whole-body Patlak plot $D/P(t) = q\int P(t)dt/P(t) + h$, where D is injected activity, and (C) $ZC = kP(0)/D$ where ZC is individual-kidney clearance and k is the slope of Patlak-Rutland plot. Clearances ZA and ZB were obtained from the heart-ROI curve only while ZC also requires the curve from the kidney ROI. Criteria of performance were mean absolute error of prediction (MAE) calculated by cross-validation (ideally 0 ml/min) and slope of regression line (SRL), ideally 1.0. Results: In posterior view, MAE and SRL were (A) 17.0 ml/min, 0.99, (B) 20.2 ml/min, 0.88, (C) 14.0 ml/min, 0.69. Method (C) was comparable with original Taylor's method (JNM 1995;36:1689) 15.7 ml/min, 0.63. In attenuation-corrected (AC) conjugate view, MAE and SRL were (A) 13.7 ml/min, 0.71, (B) 17.0 ml/min, 0.69, (C) 12.9 ml/min, 0.84, that was comparable with modified Taylor's method 13.0 ml/min, 0.90. Conclusion: The best camera-based predictor of MAG3 plasma clearance was method A in posterior view without AC and method C in conjugate view with AC. Methods for fractional plasma clearance perform well in posterior view DRS while that of renal clearance

performs better in AC conjugate view. They should be considered as technically simple and robust alternatives to regression methods.

P1095**Phenomenon of supranormal renal function in children with unilateral hydronephrosis on ^{99m}Tc-EC renoscintigraphy**

A. Nocuń, A. Kornaś, M. Nózka-Kozik, B. Chrapko; Medical University of Lublin, Lublin, POLAND.

Aim : Differential renal function (DRF) greater than 55% is referred to as supranormal. Such a kidney was first reported in 1994 by Steckler et al. Since then, there has been a lot of controversy in the literature of supranormal hydronephrotic kidney in children with unilateral hydronephrosis. The aim of our study was to assess the incidence of this phenomenon. **Materials and methods** : We retrospectively analyzed last 10 years data of children examined in our center with the diagnosis of unilateral hydronephrosis and normal contralateral kidney. Bilateral pathology, hypertension, the history of a surgery on the urinary tract were the criteria of exclusion from the studied sample. All patients underwent renoscintigraphy with ^{99m}Tc-ethylenedicycysteine, performed with the single head gamma camera Picker DC5. Examination was carried out in posterior-anterior projection, immediately after radiopharmaceutical application. For the first minute, the dynamic frames were obtained every 2 seconds, for the remaining 30 minutes, every 30 seconds. The DRF was determined with the integral method. **Results**: Sixty eight patients (33 female and 35 male) met the criteria of inclusion to the studied group. The children were 1 month to 17 years old (mean age 6.3 ±5.5 years). Nineteen (27.9%) patients were younger than 1 year. Hydronephrotic kidney was on the left side in 42 cases (61.8%), on the right side in 26 (38.2%). Affected kidney was larger than normal in 50 (73.5%) cases, smaller in 18 (26.5%). Decreased DRF (<45%) was found in 37 (54.4%) patients, normal (≥45% and ≤55%) in 28 (41.2%) children, including 6 (8.8%) cases of DRF >50%. Supranormal kidney was found in only 3 (4.4%) cases: 56%, 57% and 58%. The age of the children was respectively: 5 years, 7 months and 1 month. The side of pathology was right in 1 case, left in 2 cases. All kidneys with DRF>50% were larger than contralateral normal kidney. **Conclusion**: In opinion of the authors, supranormal renal function is the rare phenomenon. Small number of patients presented with such abnormality does not allow for statistical analysis. However, our study may support previous suggestions, that increased DRF of the hydronephrotic kidney is associated with its larger size and renal immaturity in younger children.

P1096**Usefulness of Nora in the Evaluation of Obstruction on Dilated Kidneys: Review of 150 Patients**

B. Letaief, D. Ben Sellem, Y. Mahjoub, T. Ben Ghachem, L. Zaabar, I. Slim, M. F. Ben Slimene; SALAH AZAIEZ INSTITUTE, TUNIS, TUNISIA.

Aim: Normalized residual activity (NORA) is a parameter used for estimating renal emptying during renography with ^{99m}Tc-diethylene triamine penta acetic acid (^{99m}Tc-DTPA) or ^{99m}Tc-Mercaptoacetyltryglycine (^{99m}Tc-MAG3) on dilated kidneys, since the outcome of simple urinary tract dilatation and significant obstruction are considerably different. The purpose of our study was to determine the usefulness of NORA in the diagnostic of obstructive dilated kidneys. Patients and methods: We investigated 170 kidneys on 150 patients (108 M, 42 F) referred essentially to diagnose obstruction and to determine relative function. A diuretic renal scan with ^{99m}Tc-DTPA or ^{99m}Tc-MAG3, with a maximal dose of 100 MBq, scaled on a body-surface basis, was performed for all of our patients. An adequate hydration and void of bladder prior to scintigraphy were observed. Dynamic computer data acquisition was started at the moment of injection on a large field of view scintillation camera, posteriorly in the supine position. Furosemide injection at 20 minutes (F+20) was used. Data was processed to generate renogram curves and each time the curves were suggestive of obstruction an estimation of NORA was performed. Delayed acquisition of dynamic images was performed to evaluate late emptying and to calculate NORA on its basis. Results: We classified normal, abnormal and indeterminate NORA findings as follows respectively, ≤ 1, between 1 and 2 and >2. 106/170 investigated kidney (62 %) were normal, 45/170 (26%) were indeterminate and 19/170 (11%) were abnormal. Our results enabled us to respond clearly to referring clinicians in 73 % and for the indeterminate cases we were unable to respond and have no further information about them. **Conclusion**: Evaluation of renal emptying is necessary in the investigation of dilated kidneys, since obstruction is managed surgically; while absence of obstruction needs a medical follow up. NORA as a simple parameter used for estimating renal emptying during renography helps us to respond to the question 'is there any obstruction under the dilated renal tract?'. Any suggestive signs on renal curves must lead to its calculation and to the need for delayed images.

P1097**Measured glomerular filtration rate (Tc^{99m}DTPA clearance) and renal function estimates in patients with cervical cancer**

M. Benke, J. Niewiadomska, A. Garszel, I. Kozłowicz-Gudzinska; Maria Skłodowska-Curie Memorial Cancer Center and Institute of Oncology, Warszawa, POLAND.

An assessment of renal function is important for the dosage of drugs, in particular potentially nephrotoxic chemotherapeutic agents like cisplatin. The aim of this study was to compare GFR, measured by Tc99mDTPA clearance (rsGFR), with estimates of GFR according to MDRD and Wright formulas (eGFR) and creatinine clearance according to Cockcroft-Gault formula (CrCl). This was a prospective study of patients with cervical cancer (FIGO II and III stage) who had GFR measured by Tc99mDTPA clearance. 148 patients were included in the analysis. GFR was determined prior to planned treatment and immediately after treatment. In 39 patients (26.4%) measured GFR was below 60 ml/min/1.73m², indicating impaired renal function according to K/DOQI (Group I). In 109 patients measured GFR was above 60 ml/min/1.73m² (Group II). Results In Group I we found a moderate correlation of rsGFR with eGFR calculated by MDRD and Wright formulas. The correlation coefficient was 0.46 and 0.41 respectively (p<0.02). In this group correlation was stronger after treatment, with correlation coefficient 0.60 for Wright and 0.49 for MDRD formula (p<0.02). Correlation with CrCl (Cockcroft-Gault) was weak (0.19). In group II correlation rsGFR with MDRD eGFR was 0.54 and Wright eGFR 0.58 (moderate). Correlation with CrCl was low (0.37). Both the MDRD formula and the Wright formula significantly overestimated GFR <60 ml/min (p<0.05) and underestimated GFR for patients with GFR >60 ml/min (p<0.05). Conclusions The renal clearance calculated according to MDRD, Wright, Cockcroft and Gault provide a biased and imprecise estimate of GFR in patients with cervical cancer, especially in group with impaired renal function. When a precise estimate of GFR is required then clearance should be measured using a method such as Tc99mDTPA renoscintigraphy.

P1098

Fluorine-18 Choline PET/CT in evaluation of prostate cancer. Comparison of standardized uptake values in malignant lesions compared with benign tissues.

A. Tan Eik Hock, A. Goh Soon Whatt, A. Ng, S. Yu; Singapore General Hospital, Singapore, SINGAPORE.

Positron emission tomography imaging of prostate cancer using Choline based ligands was first proven in 1998, and has seen increasing clinical adoption since. In our series of patients, we have analysed 33 sequential studies and tabulated the standardized uptake values (SUV) of unequivocal malignant lesions in the prostate, nodes and bone, and compared them with uptake values in benign tissue. Mean SUVmax values were 7.3 (SD 2.45) for histologically proven prostate adenocarcinomas, and benign prostate tissue showed a mean SUVmax of 2.6 (SD 0.57) Mean SUVmax values were 5.0 (SD 1.84) for nodal metastasis, and benign nodes had a mean SUVmax of 1.0 (SD 0.42). Mean SUVmax values were 6.8 (SD 2.67) for bony metastasis, and normal bone marrow uptake SUVmax was 3.0 (SD 0.99). Overall, our findings show statistically significant differences between malignant and benign tissues, with the malignant lesions demonstrating consistently higher SUV values.

P1099

Glomerular filtration rate (GFR) measurement with Cr-51-EDTA : comparison of the slope-intercept 2-sample method with the 10-sample kinetic plasma clearance analysis in a representative cohort of patients.

G. Arsos¹, E. Manou², G. Miserlis³, A. Sioulis⁴, I. Tsechelidis⁵, C. Sachpekidis⁵, D. Tsakiris², N. Karatzas¹; ¹3rd Department of Nuclear Medicine, Aristotle University of Thessaloniki Medical School, Papageorgiou Hospital, Thessaloniki, GREECE, ²Department of Nephrology, Papageorgiou Hospital, Thessaloniki, GREECE, ³Transplantation Clinic, Aristotle University of Thessaloniki Medical School, Hippokraton Hospital, Thessaloniki, GREECE, ⁴1st Internal Medicine Clinic, Aristotle University of Thessaloniki Medical School, AHEPA Hospital, Thessaloniki, GREECE, ⁵1st Department of Nuclear Medicine, Aristotle University of Thessaloniki Medical School, Hippokraton Hospital, Thessaloniki, GREECE.

Introduction : GFR measured as plasma clearance of an exogenous tracer is the gold standard for clinical renal function assessment. The routinely applied slope-intercept technique with bolus i.v. Cr-51-EDTA injection and 2-3 plasma samples during the 2-5 hours p.i. is more convenient but necessitates empirical correction for the fast component of the tracer elimination. On the contrary, the detailed plasma tracer elimination analysis requires multiple plasma sampling, starting soon after injection, but does not rely upon any empirical correction. The present study is aiming to compare GFR values obtained by the two methods and discuss the clinical impact of the method selection. **Subjects and methods** : In 121 subjects (106 with chronic kidney disease, 15 prospective kidney donors [PKD]), aged 61.4±13.9 years, after bolus i.v. injection of 3.7 MBq 51Cr-EDTA and 10 plasma samples obtained between 5 min-4 hours p.i., GFR was calculated with biexponential kinetic analysis of all the 10 samples (GFR10) and with 2 samples

(120 and 240 min p.i.), "slope-intercept" analysis and Brochner-Mortensen correction (GFR2). GFR values were indexed by body surface area calculated according to Haycock and expressed in ml/min/1.73 m². Test-retest repeatability of both GFR10 and GFR2 has been previously found ≤3.5 ml/min/1.73 m². Differences were assessed with t-test and paired-sample t-test as appropriate and correlation and agreement with linear regression and Bland-Altman analysis, respectively. The correlation between the GFR10-GFR2 difference (DGFR) and GFR10 was assessed for DGFR ≤0 and DGFR>0 values. Statistical significance was accepted at the p<0.05 level. **Results** : GFR10, GFR2 and DGFR (mean±SD) were 54.3±26.6, 49.5±24.6 and 4.8±4.9 (p<0.001) ml/min/1.73 m², respectively. GFR10 and GFR2 correlated strongly (r=0.984, p<0.0001) but agreed less well (95% confidence interval of DGFR -4.8 to 14.4 ml/min/1.73 m²). DGFR<0 was found in 16.5% of the cases. Negative and positive DGFR were -3.3±3.1 and 6.4±3.4 ml/min/1.73 m² (p<0.05), respectively. DGFR of the 15 PKD was 7.4±4.6 (range -0.3 to 17.4) ml/min/1.73 m². Negative DGFR values were independent from GFR10 (r=-0.106, p=0.656) but positive DGFR correlated positively with GFR10 (r=0.555, p<0.0001). **Conclusions** : The "slope-intercept" GFR measurement technique with Brochner-Mortensen correction significantly underestimates GFR. The underestimation is progressively broader as GFR increases and becomes maximum in prospective kidney donors. Our data suggest that GFR in patients with higher expected GFR values and especially in prospective kidney donors, should be measured by plasma tracer kinetic analysis rather than by the slope-intercept technique.

P1100

99mTc-DMSA planar and SPECT-CT imaging and quantification in patients with sickle cell anemia: a comparison with glomerular filtration rate

D. M. Onusic, MSc¹, S. Q. Brunetto, PhD¹, J. Pasquoto², E. M. R. Brunetto², C. M. S. Norberto², N. T. T. P. da Silva, MSc², A. O. Santos, PhD², M. C. L. de Lima, PhD², B. J. Amorim, PhD², E. C. S. C. Etchebehere, PhD², S. T. O. Saad, PhD², C. D. Ramos, PhD²; ¹Center for Biomedical Engineering - University of Campinas, Campinas, BRAZIL, ²Faculty of Medical Sciences - University of Campinas, Campinas, BRAZIL.

KEYWORDS: 51Cr-EDTA, 99mTc-DMSA ,SPECT/CT, glomerular-filtration-rate, sickle-cell-anemia **INTRODUCTION**: Different functional and structural abnormalities of the kidney are observed in patients with sickle cell anemia (SCA) and aging eventually leads to renal failure in most of these patients. Surprisingly, there is very limited data in the literature reporting the use of 99mTc-DMSA renal scintigraphy in SCA. **PURPOSE**: This study aimed to evaluate the use of planar and SPECT-CT images and 99mTc-DMSA absolute quantification in patients with SCA and compare with glomerular filtration rate (GFR). **MATERIALS AND METHODS**: Twelve patients (7 female) aged 24-58 years (43.4±/12.0 years) with SCA were studied. Doses of 110-180 MBq of 99mTc-DMSA and 10-12 MBq of 51Cr-EDTA were simultaneously injected in all patients. After 3 hours planar and SPECT-CT images were obtained using a dedicated multislice SPECT-CT. Blood samples were taken 2, 3 and 4 hours after injections and immediately counted in a well counter using the energy window of 99mTc in order to calculate DMSA clearance (DMSAcl). After 1 week (ensuring the 99mTc radioactive decay) the samples were also counted using the energy window of 51Cr to determine 51Cr-EDTA based GFR. Absolute renal uptake of DMSA (DMSAab) was calculated from SPECT-CT images as a percentage of the injected dose, using CT-based attenuation correction. Correlation curves between DMSAcl, DMSAab and GFR were performed. Planar and SPECT images were visually evaluated for identification of focal lesions in the renal parenchyma. **RESULTS**: The mean quantitative values (minimum and maximum) obtained for the 12 patients were: GFR: 87.5 +/- 26.1 ml/min (47.1 and 128.5 ml/min); DMSAcl: 81.7 +/- 39.6 ml/min (44.8 and 162.0 ml/min) ; DMSAab: 39.1% +/- 3.7% (29.7% and 44.2%). The correlation indices between DMSAcl and GRF and between DMSAab and GRF were respectively r =0.663 (p=0.024) and r=0.699(p=0.014). The images showed focal lesions in the renal parenchyma of 09/12 patients, in 4 of them evident only on SPECT images. **CONCLUSIONS**: DMSAab using SPECT-CT images presents a good correlation with GFR measured by 51Cr-EDTA clearance in patients with SCA. SPECT images are superior to planar images in identifying focal lesions in the renal parenchyma of these patients.

P1101

Impact of SPECT/CT in absolute quantification of 99mTc-DMSA uptake: a head-to-head comparison with planar and SPECT images using 51Cr-EDTA glomerular filtration rate as reference

D. M. Onusic, MSc¹, S. Q. Brunetto, PhD¹, J. Pasquoto², E. M. R. Brunetto², C. M. S. Norberto², N. T. T. P. da Silva, MSc², A. O. Santos, PhD², M. C. L. de Lima, PhD², B. J. Amorim, PhD², E. C. S. C. Etchebehere, PhD², S. T. O. Saad, PhD², C. D. Ramos, PhD²; ¹Center for Biomedical Engineering - University of Campinas, Campinas, BRAZIL, ²Faculty of Medical Sciences - University of Campinas, Campinas, BRAZIL.

KEYWORDS: [99mTc]DMSA, Plasma Clearance, SPECT/CT **INTRODUCTION:** Absolute quantification of 99mTc-DMSA renal uptake (DMSA-Quant) is traditionally calculated using the posterior view of planar acquisitions. SPECT/CT hybrid equipments have been used for accurate and reproducible quantification in different studies such as brain and myocardial perfusion studies, due to an improvement in scatter and attenuation correction. Few reports have mentioned the use of this technology in renal studies. **PURPOSE:** This study aimed to compare DMSA-Quant calculated with SPECT/CT technology with those obtained through static and SPECT acquisitions, using 51Cr-EDTA based glomerular filtration rate (GFR) as the reference method. **MATERIALS AND METHODS:** We studied 16 patients (6 male, 10 female) aged 24–59 years (45.13 \pm 11.41 years) with renal diseases of different etiologies, including diabetes mellitus, sickle cell disease and renal failure of unknown etiology. Doses of 110–180 MBq of 99mTc-DMSA and 10–12 MBq of 51Cr-EDTA were simultaneously injected in all patients and after 3 hours, planar and tomographic (SPECT/CT) acquisitions of the kidneys were obtained. Blood samples were taken 2, 3 and 4 hours after injections and counted in a well counter after 1 week (to ensure 99mTc radioactive decay) to determine 51Cr-EDTA based GFR. The SPECT acquisition followed the protocols described in the literature for calculating DMSA-Quant. A similar procedure was performed for SPECT/CT acquisition and attenuation maps were used for absolute uptake correction. Kidney depth obtained from CT images was also used for DMSA-Quant from planar images. Correlation curves between GFR and each of the DMSA-Quant methods (SPECT/CT, SPECT and static images) were performed. **RESULTS:** The mean GRF values (minimum and maximum) obtained for the 16 patients were 83.3 \pm 29.4 mL/min (31.2 and 128.5 mL/min). The mean DMSA-Quant values for the three methods were: planar images: 38.6% \pm 5.1% (30.4% and 52.5%); SPECT: 38.2% \pm 3.8% (29.1% and 44.3%); SPECT/CT: 38.6% \pm 3.7% (29.7% and 44.2%). The correlation indices between GRF and each DMSA-Quant method (planar, SPECT and SPECT/CT) were respectively: 0.535 (p = 0.0484), 0.688 (p = 0.0041) and 0.752 (p = 0.0008). **CONCLUSIONS:** DMSA-Quant obtained with the SPECT/CT presents higher correlation with GFR and lower dispersion when compared with conventional methods using planar or SPECT images. These results suggest that SPECT/CT technology should be preferred when performing 99mTc-DMSA images for absolute renal function evaluation.

P1102

Usefulness of 18F-FDG-PET-CT on Bladder Cancer

A. I. Gonzalez Ramirez, T. Morales Avellaneda, B. Rodriguez Alfonso, J. Mucientes Rasilla, I. Rodriguez Lizarbe, A. Gomez Grande, M. Beresova, J. Huertas Cuaserna; Puerta de Hierro Hospital, Madrid, SPAIN.

Aim: To assess the usefulness of PET-CT in staging of patients with bladder cancer and in suspicion of tumour relapse. **Materials and methods:** A retrospective analysis was performed reviewing bladder cancer PET-CT studies acquired between January/2009 and March/2012. Only patients with previous CT studies and with histological confirmation were included. **Results:** Seventeen patients with bladder cancer were included (mean age of 68.4 years). Twelve (61%) studies were performed for primary tumour staging. In nine of these patients the CT and PET-CT results were concordant. Four showed regional disease and five were positive for distant disease. Two patients were finally confirmed as metastatic disease, in one patient metastatic suspect disease was ruled out with histological findings and two were confirmed as second primary tumours. Two out of three discordant studies showed absence of findings in CT and metastatic disease in PET-CT that was later confirmed with histological analysis. In the other patient regional disease was describe in CT and metastatic disease was describe in PET-CT. Five patients were referred for suspicion of tumour relapse (29%). Four showed concordant results in CT and PET-CT (three metastatic disease and one regional tumor spread). One study (20%) was positive for regional disease in CT and showed metastatic disease on PET-CT which was probed as true positive in the histological confirmation. **Conclusion:** 18FDG-PET-CT in cases of bladder cancer patients improves initial staging and detection of tumour relapse. It is specially useful in detecting metastatic disease in cases of locally advanced tumours.

P78-2 - Tuesday, October 30, 2012, 16:00 - 16:30, Poster Exhibition Area

Conventional & Specialised Nuclear Medicine: Infection & Inflammation

P1103

The impact of 18F-Fluorodeoxyglucose (FDG) PET/CT in the management of patients with pyrexia of unknown origin (PUO)

P. Harris¹, M. Newport², M. Llewelyn², A. M. Peters³, S. Dizdarevic³; ¹Department of Microbiology and Infectious Diseases, Royal Sussex County Hospital, Brighton, UNITED KINGDOM, ²Department of Microbiology and Infectious Diseases, Royal Sussex County Hospital, Brighton and Sussex Medical School, Brighton, UNITED KINGDOM, ³Department of Nuclear

Medicine, Royal Sussex County Hospital, Brighton and Sussex Medical School, Brighton, UNITED KINGDOM.

Aim: To evaluate the impact of PET/CT and its role in the diagnostic and therapeutic management of patients presenting with PUO. **Methods:** Between March 2010 and May 2011, 13 PET/CT scans were performed in patients presenting with PUO at the Royal Sussex County Hospital in Brighton. Ten patients' notes were retrospectively reviewed. The impact of PET/CT on patient management was classified as a) no impact, b) confirmed proposed management or c) altered management. The impact of PET/CT results on subsequent diagnostic procedures was divided into the following options: confirmed planned investigations; cancelled planned investigations; biochemical investigations requested; imaging requested; invasive investigation requested (for example biopsy or endoscopy); or no impact on investigations. The impact of PET/CT results on subsequent therapy was also recorded as a) therapy upgraded/initiated, b) therapy downgraded or c) no change. PET/CT results were interpreted as to their relevance to the ultimate diagnosis (yes/no). **Results:** All 10 patients had a raised CRP/ESR and only 2 (20%) patients had a raised white cell count at the time of PET/CT scan. Six (60%) patients were scanned as outpatients and four (40%) were inpatients. In nine (90%) cases the use of PET/CT altered patient management. In one patient (10%) PET/CT triggered further biochemical investigations. In 6 (60%) cases PET/CT led to further invasive investigations to aid diagnosis however in 3 (30%) cases PET/CT did not help point towards subsequent diagnostic investigations. In 4 (40%) patients subsequent therapy was upgraded or initiated as a result of PET-CT, while in 6 (60%) cases PET/CT did not lead to a change in therapy. In the final diagnosis of the 10 patients presenting with PUO, four (40%) were explained by a connective tissue disorder, two (20%) by neoplastic conditions, two (20%) by infection (endocarditis and fungal infection), and one (10%) classified as miscellaneous (in this case a thyroid adenoma). The diagnosis remained unknown in two cases (20%) despite PET/CT. In half of the patients the results of the PET/CT were deemed relevant to the final diagnosis. **Conclusion:** PET/CT may change the diagnostic and therapeutic management of patients with PUO. Early use may help localise pathology and direct further investigation to reach a diagnosis more quickly and cost effectively, possibly avoiding invasive procedures, while influencing therapy. Abnormal results must however be interpreted with caution to account for those that may eventually not contribute diagnostically.

P1104

The diagnostic method value of scintigraphy with 99mTc-HMPAO labeled leukocytes in detection of osteomyelitis in various forms of diabetic foot

M. Zorkaltsev, V. Zavadovskaya, O. Kilina, A. Kourazhov, E. Krasilnikova, K. Popov; Siberian State Medical University, Tomsk, RUSSIAN FEDERATION.

The aim of the study was to evaluate the diagnostic value of scintigraphy with labeled leukocytes in detection of osteomyelitis in patients with various forms of diabetic foot (DF). **Material and methods.** The scintigraphy with 99mTc-HMPAO labeled leukocytes (370 MBq, SPECT Philips Brightview) was obtained in 76 patients (35 males and 41 females, aged 59.4 \pm 7.1 years) with diabetes mellitus type I and II, and with suspicion of osteomyelitis in neuropathic form of DF (n=25), mixed neuroischemic form of DF (n=38) and ischemic form of DF (n=13). **Results** were verified by morphological study in 36 patients. **Results.** Accumulation of WBC leukocytes at the area of suspected inflammation was found in 37 (52.1%) cases. First, the results of scintigraphy were analyzed without specifying the localization of inflammation in the bones or soft tissues. In this case, only true positive (TP) (n=37, 48.7%) and true negative (TN) results (n=38, 50%) were obtained almost exclusively. The exception was one (1.3%) false negative (FN) result identified in the ischemic form of diabetic foot. Sensitivity, specificity and accuracy were 97.4%, 100.0%, and 98.7%, respectively. In the case of diagnosis of intraosseous inflammation (the diagnostic criterion was the maximum accumulation of radiopharmaceutical in the projection of the bone), we obtained 25 (32.9%) TP, 38 (50%) TN, 12 (15.8%) false positive (FP) and 1 (1.3%) FN results. FP results were found predominantly for neuropathic (n=5) and mixed forms (n=6) of DF and were caused by difficulty in determining the localization of the pathological accumulation of WBC due to the low resolution of the method and the small size of the object. In patients with ischemic form we found one FP result and one FN result, caused by the lack of accumulation of labeled WBC in an inflammation by reducing blood flow. Sensitivity, specificity, and accuracy were calculated and found to be 96.2%, 76.0%, and 82.9%, respectively. **Conclusion.** Scintigraphy with labeled leukocytes in patients with diabetic foot is highly sensitive and specific method for identifying the existence of an inflammatory process regardless of the soft tissue or bone and of DF form. In the case of diagnosis of intraosseous inflammation the diagnostic significance of the method is reduced, especially in neuropathic and mixed forms: sensitivity, specificity, and accuracy were 100%, 62.9%, 73.7% for mixed and 100%, 55.6%, 68.0% for neuropathic form respectively.

P1105

The role of FDG PET/CT in Fever of Unknown Origin (FUO)

M. CORTES-ROMERA¹, O. Puig Calvo², A. Caresia Aróztegui¹, X. Solanich Moreno³, L. Rodríguez- Bel¹, J. Robles Barba¹, S. Rossi Seoane¹, J. Martín-Comín⁴, C. Gámez Cenzano¹; ¹PET IDI-H.U.BELLVITGE-IDIBELL, L'HOSPITALET (BARCELONA), SPAIN, ²Medicina Nuclear-H.U.B. IDIBELL, L'HOSPITALET (BARCELONA), SPAIN, ³Medicina Interna H.U.B., L'HOSPITALET (BARCELONA), SPAIN, ⁴Medicina Nuclear, H.U.BELLVITGE-IDIBELL, L'HOSPITALET (BARCELONA), SPAIN.

AIM: To assess the utility of 18F-FDG PET/CT in identifying the etiology process of fever of unknown origin (FUO). **MATERIAL AND METHODS:** Seventy two patients with FUO (from 1 week to 2 years) were included in this study from 2005 to 2011. They were 28 women (39%) and 44 men (61%), the mean age was 57 years (range 6-85). All patients underwent a whole body PET/CT at 60-120 minutes after injection of 0.1 mCi/Kg FDG. Five patients were under corticosteroids or antibiotics treatment. The results were compared with the final diagnosis based in the histopathology, microbiological assays, clinical and/or imaging follow up. PET/CT was considered clinically helpful when positive results contributed to the final diagnosis. **RESULTS:** Fifty one out of 72 patients had a positive scan (71%), the remaining 21 were negative (29%). In 40 out of 51 positive scans, PET/CT helped in identifying the cause of fever (79%) and they were classified in: infection (18), noninfectious inflammatory processes (11), neoplasm (8), and miscellanea (3). In 7 out of 11 remaining patients (false positives), the fever disappeared spontaneously without treatment and identifying the etiology. Concerning the 21 patients who had negative scan: in 8 fever disappeared during follow-up, 5 had a non-infectious inflammatory disease and 7 had diseases with non FDG avidity and/or behind the resolution limit of the equipment, and 1 drug fever. All 5 patients under treatment had a negative scan. PET/CT contributed to the final diagnosis in 56% of the patients (40/72). **CONCLUSION:** FDG-PET/CT helped to identify the etiology of FUO in patients with positive PET/CT findings (79%) and contributed to the final diagnosis in 56% of the patients.

P1106

Evaluation of vascular prosthetic graft infection by 18F-FDG PET/CT

A. M. Alvarez, J. Nogueiras, C. Martinez, D. Portela, D. Ruiz, A. M. Lopez, R. Guitián; University Hospital Complex of Vigo (CHUVI), Vigo, SPAIN.

Objective: To determine the role of 18F-FDG PET/CT in the assessment of vascular prosthetic graft infection. **Method:** Prospective cohort study with retrospective analysis. Assess to 8 patients with clinically suspected vascular prosthetic infection underwent a 18F-FDG-PET/CT scan. Angiography studies and Tc99m-HMPAO labeled leukocyte scintigraphy results were correlated with PET/CT uptake. The gold standard was based on operative/histopathological finding or a clinical follow up of >6 months. **Results:** A total of 8 patients (5 men and 3 women), with a mean age 61 ± 13.6 years and range 38-77. The location of the graft prosthesis was: Aorto-bifemoral (5), Aorto-iliacal (1), Femoro-popliteal (1) and Thoraco-abdominal (1). Seven patients presented pathological uptake in PET/CT and according to operative/histopathological findings or a clinical follow up presented vascular prosthetic graft infection. The mean SUV max was $6.4 \text{ g/ml} \pm 1.8$ and range 4.0-9.0. Positive findings for infection were observed at angio-CT or angio-MRI. However, three cases evidenced negative Tc99m-HMPAO labeled leukocyte scintigraphy. Only one patient demonstrated a negative PET/CT, concordance to a normal angio-MRI and nonclinical signs of infections at follow up for one year. **Conclusion:** PET/CT-FDG is a useful tool in the diagnosis of vascular prosthetic graft infection with excellent accuracy. The concordance between angiography studies and the tomography functional scan was high; however, the Tc99m-HMPAO labeled leukocyte scintigraphy was not helpful for the detection of vascular prosthetic graft infection.

P1107

18F-FDG PET scan in patients with IgG4-related disease: Usefulness to identify multiple organ involvements

A. Inaki, K. Nakajima, T. Mochizuki, M. Kawano, S. Kinuya; Kanazawa University Hospital, Kanazawa, JAPAN.

IgG4-related disease (IgG4-RD) is an autoimmune systemic disease which has been recognized in recent several years. It affects multiple organs including pituitary gland, lung, liver kidney, para-aorta, exocrine glands such as lacrimal glands and salivary glands. Because of the variety of symptoms, it is often difficult to diagnose affected organs of IgG4-RD. We investigated the diagnostic value of 18F-FDG PET/CT for the assessment of IgG4-RD compared with CT and MRI. **METHOD:** Fourteen patients who underwent 18F-FDG PET scan were retrospectively evaluated and then were diagnosed with IgG4-RD. **RESULTS:** Elevation of serum IgG4 level were observed in 13 patients (93%). In CT or MRI scan, abnormal findings

were detected in all patients, while abnormal FDG accumulation of any organ which can be a target organ of IgG4-RD in 13 patients (93%). Because of lack of symptoms such as swelling of glands, five CT and four MRI scan did not include information of those organs. In contrast, abnormal FDG accumulations were observed in 6 patients (43%) in lacrimal gland, 6 (43%) in salivary glands, 1 (7%) in lungs, 1 (7%) in liver, 4 (29%) in pancreas, 3 (21%) in kidneys and 5 (36%) in para-aortic fibrosis, respectively. Abnormal accumulation of lacrimal glands were identified in 2 patients even without any symptoms such as exophthalmos. Two patients without any findings of pancreas in CT or MRI scan showed a high pancreatic FDG uptake. On the other hand, 2 patients with abnormality of kidney in CT scan showed normal distribution of 18F-FDG in kidney. **CONCLUSION:** Sensitivity of 18F-FDG PET was higher than that of CT and MRI in exocrine gland, whereas lower in kidney. 18F-FDG PET appears good diagnostic tool for whole-body assessment in patients with IgG4-RD even without overt symptom, but other modalities should be appended for the evaluation of some organs.

P1108

18F-FDG PET-CT - an evolving role in management of tuberculosis

S. Singla, R. Kumar, C. S. Bal, V. S. Dhull, S. S. K C, P. Sharma, T. Jain, M. Sahoo, A. Malhotra; All India Institute of Medical Sciences, New Delhi, INDIA.

AIM : To assess the role of 18F-FDG PET-CT in evaluation of lesion extent, treatment response and identification of re-activation of latent disease. **MATERIALS AND METHODS:** Eighty-six patients of known tuberculosis underwent a total of hundred and three 18F-FDG PET-CT study. Seven patients were subjected to one follow-up and five cases to second follow-up study. 45 studies were performed for response to anti-tubercular therapy, 39 studies for disease extent and 19 studies for detection of reactivated dormant lesions. The study cohort comprised of 30 cases of genito-urinary, 17 cases of skeletal, 17 cases of disseminated tuberculosis, 14 cases of tubercular lymphadenitis, 7 cases of pulmonary tuberculosis and one patient of tubercular meningitis. Whole-body studies extending from base of skull to mid-thigh were acquired on dedicated PET-CT system (Siemens Biograph 2) 45 minutes after administration of 370 MBq of 18F-FDG. All the scans were interpreted by two experienced nuclear medicine physicians. **RESULTS :** Thirty-one males and 55 females of mean age 34.3 ± 13.9 years were recruited into study. The patients had received anti-tubercular treatment for a median duration of 18 months. A significant change in management of 65 patients who underwent 74 studies was brought about by 18F-FDG PET-CT. There were 62 true positive, 35 true negative and 6 false negative studies. The true negative studies comprised of 16 tubo-ovarian masses, 11 healed cold abscess, 5 residual lymph nodal masses, 2 cases of disseminated tuberculosis and one case of lung tuberculosis visualized on conventional imaging but with FDG uptake equal to background. Cerebral lesions and microscopic disease were not detected in three patients each which were categorized as false negatives. FDG PET-CT played a pivotal role in restarting or stopping of on-going treatment of 45 patients as well as in 18 patients with suspicion of activation of latent disease which was significantly higher than altering management in 11 patients referred for assessment of disease extent ($p < 0.0001$). **CONCLUSION:** 18F-FDG PET-CT has an important role of in evaluation of lesion extent, treatment response and identification of re-activation of latent disease. Tuberculosis is a common cause of false-positives on FDG PET-CT when patient is referred for malignancies. However, FDG PET-CT can be used to tailor the treatment of tuberculosis particularly in resistant and relapsed cases.

P79-2 - Tuesday, October 30, 2012, 16:00 - 16:30, Poster Exhibition Area

Conventional & Specialised Nuclear Medicine: Bone & Musculoskeletal

P1109

Bone SPECT/CT of the Back After Lumbar Surgery

R. García Jiménez, J. Valencia Anguita, J. Luis Simón, D. García Solís, R. Vázquez Albertino; Hospital Universitario Virgen del Rocío, Seville, SPAIN.

PURPOSE: It may be difficult to evaluate back pain in patients who have undergone spinal surgery, because symptoms may be secondary to all the possible abnormalities in patients who have not had surgery plus postoperative complications, including infection, unstable fusion sites, or transfer of biomechanical stresses to other regions. SPECT fused with computed tomography (CT) provides a new approach for more accurate diagnosis of pseudarthrosis after spinal fusion procedures. The aim of this study was to compare the findings of SPECT fused with CT (SPECT/CT) with those of CT alone for the diagnosis of pseudarthrosis. **MATERIALS AND METHODS:** Twenty-three patients, (mean age = 50.43 years (range 27-72), 9 females/14 males) with back and/or leg pain and a history of lumbar spinal surgery had bone SPECT/CT examinations. All had previously undergone anterior and/or posterior lumbar fusion techniques.

Presence of screw loosening, nonunion through or around the cages, and facet joint degeneration were assessed for diagnosis of pseudarthrosis. The clinical follow-up (mean, 12.9 months; range, 4–21 months) was evaluated according to Macnab criteria (excellent, good, fair, poor). **RESULTS:** Bone SPECT/CT excluded bony abnormalities in the operative site in 4 patients. All patients showing screw loosening on CT alone showed also an abnormal uptake on SPECT/CT. SPECT/CT was able to show increased uptake in 12 cases in which CT alone did not show pathology. SPECT/CT was able to show sacroileitis in 4 patients. **CONCLUSIONS:** In the lumbar spine, SPECT/CT seems to increase specificity and sensitivity than CT alone for detection of pathology (nonunion of interbody devices compared, facet joint degeneration, screw loosening and sacroileitis). These findings can be helpful for surgeons in planning appropriate surgical revision strategy.

P1110

Normal frontal bone uptake (FBU) seen on radionuclide scintigraphy. Age and sex-related variations.

A. Doumas¹, I. Iakovou¹, V. Balaris¹, D. Bounas², T. Christiforidis¹, V. Nikos¹, D. Lo Presti¹, S. Georga¹, N. Karatzas¹, ¹3d Nuclear Medicine Dept. of the Aristotle University, General Hospital "G. Papageorgiou", Thessaloniki, GREECE, ²"Hippocrates" Nuclear Medicine Center, Thessaloniki, GREECE.

Skull involvement in benign and malignant disorders is rare. **The aim** of this study was to identify normal variations of frontal bone uptake (FBU) and to investigate any age or sex-related variations. **Method:** All whole-body bone scans performed during the last year were evaluated. Skull was imaged at the anterior, posterior and lateral views. **Results:** A total number of 1132 bone scans were performed. One hundred twenty eight cases with known or obvious skull involvement due to metastases, or any other pathology (known metabolic bone disease, trauma, inflammation etc) were excluded. A final number of 1004 scans were evaluated (632 women). All the cases were divided into 3 age groups: Less than 30, 30–60 and more than 60 years of age. Three patterns of FBU were recognized: A. Diffuse symmetrical frontal bone uptake, B. Diffuse symmetrical frontal, temporal and parietal uptake and C. Focal (spot-like) or diffuse uptake in any of the three bones asymmetrically. **CONCLUSION:** No difference in FBU was appreciated among male population over 30 years of age. On the contrary, FBU was more evident among female patients; being almost entirely an old-age phenomenon. The most common type of FBU was the diffuse symmetrical frontal bone uptake.

P1111

The comparison of data from anteroposterior, lateral and midlateral projections in postmenopausal women: Preliminary results

S. S. Gultekin¹, S. Lacin¹, A. Dilli², ¹Diskapi Yildirim Beyazit Training and Research Hospital, Department of Nuclear Medicine, Ankara, TURKEY, ²Diskapi Yildirim Beyazit Training and Research Hospital, Department of Radiology, Ankara, TURKEY.

Aim: Bone mineral density (BMD) test with dual energy x-ray absorptiometry (DEXA) method are performed typically on anteroposterior (AP) projection in fracture risk assessment of lumbar spine. However, AP measurements may be affected by vascular calcifications, differences in the central and peripheral bone loss and in abdominal fat tissue content and pathologies belonging to posterior vertebral elements. In this study, we made a comparison among the AP, lateral (LAT) and midlateral (MLAT) projections using total vertebral BMD and T-score values in postmenopausal women. **Materials and Methods:** The study group included 109 postmenopausal women (mean age; 57 ± 8 yrs) who were made lumbar vertebra BMD measurement with DEXA method. Total BMD and T-score values for the AP, LAT and MLAT were calculated. MLAT projection images were derived from the region of interests which was drawn over the LAT projection images. The patients were classified as normal (T-score > -1), osteopenia (≤ -1 T-score < -2.5) and osteoporosis (T-score < -2.5) according to World Health Organization (WHO) criteria. All results were analyzed statistically. **Results:** When the patients were evaluated by respectively AP, LAT and MLAT the final result was normal in 20/109 (18.3%), 7/109 (6.4%) and 7/109 (6.4%) patients, was osteopenia in 53/109 (48.6%), 42/109 (38.5%) and 36/109 (33.0%) patients and was osteoporosis in 36/109 (33.0%), 60/109 (55.0%) and 66/109 (60.6%) patients. The values of total BMD and T-score were found as follows; 0.826±0.115 and -2.1±1.1 for AP, 0.627±0.101 and -2.6±1.2 for LAT, 0.582±0.128 and -3.0±1.4 for MLAT. When the average values of total BMD and T-score were compared the difference was statistically significant (p<0.001) for all groups (AP vs. LAT, AP vs. MLAT and LAT vs. MLAT). **Conclusion:** LAT and M-LAT measurements seem to may play a complementary role on AP measurements.

P1112

Added Value of SPECT-CT to Planar Bone Scintigraphy the Vertebral Column Pathology

C. Gamazo¹, P. García-Talavera¹, A. Sainz-Esteban¹, M. A. Ruiz¹, M. L. González², R. Olmos¹, P. C. García², A. Gómez²; ¹Department of nuclear medicine. Hospital Clínico Universitario de Valladolid, Valladolid, SPAIN, ²Department of Radiology. Hospital Universitario Río Hortega, Valladolid, SPAIN.

AIM: to evaluate the contribution of SPECT-CT to conventional imaging (planar bone scintigraphy -BS-) in the pathology of the spine. **MATERIAL AND METHODS:** From April 2010 to December 2011, BS and SPECT-CT were performed (SIEMENS, Symbia T2) on 45 patients (23 females, mean age= 61.9 +/- 15.1 years old). 13 of them were referred for benign bone pathology (5 for osteoarthral pain, 3 for spondylodiscitis and 5 for other causes) and 32 for malignant pathology (evaluation of bone metastatic disease in cancer (breast n=14, prostate n=4, lung n=6 and others n=8)). The indication to perform SPECT-CT was the evaluation of a detected lesion in other imaging tests not visualized in the BS and the assessment of a non-specific pathological focus. Referred to the last one, in the malignant pathology, the patients were divided into two groups. The group A, probably malignant or probably benign, and group B, with undefined diagnostic (malignant vs benign). The foci were confirmed with other imaging test (TC or MR) and the clinical follow-up (11,3 +/- 4,8 months). **RESULTS:** In 35 patients (77,8 %) SPECT-CT improved the information given by BS (53,8 % in the group of benign pathology and 87,5 % in the malignant group). For benign pathology SPECT-CT did not show new foci (sensitivity of 100% for both techniques) but dismissed three foci showed in the planar imaging (specificity of 66,6 % for BS and of 88,8 % for SPECT-CT). Besides, in two cases it improved the localization of the foci in BS and in 5 cases confirmed the suspicion of BS. In the group of malignant pathology, it showed new foci in three patients (sensitivity of 87% for BS and of 97% for SPECT-CT). From the group A, SPECT-CT confirmed the suspicion of BS in 14 patients and changed the initial diagnosis in 7 patients. In 4 patients from group B, it achieved to take a diagnostic decision (malignancy or benignity). **CONCLUSION:** Bone SPECT-CT is a valuable tool for the diagnosis of the bone spine pathology, especially in malignant disease, confirming doubtful cases, detecting new foci and even changing the diagnostic of BS.

P1113

Utility of bone scintigraphy in the response assessment and prognostification of advanced prostate cancer (APC) after orchiectomy

J. Kumar, S. Santhosh, A. Sood, A. Bhattacharya, B. Singh, B. R. Mittal; PGIMER, Chandigarh, INDIA.

Objective: To determine the utility of bone scintigraphy in the response assessment and prognostification of advanced prostate cancer (APC), after androgen ablation therapy by orchiectomy. **Methods:** Whole body bone scans of 37 patients (mean age: 62.21 yrs, range: 40 to 80 yrs) diagnosed with APC, who underwent bone scintigraphy as a part of initial staging and follow up (FU) scan after orchiectomy were retrospectively analyzed. Bone scan index (BSI) was calculated for each scan and compared with corresponding PSA levels. **Results:** All 37 patients showed skeletal metastases in the initial bone scan. The duration from orchiectomy to the FU scan ranged from 3 to 9 months. 21 / 37 patients (57%) showed disease resolution (responders) along with drop in PSA level. The median PSA level and mean BSI in pre and post orchiectomy were 71.8 & 15 and 35 & 29.7 respectively. 10 patients (27%) showed progression of disease (non-responders) with significant rise in PSA level in FU scan after orchiectomy. The median PSA level and mean BSI in pre and post orchiectomy were 58 & 161.5 and 20 and 34.75 respectively. Six patients (16%) showed significant decrease in PSA level (median pre and post orchiectomy level was 91 and 64 respectively) following orchiectomy; however, bone scan showed no significant change in the lesions (stable disease); mean BSI in pre and post orchiectomy was 34 and 36.5 respectively. There was good correlation between the PSA level and BSI in the responders and non-responders (p < 0.05). However in stable disease group, fall in PSA was not associated with response in bone lesions. Out of 27 patients who showed fall in PSA in initial FU scan, only 21 patients (78%) showed bony response. ROC analysis of PSA for disease progression showed a cut-off of < 300 with sensitivity of 100% and specificity of 30% (p=0.33), whereas BSI cut-off of < 17 had 50% sensitivity and 88% specificity (p=0.001). 11 / 21 cases (52%) with resolution in the initial FU scan, showed progression in subsequent scans (range: 1–5yrs). The median PSA level and mean BSI at pre-orchiectomy, post orchiectomy and FU were 100, 50 & 320 and 38, 32.2 & 49.75 respectively. **Conclusion:** Fall in PSA following orchiectomy may not indicate bony response in 22% of patients. Before orchiectomy, BSI can significantly predict development of progression compared to PSA level. In long run 50% of responders become androgen independent with disease progression.

P1114

Role of Tc99m MDP bone scan in evaluation of avascular necrosis of femur head in post operative cases of intracapsular fracture neck femur.

S. S. Nilegaonkar, M. Khadilkar, D. Sonawane, V. Nemade, S. Sonar; Smt Kashibai Navale Medical College and general Hospital, Narhe, Pune, INDIA.

The occurrence of avascular necrosis (AVN) of the femoral head in a case of intertrochanteric fracture of the femur is a rarely reported entity. The patients develop a painful hip due to AVN of the femoral head after fixation for the intertrochanteric fracture of the femur. Hence AVN of the femoral head a rare but distinct possibility in a case of intertrochanteric fracture of the femur. Diagnosis of AVN is mainly clinical. Computerized tomography cannot be relied upon because of artifacts associated with metallic implants. MRI cannot be performed in such cases because of metallic implant in situ. Total 10 patients were studied. Along with X ray hip, we performed 3 phase Tc99m MDP bone scan with SPECT in such patients. Patients were treated depending upon results of bone scan and clinical evaluation. Patients with demonstration of AVN on bone scan and high clinical suspicion for AVN were operated using bipolar prosthesis. Femoral head were sent to histopathology for confirmation of AVN. Other patients who were treated conservatively were followed up for 2 years. Out of 9 patients, bone scan correctly identified AVN in 3 patients which were confirmed by histopathology reports. 1 patient lost follow up. One patient, who was diagnosed as AVN post operative 2 years, improved after implant removal and is asymptomatic on clinical follow up. 4 patients showed no evidence of AVN in operated femur and on clinical follow up, these patients are doing well and asymptomatic at present. Three phase bone scan with SPECT is useful tool in evaluation of AVN in the post operative patients with implant in situ. Negative predictive value of bone scan is useful for taking decisions regarding clinical management with conservative approach. Demonstration of AVN with bone scan is useful for documentation and for making surgical decision. In clinical settings of implant in situ in which conventional imaging modalities like CT scan and MRI are difficult to perform, three phase bone scan can be a good diagnostic tool for evaluation assisting in early diagnosis and prompt institution of treatment.

P1115

Bone scan findings in Schnitzler Syndrome: analysis of a single center cohort of 14 patients.

C. Ansquer, C. Bodet-Milin, T. Eugène, M. Hamidou, S. Barbarot, A. Masseau, J. Berthelot, F. Kraeber-Bodéré, A. Néel; university hospital, Nantes, FRANCE.

Aim: Schnitzler syndrome (SS) is a rare entity, defined by the association of chronic urticaria, monoclonal gammopathy (IgM Kappa), systemic inflammation and musculoskeletal involvement (arthralgia, bone pain and osteoclerotic lesions). Whereas bone lesions have a high diagnostic value, their frequency remains unknown. Further, only few cases reports have underlined the interest of bone scan (BS) in this setting. The aim of our study was to report BS findings and its diagnostic value in a cohort of 14 patients with SS. **Materials and methods:** Between June 2000 and Jan 2012, all patients assessed in internal medicine, dermatology and rheumatology departments of our institution were investigated by BS. The diagnostic of SS relied on the classical Lipsker's criteria. The cohort comprised 14 patients including 9 men and 5 females, with median age 67 years. Clinical manifestations of SS were present since a few months to 7 years (median: 2 years). Nine patients (64%) had musculoskeletal pain. All patients underwent a total of 22 (1 to 5) planar whole body BS at diagnosis and/or during the follow-up. SPECT-CT was performed in 5 cases. All scintigraphic procedures were reviewed by a senior nuclear medicine specialist blinded to clinical data. **Results:** BS showed suggestive increased tracer uptake in 9 / 14 patients: a total number of 48 foci were detected, with a median number of 4 foci / patient (1 to 10). Among them, 44 were located on long bones of upper and lower limbs and showed a bilateral and asymmetrical distribution. Four foci involved a single iliac bone without any other foci in 3 cases. SPECT-CT confirmed that BS abnormalities were associated with osteosclerosis. Neither the intensity nor the extension of uptake correlated with disease duration. Spontaneous changes of BS findings were observed in 2 patients followed 2 and 10y. Interestingly, BS appeared to be more sensitive than clinical assessment for the detection of bone involvement. Indeed, among 5 patients who had no musculoskeletal pain, 2 exhibited suggestive abnormalities on BS. Conversely, only 2/9 patients with musculoskeletal pain had normal BS. Of note, both patients had arthralgia without bone pain. **Conclusions:** Two third of SS patients exhibit typical foci on BS, involving appendicular skeleton and/or iliac bone. This whole body scan procedure is a valuable tool for the recognition of bone involvement. BS can be informative even in patients lacking musculoskeletal symptoms and may help the identification of this under-recognized entity.

P1116

Review of Painful Prosthetic Joints Undergoing Nuclear

Medicine Imaging and Conventional Radiology at East Kent University Hospitals, United Kingdom.

S. Lewitschnig, P. Jackson, G. Shabo; Kent and Canterbury Hospital, Canterbury, UNITED KINGDOM.

Aim Patients with painful hip or knee prosthesis are often referred for Nuclear Medicine Imaging to assess peri-prosthetic infection or loosening. Bone scans and Indium labelled white cell scans with or without bone marrow imaging are performed to help differentiating between septic and aseptic loosening. This review looks at the concordance of these investigations with conventional radiology and the impact on clinical outcome. **Methods** We reviewed retrospectively 56 patients, half with hip and the other half with knee prosthesis, who had both bone and Indium labelled white cell scans with or without bone marrow scans at East Kent University Hospitals. These studies were then compared with conventional radiology findings. The comparison was carried out by a dual trained specialist in Radiology and Nuclear Medicine, using CRIS (radiology and imaging electronic system), PACS and Patient Centre Information (electronic records and ordering system). **Results** 56 patients (31 female and 25 male; mean age 75 years). 28/56 had hip and 28/56 had knee replacement. The average time post joint replacement was 36.3 months (2.5 months to 13 years). 51 patients had additionally a bone marrow scan. The results showed 8 infections, 30 aseptic loosening and 15 active remodelling. 1 scan showed synovitis as a cause of the patient's pain and 2 scans were completely normal. 7/8 with infection had a normal corresponding X-ray. The average time post surgery in the infected joints was 47.4 months (4-156 months). 18/30 with aseptic loosening had a corresponding abnormal X-ray. The average time post surgery in patients with aseptic loosening was 43.8 months (6-156 months). 13/30 with aseptic loosening underwent surgical revision. Interestingly these 13/30 patients had concordant investigations on radioisotope scanning and conventional radiology. Furthermore, 51/56 had conjoint bone marrow study with Indium white cell scans. 5/51 showed discordance and the remaining had concordant results. **Conclusion** Nuclear Medicine Imaging is helpful in determining septic and aseptic loosening of the prosthetic joint. It appears to be superior to conventional radiology in assessing periprosthetic sepsis. Bone marrow imaging definitely adds to accuracy in infection. In aseptic loosening Nuclear Medicine Imaging helped in confirming conventional radiology findings, thus increasing clinicians confidence in proceeding with surgical intervention.

P1117

The added value of SPECT-CT in equivocal bone lesions noticed on planar scintigraphy

C. J. P. Gaspar, A. H. Dias, S. Pintão, T. Martins; Centro Hospitalar Lisboa Ocidental - Hospital Santa Cruz, Lisboa, PORTUGAL.

The aim of this study was to investigate the incremental value and diagnostic impact of SPECT/CT in patients who present equivocal bone lesions in planar bone scintigraphy. **Methods:** Forty-two patients with 69 indeterminate lesions on planar scintigraphy underwent SPECT/CT imaging between August 2011 and March 2012. Whole-body, spot views, SPECT and CT images were independently evaluated by two readers, sequentially by this order. Two independent reviewers initially classified lesions as "probably malignant", "doubtful" and "probably benign" and sequentially evaluated them in order to determine the incremental value of SPECT and CT in clarifying doubtful lesions or reassuring/modifying first impressions about probably benign or malignant lesions. **Results:** There was a diverse variety of primary tumors, including breast cancer (n=17), lung cancer (n=9), colon cancer (n=5), prostate cancer (n=3) and non-neoplastic causes (n=3). Lesions were localized in vertebrae (57%), pelvis (15%), ribs (13%) and other locations (15%). On planar study reporting, reviewers rated 16 lesions as "probably malignant", 24 "doubtful" and 29 "probably benign". By adding SPECT reviewers confirmed their opinion in 26, modified their opinion in 6 and maintained in 37. When analysing SPECT-CT there were further confirmation in 57, change of opinion in 1 and 11 remained (doubtful). **Conclusion:** The use of SPECT and SPECT-CT resulted in a significant reduction of equivocal reports and allowed for increased confidence in diagnosis. In some cases it actually lead to modification of the initial opinion. While SPECT alone already brings benefit, the addition of CT resulted in a more significant reduction in doubtful studies.

P80-2 - Tuesday, October 30, 2012, 16:00 - 16:30, Poster Exhibition Area

Conventional & Specialised Nuclear Medicine: SLN (Sentinel Lymph Node)

P1118

Preoperative Identification of Sentinel Node in Head and Neck Tumors. Impact of SPECT-CT Imaging

M. Bellón Guardia, M. Talavera Rubio, B. Gonzalez García, A. Palomar Muñoz, V. Poblete García, A. García Vicente, J. Cordero García, A. Soriano Castrejon; Hospital General, Ciudad Real, SPAIN.

OBJECTIVE: To evaluate the usefulness of tomographic images of SPECT-CT versus planar imaging of the lymphoscintigraphy for identification of sentinel node (SN) in patients with head and neck cancer (HNC). **MATERIAL AND METHOD:** 14 patients were included prospectively (PI 2010/63) suffering from a HNC stage clinical and radiological T1-2N0, diagnosed by FNA and scheduled for excision and elective node dissection. Preoperative lymphoscintigraphy was performed 2-3 hours before surgery after perilesional injection of four doses of 9MBq of 99mTc-nanocolloid obtaining planar and tomographic (SPECT-CT) images, identifying and comparing the number and anatomical location of the SN obtained in both acquisitions as cervical levels (I-V). **RESULTS:** The SN detection was possible in all patients with a detection rate of 100%. The number of detected SN in planar imaging was identical to the SPECT-CT with an average of 2.5 per patient (range 1-5). However SPECT-CT provided better anatomical localization of the SN versus planar scintigraphy regarding to surgical anatomical location. We also found a total agreement of the locations on preoperative SPECT-CT with intraoperative localization of the SN, facilitating their removal. **CONCLUSION:** The SPECT-CT provides invaluable assistance in locating the SN, which is very important before node dissection, finding in our study an excellent surgical correlation.

P1119

The role of lymphoscintigraphy and Sentinel Node Biopsy in the clinical and surgical management of melanoma patients

A. Niccoli Asabella, M. A. Renna, A. Mastroiello, A. Nicoletti, C. Altini, F. luele, G. Rubini; Nuclear Medicine Unit, University of Bari "Aldo Moro", Bari, ITALY.

Aim The tumor-harboring status of the sentinel node (SN) is the most important prognostic factor for patients with early stage melanoma. The aim of this study is to evaluate the importance of preoperative lymphoscintigraphy for the identification of "unexpected" sentinel lymph nodes (UnSLNs) outside of the classic basins because these nodes pose the same risk of metastatization as SN in the usual basins. According to literature, the usual basins include the cervical, axillary and inguinal lymph node chains. In addition, isolated or small groups of lymph nodes may be found anywhere in the body (epithroclear, popliteal, jugular, scapularis region and other sites). **Materials and Methods.** From February 1998 to March 2011, 424 melanoma patients treated at the Department of Plastic and Reconstructive Surgery of Bari University Hospital were enrolled in the study. All patients with lesions between 0.75 and 4 mm (Breslow thickness) underwent preoperative lymphoscintigraphy with 99mTc-labeled human albumin colloid (18-22 MBq, intradermal injection around the scar); dynamic and planar images (anterior, posterior and lateral) were acquired using the dual-headed gamma camera, immediately after the radiopharmaceutical injection. On the same day patients were submitted to sentinel node biopsy (SNB). **Results.** A total of 48 UnSLNs were found and removed in 42 of the 424 patients. 4/42 were located in the popliteal area, 2/48 in the epithroclear region (4.1%), 8/48 in scapularis region (16.6%), 9/48 in lateral-dorsum region (18.7%), 7/48 in iliac region (14.5%), 5/48 in occipital region (10.4%), 2/48 in paravertebral region (4.1%), 6/48 in retro-auricular region (12.5%) and 1/48 in jugular region (2%), 2/48 in parasternal region (4.1%), 2/48 in intramammary region. 10/48 (20.8%) of these UnSLNs were positive for metastasis, in particular, 9/10 positive for micro-metastasis; 1/10 positive for macro-metastasis. **Conclusions.** Lymphoscintigraphy is an essential tool in identifying one or more SNs. Sometimes the lymphatic pathway is unusual and not predictable based on clinical or instrumental (ultrasonography, MRI) grounds. If the UnSLNs had been missed at the time of lymphoscintigraphy and SNB, these patients would have been under staged and the residual tumor would have remained, posing a high risk for future regional or distant metastasis. The lymphoscintigraphy remains the most reliable technique for the detection of SNs, early staging of melanoma and in the clinical and surgical management of melanoma patients to decide on the type of surgical approach and treatment, based on histological examination result of SLN.

P1120

Radioguided Surgery for Nonpalpable Breast Carcinoma: Our Institute Experience

A. M. Alvarez, D. M. Ruiz, A. Serena, A. M. Lopez J. Barandela, G. De Castro, A. De La Orden, J. C. Alvarez, R. Mallo, R. Guitian, L. Campos; University Hospital Complex of Vigo (CHUVI), Vigo, SPAIN.

AIM: To analyze the initial results from the implementation of the radioguided surgery techniques (ROLL and SNOLL) for nonpalpable breast carcinoma in our institution. **PATIENTS AND METHODS:** Review of 50 medical records of patients with nonpalpable breast carcinoma scheduled for conservative surgery and sentinel lymph node biopsy. In all cases we applied the technique SNOLL (Sentinel Node and Occult Lesion Localization), except for two patients scheduled for ROLL (Radioguided Occult Lesion Localization). The procedure for SNOLL was the

injection of two radiotracers: 99mTc-MAA (for tumoral localization) and 99mTc-nanocolloids (for sentinel node localization). For ROLL technique, we only injected 99mTc-MAA. We included the risk factors for breast cancer, pre-surgical studies, description of the technique used (ROLL / SNOLL), scintigraphy and surgical findings and subsequent histopathology results, performing statistical analysis using Epidat v.3.1. **RESULTS:** 100% of cases were women with a mean age of 59.8 ± 11 years. Only 14 cases were in pre-menopausal status. 32% had risk factors for breast carcinoma. Most breast lesions were non-palpable nodules, followed by parenchymal distortion and only one case of microcalcifications. MRI tumor size was 13.2 ± 5.3 mm. The injection of the radiotracers was performed in 85% under ultrasound guidance. For SNOLL patients, the intratumoral injection of the both tracers was preferred in 80% of cases. The tumor localization was detected correctly in all cases at the lymphoscintigraphy, except for one patient with possible failure of the radiotracer due to defective labeling. Nine patients required a subareolar re-injection of 99mTc-Nanocolloids due to no evidence of lymphatic migration or mild uptake at the sentinel nodes. In the surgical procedure, 38% patients required a margin expansion of the tumorectomy due to proximity of the primary lesion (four patients had tumor margin involved). Despite the above, on the 100% of the cases was detected the sentinel node/s (two cases that showed no activity despite subareolar reinjection, were detected by blu-dye intraoperative staining), with evidence of metastases only in four patients proceeding to axillary dissection. **CONCLUSIONS:** Our data demonstrate that ROLL/SNOLL techniques are useful for detecting non-palpable lesions and for localize the sentinel node in breast carcinoma patients, with the advantages that these procedures offer instead of the usual hookwire.

P1121

Impact of SPECT/CT in Lymphoscintigraphy of Head and Neck Squamous Cancer

M. Z. Gaino, C. T. Chone, A. O. Santos, M. C. L. Lima, E. C. S. C. Etchebehere, F. A. Hungaratto, C. D. Ramos, B. J. Amorim; State University of Campinas (Unicamp), Campinas, BRAZIL.

Introduction: The vast majority of head and neck cancers arises in mucosa of upper aerodigestive tract and are predominantly squamous cell carcinomas (SCC). About 30% to 40% of patients with head and neck SCC are diagnosed at early stages (T1 and T2). Early diagnosis of lymph node micrometastases ensures a significant improvement in prognosis of these patients. Lymphoscintigraphy has been used to localize the sentinel lymph node (SLN). The new technology SPECT/CT (single photon emission computed tomography fused with a computed tomography) can help in precise the anatomical location of the SLN. **Objective:** To evaluate the impact of SPECT/CT compared to planar images in lymphoscintigraphy in the localization of SLN from head and neck SCC. **Material and Methods:** It was studied 18 patients (13 men and 5 women), mean age 65 ± 12 years (46 a 90 years) with diagnosis of head and neck SCC. All patients had early stages cancer, with clinically negative neck and indication to lymphoscintigraphy. In each patient were made 1-2 peritumoral injections of 99mTc-phytate, 0.08 a 0.2 mCi in each syringe. After about 20 minutes were performed planar images in anterior and lateral projections from head and neck region. Then, it was performed SPECT, one step each 6 degrees performing 360 degrees, and then CT images with low radiation dose of 60 mAs. After images, patients were referred to surgical center where radioactive SLN were identified and removed with a probe help. The radiation was confirmed in the ex vivo lymph node. **Results:** During surgery, were identified 38 SLN. Of these, planar images identified 31 (82%), SPECT/CT images identified 36 (95%) (including all 31 seen in planar imaging) and 2 (5%) SLN were identified only with probe during the surgery. In the analysis of individual patients, SPECT/CT increased the number of SLN detected in 3/18 patients (16%). In addition, the SPECT/CT images allowed the accurate localization of SLN determining their cervical levels, which became surgery easier and faster. **Conclusion:** SPECT/CT images are more sensitive than conventional images in lymphoscintigraphy of head and neck cancers SCC. Moreover, different from planar images, SPECT/CT can precisely localize the SLN, which facilitates surgical resection. More studies are needed to confirm these findings.

P1122

Sentinel Lymph Node in melanoma of the head and neck

P. Paredes-Rodríguez, J. Castro-Beiras, A. Crespo-Diez; Hospital Sanitas La Moraleja, Madrid, SPAIN.

Aim To evaluate the differences between sentinel lymph node (SLN) detection in melanoma of head and neck (MNH) in comparison to melanoma in other locations. To analyze in our experience the more frequent location of the primary lesion, to determine whether detection of MNH-SLN is a more difficult technique than melanomas at other sites. Patients with MNH provides an special anatomic consideration because they often have multiple SLNs and an unpredictable pattern of involvement. **Material and methods** Detection of SLN has been performed in 188pats with melanoma, 41/188 were MNH. The more frequent site was scalp, with a male predominance. Almost all patients had previously undergone excision

or biopsy of the lesion, classified into N0 (TNM-staging). All patients underwent preoperative lymphoscintigraphy within 24 hours previously to surgery to identify the SLN and in-transit lymph nodes. There were performed dynamic scans of all nodal basins at risk with images obtained immediately after injection and statics images in anterior, oblique and lateral projections including supraclavicular region. A handheld gamma probe was used to measure radioactivity counts over the SLNs, and skin marks. Results SLN was identified in 40 over 41p. In the other patient SLN was identified in the operating room by handheld gamma probe, localized in supraclavicular region. More frequent localizations: Submaxillar: 8nodes, Upper jugular 28nodes, Intraparotid 3nodes, Mastoid (pre or retro-auricular) 14nodes and Occipital 2nodes. In 14p more than one SLN were identified. SLNs were positive for melanoma in the intraoperative biopsy in 5p. The remaining 36 (who had SLN negative) were free of metastases through lymphatic channels, but in follow-up presented haematogen metastases in brain, liver and adrenal gland, due to frequent haematogen spreading of melanoma. Conclusions Melanoma was localized in Head and Neck in about 21% of patients, there was a male predominance. Lymphatic drainage from MHN is less predictable than in other anatomical sites. The technique may need to be modified for lesions that are in close proximity to a nodal basin. Interpretation of scans is almost inaccurate, and it may be better to rely on intraoperative gamma-probe evaluation, frequently after the primary lesion has been removed, to evaluate the draining basin. Although SLN mapping is a reliable indicator of the status of the draining lymphatic basins in MHN, given the incidence of haematogen metastases, patients with negative SLNs need to be followed.

P1123

Lymphoscintigraphic patterns in lower limb lymphedema

A. Guensi^{1,2}, M. Ait Idrir, A. Sallak, M. Kebbou; ¹Ibn Rochd UH, Casablanca, MOROCCO, ²nuclear medicine department, Casablanca, MOROCCO.

Lymphedema may occur for many reasons. Primitive lymphedema may be related to a distal hypoplasia of the leg lymphatic's, sclerosis and atrophy of lymph nodes... Secondary lymphedema is related to a cause extrinsic to lymph system. Traumatism to lymphatic system, surgery, and recurrent attacks of lymphangitis or cellulitis may undermine lymph drainage. The goal of this work is to report a lymphoscintigraphic patterns in lower limb lymphedema. Eighteen patients were investigated for lymphoscintigraphy between 2009 February and 2011 December in nuclear medicine department of Ibn Rochd Universtary Hospital. Dynamic and whole body images were done after bilateral subcutaneous injection of 99mTc-labeled nanocolloids. Images were done at rest, after feet tip-toeing and after one hour walking. Images analysis to qualify appearance of lymph vessels and inguinal lymph nodes was based on qualitative interpretation. The mean age of patients was 33 years [4 to 79 years]. Ten patients were females. Indications were leg swelling in 1 patient and a lower limbs (LL) swelling in the other patients, right (5 patients), left (5) and both (8). Four patients have had a lower limb injury, Six: surgery and four: streptococcus infection. Primitive lymphoedema was suspected in 4 patients. One patient (child) has had a suspected LL lymphedema with chylous ascites. One patient has a venous insufficiency diagnosed on US echodoppler. All other patients except one have had a normal leg Doppler venous. Lymphoscintigraphy scan has shown a lymphatic impairment in unilateral lower limb in 9 patients and bilateral in 2. Lymph conducting pathways visualization was blocked in knee (1 patient) and in the 10 other patients' lymph vessels and inguinal lymph nodes weren't visualised. Dermal backflow was seen in 8 patients. Lymph transport was reduced in unilateral LL in 4 patients and in bilateral LL in 2 patients. Lymphoscintigraphy has showed a peritoneal breach in child with chylous ascite. Three patients have had a normal lymphoscintigraphy. A kind of lymph abnormalities can be seen and allowed to a kind of lymphoscintigraphic patterns. Anyway, lymphoscintigraphy is the investigation of choice for diagnosis of lymphatic impairment once other low limb swelling causes have been excluded by duplex venous Doppler, CT and MRI.

P81-2 - Tuesday, October 30, 2012, 16:00 - 16:30, Poster Exhibition Area

Conventional & Specialised Nuclear Medicine: Miscellaneous

P1124

Extracellular fluid volume (ECV) assessment by four-electrode multifrequency bioimpedance analysis (MFBIA) : comparison with ECV calculated by Cr-51-EDTA multiple sampling plasma clearance analysis

G. Arsos¹, I. Tsechlidis², C. Sachpekidis², S. Georga¹, E. Manou³, E. Karampela¹, D. Tsakiris³, N. Karatzas¹; ¹3rd Department of Nuclear Medicine, Aristotle University of Thessaloniki Medical School, Papageorgiou Hospital, Thessaloniki, GREECE, ²1st Department of Nuclear Medicine, Aristotle University of Thessaloniki Medical School, Hippokration Hospital,

Thessaloniki, GREECE, ³Department of Nephrology, Papageorgiou Hospital, Thessaloniki, GREECE.

Introduction : ECV has recently emerged as an attractive, physiologically meaningful, alternative glomerular filtration rate (GFR) indexator, compared with the widely but unjustifiably used body surface area (BSA). Cr-51-EDTA multisampling plasma clearance analysis is a reference method for clinical GFR measurement. A 2-compartment model of tracer distribution is assumed and the multiple plasma sampling data are approximated by a biexponential function allowing for both GFR and ECV (ECV-GFR) calculation. MFBIA is a convenient non-invasive body composition analysis technique assessing, among others, ECV (ECV-MFBIA). The present study is aiming to compare ECV-MFBIA with ECV-GFR values obtained in a group of adult patients. **Patients and Methods** : Sixty-four patients aged 60.4±15.2 years, submitted to GFR measurement for clinical purposes. After bolus i.v. injection of 3.7 MBq Cr-51-EDTA, 10 blood samples were drawn at 5/10/15/30/45/60/90/120/180/240 min p.i. through a closed, 2-syringe, system attached to patient's arm, invented to secure painless and sterile procedure. GFR and ECV-GFR were calculated after counting of 1 ml plasma samples for 60 min/sample in a 5-detector γ-counter (Wallac 1470 Wizard, Finland) and biexponential kinetic analysis. GFR, indexed by BSA according to Haycock, was expressed in ml/min/1.73 m² and ECV in l. ECV-MFBIA was also assessed after measuring body impedance at 5, 50, 100 and 200 kHz using a 4-electrode (hand and foot) BODYSTAT QuadScan 4000 (UK) body composition analyser. The body mass index (BMI) was calculated according to Quetelet. ECV-GFR and ECV-MFBIA values were compared with paired t-test, their correlation was assessed by linear regression analysis and their agreement by Bland-Altman analysis. The correlation of the between ECV-MFBIA and ECV-GFR difference (DECV) with age, body height, body weight, BSA and BMI was assessed by linear regression analysis and the between sexes DECV difference by t-test. Statistical significance was accepted at the p<0.05 level. **Results** : ECV-MFBIA, ECV-GFR and DECV values (mean±SD) were 18.4±3.0, 14.9±3.4 and 3.5±1.7 (p<0.0001) l respectively. ECV-MFBIA and ECV-GFR were well correlated (r=0.869, p<0.0001) but less well agreed (95% confidence interval 0.2 - 6.9 l). Neither statistically significant difference of DECV between sexes nor DECV correlation with body height, body weight, BSA and BMI was found. A weak negative correlation (r = -0.340, p<0.005) between DECV and age>50 years was detected. Conclusion: ECV-MFBIA values are systematically and body habitus independently, significantly higher than ECV-GFR values and in loose agreement with the later. As a consequence, ECV-MFBIA can not replace ECV-GFR for GFR indexing purposes.

P1125

Accuracy and reproducibility of quantified salivary gland scintigraphy in the diagnosis of Sjögren syndrome

A. Skanjeti¹, T. Angusti¹, R. Carignola², E. Trevisiol¹, S. Cauda¹, M. Manfredi¹, V. Podio¹; ¹Nuclear Medicine Unit, San Luigi Hospital, Turin, ITALY, ²Internal Medicine 1, San Luigi Hospital, Turin, ITALY.

BACKGROUND. Several quantification methods had been suggested to optimize the evaluation of Salivary gland dynamic scintigraphy (SGdS). The aim of this study was to assess accuracy and reproducibility of quantified salivary gland dynamic scintigraphy analysis (assessed with a home-made application) in the diagnosis of primary Sjögren syndrome (pSS). **MATERIALS AND METHODS.** Thirty-nine consecutive patients (4 M, 35 F; age 59±13 mean±SD) suspected for pSS were included; disease was definitively diagnosed in 13 of them. Dynamic salivary gland scintigraphy were separately assessed qualitatively and semi-quantitatively by three operators; uptake and excretion fraction for both parotids and submandibular glands of each side were studied. ROC curve analysis of these semi-quantitative data were used to establish accuracy. Finally, the intraclass correlation coefficient (ICC) was used to evaluate the inter-operator results reproducibility. **RESULTS.** Submandibular gland uptake showed good relation with diagnosis (p=0.006 for right gland, p=0.01 for left gland). Moreover, submandibular gland excretion fraction relationship with diagnosis showed p=0.03 (right) and p=0.043 (left). Data from parotid glands were far less significant: only uptake appeared weakly related (p=0.092 right, p=0.043 left). ICC showed a significant correlation (p<0.0001) among all operators with all correlation coefficients 0.87-0.96; however in all cases higher for gland uptake than for excretion fraction. **CONCLUSIONS.** This study pointed out high performances of quantified salivary gland dynamic scintigraphy analysis in primary Sjögren syndrome identification. Semi-quantitative uptake data from submandibular glands, predicted diagnosis with good accuracy. On the other hand, semi-quantitative uptake data from parotid glands did not show good relation, probably due to the delayed and less severe involvement of these glands. Moreover, the quantification of this exam was highly reproducible. These data suggests that submandibular glands semi-quantitative data could be used to reliably diagnose Sjögren syndrome.

P1126**Increased Brown Adipose Tissue (BAT) activity on FDG PET-CT examinations, factors of influence**

Z. Tóth¹, J. Varga², L. Kiss³, V. Tóth¹, P. Szabó¹, I. Garai³; ¹ScanoMed Ltd., Budapest, HUNGARY, ²Department of Nuclear Medicine, University of Debrecen Medical and Health Science Centre, Debrecen, HUNGARY, ³ScanoMed Ltd., Debrecen, HUNGARY.

Aim: The appearance characteristics of increased BAT activity on FDG PET images are influenced by numerous factors. Our aim was to evaluate the correlation of BAT activity with gender, body mass index (BMI), blood glucose level, diabetes mellitus (DM), the smoking habits in our patient population, and with the season of the study. **Methods and Materials:** We retrospectively surveyed 7243 PET-CT examinations (5563 patients; 3197 female; 2366 male) performed in 2010 and 2011, and evaluated the presence and intensity score of increased BAT activity reported. The subjects' age, weight (12-175 kg), height (67-208 cm), blood glucose level (2.1-22.6 mmol/L), medical history of diabetes mellitus (DM), and smoking were recorded. **Results:** The overall prevalence of BAT activity was 5.6%, with female predominance (odds ratio 3.7). BAT activity was more frequent in younger subjects (Kruskal-Wallis test: $p < 0.0001$), in those with lower BMI and those with lower plasma glucose levels (Mann-Whitney test: $p < 0.0001$). Quite surprisingly, none of our patients with diabetes (0/977) had increased tracer uptake suggesting BAT activity. Among subjects who gave up smoking recently, its appearance was less frequent than the average (4% vs. 5.6 %; chi-square test: $p = 0.008$). We could not find correlation of BAT uptake and the month or season of the study. **Conclusion:** Similarly to the international literature, we found female predominance, negative correlation between BAT activity and blood glucose level, BMI and diabetes (we did not detect at all BAT activity in our diabetic patients). Successful BAT activation may play an interesting role in the therapeutic modification of glucose metabolism, and lower BAT activity might be an issue in ex-smoking weight gain.

P1127**SPECT/CT with SESTAMIBI-99mTc in Head and Neck Tumors: Preliminary Study**

C. P. V. Cerqueira, L. L. Aguiar, J. G. Almeida-Filho, J. M. C. Altamiani, B. J. Amorim, C. S. P. Lima, E. M. R. Brunetto, C. R. Mudinutti, C. D. Ramos; State University of Campinas - UNICAMP, Campinas, BRAZIL.

Introduction: 99mTc-sestamibi has been demonstrated to uptake in different tumors, including squamous cell carcinoma of the head and neck (SCCHN) and it is a potential radiopharmaceutical to distinguish between necrosis, edema and fibrosis from residual tumor after cancer treatment. However, conventional scintigraphic images of this radiopharmaceutical present a major limitation due to the lack of anatomic references to accurately identify the sites of tumor uptake. Single-photon emission computed tomography/computed tomography (SPECT/CT), provides a perfect correlation between the scintigraphic functional information and patient anatomy and could be used to delineate 99mTc-sestamibi tumor uptake in patients with SCCHN. **Objective:** To study the potential use of 99mTc-sestamibi SPECT/CT in the evaluation of patients with head and neck tumors. **Methodology:** We studied 15 patients (all male, 48-85 years-old, mean age 63 years) with SCCHN clinical stages III and IV (7 in the oral cavity, 6 in the larynx and 2 in the pharynx). All patients had a high-resolution contrast-enhanced CT performed for staging purposes. SPECT/CT images using a scintillation camera integrated with a multislice computed tomography of all patients were obtained 5 minutes after an intravenous injection of 740 MBq of 99mTc-sestamibi, utilizing low-dose CT. One patient repeated SPECT/CT images after chemo and radiotherapy. Radiotracer uptake by the tumor was visually classified into three degrees of intensity: mild, moderate and marked, using background and salivary glands uptake as references. **Results:** Comparing SPECT/CT images with high-resolution contrast-enhanced CT, tumor uptake of 99mTc-sestamibi could be easily identified and distinguished from physiological uptake in all 15 patients. Eight/15 tumors showed marked uptake of the radiotracer, 6/15 moderate and 1/15 mild. The images of the single patient who repeated the study after chemo and radiotherapy, showed disappearance of 99mTc-sestamibi tumor uptake, despite the persistence of the tumor mass on CT. **Conclusion:** This preliminary study shows that SPECT/CT with 99mTc-sestamibi is a potential method to assess the metabolic activity of tumors of head and neck with clinical stage III and IV. The study of a greater number of patients is needed to establish the usefulness of this method for early evaluation of response to treatment of these tumors.

P82-2 - Tuesday, October 30, 2012, 16:00 - 16:30, Poster Exhibition Area

Therapy & Clinical Trials**P1128****Standardized Uptake Value of FDG and response to conformal hypofractionated radiotherapy (3DCRT) using a "stereotactic body frame (SBF)" in early stage NSCLC: preliminary results**

C. Tranfaglia¹, S. Zoboli¹, F. Salvi², E. Cason¹, M. Santoro¹, G. Frezza², G. Fagioli¹; ¹Nuclear Medicine Unit Maggiore Hospital, Bologna, ITALY, ²Radiotherapy Unit Bellaria Hospital, Bologna, ITALY.

Aim: The aim of this ongoing study is to evaluate the relationship between FDG uptake (expressed as body-weighted Standardized Uptake Value-SUV) and local relapse/progression (LR/PL) in patients treated with hypofractionated stereotactic radiotherapy (SRT) for early stage NSCLC. **Methods:** Thirty-six patients underwent a 18FDG-PET/CT for pre-treatment staging of primary lung tumours (24 in the superior-SL, 5 in the middle-ML and 7 in the inferior lobe-IL). Sixty minutes after intravenous injection of 4 MBq/kg of 18FDG, in eu-glycaemic conditions, images were acquired by a Discovery STE tomograph (GE Healthcare) and assessed using a GE Xeleris workstation (GE). The SUVmax value of known pulmonary lesions was calculated and collected for each patient. All patients showed no pathologic nodal uptake nor evidence of distant metastasis on PET/CT. The stage of the disease was finally: T1a-N0 in 16 patients, T1b-N0 in 11 and T2a-N0 in 9. For the radiotherapy treatment patients were positioned in a dedicated frame: the "stereotactic body frame" (SBF) developed by Elekta. A spiral CT scan of the chest was performed under shallow breathing, with a reconstructed slice thickness of 3 mm. For 3D planning the Precise Plan (Elekta) was used. The dose range was 50-60 Gy in 5 fractions. A mechanical device to reduce the movements of the diaphragm was used in tumours of the lower lobes. Response was evaluated with chest-CT after 3-4 months and CT or PET/CT at 6-8 months, and eventual subsequent follow-up chest-CT were performed every 6 months. **Results:** We observed LR/PL in only 3 male patients (8.3%), with T1a (one) and T1b (two) lesions of the right-SL, that received 55-50-60 Gy respectively. The overall SUVmax range was 1.25-19. In the 3 LR/PL patients the SUVmax was 5.7-7.8 and 9.6 respectively, while all patients with higher (>9.6) and lower (<5.7) SUVmax showed a complete local response. **Conclusions:** Hypofractionated SRT confirms to give a high response rate in early stage NSCLC. An intermediate SUVmax characterized our LR/PL patients. We can hypothesized that while a lower SUV can demonstrate a lesser biological aggressiveness, an higher SUV can correlate with an higher replication index contributing to radiosensitivity. All non-responders had small (<3cm) lesions of the SL. Although the large majority of our patients had SL lesions, this results, if confirmed, could suggest the extension of the use of the mechanical device able to reduce respiratory movements also to ML and SL lesions treatment.

P1129**SUV-volume Histogram as tool for MRgFUS bone metastasis treatment monitoring**

A. Stefano¹, G. Russo², G. Candiano¹, V. Tripoli¹, A. Vaccari³, F. Ganguzzu³, C. Messa⁴, I. Castiglioni², M. C. Gilardi⁵, G. Borasi¹; ¹LATO scari, Cefalù (PA), ITALY, ²IBFM-CNR, Segrate (MI), ITALY, ³HSR-Giglio, Cefalù (PA), ITALY, ⁴IBFM-CNR; LATO scari; Nuclear Medicine Department, San Gerardo Hospital; Tecnomed Foundation, University of Milano-Bicocca, Milano, ITALY, ⁵IBFM-CNR; Nuclear Medicine Department, Scientific Institute San Raffaele; Tecnomed Foundation, University of Milano-Bicocca, Milano, ITALY.

Aim: Aim of this study was to evaluate the Cumulative SUV-volume Histogram as a tool for Magnetic Resonance-guided Focused Ultrasound (MRgFUS) treatment monitoring. MRgFUS is an innovative method for metastasis pain palliation and for the related cancerous tissue ablation (in the regions directly accessible to the ultrasound beam). **Methods:** A patient with pelvic bone metastasis, accessible to the ultrasound beam, was studied by 18F-FDG PET/CT before (I), at 3 (II) and at 6 (III) months after the MRgFUS treatment. At the three different times, the therapy outcome was assessed by: 1) patient interview to obtain the pain perception evaluation (Visual Analog Scale), ranging from 0 to 10, 2) qualitative observation of 18F-FDG PET/CT images, and 3) the target uptake Radiotracer distribution changes. This evaluation was done by using the Cumulative SUV-volume Histograms (CSH) distribution. Similarly to the Dose-Volume Histogram (DVH) distribution in Radiotherapy, the CSH represents the % of tumor metabolic volume that is higher than a SUV threshold, variable from 0 to the maximum SUV value [Van Velden et al, Eur J Nucl Med Mol Imaging, 2011 vol.38(9):1636-47]. According to the literature, SUV threshold was set at 50% of maximum SUV and the area under the CSH curve was considered as a quantitative index of the heterogeneity in the FDG uptake inside the lesion volume. The partial volume effect was not considered because the lesion sphere-equivalent diameter was greater than 5 cm. In order to evaluate the ablation effect, the percentage change of CSH was obtained as follows: $\Delta\text{CSH}(\text{post}$

vs pre) = $100 \times (\text{CSH}_{\text{post}} - \text{CSH}_{\text{pre}}) / \text{CSH}_{\text{pre}}$. This value was compared with the patient interview results and with the Nuclear Medicine qualitative assessment. Results: The patient reported a quality-of-life marked improvement, with a pain reduction from 9 (I) to 2 (in II and III). CSH changes in I, II, and III times were observed: $\Delta\text{CSH}(\text{II vs I}) = -32.7\%$, $\Delta\text{CSH}(\text{III vs II}) = -20.4\%$ and $\Delta\text{CSH}(\text{III vs I}) = -46.4\%$. These CSH decreases were in agreement with qualitative observation of PET/CT images. Conclusion: In the considered patient, the treatment response along the follow-up stages indicated that MRgFUS therapy was effective in the reduction of the bone metastasis pain and in the ablation of accessible cancerous tissue. CSH showed a marked response in the regions treated with the ultrasound beam and seems to be a useful tool for evaluating the radiotracer uptake heterogeneity in the oncological lesions.

P1130

Evaluation of chemotherapy efficacy in patients with breast cancer by tumor visualization with ^{99m}Tc -MIBI

S. N. Novikov, S. V. Kanaev, T. U. Semiglazova, P. V. Krivorotko, V. F. Semiglazov, L. A. Jukova; N.N. Petrov Inst. Oncol., St. Petersburg, RUSSIAN FEDERATION.

Purpose: to evaluate results of breast scintigraphy (BS) with ^{99m}Tc -MIBI when it was used for monitoring of chemotherapy (CHT) efficacy in women with breast cancer (BC) **Material and methods:** 50 women were included in this study. BS was done before the start of CHT and/or after 2-6 cycles of treatment with taxane-doxorubicin based regimes +/- trastuzumab. BS was performed in planar lateral and anterior projections 10-15 min after i/v injection of 740 MBq of ^{99m}Tc -MIBI. Qualitative and semiquantitative scores were used to qualify dynamic of tracer uptake (TU). CHT efficacy according to BS results were estimated as follows: progression (grade I) - increase of area and/or intensity of TU; stabilization (II) - unchanged image of BC; partial effect (III) - intermediate (30-70%) decrease in intensity and area of TU in BC; prominent efficacy (IV) - only small foci of low residual TU in BC; complete resolution (V) - TU in BC on the level of background. **Results:** BS detected complete resolution of TU in primary tumor in 10 (20%) of 50 treated patients, in additional 12 (24%) cases efficacy of CHT was prominent, 15 (30%) women had scintigraphic signs of stabilization or progression of BC. In 20 (49%) of 41 patients with lymph node (LN) involvement CHT resulted in remarkable (grade IV-V) scintigraphic response. Of special interest is the fact that 5 women with excellent (IV-V) regression of TU in primary tumor had poor response in involved LN. Vice versa in 5 cases excellent (IV-V) LN response was accompanied by persistent TU in primary tumor. Number of CHT cycles significantly influence character of BS changes. After 2 cycles of TAC +/- trastuzumab 2 of 10 patients demonstrated signs of grade IV, one - of grade III tumor response and other 7-stabilization or progression of BC. After 3 cycles 7 (44%) of 16 women had good (grade IV-V) efficacy of CHT, in other 9 (56%) cases scintigraphic response was moderate or poor (grade I-III). After 4-6 CHT cycles TU uptake in primary tumor disappeared (V) or become markedly reduced (IV) in 13 (54%) of 24 patients. In 6 (25%) women BS data reflect non-significant efficacy of CHT. **Conclusion:** 1. BS demonstrated excellent (grade IV-V) response of BC to taxane-doxorubicin based CHT in 44% of women with advanced disease. 2. According to scintigraphic data efficacy of CHT become remarkably evident after 3 or more cycles of TAC +/- trastuzumab

P1131

Role of ^{18}F -FDG PET/CT In Radiotherapy Treatment Planning and In Predicting Response To Therapy In Locally Advanced Rectal Cancer

D. Grigolato¹, M. Zuffante¹, M. Giori², L. E. Etta³, A. Minicozzi⁴, S. Maluta³, C. Cavedon², M. Ferdeghini¹; ¹Nuclear Medicine Unit Azienda Ospedaliera Universitaria Integrata - Verona, Verona, ITALY, ²Medical Physics Unit Azienda Ospedaliera Universitaria Integrata - Verona, Verona, ITALY, ³Radiation Oncology Department Azienda Ospedaliera Universitaria Integrata - Verona, Verona, ITALY, ⁴Department of Surgery Azienda Ospedaliera Universitaria Integrata - Verona, Verona, ITALY.

AIM: To assess and correlate the metabolic change in patients with locally advanced rectal cancer (LARC) after neoadjuvant chemoradiation therapy (nCRT) and the results of tumor regression grade (TRG) according to Mandar criteria; to discriminate between inflammation reaction and viable tumor cells after nCRT; to observe the variability of ^{18}F -FDG PET derived metabolic treatment volumes with different methods: manual and automatic thresholding set on SUV max and fixed percentage of SUV max. **METHOD:** Sixteen patients with LARC, staged T3-T4 N0 and any T-N+, who were candidates for nCRT (Xeloda/5FU and 50 Gy in 25 fractions), were recruited from January 2011. FDG PET/CT was performed at baseline (PET1) for staging and metabolic planning in treatment position and PET2 after 8 weeks from nCRT with a delayed pelvic scan (PET2_{del}) in 11 patients. Standardized uptake value (SUV) of each tumor as SUV1max (PET1), SUV2 max (PET2), % SUV variation between PET1-PET2 ($\Delta 1$) and PET2- PET2_{del} ($\Delta 2$) were recorded and compared with TRG or presence of local disease at follow-up. Eleven patients underwent surgery

and 5 patients, not operated, had one year follow-up. **RESULTS:** Hystopatological results and follow-up indicated 7 responders (44%: three Mandar 2, one Mandar 1, two no local recurrences at FU) and 9 non-responders (64%: two Mandar 4; five Mandar 3; two relapse at FU). The best cut-off value to predict objective true response was SUV2 max > 4.4 with 6 TP, 6 TN, 3 FN and 1 FP, the sensibility, specificity, accuracy, NPV and PPV were 67%, 87%, 75%, 66% and 86% respectively. Choosing a lower value, SUV2 max 4, the specificity dropped to 43%, the accuracy to 56% and the sensibility remained unchanged, 50% NPV, 60% PPV. When $\Delta 1$ was 79% we obtained 8 TP, 4TN, 1 FN, 3 FP with 89% sensibility, 43% specificity, 75% accuracy, 80% NPV, 73% PPV. When $\Delta 2$ was > 30% this indicated presence of viable tumor cells and excluded inflammation. Automatic delineation methods for BTV were always smaller than manual ones. Conclusion: The accurate analysis of metabolic results after nCRT may be useful in the selection of those patients who could avoid unnecessary radical surgery. Additional late scan and $\Delta 2$ could give information in the evaluation of false negative results. Predefined PET threshold might be useful to guide boost radiation treatment and reduce BTV variability between different operators.

P1132

Case Report: Glioblastoma Imaging and Therapy with ^{64}Cu -Asparagine

C. Villano, G. Pigotti, D. Martini, E. Baldassarrini, P. Panichelli, G. Valentini; A.C.O.M SPA, MONTECOSARO, ITALY.

Glioblastoma is one of the most malignant and aggressive type of brain tumors with an average life expectancy of less than 15 months. Our aim is to demonstrate ^{64}Cu -asparagine capability to obtain both diagnosis and therapy in PET/CT imaging for a radiotargeted molecular therapy in patients with glioblastoma. We introduced the new tracer asparagine radiolabeled with copper radionuclide according to following reasons: as showed in previous experimental data, glioblastoma needs asparagine for cellular metabolic activities and ^{64}Cu is able to link DNA and to destroy tumor cells thanks to its Auger effect. In fact, it is characterized by high Linear Energy Transfer (LET) in a small spatial region that can crash the cell. We report a particular case of a 71-year-old man with cerebral craniotomy (November, 2010) for a glioblastoma in the left rolandic region. In spite of surgery, the patient showed severe epilepsy with difficult gait (lower limb palsy) and non fluent speech with urinary incontinence. Moreover, he had not exact and real thought-movement nexus. He underwent a complete radiation therapy and a partial chemo treatment due to his pharmaceutical intolerance. Prior patient's consent, ^{64}Cu -asparagine PET/CT has been evaluated in four different treatments, planned every 3 months. Two to 3 hours after 80 mCi dose injection, PET/CT acquisition was made according to cerebral protocol 15 min length with 128x128 matrix (Biograph 6 Truepoint PET/CT, Siemens). ^{64}Cu -asparagine scans showed a markedly volume reduction along all three sections (axial, coronal, sagittal): 1.42 cm, 2.6 cm and 1.5 cm. It's also verified ^{64}Cu -asparagine capability to cross the blood-brain barrier (BBB) and to link cellular DNA. Patient's life expectancy has been carried up to 15 months after tumor diagnosis with enhanced quality of life. Actually, the man is able to walk, to munch and swallow, to have a speech and his epilepsy crisis are shorter, milder and few and far between. These results are very promising but we need to extend this study to other patients to evaluate ^{64}Cu -asparagine real usefulness in glioblastoma diagnosis and therapy, mainly in pediatric population where it would be possible to obtain three-time greater efficacy.

P1133

Treatment of Keloids using Re-188 : A Pilot Study

P. Gupta¹, K. K. Verma¹, S. P. Lochab², P. Kumar¹, A. Malhotra¹, G. P. Bandopadhyaya¹, G. Bandopadhyaya¹; ¹All India Institute of Medical Sciences, New Delhi, INDIA, ²Inter University Accelerator Centre, New Delhi, INDIA.

Introduction Keloids are irregularly shaped scars composed of mainly either type III (early) or type I (late) collagen which tend to enlarge progressively. After a skin wound, both skin cells and connective tissue cells (fibroblasts) begin multiplying to repair the damage and these fibroblasts continue to multiply even after the wound is filled. No treatment is 100% effective and invasive methods like surgery lead to recurrence & increase in size. Aim The aim of the study was to test Re-188 skin bandages as a non-invasive mode of treatment for keloids. Materials and Methods Patients with clinically confirmed keloid ≤ 10 cm in longitudinal diameter were included in the study. After giving complete information about the study, patients who preferred Re-188 bandage application were included. Six patients (2 male and 4 female) aged between 22-65 years were evaluated. Surface area of the keloid was determined. Sealed skin bandages containing Re-188 (1mCi/sq.cm) were custom made according to size and shape of the lesions and applied locally over the keloid. A total of 50 Gy/sq.cm radiation dose was delivered superficially over the lesion in two fractions with an interval of two days. Patients were followed up at regular intervals upto 3 months. Results One patient showed complete remission. There was complete resolution of keloid at 10 weeks post treatment. In other five patients, there was considerable decrease in the size of the lesions (upto

80%) and marked flattening of the keloid was noted at 3 months post treatment follow up. Routine haematological and biochemical examinations did not reveal any toxicity. Conclusion Re-188 skin bandages could be used as a non-invasive method of treatment for keloids- a skin pathology with no treatment till date. However, further studies need to be done for dose optimisation and for standardising the treatment protocol.

P1134

Evaluation the effectiveness of intrapyloric BOTOX® injection in patients with chronic renal failure and severe gastric discomfort by scintigraphic study of gastric motility.

E. D. Karathanos¹, V. Kokkinou², N. Boussios³, A. Kiroudi³, I. Livaditaki³, E. Mourvati⁴, S. Panagoutsos⁴, K. Mimidis⁵, V. Vargemezis⁴, A. S. Zissimopoulos³, ¹Dptm of Nuclear Medicine, Demokritos University of Thrace University Hospital of Alexandroupolis, ALEXANDROUPOLIS, GREECE, ²Dpt of Nephrology, Demokritos University of Thrace University Hospital of Alexandroupolis, ALEXANDROUPOLIS, GREECE, ³Dpt of Nuclear Medicine, Demokritos University of Thrace University Hospital of Alexandroupolis, ALEXANDROUPOLIS, GREECE, ⁴Dpt of Nephrology, Demokritos University of Thrace University Hospital of Alexandroupolis, ALEXANDROUPOLIS, GREECE, ⁵Dpt of Gastroenterology, Demokritos University of Thrace University Hospital of Alexandroupolis, ALEXANDROUPOLIS, GREECE.

Introduction: BOTOX® (Botulinum toxin A), has been widely used in clinical and cosmetic medicine, and is also a powerful inhibitor of muscle contraction. In patients with gastroparesis and severe dyspeptic symptoms, intrapyloric BOTOX® injection through an endoscope is an alternative to ineffective pharmaceutical approach. BOTOX® relaxes muscles in the GI tract, including the lower oesophageal sphincter in achalasia, and the pylorus in gastroparesis, leading to better gastric motility and symptom relief. **Aim:** The aim of this study is to evaluate the therapeutic effectiveness of intrapyloric BOTOX® injection in patients with chronic renal failure under dialysis and gastroparesis, comparing gastric motility before and after BOTOX® injection by means of radionuclide technique. **Patients and method:** Within a period of 14 months, 25 patients (13 male, 12 female) with chronic renal failure under dialysis and severe gastric symptoms, were examined. Patients with known peptic ulcer, gastritis and gastroesophageal reflux have been excluded. The study was based on a typical solid-emptying radionuclide protocol before and after 20U BOTOX® injection: Following a fast overnight period without taking any prokinetic medication and immediately after the consumption of an omelette labelled with 1mCi 99mTc-colloid, static images of anterior and posterior stomach surface were obtained with the patient still on upright. In order to avoid movement artefacts each image had duration of 1min. The scintigraphy was completed after 90min, with 5min interval time between each anterior and posterior acquisition. (Millennium GE Milwaukee USA g-camera). Drawing regions of interest (ROI) on every gastric image, we calculated the geometrical mean and the half emptying time (T1/2). (Normal values according to our department: T1/2=70±12min). Results were presented in arithmetic values (min) and plotted out in a graph curve (percentage retention over time or/and geometrical count mean over time). **Results:** 9/25 patients who revealed prolonged T1/2 (> 120±15min) as in a typical abnormal late gastric emptying, underwent an endoscopic intrapyloric BOTOX® injection. 7 of them were re-examined 1-2 months later by scintigraphy. 4/7 patients (57%) had an important clinical and scintigraphic improvement with normal T1/2 values, whereas 3/7 showed neither symptomatic nor scintigraphic improvement. **Conclusion:** Scintigraphic measurement of gastric motility with 99mTc-colloid (solid phase) is an easy, cheap and safe way to test the efficacy of intrapyloric BOTOX® injection in end renal stage patients. Our results show a mild positive effect, but as we lack of sufficient number of patients, final conclusions have to wait. The study is still going on.